RECENT ADVANCES IN ACIDOPHILE MICROBIOLOGY: FUNDAMENTALS AND APPLICATIONS

EDITED BY: D. Barrie Johnson and Axel Schippers

PUBLISHED IN: Frontiers in Microbiology

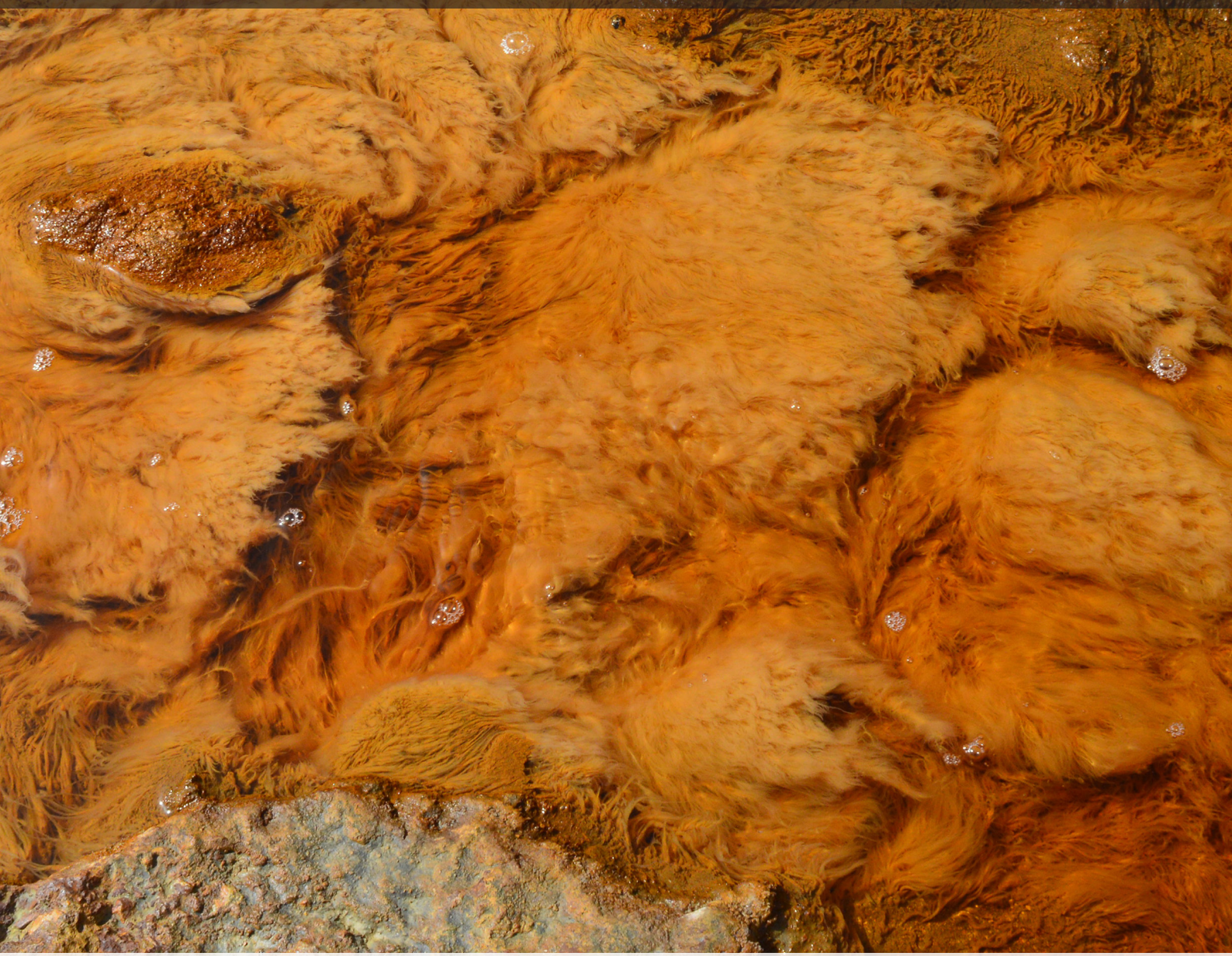

frontiers Research Topics

ISSN 1664-8714
ISBN 978-2-88945-163-0
DOI 10.3389/978-2-88945-163-0

About Frontiers

Frontiers is more than just an open-access publisher of scholarly articles: it is a pioneering approach to the world of academia, radically improving the way scholarly research is managed. The grand vision of Frontiers is a world where all people have an equal opportunity to seek, share and generate knowledge. Frontiers provides immediate and permanent online open access to all its publications, but this alone is not enough to realize our grand goals.

Frontiers Journal Series

The Frontiers Journal Series is a multi-tier and interdisciplinary set of open-access, online journals, promising a paradigm shift from the current review, selection and dissemination processes in academic publishing. All Frontiers journals are driven by researchers for researchers; therefore, they constitute a service to the scholarly community. At the same time, the Frontiers Journal Series operates on a revolutionary invention, the tiered publishing system, initially addressing specific communities of scholars, and gradually climbing up to broader public understanding, thus serving the interests of the lay society, too.

Dedication to Quality

Each Frontiers article is a landmark of the highest quality, thanks to genuinely collaborative interactions between authors and review editors, who include some of the world's best academicians. Research must be certified by peers before entering a stream of knowledge that may eventually reach the public - and shape society; therefore, Frontiers only applies the most rigorous and unbiased reviews.
Frontiers revolutionizes research publishing by freely delivering the most outstanding research, evaluated with no bias from both the academic and social point of view.
By applying the most advanced information technologies, Frontiers is catapulting scholarly publishing into a new generation.

What are Frontiers Research Topics?

Frontiers Research Topics are very popular trademarks of the Frontiers Journals Series: they are collections of at least ten articles, all centered on a particular subject. With their unique mix of varied contributions from Original Research to Review Articles, Frontiers Research Topics unify the most influential researchers, the latest key findings and historical advances in a hot research area! Find out more on how to host your own Frontiers Research Topic or contribute to one as an author by contacting the Frontiers Editorial Office: **researchtopics@frontiersin.org**

RECENT ADVANCES IN ACIDOPHILE MICROBIOLOGY: FUNDAMENTALS AND APPLICATIONS

Topic Editors:
D. Barrie Johnson, Bangor University, UK
Axel Schippers, Federal Institute for Geosciences and Natural Resources (BGR), Germany

Microbial "streamer" growths in an acidic (pH 2.5) iron-rich stream draining the abandoned San Telmo copper mine in Andalucia, Spain (image courtesy of Ana Laura Santos, Bangor University, UK).

There is considerable interest in pure and applied studies of extremophilic microorganisms, including those (acidophiles) that are active in low pH environments. As elsewhere in microbiology, this is a fast-developing field, and the proposed special issue of Frontiers highlights many of the more recent advances that have been made in this area. Authors from leading scientific groups located in North and South America, Asia and Australia and Europe have contributed to this e-book, and the topics covered include advances in molecular, biochemical, biogeochemical and industrial aspects of acidophile microbiology.

Citation: Johnson, D. B., Schippers, A., eds. (2017). Recent Advances in Acidophile Microbiology: Fundamentals and Applications. Lausanne: Frontiers Media. doi: 10.3389/978-2-88945-163-0

Table of Contents

frontiers in Microbiology

EDITORIAL
published: 14 March 2017
doi: 10.3389/fmicb.2017.00428

Editorial: Recent Advances in Acidophile Microbiology: Fundamentals and Applications

D. Barrie Johnson[1]* *and Axel Schippers*[2]

[1] School of Biological Sciences, College of Natural Sciences, Bangor University, Bangor, UK, [2] Geomicrobiology, Resource Geochemistry, Federal Institute for Geosciences and Natural Resources (BGR), Hannover, Germany

Keywords: acidophiles, *Acidithiobacillus*, biochemistry, biodiversity, biogeochemistry, extremophiles, genomics

Editorial on the Research Topic

Recent Advances in Acidophile Microbiology: Fundamentals and Applications

Acidophilic microorganisms thrive in extremely low pH natural and man-made environments such as acidic lakes, some hydrothermal systems, acid sulfate soils, sulfidic regoliths and ores, as well as metal and coal mine-impacted environments. The most widely studied acidophiles, prokaryotes that oxidize reduced iron and/or sulfur, are able to catalyze the oxidative dissolution of metal sulfide minerals such as pyrite (FeS_2), thereby severely acidify the environment (often to pH <3) in which they thrive. At such low pH values the ferric iron generated by their activities is soluble and serves as the chemical oxidant of sulfide minerals. One the one hand, this is highly beneficial, and is the core process in the biotechnology known generically as "biomining," where acidophiles are used to facilitate the extraction and recovery of base (e.g., copper, cobalt, nickel, and zinc) and precious metals (principally gold), and also uranium. On the other hand, uncontrolled microbial metal sulfide oxidation in abandoned mines and mine spoils can generate highly noxious waste-waters (acid mine/rock drainage) which, because of their low pH, elevated concentrations of potential toxic metals and metalloids, and high osmotic potentials, pose severe threats to the environment. Recent research, however, has shown that some species of acidophilic microorganisms could also be used not only to mitigate mine water pollution but also to recover metals from acidic waste-waters *via* selective biomineralization.

This *Research Topic* issue comprises 10 original research articles and presents novel data on molecular/ genomic, biochemical, physiological, and applied aspects of acidophilic prokaryotes. These extremophiles may be divided into "extreme acidophiles," which have pH growth optima at or below pH 3.0, moderate acidophiles, which grow optimally between pH 3.0 and 5.0, and acid-tolerant species which grow optimally above pH 5.0, but which also grow reasonably well at lower pH values. Eight of the papers in this *Research Topic* focus on extreme acidophiles, and most of these describe advances in our knowledge and understanding of the most widely researched class of acidophiles, the *Acidothiobacillia*. New insights into the phylogenetic structure and diversification of *Acidithiobacillus* species revealed by combining analyses of 16S rRNA gene-based ribotyping, oligotyping, and multi-locus sequencing analysis (MLSA) is described in the report of Nuñez et al., who investigated 580 strains of the seven recognized species of the genus (*Acidithiobacillus thiooxidans, A. ferrooxidans, A. albertensis, A. caldus, A. ferrivorans, A. ferridurans,* and *A. ferriphilus*) in their study. Another paper describes how bioinformatic analysis has revealed the existence of five highly conserved gene families in the core genome of the monophyletic genus *Acidithiobacillus* of the class *Acidithiobacillia* (González et al.). Insights into the quorum sensing regulon of *Acidithiobacillus ferrooxidans* revealed by transcriptomic in the

OPEN ACCESS

Edited by:
Andreas Teske, University of North Carolina at Chapel Hill, USA

Reviewed by:
Andreas Teske, University of North Carolina at Chapel Hill, USA
Jens Kallmeyer, Helmholtz Zentrum Potsdam-GFZ, Germany

***Correspondence:**
D. Barrie Johnson
d.b.johnson@bangor.ac.uk

Specialty section:
This article was submitted to Extreme Microbiology, a section of the journal Frontiers in Microbiology

Received: *13 February 2017*
Accepted: *28 February 2017*
Published: *14 March 2017*

Citation:
Johnson DB and Schippers A (2017) Editorial: Recent Advances in Acidophile Microbiology: Fundamentals and Applications. Front. Microbiol. 8:428. doi: 10.3389/fmicb.2017.00428

presence of an acyl homoserine lactone superagonist analog is described in the report of Mamani et al., while Wang et al. describe how transcriptional analysis has shown that the two-component system RsrS-RsrR regulates the tetrathionate intermediate pathway for thiosulfate oxidation in *Acidithiobacillus caldus*. A novel application of *in situ* spectroscopy carried out by Blake et al. has confirmed that acidophilic iron-oxidizing prokaryotes in different phyla use different electron transfer biomolecules to respire aerobically on soluble iron. Experiments on redox transformations of three transition metals (iron, copper, and chromium) by some *Acidithiobacillus* spp. and two other genera of acidophilic bacteria (*Leptospirillum* and *Acidiphilium*) gave some unexpected results, including the fact that reduction of ferric iron can be mediated under aerobic conditions, and that copper, like iron, can be both oxidized and reduced by acidophiles, though *via* indirect mechanisms (Johnson et al.). Quantifying numbers and activities of acidophiles in natural and anthropogenic environments is becoming increasing important, and Hedrich et al. describe novel quantitative real-time PCR assays for the quantification of *Acidithiobacillus*, *Leptospirillum*, and *Sulfobacillus* species. When combined with other molecular PCR-based methods, total cell counts and metal sulfide oxidation activity measurements *via* microcalorimetry, this allows highly accurate quantitative monitoring of different microbial species during bioleaching operations.

Another extreme acidophile considered in this *Research Topic* issue is the halotolerant species, *Acidihalobacter prosperus*, which is able to grow and catalyze sulfide mineral dissolution at elevated concentrations of salt (NaCl) and is potentially important for biomining in semi-arid and coastal areas, where only brackish and saline waters are available. The proteomic response of this acidophile to elevated chloride concentrations included the production of osmotic stress regulators that potentially induced production of the compatible solute, ectoine uptake protein, and increased iron oxidation resulting in heightened electron flow to drive proton export by the F_0F_1 ATPase. In contrast, *A. ferrooxidans* responded to low levels of chloride with a generalized stress response, decreased iron oxidation, and an increase in central carbon metabolism (Dopson et al.).

The two other papers in this *Research Topic* issue concern contrasting species of moderately acidophilic/acid-tolerant bacteria. Metagenome analysis of strains of the relatively little-researched aerobic and acidophilic iron-oxidizing species *Sideroxydans,* enriched from a pilot plant for the treatment of acid mine drainage, revealed their metabolic versatility and adaptation to low pH (Mühling et al.). Lastly, sequence analysis of the draft genome of the acid-tolerant sulfur-reducer *Desulfurella amilsii*, and comparison to the available genome sequences of other members of the *Desulfurellaceae* family, is presented by Florentino et al.

The manuscripts contained in this *Research Topic* issue illustrate how this particular area of extreme microbiology is continuing to reveal new insights into the molecular biology and evolution of acidophiles, their biochemistries and show their potential for use in new and sustainable biotechnological applications. These fascinating prokaryotes will doubtless continue to reveal new, interesting and potentially highly useful traits as they are further researched.

AUTHOR CONTRIBUTIONS

All authors listed, have made substantial, direct and intellectual contribution to the work, and approved it for publication.

Conflict of Interest Statement: The authors declare that the research was conducted in the absence of any commercial or financial relationships that could be construed as a potential conflict of interest.

frontiers in Microbiology

ORIGINAL RESEARCH
published: 19 January 2017
doi: 10.3389/fmicb.2017.00030

Molecular Systematics of the Genus *Acidithiobacillus*: Insights into the Phylogenetic Structure and Diversification of the Taxon

Harold Nuñez[1†], Ana Moya-Beltrán[1,2†], Paulo C. Covarrubias[1], Francisco Issotta[1], Juan Pablo Cárdenas[3], Mónica González[1], Joaquín Atavales[1], Lillian G. Acuña[1], D. Barrie Johnson[4] and Raquel Quatrini[1*]*

[1] Microbial Ecophysiology Laboratory, Fundación Ciencia & Vida, Santiago, Chile, [2] Faculty of Biological Sciences, Andres Bello University, Santiago, Chile, [3] uBiome, Inc., San Francisco, CA, USA, [4] College of Natural Sciences, Bangor University, Bangor, UK

The acidithiobacilli are sulfur-oxidizing acidophilic bacteria that thrive in both natural and anthropogenic low pH environments. They contribute to processes that lead to the generation of acid rock drainage in several different geoclimatic contexts, and their properties have long been harnessed for the biotechnological processing of minerals. Presently, the genus is composed of seven validated species, described between 1922 and 2015: *Acidithiobacillus thiooxidans*, *A. ferrooxidans, A. albertensis*, *A. caldus*, *A. ferrivorans*, *A. ferridurans,* and *A. ferriphilus*. However, a large number of *Acidithiobacillus* strains and sequence clones have been obtained from a variety of ecological niches over the years, and many isolates are thought to vary in phenotypic properties and cognate genetic traits. Moreover, many isolates remain unclassified and several conflicting specific assignments muddle the picture from an evolutionary standpoint. Here we revise the phylogenetic relationships within this species complex and determine the phylogenetic species boundaries using three different typing approaches with varying degrees of resolution: 16S rRNA gene-based ribotyping, oligotyping, and multi-locus sequencing analysis (MLSA). To this end, the 580 16S rRNA gene sequences affiliated to the *Acidithiobacillus* spp. were collected from public and private databases and subjected to a comprehensive phylogenetic analysis. Oligotyping was used to profile high-entropy nucleotide positions and resolve meaningful differences between closely related strains at the 16S rRNA gene level. Due to its greater discriminatory power, MLSA was used as a proxy for genome-wide divergence in a smaller but representative set of strains. Results obtained indicate that there is still considerable unexplored diversity within this genus. At least six new lineages or phylotypes, supported by the different methods used herein, are evident within the *Acidithiobacillus* species complex. Although the diagnostic characteristics of these subgroups of strains are as yet unresolved, correlations to specific metadata hint to the mechanisms behind econiche-driven divergence of some of the species/phylotypes identified. The emerging phylogenetic structure for the genus outlined in this study can be used to guide isolate selection for future population genomics and evolutionary studies in this important acidophile model.

Keywords: *Acidithiobacillus,* species complex, phylogenetic structure, diversity, 16S rRNA, MLSA, targeted metagenomics

OPEN ACCESS

Edited by:
Jesse G. Dillon, California State University, Long Beach, USA

Reviewed by:
Daniel Seth Jones, University of Minnesota, USA
Stephanus Nicolaas Venter, University of Pretoria, South Africa

***Correspondence:**
D. Barrie Johnson
d.b.johnson@bangor.ac.uk
Raquel Quatrini
rquatrini@cienciavida.org

[†] These authors have contributed equally to this work.

Specialty section:
This article was submitted to Extreme Microbiology, a section of the journal Frontiers in Microbiology

Received: *18 October 2016*
Accepted: *05 January 2017*
Published: *19 January 2017*

Citation:
Nuñez H, Moya-Beltrán A, Covarrubias PC, Issotta F, Cárdenas JP, González M, Atavales J, Acuña LG, Johnson DB and Quatrini R (2017) Molecular Systematics of the Genus Acidithiobacillus: Insights into the Phylogenetic Structure and Diversification of the Taxon. Front. Microbiol. 8:30. doi: 10.3389/fmicb.2017.00030

INTRODUCTION

The genus *Acidithiobacillus* (Kelly and Wood, 2000), recently assigned to a new class, *Acidithiobacillia,* of the phylum Proteobacteria (Williams and Kelly, 2013) includes species of Gram-negative, rod-shaped, autotrophic bacteria that are non-sporulating, obligate acidophiles, and catalyze the dissimilatory oxidation of elemental sulfur and reduced inorganic sulfur compounds (Garrity et al., 2005). For many years, this group of bacteria has been exploited in the bioleaching of metal sulfides, the desulfurization of coal, and natural gas, among other uses (Johnson, 2014). Representatives of *Acidithiobacillus* occur world-wide in a diverse range of natural (acid rock drainage, sulfur springs, etc.) and industrial settings (ore concentrates, pulps, and leaching solutions of the mining industry, etc.), with varying physicochemical characteristics (e.g., redox potentials and concentrations of dissolved solutes). A large number of strains living in these various ecological niches have been described over the years, and more recently also a vast number of sequence clones have been deposited in public databases, spanning a great deal of the inherent diversity of this taxon (Nuñez et al., 2016).

Until relatively recently, the *Acidithiobacillus* genus comprised only four validated species: *A. thiooxidans* (Waksman and Joffe, 1922), *A. ferrooxidans* (Temple and Colmer, 1951), *A. albertensis* (Bryant et al., 1983), and *A. caldus* (Hallberg and Lindström, 1994), with all isolates that could oxidize ferrous iron as well as reduced sulfur being considered as strains of *A. ferrooxidans*. However, in the last two decades, a variety of molecular tools suited for typing and identification of bacteria have been applied to further revise the taxon (reviewed in Nuñez et al., 2016). *Acidithiobacillus* strains of diverse origins have since been assigned to distinct phylogenetic subgroups and/or genomovars, thought to represent a number of unidentified cryptic species (e.g., Luo et al., 2009; Amouric et al., 2011; Wu et al., 2014). Based on a careful re-evaluation of phenotypic characteristics (e.g., capacity to oxidize molecular hydrogen, temperature, and pH tolerance profiles, tolerance to elevated concentrations of transition metals and chloride, presence of flagella, etc.) and multilocus sequence analyses, three novel iron-oxidizing species have been recently recognized, *Acidithiobacillus ferrivorans* (Hallberg et al., 2010), *Acidithiobacillus ferridurans* (Hedrich and Johnson, 2013), and *Acidithiobacillus ferriphilus* (Falagán and Johnson, 2016), enlarging the genus to a current total of seven species. Provisional recognition of a number of additional (*Acidi*)*thiobacillus* species—associated to particular niches—has occurred in the past, e.g., "(*Acidi)thiobacilus concretivorus,*" the predominant isolate during the acidification associated to the final stage of concrete corrosion (Parker, 1945a,b, 1947) and "*Acidithiobacillus cuprithermicus,*" described as a novel isolate growing on chalcopyrite obtained from the Tinto River (Fernández-Remolar et al., 2003), though the validity of some proposed novel "species" has often been questioned (e.g., Vishniac and Santer, 1957).

During the last decade, several hundreds of *Acidithiobacillus* strains have been isolated from all over the world (e.g., Ni et al., 2008) and a large number of 16S rRNA sequence clones have been obtained from environmental studies (summarized in Huang et al., 2016). Evidence is beginning to accumulate that supports both spatial and temporal variations in the occurrence and distribution of *Acidithiobacillus* species types that dominate acidophilic prokaryotic communities from different environments (e.g., Tan et al., 2009; González et al., 2014) and geographies (e.g., Jones et al., 2016). However, taxonomic assignment of many of these isolates or sequence clones remains, in many cases, elusive, and the existence of potential cryptic species calls for a more exhaustive phylogenetic revision of the taxon.

Using a broader taxon sampling that spans the *Acidithiobacillus* species complex at a global scale, the 16S rRNA gene as marker and oligotyping as a strategy to differentiate closely related taxa (Eren et al., 2013), we have explored the evolutionary relationships of the different linages within the taxon and attempted to improve the phylogenetic resolution and better define the species boundaries within the sampled repertoire of *Acidithiobacillus* strains. Inter- and intraspecific levels of divergence were further examined using multilocus sequence analysis (MLSA). Also, occurrence and distribution of lineages and sequence variants in different acidic biotopes were explored by tracing oligotype profiles of sequenced metagenomes available in public databases.

METHODS

DNA Extraction, PCR Amplification and Sequencing

General culturing techniques used were as described previously (Acuña et al., 2013). DNA isolation and routine manipulations were carried out following standard protocols (Nieto et al., 2009). All amplicons were generated by PCR using the high fidelity polymerase (*Pfu* DNA Polymerase, Promega) and amplification parameters recommended by the manufacturer. Primer annealing temperatures for each reaction are indicated in Supplementary Table 1. PCR products were purified using the QIAquick PCR purification kit (Qiagen Inc., USA). Gene sequencing was performed by the Sanger method at Macrogen Inc. (Korea).

Ribosomal Operons and 16S rRNA Gene Sequences

Ribosomal RNA operon sequences of *Acidithiobacillus* type strains (T) and reference strains (R) were obtained from publicly available genomes deposited in Genbank (*A. ferrooxidans* ATCC 23270^T NC011761, *A. ferrivorans*^{R} DSM 22755 NC015942, *A. caldus* ATCC 51756^T CP005986 and *A. thiooxidans* ATCC 19377^T NZAFOH00000000. In the absence of a complete or draft genome sequence for the type strain (NO-37) of *A. ferrivorans* (DSM 17398), strain SS3 (DSM 22755) was used as a reference. The latter was previously confirmed as a strain of the (then) newly-described species, *A. ferrivorans* (Hallberg et al., 2010). Ribosomal RNA operon sequences for *A. ferridurans* ATCC 33020^T, *A. ferriphilus* DSM 100412^T and *A. albertensis* DSM 14366^T were produced in house by PCR and

subsequently sequenced. Accession numbers, annotations and coordinates of each operon are detailed in Supplementary Table 2. Downstream phylogenetic analysis was carried out using 529 16S rRNA gene sequences assigned to the genus *Acidithiobacillus*, available at GenBank as of July 2016, meeting length and quality requirements (Supplementary Table 3). Sequences for the 16S rRNA gene of 51 additional strains from our laboratory collection obtained by PCR were also included in the analysis (Supplementary Table 3). The PCR primers used are listed in Supplementary Table 1.

16S rRNA Phylogenetic Analysis

Small subunit ribosomal RNA gene sequences of 580 *Acidithiobacillus* strains and sequenced clones (Supplementary Table 3) were aligned using the MAFFT v7.229 software using the L-INS-I method (Katoh and Standley, 2013). The resulting alignments were trimmed and masked (>50%) manually. Phylogenetic trees were generated by two methods. First, a maximum likelihood tree was reconstructed using PhyML (Guindon and Gascuel, 2003), with the following settings: Tamura–Nei (Tamura and Nei, 1993) was used as substitution model, PhyML estimated the transition/transversion ratio and the proportion of invariant nucleotides and a discrete gamma approximation with $k = 4$. The topology of the tree and the length of the branches were optimized by PhyML, using Nearest Neighbor Interchange and Subtree Pruning and Regrafting. The phylogenetic tree was assessed using 1000 bootstrap replicates. A second tree was generated using Bayesian analysis with MrBayes v.3.0b4. Bayesian analysis was run for 3,000,000 generations, and trees were saved every 100 generations. Posterior probabilities were calculated after discarding the first 30% of trees (Huelsenbeck and Ronquist, 2001). Trees were visualized and annotated in FigTree (http://tree.bio.ed.ac.uk/software/figtree/).

Oligotyping

Oligotyping of the 16S rRNA gene sequences was performed as described by Eren et al. (2013). A total of 12 positions with the highest entropy along the length of the sequence alignment (1054 nucleotides) were selected (Supplementary Figure 1), which spanned the following variable regions: V2 (46, 47, 62), V3 (257, 263, 264, 266), V4 (417, 418), V5 (588), and V6 (725, 765). Positions are defined with respect to the *Escherichia coli* 16S rRNA gene sequence. Oligotype (OT) assignment and sequence profiles for each individual strain or sequence clone, is indicated in Supplementary Table 3. Relative abundance, species-specific and lineage assignments of each of the major oligotypes (present in more than 3 individuals) and minor positional sequence variants (present in less than 3 individuals) scored from the raw data, are summarized in Supplementary Table 4.

Multi-locus Sequence Analysis (MLSA)

MLSA markers were selected as described by Nuñez et al. (2014). Internal gene fragments for each marker were amplified by PCR, using primers listed in Supplementary Table 1 and genomic DNA obtained from 32 *Acidithiobacillus* strains from our laboratory collection, and sequenced. The same markers were derived from 13 publicly available genomes of *Acidithiobacillus* strains. Sequences were aligned with the MAFFT v7.229 software (Katoh and Standley, 2013) and manually curated, when appropriate. Concatenation of the MLSA markers was done with MEGA 6. The phylogenetic trees were constructed using maximum likelihood and Bayesian analysis. Bootstrap resampling was performed using 1000 replications to estimate the confidence of the tree topologies. Optimal models for nucleotide substitution, DNA polymorphism data, mean G+C contents, Tajimas D, and dN/dS ratios values, were all calculated using MEGA 6. Bayesian trees was constructed using MrBayes v.3.0b4 (3,000,000 generations, trees saved every 100 generations and posterior probabilities calculated after discarding the first 30% of trees (Huelsenbeck and Ronquist, 2001). Trees were visualized and annotated in FigTree (http://tree.bio.ed.ac.uk/software/figtree/). Sequence type assignments for each individual strain are indicated in Supplementary Table 5.

PFGE with SpeI Digestion and Southern Hybridization Analysis

Whole cells (1×10^9 cells/ml) were embedded in agarose blocks as described by Swaminathan et al. (2001). Genomic DNA was digested with 10 U/μl of the restriction endonuclease XbaI (ThermoFischer Scientific) at 37°C for 4 h. The resulting fragments were separated by Pulsed Field Gel Electrophoresis (PFGE) on a CHEF-DR III system (BioRad) in a 1% pulse field certified agarose gel (BioRad) at 6 V/cm and 14°C for 13 h with a pulse interval of 10 s. The gel was transferred by Southern blotting onto a Hybond-XL membrane (General Electric) and hybridized by incubation at 42°C for 1 h to a PCR-generated, biotin-labeled probe spanning a 294 bp internal fragment of the 16S rRNA gene (complementary to hypervariable region V4). The blot was developed with HRP-conjugated antibody and streptavidin to recognize the biotin-labeled probe. Chemiluminescent detection of horseradish peroxidase (HRP) enzyme activity was achieved with Pierce ECL western blotting substrate (Thermo Scientific).

Statistical Analyses

Various packages within the R software (version 3.1.12; http://www.r-project.org) were used for statistical analyses of the data and metadata. Principal component analysis (PCA) was used to evaluate the contribution of different quantitative parameters (as defined in Supplementary Table 3) to the variability of the data.

RESULTS

rRNA Operons in Sequenced Genomes of the Acidithiobacilli

To assess the intra- and inter-specific diversity of *Acidithiobacillus* spp., the relationships of all known strains and sequence clones deposited in public databases (meta/genomic) were investigated using phylogenetic reconstruction strategies. Firstly, variations in copy number, operon architecture, and sequence were quantitated for each of the type (or reference) strains of the genus. This analysis showed that the number

TABLE 1 | Intraspecific comparison of the rRNA operons I vs. II for type/reference strains within the *Acidithiobacillus* species complex.

Species	Operons	Intraspecies % sequence identity (Size in bp)					Operon Context (*)
		16S	ITS-1	23S	ITS-2	5S	
A. ferrooxidans^T (ATCC 23270)	2	100 (1546)	100 (428)	99.9 (2910)	100 (80)	100 (116)	A–B C–D
A. ferridurans^T (ATCC 33020)	2	100 (1536)	100 (454)	100 (2910)	100 (58)	100 (121)	A–B C–D
A. ferrivorans (DSM 17398)	2	100 (1538)	100 (441)	100 (2910)	100 (74)	100 (121)	A–B C–D
A. ferriphilus^T (DSM 100412)	2	100 (1526)	100 (454)	100 (2910)	100 (74)	100 (121)	A–D C–B
A. thiooxidans^T (ATCC 19377)	2	100 (1536)	99 (458)	99.9 (2909)	100 (54)	100 (120)	A–D' C–B
A. albertensis^T (DSM 14366)	2	100 (1536)	100 (458)	100 (2909)	100 (56)	100 (121)	A–D' C–B
A. caldus^T (ATCC 51756)	2	100 (1540)	100 (380)	100 (2887)	100 (69)	100 (121)	A'–B C'–E

**Operon context configuration details can be found in Supplementary Table 2.*
^{T} Type strain of the species.

of rRNA operons is highly conserved within the genus (**Table 1**), with all sequenced strains having two copies of this operon. This was confirmed experimentally by Southern blot hybridization of *Xba*I digested and PFGE-fractionated genomic DNA (Supplementary Figure 2). Gene context of the operons I and II is distinctive (Supplementary Table 2) and is only partially conserved across the species reflecting lineage specific rearrangements. All operons surveyed have internal transcribed spacer (ITS-1) regions coding for $tRNA^{Ala}$ and $tRNA^{Ile}$ genes.

Intra-specifically, both operons were identical or nearly identical in size and sequence (**Table 1**). Inter-specifically, the operons analyzed varied in length by up to 130 bp (ranging from 4958 to 5088 bp), with variations correlating directly with variations in the size of ITS-1 regions (**Table 1**). Sequence differences among strains were mainly located within the ITS regions, between the $tRNA^{Ala}$ and the 23S, and the 16S rRNA gene variable regions. At the level of the 16S rRNA gene, divergence between strains belonging to the currently recognized species showed considerable variation (**Table 2**). When all 16S rRNA gene sequences were compared, the reference strains showed an overall pairwise identity of 97.6%, with 1447 conserved and 91 variable sites. Most of the differences detected in nucleotide identity were located within the variable regions V3 and V4. Given the intrinsic information content of the 16S rRNA gene and the availability of sequences for this gene in public databases with respect to the ITS regions of the acidithiobacilli (1101 16S rRNA gene sequences versus 137 ITS sequences), only this marker was used in downstream phylogenetic analysis of the *Acidithiobacillus* species complex.

Notably, when using the 16 rRNA gene as a marker to revise current species delineation (**Table 2**), a number of species pairs, namely *A. ferrooxidans-A. ferridurans*, *A. ferriphilus-A. ferridurans*, *A. ferriphilus-A. ferrivorans,* and *A. thiooxidans-A. albertensis,* exceeded the typical 97% and the conservative 98.7% sequence identity threshold values used as "gold standards" for species differentiation in the absence of DNA-DNA reassociation experiments (Stackebrandt and Goebel, 1994; Stackebrandt and Ebers, 2006).

16S rRNA Gene-Based Phylogeny of *Acidithiobacillus* Strains and Isolates

To infer the phylogenetic relationships between all available strain and clone sequences of the acidithiobacilli, a comprehensive phylogenetic tree was constructed. For this, 16S rRNA genes were amplified and sequenced from a total of 53 representative strains belonging to the seven described *Acidithiobacillus* species and 1101 other gene sequences belonging to isolates and uncultured clones, retrieved from GenBank. After filtering for redundancy and sequence length, applying masks to positions with >50% gaps and eliminating ambiguous characters, a final set of 580 sequences was obtained (Supplementary Table 3). This set encompassed 1054 bp of the full 16S rRNA gene sequence and contained 642 variable sites and 275 parsimony informative sites, (97.3% pairwise identity). Within this data set, 74.5% of the sequences had taxonomic assignment to the species level. *Thermithiobacillus tepidarius,* the type species of the single other family within the order *Acidithiobacillales*, was included as the outgroup.

TABLE 2 | 16S rRNA genes (upper half) vs. MLSA concatenate (lower half) identity matrix for *Acidithiobacillus* species complex type and reference strains.

	AFE	AFD	AFV	AFP	ATH	AAL	ACA
A. ferrooxidans^{T} (AFE)	–	**98.9**	98.3	98.5	97.8	98.0	96.1
A. ferridurans^{T}(AFD)	96.7	–	98.6	**99.2**	98.2	98.2	96.2
A. ferrivorans^{DSM17398} (AFV)	87.4	87.2	–	**99.3**	97.8	97.8	96.0
A. ferriphilus^{T}(AFP)	88.0	87.6	96.1	–	97.8	97.8	96.3
A. thiooxidans^{T}(ATH)	80.4	80.6	77.4	77.5	–	**99.9**	95.8
A. albertensis^{T}(AAL)	80.5	80.5	78.0	79.2	96.0	–	95.8
A. caldus^{T}(ACA)	77.4	75.7	75.0	73.8	71.8	73.5	–

16S rRNA Identity (%)

MLSA Concatenate Identity (%)

In bold, identity values above the accepted cutoff for species delineation (16SrRNA: > 98.7; MLSA > 97%).

^{T}Type strain of the species.

The maximum likelihood (ML) phylogenetic tree built for this dataset is shown in **Figure 1**. An additional tree built using Bayesian inference can be found in the Supplementary Material (Supplementary Figure 3). The ML tree obtained shows a clear separation of all sequenced representatives in 4 distinctive clades including the *A. caldus* strains (Clade 1; ATCC51756^{T}), the *A. ferrooxidans* strains (Clade 2; ATCC 23270^{T}), the *A. ferridurans-A. thiooxidans-A. albertensis* strains (Clade 3; ATCC 33020^{T}, ATCC 19377^{T}, DSM14366^{T}) and the *A. ferrivorans-A. ferriphilus* strains (Clade 4; DSM 22755, DSM 100412^{T}). Support values for the principal nodes were generally high (>70%). There was limited disagreement in topology between trees built with ML and Bayesian inference (Supplementary Figure 3), with discordance restricted to placement of the *A. ferriphilus-A. ferrivorans* clade and a few other less strongly supported nodes. Also, sister-clades with diverse node depth became apparent in all four branches of the tree (e.g., subclade within the *A. caldus* Clade 1). These are further analyzed below.

Sequence Entropy-Based Analysis of the Phylogenetic Structure of the Genus

Oligotyping (Eren et al., 2013) was used to improve resolution of the 16S rRNA gene tree of the *Acidithiobacillus* strains. This approach utilizes a sequence entropy-based method to identify the most informative nucleotide positions within a surveyed set of sequences. This has proven useful in subspecies-level analysis and is of value for detecting ecologically distinct organisms within closely related taxa (Eren et al., 2015). Using the depurated set of sequences that entered into the phylogenetic analysis, we explored whether there were strong correlations between the clades in the consensus tree representation and their original taxonomic assignments and the oligotypes derived for each sequence (**Figure 1**). For this purpose, the entropy at each nucleotide position in the sequence alignment was calculated, resulting in 12 information-rich positions spanning variable regions of the 16S rRNA gene V2–V9 (Supplementary Figure 1).

A total of 46 oligotypes (OTs) were derived from the dataset (Supplementary Table 4). Of these, 28 OTs were present in a single or less than 3 sequences and were omitted from further analyses. Poor representation in the dataset of the positional variants of other more abundant OTs could be indicative of randomly-generated diversity emerging from sequencing errors, especially if homogenously distributed around the tree. Interestingly, sequence variability was higher in certain clades and in those clades the positional variants map to larger branches of the tree and or to the tips of the tree. This indicates that a number of these OTs are descendants of recent origin and imply recent diversification of the dominant OT (e.g., OTs 6–13 in Clade 1). A number of the single-sequence OTs mapped to deep branches of the tree (OTs 42–46), and could possibly represent ancestral strains or still cryptic phylotypes.

All of the clades in the tree depicted in **Figure 1** were found to group 2–4 principal OTs (defined as having more than 3 representative sequences). Seven of these OT-defined groups (OTs 1, 15, 23, 24, 28, 31, 39) exactly match the tree branches defining currently recognized *Acidithiobacillus* species (**Table 3**, Supplementary Table 4). However, additional OTs matching unassigned (or mis-assigned) sequence representatives clustering in coherent subclades or sister clades within the tree were also identified (**Figure 1**, **Table 3**). This is the case of subclade 2B in the *A. ferrooxidans* branch (represented by strain DSM 1927), which accommodates sequences representing 41 strains and/or sequence clones baring a distinctively different oligotype (OT18). Sequences displaying oligotype OT6 (12 in total), OT7 (5 in total), OT12 (9 in total), and OT13 (3 in total), cluster in a shallow branch within the *A. caldus* clade, despite of the fact that a number of these had been deposited as sequence representatives of *A. thiooxidans*. These sequences are highly divergent from the 16S rRNA gene sequence of the type strain of *A. caldus* (95–96.5% % identity) and seem to comprise different (sub)species. A similar scenario applies to a number of other smaller branches within the *A. thiooxidans-A. albertensis* clade (Clade 3, OT27 and OT30) and the *A. ferriphilus-A. ferrivorans* clade (Clade 4, subclade 4B) that correlate with specific oligotypes (**Table 3**). In addition, based on this approach, most of the unassigned sequence representatives deposited in public databases can now be assigned to a species or candidate phylotype (**Table 3**, Supplementary Table 3).

Oligotypes Occurrence and Prevalence in Acidic Econiches around the Globe

Following this, we explored whether the diversity uncovered represents the global origins of isolates and clones, or whether it could be explained by niche-specific selective pressures or associated to specific environmental cues. For this, we collected all available metadata published in the literature or deposited in public databases for the strains included in the analysis (Supplementary Table 3) and performed basic statistical analyses. Also, occurrence and relative abundance of the different subclades in publically available targeted metagenomic datasets were scored (Supplementary Table 6), and the derived information was analyzed in the context of strain-specific data.

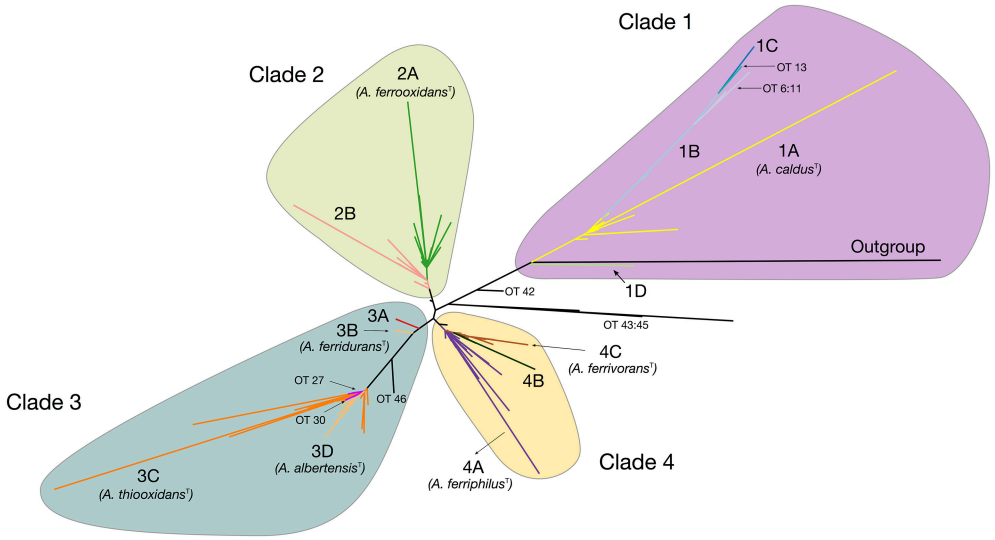

FIGURE 1 | *Acidithiobacillus* species complex consensus phylogenetic tree built using maximum likelihood inference and 16S rRNA gene sequences of 580 strains and/or sequence clones. Clade's affiliations are as follows: clade 1 (purple, *A. caldus*^{T}), clade 2 (green, *A. ferrooxidans*^{T}), clade 3 (turquoise, *A. ferridurans*^{T}, *A. thiooxidans*^{T}, *A. albertensis*^{T}), clade 4 (yellow, *A. ferriphilus*^{T}, *A. ferrivorans*^{T}). Subclades 1A through 4C are color coded according to the oligotype (OT) assigned to the strains and sequence clones that conform each cluster. Minor branches of interest are also shown in the tree and the corresponding OTs indicated. Detailed information on the sequences used in the tree construction and clade assignments can be found in Supplementary Table 3.

More than 50% of all *Acidithiobacillus* strains and sequence clones sampled can be mapped to Asiatic countries (45% of which originated in China), followed by Europe (20%), South (9%), and North America (7%), and Africa and Oceania (accounting for less than 2% each). Similarly, more than 60% of all strains and sequence clones have been obtained from industrial econiches. Both figures imply that some of the tendencies emerging from the data may be obscured by sampling biases. Despite this fact, it is clear that several subclades are ubiquitous worldwide (**Figure 2**), including the subclades represented by the type strains of *A. caldus* (subclade 1A), *A. ferrooxidans* (subclade 2A), *A. ferridurans* (subclade 3B), and *A. ferriphilus* (subclade 4A). However, differential patterns of occurrence and/or relative abundance are also evident from the map in **Figure 2A** and are generally consistent between natural and industrial econiches (Supplementary Figure 4). The strongest apparent tendency is the decrease in the diversity of subclades detectable at increasing latitudes (**Figures 2A,B**), which is also evident from the subclade assignments derived from targeted metagenomic data (Supplementary Table 6). Prevalence of the *A. ferriphilus* (4A) subclade in China, the *A. ferrooxidans* (2A) subclade in European countries and India, the *A. thiooxidans* (3C) subclade in Europe and Brazil and the *A. ferrooxidans*–like (2B) subclade in South and North America is notably high. In contrast, subclade 4C represented by *A. ferrivorans* SS3 and related strains, is restricted to high latitudes and high altitudes (**Figure 2B**, Supplementary Table 3), being the only *Acidithiobacillus* type found at the most extreme latitudes. This is in agreement with the psychrotolerance of known strains from the clade (Hallberg et al., 2010). Further support for this finding emerges from targeted metagenomic data obtained at the coal mine in Svalbard, Norway, and a copper tailing in Ontario, Canada, were every representative of the genus *Acidithiobacillus* detected matches the 16S rRNA gene oligotype of clade 4C, represented by *A. ferrivorans* SS3.

Evidence for niche-specific diversification of certain clades is also apparent from the available data, as in the case of Clade 1, grouping *A. caldus*-like strains. While subclade 1A, represented by the *A. caldus* type strain, is present in different global locations and mostly associated with industrial operations involved in copper and gold recovery or in coal exploitation, subclades 1B and 1C are restricted to copper sulfide mining sites in China and subclade 1D to zinc/lead ores mined in USA (Supplementary Table 3), suggesting that local selection pressures (eventually process-specific) are driving differentiation of ecotypes. Occurrence of the 1D subclade in the targeted metagenomes obtained from the Iron King Mine tailings in Arizona (USA) and dominance of clade 1D over other *Acidithiobacillus* species in the metagenomes obtained from the Chinese mine tailings in the Tongling region, both of which are heavily polluted with metalloids (Huang et al., 2012; Hayes et al., 2014), could provide further hints on the drivers behind the diversification of the *A. caldus* linage. The same argument stands for the 1B subclade, which is highly abundant in sulfidic caves from Mexico and also dominate the *Acidithiobacillus* population in concrete pipes in Ala Moana Park (Hawaii), as assessed by targeted metagenomics (Supplementary Figure 4; Supplementary Table 3). In agreement with this finding, strains originating in Mexico were recently suggested to represent a new species (Jones et al., 2016).

TABLE 3 | Oligotype distribution with respect to original taxonomic assignments and subclades in the consensus tree representation.

Subclade		Oligotype	*A. caldus*	*A. ferrooxidans*	*A. ferridurans*	*A. thiooxidans*	*A. albertensis*	*A. ferriphilus*	*A. ferrivorans*	*Acidithiobacillus* spp.	Total	Rep. strains
1A	1	AGCCCGTCGTCG	**30**	0	0	0	0	0	0	19	49	ATCC 51756^T
2A	15	GACTCATTTACG	0	**99**	0	0	0	0	0	22	121	ATCC 23270^T
3B	23	GGTTCATCGCCG	0	27	**8**	0	0	0	0	3	38	ATCC 33020^T
3C	24	AATGTCCTTATA	0	1	0	**71**	0	0	0	15	87	ATCC19377^T
3D	28	AATGACCTTATA	0	2	0	14	**10**	0	0	12	38	DSM 14366^T
4A	31	GGTCCGTCCACG	0	76	0	0	0	**8**	1	10	95	DSM 100412^T
4C	39	GATCCGGCAACG	0	4	0	0	0	0	**12**	5	21	DSM 22755^T
1B	6	AGCGTCTCGTAT	1	0	0	0	0	0	0	11	12	LA10A
1B	7	GGCGTCTCGTAT	0	0	0	0	0	0	0	5	5	NJU-AMD3
1C	12	TGCGTCGCGTGC	0	0	0	4	0	0	0	5	9	ZMB
1C	13	AGCCTGTCGTGC	1	0	0	0	0	0	0	2	3	ORCS6
1D	14	GACCCGTTGACG	0	0	0	0	0	0	0	3	3	NJU-T1
2B	18	GACTCATCCACG	0	37	0	0	0	0	0	4	41	DSM 1927
3A	22	GGTCCGTCCCCG	0	1	0	0	0	0	0	4	5	LMT1
3D	27	AATGTCCTTCTA	0	0	0	8	0	0	0	1	9	GG1/14
3D	30	AATGCCCTTATA	0	0	0	4	0	0	0	0	4	ATCC 21835
4B	37	GGTCCGGCCACG	0	0	0	0	0	0	0	7	7	BER_D10
4C	40	GATCCGGCCACG	0	0	0	0	0	0	0	3	3	NJUST22
Rest		NNNNNNNNNNNN	0	10	0	2	0	0	0	18	30	All others
Correctly assigned[a]			30	99	8	71	10	8	12	–		
Unassigned[b]			19	22	3	15	12	10	5	149		
Mis-assigned[c]			2	158	27	32	16	77	4	31		

^{T}*Type strain of the species*

[a]*Number of strains assigned to the taxon that possess the oligotype of the type strain of the species (bold).*

[b]*Number of strains without a specific assignment that possess the oligotype of the type strain of the species.*

[c]*Number of strains assigned to the taxon that possess the oligotype of the type strain of a different species.*

MLSA-Marker Based Phylogeny of Sequences from Strains and Isolates

MLSA was used to gain deeper insight into the genetic structure of the *Acidithiobacillus* species complex at a higher resolution level. Informative markers were selected using a previously developed scheme for identification of housekeeping genes suitable for MLSA (Nuñez et al., 2014). All 10 genomic sequences of validated *Acidithiobacillus* spp. available in public databases as of July 2016 were used as input in this analysis (Valdés et al., 2008, 2009, 2011; Liljeqvist et al., 2011; You et al., 2011; Talla et al., 2014; Travisany et al., 2014; Yin et al., 2014; Yan et al., 2015; Latorre et al., 2016). Eight HKG that met the amplicon size requirements of the pipeline were selected for further phylogenetic analysis. Internal gene sequences of the 8 markers were amplified from genomic DNA obtained from an additional set of 35 *Acidithiobacillus* strains and industrial isolates of diverse geographical origins by PCR, using a high fidelity polymerase. Details on the marker genes, the allelic profiles, and the sequence types (ST) derived from sequence analyses, are summarized in **Table 4**, and the GenBank accession numbers for the sequences generated in this study are listed in Supplementary Table 5. The concatenate comprised 4086 nucleotides and consisted of 1832 variable sites. The eight protein-coding gene loci showed a mean nucleotide sequence diversity of 34.2%, in contrast with that using the 16S rRNA gene alone, which yielded only 5.4% polymorphic sites. Parsimony informative sites, i.e., positions in the sequence set under comparison that contain at least two types of nucleotides in at least two different sequences, varied form a maximum of 368 (*ruvB*) to a minimum of 79 (*ihfB*).

Maximum likelihood and Bayesian inference based phylogenetic trees were constructed using a sequence concatenate of all eight markers. Topology of the concatenate-based tree was congruent between methods and with the topology of single-gene trees generated with most informative markers, suggesting that none of the markers utilized was the object of active gene flow (Supplementary Figure 5). Phylogenetic analysis of the concatenate produced 6 major clades supported by bootstrap values of > 93% (**Figure 3**). Despite

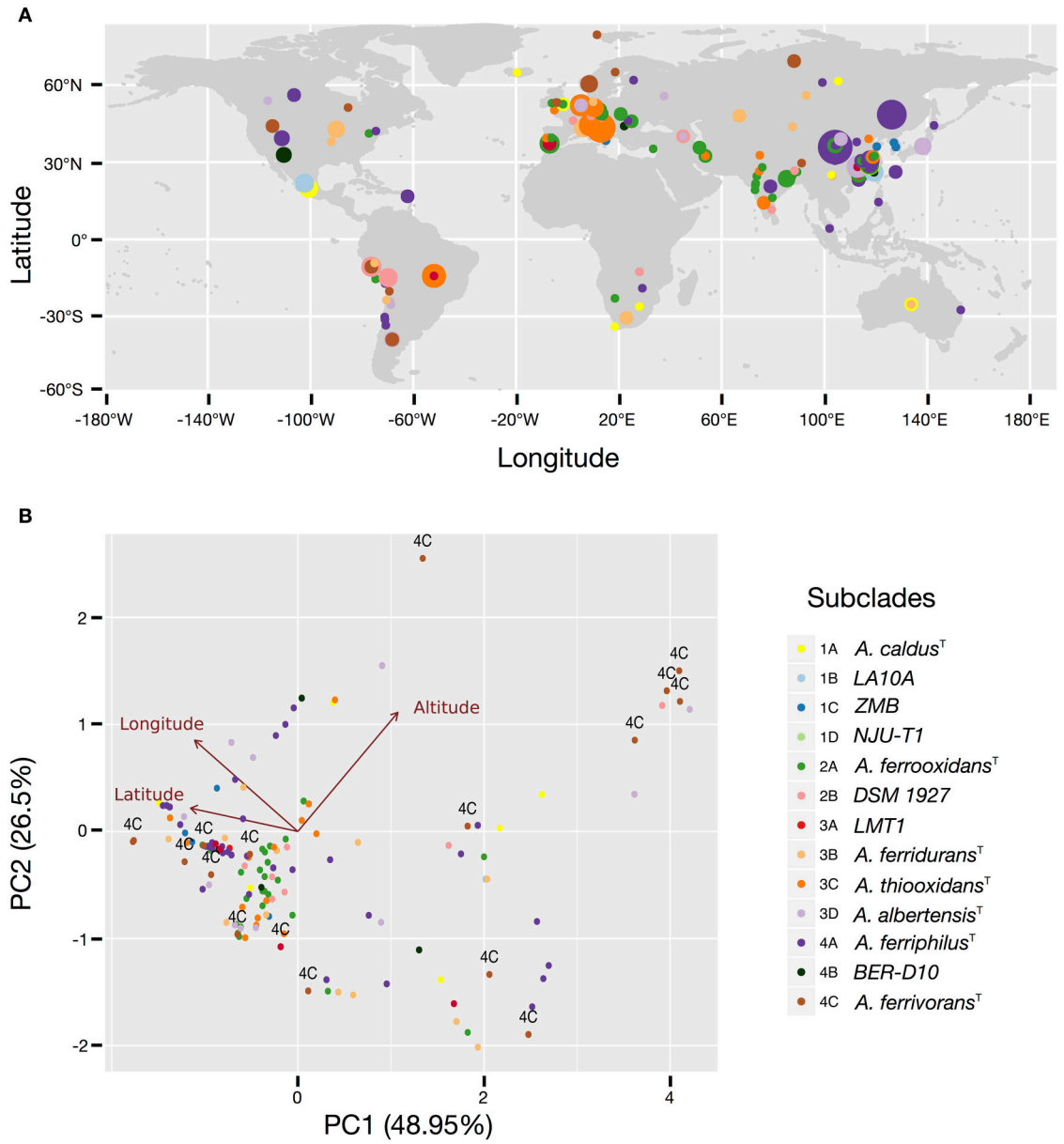

FIGURE 2 | Occurrence and prevalence of the *Acidithiobacillus* species complex subclades in acidic econiches around the globe. (A) Location and relative abundance of each subclade according to latitude and longitude coordinates. **(B)** Principal component analysis (PCA) biplot showing arrangement of the isolates and sequence clones according to variations in latitude, longitude and elevation. Individuals are color coded according to the 16S rRNA gene tree subclade they belong to. Taxon assignment of the different subclades is indicated in the figure, by the species name or the name of a representative strain. Arrows represent the relationship (direction and strength) of the parameters with the individuals. The direction of each arrow indicates an increase in that variable.

some disagreement in the topology of the MLSA-based tree and the 16S rRNA gene-based tree, mostly due to difference in the divergence times between sister clades, all clades identified coincided with the major clades emerging from the 16S rRNA gene phylogenetic analysis (see **Figure 1**). Discordance occurred in the placement of the *A. ferridurans* subclade in both trees.

Based on the concatenate alignment, the 45 isolates were resolved into 30 STs (Supplementary Table 5). All clades showed high variability in terms of STs, which may be explained by the non-clonal nature of the strains analyzed, many originated from different sources and environments (Supplementary Table 3). All eight protein-coding loci that comprised the concatenate have nucleotide substitution ratios (dN/dS) well below 1, indicating pressure to conserve the gene sequences (**Table 4**). Overall, these values indicate that most of the sequence variability identified can be explained by strong negative selection, typical of housekeeping genes. However, inspection of the dN/dS ratios within specific branches of the trees generated with single genes showed positive

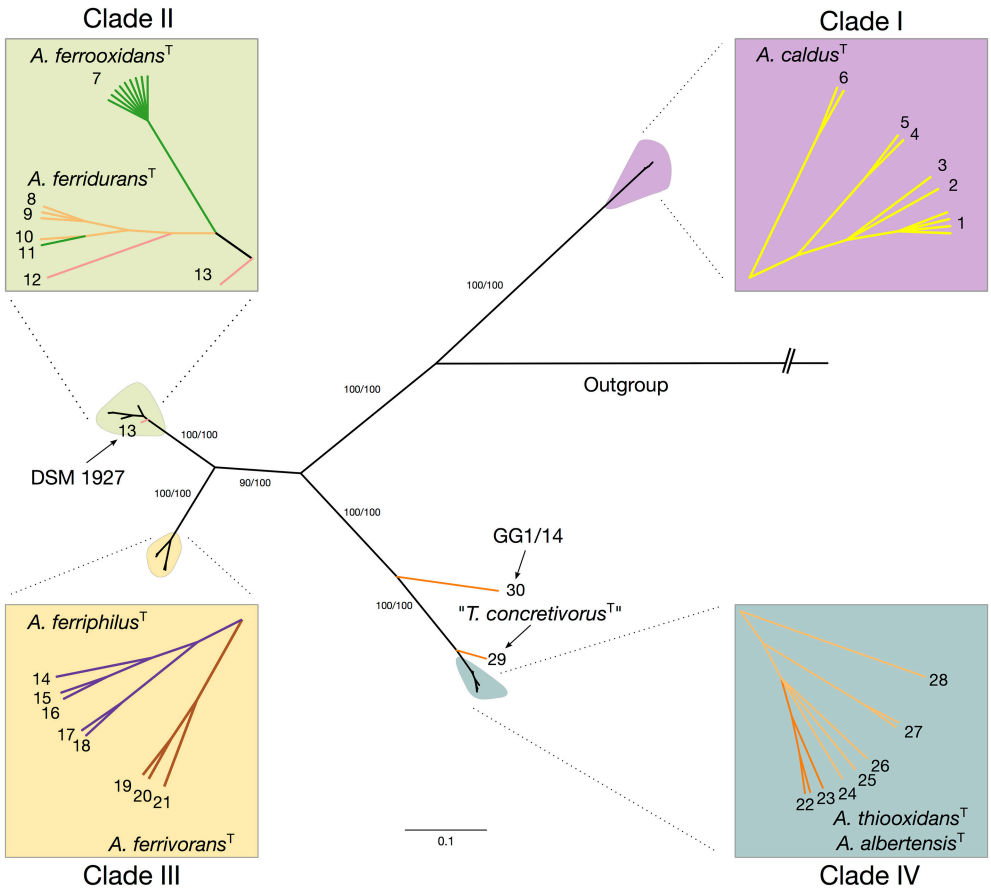

FIGURE 3 | Maximum likelihood tree inferred from the concatenate of eight selected MLSA markers. The *ilvE, trx, rpsE, ruvB, rplU, ihfB, hslV,* and *fdx* gene sequences (4086 bp) from 45 *Acidithiobacillus* strains representative of available subclades undercovered in the 16S rRNA analysis were concatenated and analyzed using MEGA 6. Numbers at the nodes indicate the bootstrap values of 1000 replicates (%). The bar represents expected nucleotide substitutions per site.

TABLE 4 | Sequence analysis of the MLSA selected markers and the 16S rRNA gene.

Locus	Length (bp)	N° Alleles	Parsimony informative sites		Mean G+C	Tajima's D	dN/dS
			N°	%			
rrs	1216		66	5.4	56.7	1.080	–
IlvE	890	22	322	36.2	57.9	0.724	0.095
trx?	296	20	108	36.5	50.7	1.006	0.060
rpsE	485	26	190	39.2	56.6	0.808	0.585
ruvB	848	27	324	38.2	62.3	0.647	0.522
rplU	290	22	104	35.9	57.9	1.051	0.141
ihfb	225	22	81	36.0	54.2	1.428	0.066
hslV	434	24	153	35.3	61.5	0.571	0.089
fdx	281	22	111	39.5	58.0	1.140	0.185

values in some clades and subclades. Specifically, 7 out of 8 trees showed dN/dS ratios above 1, indicating positive selection for the selected genes analyzed within clade IV. The same holds true for clade III in 3 out of 8 trees. These differences between general ratios and ratios observed at individual branches of the tree, may be explained by the lesser time since divergence of the subclades conforming each of these two clades. MLSA distances between subclades within each clade are near the threshold for species delineation, hinting that events of speciation are still ongoing, supporting the observation of high levels of adaptive evolution on the analyzed markers.

Levels of Diversity within and across Lineages

To further assess the levels of diversity within and across lineages at a higher resolution level, pairwise distances between a set of 45 *Acidithiobacillus* strains, including the reference strains of all seven validated species of the genus (**Table 2**; **Figure 4**), were calculated using the MLSA concatenate as molecular marker. As shown in **Table 2**, all seven *Acidithiobacillus* species are supported by MLSA concatenate divergence values larger that the 3% threshold value (meeting the 70% DNA-DNA hybridization threshold) used to differentiate strains into species in other microbial groups (Vandamme and Peeters, 2014).

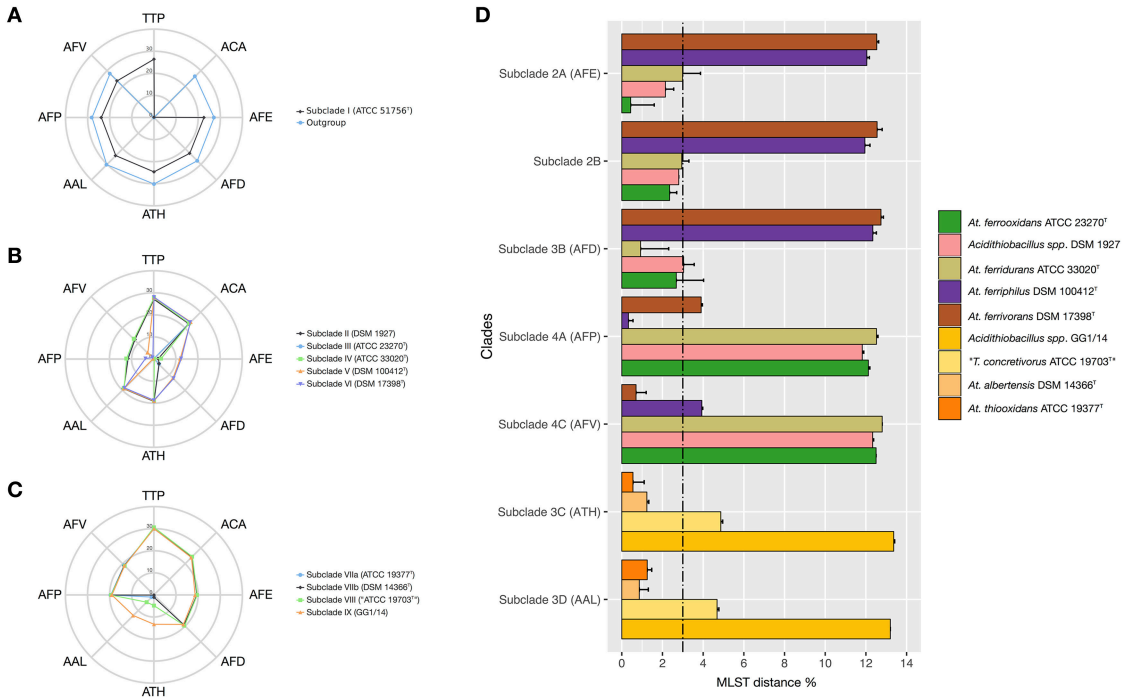

FIGURE 4 | Average nucleotide divergence of the MLSA concatenate (%) between strains conforming each of the MLSA clades against all reference species in the *Acidithiobacillus* species complex and the outgroup *Thermithiobacillus tepidarius*. (A) *T. tepidarius* and Clade I strains: (10 *A. caldus* strains); **(B)** Clades II and III strains: *A. ferrooxidans* (9 strains), *A. ferridurans* (7), *A. ferriphilus* (5 strains), *A. ferrivorans* (3 strains), and the variant lineage represented by strain DSM 1927; **(C)** Clade IV strains: *A. thiooxidans* (3 strains), *A. albertensis* (6 strains), and variant lineages represented by strains ATCC 19703 ex. *T. concretivorus*^{T} and GG1/14; **(D)** Average nucleotide divergence of the MLSA concatenate (%) within and between *Acidithiobacillus* species complex 16S rRNA subclades 2A-2B, 3A-3D; 4A, 4C. For each bar, the standard deviation is indicated. The 3% divergence threshold value is indicated (Vandamme and Peeters, 2014). Abbreviations: *Thermithiobacillus tepidarius* (TTP), *A. caldus* (ACA), *A. thiooxidans* (ATH), *A. albertensis* (AAL), *A. ferrooxidans* (AFE), *A. ferridurans* (AFD), *A. ferriphilus* (AFP), *A. ferrivorans* (AFV).

The intergroup average divergence levels varied significantly depending on the lineage considered (**Figure 4**). Average divergence between *A. caldus* strains and the rest of the *Acidithiobacillus* species complex was almost as high as that observed for the related genus *Thermithiobacillus tepidarius* ATCC 43215^T (**Figure 4A**), raising the question if intrinsic differences are larger than those expected for species of the same genus. In turn, *A. ferrooxidans* was strongly differentiated from both *A. ferriphilus* (12.1 ± 0.1% divergence) and *A. ferrivorans* (12.5 ± 0.0% divergence), but only 3.0% divergent from *A. ferridurans*.

When additional strains were considered, the average within-group divergence for most lineages emerging from the 16S rRNA gene and/or the MLSA phylogenetic analyses (**Figure 4**) remained below the 3% threshold, with one exception. A considerable level of intragroup diversity distributed in 3 recognizable subclades was apparent within the *A. thiooxidans* clade (**Figure 3**). One subclade spanned the acknowledged species *A. thiooxidans* and *A. albertensis*, which were less than 3% divergent between each other. The other two subclades encompassed two potentially new species represented by strains ATCC 19703 ("*Thiobacillus concretivorus*") and strain GG1-14, respectively. For these two novel taxons the average sequence divergence of the concatenate toward its nearest neighbor, *A. thiooxidans*^{T}, was 4.9 ± 0.1% and 13.35 ± 0.05%, respectively. These figures supported their assignment as distinct *Acidithiobacillus* species. On the other hand, the *A. ferrooxidans*-like subclade 2B represented by strain DSM 1927, emerging from the combined 16S rRNA gene phylogenetic analysis and the oligotyping analysis, had an intertaxon divergence of 2.8% from the *A. ferrooxidans* subclade 2A (**Figures 4C,D**) which did not support recognition of separate species, even though levels of divergence at the MLSA concatenate level and the 16S rRNA gene levels indicated ongoing differentiation.

DISCUSSION

The class *Acidithiobacillia* currently consists of 9 validly described species arranged within a single order, the *Acidithiobacillales*. This order contains two genera: *Thermithiobacillus*, with two validated species [*T. tepidarius* (Hudson et al., 2014) and *T. plumbiphilus* (Watanabe et al., 2016) and *Acidithiobacillus* (Kelly and Wood, 2000)], which currently accommodates seven validated species. Despite the extensive work that has been carried out on the acidithiobacilli, the evolutionary relationships amongst members of this group

remain poorly understood. In this study, we have generated the most thoroughly sampled species-level phylogeny to date for this group, using 16S rRNA gene sequence data and a MLSA scheme based on 8 single-copy orthologous genes represented across members of the *Acidithiobacillales*. Our aim was to produce a robust phylogeny by enabling rooting of the trees and to obtain a better understanding of the evolution of the taxon. In order to span both inter- and intra-species variation we assembled a diverse set of strains and sequence clones (>580) originating from sites throughout the world and encompassing all currently recognized *Acidithiobacillus* species, as well as neglected candidate species (e.g., "*T. concretivorus*"). The phylogeny resulting from the 16S rRNA gene data achieved a high coverage of the diversity of the group, while the oligotyping and the MLSA typing approaches enabled a more thorough inspection of the intra-clade diversity for a set of well sampled clades.

Based both on 16S rRNA gene- and the MLSA-based phylogenies, the majority of the sampled diversity clustered together with known reference strains and formed well-defined clades, supporting the seven (species) fundamental units previously described. However, a number of additional lineages (phylotypes) with statistically well-supported nodes also became apparent in either, or in both, analyses, uncovering further inherent diversity for this taxon. This is in agreement with evidence derived from phylogenetic studies encompassing more restricted sets of strains, mostly focused on iron-oxidizing strains of the group (Amouric et al., 2011; Wu et al., 2014 and references therein), which have resulted in recent reclassification of a number of strains of *A. ferrooxidans* into the new species referred to above. In this work a total of 6 new phylotypes (16S rRNA clades 1B, 1C, 1D, 2B, 3A, 4B, Supplementary Table 4) were identified that are readily distinguishable by phylogenetic clustering and important levels of sequence divergence. Taken as a whole, the evidence suggests that the *Acidithiobacillus* genus is better defined as a species complex made up of at least 13 phylotypes in diverse stages of differentiation (speciation) that can be distinguished from each other on the basis of divergent phenotypic and/or genotypic characters. Nonetheless, due to the continuous nature of evolution and in some cases the under-sampling of isolates or the scarcity of sequence representatives of certain phylotypes available, several of these phylotypes have remained cryptic and have not yet been adequately framed as discrete units or species.

Recognition of these new lineages has been further obscured by the extensive taxonomic mis-assignment of strains to named species, which has hidden a great deal of the inherent diversity of the *Acidithiobacilliae*. For many years, knowledge on the taxonomic structure of the *Acidithiobacillus* species complex has relied on classifications achieved on the basis of morphological and physiological characteristics. Acidophilic rods catalyzing the dissimilatory oxidation of both iron and sulfur have almost always been classified as strains of *A. ferrooxidans*, while those that only oxidize sulfur have been assigned to *A. thiooxidans* or *A. caldus*, depending on the optimal temperature of growth of the isolate. According to our 16S rRNA gene oligotyping results, 35.6% of the isolates, which presumably have been experimentally diagnosed before being assigned to a particular taxon, were actually incorrectly classified (e.g., *A. caldus* 1B as *A. thiooxidans*). This indicates that in many cases strains are not thoroughly evaluated in terms of their phenotypic features, and are somewhat arbitrarily assigned to one of these taxons without a systematic assessment of diagnostic characteristics (such as their optimal temperature ranges). Even in the case of sequence clones, where 16S rRNA gene data are the only piece of information available on the individual being sampled, major mistakes in the specific assignment were detected (17.6% of mis-assignments). A certain degree of mis-assignment is expected for data originating before the revision of the taxon, yet many of the mistakes correlate to recent data. In addition, a large number of sequences deposited in public databases (∼40%) remain unclassified, while our data strongly support their specific assignments.

According to polyphasic taxonomy, strains of the same species should have similar phenotypes, genotypes, and chemotaxonomic features (Gillis et al., 2005). Currently, genotypic criteria required to differentiate species require strains to have <70% DNA-DNA hybridization similarity, > 5°C ΔT_m, > 5% mol G + C difference of total genomic DNA, and a 16S rRNA gene divergence larger than 1.3% (Stackebrandt and Ebers, 2006). Measurement of all these parameters is seldom achieved for any particular strain, unless phenotypic, molecular and/or available genomic data support a specific reassignment, and confirmation is deemed necessary. From the genotypic standpoint, currently recognized *Acidithiobacillus* species have been evaluated only in some of these aspects, and in those actually tested thresholds values are not always met, making species delineation further unclear. DNA–DNA hybridization between *A. ferrooxidans* and either *A. thiooxidans* (9%, Harrison, 1982), *A. ferrivorans* (37%, Hallberg et al., 2010), or *A. ferridurans* (63%, Amouric et al., 2011) meet the 70% gold standard that serves as a boundary to differentiate species. Conversely, mean differences in total G + C content between each of the newly designated iron-oxidizing species and *A. ferrooxidans sensu stricto*, are in all cases lower than the 5% required to differentiate species. Mean differences in this parameter for the non iron-oxidizing species *A. thiooxidans, A. caldus* and *A. albertensis* with respect to *A. ferrooxidans* (6.8, 5.1, and 2.7 % respectively) have also a certain degree of ambiguity. These differences could result from varying degrees of horizontal gene transfer (HGT), blurring the boundaries at the level of the core genome between bacterial groups. In recent years, evidence has accumulated for the extensive contribution of HGT to the genomic evolution of the *Acidithiobacillus* species complex (e.g., Bustamante et al., 2012; Acuña et al., 2013; Travisany et al., 2014).

Our 16S rRNA gene sequence data support the differentiation of *A. ferrooxidans, A. ferrivorans, A. thiooxidans,* and *A. caldus*, all of which are more than 1.3% divergent with respect to all other currently recognized species in the complex, though this parameter failed to differentiate *A. ferrivorans* from *A. ferridurans, A. ferriphilus* from both *A. ferridurans* and *A. ferrivorans,* and *A. albertensis* from *A. thiooxidans*. Despite this fact, all seven acknowledged species in the complex are individualized as neat clades in the 16S rRNA tree and identified by a principal/predominant oligotype, supporting

actual differentiation of these phylotypes. Overall the topology of our 16S rRNA-based tree is similar to those reported previously (e.g., Ni et al., 2008), with differences attributable mostly to the number of sequences, the wider diversity of sequences considered in the analysis and rooting using *Thermithiobacillus tepidarius* as outgroup. One interesting observation emerging from this deep coverage and rooted 16S rRNA tree is the relationship between species that can and cannot oxidize sulfur. Historically, *A. caldus* and *A. thiooxidans* have been considered to be more closely related to each other than to *A. ferrooxidans* (Goebel and Stackebrandt, 1994). However, the 16S rRNA gene phylogeny constructed herein placed *A. caldus* far from the rest of the acidithiobacilli and actually much closer to the outgroup species (*T. tepidarius*). In turn, based on this marker all *A. thiooxidans* related strains appear to have shared a more recent common ancestor with the iron-oxidizing lineages.

To achieve a more precise delineation of relevant operational units, microbial taxonomists are rapidly turning to genome-wide molecular markers, such as MLSA genes, genomic signatures, or even full sequences (Vandamme and Peeters, 2014). Genome sequences for number of *Acidithiobacillus* spp. have become available in public databases since 2008, including the type strains of *A. ferrooxidans*, *A. caldus*, *A. thiooxidans,* and *A. ferrivorans* strain SS3 (Valdés et al., 2008, 2009, 2011; Liljeqvist et al., 2011; You et al., 2011; Talla et al., 2014; Travisany et al., 2014; Yin et al., 2014; Yan et al., 2015; Latorre et al., 2016; Zhang et al., 2016a). However, no genome, complete or draft, has yet been reported for *A. ferridurans*, *A. ferriphilus* and *A. albertensis*. This poor representation of the acidithiobacilli in genomic databases hampers the detailed investigation of the evolutionary relationships of its members through thorough phylogenomic analyses (although efforts in this direction have recently been published; Zhang et al., 2016a,b), and prevents the unraveling of the ambiguities addressed above without further genome sequencing. Therefore, to achieve a high degree of resolution and at the same time restrict our view on the evolution of the taxon to its core genome (preventing biases introduced by HGT and recombination) we used single copy orthologous genes shared by all members of the complex as MLSA markers for further phylogenetic reconstruction. In the absence of robust genomic data, core genes-based MLSA has proven useful in understanding the evolutionary relationships and classification of other complex taxonomic groups (Konstantinidis et al., 2006).

Using MLSA analysis, the type/reference strains of all validated species clustered to discrete branches of the tree, regardless of the tree construction method used. However, at this level of resolution inclusion of some lineages as species of the genus appears unrealistic (*A. caldus*), and individualization of others (*A. thiooxidans-A. albertensis*), questionable. MLSA-based phylogenetic analysis divided the strains in 4 groups, all of which encompassed different levels of genetic diversity. The first clade encompassed all sampled *A. caldus* strains available to us, which happened to pertain exclusively to 16S rRNA tree subclade 1A. Homogeneity of this group of strains from a genomic point of view, was demonstrated previously using species-specific MLSA markers (Nuñez et al., 2014). Notably, none of the strains in our collection was affiliated with the 1B, 1C, or 1D subclades, which are mostly Asiatic or American in origin, and seem to be considerably less common than subclade 1A strains. Strains from the rare subclades that can be traced to natural environments seem to be associated to sulfidic caves (Jones et al., 2016) or geothermal sites (Urbieta et al., 2015). Strains from these subclades are as much as 3.7–5.2% divergent with respect to the type strain of *A. caldus* (ATCC 51756) at the level of the 16S rRNA gene, indicating that they comprise distinct species or even distinct genera. Divergence between *A. caldus* and *A. thiooxidans* is also close to the 5% limit value, generally accepted as boundary to discriminate genera.

According to recent studies, only 10% of the current bacterial species with validly published names conform to the established species or even the genus thresholds (Rossi-Tamisier et al., 2015). These cutoffs were originally established under the assumption that the level of inter-species 16S rRNA gene sequence variation was homogeneous among genera. However, in the light of the variations in the speed of evolution of these genes between phyla (e.g., Clarridge, 2004), their adequacy has been challenged. Our MLSA data support the view that the clade that groups the type strain of *A. caldus* and other 16S rRNA gene-defined subclades, is almost as divergent with respect to the other *Acidithiobacillus* species as it is to *T. tepidarius*. While *T. tepidarius* is 26.4% divergent from *A. caldus*, 27.6% divergent (on average) from the iron-oxidizing acidithiobacilli and 30.3% divergent (on average) from the *A. thiooxidans* clade members, *A. caldus* diverges from all other *Acidithiobacillus* species by an average of 24%. These results strongly suggest that this whole lineage should be reassigned to a new genus. However, divergence at the 16S rRNA gene level is above the 94% divergence limits identity cutoff generally used to distinguish genera (Yarza et al., 2008). Clearly, additional criteria will need to be considered to further clarify this situation.

While MLSA supported the distinction of clade II and III lineages (represented respectively by the type/reference strains of *A. ferrooxidans* and *A. ferridurans*, and *A. ferriphilus* and *A. ferrivorans*), as distinct species, *A. thiooxidans* and *A. albertensis,* with a global divergence lower than 3%, generally considered as threshold value for species distinction, appeared almost indistinguishable. *A. ferridurans* seems to have become distinct from *A. ferrooxidans* quite recently (3.4% divergence at the level of the 8-gene concatenate) and likewise *A. ferrivorans* from *A. ferriphilus* (3.9% divergent), implying some degree of niche-driven specialization or biogeographical isolation. Metadata and targeted metagenomic data suggest that this is indeed the case for the psychrotolerant species, *A. ferrivorans*, which seems to be mostly restricted to environments experiencing extensive periods of cold temperature, for example at high latitudes or altitudes. Further evidence needs to be generated to explain factors driving *A. ferridurans* differentiation from *A. ferrooxidans*. For the moment, metadata are too poor to derive relevant conclusions in this respect, although the greater tolerance of some *A. ferridurans* strains to extreme acidity, and a greater propensity of growth on hydrogen as sole electron donor with respect to *A. ferrooxidans* have been proposed as diagnostic characteristics of the species (Hedrich and Johnson, 2013).

In turn, differentiation of *A. albertensis* from *A. thiooxidans* seems to be ongoing, as suggested by the nucleotide substitution ratios in the protein-coding loci analyzed. At the level of the single gene trees, the dN/dS ratios for the *A. thiooxidans*-*A. albertensis* clade had values > 1, indicating that positive selection is ongoing in this branch. This statement is also supported by clearly distinguishable oligotypes between the two lineages at the level of the 16S rRNA gene, implying probable ecotype level differentiation (e.g., Sintes et al., 2016). Some obvious phenotypic features between the two lineages support this view. In particular, *A. albertensis* has a bundle of polar flagella that are unique in the genus, while other flagellated bacteria, like *A. thiooxidans*, only have a single polar flagellum (unpublished). Different types of flagellation have been shown to provide diverse advantages under different environmental conditions (Kearns, 2010). A flagellar bundle in *A. albertensis* may add propulsion forces for displacement in viscous environments or enable more efficient spreading along surfaces, as shown in other bacteria (Bubendorfer et al., 2014), which may in turn, convey greater fitness to *A. albertensis* strains under specific mineral leaching conditions. Further efforts to evaluate niche partitions and relative fitness of these two types of mesophilic sulfur-oxidizers need to be carried out to test this hypothesis.

Even if not all new clades represented in the 16S rRNA gene tree were represented in our culture collection, or available to us from our colleagues, a number of them could be tested at higher molecular resolution. MLSA evidence further supported divergence of several of the emergent lineages and currently recognized species, uncovered using the combined 16S rRNA gene and oligotyping strategies. Using the 3% divergence cutoff, lineages represented by *A. thiooxidans*-like strains ATCC 19703 and GG1-14, and the *A. ferrooxidans*-like strain DSM 1927, emerge as new candidate species. Interestingly, strain ATCC 19703 was described as a sulfuric acid-forming bacterium isolated from moist corroded concrete exposed to atmospheres containing H_2S (Parker, 1945a). Based on morphological, cultural and biochemical properties this strain was considered to be a different species from *A. thiooxidans*, and was designated as *Thiobacillus concretivorus*. This new candidate species was described as one of the relevant members in a microbial succession driving the corrosion of concrete sewers (Parker, 1945b, 1947), and strain ATCC 19703 was accepted as the type strain of the species (Sneath and Skerman, 1966). Common features between "*T. concretivorus*" and *A. thiooxidans* included their capacity to oxidize thiosulfate, elementary sulfur and hydrogen sulfide (Parker and Prisk, 1953). Distinguishing features included the ability of "*T. concretivorus*" to utilize nitrate, in addition to ammonium, as a nitrogen source for growth, to occasionally precipitate sulfur from thiosulfate instead of directly forming sulfuric acid as *A. thiooxidans* (Parker, 1945a) and its higher tolerance to high concentrations of thiosulfate (Parker and Prisk, 1953). In 1957, Vishniac and colleagues questioned the pertinence of these discriminating criteria (Vishniac and Santer, 1957) and after evaluation of the 16S rRNA gene sequence Kelly reassigned all "*T. concretivorus*" strains to *A. thiooxidans* (Kelly and Wood, 2000). According to our molecular analyses, strain ATCC 19703 cannot be distinguished from *A. thiooxidans* on the basis of 16S rRNA gene analysis nor oligotyping. However, MLSA data uncovered a significant divergence (4.8%) between strain ATCC 19703 and the *A. thiooxidans* subclade that exceeds the currently accepted threshold for species differentiation and points to a genetic distinction between the two groups. Further physiological, chemotaxonomic and genomic analysis should be performed on this strain and its close relatives to resolve this issue.

A much clearer distinction was found at the MLSA concatenate level for strain GG1-14, which is as much as 13.3% divergent with respect to *A. thiooxidans*, a level of divergence that is comparable to that existing between *A. ferrooxidans* and *A. ferrivorans*. This strain was isolated from an acidic (pH 1.9; 25°C) pool on the island of Montserrat (W.I.), but no further physiological or cultural data have been obtained so far that hints on its diagnostic characteristics (Atkinson et al., 2000).

A new lineage, possibly representing a new species, was also found among the iron-oxidizing strains. This lineage, called 2B on the basis of the 16S rRNA gene phylogeny and which groups strains DSM 1927 (strain F221) and CF3 among 39 other isolates and sequence clones, was clearly distinguishable from the *A. ferrooxidans* subclade 2A and the *A. ferridurans* subclade 3B, both according to 16S rRNA gene oligotyping and MLSA sequence typing. In agreement with our findings, strain CF3 has been shown to group as a sister branch with respect to the type strain of *A. ferroxidans* in neighbor-joining phylogenetic trees derived from the same molecular marker (Hedrich and Johnson, 2013). However, according to the same study strain DSM 1927 clusters together with the type strain of *A. ferridurans*. Branching order of these strains had earlier been shown to be unstable (Lane et al., 1992). Previous studies have also shown divergence between strain CF3 and *A. ferrooxidans* using rep-PCR (Paulino et al., 2001). At the level of the MLSA concatenate, strains DSM 1927 and CF3 were below the species divergence threshold cutoff with respect to *A. ferrooxidans* and just above the cutoff with respect to *A. ferridurans*, suggesting they comprise an intermediate group to both in a presently unclear state of differentiation from both these species. Further, phylogenomic studies should cast light on this matter and better resolve if this is a case of ongoing or achieved differentiation. There are a number of physiological characteristics support differentiation of strain DSM 1927, which was originally isolated from a uranium mine drainage in Austria, from both *A. ferrooxidans* and *A. ferridurans*. It is tolerant to uranium (up to 2400 ppm; ∼10 mM) and, while it shares 85% DNA-DNA hybridization homology to *A. ferrooxidans* strain ATCC 19859 (subclade 2A) and has numerous features in common with this strain, strain DSM 1927 was able to tolerate 65°C for 5 min without losing viability in contrast with strain ATCC 19859 which perished in the process (Harrison, 1982). Other studies have shown that colonies of strain DSM 1927 are differently pigmented (gray colored) during aerobic growth on hydrogen, in contrast with those of *A. ferridurans* ATCC 33020^T which were dark brown and *A. ferrooxidans* ATCC 23270^T which remained unpigmented (Hedrich and Johnson, 2013).

Other lineages uncovered by the 16S rRNA gene phylogeny and further supported by the oligotyping data, that could not

be evaluated by MLSA in this study and that deserve further attention are subclades 1B, 1C, and 1D, branching close to the *A. caldus* type strain, subclade 4B branching as a sister clade of *A. ferrivorans* and subclade 3A branching next to *A. ferridurans*. Although presently mostly occupied by uncultured clones, all these clades have at least one cultured representative and could be targeted for deeper experimental characterization in order to better span the genetic diversity of the *Acidithiobacillus* species complex.

CONCLUSIONS

The hierarchical relationships among members of the genus *Acidithiobacillus*, all of which are part of a single order and a single family, have remained poorly understood in the past. Using molecular systematics approaches and an extensive set of strains and sequence clones from diverse global locations, we have revised the inherent diversity of the acidithiobacilli and reconstructed a robust genus-level phylogeny. Results obtained in this study confirm, at a much wider scale, the inherent diversity of this taxon and support the recognition of the acidithiobacilli as a species complex. These phylogenetic analyses, utilizing different molecular markers and typing approaches, suggest that this species complex includes hitherto unrecognized genera and species, and also ecotypes in the process of differentiation. The availability of genome sequences from a larger number of strains spanning the complex should enable future detailed phylogenomic studies to resolve the evolutionary relationships with a greater degree of precision and gain insight into the factors driving population differentiation in extremely acidic environments.

AUTHOR CONTRIBUTIONS

RQ and DBJ conceived and supervised the study. HN and AM designed and carried out the bioinformatic analyses. PC, JA, and LA performed the molecular biology experiments. MG prepared and maintained the strains. FI and JC supported the sequence and statistical analyses. All authors analyzed the data. HN, AM, and RQ analyzed and interpreted the data and wrote the paper. All authors read and approved the final manuscript.

FUNDING

FONDECYT 1140048 and 3130376. CONICYT Basal CCTE PFB16 and CONICYT and UNAB graduate study fellowships.

ACKNOWLEDGMENTS

The authors thank Douglas Rawlings, Violaine Bonnefoy, Pablo Ramirez, Mario Vera, Jiri Kucera, and Francisco Remosellez for providing strains of *Acidithiobacillus* spp.

SUPPLEMENTARY MATERIAL

The Supplementary Material for this article can be found online at: http://journal.frontiersin.org/article/10.3389/fmicb.2017.00030/full#supplementary-material

REFERENCES

Acuña, L. G., Cárdenas, J. P., Covarrubias, P. C., Haristoy, J. J., Flores, R., Nuñez, H., et al. (2013). Architecture and gene repertoire of the flexible genome of the extreme acidophile *Acidithiobacillus caldus*. *PLoS ONE* 8:e78237. doi: 10.1371/journal.pone.0078237

Amouric, A., Brochier-Armanet, C., Johnson, D. B., Bonnefoy, V., and Hallberg, K. B. (2011). Phylogenetic and genetic variation among Fe(II)-oxidizing acidithiobacilli supports the view that these comprise multiple species with different ferrous iron oxidation pathways. *Microbiology* 157, 111. doi: 10.1099/mic.0.044537-0

Atkinson, T., Cairns, S., Cowan, D. A., Danson, M. J., Hough, D. W., Johnson, D. B., et al. (2000). A microbiological survey of Montserrat island hydrothermal biotopes. *Extremophiles* 4, 305–313. doi: 10.1007/s007920070018

Bryant, R. D., McGroarty, K. M., Costerton, J. W., and Laishley, E. J. (1983). Isolation and characterization of a new acidophilic *Thiobacillus* species (*T. albertis*). *Can. J. Microbiol.* 29, 1159. doi: 10.1139/m83-178

Bubendorfer, S., Koltai, M., Rossmann, F., Sourjik, V., and Thormann, K. M. (2014). Secondary bacterial flagellar system improves bacterial spreading by increasing the directional persistence of swimming. *Proc. Natl. Acad. Sci. U.S.A.* 111, 11485. doi: 10.1073/pnas.1405820111

Bustamante, P., Covarrubias, P. C., Levicán, G., Katz, A., Tapia, P., Holmes, D., et al. (2012). ICE*Afe*1, an actively excising genetic element from the biomining bacterium *Acidithiobacillus ferrooxidans*. *J. Mol. Microbiol. Biotechnol.* 22, 399. doi: 10.1159/000346669

Clarridge, J. E. III (2004). Impact of 16S rRNA gene sequence analysis for identification of bacteria on clinical microbiology and infectious diseases. *Clin. Microbiol. Rev.* 17, 840. doi: 10.1128/CMR.17.4.840-862.2004

Eren, A. M., Maignien, L., Sul, W. J., Murphy, L. G., Grim, S. L., Morrison, H. G., et al. (2013). Oligotyping: differentiating between closely related microbial taxa using 16S rRNA gene data. *Methods Ecol. Evol.* 4, 1111. doi: 10.1111/2041-210X.12114

Eren, A. M., Sogin, M. L., Morrison, H. G., Vineis, J. H., Fisher, J. C., Newton, R. J., et al. (2015). A single genus in the gut microbiome reflects host preference and specificity. *ISME J.* 9, 90. doi: 10.1038/ismej.2014.97

Falagán, C., and Johnson, D. B. (2016). *Acidithiobacillus ferriphilus* sp. nov., a facultatively anaerobic iron- and sulfur-metabolizing extreme acidophile. *Int. J. Syst. Evol. Microbiol.* 66, 206. doi: 10.1099/ijsem.0.000698

Fernández-Remolar, D. C., Rodriguez, N., Gómez, F., and Amils, R. (2003). Geological record of an acidic environment driven by iron hydrochemistry: the Tinto River system. *J. Geophys. Res.* 108, 5080. doi: 10.1029/2002JE001918

Garrity, G. M., Bell, J. A., and Lilburn, T. (2005). "Order II. *Acidithiobacillales* ord. nov," in *Bergey's Manual of Systematic Bacteriology*, ed D. Brenner, N. Krieg, J. Staley, and G. Garrity (New York, NY: Springer), 60–62.

Gillis, M., Vandamme, P., De Vos, P., Swings, J., and Kersters, K. (2005). "Polyphasic taxonomy," in *Bergey's Manual of Systematic Bacteriology*, ed D. Brenner, N. Krieg, J. Staley, and G. Garrity (New York, NY: Springer), 43–48.

Goebel, B. M., and Stackebrandt, E. (1994). Cultural and phylogenetic analysis of mixed microbial populations found in natural and commercial bioleaching environments. *Appl. Environ. Microbiol.* 60, 1614–1621.

González, C., Yanquepe, M., Cardenas, J. P., Valdes, J., Quatrini, R., Holmes, D. S., et al. (2014). Genetic variability of psychrotolerant *Acidithiobacillus ferrivorans* revealed by (meta)genomic analysis. *Res. Microbiol.* 165, 726. doi: 10.1016/j.resmic.2014.08.005

Guindon, S., and Gascuel, O. (2003). A simple, fast, and accurate algorithm to estimate large phylogenies by maximum likelihood. *Syst. Biol.* 52, 696. doi: 10.1080/10635150390235520

Hallberg, K. B., González-Toril, E., and Johnson, D. B. (2010). *Acidithiobacillus ferrivorans*, sp. nov.; facultatively anaerobic, psychrotolerant iron-, and sulfur-oxidizing acidophiles isolated from metal mine-impacted environments. *Extremophiles* 14, 9: doi: 10.1007/s00792-009-0282-y

Hallberg, K. B., and Lindström, E. B. (1994). Characterization of *Thiobacillus caldus* sp. nov., a moderately thermophilic acidophile. *Microbiology* 140, 3451–3456. doi: 10.1099/13500872-140-12-3451

Harrison, A. P. (1982). Genomic and physiological diversity amongst strains of *Thiobacillus ferrooxidans*, and genomic comparison with *Thiobacillus thiooxidans*. *Arch. Microbiol.* 131, 68: doi: 10.1007/BF00451501

Hayes, S. M., Root, R. A., Perdrial, N., Maier, R. M., and Chorover, J. (2014). Surficial weathering of iron sulfide mine tailings under semi-arid climate. *Geochim. Cosmochim. Acta* 141, 240: doi: 10.1016/j.gca.2014.05.030

Hedrich, S., and Johnson, D. B. (2013). *Acidithiobacillus ferridurans* sp. nov., an acidophilic iron-, sulfur- and hydrogen-metabolizing chemolithotrophic gammaproteobacterium. *Int. J. Syst. Evol. Microbiol.* 63, 4018: doi: 10.1099/ijs.0.049759-0

Huang, J. Y., Xu, X. C., Chen, L. W., and Zhou, Y. X. (2012). Heavy metal migration rule in Yangshanchong tailings of Tongling. *Adv. Mater. Res.* 573–574, 421–426. doi: 10.4028/www.scientific.net/AMR.573-574.421

Huang, L.-N., Kuang, J.-L., and Shu, W.-S. (2016). Microbial ecology and evolution in the acid mine drainage model system. *Trends Microbiol.* 24, 581. doi: 10.1016/j.tim.2016.03.004

Hudson, C. M., Williams, K. P., and Kelly, D. P. (2014). Definitive assignment by multigenome analysis of the gammaproteobacterial genus *Thermithiobacillus* to the class *Acidithiobacillia*. *Pol. J. Microbiol.* 63, 245–247.

Huelsenbeck, J. P., and Ronquist, F. (2001). MRBAYES: bayesian inference of phylogenetic trees. *Bioinformatics* 17:754. doi: 10.1093/bioinformatics/17.8.754

Johnson, D. B. (2014). Biomining-biotechnologies for extracting and recovering metals from ores and waste materials. *Curr. Opin. Biotechnol.* 30, 24. doi: 10.1016/j.copbio.2014.04.008

Jones, D. S., Schaperdoth, I., and Macalady, J. L. (2016). Biogeography of sulfur-oxidizing *Acidithiobacillus* populations in extremely acidic cave biofilms. *ISME J.* 10, 2879. doi: 10.1038/ismej.2016.74

Katoh, K., and Standley, D. M. (2013). MAFFT multiple sequence alignment software version 7: improvements in performance and usability. *Mol. Biol. Evol.* 30, 772. doi: 10.1093/molbev/mst010

Kearns, D. B. (2010). A field guide to bacterial swarming motility. *Nat. Rev. Microbiol.* 8, 634. doi: 10.1038/nrmicro2405

Kelly, D. P., and Wood, A. P. (2000). Reclassification of some species of *Thiobacillus* to the newly designated genera *Acidithiobacillus* gen. nov., *Halothiobacillus* gen. nov. *and Thermithiobacillus* gen. nov. *Int. J. Syst. Evol. Microbiol.* 50:511. doi: 10.1099/00207713-50-2-511

Konstantinidis, K. T., Ramette, A., and Tiedje, J. M. (2006). The bacterial species definition in the genomic era. *Philos. Trans. R. Soc. Lond. B. Biol. Sci.* 361:1929. doi: 10.1098/rstb.2006.1920

Lane, D. J., Harrison, A. P., Stahl, D., Pace, B., Giovannoni, S. J., Olsen, G. J., et al. (1992). Evolutionary relationships among sulfur- and iron-oxidizing eubacteria. *J. Bacteriol.* 174, 269–278.

Latorre, M., Ehrenfeld, N., Cortés, M. P., Travisany, D., Budinich, M., Aravena, A., et al. (2016). Global transcriptional responses of *Acidithiobacillus ferrooxidans* Wenelen under different sulfide minerals. *Bioresour. Technol.* 200, 29. doi: 10.1016/j.biortech.2015.09.110

Liljeqvist, M., Valdés, J., Holmes, D. S., and Dopson, M. (2011). Draft genome of the psychrotolerant acidophile *Acidithiobacillus ferrivorans* SS3. *J. Bacteriol.* 193, 4304. doi: 10.1128/jb.05373-11

Luo, H., Shen, L., Yin, H., Li, Q., Chen, Q., Luo, Y., et al. (2009). Comparative genomic analysis of *Acidithiobacillus ferrooxidans* strains using the *A. ferrooxidans* ATCC 23270 whole-genome oligonucleotide microarray. *Can. J. Microbiol.* 55, 587. doi: 10.1139/w08-158

Ni, Y.-Q., He, K.-Y., Bao, J.-T., Yang, Y., Wan, D.-S., and Li, H.-Y. (2008). Genomic and phenotypic heterogeneity of *Acidithiobacillus* spp. strains isolated from diverse habitats in China. *FEMS Microbiol. Ecol.* 64, 248. doi: 10.1111/j.1574-6941.2008.00457.x

Nieto, P. A., Covarrubias, P. C., Jedlicki, E., Holmes, D. S., and Quatrini, R. (2009). Selection and evaluation of reference genes for improved interrogation of microbial transcriptomes: case study with the extremophile *Acidithiobacillus ferrooxidans*. *BMC Mol. Biol.* 10:63. doi: 10.1186/1471-2199-10-63

Nuñez, H., Covarrubias, P. C., Moya-Beltrán, A., Issotta, F., Atavales, J., Acuña, L. G., et al. (2016). Detection, identification and typing of *Acidithiobacillus* species and strains: a review. *Res. Microbiol.* 167, 555. doi: 10.1016/j.resmic.2016.05.006

Nuñez, H., Loyola, D., Cárdenas, J. P., Holmes, D. S., Johnson, D. B., and Quatrini, R. (2014). Multi locus sequence typing scheme for *Acidithiobacillus caldus* strain evaluation and differentiation. *Res. Microbiol.* 165, 735. doi: 10.1016/j.resmic.2014.07.014

Parker, C. D. (1945a). The corrosion of concrete. I. The isolation of a species of bacterium associated with the corrosion of concrete exposed to atmosphere containing hydrogen sulphide. *Aust. J. Biol. Med. Sci.* 23, 81–90.

Parker, C. D. (1945b). The corrosion of concrete 2. The function of *Thiobacillus concretivorus* (nov. spec.) in the corrosion of concrete exposed to atmospheres containing hydrogen sulphide. Aust. J. Biol. Med. Sci. 23, 91–98.

Parker, C. D. (1947). Species of sulphur bacteria associated with the corrosion of concrete. *Nature* 159, 439–440.

Parker, C. D., and Prisk, J. (1953). The oxidation of inorganic compounds of sulphur by various sulphur bacteria. *J. Gen. Microbiol.* 8, 344–364.

Paulino, L. C., Bergamo, R. F., de Mello, M. P., Garcia, O. Jr., Manfio, G. P., and Ottoboni, L. M. M. (2001). Molecular characterization of *Acidithiobacillus ferrooxidans* and *A. thiooxidans* strains isolated from mine wastes in Brazil. *Antonie Van Leeuwenhoek* 80, 65. doi: 10.1023/A:1012247325537

Rossi-Tamisier, M., Benamar, S., Raoult, D., and Fournier, P.-E. (2015). Cautionary tale of using 16S rRNA gene sequence similarity values in identification of human-associated bacterial species. *Int. J. Syst. Evol. Microbiol.* 65, 1929. doi: 10.1099/ijs.0.000161

Sintes, E., De Corte, D., Haberleitner, E., and Herndl, G. J. (2016). Geographic distribution of archaeal ammonia oxidizing ecotypes in the Atlantic ocean. *Front. Microbiol.* 7:77. doi: 10.3389/fmicb.2016.00077

Sneath, P. H. A., and Skerman, V. B. D. (1966). A list of type and reference strains of bacteria. *Int. J. Syst. Bacteriol.* 16:1. doi: 10.1099/00207713-16-1-1

Stackebrandt, E., and Ebers, J. (2006). Taxonomic parameters revisited: tarnished gold standards. *Microbiol. Today.* 33, 152–155.

Stackebrandt, E., and Goebel, B. M. (1994). Taxonomic note: a place for DNA-DNA reassociation and 16S rRNA sequence analysis in the present species definition in bacteriology. *Int. J. Syst. Evol. Microbiol.* 44:846. doi: 10.1099/00207713-44-4-846

Swaminathan, B., Barrett, T. J., Hunter, S. B., Tauxe, R. V., and CDC PulseNet Task Force (2001). PulseNet: the molecular subtyping network for foodborne bacterial disease surveillance, United States. *Emerg. Infect. Dis.* 7, 382. doi: 10.3201/eid0703.010303

Talla, E., Hedrich, S., Mangenot, S., Ji, B., Johnson, D. B., Barbe, V., et al. (2014). Insights into the pathways of iron- and sulfur-oxidation, and biofilm formation from the chemolithotrophic acidophile *Acidithiobacillus ferrivorans* CF27. *Res. Microbiol.* 165, 753. doi: 10.1016/j.resmic.2014.08.002

Tamura, K., and Nei, M. (1993). Estimation of the number of nucleotide substitutions in the control region of mitochondrial DNA in humans and chimpanzees. *Mol. Biol. Evol.* 10:512.

Tan, G.-L., Shu, W.-S., Zhou, W.-H., Li, X.-L., Lan, C.-Y., and Huang, L.-N. (2009). Seasonal and spatial variations in microbial community structure and diversity in the acid stream draining across an ongoing surface mining site. *FEMS Microbiol. Ecol.* 70, 121. doi: 10.1111/j.1574-6941.2009.00744.x

Temple, K. L., and Colmer, A. R. (1951). The autotrophic oxidation of iron by a new bacterium, *Thiobacillus ferrooxidans*. *J. Bacteriol.* 62, 605–611.

Travisany, D., Cortés, M. P., Latorre, M., Di Genova, A., Budinich, M., Bobadilla-Fazzini, R. A., et al. (2014). A new genome of *Acidithiobacillus thiooxidans* provides insights into adaptation to a bioleaching environment. *Res. Microbiol.* 165, 743. doi: 10.1016/j.resmic.2014.08.004

Urbieta, M. S., Porati, G., Segretín, A., González-Toril, E., Giaveno, M., and Donati, E. (2015). Copahue geothermal system: a volcanic environment with rich extreme prokaryotic biodiversity. *Microorganisms* 3, 344. doi: 10.3390/microorganisms3030344

Valdés, J., Ossandon, F., Quatrini, R., Dopson, M., and Holmes, D. S. (2011). Draft genome sequence of the extremely acidophilic biomining bacterium *Acidithiobacillus thiooxidans* ATCC 19377 provides insights into the evolution of the *Acidithiobacillus* genus. *J. Bacteriol.* 193, 7003. doi: 10.1128/JB.06281-11

Valdés, J., Pedroso, I., Quatrini, R., Dodson, R. J., Tettelin, H., Blake, R., et al. (2008). *Acidithiobacillus ferrooxidans* metabolism: from genome sequence to industrial applications. *BMC Genomics.* 9:597. doi: 10.1186/1471-2164-9-597

Valdés, J., Quatrini, R., Hallberg, K., Dopson, M., Valenzuela, P. D. T., and Holmes, D. S. (2009). Draft genome sequence of the extremely acidophilic bacterium *Acidithiobacillus caldus* ATCC 51756 reveals metabolic versatility in the genus *Acidithiobacillus*. *J. Bacteriol.* 191, 5877. doi: 10.1128/JB.00843-09

Vandamme, P., and Peeters, C. (2014). Time to revisit polyphasic taxonomy. *Antonie Van Leeuwenhoek* 106, 57. doi: 10.1007/s10482-014-0148-x

Vishniac, W., and Santer, M. (1957). The thiobacilli. *Bacteriol. Rev.* 21, 195–213.

Waksman, S. A., and Joffe, J. S. (1922). Microorganisms concerned in the oxidation of sulfur in the soil: II. *Thiobacillus thiooxidans*, a new sulfur-oxidizing organism isolated from the soil. *J. Bacteriol.* 7, 239–256.

Watanabe, T., Miura, A., Shinohara, A., Kojima, H., and Fukui, M. (2016). *Thermithiobacillus plumbiphilus* sp. nov., a sulfur-oxidizing bacterium isolated from lead sulfide. *Int. J. Syst. Evol. Microbiol.* 66, 1986. doi: 10.1099/ijsem.0.000972

Williams, K. P., and Kelly, D. P. (2013). Proposal for a new class within the phylum *Proteobacteria*, *Acidithiobacillia* classis nov., with the type order *Acidithiobacillales*, and emended description of the class *Gammaproteobacteria*. *Int. J. Syst. Evol. Microbiol.* 63, 2901. doi: 10.1099/ijs.0.049270-0

Wu, X., Liu, L., Zhang, Z., Deng, F., and Liu, X. (2014). Phylogenetic and genetic characterization of *Acidithiobacillus* strains isolated from different environments. *World J. Microbiol. Biotechnol.* 30, 3197. doi: 10.1007/s11274-014-1747-4

Yan, L., Zhang, S., Wang, W., Hu, H., Wang, Y., Yu, G., et al. (2015). Draft genome sequence of *Acidithiobacillus ferrooxidans* YQH-1. *Genom Data* 6, 269. doi: 10.1016/j.gdata.2015.10.009

Yarza, P., Richter, M., Peplies, J., Euzeby, J., Amann, R., Schleifer, K. H., et al. (2008). The all-species living tree project: a 16S rRNA-based phylogenetic tree of all sequenced type strains. *Syst. Appl. Microbiol.* 31, 241. doi: 10.1016/j.syapm.2008.07.001

Yin, H., Zhang, X., Liang, Y., Xiao, Y., Niu, J., and Liu, X. (2014). Draft genome sequence of the extremophile *Acidithiobacillus thiooxidans* A01, isolated from the wastewater of a coal dump. *Genome Announc.* 2, e00222–e00214. doi: 10.1128/genomeA.00222-14.

You, X.-Y., Guo, X., Zheng, H.-J., Zhang, M.-J., Liu, L.-J., Zhu, Y.-Q., et al. (2011). Unraveling the *Acidithiobacillus caldus* complete genome and its central metabolisms for carbon assimilation. *J. Genet. Genomics* 38, 243. doi: 10.1016/j.jgg.2011.04.006

Zhang, X., Feng, X., Tao, J., Ma, L., Xiao, Y., Liang, Y., et al. (2016a). Comparative genomics of the extreme acidophile *Acidithiobacillus thiooxidans* reveals intraspecific divergence and niche adaptation. *Int. J. Mol. Sci.* 17, E1355. doi: 10.3390/ijms17081355

Zhang, X., She, S., Dong, W., Niu, J., Xiao, Y., Liang, Y., et al. (2016b). Comparative genomics unravels metabolic differences at the species and/or strain level and extremely acidic environmental adaptation of ten bacteria belonging to the genus *Acidithiobacillus*. *Syst. Appl. Microbiol.* 39, 493. doi: 10.1016/j.syapm.2016.08.007

Conflict of Interest Statement: The authors declare that the research was conducted in the absence of any commercial or financial relationships that could be construed as a potential conflict of interest.

frontiers in Microbiology

ORIGINAL RESEARCH
published: 27 December 2016
doi: 10.3389/fmicb.2016.02035

Bioinformatic Analyses of Unique (Orphan) Core Genes of the Genus *Acidithiobacillus*: Functional Inferences and Use As Molecular Probes for Genomic and Metagenomic/Transcriptomic Interrogation

Carolina González[1,2†], *Marcelo Lazcano*[1,2†], *Jorge Valdés*[3*] and *David S. Holmes*[1,2*]

[1] Center for Bioinformatics and Genome Biology, Fundación Ciencia & Vida, Santiago, Chile, [2] Facultad de Ciencias Biologicas, Universidad Andres Bello, Santiago, Chile, [3] Center for Genomics and Bioinformatics, Faculty of Sciences, Universidad Mayor, Santiago, Chile

Using phylogenomic and gene compositional analyses, five highly conserved gene families have been detected in the core genome of the phylogenetically coherent genus *Acidithiobacillus* of the class *Acidithiobacillia*. These core gene families are absent in the closest extant genus *Thermithiobacillus tepidarius* that subtends the *Acidithiobacillus* genus and roots the deepest in this class. The predicted proteins encoded by these core gene families are not detected by a BLAST search in the NCBI non-redundant database of more than 90 million proteins using a relaxed cut-off of $1.0e^{-5}$. None of the five families has a clear functional prediction. However, bioinformatic scrutiny, using pI prediction, motif/domain searches, cellular location predictions, genomic context analyses, and chromosome topology studies together with previously published transcriptomic and proteomic data, suggests that some may have functions associated with membrane remodeling during cell division perhaps in response to pH stress. Despite the high level of amino acid sequence conservation within each family, there is sufficient nucleotide variation of the respective genes to permit the use of the DNA sequences to distinguish different species of *Acidithiobacillus*, making them useful additions to the armamentarium of tools for phylogenetic analysis. Since the protein families are unique to the *Acidithiobacillus* genus, they can also be leveraged as probes to detect the genus in environmental metagenomes and metatranscriptomes, including industrial biomining operations, and acid mine drainage (AMD).

Keywords: ***Acidithiobacillus***, ***Thermithiobacillus***, **extreme acidophile, Orphan (ORFan) genes, horizontal gene transfer (HGT), biomining bioleaching and acid mine drainage (AMD), acid resistance, metagenome and metatranscriptome**

OPEN ACCESS

Edited by:
Axel Schippers, Federal Institute for Geosciences and Natural Resources, Germany

Reviewed by:
Zheng Wang, Yale University, USA
Jeannette Marrero-Coto, Leibniz University of Hanover, Germany

***Correspondence:**
Jorge Valdés
jorge.valdes@gmail.com
David S. Holmes
dsholmes2000@yahoo.com

[†] *These authors have contributed equally to this work.*

Specialty section:
This article was submitted to Extreme Microbiology, a section of the journal Frontiers in Microbiology

Received: *10 October 2016*
Accepted: *02 December 2016*
Published: *27 December 2016*

Citation:
González C, Lazcano M, Valdés J and Holmes DS (2016) Bioinformatic Analyses of Unique (Orphan) Core Genes of the Genus Acidithiobacillus: Functional Inferences and Use As Molecular Probes for Genomic and Metagenomic/Transcriptomic Interrogation. Front. Microbiol. 7:2035. doi: 10.3389/fmicb.2016.02035

INTRODUCTION

The power of comparative genomics to enlighten evolutionary processes through hypotheses has emerged based on the enormous availability of complete and partial genome sequences from both early and late branching lineages at different taxonomic levels (MacLean et al., 2009). At present, we are able to exploit the powerful analytical methods of molecular evolution and population genomics to determine the relative contribution of the different evolutionary forces that shape genome organization, structure, and diversity. These methods also offer an exceptional opportunity to explore the genetic and genomic determinants of lifestyle diversity in bacteria, especially for polyextremophiles including those that thrive in extremely acidic environments and for which there are genome sequences available (Cárdenas et al., 2016a,b).

The genus *Acidithiobacillus* (termed *Acidithiobacilli*) consists of seven recognized species; *Acidithiobacillus ferrooxidans, A. ferridurans, A. ferrivorans, A. ferriphilus, A. thiooxidans, A. caldus and A. albertensis* (reviewed in Nuñez et al., 2016). The *Acidithiobacilli* together with *Thermithiobacillus tepidarius* constitute the class *Acidithiobacillia* (Williams and Kelly, 2013; Hudson et al., 2014).

The *Acidithiobacilli* have been found principally in industrial biomining and coal processing operations, the deep subsurface of the Spanish pyritic belt and in natural and man-made acid drainages including acid mine drainage (AMD; Méndez-García et al., 2015; Hedrich, 2016). All are extreme acidophiles with a pH optima for growth of 3.5 or less (Barrie Johnson and Quatrini, 2016). In contrast, *T. tepidarius* is a neutrophile that was recovered from a terrestrial thermal spring (Wood and Kelly, 1985). All the other extant bacterial lineages phylogenetically closely related to *T. tepidarius* are also neutrophiles, making it likely that the last common ancestor before the split between *T. tepidarius* and the *Acidithiobacilli* was also a neutrophile. This raises questions about the origin and evolution of genes and mechanisms that allowed the transition to be made from a neutral pH environment to an extremely acidic environment eventually giving rise to the *Acidithiobacilli*.

Mechanisms used by extreme acidophiles to mitigate the effect of low pH have been extensively investigated (Baker-Austin and Dopson, 2007). However, there are no studies that use comparative genomics to discover new genetic determinants of pH homeostasis in the *Acidithiobacilli*, although one study used multiple strains of *A. thiooxidans* to confirm known acid resistant determinants and assign them to the core or accessory genome (Zhang et al., 2016).

The study of unique gene families from extreme acidophile representatives could provide evidence about events of protein lineage specification involving many structural rearrangements needed to survive under extreme life conditions. Gene tree analyses suggest recent, lineage-specific expansion, and diversification among homologs encoding yet unknown functions for pathway and processes that might be unique requirements in *Acidithiobacilli.* Their analysis could help close gaps in our understanding of genetic and metabolic requirements that support extremophile lifestyles and they could also provide novel candidate sequences for prospecting for new DNA-based screenings and other production avenues (Sabir et al., 2016).

In the present study, we perform an extensive bioinformatic characterization of five protein families taxonomically restricted to the *Acidithiobacilli*. Analyses of their fundamental properties combined with comparative genomics and phylogenomics suggest potential functional roles and allow evolutionary models to be built. The sequences of the five families are also exploited as molecular probes for phylogenetic scrutiny and interrogation of metagenomes and metatranscriptomes including AMD and biomining operations.

MATERIALS AND METHODS

Genomes Used

Table 1 provides information about the genomes.

Pipeline Used for Compiling and Analyzing the Data Set

Predicted protein sequences corresponding to all *Acidithiobacilli* proteomes were sorted using an all-vs.-all BLASTP script based on Best Bidirectional BLAST Hit (BBBH; Altschul et al., 1997) with an *E*-value of 1e-5. Protein families were constructed based on 50% of identity and 50% of coverage in the alignments (Altschul et al., 1997), assigning each protein to one protein family. The families with predicted proteins shared by all strains were selected and denominated the core-genome (Williams and Kelly, 2013; Hudson et al., 2014). The *Acidithiobacillus* core-genome was compared using BLASTP version 2.2.26 (Altschul et al., 1997) against NCBI non-redundant (NR) database in August of 2015, using a minimal *E*-value of 1e-5. Core families with exclusive similarity with *Acidithiobacillus* members, and not associated with any other microorganism, were selected and denominated unique (orphan) core genes. The selected unique protein families were checked manually using BLASTP, Psi-BLAST (Altschul et al., 1997) and HMMer version 3.0 (Eddy, 1998) against NR database with an *E*-value of 1e-4 to confirm their exclusive association with the *Acidithiobacillus* genus. The locus tags of the respective genes are provided in **Table 2**.

Genomic Contexts of Unique Core Genes

Collinear blocks between the genomes and conservation of gene neighbors were determined by MAUVE (Darling et al., 2010), RAST (Aziz et al., 2008; Overbeek et al., 2014; Markowitz et al., 2014a) and IMG-JGI (Markowitz et al., 2014b; Dhillon et al., 2015). Genomic contexts were visualized using Artemis of Sanger (Brettin et al., 2015).

Evaluation of HGT

IslandViewer (Rutherford et al., 2000) was used to predict genomic islands.

Annotation of Unique Core Genes (Families I–V)

Protein coding sequences were annotated using an integrated pipeline consisting of BLASTP (Altschul et al., 1997) searches against NR database of NCBI with an *E*-value cutoff of 1e-3,

TABLE 1 | Genomes used in this study.

Microorganism	Genome size (Mbp)	Predicted protein coding sequences	Genome G+C (%)	Genome accession number (NCBI)	References
Acidithiobacillus ferrooxidans ATCC 23270^T	2.98	3147	58.8	CP001219	Valdés et al., 2008
Acidithiobacillus ferrooxidans ATCC 53993	2.88	2826	58.9	CP001132	Lucas et al., 2008, Unpublished
Acidithiobacillus ferrivorans SS3^T	3.2	3093	56.6	CP002985	Liljeqvist et al., 2011
Acidithiobacillus ferrivorans CF27	3.42	3854	56.4	CCCS020000000	Talla et al., 2014
Acidithiobacillus thiooxidans A01	3.82	3826	53.1	AZMO00000000	Yin et al., 2014
Acidithiobacillus thiooxidans ATCC 19377^T	3.01	3041	53.1	AFOH00000000	Valdés et al., 2011
Acidithiobacillus thiooxidans Licanantay	3.93	4191	52.8	JMEB00000000	Travisany et al., 2014
Acidithiobacillus caldus ATCC 51756^T	2.77	2681 (0.21)^P	61.4	CP005986-CP005989	Valdes et al., 2009
Acidithiobacillus caldus SM-1	2.93	2881 (0.31)^P	61.3	CP002573-CP002577	You et al., 2011
Thermithiobacillus tepidarius DSM 3134^T	2.96	2750	66.8	AUIS00000000	Kelly and Wood, 2000
Acidithiobacillus ferrooxidans strain BY0502	2.97	2822	56.8	LVXZ00000000	Zhou, 2016, Unpublished
Acidithiobacillus ferrooxidans strain DLC-5	4.23	5600	57.6	JNNH00000000*	Chen et al., 2015
Acidithiobacillus ferrooxidans strain YQH-1	3.11	2949	58.6	LJBT00000000	Yan et al., 2015
Acidithiobacillus ferrooxidans strain Hel18	3.11	2939	58.6	LQRJ00000000	Schopf, 2016, Unpublished
Acidithiobacillus caldus strain MTH-04	2.87	2646	61.4	LXQG00000000	Mi et al., 2006, Unpublished
Acidithiobacillus thiooxidans DMC	3.85	3768	53.1	LWSB00000000	Zhang et al., 2016

*T, denotes type strain; P, denotes plasmid information. *Denotes JGI accession number.*

Pfam (Punta et al., 2012), TigrFAM (Consortium, 2014), and Uniprot (Hofmann and Stoffel, 1993) database comparisons. Transmembrane regions in protein sequences were predicted with TMHMM (Haft et al., 2003) and TMPRED (Krogh et al., 2001). Computation of isoelectric point and molecular weight were made with ExPASy web tool (Bjellqvist et al., 1993; Nakai and Horton, 1999; Gasteiger et al., 2005).

Estimation of Mutation Rates

Synonymous and non-synonymous substitution rates were calculated as follows: amino acid alignments of unique (orphan) core genes were constructed using MUSCLE (Edgar, 2004), and used as input for PAL2NAL (Suyama et al., 2006) with the nucleotide sequences to create the codon alignments of gene core families. The ratio of non-synonymous (K_a) to synonymous (K_s) nucleotide substitution rates (K_a/K_s ratios) were calculated using SeqinR package of R project (Charif and Lobry, 2007). Mean K_a/K_s ratios were assigned for individual unique (orphan) core genes (families I–V) by averaging all pairwise ratios within each family.

Signal Peptide and Subcellular Location Predictions

A combination of computational prediction tools PSORTb (Nakai and Horton, 1999; Yu et al., 2010), CELLO (Yu et al., 2006) and ProtCompB[1] (Yu et al., 2004) were used to perform whole genome analysis of unique core protein subcellular localization via the Sec Mechanism and Tat signal prediction (Natale et al., 2008; Bagos et al., 2010). The results derived from three prediction algorithms tools were combined according to majority to obtain a more accurate protein subcellular localization prediction.

[1]http://linux1.softberry.com/berry.phtml?topic=pcompb&group=programs&subgroup=proloc

Lipoproteins Signal Prediction

Prediction of lipoproteins signals was made with LipoP Server (Juncker et al., 2003).

Phylogenetic Analyses

16S rRNA sequences from *Acidithiobacillus* genomes were identified by BLASTN-based script using an *E*-value threshold of 1e-5 and the databases GREENGENES (DeSantis et al., 2006), RDP (Cole et al., 2009) and SILVA (Pruesse et al., 2007) and were aligned using MAFFT (Katoh et al., 2002, 2005) alignment tool with L-INS strategy. Phylogenetic trees were constructed with MrBayes (Huelsenbeck and Ronquist, 2001; Ronquist and Huelsenbeck, 2003) and PHYML (Guindon et al., 2010), using the substitution model predicted for jModelTest2 (Guindon and Gascuel, 2003; Darriba et al., 2012).

Mapping of Genes for Families I–V onto Circular Genomes

The genes encoding families I–V were mapped onto the genomes *A. ferrooxidans* ATCC 23270, *A. ferrivorans* SS3, *A. caldus* ATCC 51756, and *A. caldus* SM-1 using DNAplotter (Carver et al., 2009). The origin of replication (Ori) of each genome was predicted between *dnaN* and *dnaA* as previously described (Valdés et al., 2008) and was used as the zero coordinate to orient the genome maps.

Metagenomic Analysis

Metagenomic and metatranscriptomic sequences were downloaded from NCBI, JGI (Nordberg et al., 2014), and

TABLE 2 | Predicted properties of the proteins of families I–V.

	Microorganism	Locus tag or contig	pI	Size (aa)	TM regions	Signal peptide	Subcellular location	Lipoprotein signature
Family I	*A. ferrooxidans* ATCC 23270	AFE_0294	8.06	250	5	–	IM	–
	A. ferrooxidans ATCC 53993	Lferr_0470	8.06	251	5	–	IM	–
	A. ferrivorans SS3	Acife_2737	9.47	259	5	–	IM	–
	A. ferrivorans CF27	CDQ10770.1	9.26	259	5	–	IM	–
	A. thiooxidans ATCC 19377	AFOH01000117	8.21	261	5	–	IM	–
	A. thiooxidans A01	AZMO01000067	8.06	263	5	–	IM	–
	A. thiooxidans Licanantay	JMEB01000250	8.21	261	5	–	IM	–
	A. caldus SM-1	Atc_0578	9.25	257	5	–	IM	–
	A. caldus ATCC 51756	Acaty_c0588	8.85	249	5	–	IM	–
Family II	*A. ferrooxidans* ATCC 23270	AFE_2894	9.52	103	1	–	IM/P/C	–
	A. ferrooxidans ATCC 53993	Lferr_2514	9.52	103	1	–	IM	–
	A. ferrivorans SS3	Acife_0262	10.26	103	1	–	IM/P/C	–
	A. ferrivorans CF27	CDQ10832.1	9.98	103	1	–	IM/P/C	–
	A. thiooxidans ATCC 19377	AFOH01000056	10.94	103	1	–	IM/P/C	–
	A. thiooxidans A01	AZMO01000007	10.63	103	1	–	IM/P/C	–
	A. thiooxidans Licanantay	JMEB01000152	10.90	103	1	–	IM/P/C	–
	A. caldus SM-1	Atc_0665	10.37	103	1	–	IM/P/C	–
	A. caldus ATCC 51756	Acaty_c0696	9.97	91	1	–	IM/P/C	–
Family III	*A. ferrooxidans* ATCC 23270	AFE_2918	6.82	128	1	Yes	P	Yes
	A. ferrooxidans ATCC 53993	Lferr_2533	6.82	128	1	Yes	P	Yes
	A. ferrivorans SS3	Acife_0237	8.79	128	1	Yes	P/C	Yes
	A. ferrivorans CF27	CDQ10857.1	7.88	128	1	Yes	P	Yes
	A. thiooxidans ATCC 19377	AFOH01000056	8.76	128	1	Yes	P	Yes
	A. thiooxidans A01	AZMO01000007	8.07	128	1	Yes	P	Yes
	A. thiooxidans Licanantay	JMEB01000332	8.76	128	1	Yes	P	Yes
	A. caldus SM-1	Atc_2682	8.58	129	1	Yes	P/C	Yes
	A. caldus ATCC 51756	Acaty_c2529	8.59	129	1	Yes	P/C	Yes
Family IV	*A. ferrooxidans* ATCC 23270	AFE_3261	6.33	172	–	Yes	P/IM	Yes
	A. ferrooxidans ATCC 53993	Lferr_2861	6.48	172	–	Yes	P	Yes
	A. ferrivorans SS3	Acife_0197	8.80	170	–	Yes	P/E	Yes
	A. ferrivorans CF27	CDQ11656.1	8.80	170	–	Yes	P/E	Yes
	A. thiooxidans ATCC 19377	AFOH01000137	6.33	172	–	Yes	P	Yes
	A. thiooxidans A01	AZMO01000008	8.21	171	–	Yes	P	Yes
	A. thiooxidans Licanantay	JMEB01000258	8.22	171	–	Yes	P	Yes
	A. caldus SM-1	Atc_0064	8.80	170	–	Yes	P/IM	Yes
	A. caldus ATCC 51756	Acaty_c0059	8.80	170	–	Yes	P	Yes
Family V	*A. ferrooxidans* ATCC 23270	AFE_2816	9.30	146	1	–	P/IM	–
	A. ferrooxidans ATCC 53993	Lferr_2439	9.31	146	1	–	P/IM	–
	A. ferrivorans SS3	Acife_0333	9.75	145	1	–	P	–
	A. ferrivorans CF27	CDQ09308.1	9.70	145	1	–	P	–
	A. thiooxidans ATCC 19377	AFOH01000029	9.52	86	1	–	C/P	–
	A. thiooxidans A01	AZMO01000004	9.56	119	1	–	P	–
	A. thiooxidans Licanantay	JMEB01000081	9.40	119	1	Yes	P	–
	A. caldus SM-1	Atc_0233	9.21	128	1	–	P	–
	A. caldus ATCC 51756	Acaty_c0260	9.21	128	1	–	P	–

IM, inner membrane; C, cytoplasm; P, periplasm.

MG-RAST (Meyer et al., 2008; additional information can be found in **Table 4**) and were interrogated by BLASTX (Altschul et al., 1997) against the five core protein families with an *E*-value cut-off of 1e-5. The percent identity and coverage of sequences were analyzed for each alignment.

RESULTS AND DISCUSSION

Pipeline for Discovery of Protein Families Unique to the Core Genome of the Genus *Acidithiobacillus*

Figure 1 summarizes the bioinformatics pipeline used to recover five families of proteins and their corresponding genes that are taxonomically restricted to the genus *Acidithiobacillus*. Using a relaxed cutoff (1e-5) in a BLAST search, they were not detected in the NCBI nr database of more than 90 million proteins that includes the predicted proteins of *Thermithiobacillus tepidarius*, the nearest extant relative of the *Acidithiobacilli*.

Integrative Bioinformatics Approaches Can Suggest Functions for the Unique *Acidithiobacillus* Gene Families I–V

Since *Acidithiobacilli*-specific protein families have almost no similarity with known proteins for other non-*Acidithiobacilli* representatives, we used a collection of bioinformatics resources in order to gain insights into potential protein functions based on hydrophobicity profiles, secondary structure predictions, predicted protein cell localizations and the comparison of consensus and profile sequences to pattern and domain databases (see Section Materials and Methods). Protein function predictions of the five *Acidithiobacilli*-specific protein families were examined using an analysis of their genomic contexts. Their differential expression was linked to previously published proteomic data derived from cells subjected to changes of pH, which is known to be a major selective pressure for members of the *Acidithiobacillus* genus (Baker-Austin and Dopson, 2007; see **Table 3**).

Figure 2 provides an example of the predicted protein properties deduced with bioinformatics tools and comparative genomic analysis for members of family II. Additional information for all five families I–V can be found in Supplemental Files 1, 2. *In silico* predictions demonstrate the power of integrative genomics approaches to gain insights into gene function. A significant prediction was made for an integral membrane segment with a moderate conservation profile within the family II. From the non-membrane associated portion of the protein, profile sequences were generated that have similarity to a pattern present in periplasmic binding proteins (Dwyer and Hellinga, 2004) and also solute carrier organic anion transporter family member 4A1 (Pizzagalli et al., 2003).

Comparative genome organization data demonstrated that there is conservation of gene neighborhood profiles that include genes predicted for cell division, surface proteins and ABC transport systems (**Figure 2** and Supplemental File 3). **Table 2** shows a detailed overview of the predicted properties based on amino acid sequences for families I–V.

Gene Expression of Families I–V

Information regarding the expression of the genes encoding the five families was extracted from the literature and is presented in **Table 3**. RNA transcript analysis indicates that all five family genes are expressed in *A. ferrivorans* SS3 in two different conditions: continuous culture at 20°C (Christel et al., 2016a) and at 8°C (Christel et al., 2016b), adjusted to pH 2.5 with sulfuric acid plus trace elements. A proteomic study of *A. ferrooxidans* ATCC 23270 on elemental sulfur as electron donor under aerobic and anaerobic conditions (Osorio et al., 2013) showed that family III was expressed in this strain. A proteomic study of *A. caldus* ATCC 51756 using cells grown at pH 2.5 (optimum growth pH) vs. pH 1 and 4, demonstrated up-regulation of core families I, III, and IV when cells were shifted from pH 2.5 to 1 and that family V was upregulated when cells were shifted from pH 2.5 to 4 (**Table 3**; Mangold et al., 2013). These data show that the genes for

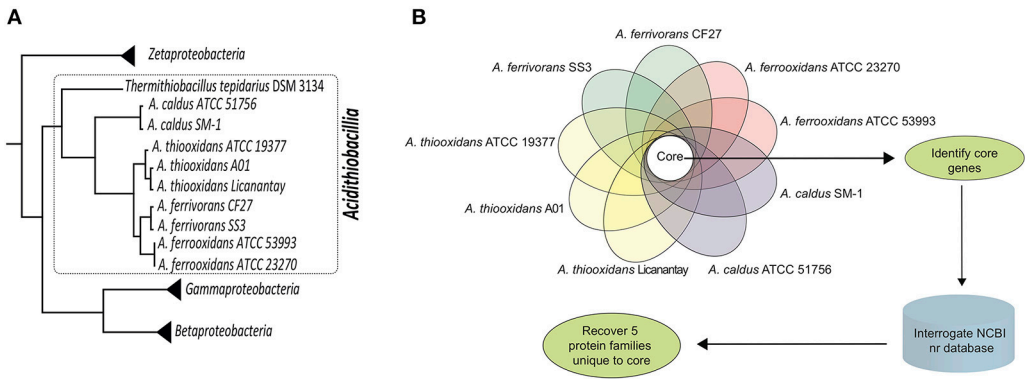

FIGURE 1 | Work Flow. (A) Phylogenetic tree of the class *Acidithiobacillia* (within the dotted line) showing the clustering of the acidophilic *Acidithiobacillus* genus (*Acidithiobacilli*) subtended by the neutrophilic *Thermithiobacillus tepidarius*. The tree is based on genome-scale maximum-likelihood analysis of 98 universal protein families (housekeeping) conserved in *Zeta-*, *Gamma-*, *Betaproteobacteria,* and *Acidithiobacillia* class according to references Williams and Kelly (2013) and Hudson et al. (2014). **(B)** Pipeline for the identification and recovery of five protein families (termed I-V) unique to the genus *Acidithiobacillus*.

TABLE 3 | Gene expression evidence.

	Microorganism	Locus tag or contig	Gene expressed[a]	Protein abundance with pH change[b]		Meta-transcriptomic evidence[c]
Family I	*A. ferrooxidans* ATCC 23270	AFE_0294	ND	ND	Family I	AFE sp. Yes
	A. ferrooxidans ATCC 53993	Lferr_0470	ND	ND		
	A. ferrivorans SS3	Acife_2737	Yes	ND		
	A. ferrivorans CF27	CDQ10770.1	ND	ND		AFV sp. Yes
	A. thiooxidans ATCC 19377	AFOH01000117	ND	ND		
	A. thiooxidans A01	AZMO01000067	ND	ND		
	A. thiooxidans Licanantay	JMEB01000250	ND	ND		ATHIO sp. Yes
	A. caldus SM-1	Atc_0578	ND	ND		
	A. caldus ATCC 51756	Acaty_c0588	Yes	Up at pH 1		
Family II	*A. ferrooxidans* ATCC 23270	AFE_2894	ND	ND	Family II	AFE sp. Yes
	A. ferrooxidans ATCC 53993	Lferr_2514	ND	ND		
	A. ferrivorans SS3	Acife_0262	Yes	ND		
	A. ferrivorans CF27	CDQ10832.1	ND	ND		AFV sp. Yes
	A. thiooxidans ATCC 19377	AFOH01000056	ND	ND		
	A. thiooxidans A01	AZMO01000007	ND	ND		
	A. thiooxidans Licanantay	JMEB01000152	ND	ND		ATHIO sp. Yes
	A. caldus SM-1	Atc_0665	ND	ND		
	A. caldus ATCC 51756	Acaty_c0696	Yes	No change		
Family III	*A. ferrooxidans* ATCC 23270	AFE_2918	Yes	ND	Family III	AFE sp. Yes
	A. ferrooxidans ATCC 53993	Lferr_2533	ND	ND		
	A. ferrivorans SS3	Acife_0237	Yes	ND		
	A. ferrivorans CF27	CDQ10857.1	ND	ND		AFV sp. Yes
	A. thiooxidans ATCC 19377	AFOH01000056	ND	ND		
	A. thiooxidans A01	AZMO01000007	ND	ND		
	A. thiooxidans Licanantay	JMEB01000332	ND	ND		ATHIO sp. Yes
	A. caldus SM-1	Atc_2682	ND	ND		
	A. caldus ATCC 51756	Acaty_c2529	Yes	Up at pH 1		
Family IV	*A. ferrooxidans* ATCC 23270	AFE_3261	ND	ND	Family IV	AFE sp. Yes
	A. ferrooxidans ATCC 53993	Lferr_2861	ND	ND		
	A. ferrivorans SS3	Acife_0197	Yes	ND		
	A. ferrivorans CF27	CDQ11656.1	ND	ND		AFV sp. Yes
	A. thiooxidans ATCC 19377	AFOH01000137	ND	ND		
	A. thiooxidans A01	AZMO01000008	ND	ND		
	A. thiooxidans Licanantay	JMEB01000258	ND	ND		ATHIO sp. Yes
	A. caldus SM-1	Atc_0064	ND	ND		
	A. caldus ATCC 51756	Acaty_c0059	Yes	Up at pH 1		
Family V	*A. ferrooxidans* ATCC 23270	AFE_2816	ND	ND	Family V	AFE sp. Yes
	A. ferrooxidans ATCC 53993	Lferr_2439	ND	ND		
	A. ferrivorans SS3	Acife_0333	Yes	ND		
	A. ferrivorans CF27	CDQ09308.1	ND	ND		AFV sp. Yes
	A. thiooxidans ATCC 19377	AFOH01000029	ND	ND		
	A. thiooxidans A01	AZMO01000004	ND	ND		
	A. thiooxidans Licanantay	JMEB01000081	ND	ND		ATHIO sp. Yes
	A. caldus SM-1	Atc_0233	ND	ND		
	A. caldus ATCC 51756	Acaty_c0260	Yes	Up at pH 4		

Expression of members of the five orphan families in different environmental conditions. Locus tags for the five families are provided.

[a] *Gene expression for families I–V was extracted from Christel et al. (2016a,b) and Osorio et al. (2013).*

[b] *Information regarding protein abundance levels when A. caldus was subjected to growth at pH 1, 2, or 4 was taken from Mangold et al. (2013). Abundance of proteins is expressed as "up in low pH" or "up in high pH" relative to protein levels found at pH 2 (Mangold et al., 2013). Note that the gene accession numbers in Mangold et al. (2013) have been replaced recently by the locus tags provided in this Table.*

[c] *RNA transcript expression as determined by examination of published metatranscriptomics data (Chen et al., 2015) using the families I–V as probes (see **Table 4** for details).*

AFE, Acidithiobacillus ferrooxidans; AFV, Acidithiobacillus ferrivorans; ATHIO, Acidithiobacillus thiooxidans; ND, Not detected.

TABLE 4 | Detection of *Acidithiobacilli* in (A) various metagenomes and (B) metatranscriptomes using families I–V as molecular probes.

(A) Study name	Sample type	Source	pH	Database source	ID	*Acidithiobacilli* reported	*Acidithiobacilli* detected using Families I–V (this study) in reference
Kristineberg Mine	P	Malå, Sweden	2.5–2.7	NCBI nr	AOMQ00000000	AFV, AFE, ATHIO, ACAL (Liljeqvist et al., 2015)	AFV, AFE, ATHIO, ACAL
Kristineberg Mine	B	Malå, Sweden	2.5–2.7	NCBI nr	AOMP00000000	AFV, AFE, ATHIO, ACAL (Liljeqvist et al., 2015)	AFV, AFE, ATHIO, ACAL
Pink biofilm Richmond Mine	AMD	California, USA	0.83	NCBI nr	AADL00000000	None (Tyson et al., 2004)	Not detected
Carnoulès Mine (bin 5)	AMD	Gard, France	3.5–3.8	NCBI nr	PRJNA62261	AFE (Bertin et al., 2011)	AFE, ATHIO, ACAL
Snottites in Frasassi Cave	AMD	Ancona, Italy	0–1	NCBI nr	SRP006444	ATHIO, AT (Jones et al., 2012)	ATHIO
Acquasanta Terme AS5	SB	Grotta Nuova di Rio Garrafo, Italy	0–1.5	IMG/M	3300000825	ATHIO (Jones et al., 2016)	ATHIO
Black Soud Mine	AMD	Minnesota, USA	6.7	NCBI nr	ABLV00000000	None (Edwards et al., 2006)	Not detected
Black smokers (Tui Malila)	HVP	Lau Basin, Pacific Ocean	3.8–5.7	IMG/M	3300001676	None (Sheik et al., 2015)	Not detected
Hydrothermal vent (Guaymas Basin)	HVP	Guaymas Basin, Pacific Ocean	6.5–8	IMG/M	3300003086	None (Li et al., 2016)	Not detected
Marine Microbial communities (Loihi)	HVP	Loihi Seamount, Hawaii	8	IMG/M	3300000327	None (Singer et al., 2013)	Not detected
Deep Oceanic Microbial Communities (Juan de Fuca)	HVP	Juan de Fuca, Pacific Ocean	4.2	IMG/M	3300002481	None (Jungbluth et al., 2013)	Not detected
Marine Microbial communities (Lost City)	HVP	Lost City, Atlantic Ocean	9–11	IMG/M	3300003136	None (Anantharaman et al., 2014)	Not detected
(B) Study	**Sample type**	**Origin**	**pH**	**Database source**	**ID**	***Acidithiobacillus* reported**	***Acidithiobacillus* detected with family probes in reference**
Dabaoshan Mine	AMD	Guangdong, China	1.9–2.3	MG-RAST	4481316.3	AFE, AFV (Chen et al., 2015)	AFE, AFV, ATHIO
Yunfu Mine	AMD	Guangdong, China	2.5	MG-RAST	4481318.3	AFE, AFV (Chen et al., 2015)	AFE, AFV, ATHIO

AMD, Acid Mine Drainage; ACAL, A. caldus; AFV, A. ferrivorans; AFE, A. ferrooxidans; ATHIO, A. thiooxidans; AT, Acidithiobacillus genus; P, Planktonic; B, Biofilm; SB, Subaerial biofilm; HVP, Hydrothermal vent plume; NCBI nr, National Center for Biotechnology Information, non-redundant database; IMG/M, Integrated Microbial Genomes/ Metagenomes; MG-RAST, Metagenomes- Rapid Annotation using Subsystem Technology.

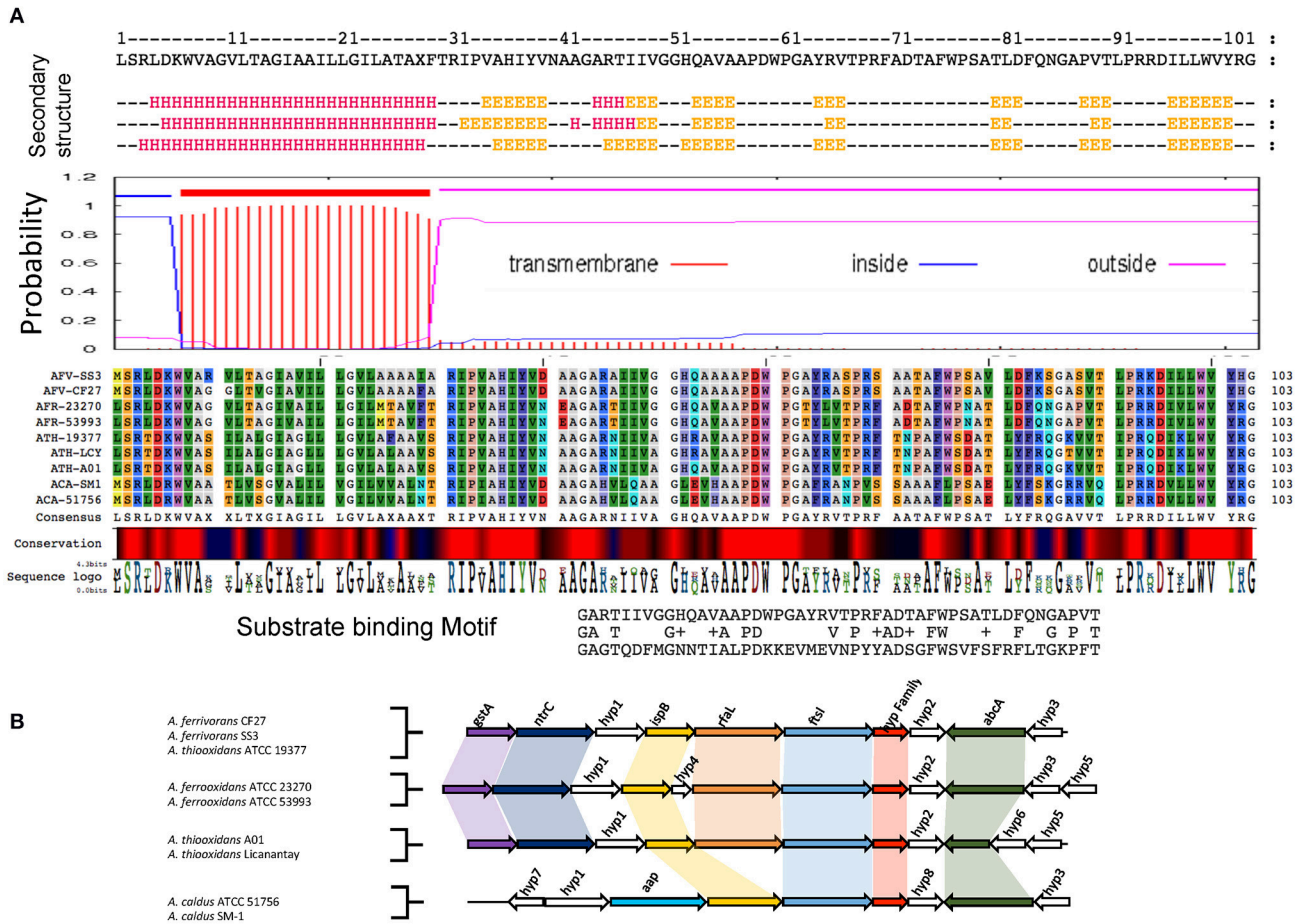

FIGURE 2 | Example of functional prediction based on multiple bioinformatics and genome-based evidence for members of family II. (A) Bioinformatics analysis of members of family II based on secondary structure prediction, hydrophobicity profiles and transmembrane segments prediction, multiple alignments and conservation profiles for the generation of consensus and profile sequences and their comparison to specific substrate binding protein profiles found in public databases. **(B)** Genomic context analysis of members of family II including functional annotations of the closest neighborhood genes for functional association. gstA, Glutathione S-transferase; ntrC, Nitrogen assimilation regulatory protein; ispB, Octaprenyl-diphosphate synthase; rfaL, O-antigen ligase; ftsI, Cell division protein; Hyp family II, Hypothetical protein; abcA, ABC transporter A family; app, Amino acid permease; Hyp (1–8), Hypothetical protein (1–8). **Table 2** provides a complete overview of the predicted properties from amino acid sequences for member of the five families.

the five families (i) are expressed and thus are unlikely to be misannotated open reading frames with no coding capacity and (ii) provide evidence that families I, III, IV, and V could be involved in responses to acid stress at least in *A. caldus*. It remains to be determined if changes in RNA levels are associated with these genes in the other *Acidithiobacilli*.

In addition, RNA transcripts in metatranscriptomes of the Dabaoshan and Yunfu Pond mines in China (Chen et al., 2015) were detected that exhibited sequences similar to families I–V (**Table 3**, right hand side) from *A. ferrooxidans*, *A. ferrivorans*, and *A. thiooxidans*, although no strain specificity could be determined. This supports the idea that the five families are bona fide genes.

Insights into Protein Functions

In order to make a comprehensive summary of the potential gene function inferred from all the evidence presented, a schematic summary is presented in **Figure 3**. Families I, II, and V, have predicted transmembrane segments that, in conjunction with protein sorting signal identification, provide preliminary information about their cellular location. Profile and consensus sequences comparisons against public databases only provided information about family II. Family II sequences have motifs similar to those of periplasmic binding proteins, usually associated with ABC transport for the substrate specific incorporation of nutrients and scarce molecules or beneficial solutes under extreme environmental conditions (Cuneo et al., 2008). We suggest that members of family II could be distant relatives of periplasmic binding proteins whose specific substrate(s) and functional role remains to be investigated.

Families III and IV have predicted protein localizations associated with inner membrane and periplasmic spaces and their strong lipoprotein signatures, in addition to genomic context information, provide clues for their potential role

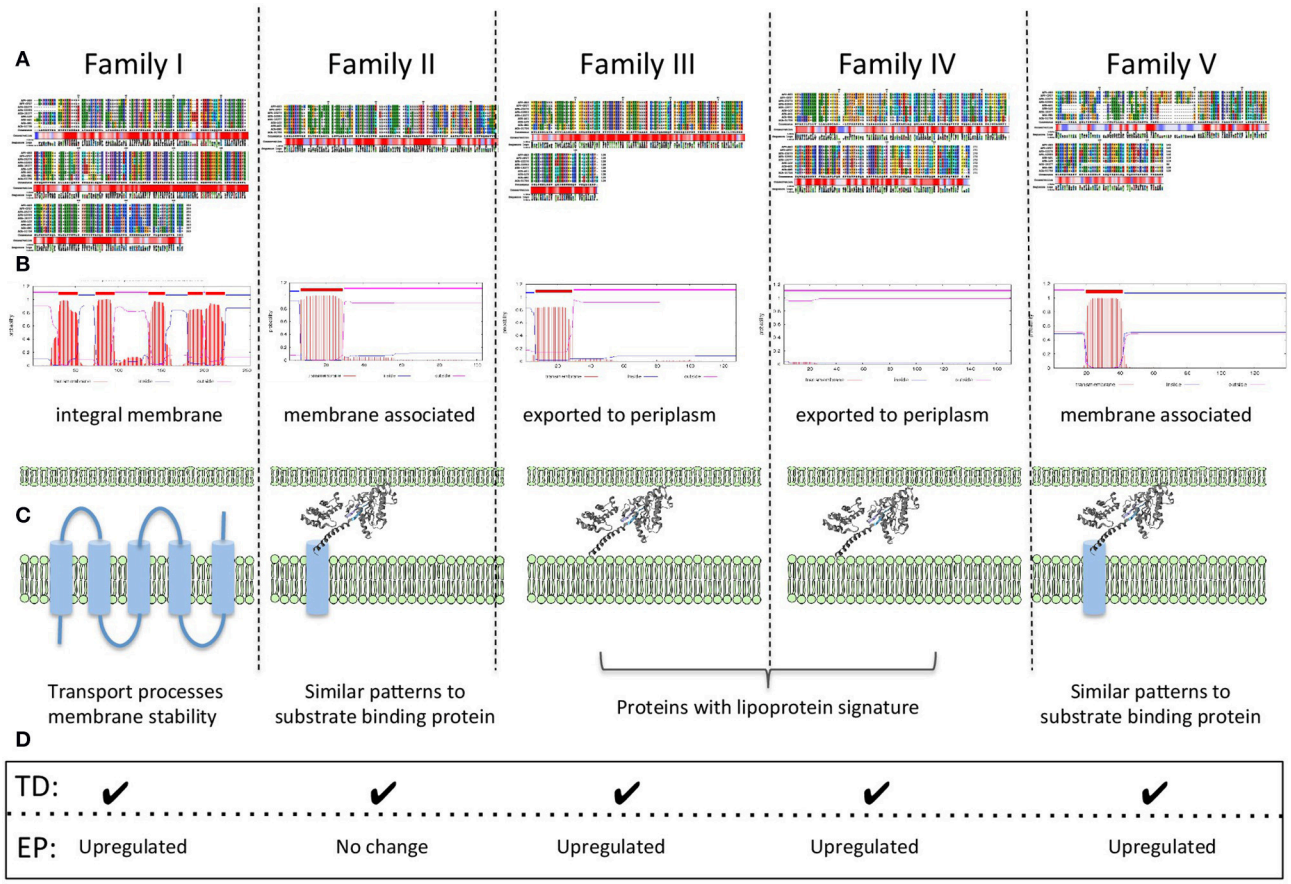

FIGURE 3 | Schematic summary of functional associations found in families I–V. (A) Multiple alignments, conservation profiles and consensus sequences. **(B)** Transmembrane topology predictions. **(C)** Predicted protein localization and deduced general functions. **(D)** Expression data TD: RNA transcript detected; EP: protein expression profile.

in key physiological processes, such as lipid metabolism. We hypothesize a potential connection between membrane associated lipoproteins, lipid metabolism and membrane stability as a requirement for low pH lifestyle (Baker-Austin and Dopson, 2007; Liljeqvist et al., 2015).

Predicted protein properties of all families I–V, suggest a general involvement in functions associated with membrane processes perhaps involving roles in membrane stability, transport processes, and/or the generation of molecular components to allow the synthesis and incorporation of hydrophobic molecules into the membrane increasing its stability in low pH.

Chromosome Architecture is Consistent with Functional Inferences (Involvement in Cell Envelope Remodeling during Cell Division)

It has been observed in many bacteria that the gene order relative to OriC is highly conserved along the chromosomal replicores (Sobetzko et al., 2012). Also, essential and highly expressed genes tend to be encoded close to oriC (Rocha, 2004). This heightened activity can be attributed to gene dosage effects during chromosome replication especially in rapidly dividing cells, but underlying physical properties of the circular chromosome, including an inferred gradient of DNA superhelical density from the origin to the terminus, are also known to be involved in influencing gene expression (Sobetzko et al., 2012).

In particular, it has been observed that several genes involved in acid stress, including envelope remodeling, are located close to oriC in the gammaproteobacterium *Dickeya dadantii* (Jiang et al., 2015). Given the possibility that genes of families I–V could be involved in acid stress response and that this response might be associated with chromosome topology, we determine their chromosomal locations on the closed circular chromosomes of *A. ferrooxidans* ATCC 23270^T, *A. ferrivorans* SS3^T, *A. caldus* ATCC 51756^T, and *A. caldus* SM-1 using DNAplotter (Carver et al., 2009; **Figure 4**). In all these chromosomes, the five family genes exhibit a tendency to be located nearer Ori rather than the terminus, especially in the cases of *A. ferrooxidans* and *A. ferrivorans*. In the latter two chromosomes, the gene order

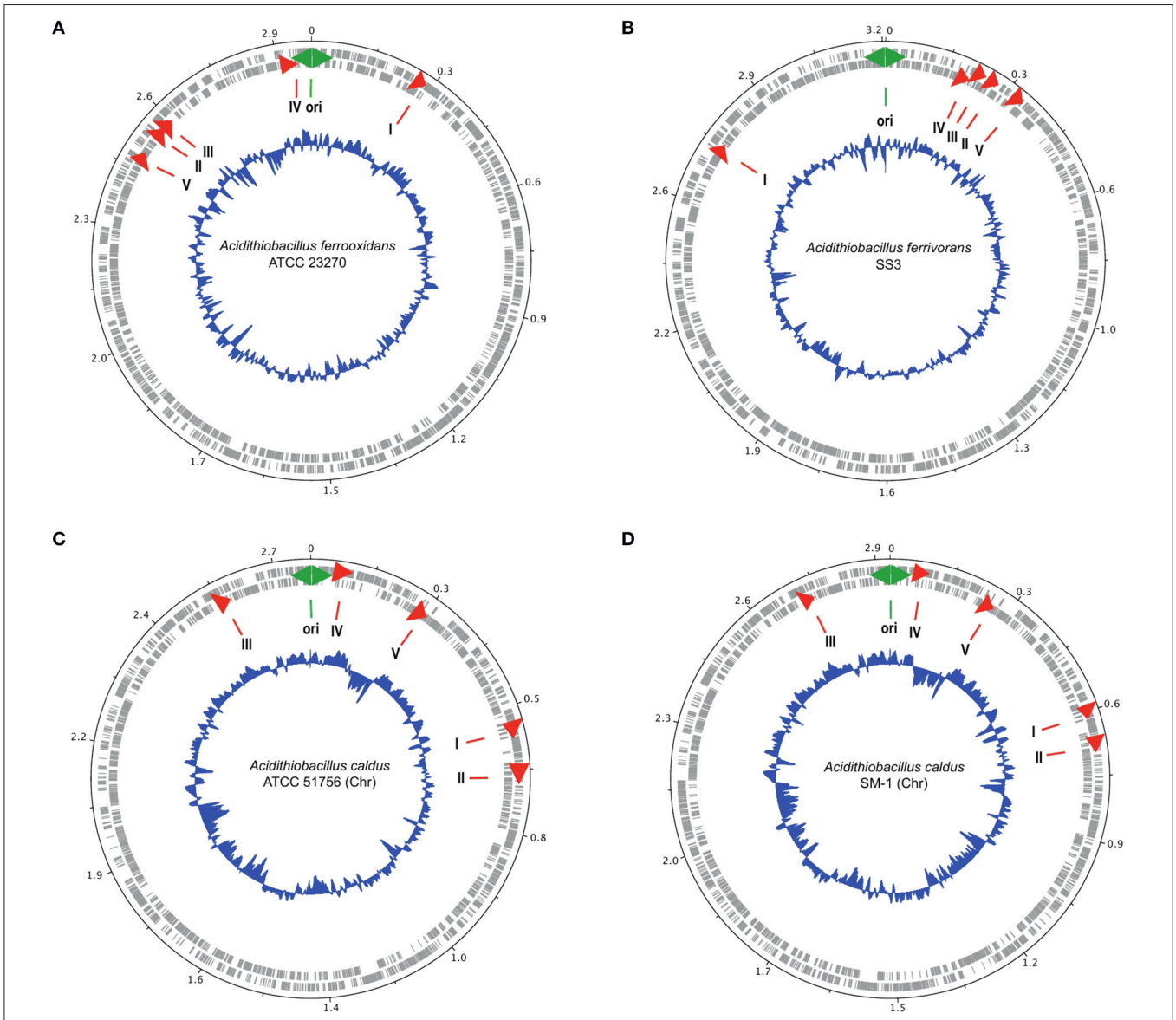

FIGURE 4 | Location of the genes encoding families I–V (red arrows) in the genomes of (A) *A. ferrooxidans* ATCC 23270, **(B)** *A. ferrivorans* SS3, **(C)** *A. caldus* ATCC 51756, and **(D)** *A. caldus* SM-1. The outer two circles show the genes on both strands of DNA of the chromosome. The inner blue circle indicates the G+C content. The green two-headed arrow indicates the predicted origin of replication of the chromosome. The red arrows indicate the position of the families I–V genes.

relative to Ori is conserved but is inverted, perhaps due to inter-replicore translocation that is known to be common around Ori in other microorganisms (Eisen et al., 2000; Khedkar and Seshasayee, 2016). Three of the families have genes predicted to DNA handling functions in their gene neighborhoods ordered in tightly clustered associations that could be operons; for example, *rmuC* (DNA recombination) near family IV, and *dnaB* and *radA* (DNA helicase and DNA repair, respectively) near family V. These genes are usually associated with DNA replication and cell division (**Figure 4**). The juxtaposition of *ftsL*, an essential cell division protein (Guzman et al., 1992), to the gene encoding family II and its closeness to the family III gene (**Figure 4**) strongly suggests that family II and III are involved in cell division perhaps through cell envelope remodeling. Their proximity to Ori could enhance the ability of the *Acidithiobacilli* to respond to changes in environmental acidity at early stages of cell division. Such changes might be more difficult to accomplish during later stages of cell division or at the resting stage.

Families I–V Are Protein Coding Genes

Taxonomically restricted genes, such as families I–V, are referred to as orphans genes or ORFans (orphan open reading frames; Fischer and Eisenberg, 1999; Pedroso et al., 2008; Tautz and Domazet-Loso, 2011). ORFans can be artifacts of annotation,

non-coding RNA genes or protein encoding genes (Prabh and Rodelsperger, 2016). In the case of families I–V, there is evidence that those from *A. caldus* encode proteins and that families I–V from *A. ferrooxidans*, *A. ferrivorans,* and *A. thiooxidans* express RNA (**Table 3**). Given the highly conserved sequences similarity between the respective families from the different *Acidithiobacillus* species, it is reasonable to suggest that all are protein coding genes, as observed for the *A. caldus* families and are not "merely" RNA genes. However, in order to provide additional evidence for protein coding capacity, selection pressure was measured as the ratio of the synonymous and non-synonymous rates of amino acid substitution (dN/dS), also called omega (ω) for all families. The omega values for families I–V are 0.07, 0.05, 0.03, 0.05, and 0.08 respectively. An $\omega < 1$ can be interpreted as evidence for negative selection and most likely such a sequence would correspond to a protein encoding gene (Prabh and Rodelsperger, 2016). The omega values are considerably <1 for all five families providing compelling evidence that they are protein-encoding genes.

Origin of Families I–V

The genes encoding families I–V are not found in *T. tepidarius* that subtends the genus *Acidithiobacillus* and shares the last common ancestor with it, nor are they found in any other organism that has sequence information in the NCBI nr database. So questions arise as to the origin and evolution of the five families.

We propose three main hypotheses.

i The genes arose *de novo* in the *Acidithiobacillus* genus, after its split with *T. tepidarius* perhaps by gene duplication and divergence (Long et al., 2003; Tautz and Domazet-Loso, 2011; Klasberg et al., 2016). If this happened, then the duplication events occurred so long ago and/or involved such fast divergence that sequence similarities to the original genes have been blurred by subsequent evolutionary events.

ii The genes entered the last common ancestor of the *Acidithiobacillus* genus by horizontal gene transfer (HGT). IslandViewer (Rutherford et al., 2000) was employed to search for evidence of HGT with no positive results. Also, the annotated gene neighborhoods of families I–V were searched by hand for evidence of signatures of HGT such as transposases (Riadi et al., 2012; Acuña et al., 2013), integrases, conjugative and viral functions, and tRNAs but only one transposase was detected in the vicinity of family IV, (Supplemental File 3). Although little evidence of HGT could be found, it can be argued that it occurred so long ago that its molecular signatures have been lost. If HGT occurred, who were the donor organisms? There is no obvious donor lineage represented in the NCBI nr database, but other organisms could remain to be discovered whose study could help shed light on the evolutionary history of the genes of families I–V genes. The increasing metagenomic sequencing efforts offer the best opportunities for discovering such potential donors.

iii Other lineages of Bacteria and Archaea including the ancestors of *T. tepidarius*, once contained the genes but all subsequently lost them except the *Acidithiobacillus* genus. We think that this is the least likely explanation because it requires many independent gene loss events to have occurred. Also, if the proposed association of families I–V with functions involved in acid related response is correct, it would suggest that many ancestral lineages of the *Acidithiobacillus* genus were acidophiles for which there is no evidence.

Although a lack of definitive evidence leaves all three hypothesis unimpaired, we speculate that the emergence of families I–V could have helped promote by whatever means (direct activity of the encoded proteins, or via sensing or regulatory mechanisms) the ability of the last common ancestor of the *Acidithiobacillus* genus and *T. tepidarius* to transition from a neutral pH environment to one that was increasingly acidic and finally to one that was extremely acidic. In this scenario, the transition process could have provided opportunities for the *Acidithiobacillus* genus to diverge from the *T. tepidarius* lineage. This hypothesis requires additional evidence, especially experimental evidence, to clearly pinpoint the specific functions and physiological roles of the five families.

Use of Families I–V As Genetic Probes for *Acidithiobacillus* Genus and Species Identification

In order to evaluate the sensitivity and specificity of the families to discriminate between *Acidithiobacillus* species, the DNA sequences of families I–V were concatenated for each *Acidithiobacillus* species and compared by BLASTN against each *Acidithiobacillus* species. The results are reported as % nucleotide identity between the concatenated probe and each *Acidithiobacillus* species (**Figure 5**). The dark blue diagonal indicates high nucleotide identity, as expected, between the concatenated probe and its respective sequences in the corresponding genome. Importantly, the concatenated probes from one species have lower levels of sequence identity when compared to other species. For example, the concatenated probe from *A. caldus* has only 69% identity (white cell) when compared to sequences present in the genome of *A. ferrivorans*.

These data indicate that the concatenated families are capable of discriminating between the different *Acidithiobacilli* species used to build the concatenated probes, but are they capable of phylotyping new genomes that did not contribute to building the probes?

During the course of this investigation four new genomes of *A. ferrooxidans* (strains BY0502, DLC-5, YQH-1, and Hel18), one *A. caldus* genome (strain MTH-04) and six genomes of *A. thiooxidans* were released (**Table 1**), providing an opportunity to test the discriminatory powers of the family probes on new genomes.

First, the concatenated family probes, described in the previous experiment, were used in BLASTN comparisons with the new genomes. The results are reported as % nucleotide identity between the concatenated probe and each *Acidithiobacillus* species (leftmost four columns, **Figure 6**). The concatenated probes clearly have the ability to discriminate between *A. caldus* MTH-04, *A. thiooxidans* DMC, *A. ferrooxidans* BY0502, *A. ferrooxidans* YQH-1, and *A. ferrooxidans* Hel18,

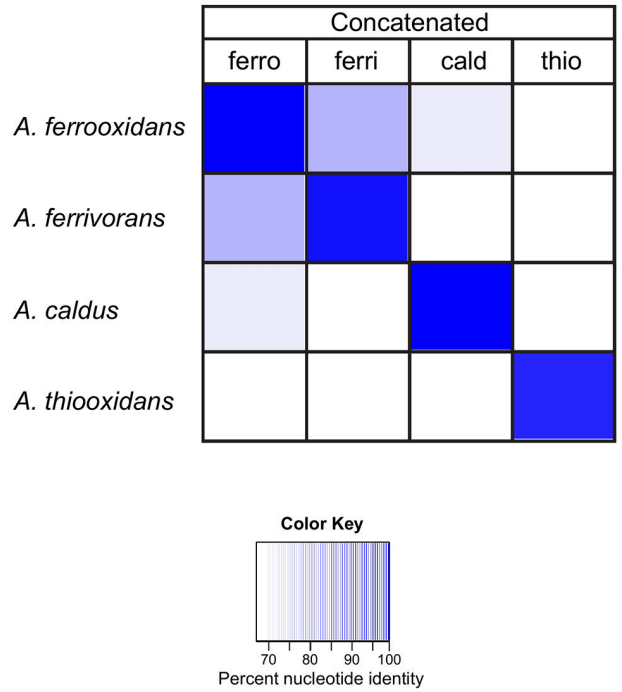

FIGURE 5 | Heat map showing the percent nucleotide similarity (from 100% to <70%, see color key) between families I–V genes, concatenated for each *Acidithiobacillus* species (top row) vs. families I–V in each genome (left). ferro: *A. ferrooxidans*; ferri: *A. ferrivorans*; thio: *A. thiooxidans* and cald: *A. caldus*.

indicated by the dark blue color (close to 100% sequence identity). However, there is one anomalous identification. *A. ferrooxidans* BY0502 exhibits the best match with the *A. ferrivorans* concatenated probe (bottom row), suggesting that this species might not be *A. ferrooxidans*.

In order to determine if this anomaly could be attributed to one (or more) of the families in particular, the experiment was repeated with each individual family (**Figure 6**). Each family correctly identified the new genomes of *A. ferrooxidans*, *A. thiooxidans* and *A. caldus* with the exception of *A. ferrooxidans* BY0502. The highest percentage matches of all five families to *A. ferrooxidans* BY0502 were to the probes built from *A. ferrivorans,* confirming the results using the concatenated family probe.

Because of the vexing problem of the anomalous *A. ferrooxidans* BY0502 in which the family I–V probes place it closer to *A. ferrivorans* than *A. ferrooxidans*, it was decided to use other approaches to investigate its phylogeny using ANI (Goris et al., 2007) and TETRA (Richter and Rosselló-Móra, 2009). Both approaches indicate that *A. ferrooxidans* BY0502 is not related to *A. ferrooxidans* because of the low values of ANI and TETRA, 83.4 and 0.988, respectively, between the two genomes. Nor can it be classified in the *A. ferrivorans* clade, with low values of 91.7/0.996 (ANI/TETRA values), although it is more closely related to *A. ferrivorans* than *A. ferrooxidans*. In order to investigate further the phylogeny of *A. ferrooxidans* BY0502, 16S rRNA sequence analysis was carried out that placed it in a clade with *A. ferriphilus*, subtended by the clade *A. ferrivorans* with a bayesian posterior probability node support of 1 that strongly endorses the proposed phylogeny (**Figure 7**). Therefore, we suggest that *A. ferrooxidans* BY0502 is more likely to be an *A. ferriphilus-like* microorganism; an hypothesis that requires confirmation using other phylogenetic approaches. This example demonstrates the power of the family probes to aid in the identification of the *Acidithiobacillus* genus with discriminatory powers to suggest species at least for those under interrogation in the present study.

Use of Families I–V As Genetic Probes for Interrogation of Metagenomes and Metatranscriptomes

Gaining insight into the structure, organization, and function of microbial communities (microbiomes) has been proposed as one of the major research challenges of the current decade (2020 visions, 2010) and metagenomic and metatranscriptomic approaches present major opportunities for advancing our knowledge in this area. One of the most promising areas of metagenomics research is the use of shotgun methods to sequence random fragments of DNA (or RNA) in an environmental sample. This information can then be analyzed for microbial diversity, prediction of gene functions and biochemical pathway model building. Many bioinformatic approaches have been developed to handle the typically enormous amounts of data generated by metagenomics investigations (e.g., reviewed in Hiraoka et al., 2016).

One of the most straightforward and computationally less demanding approaches to estimate microbial diversity in a microbiome is the use of marker genes (molecular probes; Wu and Eisen, 2008; Liu et al., 2011; Wu and Scott, 2012; Kim et al., 2013; Darling et al., 2014). For example, rRNA sequences from known organisms can be used to computationally search the shotgun sequences for similar sequences or can be coupled with rRNA-PCR to pull out and extend specific sequences. These methods provide an overview of the phylogenetic distribution (phylotyping) of the cell-based life present in a sample but they have their limitations (reviewed in Fabrice and Didier, 2009).

Taxonomically restricted protein encoding genes have been used for phylotyping, including the recombinase A gene family and the RNA polymerase beta subunit (Wu et al., 2011), genes specifically targeting the *Acidithiobacilli* (Nieto et al., 2009; Nuñez et al., 2014, 2016) and many other examples (Liu et al., 2011; Segata et al., 2011; Wu et al., 2013; Darling et al., 2014). However, such marker genes are subject to HGT and evolutionary rate differences that can exacerbate the interpretation of phylogenies. Since the five families are taxonomically restricted to the *Acidithiobacilli* and do not appear to be prone to HGT, we decided to examine their ability to identify the *Acidithiobacillus* genus and to discriminate between different species of the *Acidithiobacilli* (**Figures 6**, **7**) in environmental metagenomic and metatranscriptomic samples. For the first objective, the amino acid sequence of all five families from all participating *Acidithiobacillus* species (*A. ferrooxidans*, *A. ferrivorans*, *A. thiooxidans,* and *A. caldus*) was

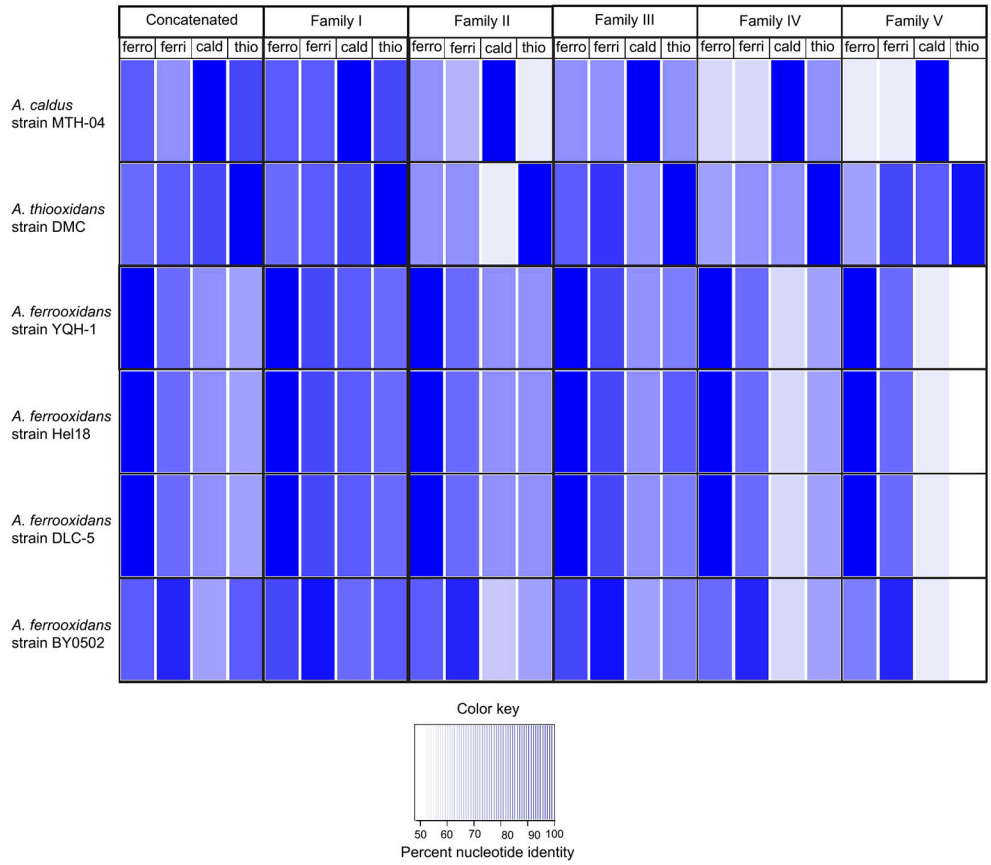

FIGURE 6 | Heat map illustrating the percent nucleotide similarity (from 100% to <50%, see color key) between families I–V genes and the best BLAST hit of four newly identified *A. ferrooxidans* genomes (strain BY0502, strain DLC-5, strain YQH-1, and strain Hel18) and one *A. caldus* genome (strain MTH-04).

concatenated (five families × nine species). This was considered as a general probe for the *Acidithiobacillus* genus (genus-level probe). A second series of probes was constructed where the protein sequences of the five families was concatenated according to species, generating five different probes each one specific for an *Acidithiobacillus* species (e.g., *A. ferrooxidans* probe = the concatenation of families I–V of *A. ferrooxidans*). These probes were then used in a BLASTX searches to interrogate several environmental metagenomes and metatranscriptomes listed in **Table 4**.

The metagenomes were chosen to include low pH environments such as mining operations and AMD, where *Acidithiobacilli* have previously been reported, and also environments of intermediate acidity (e.g., Black Smokers, Tui Malila), neutral pH (e.g., Hydrothermal vent, Guaymas Basin), and high pH (e.g., Marine Microbial Communities, Lost City) where *Acidithiobacilli* have not been detected. Two low pH metatranscriptomes were also included in the analysis. The results of the BLASTX interrogations are shown in **Figure 8** and the results are summarized in **Table 4**.

Inspection of the left hand column of **Figure 8** indicates that the genus-level probe detects sequence similarity in all the samples except for the Pink Biofilm from the Richmond mine. This is in agreement with the report that no *Acidithiobacilli* were detected in the Pink Biofilm but were detected in all the other samples (references provided in **Table 4**). The absence of *Acidithiobacilli* in the Pink Biofilm sample could be due to its extremely low pH (pH 0.83) which is thought to be too acidic to support their growth (Tyson et al., 2004). In addition no *Acidithiobacilli* were detected in samples from the Black Soud Mine, Black Smokers (Tui Malila), Hydrothermal Vent (Guaymas Basin), Marine Microbial Communities (Loihi), Deep Ocean Microbial Communities (Juan de Fuca), Marine Microbial Communities (Lost City), which is also in agreement with the published literature (references found in **Table 4**). The conclusion is that the *Acidithiobacilli* genus-level probe appears to have good specificity and sensitivity in detecting *Acidithiobacilli* in environmental metagenomes but more samples are required to develop statistical support for this assertion.

Table 4 also indicates that the families can be used to interrogate metatranscriptomes and provides additional evidence that the genes of family I–V are transcribed. This evidence was

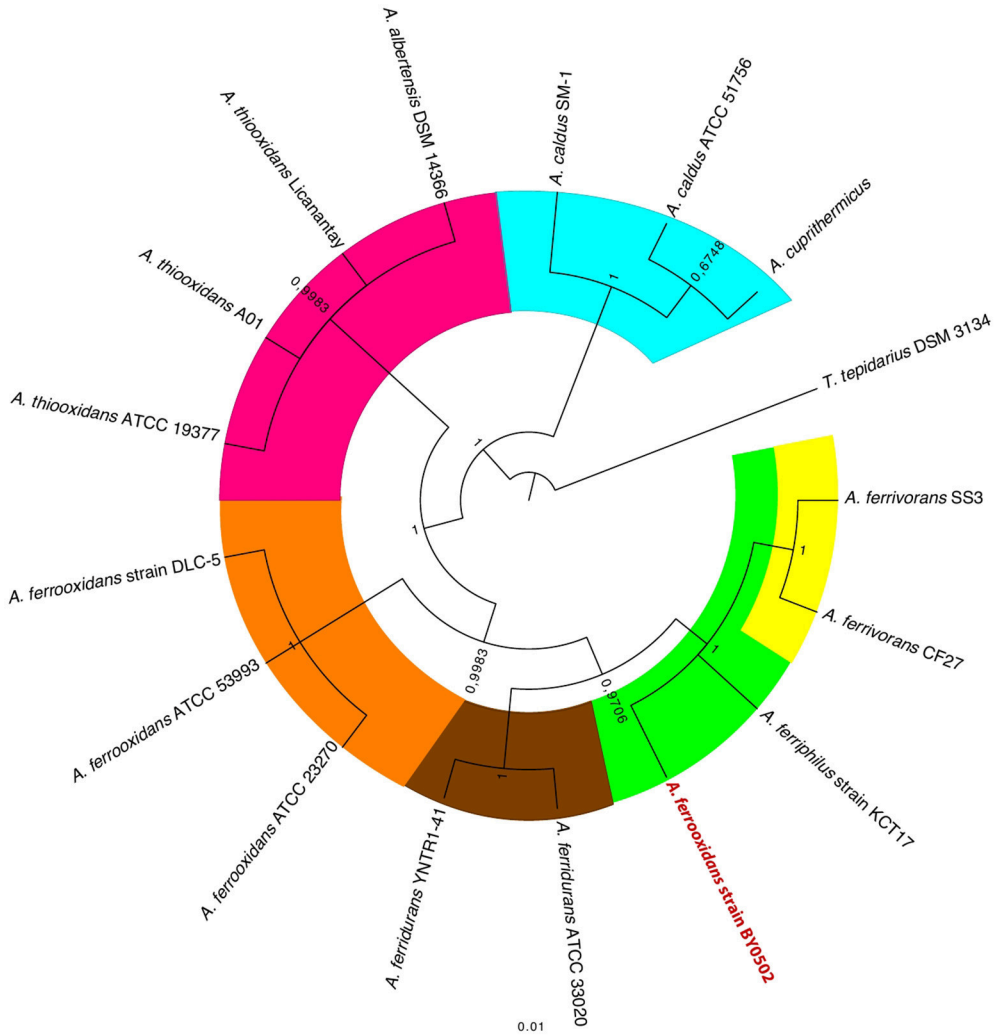

FIGURE 7 | 16S rRNA gene tree of selected *Acidithiobacilli* showing the anomalous location of *A. ferrooxidans* BY0502 within the *A. ferriphilus* clade. The tree was constructed using bayesian inference with MrBayes (Huelsenbeck and Ronquist, 2001). The posterior probability node support is given for all nodes.

used to construct the right hand column presented earlier in **Table 3**.

However, caution is required in the interpretation of the use of the species-specific probes. In case A (see **Figure 8**), both the sequence identity (100%) and sequence coverage (83.5–95.1%) of the *A. ferrooxidans* probes of families II and III strongly support the contention that sequences corresponding to them are present in the Carnoulès metagenome. However, in case B, although there is good coverage of the *A. ferrooxidans* family I and V probes (99.3–99.6%), the sequence identity is lower (80–83%). This suggests that these families probably belong to *A. ferrooxidans* in the metagenome but that they have diverged somewhat from the probe sequences. Recovery of such sequences would expand the number and diversity of such sequences that could be helpful for elucidating their function and shedding light on their evolution. In case C, both the coverage and identity are lower and the hits are to probes developed for *A. thiooxidans* and *A. caldus* family III and family IV. This suggests that the Carnoulès metagenome contains *A. thiooxidans*-like and *A. caldus*-like organisms that exhibit low sequence similarity to families III and IV, but not to the other families. As in case B, these sequences could be helpful for later studies to help unravel sequence function and evolution. A final case marked by asterisks in **Figure 8** illustrates the common finding of sequence similarity to metagenomic reads that are truncated. Truncated sequences that have high similarity to the probes could potentially be extended by PCR using primers designed from the probes and subsequently analyzed.

With these caveats in mind, families I–V satisfy a number of criteria for use as identification markers for *Acidithiobacilli* in genomic, metagenomic/metatranscriptomic investigations. They are universally present in the genus, not present in other genera and are not subject to HGT. Preliminary evidence also points to association of at least three of the

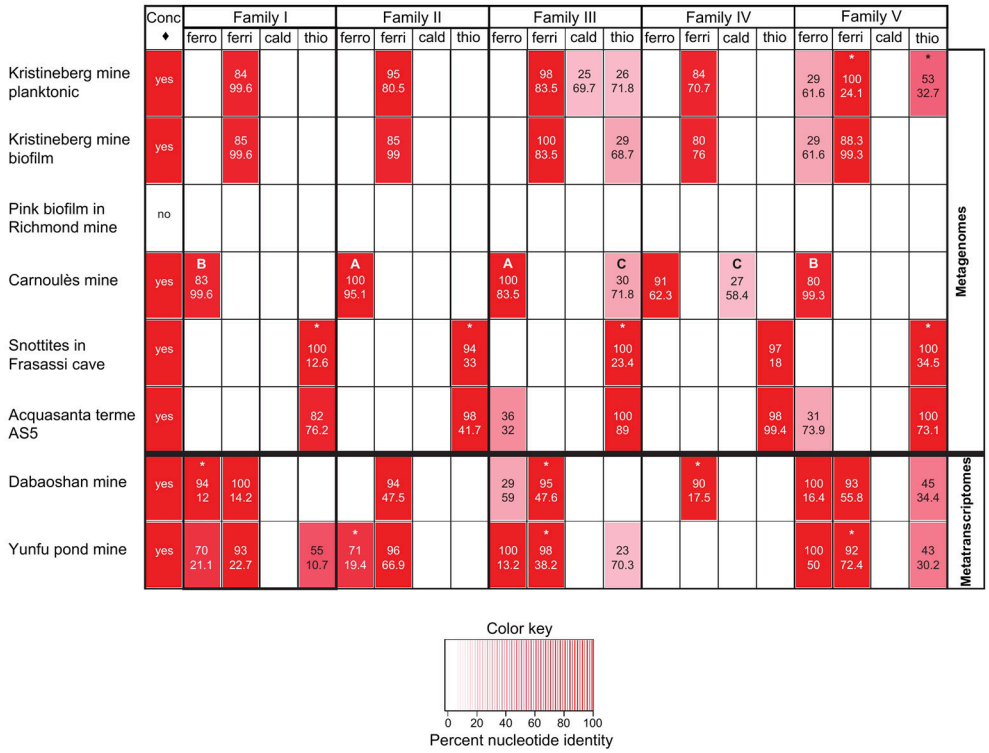

FIGURE 8 | Heat map indicating the percent nucleotide identity (top number in respective cells) and sequence coverage (lower number in respective cells) between families I–V and environmental metagenomes and metatranscriptomes as assayed by BLASTX. The figure also shows (leftmost column, ◊ = concatenated probe) the presence or absence of the *Acidithiobacillus* genus in the metagenomes and metatranscriptomes determined by BLASTX, using as a probe the concatenated sequences of all five families of all *Acidithiobacilli* used in the study (5 families × 9 *Acidithiobacilli* species = 45 concatenated sequences), where positive matching is indicated with a "yes." The letters A to C refer to specific cases described in the text. The * refers to sequences that are truncated in the respective metagenome/transcriptome databases.

families (Families I, III, and IV) in envelope remodeling and lipid metabolism possibly associated with acid stress response and so could serve as PhyEco (for phylogenetic and phylogenetic ecology; Wu et al., 2013) markers for certain acidic environments including AMD and biomining operations.

CONCLUSIONS

This study:

- Used comparative genomics approaches to discover five protein families that are taxonomically restricted to the genus *Acidithiobacillus* (*Acidithiobacilli*), a group of extreme acidophiles.
- Highlighted and examined the potential functions of the five families. Although functional assignments could not be made with confidence for any of the families, it was hypothesized that they are involved in cell envelope restructuring that in four families may be associated with responses to changing pH conditions, at least in *A. caldus*.
- Reflected on the possible evolution of the five families. It was suggested that the five families emerged after the split of the *Acidithiobacilli* lineage from the neutrophile *T. tepidarius*, allowing the *Acidithiobacilli* lineage to colonize acidic econiches.
- Considered how the five families can be used as molecular probes to interrogate genomic and metagenomic/metatranscriptomic data.
- Served as a springboard for testing hypotheses and for guiding future research, for example to: (i) investigate experimentally the hypothesis that some of the orphan family genes could be involved in acid stress response(s) and/or membrane remodeling, (ii) explore further the concept that the orphan family genes have played a role in the evolution of the *Acidithiobacilli* from neutral ancestors to modern day extreme acidophiles, and (iii) use additional tools to investigate the phylogeny of *A. ferrooxidans* BY0502 that our study suggests is more likely to be a *Ferriphilus*-like microorganism.

FUTURE PERSPECTIVES

As more data become available from genomic and metagenome sequencing projects, it will be possible to determine if families I–V maintain their ability to be specific

probes for the genus *Acidithiobacillus*. The availability of additional examples of families I–V could advance our understanding of their function, origin and evolutionary trajectory.

AUTHOR CONTRIBUTIONS

DH and JV conceived the project. DH and CG designed the experiments. ML and CG carried out the experiments. All authors analyzed the data. DH drafted the manuscript. All authors contributed to subsequent drafts of the manuscript. All authors read and approved the final manuscript.

ACKNOWLEDGMENTS

Fondecyt 1130683 and Conicyt Basal CCTE PFB16 (DH, CG, and ML), FIDUM OI101002 (JV), CONICYT doctoral fellowship (CG). We thank Dr. Mark Dopson for drawing our attention to the proteomic data for *A. caldus* and the transcriptomic data for *A. ferrivorans*.

SUPPLEMENTARY MATERIAL

The Supplementary Material for this article can be found online at: http://journal.frontiersin.org/article/10.3389/fmicb.2016.02035/full#supplementary-material

REFERENCES

2020 visions (2010). *Nature* 463, 26–32. doi: 10.1038/463026a

Acuña, L. G., Cárdenas, J. P., Covarrubias, P. C., Haristoy, J. J., Flores, R., Nunez, H., et al. (2013). Architecture and gene repertoire of the flexible genome of the extreme acidophile *Acidithiobacillus caldus*. *PLoS ONE* 8:e78237. doi: 10.1371/journal.pone.0078237

Altschul, S. F., Madden, T. L., Schäffer, A. A., Zhang, J., Zhang, Z., Miller, W., et al. (1997). Gapped BLAST and PSI-BLAST: a new generation of protein database search programs. *Nucleic Acids Res.* 25, 3389–3402. doi: 10.1093/nar/25.17.3389

Anantharaman, K., Duhaime, M. B., Breier, J. A., Wendt, K. A., Toner, B. M., and Dick, G. J. (2014). Sulfur oxidation genes in diverse deep-sea viruses. *Science* 344, 757–760. doi: 10.1126/science.1252229

Aziz, R. K., Bartels, D., Best, A. A., DeJongh, M., Disz, T., Edwards, R. A., et al. (2008). The RAST server: rapid annotations using subsystems technology. *BMC Genomics* 9:75. doi: 10.1186/1471-2164-9-75

Bagos, P. G., Nikolaou, E. P., Liakopoulos, T. D., and Tsirigos, K. D. (2010). Combined prediction of Tat and Sec signal peptides with hidden Markov models. *Bioinformatics* 26, 2811–2817. doi: 10.1093/bioinformatics/btq530

Baker-Austin, C., and Dopson, M. (2007). Life in acid: pH homeostasis in acidophiles. *Trends Microbiol.* 15, 165–171. doi: 10.1016/j.tim.2007.02.005

Barrie Johnson, D., and Quatrini, R. (2016). "Acidophile microbiology in space and tim," in *Acidophile Life in Extremely Acidic Environment,* eds R. Quatrini and D. Barrie Johnson (Norfolk, VA: Caister Academic Press), 3–16.

Bertin, P. N., Heinrich-Salmeron, A., Pelletier, E., Goulhen-Chollet, F., Arsène-Ploetze, F., Gallien, S., et al. (2011). Metabolic diversity among main microorganisms inside an arsenic-rich ecosystem revealed by meta- and proteo-genomics. *ISME J.* 5, 1735–1747. doi: 10.1038/ismej.2011.51

Bjellqvist, B., Hughes, G. J., Pasquali, C., Paquet, N., Ravier, F., Sanchez, J. C., et al. (1993). The focusing positions of polypeptides in immobilized pH gradients can be predicted from their amino acid sequences. *Electrophoresis* 14, 1023–1031. doi: 10.1002/elps.11501401163

Brettin, T., Davis, J. J., Disz, T., Edwards, R. A., Gerdes, S., Olsen, G. J., et al. (2015). RASTtk: a modular and extensible implementation of the RAST algorithm for building custom annotation pipelines and annotating batches of genomes. *Sci. Rep.* 5:8365. doi: 10.1038/srep08365

Cárdenas, J. P., Quatrini, R., and Holmes, D. S. (2016a). Genomic and metagenomic challenges and opportunities for bioleaching: a mini-review. *Res. Microbiol.* 167, 529–538. doi: 10.1016/j.resmic.2016.06.007

Cárdenas, J. P., Quatrini, R., and Holmes, D. S. (2016b). "The Genomics of Acidophile," in *Acidophile Life in Extremely Acidic Environment,* eds R. Quatrini and D. B. Johnson (Norfolk, VA: Caister Academic Press), 179–197.

Carver, T., Thomson, N., Bleasby, A., Berriman, M., and Parkhill, J. (2009). DNAPlotter: circular and linear interactive genome visualization. *Bioinformatics* 25, 119–120. doi: 10.1093/bioinformatics/btn578

Charif, D., and Lobry, J. R. (2007). "A Contributed package to the R Project for statistical computing devoted to biological sequences retrieval and analysi," in *Structural Approaches to Sequence Evolution,* eds U. Bastoll, M. Port, H. E. Roma, and M. Vendruscolo (Berlin; Heidelberg: Springer), 207–232.

Chen, L. X., Hu, M., Huang, L. N., Hua, Z. S., Kuang, J. L., Li, S. J., et al. (2015). Comparative metagenomic and metatranscriptomic analyses of microbial communities in acid mine drainage. *ISME J.* 9, 1579–1592. doi: 10.1038/ismej.2014.245

Christel, S., Fridlund, J., Buetti-Dinh, A., Buck, M., Watkin, E. L., and Dopson, M. (2016a). RNA transcript sequencing reveals inorganic sulfur compound oxidation pathways in the acidophile *Acidithiobacillus* ferrivorans. *FEMS Microbiol. Lett.* 363:fnw057. doi: 10.1093/femsle/fnw057

Christel, S., Fridlund, J., Watkin, E. L., and Dopson, M. (2016b). *Acidithiobacillus ferrivorans* SS3 presents little RNA transcript response related to cold shock during growth at 8°C suggesting it is a eurypsychrophile. *Extremophiles* 20, 903–913. doi: 10.1007/s00792-016-0882-2

Cole, J. R., Wang, Q., Cardenas, E., Fish, J., Chai, B., Farris, R. J., et al. (2009). The Ribosomal Database Project: improved alignments and new tools for rRNA analysis. *Nucleic Acids Res.* 37(Suppl. 1), D141–D145. doi: 10.1093/nar/gkn879

Consortium, T. U. (2014). Activities at the Universal Protein Resource (UniProt). *Nucleic Acids Res.* 42, D191–D198. doi: 10.1093/nar/gkt1140

Cuneo, M. J., Beese, L. S., and Hellinga, H. W. (2008). Ligand-induced conformational changes in a thermophilic ribose-binding protein. *BMC Struct. Biol.* 8:50. doi: 10.1186/1472-6807-8-50

Darling, A. E., Jospin, G., Lowe, E., Matsen, F. A. IV., Bi, H. M., and Eisen, J. A. (2014). PhyloSift: phylogenetic analysis of genomes and metagenomes. *PeerJ.* 2:e243. doi: 10.7717/peerj.243

Darling, A. E., Mau, B., and Perna, N. T. (2010). Progressivemauve: multiple genome alignment with gene gai loss and rearrangement. *PLoS ONE* 5:e11147. doi: 10.1371/journal.pone.0011147

Darriba, D., Taboada, G. L., Doallo, R., and Posada, D. (2012). jModelTest 2: more model new heuristics and parallel computing. *Nat. Methods* 9, 772. doi: 10.1038/nmeth.2109

DeSantis, T. Z., Hugenholtz, P., Larsen, N., Rojas, M., Brodie, E. L., Keller, K., et al. (2006). Greengene a chimera-checked 16S rRNA gene database and workbench compatible with ARB. *Appl. Environ. Microbiol.* 72, 5069–5072. doi: 10.1128/AEM.03006-05

Dhillon, B. K., Laird, M. R., Shay, J. A., Winsor, G. L., Lo, R., Nizam, F., et al. (2015). IslandViewer 3: more flexibl interactive genomic island discover visualization and analysis. *Nucleic Acids Res.* 43, W104–W108. doi: 10.1093/nar/gkv401

Dwyer, M. A., and Hellinga, H. W. (2004). Periplasmic binding proteins: a versatile superfamily for protein engineering. *Curr. Opin. Struct. Biol.* 14, 495–504. doi: 10.1016/j.sbi.2004.07.004

Eddy, S. R. (1998). Profile hidden Markov models. *Bioinformatics* 14, 755–763. doi: 10.1093/bioinformatics/14.9.755

Edgar, R. C. (2004). MUSCLE: multiple sequence alignment with high accuracy and high throughput. *Nucleic Acids Res.* 32, 1792–1797. doi: 10.1093/nar/gkh340

Edwards, R. A., Rodriguez-Brito, B., Wegley, L., Haynes, M., Breitbart, M., Peterson, D. M., et al. (2006). Using pyrosequencing to shed light on

deep mine microbial ecology. *BMC Genomics* 7:57. doi: 10.1186/1471-2164-7-57

Eisen, J. A., Heidelberg, J. F., White, O., and Salzberg, S. L. (2000). Evidence for symmetric chromosomal inversions around the replication origin in bacteria. *Genome Biol.* 1:RESEARCH0011. doi: 10.1186/gb-2000-1-6-research0011

Fabrice, A., and Didier, R. (2009). Exploring Microbial Diversity Using 16S rRNA High-Throughput Methods. *J. Comput. Sci. Syst. Biol.* 2, 074–092. doi: 10.4172/jcsb.1000019

Fischer, D., and Eisenberg, D. (1999). Finding families for genomic ORFans. *Bioinformatics* 15, 759–762. doi: 10.1093/bioinformatics/15.9.759

Gasteiger, E., Hoogland, C., Gattiker, A., Duvaud, S., Wilkins, M. R., Appel, R. D., et al. (2005). "Protein identification and analysis tools on the ExPASy Serve" in *The Proteomics Protocols Handbook*, eds J. M. Walke and N. J. Totowa (New York, NY: Humana Press), 571–607.

Goris, J., Konstantinidis, K. T., Klappenbach, J. A., Coenye, T., Vandamme, P., and Tiedje, J. M. (2007). DNA-DNA hybridization values and their relationship to whole-genome sequence similarities. *Int. J. Syst. Evol. Microbiol.* 57, 81–91. doi: 10.1099/ijs.0.64483-0

Guindon, S., Dufayard, J.-F, Lefort, V., Anisimova, M., Hordijk, W., and Gascuel, O. (2010). New algorithms and methods to estimate maximum-likelihood phylogenies: assessing the performance of PhyML 3.0. *Syst. Biol.* 59, 307–321. doi: 10.1093/sysbio/syq010

Guindon, S., and Gascuel, O. (2003). A simple, fast and accurate algorithm to estimate large phylogenies by maximum likelihood. *Syst. Biol.* 52, 696–704. doi: 10.1080/10635150390235520

Guzman, L. M., Barondess, J. J., and Beckwith, J. (1992). Fts an essential cytoplasmic membrane protein involved in cell division in *Escherichia coli*. *J. Bacteriol.* 174, 7716–7728. doi: 10.1128/jb.174.23.7717.1992

Haft, D. H., Selengut, J. D., and White, O. (2003). The TIGRFAMs database of protein families. *Nucleic Acids Res.* 31, 371–373. doi: 10.1093/nar/gkg128

Hedrich, S. S. A. (2016). "Distribution of acidophilic microorganisms in natural and man-made acidic environment" in *Acidophile Life in Extremely Acidic Environment*, ed R. J. D. B. Quatrini (Norfolk, VA: Caister Academic Press), 153–176.

Hiraoka, S., Yang, C. C., and Iwasaki, W. (2016). Metagenomics and bioinformatics in microbial ecology: current status and beyond. *Microbes Environ.* 31, 204–212. doi: 10.1264/jsme2.ME16024

Hofmann, K., and Stoffel, W. (1993). TMbase - A database of membrane spanning proteins segments. *Biol Chem Hoppe-Seyler.* 374.

Hudson, C. M., Williams, K. P., and Kelly, D. P. (2014). Definitive assignment by multigenome analysis of the gammaproteobacterial genus Thermithiobacillus to the class Acidithiobacillia. *Pol. J. Microbiol.* 63, 245–247.

Huelsenbeck, J. P., and Ronquist, F. (2001). MRBAYES: Bayesian inference of phylogenetic trees. *Bioinformatics* 17, 754–755. doi: 10.1093/bioinformatics/17.8.754

Jiang, X., Sobetzko, P., Nasser, W., Reverchon, S., and Muskhelishvili, G. (2015). Chromosomal "stress-response" domains govern the spatiotemporal expression of the bacterial virulence program. *Mbio* 6, e00353–e00315. doi: 10.1128/mBio.00353-15

Jones, D. S., Albrecht, H. L., Dawson, K. S., Schaperdoth, I., Freeman, K. H., Pi, Y., et al. (2012). Community genomic analysis of an extremely acidophilic sulfur-oxidizing biofilm. *ISME J.* 6, 158–170. doi: 10.1038/ismej.2011.75

Jones, D. S., Schaperdoth, I., and Macalady, J. L. (2016). Biogeography of sulfur-oxidizing Acidithiobacillus populations in extremely acidic cave biofilms. *ISME J.* 10, 2879–2891. doi: 10.1038/ismej.2016.74

Juncker, A. S., Willenbrock, H., Von Heijne, G., Brunak, S., Nielsen, H., and Krogh, A. (2003). Prediction of lipoprotein signal peptides in Gram-negative bacteria. *Protein Sci.* 12, 1652–1662. doi: 10.1110/ps.0303703

Jungbluth, S. P., Grote, J., Lin, H. T., Cowen, J. P., and Rappé, M. S. (2013). Microbial diversity within basement fluids of the sediment-buried Juan de Fuca Ridge flank. *ISME J.* 7, 161–172. doi: 10.1038/ismej.2012.73

Katoh, K., Kuma, K., Toh, H., and Miyata, T. (2005). MAFFT version 5: improvement in accuracy of multiple sequence alignment. *Nucleic Acids Res.* 33, 511–518. doi: 10.1093/nar/gki198

Katoh, K., Misawa, K., Kuma, K. Ä., and Miyata, T. (2002). MAFFT: a novel method for rapid multiple sequence alignment based on fast Fourier transform. *Nucleic Acids Res.* 30, 3059–3066. doi: 10.1093/nar/gkf436

Kelly, D. P., and Wood, A. P. (2000). Reclassification of some species of Thiobacillus to the newly designated genera Acidithiobacillus gen. nov., Halothiobacillus gen. nov. and Thermithiobacillus gen. nov. *Int. J. Syst. Evol. Microbiol.* 50(Pt 2), 511–516. doi: 10.1099/00207713-50-2-511

Khedkar, S., and Seshasayee, A. S. (2016). Comparative genomics of interreplichore translocations in bacteria: a measure of chromosome topology? *G3 (Bethesda)* 6, 1597–1606. doi: 10.1534/g3.116.028274

Kim, M., Lee, K. H., Yoon, S. W., Kim, B. S., Chun, J., and Yi, H. (2013). Analytical tools and databases for metagenomics in the next-generation sequencing era. *Genomics Inform.* 11, 102–113. doi: 10.5808/GI.2013.11.3.102

Klasberg, S., Bitard-Feildel, T., and Mallet, L. (2016). Computational identification of novel genes: current and future perspectives. *Bioinform. Biol. Insights* 10, 121–131. doi: 10.4137/BBI.S39950

Krogh, A., Larsson, B., von Heijne, G., and Sonnhammer, E. L. (2001). Predicting transmembrane protein topology with a hidden markov model: application to complete genomes. *J. Mol. Biol.* 305, 567–580. doi: 10.1006/jmbi.2000.4315

Li, M., Jain, S., and Dick, G. J. (2016). Genomic and transcriptomic resolution of organic matter utilization among deep-sea bacteria in guaymas basin hydrothermal plumes. *Front. Microbiol.* 7:1125. doi: 10.3389/fmicb.2016.01125

Liljeqvist, M., Ossandon, F. J., Gonzalez, C., Rajan, S., Stell, A., Valdes, J., et al. (2015). Metagenomic analysis reveals adaptations to a cold adapted lifestyle in a low temperature acid mine drainage stream. *FEMS Microbiol. Ecol.* 91:fiv011. doi: 10.1093/femsec/fiv011

Liljeqvist, M., Valdes, J., Holmes, D. S., and Dopson, M. (2011). Draft genome of the psychrotolerant acidophile *Acidithiobacillus ferrivorans* SS3. *J. Bacteriol.* 193, 4304–4305. doi: 10.1128/JB.05373-11

Liu, B., Gibbons, T., Ghodsi, M., Treangen, T., and Pop, M. (2011). Accurate and fast estimation of taxonomic profiles from metagenomic shotgun sequences. *BMC Genomics.* 12(Suppl. 2):S4. doi: 10.1186/1471-2164-12-S2-S4

Long, M., Betran, E., Thornton, K., and Wang, W. (2003). The origin of new genes: glimpses from the young and old. *Nat. Rev. Genet.* 4, 865–875. doi: 10.1038/nrg1204

MacLean, D., Jones, J. D., and Studholme, D. J. (2009). Application of 'next-generation' sequencing technologies to microbial genetics. *Nat. Rev. Microbiol.* 7, 287–296. doi: 10.1038/nrmicro2122

Mangold, S., Rao Jonna, V., and Dopson, M. (2013). Response of *Acidithiobacillus caldus* toward suboptimal pH conditions. *Extremophiles* 17, 689–696. doi: 10.1007/s00792-013-0553-5

Markowitz, V. M., Chen, I. M., Chu, K., Szeto, E., Palaniappan, K., Pillay, M., et al. (2014a). IMG/M 4 version of the integrated metagenome comparative analysis system. *Nucleic Acids Res.* 42, D568–D573. doi: 10.1093/nar/gkt919

Markowitz, V. M., Chen, I. M., Palaniappan, K., Chu, K., Szeto, E., Pillay, M., Ratner, A., et al. (2014b). IMG 4 version of the integrated microbial genomes comparative analysis system. *Nucleic Acids Res.* 42, D560–D567. doi: 10.1093/nar/gkt963

Méndez-García, C., Peláez, A. I., Mesa, V., Sánchez, J., Golyshina, O. V., and Ferrer, M. (2015). Microbial diversity and metabolic networks in acid mine drainage habitats. *Front. Microbiol.* 6:475. doi: 10.3389/fmicb.2015.00475

Meyer, F., Paarmann, D., D'Souza, M., Olson, R., Glass, E. M., Kubal, M., et al. (2008). The metagenomics RAST server - a public resource for the automatic phylogenetic and functional analysis of metagenomes. *BMC Bioinformatics* 9:386. doi: 10.1186/1471-2105-9-386

Nakai, K., and Horton, P. (1999). PSORT: a program for detecting sorting signals in proteins and predicting their subcellular localization. *Trends Biochem. Sci.* 24, 34–35. doi: 10.1016/S0968-0004(98)01336-X

Natale, P., Brüser, T., and Driessen, A. J. (2008). Sec- and Tat-mediated protein secretion across the bacterial cytoplasmic membranÄiDistinct translocases and mechanisms. *Biochim. Biophys. Acta* 1778, 1735–1756. doi: 10.1016/j.bbamem.2007.07.015

Nieto, P. A., Covarrubias, P. C., Jedlicki, E., Holmes, D. S., and Quatrini, R. (2009). Selection and evaluation of reference genes for improved interrogation of microbial transcriptomes: case study with the extremophile *Acidithiobacillus ferrooxidans*. *BMC Mol. Biol.* 10:63. doi: 10.1186/1471-2199-10-63

Nordberg, H., Cantor, M., Dusheyko, S., Hua, S., Poliakov, A., Shabalov, I., et al. (2014). The genome portal of the Department of Energy

Joint Genome Institute: 2014 updates. *Nucleic Acids Res.* 42, D26–D31. doi: 10.1093/nar/gkt1069

Nuñez, H., Covarrubias, P. C., Moya-Beltrán, A., Issotta, F., Atavales, J., Acuna, L. G., et al. (2016). Detectio identification and typing of Acidithiobacillus species and strains: a review. *Res. Microbiol.* 167, 555–567. doi: 10.1016/j.resmic.2016.05.006

Nuñez, H., Loyola, D., Cárdenas, J. P., Holmes, D. S., Johnson, D. B., and Quatrini, R. (2014). Multi locus sequence typing scheme for *Acidithiobacillus caldus* strain evaluation and differentiation. *Res. Microbiol.* 165, 735–742. doi: 10.1016/j.resmic.2014.07.014

Osorio, H., Mangold, S., Denis, Y., Ñancucheo, I., Esparza, M., Johnson, D. B., et al. (2013). Anaerobic sulfur metabolism coupled to dissimilatory iron reduction in the extremophile *Acidithiobacillus ferrooxidans*. *Appl. Environ. Microbiol.* 79, 2172–2181. doi: 10.1128/AEM.03057-12

Overbeek, R., Olson, R., Pusch, G. D., Olsen, G. J., Davis, J. J., Disz, T., et al. (2014). The SEED and the Rapid Annotation of microbial genomes using Subsystems Technology (RAST). *Nucleic Acids Res.* 42, D206–D214. doi: 10.1093/nar/gkt1226

Pedroso, I., Rivera, G., Lazo, F., Chacón, M., Ossandon, F., Veloso, F. A., et al. (2008). AlterORF: a database of alternate open reading frames. *Nucleic Acids Res.* 36, D517–D518. doi: 10.1093/nar/gkm886

Pizzagalli, F., Varga, Z., Huber, R. D., Folkers, G., Meier, P. J., and St-Pierre, M. V. (2003). Identification of steroid sulfate transport processes in the human mammary gland. *J. Clin. Endocrinol. Metab.* 88, 3902–3912. doi: 10.1210/jc.2003-030174

Prabh, N., and Rodelsperger, C. (2016). Are orphan genes protein-codin prediction artifact or non-coding RNAs? *BMC Bioinformatics* 17:226. doi: 10.1186/s12859-016-1102-x

Pruesse, E., Quast, C., Knittel, K., Fuchs, B. M., Ludwig, W., Peplies, J., et al. (2007). SILVA: a comprehensive online resource for quality checked and aligned ribosomal RNA sequence data compatible with ARB. *Nucleic Acids Res.* 35, 7188–7196. doi: 10.1093/nar/gkm864

Punta, M., Coggill, P. C., Eberhardt, R. Y., Mistry, J., Tate, J., Boursnell, C., et al. (2012). The Pfam protein families database. *Nucleic Acids Res.* 40, D290–D301. doi: 10.1093/nar/gkr1065

Riadi, G., Medina-Moenne, C., and Holmes, D. S. (2012). TnpPred: a web service for the robust prediction of prokaryotic transposases. *Comp. Funct. Genomics.* 2012:678761. doi: 10.1155/2012/678761

Richter, M., and Rosselló-Móra, R. (2009). Shifting the genomic gold standard for the prokaryotic species definition. *Proc. Natl. Acad. Sci. U.S.A.* 106, 19126–19131. doi: 10.1073/pnas.0906412106

Rocha, E. P. (2004). The replication-related organization of bacterial genomes. *Microbiology* 150, 1609–1627. doi: 10.1099/mic.0.26974-0

Ronquist, F., and Huelsenbeck, J. P. (2003). MrBayes 3: Bayesian phylogenetic inference under mixed models. *Bioinformatics* 19, 1572–1574. doi: 10.1093/bioinformatics/btg180

Rutherford, K., Parkhill, J., Crook, J., Horsnell, T., Rice, P., Rajandream, M. A., et al. (2000). Artemis: sequence visualization and annotation. *Bioinformatics* 16, 944–945. doi: 10.1093/bioinformatics/16.10.944

Sabir, J. S., Jansen, R. K., Arasappan, D., Calderon, V., Noutahi, E., Zheng, C., et al. (2016). The nuclear genome of *Rhazya stricta* and the evolution of alkaloid diversity in a medically relevant clade of Apocynaceae. *Sci. Rep.* 6:33782. doi: 10.1038/srep33782

Segata, N., Izard, J., Waldron, L., Gevers, D., Miropolsky, L., Garrett, W. S., et al. (2011). Metagenomic biomarker discovery and explanation. *Genome Biol.* 12:R60. doi: 10.1186/gb-2011-12-6-r60

Sheik, C. S., Anantharaman, K., Breier, J. A., Sylvan, J. B., Edwards, K. J., and Dick, G. J. (2015). Spatially resolved sampling reveals dynamic microbial communities in rising hydrothermal plumes across a back-arc basin. *ISME J.* 9, 1434–1445. doi: 10.1038/ismej.2014.228

Singer, E., Heidelberg, J. F., Dhillon, A., and Edwards, K. J. (2013). Metagenomic insights into the dominant Fe(II) oxidizing Zetaproteobacteria from an iron mat at Lo ih Hawai l. *Front. Microbiol.* 4:52. doi: 10.3389/fmicb.2013.00052

Sobetzko, P., Travers, A., and Muskhelishvili, G. (2012). Gene order and chromosome dynamics coordinate spatiotemporal gene expression during the bacterial growth cycle. *Proc. Natl. Acad. Sci. U.S.A.* 109, E42–E50. doi: 10.1073/pnas.1108229109

Suyama, M., Torrents, D., and Bork, P. (2006). PAL2NAL: robust conversion of protein sequence alignments into the corresponding codon alignments. *Nucleic Acids Res.* 34(Suppl. 2), W609–W612. doi: 10.1093/nar/gkl315

Talla, E., Hedrich, S., Mangenot, S., Ji, B., Johnson, D. B., Barbe, V., et al. (2014). Insights into the pathways of iron- and sulfur-oxidatio and biofilm formation from the chemolithotrophic acidophile *Acidithiobacillus ferrivorans* CF27. *Res. Microbiol.* 165, 753–760. doi: 10.1016/j.resmic.2014.08.002

Tautz, D., and Domazet-Loso, T. (2011). The evolutionary origin of orphan genes. *Nat. Rev. Genet.* 12, 692–702. doi: 10.1038/nrg3053

Travisany, D., Cortés, M. P., Latorre, M., Di Genova, A., Budinich, M., Bobadilla-Fazzini, R. A., et al. (2014). A new genome of *Acidithiobacillus thiooxidans* provides insights into adaptation to a bioleaching environment. *Res. Microbiol.* 165, 743–752. doi: 10.1016/j.resmic.2014.08.004

Tyson, G. W., Chapman, J., Hugenholtz, P., Allen, E. E., Ram, R. J., Richardson, P. M., et al. (2004). Community structure and metabolism through reconstruction of microbial genomes from the environment. *Nature* 428, 37–43. doi: 10.1038/nature02340

Valdés, J., Ossandon, F., Quatrini, R., Dopson, M., and Holmes, D. S. (2011). Draft genome sequence of the extremely acidophilic biomining bacterium Acidithiobacillus thiooxidans ATCC 19377 provides insights into the evolution of the Acidithiobacillus genus. *J. Bacteriol.* 193, 7003–7004. doi: 10.1128/JB.06281-11

Valdés, J., Pedroso, I., Quatrini, R., Dodson, R. J., Tettelin, H., Blake, R., et al. (2008). *Acidithiobacillus ferrooxidans* metabolism: from genome sequence to industrial applications. *BMC Genomics* 9:597. doi: 10.1186/1471-2164-9-597

Valdes, J., Quatrini, R., Hallberg, K., Dopson, M., Valenzuela, P. D., and Holmes, D. S. (2009). Draft genome sequence of the extremely *Acidophilic Bacterium Acidithiobacillus caldus* ATCC 51756 reveals metabolic versatility in the genus Acidithiobacillus. *J. Bacteriol.* 191, 5877–5878. doi: 10.1128/JB.00843-09

Williams, K. P., and Kelly D. P. (2013). Proposal for a new class within the phylum Proteobacteri Acidithiobacillia classis nov., with the type order Acidithiobacillale and emended description of the class Gammaproteobacteria. *Int. J. Syst. Evol. Microbiol.* 63(Pt 8), 2901–2906. doi: 10.1099/ijs.0.049270-0

Wood, A. P., and Kelly, D. P. (1985). Physiological characteristics of a new thermophilic obligately chemolithotrophic Thiobacillus Species *Thiobacillus tepidarius*. *Int. J. Syst. Bacteriol.* 35, 434–437. doi: 10.1099/00207713-35-4-434

Wu, D., Jospin, G., and Eisen, J. A. (2013). Systematic identification of gene families for use as "markers" for phylogenetic and phylogeny-driven ecological studies of bacteria and archaea and their major subgroups. *PLoS ONE* 8:e77033. doi: 10.1371/journal.pone.0077033

Wu, D., Wu, M., Halpern, A., Rusch, D. B., Yooseph, S., Frazier, M., et al. (2011). Stalking the fourth domain in metagenomic data: searching fo discoverin and interpreting nove deep branches in marker gene phylogenetic trees. *PLoS ONE* 6:e18011. doi: 10.1371/journal.pone.0018011

Wu, M., and Eisen J. A. (2008). A simpl fas and accurate method of phylogenomic inference. *Genome Biol.* 9:R151. doi: 10.1186/gb-2008-9-10-r151

Wu, M., and Scott A. J. (2012). Phylogenomic analysis of bacterial and archaeal sequences with AMPHORA2. *Bioinformatics* 28, 1033–1034. doi: 10.1093/bioinformatics/bts079

Yan, L., Zhang, S., Wang, W., Hu, H., Wang, Y., Yu, G., et al. (2015). Draft genome sequence of *Acidithiobacillus ferrooxidans* YQH-1. *Genom Data* 6, 269–270. doi: 10.1016/j.gdata.2015.10.009

Yin, H., Zhang, X., Liang, Y., Xiao, Y., Niu, J., and Li X. (2014). Draft Genome sequence of the extremophile *Acidithiobacillus thiooxidans* A01, isolated from the wastewater of a coal dump. *Genome Announc.* 2:e00222-14. doi: 10.1128/genomeA.00222-14

You, X. Y., Guo, X., Zheng, H. J., Zhang, M. J., Liu, L. J., Zhu, Y. Q., et al. (2011). Unraveling the *Acidithiobacillus caldus* complete genome and its central metabolisms for carbon assimilation. *J. Genet. Genomics* 38, 243–252. doi: 10.1016/j.jgg.2011.04.006

Yu, C. S., Che, Y. C., Lu, C. H., and Hwan, J. K. (2006). Prediction of protein subcellular localization. *Proteins* 64, 643–651. doi: 10.1002/prot.21018

Yu, C. S., Li, C. J., and Hwan, J. K. (2004). Predicting subcellular localization of proteins for Gram-negative bacteria by support vector machines based

on n-peptide compositions. *Protein Sci.* 13, 1402–1406. doi: 10.1110/ps.03479604

Yu, N. Y., Wagner, J. R., Laird, M. R., Melli, G., Rey, S., Lo, R., et al. (2010). PSORTb 3.0: improved protein subcellular localization prediction with refined localization subcategories and predictive capabilities for all prokaryotes. *Bioinformatics* 26, 1608–1615. doi: 10.1093/bioinformatics/btq249

Zhang, X., Feng, X., Tao, J., Ma, L., Xiao, Y., Liang, Y., et al. (2016). Comparative genomics of the extreme acidophile *Acidithiobacillus thiooxidans* reveals intraspecific divergence and niche adaptation. *Int. J. Mol. Sci.* 17:1355. doi: 10.3390/ijms17081355

Conflict of Interest Statement: The authors declare that the research was conducted in the absence of any commercial or financial relationships that could be construed as a potential conflict of interest.

frontiers in Microbiology

ORIGINAL RESEARCH
published: 14 September 2016
doi: 10.3389/fmicb.2016.01365

Insights into the Quorum Sensing Regulon of the Acidophilic *Acidithiobacillus ferrooxidans* Revealed by Transcriptomic in the Presence of an Acyl Homoserine Lactone Superagonist Analog

Sigde Mamani[1,2], Danielle Moinier[1], Yann Denis[3], Laurent Soulère[4], Yves Queneau[4], Emmanuel Talla[1], Violaine Bonnefoy[1]† and Nicolas Guiliani[2]*†*

[1] Laboratoire de Chimie Bactérienne, Institut de Microbiologie de la Méditerranée, Aix Marseille Université, Centre National de la Recherche Scientifique, Marseille, France, [2] Laboratorio de Comunicación Bacteriana, Departamento de Biología, Facultad de Ciencias, Universitad de Chile, Santiago, Chile, [3] Plateforme Transcriptome, Institut de Microbiologie de la Méditerranée, Aix Marseille Université, Centre National de la Recherche Scientifique, Marseille, France, [4] Université Lyon, Institut National des Sciences Appliquées de Lyon, UMR 5246, Centre National de la Recherche Scientifique, Université Lyon 1, École Supérieure de Chimie Physique Electronique de Lyon, Institut de Chimie et de Biochimie Moléculaires et Supramoléculaires, Villeurbanne, France

While a functional quorum sensing system has been identified in the acidophilic chemolithoautotrophic *Acidithiobacillus ferrooxidans* ATCC 23270^T and shown to modulate cell adhesion to solid substrates, nothing is known about the genes it regulates. To address the question of how quorum sensing controls biofilm formation in *A. ferrooxidans*^{T}, the transcriptome of this organism in conditions in which quorum sensing response is stimulated by a synthetic superagonist AHL (N-acyl homoserine lactones) analog has been studied. First, the effect on biofilm formation of a synthetic AHL tetrazolic analog, tetrazole **9c,** known for its agonistic QS activity, was assessed by fluorescence and electron microscopy. A fast adherence of *A. ferrooxidans*^{T} cells on sulfur coupons was observed. Then, tetrazole **9c** was used in DNA microarray experiments that allowed the identification of genes regulated by quorum sensing signaling, and more particularly, those involved in early biofilm formation. Interestingly, *afeI* gene, encoding the AHL synthase, but not the *A. ferrooxidans* quorum sensing transcriptional regulator AfeR encoding gene, was shown to be regulated by quorum sensing. Data indicated that quorum sensing network represents at least 4.5% (141 genes) of the ATCC 23270^T genome of which 42.5% (60 genes) are related to biofilm formation. Finally, AfeR was shown to bind specifically to the regulatory region of the *afeI* gene at the level of the palindromic sequence predicted to be the AfeR binding site. Our results give new insights on the response of *A. ferrooxidans* to quorum sensing and on biofilm biogenesis.

Keywords: quorum sensing regulon, acyl homoserine lactone, superagonist, extracellular polymeric substances, biofilm, transcriptomic, *Acidithiobacillus ferrooxidans*, acidophile

OPEN ACCESS

Edited by:
Axel Schippers, Federal Institute for Geosciences and Natural Resources, Germany

Reviewed by:
Jeannette Marrero-Coto, Leibniz University of Hanover, Germany
Soeren Bellenberg, University of Duisburg, Germany

***Correspondence:**
Violaine Bonnefoy
bonnefoy@imm.cnrs.fr
Nicolas Guiliani
nguilian@uchile.cl

† These authors have contributed equally to this work.

Specialty section:
This article was submitted to Extreme Microbiology, a section of the journal Frontiers in Microbiology

Received: *30 June 2016*
Accepted: *17 August 2016*
Published: *14 September 2016*

Citation:
Mamani S, Moinier D, Denis Y, Soulère L, Queneau Y, Talla E, Bonnefoy V and Guiliani N (2016) Insights into the Quorum Sensing Regulon of the Acidophilic Acidithiobacillus ferrooxidans Revealed by Transcriptomic in the Presence of an Acyl Homoserine Lactone Superagonist Analog. Front. Microbiol. 7:1365. doi: 10.3389/fmicb.2016.01365

INTRODUCTION

Due to its low operating cost, biomining is a very successful geobiotechnology that actually produces approximately 15 per cent of the world's extracted copper (Johnson, 2014). Withstanding low pH and high heavy metal concentrations, *Acidithiobacillus* species are acidophilic key players in biomining industry recovering valuable metals from sulfidic ores such as copper or gold (Jerez, 2009). However, these bacteria are also involved in Acid Mine/Rock Drainage (AM/RD), which represents a worldwide problem of water pollution, from natural and anthropogenic environments (Johnson, 2009, 2012). Indeed, several studies recently indicated that *Acidithiobacillus* species play a pivotal and structural role in acidophilic communities ranging from 6°C to 90°C (Chen et al., 2015; Liljeqvist et al., 2015; Menzel et al., 2015). Nevertheless, due to an insufficient understanding of the microbiological processes, most biohydrometallurgical plants operate far from maximum efficiency and natural AM/RD are to a large extent uncontrolled.

Acidithiobacillia has been recently defined as a new class of *Proteobacteria* in which the genus *Acidithiobacillus* is the main one characterized (Williams and Kelly, 2013). Actually, the genus *Acidithiobacillus* encompasses seven closely related Gram-negative, chemolithoautotrophic bioleaching species: (i) *Acidithiobacillus thiooxidans*, *A. caldus,* and *A. albertensis*, which oxidize only reduced inorganic sulfur compounds (RISC) and (ii) *A ferrooxidans, A. ferrivorans*, *A. ferridurans,* and *A. ferriphilus* that oxidize both ferrous iron and RISC (Amouric et al., 2011; Hedrich and Johnson, 2013; Williams and Kelly, 2013; Falagan and Johnson, 2015). It has been well established that all *Acidithiobacillus* species are able to form biofilms on the surface of ores. This bacterial attachment on the mineral has been reported to increase metal leaching due to the formation of a close and enlarged "reaction space" between the metal sulfide surface and the cell (Pogliani and Donati, 1999; Harneit et al., 2006; Rohwerder and Sand, 2007). Therefore, deciphering molecular mechanisms underlying biofilm formation in acidophilic leaching bacteria has been early pointed out as an important field of investigation.

Quorum sensing (QS) and the secondary messenger c-di-GMP signaling pathway [for recent reviews see (Hengge, 2009; Decho et al., 2011; Kalia et al., 2013; Romling et al., 2013; Hengge et al., 2015)] are the most studied mechanisms controlling biofilm development in bacteria. Both pathways have been shown to be linked in several bacterial species (Ryan et al., 2006; Waters et al., 2008; Ueda and Wood, 2009; Zhang, 2010; Kozlova et al., 2011) and to control more particularly polysaccharide production and biofilm formation (Ueda and Wood, 2009). QS is an important mechanism for the timing of collective behaviors through the regulation of population density-dependent cellular processes, such as the production of virulence factors, motility, exopolysaccharide production and biofilm formation (Parsek and Greenberg, 2005; Waters and Bassler, 2005; Ng and Bassler, 2009). In Gram-negative bacteria, the main characterized QS system involves three key molecular elements (Venturi and Subramoni, 2009): (i) N-acyl homoserine lactones (AHLs), which act as autoinducers (AIs); (ii) the AHLs synthase encoded by a *luxI*-like gene; (iii) a transcriptional regulator, which is encoded by a *luxR*-like gene and which binds AHL molecules and modulates the expression of different target genes that constitute the QS regulon. Depending on the bacterial species and also on the experimental strategies (transcriptomic or proteomic), the size of the QS regulons oscillates between 3 and 8% of the identified ORFs (Vasil, 2003; Wagner et al., 2003; Cantero et al., 2006; Qin et al., 2007; Stevens et al., 2011; Majerczyk et al., 2014).

Even if several reports related to biofilm formation regulation by acidophilic bacteria belonging to *Acidithiobacillus* genus have been released recently (Farah et al., 2005; Bellenberg et al., 2012, 2014; Ruiz et al., 2012; Diaz et al., 2013; Montgomery et al., 2013; Vera et al., 2013; Castro et al., 2015), the molecular cascade involved in exopolysaccharide production and biofilm formation by *Acidithiobacillus* species is still undeciphered. While c-di-GMP pathway has been identified in all *Acidithiobacillus* spp. (Ruiz et al., 2012; Diaz et al., 2013; Castro et al., 2015), the species that oxidize only RISC do not possess the genes related to canonical QS systems (Valdés et al., 2008). Indeed, a functional QS system has been reported only in the iron/RISC-oxidizing species *A. ferrooxidans* (Farah et al., 2005; Rivas et al., 2005; Valenzuela et al., 2007). In addition, it has been recently reported that the RISC-oxidizing species *A. thiooxidans* cannot adhere to pyrite if this mineral is not previously colonized by an iron-oxidizing species (Bellenberg et al., 2014) pointing out *A. ferrooxidans* as a key player for mineral colonization.

Acidithiobacillus ferrooxidans ATCC 23270^T QS system involves two divergent genes *afeI* and *afeR* coding for the AHL synthase and the transcriptional regulator, respectively (Farah et al., 2005). AfeR has the conserved amino acid residues located in the active site of LuxR-protein family and possesses the canonical AHL and DNA binding domains based on a 3D-structural model (Soulere et al., 2008). In *A. ferrooxidans* ATCC 23270^T, nine different AHL molecules are synthesized with medium or large acyl side chains (Valenzuela et al., 2007). In this strain, transcription of *afeI* is increased under the physiological conditions that promote biofilm formation, such as growth in the presence of sulfur (solid energetic substrate) or in low phosphate medium (Farah et al., 2005), suggesting a role of QS system in the attachment of *A. ferrooxidans* to ores (e.g., pyrite). In agreement with this hypothesis, addition of synthetic AHL that are AIs naturally synthesized by *A. ferrooxidans* such as C14-AHL and 3-hydroxy-C14-AHL has been shown to enhance *A. ferrooxidans* ATCC 23270^T cell adhesion, exopolysaccharide production and biofilm development on elemental sulfur and pyrite (Ruiz et al., 2008; Gonzalez et al., 2013).

However, to date this phenotypic result is still uncoupled with genotypic data that will allow the understanding of the molecular chain reaction going from the AHL-sensing by AfeR to ore colonization. A bioinformatics analysis has recently allowed the identification of a putative QS regulon in *A. ferrooxidans* ATCC 23270^T that encompasses 75 possible AfeR target-genes, including genes likely involved in polysaccharide biosynthesis (Banderas and Guiliani, 2013). However, biological data are

required to fully identify the *A. ferrooxidans* genes whose expression is modulated by AHL signaling.

Here, we report the first biological study focused on deciphering the QS regulon of *A. ferrooxidans* ATCC 23270^T. The effects of AI 3-hydroxy-C14-AHL and of tetrazolic AHL-analog **9c**, on *A. ferrooxidans* adhesion to sulfur were first compared by fluorescence and scanning electronic microscopy. Then, DNA microarray experiments were performed to compare total RNA of *A. ferrooxidans* ATCC 23270^T cells induced or not by tetrazole **9c**. These allowed the identification of 141 genes from which at least 48 can be linked with QS pathway, exopolysaccharide production and biofilm development. If we include the genes encoding hypothetical proteins that colocalized and are coregulated with these 48 genes, this number would increase to 60 and represents 1.9% of the ATCC 23270^T genome.

MATERIALS AND METHODS

Bacterial Strains, Plasmids, and Growth Conditions

Acidithiobacillus ferrooxidans ATCC 23270^T was used throughout this study. *Escherichia coli* TG1 [(*supE*, *hsd*Δ5, *thi*, Δ (*lac-proAB*), F':*traD36*, *proAB*$^+$, *lacI*^{q}, *lacZ*ΔM15) was used for plasmid propagation. Rosetta (DE3)/pLysS strain (F^- *ompT hsd*S_B(r_B^- m_B^-) *gal dcm* λ [DE3 (*lacI lacUV5*-T7 gene *1 ind1 sam7 nin5*)] pLysSRARE (Cam^R)] and the pET21 plasmid from Novagen were used to produce the recombinant AfeR with a hexahistidine tag fused to its C terminus (AfeR-Histag).

Acidithiobacillus ferrooxidans was grown at 30°C under oxic conditions in modified 9K medium [(0.1 g L^{-1} $(NH_4)_2SO_4$, 0.4 g L^{-1} $MgSO_4 \cdot 7H_2O$; 0.04 g L^{-1} K_2HPO_4, pH 2,5] with sulfur (S^0) coupons (0.5 cm^2 obtained by S^0 fusion) for fluorescence and electron microscopy or 200 g L^{-1} S^0 prills for real-time PCR or microarrays analysis (Amaro et al., 1991) in the presence (5 μM) or the absence of the AHL analogs. The ferrous iron [Fe(II)] growth conditions were described in (Yarzabal et al., 2003). *E. coli* strains were usually grown at 37°C under oxic conditions in Luria-Bertani broth (LB) supplemented with 100 μg ml^{-1} ampicillin and 34 μg ml^{-1} chloramphenicol when necessary (Ausubel et al., 1998).

Synthesis of AHL-Signaling Molecules

Due to its high agonistic effect reported on *Vibrio fischeri* QS system (Sabbah et al., 2012), the tetrazolic AHL analog (tetrazole **9c**; **Supplementary Figure S1**) was selected to test its biological activity on biofilm formation by *A. ferrooxidans*. It was synthesized according to the protocol described by Sabbah et al. (2012). Briefly, this synthesis was achieved from racemic α-amino-γ-butyrolactone hydrobromide that was acylated with heptanoyl chloride. The intermediate was then cyclized with sodium azide (Biot et al., 2004) to afford tetrazole **9c** (**Supplementary Figure S1**). *A. ferrooxidans* natural AI 3-hydroxy-C14-AHL was also obtained by chemical synthesis according to the protocol described previously (Chhabra et al., 2003).

Cell Adhesion Assays on Sulfur Coupons and Microscopy Visualizations

Experimental procedures have been previously described (Gonzalez et al., 2013). *A. ferrooxidans* was grown at 30°C in modified 9K medium (Ruiz et al., 2012) at pH 2.5 with 5% (wt/vol) sulfur (S^0) prills. To assess adhesion levels, sterilized S^0 coupons were initially added to cell cultures. S^0 coupons were daily extracted from day 1 (lag phase) to day 7 (end of the exponential phase) and adhered cells were fixed. Staining was performed with fluorochrome Syto9 for epifluorescence microscopy observations. Epifluorescence visualizations of stained coupons were performed by using fluorescence microscope (ZEISS Axiovert 200 M) equipped with a filter set 10 (FITC, emission BP 515–565) and 20 (Rhodamine, emission BP 575–640) and a digital microscope camera (Axiocam ZEISS). For scanning electronic microscopy (SEM) visualizations, S^0 coupons colonized by *A. ferrooxidans* cells were submitted to critical point drying to avoid cell shrinking and damage. Then, dried samples were coated with a thin conductive film of gold and analyzed with a scanning electron microscope (HITACHI TM 3000, Japan) at the Pontificia Universidad Católica de Chile.

General DNA Manipulations

Genomic DNA from *A. ferrooxidans* was prepared with the NucleoSpin Tissue kit (Macherey Nagel). Plasmid DNA was obtained using a Wizard Plus SV DNA purification system from Promega. DNA digestions with restriction enzymes and ligation with T4 DNA ligase were performed according to New England BioLabs' recommendations. Primers (Sigma) used in this study are described in Supplementary Table S1. For routine PCR, Go *Taq* polymerase (Promega) was used. For *afeR* cloning, PCR amplifications were carried out with Platinum *Taq* polymerase (Invitrogen) on genomic DNA. DNA products were analyzed on an 1% agarose gel, then concentrated and purified using Amicon® Ultra-0.5 centrifugal filter units (Millipore). Recombinant plasmids were introduced into *E. coli* competent cells as previously described (Chung and Miller, 1988).

Nucleotide sequence of the amplified DNA was determined by GATC Biotech (Germany).

RNA Manipulations

To get reproducible results, the following experimental growth protocol was performed. The starting inoculum was obtained by growing 1×10^7 cells on 150 ml Fe (II) medium for 3 days. From this culture, 1×10^7 cells were washed three times with basal salts to remove iron traces and inoculated in 250 ml 9K modified medium containing 200 g L^{-1} S^0 prills for 5–6 days (adaptation step). This culture was used to inoculate the same medium (400 ml) for 4 days (pre-inoculum step). This step was repeated in larger volumes in the presence of superagonist AHL analog (adding 5 μM tetrazole **9c**) and in its absence (adding DMSO which is the tetrazole **9c** solvent) and the cultures were grown for 2, 3, and 4 days.

The cultures were centrifuged at low speed (1,000 rpm, 5 min) to recover S^0 prills. Planktonic cells were harvested from the supernatant by centrifugation and washed several times with acid

water (pH 1.5) to remove S^0. To get sessile cells, the collected S^0 prills were washed several times with acid water to remove the remaining planktonic cells. Then, S^0 prills were incubated for 5 min in acid water with 0.04% Triton X-100. They were vortexed every min and then, sonicated every 4 sec for 2 min at 4°C to recover adhered cells. S^0 prills were removed by low speed centrifugation (1,000 rpm, 5 min). Sessile cells, harvested by centrifugation from the supernatant, were washed three times with acid water to remove Triton X-100.

Acidithiobacillus. ferrooxidans total RNA was extracted from planktonic and sessile cells by using a modified acid-phenol extraction method (Aiba et al., 1981) according to Quatrini et al. (2006, 2009). The modifications included a preliminary TRIZOL® reagent (Invitrogen) extraction step, a final purification step with the High Pure RNA isolation kit (Roche Applied Biosystem) and DNAse I treatments [twice with the DNAse I provided in the kit and once with the reagents from a Turbo DNA-free kit (Applied Biosystems)]. The lack of DNA contamination was checked by PCR on each RNA sample. The RNA integrity was controlled on an agarose gel.

Quantitative Real-Time PCR

The relative expression levels of the *afeI*, *afeR*, *zwf*, AFE_0233, and AFE_1339 genes were compared to that of the 16S rRNA *rrs* gene used as a reference standard by quantitative real-time PCR. RNAs were extracted from planktonic cells grown on S^0 prills after 2, 3, and 4 days of growth and from sessile cells after 3 days of growth on sulfur prills, as described below. The real-time PCR analysis was performed on a CFX96 real-time PCR detection system with the C1000^{TM} thermal cycler (BioRad) with the "SsoFast EvaGreen Supermix 2X" kit (Bio-Rad) following the manufacturer's instructions and as described in (Slyemi et al., 2013). The results were analyzed with the Bio-Rad CFX Manager Software 3.0. The real-time quantitative PCR experiments were performed on RNA extracted from at least three independent cultures and duplicated for each RNA preparation with the oligonucleotides listed in Supplementary Table S1. The calculated threshold cycle (Ct) for each gene was normalized to the Ct of the *rrs* gene. The results are expressed in arbitrary units.

Microarray Construction: Oligonucleotide Design and Arraying

The complete genome (gene annotations and sequences) of *A. ferrooxidans* ATCC 23270^T chromosome was downloaded from the NCBI ftp site[1]. The *OliD* program (Talla et al., 2003) was used to design oligonucleotide probe sequences matching defined criteria. An effort was placed to design oligonucleotide probes of similar lengths, with the aim to reduce cross-hybridization between related sequences. Most oligonucleotides are 55 nt long with predicted melting temperatures between 80–100°C in standard hybridization buffer (G + C contents between 30 and 70%). Oligonucleotides were selected such as to avoid self-complementary structures at 65–70°C, and cross-hybridization with the rest of the genome, and were positioned less than 1500 bp upstream of the stop codon of the CDS. The program successfully designed specific oligonucleotide probes for 3044 protein encoding genes, representing 96.7% of the total number of genes. Due to the high similarity with other sequenced regions of the ATCC 23270^T genome, 103 genes (3.3%) failed to be represented by a specific oligonucleotide probe. When possible, each gene was represented by two distinct oligonucleotide probes separated by a minimum of 100 nucleotides. A total of 6294 probes from 3147 genes were thus designed. The probes were spotted twice on slides using the Agilent technology[2]. The array design, the experimental design, and the data for all hybridizations are available in Array Express database under accession numbers A-MTAB-592 and E-MTAB-4896.

Transcriptome Assay

Twelve independent hybridizations using total RNA obtained from three different cultures grown without or with 5 μM of tetrazole **9c** were performed on Agilent microarrays. Total RNA was used for the synthesis of cDNA fluorescent labeled with Cy®3 and Cy®5 as previously described (Quatrini et al., 2006, 2009). Microarray hybridizations were performed at 42°C for 16 h in a microarray hybridization chamber (Agilent G2534A) following the manufacturer's instruction. Slides were washed in washing buffer serial dilutions. Arrays were scanned for the Cy®3 and Cy®5 fluorescent signals using an Axion 4400A scanner (Molecular Devices). The data were analyzed with the image quantification software package GenePix Pro 6.0 (Axon Instruments, Inc.) as previously described (Quatrini et al., 2006, 2009). Each gene expression ratio was calculated from 12 values calculated from three biological and four technical replicates and normalized using Acuity 4.0 package (Molecular Devices). Only the four best hybridizations (in term of reproducibility) out of the six were taken into account. Genes with weak expression (median intensity <250) were discarded. A onefold deviation from the 1:1 hybridization ($\log_2$) ratio (corresponding to twofold change) was taken as indicative of differential gene expression in the conditions analyzed. The values of one Sample *t*-test – Benjamini–Hochberg (Adv) $\leq$0.05 (corresponding to 95% confidence) for at least one oligonucleotide were considered statistically significant. Only the genes filling the conditions described above were analyzed. Hierarchical cluster analysis (Pearson correlation, average linkage) was performed using Genesis software suit (Peterson et al., 2001).

Bioinformatic Analysis

Bioinformatic analyses were performed with the tools available in the MaGe annotation platform[3] (Vallenet et al., 2013).

General Biochemical Procedures

The protein concentration was determined by the modified Bradford method (Bio-Rad protein assay). The purity of the preparation was checked by 12.5% SDS-PAGE stained with Coomassie blue and by immunodetection with antibodies directed against the hexa-histidine tag using a SuperSignal West

[1] ftp://ftp.ncbi.nlm.nih.gov/

[2] http://www.agilent.com/home

[3] https://www.genoscope.cns.fr/agc/microscope/home/

Hisprobe kit (Thermo Scientific) following the manufacturer's instructions.

Cloning and Overexpression of *afeR*

To produce wild-type AfeR fused to a hexa-histidine tag at the C-terminus, the DNA fragment corresponding to the AfeR peptide was amplified by PCR with the AFERC1 and AFERC2 oligonucleotides (Supplementary Table S1). The amplified product was digested with *Hin*dIII and *Xho*I and cloned into pET21 to give pET21-AfeR-Histag plasmid. Cloning was done in *E. coli* TG1 strain. The construction was checked by nucleotide sequencing with the petT7 and T7ter oligonucleotides (Supplementary Table S1). The recombinant plasmid was then introduced into *E. coli* Rosetta (DE3)/pLysS strain.

The Rosetta (DE3)/pLysS strain carrying pET21-AfeR-Histag was grown at 37°C with 100 μg ml^{-1} ampicillin and 34 μg ml^{-1} chloramphenicol to an OD_{600} of 0.6. Ampicillin (100 μg ml^{-1}) and 3-hydroxy-C14-AHL (Gonzalez et al., 2013) to a final concentration of 1 μM were then added. Cells were grown 30 min at 30°C. At this stage, 0.4 mM IPTG was added and the culture was grown for a further 3 h at 30°C. The cells were harvested by centrifugation and stored at −80°C until use.

Production of His-Tagged Recombinant AfeR Protein

To lyse the cells, the cell pellet previously resuspended in lysis solution [50 mM Tris-HCl pH 7.4, 300 mM NaCl, 5 mM imidazole, 2% Tween-20, 1 mM phenylmethylsulfonyl fluoride (PMSF), 0.1 mg ml^{-1} DNase, 0.1 mg ml^{-1} lysosyme, and 5 μM 3-hydroxy-C14-AHL] was incubated 30 min at 4°C with gentle shaking and then sonicated. Inclusion bodies, unbroken cells, and cellular debris were removed by centrifugation at 13,000 rpm for 30 min at 4°C. The pellet was dissolved with 4 M urea in 40 mM sodium phosphate pH 7.4, 300 mM NaCl, 1 mM PMSF, 5 μM 3-hydroxy-C14-AHL, and 0.1 mg ml^{-1} DNase, kept on ice for 30 min with gentle stirring, and then centrifuged at 13,000 rpm for 20 min at 4°C. The supernatant, corresponding to the solubilized inclusion bodies, was filtered through a 0.45 μm membrane before loading onto a cobalt column (HisTrap™ Talon®; GE Healthcare) according to the manufacturer's instructions. The fractions were eluted with 5, 50, 150, 250, and 500 mM imidazole, in 40 mM sodium phosphate pH 7.4, 300 mM NaCl, 1 mM PMSF, 4 M urea, and 25 μM 3-hydroxy-C14-AHL buffer. The 150 mM fractions containing the recombinant AfeR-His tag was dialysed with decreasing urea concentrations (2 M, 0.5 M, 0 M) in 50 mM HEPES pH 8, 150 mM NaCl, 10 mM DTT, and 5 μM 3-hydroxy-C14-AHL. These fractions were kept at 4°C until use.

Electrophoretic Mobility Shift Assays (EMSA)

DNA substrates for band shift assays were produced by PCR amplification with PrimeSTAR Max DNA Polymerase (Clontech) using 5′ Cy5-labeled reverse oligonucleotide (Sigma; Supplementary Table S1). The Cy5 labeled DNA (2.3 ng) was incubated in a total volume of 10 μl with increasing concentrations of the enriched recombinant AfeR-Histag preparation as indicated in the Figure. The binding reaction contained 20 mM Tris-HCl pH 8, 50 mM KCl, 1 mM DTT, 0.05 % Nonidet P40, 1 mM EDTA, 10 % glycerol, 5 μM 3-hydroxy-C14-AHL, 30 ng μl^{-1} herring sperm, and bovine serum albumin 100 μg ml^{-1}. After 30 min at room temperature, the reaction mixtures were separated by electrophoresis on a 6% native polyacrylamide gel previously prerun 5 min and run for 1–2 h more in 25 mM Tris-HCl pH 8.3, 0.19 M glycine, 1 mM EDTA, 200 μM spermidine at 30 mA at 4°C. The gel was then scanned using a 635 nm laser and a LPR filter (FLA5100, Fujifilm).

RESULTS AND DISCUSSION

To develop biological strategies for improving biomining activities and preventing environmental damages caused by AM/RD, it is well documented that mineral colonization by acidophilic bacteria such as *Acidithiobacillus* species is a key step to decipher (Rohwerder and Sand, 2007). If synthesis of specific exopolysaccharides rich in α-mannopyranosyl and α-glucopyranosyl sugar residues has been revealed by fluorescently labeled lectin Concanavalin A within 1 day for EPS (extracellular polymeric substances)-deficient ferrous-iron grown cells after transfer to cultures with pyrite as sole nutrient (Bellenberg et al., 2014), a clear understanding of the molecular cascade involved in exopolysaccharide production and biofilm formation by *Acidithiobacillus* species is actually missing. However, as a molecular relationship between QS and cell adhesion has been clearly established in *A. ferrooxidans* (Gonzalez et al., 2013) and it has to be pointed out that the canonical QS systems are missing in *Acidithiobacillus* species that can oxidize only RISC (Valdés et al., 2008), the iron-oxidizing species such as *A. ferrooxidans* as primary colonizers are now considered fundamental players for mineral colonization by the bioleaching community. Therefore, to address the question of how *A. ferrooxidans* regulates the physiological processes involved in cell adhesion, EPS production and biofilm formation, we focused on the deciphering of the QS molecular network by using a synthetic QS-activator molecule and DNA array technology.

The Tetrazolic AHL Analog 9c Accelerates Cellular Adhesion of *Acidithiobacillus ferrooxidans* on Sulfur Coupons

To further investigate the molecular mechanisms underlying this pathway, we first challenged the identification of synthetic AHL analogs capable to induce better *A. ferrooxidans* cell adhesion than natural AIs previously tested (Gonzalez et al., 2013). Thus, a tetrazolic derivative that displays a much higher affinity to the LuxR protein than the natural AI and acts as a superagonist of AHL signaling molecules (Sabbah et al., 2012) was tested. Its effect on biofilm formation by *A. ferrooxidans* was compared to the natural AI 3-hydroxy-C14-AHL (**Figure 1**). Growth curves revealed that both tetrazolic

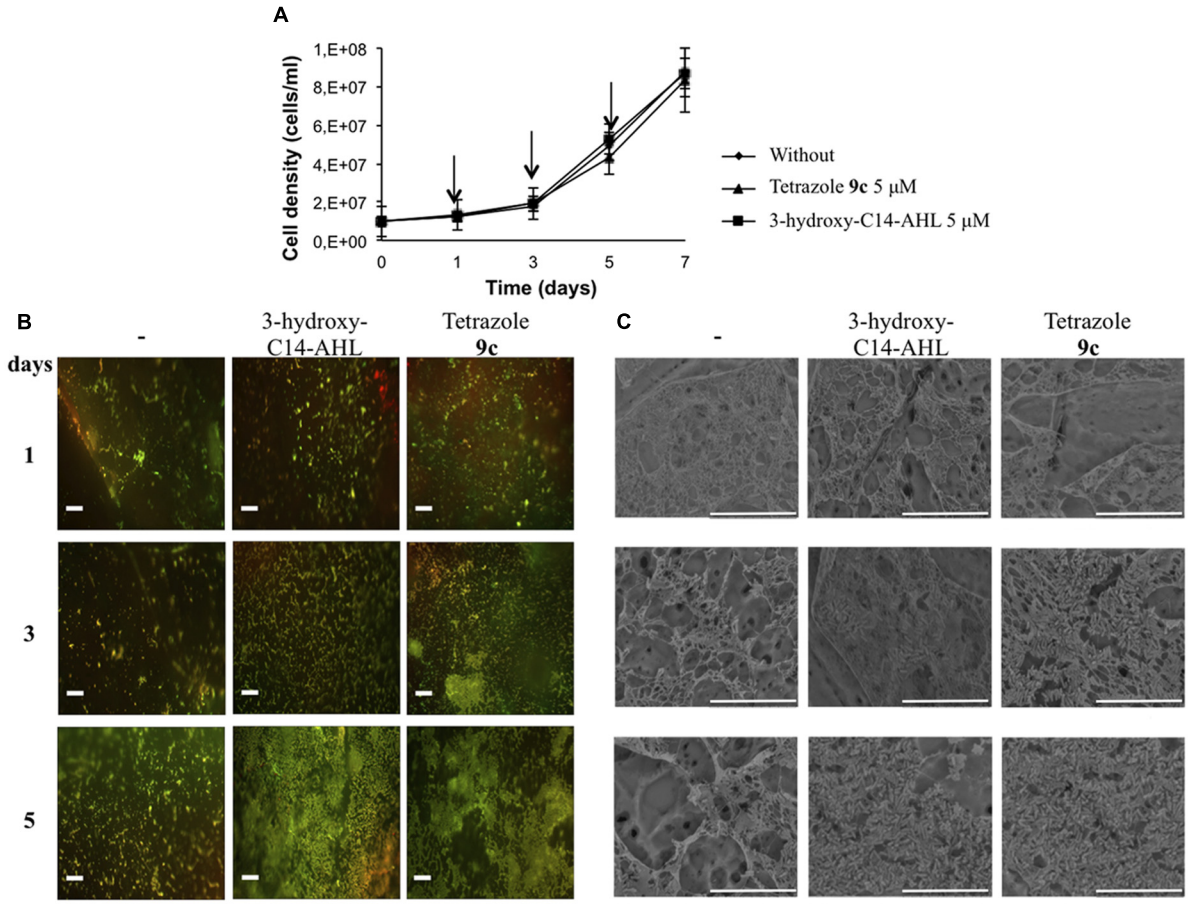

FIGURE 1 | Effect of tetrazole 9c on biofilm formation. **(A)** Growth curves in the absence or the presence of 5 μM 3-hydroxy-C14-AHL or tetrazole **9c**. Arrows indicate when aliquots were sampled for microscopy analysis. **(B)** Fluorescence microscopy of sulfur coupons after 1, 3, or 5 days of *Acidithiobacillus ferrooxidans* ATCC 23270^T cells grown in the absence (-) or the presence of 5 μM 3-hydroxy-C14-AHL or tetrazole **9c**. Cells were stained with fluochrome Syto9. **(C)** Electron microscopy of sulfur coupons treated as above. White bars represent 20 μm.

AHL analog and 3-hydroxy-C14-AHL have no effect on *A. ferrooxidans* growth compared to the control in the absence of exogenous AHL (**Figure 1A**). Fluorescence (**Figure 1B**) and SEM (**Figure 1C**) clearly indicated that tetrazole **9c** also promoted cell adhesion. Moreover, confirming in the *A. ferrooxidans* model the superagonistic behavior of tetrazole **9c** previously found in *V. fisheri* (Sabbah et al., 2012), the results obtained on day 3 strongly suggest that tetrazole **9c** is biologically more efficient than the natural AI 3-hydroxy-C14-AHL in promoting biofilm formation (**Figure 1C**).

The QS System is Triggered after 3 days in the Presence of the Tetrazolic AHL Analog 9c in Planktonic Cells

The results presented in **Figure 1** suggest that QS was triggered by 5 μM tetrazole **9c** between 2 and 3 days of growth versus 4–5 days in the absence of this AHL analog. To assess whether the tetrazole **9c** indeed switched on QS system by inducing the transcription of the genes known to be involved in QS response (Farah et al., 2005), i.e. *afeI* (AFE_1999) and *afeR* (AFE_1997), the transcription of these genes was analyzed by quantitative real-time PCR after 2, 3, and 4 days of growth in the presence or the absence of 5μM tetrazole **9c**. The results indicated that *afeR* expression was constitutively expressed under the conditions analyzed, while *afeI* was induced by tetrazole **9c** from the third day of growth in planktonic cells (**Table 1**).

Biofilm formation after 3 days was strongly enhanced in cells treated with 5 μM tetrazole **9c** compared to cells from control experiments without agonist (**Figure 1**). Therefore, expression of some genes predicted to be linked to EPS biosynthesis [*zwf* (AFE_2025), AFE_0233, and AFE_1339] was also monitored in planktonic (**Table 1**) and sessile (Supplementary Table S2) cells after 3 days of growth with 5 μM tetrazole **9c**. The gene *zwf* encodes glucose-6-phosphate 1-dehydrogenase that is involved in the intracellular levels of glucose-6P, a precursor of the EPS. AFE_0233 encodes a glycosyl transferase and is located in a gene cluster predicted to encode cell wall constituents (polysaccharides, and lipopolysaccharides). AFE_1339 encodes the putative polysaccharide export protein Wza and is located

TABLE 1 | Quantitative real-time PCR expression data for *afeI, afeR, zwf*, AFE_0233 (glycosyl transferase), and AFE_1339 (putative polysaccharide export protein) genes from *Acidithiobacillus ferrooxidans* ATCC 23270^T planktonic cells grown with sulfur prills in the presence or the absence of 5 μM tetrazole 9c after 2, 3, and 4 days of growth.

Gene or locus name	Growth condition	Day of growth	Gene mRNA/*rrs* ± *SD*[a]
afeI (AFE_1999)	DMSO	2	1 ± 0
	Tetrazole **9c**	2	1.69 ± 0.15
	DMSO	3	4.49 ± 0.58
	Tetrazole **9c**	3	12.75 ± 1.66
	DMSO	4	5.19 ± 6.95
	Tetrazole **9c**	4	49.35 ± 5.72
afeR (AFE_1997)	DMSO	2	1 ± 0
	Tetrazole **9c**	2	1.58 ± 0.19
	DMSO	3	1.59 ± 0.19
	Tetrazole **9c**	3	1.21 ± 0.08
	DMSO	4	1.64 ± 0.11
	Tetrazole **9c**	4	1.78 ± 0.21
zwf (AFE_2025)	DMSO	2	1 ± 0
	Tetrazole **9c**	2	1.43 ± 0.12
	DMSO	3	2.70 ± 1.11
	Tetrazole **9c**	3	1.66 ± 0.16
	DMSO	4	2.82 ± 0.32
	Tetrazole **9c**	4	3.90 ± 0.58
AFE_0233	DMSO	2	1 ± 0
	Tetrazole **9c**	2	1.04 ± 0.01
	DMSO	3	1.13 ± 0.13
	Tetrazole **9c**	3	1.00 ± 0.13
	DMSO	4	1.14 ± 0.17
	Tetrazole **9c**	4	0.91 ± 0.02
AFE_1339	DMSO	2	1 ± 0
	Tetrazole **9c**	2	1.72 ± 0.02
	DMSO	3	1.58 ± 0.32
	Tetrazole **9c**	3	1.62 ± 0.32
	DMSO	4	1.56 ± 0.11
	Tetrazole **9c**	4	1.69 ± 0.12

[a]*Values were related to those obtained after 2 days of growth in the absence of tetrazole* ***9c****.*

close to the *gal* operon proposed to be involved in the formation of EPS in iron-grown cells (Barreto et al., 2005). Besides, AfeR-AHL binding sites were predicted in the regulatory region of *zwf*, AFE_0233, and AFE_1339 (Banderas and Guiliani, 2013). Surprisingly, tetrazole **9c** had no effect on AFE_0233, AFE_1339 and *zwf* transcription and only the expression of the *afeI* gene was induced by tetrazole **9c** (**Table 1**; Supplementary Table S2). These data indicate that *afeI*, and not *afeR*, is regulated by QS and suggest either that *zwf*, AFE_0233, and AFE_1339 genes were not regulated by AfeR or that their expression was induced later during biofilm biogenesis.

QS Regulon in *Acidithiobacillus ferrooxidans* Cells

Quorum sensing response and biofilm formation were obvious within 3 days of growth in the presence of the tetrazolic AHL analog **9c** (**Figure 1**; **Table 1**). Consequently, total RNAs from planktonic and sessile cells of *A. ferrooxidans* ATCC 23270^T were isolated from 3-days cultures in the presence or the absence of the superagonist AHL analog **9c**. They were used to probe gene expression using microarrays displaying two specific oligonucleotides for each gene of this bacterium (3147 predicted genes). Only the genes filling the conditions described in the Materials and Methods section were analyzed. It has to be pointed out that the microarray and quantitative real-time PCR data agreed with the constitutive expression of *afeR*, *zwf*, AFE_0233, and AFE_1339 genes under the conditions tested (**Table 1**; Supplementary Tables S2–S4).

In planktonic cells, a total of 133 genes were differentially expressed, 34 induced and 99 repressed by tetrazole **9c** (Supplementary Table S3). In sessile cells under the same conditions, only eight genes presented significant differences in expression, four induced and four repressed by tetrazole **9c** (Supplementary Table S4). Therefore, 141 genes were QS regulated, which represent 4.5% of the total number of *A. ferrooxidans* gene analyzed in this study (see Materials and Methods). These genes were grouped according to their COG classification. Their percentage relative to all the *A. ferrooxidans* ATCC 23270^T genes present in the same COG class is given in **Table 2**. In planktonic cells, mainly the genes involved in inorganic ion transport and metabolism (4.86%), and nucleotide transport and metabolism (3.39%) were induced in the presence of tetrazole **9c**. Mainly those involved in carbohydrate transport and metabolism (11.11%), posttranslational modification, protein turnover, chaperones (8.27%), energy production and conversion (5.76%), cell motility (3.70%), and transcription (2.92%) as well as poorly characterized proteins (11%) were repressed by this AHL analog. In sessile cells, mainly induction by tetrazole **9c** of secondary metabolites biosynthesis, transport and catabolism (1.61%), and signal transduction mechanisms (1.15%) was observed while repression was detected for energy production and conversion genes (1.05%). Only the genes differentially expressed in cells that were cultivated with or without the tetrazolic AHL analog and which have known or reliable predicted function are presented in **Table 3** for the planktonic cells and in **Table 4** for the sessile cells and are discussed below.

Genes Differentially Expressed in the Presence of Tetrazole 9c in Planktonic Cells

In planktonic cells, tetrazole **9c** modified the expression of a number of genes related to biofilm formation, few being induced and several repressed. Among the induced genes, those involved in inorganic ion transport and energy conversion were mainly found. Not surprisingly, genes involved in the transport of phosphate [*pstS* (AFE_1939) and *pstC* (AFE_1940)] and ammonium [*glnK* (AFE_2915) and *amt* (AFE_2916)] were upregulated. The phosphate specific transport (Pst) system is known to be important in biofilm formation in a number of bacteria [see (O'May et al., 2009; Heindl et al., 2014) and references therein] including *Leptospirillum ferrooxidans* (Moreno-Paz et al., 2010) and *A. ferrooxidans* (Vera et al., 2013),

TABLE 2 | COG classification of the genes differentially expressed in planktonic and sessile cells grown with (+) and without (–) tetrazole 9c.

Process	COG functional categories	COG class	Planktonic cells[a,b]		Sessile cells[a,b]	
			+	–	+	–
Cellular processes and signaling	Cell cycle control, cell division, chromosome partitioning	D	0.00%	0.00%	0.00%	0.00%
	Cell wall/membrane/envelope biogenesis	M	0.93%	0.93%	0.00%	0.00%
	Cell motility	N	0.00%	**3.70%**	0.00%	0.00%
	Posttranslational modification, protein turnover, chaperones	O	0.00%	**8.27%**	**0.75%**	0.00%
	Signal transduction mechanisms	T	0.00%	**1.15%**	**1.15%**	0.00%
	Intracellular trafficking, secretion, and vesicular transport	U	**1.89%**	0.94%	0.00%	0.00%
	Defense mechanisms	V	0.00%	0.00%	0.00%	0.00%
	Extracellular structures	W	0.00%	0.00%	0.00%	0.00%
Information storage and processing	RNA processing and modification	A	0.00%	0.00%	0.00%	0.00%
	Chromatin structure and dynamics	B	0.00%	0.00%	0.00%	0.00%
	Translation, ribosomal structure, and biogenesis	J	**1.89%**	0.00%	0.00%	0.00%
	Transcription	K	0.00%	**2.92%**	0.00%	0.00%
	Replication, recombination, and repair	L	0.00%	**1.35%**	0.00%	0.00%
Metabolism	Energy production and conversion	C	2.09%	**5.76%**	0.00%	**1.05%**
	Amino acid transport and metabolism	E	1.01%	1.52%	0.00%	0.00%
	Nucleotide transport and metabolism	F	**3.39%**	0.00%	0.00%	0.00%
	Carbohydrate transport and metabolism	G	1.59%	**11.11%**	0.00%	0.00%
	Coenzyme transport and metabolism	H	0.00%	**1.74%**	0.00%	0.00%
	Lipid transport and metabolism	I	0.00%	**1.41%**	0.00%	0.00%
	Inorganic ion transport and metabolism	P	**4.86%**	1.62%	0.54%	0.54%
	Secondary metabolites biosynthesis, transport, and catabolism	Q	0.00%	**1.61%**	**1.61%**	0.00%
Poorly characterized	General function prediction only	R	0.31%	**4.97%**	**0.62%**	0.31%
	Function unknown	S	0.00%	**6.03%**	0.00%	0.00%

[a]*The numbers represent the percentage relative to all the A. ferrooxidans ATCC 23270*^{T} *genes present in this COG class.* [b]*Bold numbers are discussed in the text.*

in which phosphate metabolism was early linked to QS regulatory pathway (Farah et al., 2005). Deep cDNA sequencing experiments also revealed that several genes related to ammonium metabolism (*amt-1*, *amt-2,* and *glnK-1*) were upregulated in *A. ferrooxidans* planktonic cells induced by hydroxyl-C14-AHL compared to not induced (unpublished data). Biofilm formation occurs also in response to the availability of nutrients supplied by the ammonium transporter (AFE_2916) which expression is regulated by GlnK (AFE_2915), as shown recently in *Streptococcus mutans* (Ardin et al., 2014). This might anticipate gradient of inorganic ions within and around microbial biofilm. The other gene class that was induced by tetrazole **9c** in planktonic cells is involved in energy production and conversion, in particular the genes *atpBEF* (AFE_3207–3209) encoding the membrane-embedded proton channel F0 of the ATPase. This upregulation could allow more protons to pass through the ATP synthase complex generating a proton motive force (PMF) rather than ATP. PMF is required not only for early biofilm formation (Saville et al., 2011), but also in influx and efflux involved in QS since PMF inhibition enhances the intracellular accumulation of AHL leading to decrease in biofilm formation (Ikonomidis et al., 2008; Varga et al., 2012). Along the same lines, genes encoding a putative MolA/TolQ/ExbB proton channel family protein (AFE_2273) and TonB family protein (AFE_2275) were upregulated in the presence of the tetrazole **9c** and could contribute to PMF-dependent import through the outer membrane of substrates necessary for QS and/or early EPS synthesis. Another interesting gene that was more expressed in the presence of the tetrazolic AHL analog in planktonic cells is *ndk* (AFE_1929) encoding a nucleoside diphosphate kinase. A *ndk* knockout mutant of *Pseudomonas aeruginosa* was shown to be deficient in polysaccharide synthesis (Kapatral et al., 2000), because it was unable to provide GTP necessary for the incorporation of mannuronate in alginate. It is therefore possible that nucleotide triphosphates are required in an early step of *A. ferrooxidans* EPS biosynthesis.

The genes that were repressed in the presence of the tetrazolic AHL analog in planktonic cells were mainly involved in energy production and conversion, carbohydrate transport and metabolism, posttranslational modification, protein turnover, chaperones, and transcription. Most of the energy production and conversion class genes encoded two out of the four hydrogenases described in *A. ferrooxidans*. One is a group one membrane-bound respiratory enzyme enabling the cell to use H_2 as an energy source [*hynS* (AFE_3283) and *hynL* (AFE_3286)]. The genes encoding this hydrogenase physiological partners [*isp1* (AFE_3284) and *isp2* (AFE_3285)] and biogenesis machinery [*hynD* (AFE_3281), *hynH* (AFE_3282), *hynL* (AFE_3286), *hypA* (AFE_3287), *hypB* (AFE_3288), *hypC* (AFE_3289), and *hypD* (AFE_3290)] were also repressed under this condition. The second hydrogenase is a sulfhydrogenase, a group 3b cytoplasmic hydrogenase [*hoxH* (AFE_0937) and *hoxF* (AFE_0940)], with

TABLE 3 | Microarray expression data for genes with known or predicted function differentially expressed in planktonic cells in the presence of tetrazole 9c.

Oligonucleotides[a]	Gene	Protein description	COG identity: Functional description	COG class	One sample *t*-test (Adv) median (Stats)	One sample *t*-test Benjamini–Hochberg (Adv)[b]
Genes induced by tetrazole 9c						
Inorganic ion transport and metabolism						
AFE_1939_860-914	*pstS*	Phosphate ABC transporter substrate-binding protein	COG0226: ABC-type phosphate transport system, periplasmic component	P	**−1.961**	**2.31E−03**
AFE_1939_990-1044					**−1.098**	**2.20E−02**
AFE_1940_802-856	*pstC*	Phosphate ABC transporter permease	COG0573: ABC-type phosphate transport system, permease component	P	**−1.544**	**3.55E−03**
AFE_1940_902-956 ↓					**−1.424**	**2.49E−03**
AFE_2915_146-200	*glnK*	Nitrogen regulatory protein P-II	COG0347: Nitrogen regulatory protein PII	P	**−2.191**	**4.42E−04**
AFE_2915_29-83					**−2.074**	**4.32E−04**
AFE_2916_1123-1177	*amt*	Ammonium transporter	COG0004: Ammonia permease	P	**−1.642**	**1.02E−03**
AFE_2916_765-819 ↓					**−1.438**	**5.10E−03**
Energy production and conversion						
AFE_2131_1122-1176	*aldA*	Aldehyde dehydrogenase (NAD) family protein	COG1012: NAD-dependent aldehyde dehydrogenases	C	−1.093	**1.63E−02**
AFE_2131_1342-1396					**−0.984**	**1.79E−03**
AFE_3207_413-467 ↑	*atpF*	ATP synthase F0 subunit B	COG0711: F0F1-type ATP synthase, subunit b	C	**−1.082**	**8.45E−03**
AFE_3207_85-139					−0.97	**2.45E−03**
AFE_3208_192-246	*atpE*	ATP synthase F0 subunit C	COG0636: F0F1-type ATP synthase, subunit c/Archaeal/vacuolar-type H^+-ATPase, subunit K	C	**−1.408**	**3.36E−04**
AFE_3208_65-119					−0.939	**9.09E−04**
AFE_3209_429-483	*atpB*	ATP synthase F0 subunit A	COG0356: F0F1-type ATP synthase, subunit a	C	**−1.735**	**3.92E−04**
AFE_3209_530-584					**−1.38**	**1.03E−03**
Translation, ribosomal structure and biogenesis						
AFE_1904_132-186a	*rpmF*	50S ribosomal protein L32	COG0333: Ribosomal protein L32	J	**−1.077**	**6.19E−04**
AFE_1904_132-186b					**−1.058**	**6.19E−04**
AFE_2670_163-217a	*rpmB*	50S ribosomal protein L28	COG0227: Ribosomal protein L28	J	**−1.106**	**9.95E−03**
AFE_2670_163-217b					**−1.124**	**1.15E−02**
Other COG classes						
AFE_1929_175-229	*ndk*	Nucleoside diphosphate kinase	COG0105: Nucleoside diphosphate kinase	F	−0.934	**4.54E−04**
AFE_1929_322-376					**−1.227**	**4.54E−04**
AFE_2273_388-442		Putative MotA/TolQ/ExbB proton channel family protein	COG0811: Biopolymer transport proteins	U	**−1.516**	**5.19E−04**
AFE_2273_553-607					**−1.081**	**5.29E−04**
AFE_2275_252-306		Putative TonB family protein	COG0810: Periplasmic protein TonB, links inner and outer membranes	M	**−1.788**	**2.30E−02**
AFE_2275_675-729 ↓					**−1.674**	**3.05E−04**

(Continued)

TABLE 3 | Continued

Oligonucleotides[a]	Gene	Protein description	COG identity : Functional description	COG class	One sample *t*-test (Adv) median (Stats)	One sample *t*-test Benjamini–Hochberg (Adv)[b]
Genes repressed by tetrazole 9c						
Energy production and conversion						
AFE_0808_719-773 ↑		Oxidoreductase, FAD-binding subunit	COG1319: Aerobic-type carbon monoxide dehydrogenase, middle subunit CoxM/CutM homologs	C	**1.385**	**2.85E−02**
AFE_0808_948-1002					**1.929**	**4.37E−02**
AFE_0809_1969-2023		Oxidoreductase, molybdopterin binding subunit	COG1529: Aerobic-type carbon monoxide dehydrogenase, large subunit CoxL/CutL homologs	C	**1.78**	**2.32E−02**
AFE_0809_2151-2205					**1.092**	**8.41E−04**
AFE_0810_397-451		Oxidoreductase, iron-sulfur binding subunit	COG2080: Aerobic-type carbon monoxide dehydrogenase, small subunit CoxS/CutS homologs	C	**1.433**	**2.92E−02**
AFE_0810_41-95					**1.507**	9.86E−02
AFE_0937_1209-1263 ↑	*hoxH*	[NiFe] hydrogenase subunit alpha	COG3259: Coenzyme F420-reducing hydrogenase, alpha subunit	C	**1.177**	1.82E−01
AFE_0937_768-822					**1.262**	**6.19E−04**
AFE_0940_383-437	*hoxF*	[NiFe] hydrogenase subunit beta	COG1145: Ferredoxin	C	**1.083**	**1.64E−02**
AFE_0940_882-936					**1.587**	1.67E−01
AFE_1854_267-321		Putative FAD-dependent pyridine nucleotide-disulfide oxidoreductase	COG1252: NADH dehydrogenase, FAD-containing subunit	C	**1.349**	**6.47E−04**
AFE_1854_900-954					**1.49**	**2.77E−03**
AFE_3281_134-188 ↑	*hynD*	Hydrogenase maturation protease	COG0680: Ni,Fe-hydrogenase maturation factor	C	**1.539**	**1.83E−02**
AFE_3281_20-74					**2.414**	5.27E−02
AFE_3283_231-285	*hynS*	[Ni/Fe] hydrogenase, small subunit	COG1740: Ni,Fe-hydrogenase I small subunit	C	**1.539**	1.24E−01
AFE_3283_695-749					**1.593**	**4.01E−02**
AFE_3284_219-273	*isp1*	Putative cytochrome *b* subunit of membrane-bound hydrogenase Isp1	COG2181: Nitrate reductase gamma subunit	C	**1.87**	**1.40E−02**
AFE_3284_462-516					**1.747**	**3.96E−02**
AFE_3285_245-299	*isp2*	Putative Isp2 (Iron sulfur protein) of HydSL-type hydrogenase	COG0247: Fe-S oxidoreductase	C	**1.331**	**3.96E−03**
AFE_3285_730-784					**1.486**	**1.83E−02**
AFE_3286_1372-1426	*hynL*	[Ni/Fe] hydrogenase, large subunit	COG0374: [Ni/Fe]-hydrogenase I large subunit	C	**1.586**	**2.48E−03**
AFE_3286_1498-1552					**1.844**	**8.88E−03**
Carbohydrate transport and metabolism						
AFE_0419_495-549	*tal*	Transaldolase	COG0176: Transaldolase	G	**1.1**	**1.27E−02**
AFE_0419_595-649					**1.322**	**2.48E−02**
AFE_1799_2258-2312 ↑		Putative glycogen phosphorylase GlgP	COG0058: Glucan phosphorylase	G	**1.077**	**6.19E−04**
AFE_1799_2377-2431					**1.311**	**2.04E−04**
AFE_1801_1309-1363	*pyk*	Pyruvate kinase	COG0469: Pyruvate kinase	G	**1.297**	**3.89E−03**
AFE_1801_612-666					**2.245**	1.35E−01
AFE_1802_294-348		Putative fructose-bisphosphate aldolase Fba	COG1830: DhnA-type fructose-1,6-bisphosphate aldolase and related enzymes	G	**1.205**	**1.83E−02**
AFE_1802_822-876					**1.124**	**1.86E−03**
AFE_1815_455-509	*gpmI*	Phosphoglyceromutase	COG0696: Phosphoglyceromutase	G	**1.629**	**3.49E−03**
AFE_1815_745-799					0.911	**2.78E−03**

(Continued)

TABLE 3 | Continued

Oligonucleotides[a]	Gene	Protein description	COG identity : Functional description	COG class	One sample *t*-test (Adv) median (Stats)	One sample *t*-test Benjamini–Hochberg (Adv)[b]
AFE_2024_274-328		Putative 6-phosphogluconate dehydrogenase Gnd	COG1023: Predicted 6-phosphogluconate dehydrogenase	G	**1.109**	**1.63E−02**
AFE_2024_515-569					**1.209**	**3.09E−03**
AFE_2082_558-612		Putative malto-oligosyltrehalose trehalohydrolase TreZ	COG0296: alpha-glucan branching enzyme	G	**1.253**	**1.17E−03**
AFE_2082_882-936					**1.597**	**2.22E−02**
AFE_2836_1869-1923	*glgB*	1,4-alpha-glucan-branching protein	COG0296: alpha-glucan branching enzyme	G	**1.018**	1.85E−01
AFE_2836_2041-2095					**1.257**	**4.76E−02**
AFE_3019_176-230	*ptsH*	Phosphocarrier protein HPr	COG1925: Phosphotransferase system, HPr-related proteins	G	**1.451**	5.82E−02
AFE_3019_2-56					**1.335**	**1.00E−02**
Posttranslational modification, protein turnover, chaperones						
AFE_0123_409-463	*gcp*	*O*-sialoglycoprotein endopeptidase	COG0533: Metal-dependent proteases with possible chaperone activity	O	0.711	**6.93E−03**
AFE_0123_848-902					**1.708**	**3.52E−02**
AFE_0871_233-287		Putative heat shock protein, Hsp20 family	COG0071: Molecular chaperone (small heat shock protein)	O	**1.525**	**1.89E−02**
AFE_0871_351-405					**1.475**	**8.58E−03**
AFE_0872_2007-2061	*lon*	ATP-dependent protease La	COG0466: ATP-dependent Lon protease, bacterial type	O	**1.328**	4.87E−01
AFE_0872_2290-2344					**1.352**	**1.18E−02**
AFE_2086_217-271		Putative small heat shock protein, Hsp20 family	COG0071: Molecular chaperone (small heat shock protein)	O	**1.957**	**9.36E−03**
AFE_2086_350-404					**1.261**	**5.02E−03**
AFE_2600_146-200		Putative sulfurtransferase TusA homolog	COG0425: Predicted redox protein, regulator of disulfide bond formation	O	**1.545**	**1.05E−03**
AFE_2600_44-98					**2.053**	**1.88E−02**
AFE_3117_146-200		Putative sulfurtransferase TusA homolog	COG0425: Predicted redox protein, regulator of disulfide bond formation	O	**1.547**	**1.05E−03**
AFE_3117_44-98					**2.017**	**1.82E−02**
AFE_3288_24-78	*hypB*	Hydrogenase nickel incorporation protein HypB	COG0378: Ni^{2+}-binding GTPase involved in regulation of expression and maturation of urease and hydrogenase	OK	**1.239**	**1.67E−04**
AFE_3288_673-727					**1.091**	**3.31E−03**
AFE_3289_109-163	*hypC*	Hydrogenase assembly chaperone HypC	COG0298: Hydrogenase maturation factor	O	**1.634**	**3.00E−03**
AFE_3289_3-57					**1.705**	**1.47E−02**
AFE_3290_585-639	*hypD*	Hydrogenase expression/formation protein HypD	COG0409: Hydrogenase maturation factor	O	**1.216**	**1.67E−04**
AFE_3290_687-741					**1.077**	**3.05E−04**
Transcription						
AFE_2209_459-513		Putative TetR family transcriptional regulator	COG1309: Transcriptional regulator	K	**1.356**	**9.40E−03**
AFE_2209_561-615					0.976	**1.03E−02**
AFE_2641_112-166		Putative transcriptional regulator	COG0640: Predicted transcriptional regulators	K	**1.498**	**1.27E−03**
AFE_2641_241-295					**1.2**	**9.57E−03**
AFE_2750_389-443	*rpoH*	RNA polymerase sigma-32 factor	COG0568: DNA-directed RNA polymerase, sigma subunit (sigma70/sigma32)	K	**1.529**	1.10E−01
AFE_2750_514-568					**1.41**	**4.43E−02**

(Continued)

TABLE 3 | Continued

Oligonucleotides[a]	Gene	Protein description	COG identity : Functional description	COG class	One sample *t*-test (Adv) median (Stats)	One sample *t*-test Benjamini–Hochberg (Adv)[b]
Other COG classes						
AFE_0029_1279-1333	*tetH*	Tetrathionate hydrolase	COG1520: FOG: WD40-like repeat	S	**1.631**	**1.24E−03**
AFE_0029_705-759					**1.905**	**2.72E−02**
AFE_0572_345-399		Putative mediator of cell motility MEMO1 family protein	COG1355: Predicted dioxygenase	R	**1.215**	1.19E−01
AFE_0572_577-631					**1.716**	**4.26E−02**
AFE_0696_110-164	*gfa*	Glutathione-dependent formaldehyde-activating protein	COG3791: Uncharacterized conserved protein	S	**1.203**	**3.23E−03**
AFE_0696_227-281					**1.474**	**3.06E−02**
AFE_0751_106-160		Putative universal stress protein UspA family	COG0589: Universal stress protein UspA and related nucleotide-binding proteins	T	**2.053**	**2.64E−02**
AFE_0751_275-329					**1.736**	**5.06E−03**
AFE_0846_381-435	*yahK*	Aldehyde reductase	COG1064: Zn-dependent alcohol dehydrogenases	R	**1.607**	**9.32E−04**
AFE_0846_934-988					**1.134**	**2.10E−03**
AFE_1034_1318-1372		Putative transposon transposase	COG0675: Transposase and inactivated derivatives	L	**1.461**	**6.19E−04**
AFE_1034_1429-1483					**1.279**	**4.27E−03**
AFE_1675_264-318	*bioD-1*	Dethiobiotin synthetase	COG0132: Dethiobiotin synthetase	H	0.934	1.39E−01
AFE_1675_531-585					**1.551**	**5.40E−03**
AFE_1857_486-540		Putative glucose 1-dehydrogenase Gdh	COG1028: Dehydrogenases with different specificities (related to short-chain alcohol dehydrogenases)	IQR	**1.068**	**6.70E−04**
AFE_1857_605-659					**1.525**	**3.20E−03**
AFE_2083_267-321		Putative trehalose synthase TreT	COG0438: Glycosyltransferase	M	**1.233**	**6.19E−04**
AFE_2083_657-711					**1.637**	**1.20E−02**
AFE_2088_775-829		Putative zinc-binding alcohol dehydrogenase family protein Adh	COG1064: Zn-dependent alcohol dehydrogenases	R	0.94	**4.62E−03**
AFE_2088_875-929					**1.086**	**1.51E−03**
AFE_2464_447-501	*proB-1*	Glutamate 5-kinase	COG0263: Glutamate 5-kinase	E	**1.036**	**6.19E−04**
AFE_2464_594-648					**1.023**	**1.66E−03**
AFE_2931_2329-2383	*recC*	Exodeoxyribonuclease V subunit gamma	COG1330: Exonuclease V gamma subunit	L	**1.206**	**6.65E−04**
AFE_2931_3238-3292					**1.108**	**1.10E−02**
AFE_3086_2008-2062		Putative cytoplasmic membrane cation-transporting ATPase	COG0474: Cation transport ATPase	P	**1.085**	1.48E−01
AFE_3086_2207-2261					**1.106**	**4.77E−03**
AFE_3282_160-214	*hynH*	Hydrogenase expression protein			**2.056**	1.89E−01
AFE_3282_319-373					**2.066**	**4.74E−02**
AFE_3287_288-342	*hypA*	Hydrogenase nickel incorporation protein HypA	COG0375: Zn finger protein HypA/HybF (possibly regulating hydrogenase expression)	R	**1.247**	**1.98E−04**
AFE_3287_39-93					**2.562**	9.70E−02

[a]*Arrow shows co-localized genes transcribed in the same direction.* [b]*Result values are expressed in log2.*
One sample t-test (Adv) median (Stats) value ≤−1 or ≥1 and One sample t-test Benjamini–Hochberg (Adv) value ≤0.05 are indicated in bold.

TABLE 4 | Microarray expression data for genes with known or predicted function differentially expressed in sessile cells in the presence of tetrazole 9c.

Oligonucleotides[a]	Gene	Protein description	COG identity: functional description	COG class	One sample *t*-test (Adv) median (Stats)	One sample *t*-test Benjamini–Hochberg (Adv)[b]
Genes induced by tetrazole 9c						
AFE_1999_222-276	*afeI*	Autoinducer synthesis protein	COG3916 : *N*-acyl-L-homoserine lactone synthetase	TQ	**−3.178**	**1.48E−03**
AFE_1999_445-499					**−3.149**	**4.73E−04**
Genes repressed by tetrazole 9c						
AFE_0690_373-427	*fdhD*	Formate dehydrogenase family accessory protein FdhD	COG1526 : Uncharacterized protein required for formate dehydrogenase activity	C	**1.236**	**1.06E−02**
AFE_0690_725-779					**1.24**	**1.40E−02**
AFE_0697_766-820	*adhI*	Alcohol dehydrogenase class-3/*S*-(hydroxymethyl) glutathione dehydrogenase	COG1062 : Zn-dependent alcohol dehydrogenases, class III	C	**1.099**	**1.72E−02**
AFE_0697_1027-1081					0.993	**1.31E−02**
AFE_0698_289-343	*fghA*	S-formylglutathione hydrolase	COG0627 : Predicted esterase	R	**1.137**	**8.57E−03**
AFE_0698_497-551					**1.255**	**5.56E−03**

[a]*Arrow shows co-localized genes transcribed in the same direction.* [b]*Result values are expressed in log2.*
One sample t-test (Adv) median (Stats) value ≤ −1 or ≥1 and One sample t-test Benjamini–Hochberg (Adv) value ≤0.05 are indicated in bold.

both hydrogenase and sulfur reductase activities, likely serving as an electron sink under highly reducing conditions by recycling redox cofactors using either protons or polysulfides as the electron acceptor. It is worth mentioning that, in different bacteria, some hydrogenases were shown to be upregulated in sessile cells, others in planktonic cells (Caffrey et al., 2008; Clark et al., 2012; Kassem et al., 2012). Our data suggest that the groups 1 and 3 hydrogenases of *A. ferrooxidans* are specific to the non-attached cells.

The number of genes belonging to the carbohydrate transport and metabolism class that were differentially expressed with/without tetrazole **9c** agrees with an alteration in the carbon flow when planktonic cells switched to sessile state. It has to be pointed out that all these genes were downregulated in the presence of the tetrazole **9c**.Three pathways seemed to be affected: the glycolysis [*pyk* (AFE_1801), AFE_1802, *gpmL* (AFE_1815)], the pentose phosphate pathway [*tal* (AFE_0419), AFE_1857, and AFE_2024] and the glycogen biosynthesis/degradation pathway [AFE_1799, AFE_2082, AFE_2083, and *glgB* (AFE_2836)]. In the case of glycolysis, this could mean that the pathway was directed toward β-D-fructose-1,6-bisphosphate, β-D-fructose-6-phosphate, α-D-glucose-6-phosphate, and α-D-glucose-1-phosphate production (**Figure 2A**). Similarly, in the pentose phosphate pathway, the repression would lead toward β-D-glucose, β-D-glucose-6-phosphate and β-D-fructose-6-phosphate direction and therefore to α-D-glucose-6-phosphate and α-D-glucose-1-phosphate accumulation (**Figure 2A**). Noteworthy, α-D-glucose-6-phosphate and α-D-glucose-1-phosphate are the precursors of UDP glucose, UDP-galactose, dTDP-rhamnose and GDP-mannose, which are the building blocks in EPS biosynthesis (Quatrini et al., 2007). Another interesting results was the repression of three genes predicted to be involved in trehalose synthesis [*treT* (AFE_2083), *treZ* (AFE_2082) and *treY* (AFE_2081)] by tetrazole **9c**. In the first case, α-D-glucose-1-phosphate consumption will be prevented, in agreement with the data presented above, and, in addition, maltodextrin synthesis will be favored. In the second case, maltodextrin consumption will be avoided (**Figure 2B**). Notably, maltodextrin has been shown to increase *E. coli* adhesion (Nickerson and McDonald, 2012). Along the same lines, genes involved in maltodextrin consumption [AFE_1799 and *glgB* (AFE_2836)] were repressed in the presence of tetrazole **9c** (**Figure 2B**). Therefore, in planktonic cells, it appears that tetrazole **9c** directed the carbon flow toward adhesion (maltodextrin), EPS precursor biosynthesis (α-D-glucose-6-phosphate, α-D-glucose-1-phosphate) and therefore biofilm formation.

In a number of microorganisms, including *L. ferrooxidans*, heat shock chaperones (Moreno-Paz et al., 2010; Singh et al., 2012; Becherelli et al., 2013; Grudniak et al., 2013) and proteases (Doern et al., 2009; Moreno-Paz et al., 2010; Singh et al., 2012; Yepes et al., 2012), in particular O-sialoglycoprotein endopeptidase (Wickstrom et al., 2013), have been shown to be required in sessile cells for biofilm development. Furthermore, the *uspA* gene, encoding an universal stress protein, is necessary for optimal biofilm formation in *Porphyromonas gingivalis* (Chen et al., 2006). In *A. ferrooxidans*, tetrazole **9c** repressed the genes

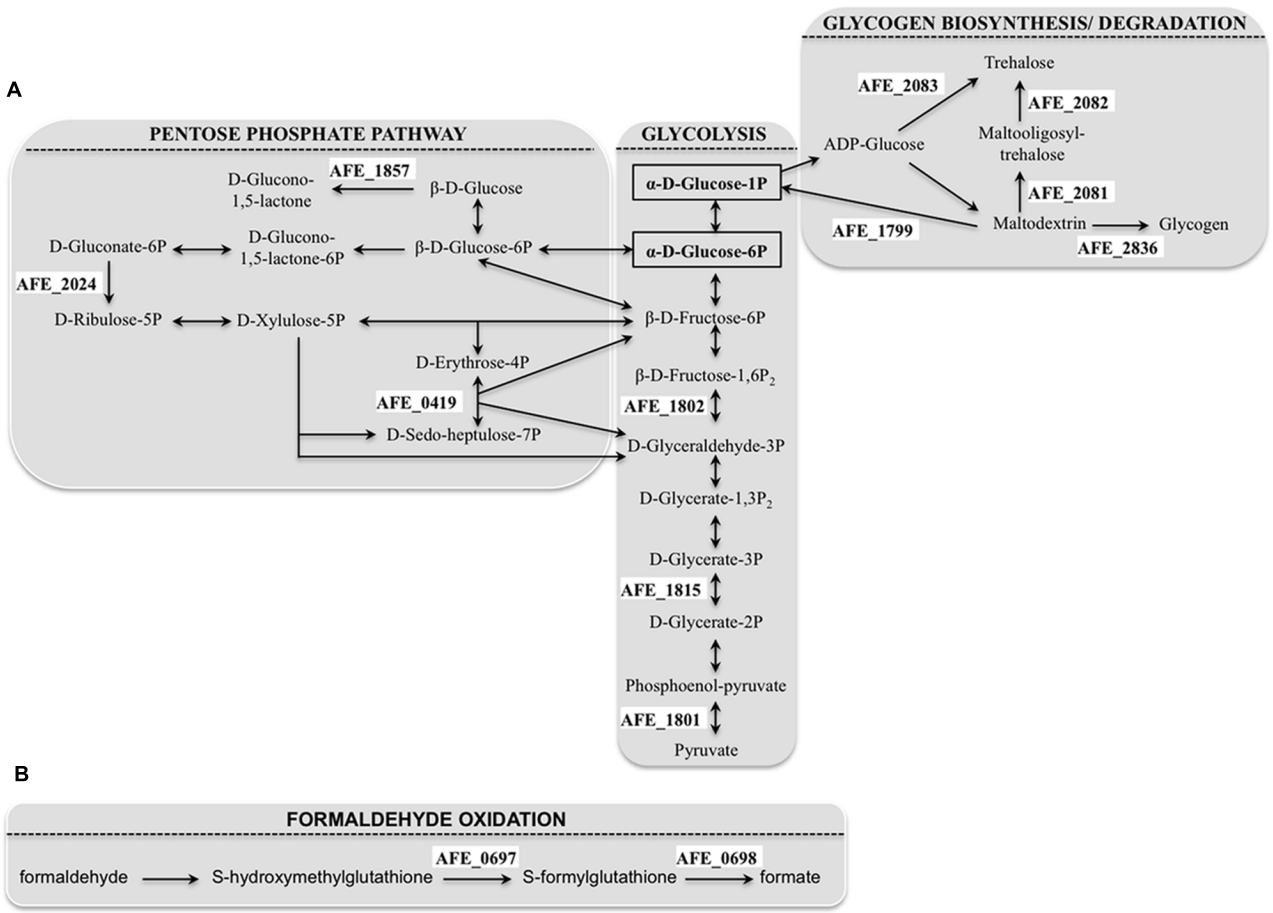

FIGURE 2 | *Acidithiobacillus ferrooxidans* pathways showing gene repression by tetrazole 9c. (A) Genes involved in carbon flow that were downregulated in planktonic cells (for clarity, only the connections of the pathways discussed in the text have been shown). **(B)** Genes involved in formaldehyde oxidation that were downregulated in sessile cells. The precursors of the EPS (extracellular polymeric substances) building blocks are surrounded by a black rectangle. The genes that were repressed by tetrazole **9c** are indicated in a white background.

encoding the heat shock response RNA polymerase σ32 factor [*rpoH* (AFE2750)], Hsp20 family heat shock proteins (AFE_0871 and 2086), a putative universal stress protein (AFE_0751), as well as protease [*lon* (AFE_0872)] and O-sialoglycoprotein endopeptidase [*gcp* (AFE_0123)] in planktonic cells, indicating that these proteins are not required at the early step of biofilm biogenesis. Interestingly, *bioD* (AFE_1675) was repressed in the presence of the tetrazolic analog. This gene encodes dethiobiotin synthetase involved in biotin synthesis from 7-keto-8-aminopelargonate. This pathway consumes *S*-adenosyl-L-methionine (Streit and Entcheva, 2003). The down-regulation in the presence of tetrazole **9c** of this gene could save this substrate that is required for AHL biosynthesis. Another important data is the repression of *proB* (AFE_2464) in the presence of tetrazole **9c**. The *proB* gene encodes glutamate-5-kinase and its repression could lead to glutamate accumulation. Glutamate metabolism has been reported to be essential for biofilm formation. Amino acid levels in general increased in biofilm cells and are used as precursors for energy production with gluconeogenesis (Yeom et al., 2013). In harsh environments, such as acidic conditions, a high demand for amino acids as substrates for energy production may indeed exist in biofilms. Very recently, it has been proposed that amino acids, including glutamate, may also have another role as a signal for biofilm maturation and eventual disassembly (Wong et al., 2015). Finally, two genes encoding transcriptional regulators (AFE_2209 and AFE_2641) were repressed in planktonic cells in the presence of tetrazolic AHL analog. Therefore, we cannot exclude the possibility that genes differentially expressed in the presence of this superagonist AHL analog were indirectly regulated by one of these regulators rather than directly by the AfeR/AfeI QS system. It is noteworthy that members of the TetR-protein family, as is the case for AFE_2209, have been directly involved in the regulation of cellular processes and in particular the QS in different Gram-negative species (Cuthbertson and Nodwell, 2013; Longo et al., 2013).

To summarize, in planktonic cells, tetrazole **9c** led to the induction of genes encoding (i) proton channel proteins to allow PMF energized transport system of AHL and substrates required for EPS synthesis, (ii) an enzyme required in an

early step of polysaccharide synthesis, and (iii) transport system to anticipate phosphate and ammonium gradients within the biofilm. On the other hand, it repressed genes involved in (i) biofilm maturation (heat-shock proteins and chaperone encoding genes), (ii) biotin synthesis to prevent the consumption of *S*-adenosyl-L-methionine required for AHL biosynthesis, (iii) glutamate conversion to proline to use it as an energy source and/or as a signal for biofilm maturation, and (iv) carbohydrate metabolism to redirect the carbon flow toward proteins necessary for adhesion and EPS precursor biosynthesis. It seems therefore reasonable to conclude that tetrazole **9c** reprograms planktonic cells toward early biofilm formation.

Genes Differentially Expressed In the Presence of Tetrazole 9c in Sessile Cells

In sessile cells, only four genes, encoding proteins with known or predicted functions, presented significant differences in expression. Not surprisingly, the gene with the highest fold difference was *afeI* (AFE_1999) encoding the AHL synthase, with at least an eight-fold expression increase in the presence of tetrazole **9c** indicating that indeed the QS was triggered. The three other genes *fdhD* (AFE_0690), *adhI* (AFE_0697), and *fghA* (AFE_0698) encoding a putative formate dehydrogenase family accessory protein FdhD, a *S*-(hydroxymethyl) glutathione dehydrogenase, and a *S*-formylglutathione hydrolase, respectively, are involved in formaldehyde oxidation to formate (**Figure 2B**). Their repression could lead to the accumulation of formaldehyde, shown to lead to higher biofilm density in a biofilm reactor (Ong et al., 2006). Another not exclusive possibility is that this system is to prevent formate formation that could acidify *A. ferroxidans* cytoplasm and lead to cell death.

Surprisingly, only three genes differentially expressed in the presence of tetrazole **9c** (Supplementary Tables S3 and S4) have the AfeR binding site inferred from bioinformatic prediction (Farah et al., 2005; Banderas and Guiliani, 2013): AFE_0582 and AFE_1998 encoding hypothetical proteins as well as *afeI* (AFE_1999). This could be due to an indirect regulation through a regulator whose expression is controlled by QS. However, the two genes encoding a transcription regulator whose expression was downregulated in the presence of tetrazole **9c** (AFE_2209 and AFE_2641) do not exhibit this predicted AfeR binding site. On the other hand, three genes [*zwf* (AFE_2025), AFE_0233, and AFE_1339] in which this site was predicted, are constitutively expressed in the conditions analyzed. Therefore, another possibility is that a different transcriptional regulator than AfeR binds to the proposed AfeR binding site. All in all, the QS regulon of *A. ferrooxidans* seems to involve a complex regulatory cascade.

AfeR Binds Specifically to the *afeI* Regulatory Region

To check that the *afeI* induction in the presence of tetrazole **9c** observed by transcriptomic data was mediated by the QS regulator AfeR, we have produced AfeR in *E. coli* and analyzed its binding to the regulatory region of the *afeI* gene. AfeR with a hexa-histidine tag fused to its C terminus (AfeR-Histag) was mainly found in the inclusion bodies, even when the 3-hydroxy-C14-AHL (Gonzalez et al., 2013) was added at the induction time. The recombinant AfeR-Histag produced in the presence of 3-hydroxy-C14-AHL was purified on an affinity cobalt column. As shown in **Figure 3A**, a major band of the expected mass (theoretical molecular mass: 27,876 Da including one molecule of 3-hydroxy-C14-AHL) was visualized on Coomassie blue-stained SDS-polyacrylamide gels. This same protein was recognized by anti-hexahistidine tag antibodies (**Figure 3A**) strongly suggesting that it was AfeR-Histag. The analysis by MALDI-TOF mass spectrometry of this protein digested with Trypsin after reduction by DTT and alkylation by iodoacetamide confirmed that it was AfeR-Histag (54% sequence coverage).

Binding of AfeR-Histag to the regulatory region of *afeI* was analyzed by EMSA in the presence of 3-hydroxy-C14-AHL. A retarded band was detected with 1.3 μM AfeR-Histag and higher concentrations (**Figure 3C**) with DNA fragments encompassing the palindromic sequence predicted to be the AfeR binding site (Farah et al., 2005; Banderas and Guiliani, 2013) in the *afeI* regulatory region (**Figure 3B**). This binding was specific to this region since no binding was observed on an internal fragment of the *rrs* gene of *Thiomonas arsenitoxydans* (**Figure 3C**). These results indicate that AfeR-Histag binds to the regulatory region of *afeI* in the presence of 3-hydroxy-C14-AHL, in agreement with the induction of this gene in the presence of tetrazole superagonist AHL analog **9c**. Since AfeR was constitutively expressed under the conditions analyzed (i.e., with or without tetrazole **9c**), these results suggest that the binding of 3-hydroxy-C14-AHL to AfeR induces a conformational change allowing its specific binding to the target DNA, as it has been proposed for several members of LuxR-like protein family (Choi and Greenberg, 1991).

CONCLUSION

The exogenous use of tetrazole superagonist AHL analog **9c** allowed the first overview of the QS regulon of *A. ferrooxidans*, an acidophilic bacterial species involved in bioleaching processes. This study gave some insights into the molecular chain reactions involved in the first steps of mineral adherence and colonization of this bacterium. As expected, tetrazole **9c** activates the positive feedback previously reported (Rivas et al., 2005) by inducing the transcription of *afeI* gene, likely through its binding to the transcriptional regulator AfeR, and therefore its activation, as early as the third day of growth.

The data obtained from planktonic cells revealed that tetrazole **9c** triggers the QS system to drive gene expression toward sessile state by reprogramming some cellular processes. These mainly include: (i) induction of the genes encoding the F0-ATPase subunit leading to the PMF allowing AHL efflux and influx, (ii) repression of several genes involved in carbohydrate metabolism to orientate carbon flow to maltodextrin and EPS building block precursor synthesis for adhesion and biofilm formation, respectively; (iii) induction of phosphate and ammonium transporters to anticipate inorganic ion gradient

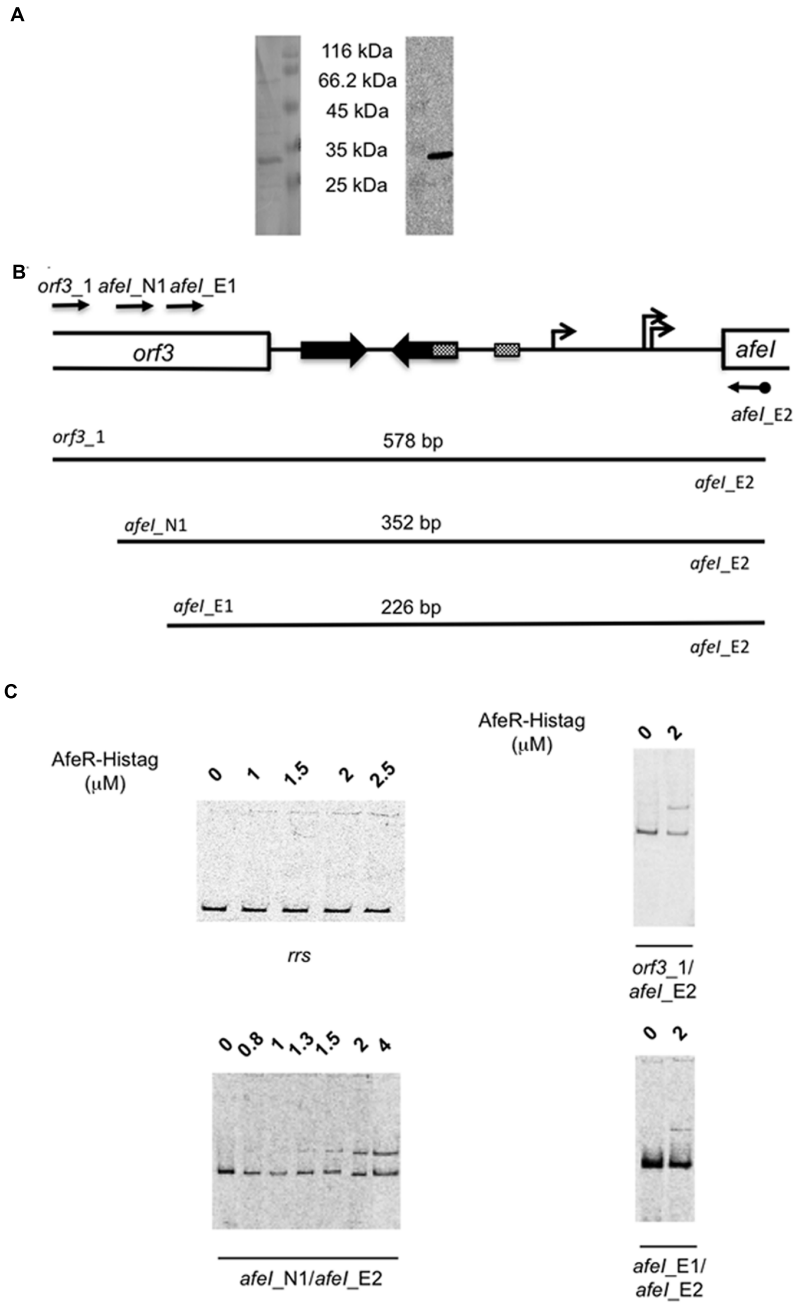

FIGURE 3 | Production of the recombinant AfeR-Histag in *Escherichia coli* and its binding on the *afeI* regulatory region. (A) Coomassie brilliant blue stained SDS-PAGE (left) and Western immunoblot with antisera raised against the hexahistidine tag (right). The size of the unstained protein molecular weight marker standards (Euromedex) is indicated. **(B)** Schematic representation of the *afeI* locus with the DNA fragments analysed. **(C)** Gel mobility shift assays with an internal DNA fragment of the *rrs* gene of *Thiomonas arsenitoxydans* (left upper part) and the DNA fragments depicted in **(B)**.

within and around the biofilm structure. Whereas QS and c-di-GMP pathway have been linked in different bacterial species (Waters et al., 2008; Zhang, 2010; Kozlova et al., 2011; Suppiger et al., 2016), it is noteworthy that no change in the transcriptional profiling of the seven genes related to the c-di-GMP pathway in *A. ferrooxidans* (Ruiz et al., 2012; Castro et al., 2015) has been observed in the presence of tetrazole **9c.** This result indicates that QS does not modulate c-di-GMP signaling in this Gram-negative species. Finally, the high transcription level of *afeI* gene in sessile cells observed after 3 days of growth lead not only to *A. ferrooxidans* biofilm stabilization but also to the synthesis of a large spectrum of AHL molecules (Farah et al., 2005; Valenzuela et al., 2017), some of which are sensed by secondary colonizers such as *A. thiooxidans* to form a mixed biofilm

(Bellenberg et al., 2014) through a not yet identified non-canonical AHL-binding protein.

AUTHOR CONTRIBUTIONS

VB and NG conceived and designed the experiments. SM, DM, YD, and ET performed the experiments. VB, SM, NG, and DM analyzed the data. LS and YQ performed the chemical synthesis. NG, VB, YD, LS, YQ, and ET contributed to the reagents/materials/analysis tools. VB, NG, and ET wrote the paper. All authors read and approved the final manuscript.

FUNDING

SM acknowledges CONICYT to support her doctoral studies in Chile (scholarship N°21090736, 2009) and France (cotutorship "Becas Chile" N°78110005, 2011) and to allow attending international meeting. ET and VB are supported by Aix Marseille Université (AMU) and Centre National de la Recherche Scientifique (CNRS). NG is supported by Universidad de Chile (UCH). This work was partly performed in the frame of the PICS 5270 entitled "Studies of the Quorum Sensing and its function during the bioleaching process in the bacterium *Acidithiobacillus ferrooxidans*. An interdisciplinary challenge at the chemical/Biology/Biotechnology frontier." This work was mainly supported by FONDECYT grants 1120295 and 1160702.

ACKNOWLEDGMENTS

We thank M. Bauzan (Fermentation plant unit, IMM, Marseille, France) for growing the *Escherichia coli* Rosetta (DE3)/pLysS strain carrying pET21-AfeR-His tag in bioreactor and the Proteomic facility of IMM (Marseille, France) for proteomic analysis.

SUPPLEMENTARY MATERIAL

The Supplementary Material for this article can be found online at: http://journal.frontiersin.org/article/10.3389/fmicb.2016.01365

FIGURE S1 | Chemical structure of tetrazole 9c.

REFERENCES

Aiba, H., Adhya, S., and de Crombrugghe, B. (1981). Evidence for two functional *gal* promoters in intact *Escherichia coli* cells. *J. Biol. Chem.* 256, 11905–11910.

Amaro, A. M., Chamorro, D., Seeger, M., Arredondo, R., Peirano, I., and Jerez, C. A. (1991). Effect of external pH perturbations on in vivo protein synthesis by the acidophilic bacterium *Thiobacillus ferrooxidans*. *J. Bacteriol.* 173, 910–915.

Amouric, A., Brochier-Armanet, C., Johnson, D. B., Bonnefoy, V., and Hallberg, K. B. (2011). Phylogenetic and genetic variation among Fe(II)-oxidizing acidithiobacilli supports the view that these comprise multiple species with different ferrous iron oxidation pathways. *Microbiology* 157, 111–122. doi: 10.1099/mic.0.044537-0

Ardin, A. C., Fujita, K., Nagayama, K., Takashima, Y., Nomura, R., Nakano, K., et al. (2014). Identification and functional analysis of an ammonium transporter in *Streptococcus mutans*. *PLoS ONE* 9:e107569. doi: 10.1371/journal.pone.0107569

Ausubel, F. M., Brent, R., Kingston, R. E., Moore, D. D., Seidman, J. G., Smith, J. A., et al. (1998). *Current Protocols in Molecular Biology*. New York, NY: Greene publishing.

Banderas, A., and Guiliani, N. (2013). Bioinformatic prediction of gene functions regulated by quorum sensing in the bioleaching bacterium *Acidithiobacillus ferrooxidans*. *Int. J. Mol. Sci.* 14, 16901–16916. doi: 10.3390/ijms140816901

Barreto, M., Jedlicki, E., and Holmes, D. S. (2005). Identification of a gene cluster for the formation of extracellular polysaccharide precursors in the chemolithoautotroph *Acidithiobacillus ferrooxidans*. *Appl. Environ. Microbiol.* 71, 2902–2909. doi: 10.1128/AEM.71.6.2902-2909.2005

Becherelli, M., Tao, J., and Ryder, N. S. (2013). Involvement of heat shock proteins in *Candida albicans* biofilm formation. *J. Mol. Microbiol. Biotechnol.* 23, 396–400. doi: 10.1159/000351619

Bellenberg, S., Diaz, M., Noel, N., Sand, W., Poetsch, A., Guiliani, N., et al. (2014). Biofilm formation, communication and interactions of leaching bacteria during colonization of pyrite and sulfur surfaces. *Res. Microbiol.* 165, 773–781. doi: 10.1016/j.resmic.2014.08.006

Bellenberg, S., Leon-Morales, C. F., Sand, W., and Vera, M. (2012). Visualization of capsular polysaccharide induction in *Acidithiobacillus ferrooxidans*. *Hydrometallurgy* 129–130, 82–89. doi: 10.1016/j.hydromet.2012.09.002

Biot, C., Bauer, H., Schirmer, R. H., and Davioud-Charvet, E. (2004). 5-substituted tetrazoles as bioisosteres of carboxylic acids. Bioisosterism and mechanistic studies on glutathione reductase inhibitors as antimalarials. *J. Med. Chem.* 47, 5972–5983. doi: 10.1021/jm0497545

Caffrey, S. M., Park, H. S., Been, J., Gordon, P., Sensen, C. W., and Voordouw, G. (2008). Gene expression by the sulfate-reducing bacterium *Desulfovibrio vulgaris* Hildenborough grown on an iron electrode under cathodic protection conditions. *Appl. Environ. Microbiol.* 74, 2404–2413. doi: 10.1128/AEM.02469-07

Cantero, L., Palacios, J. M., Ruiz-Argueso, T., and Imperial, J. (2006). Proteomic analysis of quorum sensing in *Rhizobium leguminosarum* biovar viciae UPM791. *Proteomics* 6(Suppl. 1), S97–S106. doi: 10.1002/pmic.200500312

Castro, M., Deane, S. M., Ruiz, L., Rawlings, D. E., and Guiliani, N. (2015). Diguanylate cyclase null mutant reveals that c-di-GMP pathway regulates the motility and adherence of the extremophile bacterium *Acidithiobacillus caldus*. *PLoS ONE* 10:e0116399. doi: 10.1371/journal.pone.0116399

Chen, L. X., Hu, M., Huang, L. N., Hua, Z. S., Kuang, J. L., Li, S. J., et al. (2015). Comparative metagenomic and metatranscriptomic analyses of microbial communities in acid mine drainage. *ISME J.* 9, 1579–1592. doi: 10.1038/ismej.2014.245

Chen, W., Honma, K., Sharma, A., and Kuramitsu, H. K. (2006). A universal stress protein of *Porphyromonas gingivalis* is involved in stress responses and biofilm formation. *FEMS Microbiol. Lett.* 264, 15–21. doi: 10.1111/j.1574-6968.2006.00426.x

Chhabra, S. R., Harty, C., Hooi, D. S., Daykin, M., Williams, P., Telford, G., et al. (2003). Synthetic analogues of the bacterial signal (quorum sensing) molecule N-(3-oxododecanoyl)-L-homoserine lactone as immune modulators. *J. Med. Chem.* 46, 97–104. doi: 10.1021/jm020909n

Choi, S. H., and Greenberg, E. P. (1991). The C-terminal region of the *Vibrio fischeri* LuxR protein contains an inducer-independent *lux* gene activating domain. *Proc. Natl. Acad. Sci. U.S.A.* 88, 11115–11119. doi: 10.1073/pnas.88.24.11115

Chung, C. T., and Miller, R. H. (1988). A rapid and convenient method for the preparation and storage of competent bacterial cells. *Nucleic Acids Res.* 16:3580. doi: 10.1093/nar/16.8.3580

Clark, M. E., He, Z., Redding, A. M., Joachimiak, M. P., Keasling, J. D., Zhou, J. Z., et al. (2012). Transcriptomic and proteomic analyses of *Desulfovibrio vulgaris* biofilms: carbon and energy flow contribute to the distinct biofilm growth state. *BMC Genomics* 13:138. doi: 10.1186/1471-2164-13-138

Cuthbertson, L., and Nodwell, J. R. (2013). The TetR family of regulators. *Microbiol. Mol. Biol. Rev.* 77, 440–475. doi: 10.1128/MMBR.00018-13

Decho, A. W., Frey, R. L., and Ferry, J. L. (2011). Chemical challenges to bacterial AHL signaling in the environment. *Chem. Rev.* 111, 86–99. doi: 10.1021/cr100311q

Diaz, M., Copaja, S., and Guiliani, N. (2013). Functional analysis of c-di-GMP pathway in biomining bacteria *Acidithiobacillus thiooxidans*. *Adv. Mater. Res.* 825, 133–136. doi: 10.4028/www.scientific.net/AMR.825.133

Doern, C. D., Roberts, A. L., Hong, W., Nelson, J., Lukomski, S., Swords, W. E., et al. (2009). Biofilm formation by group A *Streptococcus*: a role for the streptococcal regulator of virulence (Srv) and streptococcal cysteine protease (SpeB). *Microbiology* 155, 46–52. doi: 10.1099/mic.0.021048-0

Falagan, C., and Johnson, D. B. (2015). *Acidithiobacillus ferriphilus* sp. nov., a facultatively anaerobic iron- and sulfur-metabolising extreme acidophile. *Int. J. Syst. Evol. Microbiol* 66, 206–211. doi: 10.1099/ijsem.0.000698

Farah, C., Vera, M., Morin, D., Haras, D., Jerez, C. A., and Guiliani, N. (2005). Evidence for a functional quorum-sensing type AI-1 system in the extremophilic bacterium *Acidithiobacillus ferrooxidans*. *Appl. Environ. Microbiol.* 71, 7033–7040. doi: 10.1128/AEM.71.11.7033-7040.2005

Gonzalez, A., Bellenberg, S., Mamani, S., Ruiz, L., Echeverria, A., Soulere, L., et al. (2013). AHL signaling molecules with a large acyl chain enhance biofilm formation on sulfur and metal sulfides by the bioleaching bacterium *Acidithiobacillus ferrooxidans*. *Appl. Microbiol. Biotechnol.* 97, 3729–3737. doi: 10.1007/s00253-012-4229-3

Grudniak, A. M., Pawlak, K., Bartosik, K., and Wolska, K. I. (2013). Physiological consequences of mutations in the *htpG* heat shock gene of *Escherichia coli*. *Mutat. Res.* 745–746, 1–5. doi: 10.1016/j.mrfmmm.2013.04.003

Harneit, K., Göksel, A., Klock, J. -H., Gehrke, T., and Sand, W. (2006). Adhesion to metal sulfide surfaces by cells of *Acidithiobacillus ferrooxidans*, *Acidithiobacillus thiooxidans* and *Leptospirillum ferrooxidans*. *Hydrometallurgy* 83, 245–254. doi: 10.1016/j.hydromet.2006.03.044

Hedrich, S., and Johnson, D. B. (2013). *Acidithiobacillus ferridurans* sp. nov., an acidophilic iron-, sulfur- and hydrogen-metabolizing chemolithotrophic gammaproteobacterium. *Int. J. Syst. Evol. Microbiol.* 63, 4018–4025. doi: 10.1099/ijs.0.049759-0

Heindl, J. E., Wang, Y., Heckel, B. C., Mohari, B., Feirer, N., and Fuqua, C. (2014). Mechanisms and regulation of surface interactions and biofilm formation in *Agrobacterium*. *Front. Plant Sci.* 5:176. doi: 10.3389/fpls.2014.00176

Hengge, R. (2009). Principles of c-di-GMP signalling in bacteria. *Nat. Rev. Microbiol.* 7, 263–273. doi: 10.1038/nrmicro2109

Hengge, R., Grundling, A., Jenal, U., Ryan, R., and Yildiz, F. (2015). Bacterial signal transduction by c-di-GMP and other nucleotide second messengers. 198:15–26 *J. Bacteriol.* doi: 10.1128/JB.00331-15

Ikonomidis, A., Tsakris, A., Kanellopoulou, M., Maniatis, A. N., and Pournaras, S. (2008). Effect of the proton motive force inhibitor carbonyl cyanide-m-chlorophenylhydrazone (CCCP) on *Pseudomonas aeruginosa* biofilm development. *Lett. Appl. Microbiol.* 47, 298–302. doi: 10.1111/j.1472-765X.2008.02430.x

Jerez, C. A. (2009). "Biomining microorganisms: molecular aspects and applications in biotechnology and bioremediation," in *Advances in Applied Bioremediation*, eds A. Singh, R. C. Kuhad, and O. P. Ward (Berlin: Springer-Verlag), 239–256.

Johnson, D. B. (2009). "Extremophiles: acidic environments," in *Encyclopaedia of Microbiology* ed. M. Schaechter (Oxford: Elsevier), 107–126.

Johnson, D. B. (2012). Geomicrobiology of extremely acidic subsurface environments. *FEMS Microbiol. Ecol.* 81, 2–12. doi: 10.1111/j.1574-6941.2011.01293.x

Johnson, D. B. (2014). Biomining-biotechnologies for extracting and recovering metals from ores and waste materials. *Curr. Opin. Biotechnol.* 30, 24–31. doi: 10.1016/j.copbio.2014.04.008

Kalia, D., Merey, G., Nakayama, S., Zheng, Y., Zhou, J., Luo, Y., et al. (2013). Nucleotide, c-di-GMP, c-di-AMP, cGMP, cAMP, (p)ppGpp signaling in bacteria and implications in pathogenesis. *Chem. Soc. Rev.* 42, 305–341. doi: 10.1039/c2cs35206k

Kapatral, V., Bina, X., and Chakrabarty, A. M. (2000). Succinyl coenzyme A synthetase of *Pseudomonas aeruginosa* with a broad specificity for nucleoside triphosphate (NTP) synthesis modulates specificity for NTP synthesis by the 12-kilodalton form of nucleoside diphosphate kinase. *J. Bacteriol.* 182, 1333–1339. doi: 10.1128/JB.182.5.1333-1339.2000

Kassem, I. I., Khatri, M., Esseili, M. A., Sanad, Y. M., Saif, Y. M., Olson, J. W., and Rajashekara, G. (2012). Respiratory proteins contribute differentially to *Campylobacter jejuni*'s survival and *in vitro* interaction with hosts' intestinal cells. *BMC Microbiol.* 12:258. doi: 10.1186/1471-2180-12-258

Kozlova, E. V., Khajanchi, B. K., Sha, J., and Chopra, A. K. (2011). Quorum sensing and c-di-GMP-dependent alterations in gene transcripts and virulence-associated phenotypes in a clinical isolate of *Aeromonas hydrophila*. *Microb. Pathog.* 50, 213–223. doi: 10.1016/j.micpath.2011.01.007

Liljeqvist, M., Ossandon, F. J., Gonzalez, C., Rajan, S., Stell, A., Valdes, J., et al. (2015). Metagenomic analysis reveals adaptations to a cold-adapted lifestyle in a low-temperature acid mine drainage stream. *FEMS Microbiol. Ecol.* 91:fiv011. doi: 10.1093/femsec/fiv011

Longo, F., Rampioni, G., Bondi, R., Imperi, F., Fimia, G. M., Visca, P., et al. (2013). A new transcriptional repressor of the *Pseudomonas aeruginosa* quorum sensing receptor gene LasR. *PLoS ONE* 8:e69554. doi: 10.1371/journal.pone.0069554

Majerczyk, C., Brittnacher, M., Jacobs, M., Armour, C. D., Radey, M., Schneider, E., et al. (2014). Global analysis of the *Burkholderia thailandensis* quorum sensing-controlled regulon. *J. Bacteriol.* 196, 1412–1424. doi: 10.1128/JB.01405-13

Menzel, P., Gudbergsdottir, S. R., Rike, A. G., Lin, L., Zhang, Q., Contursi, P., et al. (2015). Comparative metagenomics of eight geographically remote terrestrial hot springs. *Microb. Ecol.* 70, 411–424. doi: 10.1007/s00248-015-0576-9

Montgomery, K., Charlesworth, J. C., LeBard, R., Visscher, P. T., and Burns, B. P. (2013). Quorum sensing in extreme environments. *Life (Basel)* 3, 131–148. doi: 10.3390/life3010131

Moreno-Paz, M., Gomez, M. J., Arcas, A., and Parro, V. (2010). Environmental transcriptome analysis reveals physiological differences between biofilm and planktonic modes of life of the iron oxidizing bacteria *Leptospirillum* spp. in their natural microbial community. *BMC Genomics* 11:404. doi: 10.1186/1471-2164-11-404

Ng, W. L., and Bassler, B. L. (2009). Bacterial quorum-sensing network architectures. *Annu. Rev. Genet.* 43, 197–222. doi: 10.1146/annurev-genet-102108-134304

Nickerson, K. P., and McDonald, C. (2012). Crohn's disease-associated adherent-invasive *Escherichia coli* adhesion is enhanced by exposure to the ubiquitous dietary polysaccharide maltodextrin. *PLoS ONE* 7:e52132. doi: 10.1371/journal.pone.0052132

O'May, G. A., Jacobsen, S. M., Longwell, M., Stoodley, P., Mobley, H. L., and Shirtliff, M. E. (2009). The high-affinity phosphate transporter Pst in *Proteus mirabilis* HI4320 and its importance in biofilm formation. *Microbiology* 155, 1523–1535. doi: 10.1099/mic.0.026500-0

Ong, S. L., Sarkar, S. K., Lee, L. Y., Hu, J. Y., Ng, H. Y., and van Loosdrecht, M. (2006). Effect of formaldehyde on biofilm activity and morphology in an ultracompact biofilm reactor for carbonaceous wastewater treatment. *Water Environ. Res.* 78, 372–380. doi: 10.2175/106143006X98787

Parsek, M. R., and Greenberg, E. P. (2005). Sociomicrobiology: the connections between quorum sensing and biofilms. *Trends Microbiol.* 13, 27–33. doi: 10.1016/j.tim.2004.11.007

Peterson, J. D., Umayam, L. A., Dickinson, T., Hickey, E. K., and White, O. (2001). The comprehensive microbial resource. *Nucleic Acids Res.* 29, 123–125. doi: 10.1093/nar/29.1.123

Pogliani, C., and Donati, E. (1999). The role of exopolymers in the bioleaching of a non-ferrous metal sulphide. *J. Ind. Microbiol. Biotechnol.* 22, 88–92. doi: 10.1038/sj.jim.2900610

Qin, N., Callahan, S. M., Dunlap, P. V., and Stevens, A. M. (2007). Analysis of LuxR regulon gene expression during quorum sensing in *Vibrio fischeri*. *J. Bacteriol.* 189, 4127–4134. doi: 10.1128/JB.01779-06

Quatrini, R., Appia-Ayme, C., Denis, Y., Jedlicki, E., Holmes, D. S., and Bonnefoy, V. (2009). Extending the models for iron and sulfur oxidation in the extreme acidophile *Acidithiobacillus ferrooxidans*. *BMC Genomics* 10:394. doi: 10.1186/1471-2164-10-394

Quatrini, R., Appia-Ayme, C., Denis, Y., Ratouchniak, J., Veloso, F., Valdes, J., et al. (2006). Insights into the iron and sulfur energetic metabolism of *Acidithiobacillus ferrooxidans* by microarray transcriptome profiling. *Hydrometallurgy* 83, 263–272. doi: 10.1007/s12223-011-0067-4

Quatrini, R., Valdes, J., Jedlicki, E., and Holmes, D. S. (2007). "The use of bioinformatics and genomic biology to advance our understanding of bioleaching microorganisms," in *Microbial Processing of Metal Sulfides*, eds E. R. Donati and W. Sand (Dordrecht: Springer), 221–239.

Rivas, M., Seeger, M., Holmes, D. S., and Jedlicki, E. (2005). A Lux-like quorum sensing system in the extreme acidophile *Acidithiobacillus ferrooxidans*. *Biol. Res.* 38, 283–297. doi: 10.4067/S0716-97602005000200018

Rohwerder, T., and Sand, W. (2007). "Mechanisms and biochemical fundamentals of bacterial metal sulfide oxidation," in *Microbial Processing of Metal Sulfides*, eds E. R. Donati and W. Sand (Dordrecht: Springer), 35–58.

Romling, U., Galperin, M. Y., and Gomelsky, M. (2013). Cyclic di-GMP: the first 25 years of a universal bacterial second messenger. *Microbiol. Mol. Biol. Rev.* 77, 1–52. doi: 10.1128/MMBR.00043-12

Ruiz, L. M., Castro, M., Barriga, A., Jerez, C. A., and Guiliani, N. (2012). The extremophile *Acidithiobacillus ferrooxidans* possesses a c-di-GMP signalling pathway that could play a significant role during bioleaching of minerals. *Lett. Appl. Microbiol.* 54, 133–139. doi: 10.1111/j.1472-765X.2011.03180.x

Ruiz, L. M., Valenzuela, S., Castro, M., Gonzalez, A., Frezza, M., Soulere, L., et al. (2008). AHL communication is a widespread phenomenon in biomining bacteria and seems to be involved in mineral-adhesion efficiency. *Hydrometallurgy* 94, 133–137. doi: 10.1016/j.hydromet.2008.05.028

Ryan, R. P., Fouhy, Y., Lucey, J. F., Crossman, L. C., Spiro, S., He, Y. W., et al. (2006). Cell-cell signaling in *Xanthomonas campestris* involves an HD-GYP domain protein that functions in cyclic di-GMP turnover. *Proc. Natl. Acad. Sci. U.S.A.* 103, 6712–6717. doi: 10.1073/pnas.0600345103

Sabbah, M., Fontaine, F., Grand, L., Boukraa, M., Efrit, M. L., Doutheau, A., et al. (2012). Synthesis and biological evaluation of new N-acyl-homoserine-lactone analogues, based on triazole and tetrazole scaffolds, acting as LuxR-dependent quorum sensing modulators. *Bioorg. Med. Chem.* 20, 4727–4736. doi: 10.1016/j.bmc.2012.06.007

Saville, R. M., Rakshe, S., Haagensen, J. A., Shukla, S., and Spormann, A. M. (2011). Energy-dependent stability of *Shewanella oneidensis* MR-1 biofilms. *J. Bacteriol.* 193, 3257–3264. doi: 10.1128/JB.00251-11

Singh, V. K., Syring, M., Singh, A., Singhal, K., Dalecki, A., and Johansson, T. (2012). An insight into the significance of the DnaK heat shock system in *Staphylococcus aureus*. *Int. J. Med. Microbiol.* 302, 242–252. doi: 10.1016/j.ijmm.2012.05.001

Slyemi, D., Moinier, D., Talla, E., and Bonnefoy, V. (2013). Organization and regulation of the arsenite oxidase operon of the moderately acidophilic and facultative chemoautotrophic *Thiomonas arsenitoxydans*. *Extremophiles* 17, 911–920. doi: 10.1007/s00792-013-0573-1

Soulere, L., Guiliani, N., Queneau, Y., Jerez, C. A., and Doutheau, A. (2008). Molecular insights into quorum sensing in *Acidithiobacillus ferrooxidans* bacteria via molecular modelling of the transcriptional regulator AfeR and of the binding mode of long-chain acyl homoserine lactones. *J. Mol. Model* 14, 599–606. doi: 10.1007/s00894-008-0315-y

Stevens, A. M., Queneau, Y., Soulere, L., von Bodman, S., and Doutheau, A. (2011). Mechanisms and synthetic modulators of AHL-dependent gene regulation. *Chem. Rev.* 111, 4–27. doi: 10.1021/cr100064s

Streit, W. R., and Entcheva, P. (2003). Biotin in microbes, the genes involved in its biosynthesis, its biochemical role and perspectives for biotechnological production. *Appl. Microbiol. Biotechnol.* 61, 21–31. doi: 10.1007/s00253-002-1186-2

Suppiger, A., Eshwar, A. K., Stephan, R., Kaever, V., Eberl, L., and Lehner, A. (2016). The DSF type quorum sensing signalling system RpfF/R regulates diverse phenotypes in the opportunistic pathogen *Cronobacter*. *Sci. Rep.* 6:18753. doi: 10.1038/srep18753

Talla, E., Tekaia, F., Brino, L., and Dujon, B. (2003). A novel design of whole-genome microarray probes for *Saccharomyces cerevisiae* which minimizes cross-hybridization. *BMC Genomics* 4:38. doi: 10.1186/1471-2164-4-38

Ueda, A., and Wood, T. K. (2009). Connecting quorum sensing, c-di-GMP, pel polysaccharide, and biofilm formation in *Pseudomonas aeruginosa* through tyrosine phosphatase TpbA (PA3885). *PLoS Pathog.* 5:e1000483. doi: 10.1371/journal.ppat.1000483

Valdés, J., Pedroso, I., Quatrini, R., and Holmes, D. S. (2008). Comparative genome analysis of *Acidithiobacillus ferrooxidans*, *A. thiooxidans* and *A. caldus*: insights into their metabolism and ecophysiology. *Hydrometallurgy* 94, 180–184. doi: 10.1016/j.hydromet.2008.05.039

Valenzuela, S., Banderas, A., Jerez, C. A., and Guiliani, N. (2007). "Cell-cell communication in bacteria," in *Microbial Processing of Metal Sulfides*, eds E. R. Donati and W. Sand (Dordrecht: Springer), 253–264.

Valenzuela, S., Banderas, A., Jerez, C. A., and Guiliani, N. (2017). "Cell-cell communication in bacteria: a promising new approach to improve bioleaching efficiency?," in *Microbial Processing of Metal Sulfides*, eds E. R. Donati and W. Sand (Dordrecht: Springer), 253–264.

Vallenet, D., Belda, E., Calteau, A., Cruveiller, S., Engelen, S., Lajus, A., et al. (2013). MicroScope–an integrated microbial resource for the curation and comparative analysis of genomic and metabolic data. *Nucleic Acids Res.* 41, D636–D647. doi: 10.1093/nar/gks1194

Varga, Z. G., Armada, A., Cerca, P., Amaral, L., Mior Ahmad Subki, M. A., Savka, M. A., et al. (2012). Inhibition of quorum sensing and efflux pump system by trifluoromethyl ketone proton pump inhibitors. *In Vivo* 26, 277–285.

Vasil, M. L. (2003). DNA microarrays in analysis of quorum sensing: strengths and limitations. *J. Bacteriol.* 185, 2061–2065. doi: 10.1128/JB.185.7.2061-2065.2003

Venturi, V., and Subramoni, S. (2009). Future research trends in the major chemical language of bacteria. *HFSP J.* 3, 105–116. doi: 10.2976/1.3065673

Vera, M., Krok, B., Bellenberg, S., Sand, W., and Poetsch, A. (2013). Shotgun proteomics study of early biofilm formation process of *Acidithiobacillus ferrooxidans* ATCC 23270 on pyrite. *Proteomics* 13, 1133–1144. doi: 10.1002/pmic.201200386

Wagner, V. E., Bushnell, D., Passador, L., Brooks, A. I., and Iglewski, B. H. (2003). Microarray analysis of *Pseudomonas aeruginosa* quorum-sensing regulons: effects of growth phase and environment. *J. Bacteriol.* 185, 2080–2095. doi: 10.1128/JB.185.7.2080-2095.2003

Waters, C. M., and Bassler, B. L. (2005). Quorum sensing: cell-to-cell communication in bacteria. *Annu. Rev. Cell Dev. Biol.* 21, 319–346. doi: 10.1146/annurev.cellbio.21.012704.131001

Waters, C. M., Lu, W., Rabinowitz, J. D., and Bassler, B. L. (2008). Quorum sensing controls biofilm formation in *Vibrio cholerae* through modulation of cyclic di-GMP levels and repression of *vpsT*. *J. Bacteriol.* 190, 2527–2536. doi: 10.1128/JB.01756-07

Wickstrom, C., Chavez de Paz, L., Davies, J. R., and Svensater, G. (2013). Surface-associated MUC5B mucins promote protease activity in *Lactobacillus fermentum* biofilms. *BMC Oral Health* 13:43. doi: 10.1186/1472-6831-13-43

Williams, K. P., and Kelly, D. P. (2013). Proposal for a new class within the phylum Proteobacteria, Acidithiobacillia classis nov., with the type order Acidithiobacillales, and emended description of the class Gammaproteobacteria. *Int. J. Syst. Evol. Microbiol.* 63, 2901–2906. doi: 10.1099/ijs.0.049270-0

Wong, H. S., Maker, G. L., Trengove, R. D., and O'Handley, R. M. (2015). Gas chromatography-mass spectrometry-based metabolite profiling of *Salmonella enterica* serovar typhimurium differentiates between biofilm and planktonic phenotypes. *Appl. Environ. Microbiol.* 81, 2660–2666. doi: 10.1128/AEM.03658-14

Yarzabal, A., Duquesne, K., and Bonnefoy, V. (2003). Rusticyanin gene expression of *Acidithiobacillus ferrooxidans* ATCC 33020 in sulfur- and in ferrous iron-media. *Hydrometallurgy* 71, 107–114. doi: 10.1016/S0304-386X(03)00146-4

Yeom, J., Shin, J. H., Yang, J. Y., Kim, J., and Hwang, G. S. (2013). (1)H NMR-based metabolite profiling of planktonic and biofilm cells in *Acinetobacter baumannii* 1656-2. *PLoS ONE* 8:e57730. doi: 10.1371/journal.pone.0057730

Yepes, A., Schneider, J., Mielich, B., Koch, G., Garcia-Betancur, J. C., Ramamurthi, K. S., et al. (2012). The biofilm formation defect of a *Bacillus subtilis* flotillin-defective mutant involves the protease FtsH. *Mol. Microbiol.* 86, 457–471. doi: 10.1111/j.1365-2958.2012.08205.x

Zhang, L. H. (2010). A novel c-di-GMP effector linking intracellular virulence regulon to quorum sensing and hypoxia sensing. *Virulence* 1, 391–394. doi: 10.4161/viru.1.5.12487

Conflict of Interest Statement: The authors declare that the research was conducted in the absence of any commercial or financial relationships that could be construed as a potential conflict of interest.

frontiers in Microbiology

ORIGINAL RESEARCH
published: 22 December 2016
doi: 10.3389/fmicb.2016.02082

Reconstruction of the Metabolic Potential of Acidophilic *Sideroxydans* Strains from the Metagenome of an Microaerophilic Enrichment Culture of Acidophilic Iron-Oxidizing Bacteria from a Pilot Plant for the Treatment of Acid Mine Drainage Reveals Metabolic Versatility and Adaptation to Life at Low pH

***Martin Mühling*[1]*, *Anja Poehlein*[2], *Anna Stuhr*[1], *Matthias Voitel*[1], *Rolf Daniel*[2] and *Michael Schlömann*[1]**

[1] *Institute of Biological Sciences, Technische Universität Bergakademie Freiberg, Freiberg, Germany,*
[2] *Georg-August-University Göttingen, Genomic and Applied Microbiology and Göttingen Genomics, Laboratory, Göttingen, Germany*

OPEN ACCESS

Edited by:
Robert Duran, University of Pau and Pays de l'Adour, France

Reviewed by:
Mario A. Vera, Pontifical Catholic University of Chile, Chile
Daniel Seth Jones, University of Minnesota, USA

***Correspondence:**
Martin Mühling
martin.muehling@ioez.tu-freiberg.de

Specialty section:
This article was submitted to Extreme Microbiology, a section of the journal Frontiers in Microbiology

Received: *30 September 2016*
Accepted: *08 December 2016*
Published: *22 December 2016*

Citation:
Mühling M, Poehlein A, Stuhr A, Voitel M, Daniel R and Schlömann M (2016) Reconstruction of the Metabolic Potential of Acidophilic Sideroxydans Strains from the Metagenome of an Microaerophilic Enrichment Culture of Acidophilic Iron-Oxidizing Bacteria from a Pilot Plant for the Treatment of Acid Mine Drainage Reveals Metabolic Versatility and Adaptation to Life at Low pH. Front. Microbiol. 7:2082. doi: 10.3389/fmicb.2016.02082

Bacterial community analyses of samples from a pilot plant for the treatment of acid mine drainage (AMD) from the lignite-mining district in Lusatia (East Germany) had previously demonstrated the dominance of two groups of acidophilic iron oxidizers: the novel candidate genus "*Ferrovum*" and a group comprising *Gallionella*-like strains. Since pure culture had proven difficult, previous studies have used genome analyses of co-cultures consisting of "*Ferrovum*" and a strain of the heterotrophic acidophile *Acidiphilium* in order to obtain insight into the life style of these novel bacteria. Here we report on attempts to undertake a similar study on *Gallionella*-like acidophiles from AMD. Isolates belonging to the family *Gallionellaceae* are still restricted to the microaerophilic and neutrophilic iron oxidizers *Sideroxydans* and *Gallionella*. Availability of genomic or metagenomic sequence data of acidophilic strains of these genera should, therefore, be relevant for defining adaptive strategies in pH homeostasis. This is particularly the case since complete genome sequences of the neutrophilic strains *G. capsiferriformans* ES-2 and *S. lithotrophicus* ES-1 permit the direct comparison of the metabolic capacity of neutrophilic and acidophilic members of the same genus and, thus, the detection of biochemical features that are specific to acidophilic strains to support life under acidic conditions. Isolation attempts undertaken in this study resulted in the microaerophilic enrichment culture ADE-12-1 which, based on 16S rRNA gene sequence analysis, consisted of at least three to four distinct *Gallionellaceae* strains that appear to be closely related

to the neutrophilic iron oxidizer *S. lithotrophicus* ES-1. Key hypotheses inferred from the metabolic reconstruction of the metagenomic sequence data of these acidophilic *Sideroxydans* strains include the putative role of urea hydrolysis, formate oxidation and cyanophycin decarboxylation in pH homeostasis.

Keywords: acid mine drainage, metagenomics, iron oxidation, microaerophilic bacteria, *Gallionella*, *Sideroxydans*, pH homeostasis, cyanophycin

INTRODUCTION

The lignite-mining district in Lusatia (Germany) is rich in pyrite and marcasite. Mining activities, therefore, cause a dramatic increase in pyrite/marcasite surface exposure and subsequent oxidative processes which, in turn, result in acidic waters with high sulfate and ferrous iron loads. Remediation of these acidic waters is required in order to avoid environmental damage following drainage from active and abandoned mines. Key to the unceasing formation of these acid mine drainage (AMD) waters is the continuous oxidation of ferrous iron to ferric iron which itself is the main oxidant in this process. Acidophilic iron-oxidizing bacteria that gain energy for their metabolic activities from the oxidation of ferrous iron to ferric iron at low pH play a pivotal part, because their activity ensures sustained ferrous iron oxidation at pH levels where ferrous iron becomes stable even in the presence of oxygen.

Although, acidophilic iron-oxidizing bacteria are largely responsible for the generation of AMD, they can also contribute to the reduction of its iron and of some of its sulfate load *via* ferrous iron oxidation with subsequent precipitation of ferric iron hydroxysulfate minerals (Janneck et al., 2010). An example of such a biotechnological process is provided by the treatment plant Tzschelln (Janneck et al., 2010), a 10-qm^3 pilot-scale operation (**Figure 1**) for the bioremediation of AMD water from the open-pit lignite mine Nochten (Lusatia, Germany). This process involves, in essence, the aeration of AMD water and subsequent ferrous iron oxidation by acidophilic iron-oxidizing microorganisms. The resulting ferric iron then precipitates as the amorphous iron hydroxy sulfate mineral schwertmannite ($Fe_{16}[O_{16}|(OH)_{10}|(SO_4)_3] \bullet 10\ H_2O$; Bigham et al., 1996), because the average hydraulic retention time (8 h) of the AMD water within the treatment plant ensures that the pH is maintained at approximately 3 (pH 2.85–3.1). Schwertmannite has various applications as a pigment or as a sorbent for the removal of arsenic from aqueous solutions (Janneck et al., 2010).

Since the microbial community within this treatment plant is likely to play a fundamental role in the performance of the biotechnological process, it has been investigated in a series of studies covering almost 10 years. Employing culture independent molecular techniques, surveys of the bacterial diversity within the treatment plant Tzschelln previously revealed the dominance of two bacterial groups: strains belonging to the novel putative genus "*Ferrovum*" (Johnson et al., 2014) and strains that are, based on their 16S rRNA gene sequences, related to neutrophilic iron-oxidizing strains of the genus *Gallionella* (Heinzel et al., 2009a,b). *Acidithiobacillus* strains were also detected in the AMD entering the treatment plant, though these only played a minor role within the oxidation basin of the treatment plant (Heinzel et al., 2009a). Moreover, the same observations were made following the commissioning of a new pilot plant where "*Ferrovum*" and *Gallionella*-like strains also dominated the bacterial diversity throughout an annual cycle (Heinzel et al., 2009b). Both bacterial groups belong to the *Betaproteobacteria* and, therefore, represent the first acidophilic iron oxidizers within this phylogenetic class (Hallberg et al., 2006; Mosler et al., 2013; Johnson et al., 2014; Ullrich et al., 2016a,b). At that time, the genus *Gallionella* was only known to comprise iron oxidizing strains that occur in circumneutral and microaerobic environments rich in ferrous iron (e.g., Hanert, 1968). In contrast to this, much less was known of the genus "*Ferrovum*" which was newly proposed to accommodate streamer forming acidophilic iron oxidizing strains with an autotrophic life style (e.g., Hallberg et al., 2006; Johnson et al., 2014).

Attempts to isolate "*Ferrovum*" strains or representatives of the acidophilic *Gallionella* relatives were initially based on the use of the overlay-plate technique in combination with the iFe medium (e.g., Johnson et al., 2014), which is a modified version of a medium developed for a broad range of acidophilic iron oxidizers (Johnson and McGinness, 1991; Johnson and Hallberg, 2007). However, the subsequent development and use of a novel medium (Artificial Pilot Plant Water – APPW – medium) that simulates the chemical composition of the water within the treatment plant resulted in cultures composed of two strains, a "*Ferrovum*" and an *Acidiphilium* strain (Tischler et al., 2013; Ullrich et al., 2015). All attempts to obtain clonal cultures of "*Ferrovum*" strains from these mixed cultures failed, though this did not prevent detailed genome analyses of three "*Ferrovum*" strains (Ullrich et al., 2016a,b). The presence of *Acidiphilium* in any of the "*Ferrovum*"-containing cultures may partially be explained by hydrolysis of agar or agarose (used as solidifying agent) at pH 3 which results in the release of organic acids that seem to be toxic to "*Ferrovum.*" The heterotrophic *Acidiphilium* contaminant is capable of oxidizing these organic acids to carbon dioxide and, by doing so, provides an improved environment for growth of "*Ferrovum*" (Ullrich et al., 2015). This also indicates that *Acidiphilium* in the lower layer of the overlay-plate (Johnson and McGinness, 1991; Johnson and Hallberg, 2007) was in these cases insufficient to remove all of the organic molecules from the top layer where the samples were plated on. Once present within a "*Ferrovum*" colony on solidified media, *Acidiphilium* can apparently not easily be removed in subsequent efforts that merely favor growth of the iron oxidizers in the mixed culture, an observation that has also been made by others (Johnson et al., 2014).

Using the same approach the isolation of the acidophilic *Gallionella* relatives proved even more difficult and did not even result in a mixed culture, though colonies on overlay-plates screened by PCR with *Gallionella*-specific primers indicated in some instances their presence (Gelhaar, 2012). Interestingly, comparative media tests also showed that most colonies harboring acidophilic *Gallionella* relatives were obtained with a modified version of the APPW medium in which the phosphate concentration was adapted to that of the iFe medium (APPW-PO4 medium: Tischler et al., 2013). Whether phosphate addition is the most important trigger for improved recovery of acidophilic *Gallionella* relatives remains to be determined since an overall reduction of the number of colonies, in particular those comprising *Acidithiobacillus* strains, may indicate potential indirect effects.

Nevertheless, all subsequent enrichment campaigns for *Gallionella* relatives were built on the use of APPW-PO4, but—assuming a microaerophilic life style similar to that of the neutrophilic iron oxidizer *Gallionella ferruginea*—in combination with the gradient tube technique developed by Kucera and Wolfe (1957) for the isolation of neutrophilic iron-oxidizing *Gallionella* strains. Additionally, the pH of the APPW-PO4 was adjusted to 3.5 in order to simulate the acidic pH of the AMD within treatment plant Tzschelln. Given the difficulties with respect to isolation of clonal cultures, we aimed to employ a metagenomic approach for the analysis of such an enrichment culture followed by subsequent reconstruction of metabolic features of acidophilic *Gallionellaceae* strains.

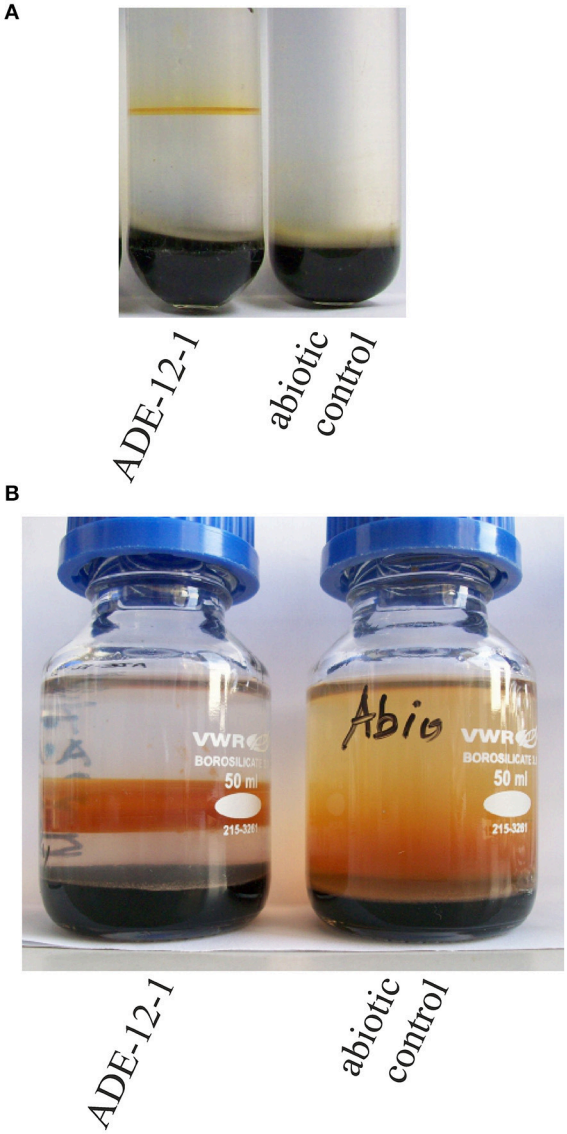

FIGURE 1 | Photographs of enrichment culture ADE-12-1 in gradient tube (A) and as 50-mL volume gradient culture **(B)**. Photographs were taken after 14 days **(A)** or 35 days **(B)** of incubation.

MATERIALS AND METHODS

Origin of Samples and Enrichment of Microaerophilic Strains

The AMD sample used to obtain enrichment cultures was collected on 19 March 2014 from the inflow into the treatment plant Tzschelln. A 100-μL aliquot of the AMD was used to inoculate gradient tubes (see below) on 20 March 2014.

Enrichment of microaerophilic and acidophilic iron-oxidizing microorganisms was achieved using gradient tubes of semi-solid APPW-PO4 and incubation in microaerobic chambers (2.5 L Anaerojar with Campygen pads, OXOID). This approach was based on the assumption that the acidophilic *Gallionella*-like strains are physiologically similar to neutrophilic *Gallionella* which have long been known to occur mainly under ferrous iron rich and oxygen limiting conditions (Engel and Hanert, 1967). Gradient tubes originally developed by Kucera and Wolfe (1957) were produced by encapsulating iron sulfide (prepared according to Emerson and Floyd, 2005) within agarose (0.5% w/v) at the bottom of a glass tube, with a semi-solid [0.15% (w/v) agarose] layer of APPW-PO4 medium (pH 3.5) atop. Tests had shown that this setup led to better results than those using, for instance, iron carbonate as source of ferrous iron (data not shown). Additionally, a semisolid layer proved also to be superior for the isolation of microaerophilic enrichment cultures in comparison to a liquid layer of APPW-PO4 medium, similar to what has been suggested by Hallbeck et al. (1993). The pH within the semi-solid medium in uninoculated control tubes was found to be constant. Although, the pH was not determined within enrichment culture ADE-12-1 we believe that it did not increase since precipitation of ferric iron results in the release of protons.

Analysis of the Bacterial Diversity

Genomic DNA extraction from the microaerophilic enrichment culture ADE-12-1 was carried out using the PowerSoil DNA Isolation Kit (MoBio). PCR amplification of approx. 1300-bp 16S rRNA gene fragments was achieved using primers 27f (5′-AGAGTTTGATCCTGGCTCA) and 1387r

(5′-GGGCGG(AT)GTGTACAAGGC) and a cycle protocol consisting of an initial denaturing step at 95°C for 5 min followed by 30 cycles (95°C for 30 s, 55°C for 30 s, 72°C for 90 s) and a final extension step at 72°C for 5 min. PCRs were carried out in 25-μL volumes containing 20 μmol L^{-1} of each of the two primers, 1.5 mmol L^{-1} $MgCl_2$, 8 μmol L^{-1} of each of the dNTPs, 2 U of DreamTaq DNA polymerase and 15 ng of genomic DNA as template for amplification. The PCR amplicons of two independent PCRs were combined in order to limit the impact of potential differences between the setups for the PCRs. PCR amplicons were subsequently purified using the Ultra Clean PCR Clean-Up Kit (MoBio) and ligated into the pSC-A-amp/kan Vektor using the StrataClone PCR Cloning Kit (Stratagene) according to the manufacturer's protocol. These constructs were finally transformed into the StrataClone SoloPack competent cells (Stratagene). 100 clones were screened by amplified ribosomal DNA restriction analysis (ARDRA). In brief, 4 μL of a PCR product obtained with vector primers T3 and T7 were digested in a 10-μL reaction with 1 U of restriction endonuclease BsuRI (Fermentas). The nucleotide sequence of a total of 30 clones representing the 18 observed restriction patterns were subsequently determined using Sanger sequencing (Eurofins Genomics, Germany).

Alignment of the 16S rRNA gene sequences and amino acid sequences was performed within ARB (Ludwig et al., 2004) against the SILVA database (Pruesse et al., 2007) or within MEGA 6 (Tamura et al., 2013), respectively. Phylogenetic analyses were carried out using the neignor-joining approach within MEGA 6 (Tamura et al., 2013).

16S-tag amplicons for subsequent Illumina sequence analysis were obtained according to Illumina's 16S Metagenomic Sequencing Library Preparation protocol which aims at PCR amplification of the V3-V4 region of the 16S rRNA gene using the PCR primers recommended by Klindworth et al. (2013). However, instead of an aliquot of the genomic DNA preparations an approx. 1300-bp PCR product (obtained with primers 27f/1387r) was used as template for the index PCR during Nextera library preparation. This was necessary since direct amplification of the V3-V4 region from genomic DNA using the PCR primers of Klindworth et al. (2013) did not result in any PCR product. Although, this represents a nested PCR approach, it should still permit a reliable comparison of the results with those from the sequence analysis of the clone library of 16S rRNA gene fragments which was based on the same 1300-bp PCR amplicons (see above).

16S-tag Illumina datasets were processed with Usearch version 8.1.1861 (Edgar, 2010). Paired-end reads were truncated to 250 bp to remove low-quality sequence tails, subsequently merged and quality-filtered. Filtering included the removal of low quality reads (maximum number of expected errors >1 and more than 1 ambiguous base). Processed sequences of all samples were joined and clustered into operational taxonomic units (OTUs) at 3% genetic divergence using the UPARSE algorithm implemented in Usearch. Chimeric sequences were identified *de novo* during clustering and removed together with singletons (OTUs consisting of only one sequence). Afterwards, putative chimeric sequences were removed using the Uchime algorithm implemented in Usearch in reference mode with the most recent RDP training set (version 15) as reference dataset (Cole et al., 2009). Afterwards, OTU sequences were taxonomically classified using a BLAST alignment against the most recent SILVA database (SILVA SSURef 123 NR) (Quast et al., 2013). All non-bacterial OTUs were removed based on their taxonomic classification in the database. Subsequently, processed sequences were mapped to OTU sequences to calculate the distribution and abundance of each OTU in every sample.

Metagenome Sequencing, Assembly and Annotation

Metagenome sequencing of the microaerophilic enrichment culture ADE-12-1 was performed at the Göttingen Genomics Laboratory (G2L, Göttingen University, Germany) *via* a hybrid approach using the Genome Analyzer (GA) II and the MiSeq (Illumina). The shotgun library was prepared according to the manufacturers' protocol. This involved the use of the Nextera library preparation. The library was sequenced on the Genome Analyzer IIx using the TruSeq SBS Kit V5-GA and on the Miseq instrument using MiSeq reagent kit version 3 as recommended by the manufacturer (Illumina, San Diego, CA, USA). Sequencing resulted in 8,364,879 reads (2 × 112 bp) sequenced on the GA IIx and 11,075,962 reads (2 × 301 bp) on the MiSeq. The paired-end Illumina sequence reads were pre-processed using Trimmomatic with quality filter Phred33 (Bolger et al., 2014) resulting in trimmed sequence reads with a mean length of 92.7 and 201 bp, respectively.

De novo assembly of the total of 8,184,130 trimmed paired-end GA II and 10,406,346 MiSeq reads was achieved using SPAdes 3.7.0. (This version includes the metaSPAdes metagenomic pipeline, Bankevich et al., 2012). The assembly were inspected and quality checked using Qualimap (García-Alcalde et al., 2012).

Automated gene prediction and annotation was conducted with PROKKA (Seemann, 2014). Phylogenetic assignment of annotated contigs was achieved *via* Blast comparison with the NCBI database using Blobology (https://github.com/blaxterlab/blobology). These analyses were performed using the default settings of the various programs. This Whole Genome Shotgun project has been deposited at DDBJ/ENA/GenBank under the accession MLJW00000000. The version described in this paper is version MLJW01000000. The unassembled nucleotide sequence reads are available at the Sequence Read Archive of the NCBI *via* accession numbers SRR5040535 (GAII sequence reads) and SRR5040536 (MiSeq sequence reads).

Transmembrane helices in protein sequences were identified by TMHMM 2.0 using the default settings (Möller et al., 2001, http://www.cbs.dtu.dk/services/TMHMM/ which was accessed on 19 September 2016).

RESULTS AND DISCUSSION

Attempts to enrich microaerophilic strains from AMD collected at the inflow into the treatment plant Tzschelln were based on

the previous finding using culture-independent approaches that *Gallionella*-like strains were more abundant in the near-anoxic inflow AMD than in samples collected from the oxidation basin of the treatment plant Tzschelln (Gelhaar, 2012). These attempts resulted in various cultures of which enrichment culture ADE-12-1 (**Figure 1A**) was chosen for further metagenomic analysis. An aliquot of culture ADE-12-1 was transferred into an oxygen-ferrous iron-gradient in a 50-mL bottle (**Figure 1B**) in order to obtain sufficient biomass for subsequent isolation of total genomic DNA. Extraction of the total nucleic acid fraction of this 50-mL culture after 35 days of incubation provided 1.2 μg of DNA.

Metagenome Assembly of *Sideroxydans* Related Contigs

Illumina-based sequence analysis of the metagenomic DNA extracted from enrichment culture ADE-12-1 provided 20,563,010 GAII and 10,406,346 MiSeq sequence reads which were assembled into 9456 contigs totalling 56.8 Mb of metagenomic sequence information. Although, only 762 of these contigs were larger than 10 kb, these still represent approximately two thirds (38 Mb) of the total sequence information. Therefore, and due to the fact that the contigs < 10 kb encode only up to 10 ORFs further detailed analyses focused on contigs > 10 kb (Supplementary Table 1A). Key information on the metagenomic sequence data obtained for enrichment culture ADE-12-1 are summarized in **Table 1**.

Blast-based sequence comparison of the individual contig sequences assigned 738 of the 762 contigs (Supplementary Table 1A) to phylogenetic groups (in general to genus or species level) that were largely also detected by sequence analysis of PCR-amplified 16S rRNA gene fragments (Supplementary Table 2, **Table 2**). Only 64 of these remaining 738 contigs (8.8%) seem to have derived from *Sideroxydans* or *Sideroxydans*-like strains (**Table 1**, Supplementary Table 1B). However, these 738 contigs comprise approximately a quarter of the metagenomic sequence information (9.8 Mb of the 38 Mb of total metagenomic sequence data encoded within contigs > 10 kb: **Table 1**, Supplementary Table 1B) since most of the largest contigs are among those. For example, the 13 largest contigs assigned to *Sideroxydans* total more than half (5.01 Mb) of the sequence information encoded by the 64 contigs > 10 kb. Therefore, and despite 12 contigs being < 50 kb, the 64 contigs averaged 155 kb in size and were sequenced with an approximately 150-fold coverage. In total, the 64 contigs encode 9673 ORFs (**Table 1**).

Bacterial Diversity within the AMD Sample and within the Microaerophilic Enrichment Culture ADE-12-1

The metagenomic dataset (**Table 1**) contains only 13 contigs that harbor a 16S rRNA gene or gene fragment, with four instances in which the 16S rRNA sequence was part of a large contig (> 100 kb). In the other cases the 16S rRNA sequences were individual sequence reads or within small contigs (up to ca. 32 kb, Supplementary Table 3). This is not surprising since ribosomal gene clusters often occur in multiple copies within genomes which, in turn, affects the assembly of the raw data. The genomes of the microaerophilic strains *S. lithotrophicus* ES-1 and *G. capsiferriformans* ES-2, are, for instance, known to harbor two (ES-1) or three (ES-2) ribosomal RNA operons (Emerson et al., 2013). Blast analysis of these 16S rRNA gene fragments from the metagenomic dataset confirmed the presence of eight genera (*Sideroxydans*, *Telmatospirillum*, *Cellulomonas*, *Sulfuritalea*, *Sediminibacterium*, *Thiomonas*, *Methylotenera*, *Opitutus*) from four phyla (*Proteobacteria*, *Actinobacteria*, *Bacteroidetes*, *Verrucomicrobia*). However, the 16S rRNA gene

TABLE 1 | Metagenomic sequence information obtained for the microaerophilic enrichment culture ADE-12-1.

General information on the metagenomic sequence data	Total		*Sideroxydans*	
	Value or range	Average	Value or range	Average
Total sequence length (Mb)	56.8	–	10.1	–
Contigs	9456	–	92	–
Contigs > 10 kb	762[a]	–	64[b]	–
Total sequence length (Mb)[c]	38.1	–	9.8	–
Contig size (kb)[c]	10–901.1	49.9 kb	15.3–901.1	155
Coverage (fold)[c]	5.2–280.3	68.7[d]	73.9–222	150.2[d]
GC content (%)[c]	73.6–34.8	58.9[d]	51–61%	58.6%[d]
ORFs[c]	35,340	–	9673	–
ORFs per contig[c]	10–891	46.5	12–891	151.1

[a] *24 of these contigs could not be assigned to specific taxa.*
[b] *Contig GALL_all_contig000366 was removed from the dataset due to low coverage (8-fold); it also had the highest average GC content (61.5%).*
[c] *Of those > 10 kb.*
[d] *The average was calculated taking the contig length into consideration (i.e., values per base).*

TABLE 2 | 16S rRNA based analysis of the bacterial diversity within the microaerophilic enrichment culture ADE-12-1.

	16S rRNA library[a]	16S-tag Illumina[b]
–Total number of clones or sequence reads	100	42,639
–Most abundant taxa within ADE-12-1 and *Gallionella*		
• *Telmatospirillum*	14 (14%)	19,680 (46.2%)
• *Opitutus*	13 (13%)	9261 (21.7%)
• *Sideroxydans* (total)[c]	70 (70%)	4133 (9.7%)
OTU_31[d]	–	4131 (99.95%)
OTU_1160[d]	–	1 (0.002%)
OTU_1869[d]	–	1 (0.002%)
• *Gallionellaceae*	70 (70%)	4178 (9.8%)
Percentage *Sideroxydans* of *Gallionellaceae*[c]	100%	98.92%
• *Gallionella*[c]	0 (0%)	0 (0%)

[a] *Number of clones screened by ARDRA with subsequent sequence analysis of representatives of each ARDRA group.*
[b] *Numbers represent 16S-tag sequence reads.*
[c] *Only those reads were considered that were assigned to genus level.*
[d] *Of total Sideroxydans reads.*

fragments of neither neutrophilic *Gallionella* nor acidophilic *Gallionella*-like strains (Heinzel et al., 2009a) were closest (BLAST) hits to any of the 16S rRNA sequences detected in the metagenomic data. One of the 16S rRNA gene fragments showed highest sequence similarity to *Sideroxydans lithotrophicus* strain ES-1 (Supplementary Table 3).

To obtain more information on the bacterial diversity within enrichment culture ADE-12-1, sequence analysis of PCR-amplified 16S ribosomal RNA gene fragments was used in a two-tier approach that aimed at providing both: robust assignment of sequence reads to specific taxa (i.e., Sanger sequence analysis of clones from a clone library of large gene fragments) and (near) complete coverage of the diversity (i.e., 16S-tag Illumina sequence analysis). Blast-based comparison of the nucleotide sequences obtained from the clone library of approx. 1300-bp 16S rRNA gene fragments with the entries in the SILVA database (Pruesse et al., 2007) confirmed that *Sideroxydans*-like strains were abundant in enrichment culture ADE-12-1 and that no close *Gallionella* strains seem to be present (**Table 2**). Although, the extent of their dominance was found to be lower, *Sideroxydans* strains still represent almost 10 % of the bacterial cells within enrichment culture ADE-12-1 when analyzed by 16S-tag Illumina sequencing (**Table 2**), an approach that avoids a potential bias caused by the preparation of a clone library (i.e., cloning). Taxa that, based on the 16S-tag Illumina sequencing approach, were found to dominate enrichment culture ADE-12-1 were *Telmatospirillum* (*Alphaproteobacteria*) and *Opitutus* (*Verrucomicrobia*) (**Table 2**). Again, *Gallionella*-derived sequences were not detected among the 42,639 Illumina sequence reads (**Table 2**). A phylogenetic analysis of the 16S rRNA sequences from the clone library and from the metagenomic data further confirmed the results and indicates the presence of at least three to four different *Sideroxydans* and *Sideroxydans*-like groups of strains (**Figure 2**).

In summary, the application of the gradient tube technique proved to be successful for the cultivation and enrichment of microaerophilic iron-oxidizing *Sideroxydans*-like strains from AMD. The absence of any *Gallionella* strains raises, however, the question as to the reasons for the observed discrepancy to the results previously reported for the same environment; that is, the abundance of *Sideroxydans* strains *versus* that of *Gallionella*-like strains (Heinzel et al., 2009a,b; Gelhaar, 2012). Clearly, the samples tested in previous studies (Heinzel et al., 2009a,b) and that used as inoculum for enrichment culture ADE-12-1 were collected at different times (2007 vs. 2014, respectively) and the observed results may indeed reflect a shift in the bacterial community within the AMD inflow to the treatment plant Tzschelln. However, the methodological approaches used by Heinzel et al. (2009a,b) for the analysis of the bacterial diversity (ARDRA analysis of clones from a library of 16S rRNA gene fragments: Heinzel et al., 2009a) and the quantification of *Gallionella*-like strains (terminal restriction fragment length polymorphism (TRFLP) analysis and real-time qPCR: Heinzel et al., 2009b) were also scrutinized in order to uncover potential causes for the different results. This examination revealed that neither the ARDRA nor the TRFLP approach distinguishes between *Gallionella* and *Sideroxydans* strains (results not shown). In contrast to this, the real-time qPCR approach withstands this scruntiny, in particular due to a mismatch between the 3′-end base of reverse primer 384r (Heinzel et al., 2009b) and its corresponding binding site within *Sideroxydans* strains (results not shown). The discrepancy between the results obtained by Heinzel et al. (2009b) from real-time qPCR and TRFLP analyses may, therefore, be explained by the possible detection of *Sideroxydans* strains in the samples from the treatment plant Tzschelln by one (TRFLP) but not the other (real-time qPCR) methodological approach.

Nevertheless, the culture conditions applied and the observation of rust-like precipitates, which most likely represent ferric iron hydroxy-like compounds, and the close 16S rRNA sequence similarity to that of *S. lithotrophicus* strain ES-1 indicate that microaerophilic iron-oxidizing microorganisms were enriched that can withstand low pH conditions. Moreover, the metagenomic sequence data obtained for enrichment culture ADE-12-1 proved to be particularly relevant in defining adaptive strategies to pH homeostasis, since the family *Gallionellaceae* had previously only been known to consist of the microaerophilic and neutrophilic iron oxidizers *Gallionella* and *Sideroxydans*. That is, the availability of the complete genome of the neutrophilic *S. lithotrophicus* strain ES-1 (Emerson et al., 2013) now permits the detailed comparison of the metabolic capacity of neutrophilic and acidophilic members of the same genus and, thus, the detection of biochemical features that are present in acidophilic strains to support life under acidic conditions. Attempts were therefore undertaken to reconstruct the metabolic potential of these acidophilic strains from the metagenomic sequence data assigned to *Sideroxydans* strains.

Metabolic Reconstruction from *Sideroxydans* Metagenomic Contigs

Reconstruction of metabolic traits was based on the analysis of the automated annotation of the 9673 ORFs assigned to members of this genus (**Table 1**) and provided new insights into the life style of acidophilic representatives of the genus *Sideroxydans*. Overall, the analysis of this fraction of the metagenomic dataset focused on nutrient assimilation, energy production and strategies for pH homeostasis. The findings reported here indicate that acidophilic *Sideroxydans* strains have a wider repertoire of metabolic features available in this respect than found in the genome sequence of the neutrophilic *S. lithotrophicus* strain ES-1 (Emerson et al., 2013). However, this has to be seen in the context of the obvious imbalance of available genome data of neutrophilic strains (i.e., only that of strain ES-1) versus the metagenome comprised of presumably several strains. This has to be taken into account throughout the following discussions which directly compare metabolic features reconstructed from the metagenomic dataset with those of the neutrophilic strain ES-1. In this context, it should be noted that reference is made to acidophilic *Sideroxydans* strains independent of the fact that the genomic and metabolic features which are discussed may be present only in one strain or are shared by several strains. Similarly, it remains inconclusive

FIGURE 2 | Evolutionary relationship of strains detected within culture ADE-12-1 based on an alignment of 16S rRNA gene fragments. Sequences were obtained from the metagenomic dataset (see Supplementary Table 3) and from the sequence analysis of the clone library of 16S rRNA gene fragments (see **Table 2**). The position of three 16S rRNA gene fragments (out of the total of 13) from the metagenomic dataset was determined separately due to the short overlapping region (ca. 205 bp) with the other sequences. This was achieved by adding them to an identical neighbor-joining tree using the parsimony option within ARB. Their positions within the tree are indicated by arrows. Calculation of phylogenetic trees was conducted within MEGA 6 (Tamura et al., 2013). The position of *S. lithotrophicus* ES-1 is highlighted in bold and red characters.The bars next to the position of *S. lithotrophicus* ES-1 and related strains indicate potential clusters. The evolutionary history was inferred using the Neighbor-Joining method in combination with the Jukes-Cantor model (Saitou and Nei, 1987) and bootstrap tests (1000 replicates; Felsenstein, 2004). Only bootstrap values > 70 % are shown next to the branches. There were a total of 683 positions in the final dataset. The 16S rRNA gene fragment of *Pyrococcus furiosus* was used as outgroup.

whether all or only some of the metabolic features are present within a particular strain.

Nutrient Assimilation and Biomass Production

As mentioned above, the metagenomic sequence data assigned to acidophilic *Sideroxydans* strains indicate a more extensive metabolic potential for nutrient assimilation than predicted for the neutrophilic strain ES-1 based on its genome sequence. An example for this is provided by the fact that strain ES-1 seems to be limited to inorganic phosphate as source of phosphorus while acidophilic *Sideroxydans* strains represented in the metagenomic dataset appear to have the potential to use phosphonates in addition to inorganic phosphate. Contig Gall_all_000077 contains a gene cluster comprising 14 genes (GALL_all_158100 - GALL_all_158230) which encode an ABC transporter for phosphonate uptake, a phosphonate lyase (C-P lyase, encoded by *phnJ*) together with all required accessory proteins (encoded by *phnGHIKLMNP*) (Supplementary Table 4A). In contrast to this, the genome of the neutrophilic strain ES-1 does not contain a homolog of this gene cluster, but only encodes three proteins with high sequence similarity to phosphonate uptake (Slit_1183) or to putative phosphonate utilization (Slit_1659, Slit_2972). In any case, psi-Blast searches with C-P lyases as query, including that from the metagenomic dataset, did not reveal any C-P lyase gene within the *Sideroxydans* ES-1 genome, thus indicating that, if strain ES-1 should be able to utilize phosphonates, it would be *via* a different route. Interestingly, the close localization of genes encoding a tRNA(-Met) (GALL_all_158020) and a transposase (GALL_all_158310) upstream and downstream of the phosphonate encoding gene cluster on contig000077, respectively, indicates that this gene cluster in the acidophilic *Sideroxydans* strain may have been acquired *via* horizontal gene transfer. Similarly, a transposase and an integrase are also located upstream and downstream of the phosphonate encoding gene cluster in the genome of *G. capsiferriformans* strain ES-2 which is highly similar to that on contig_000077. A possible explanation for this observation may be that the common ancestor of the *Gallionellaceae* has acquired the genetic ability to utilize phosphonates as a source of phosphorus which was later lost by the neutrophilic *S. lithotrophicus* strain ES-1. Following its uptake phosphate can then be stored in form of polyphosphate granules synthesized by the polyphosphate kinase (encoded by *ppk*) and liberated upon cellular phosphate depletion (*via* action of an exopolyphosphatase, encoded by *ppx*; Supplementary Table 4A).

Similar to the situation described for the utilization of phosphorus sources, the metagenomic sequence data assigned to *Sideroxydans* strains also indicate that the acidophilic strains seem to be more versatile regarding nitrogen assimilation than the neutrophile *S. lithotrophicus* ES-1, though—as mentioned above—the former may comprise several genetically different strains. The metagenomic dataset as well as the genome of strain ES-1 harbors genes that are predicted to code for the ability to assimilate ammonium, nitrate and nitrite and to fix elementary nitrogen *via* nitrogenase activity (Supplementary Table 4B). Genes related to nitrogen fixation are organized in several small gene clusters within each of the three contigs (contig000009, contig000013, contig000035) encoding a nitrogenase (Supplementary Table 4B), though all within close proximity to each other and to a Rnf complex encoding gene cluster. Expression of the nitrogenase may be regulated *via* reversible ADP-glycosylation of a specific arginine residue in the nitrogenase complex catalyzed by a dinitrogenase reductase glycohydrolase (DraG) and a dinitrogenase reductase ADP-ribosylation transferase (DraT). DraG and DraT are also encoded on contig000009 in close proximity to the nitrogenase. Such a mechanism has been described in detail for the alphaproteobacterium *Rhodospirillum rubrum* (Wang and Norén, 2006). Both the neutrophilic *Sideroxydans* strain ES-1 (Emerson et al., 2013) and the metagenomic data indicate that recycling (i.e., reduction) of ferredoxin, which is required by the dinitrogenase reductase as low potential reduction equivalents, is achieved *via* a Rnf membrane-integral protein complex. The energy for the uphill electron transport from NADH to ferredoxin, which is mediated by the Rnf complex, may be obtained through ion (H^+ or Na^+) influx across the membrane-bound Rnf complex (e.g., Biegel and Müller, 2010). However, the stoichiometric ratio of inflowing protons required for electron transfer from NADH to ferredoxin remains unclear since it depends on the prevailing membrane potential.

One of the acidophilic *Sideroxydans*-derived contigs (contig000112) also encodes a urease gene cluster (Supplementary Table 4B). The host cell of contig000112 therefore seems to be able to utilize urea as alternative nitrogen source, with urea being taken up *via* an ABC transporter (Gall_all_190370, Gall_all_190380, Gall_all_190390) encoded upstream of the urease gene cluster on the same contig (Supplementary Table 4B). In contrast to this, the genome of strain ES-1, which lacks a homolog of the urease gene cluster, harbors a four-gene cluster (Slit_0078 - Slit_0081) encoding an alternative urea utilization pathway which is not found among the *Sideroxydans*-assigned metagenomic contigs. This pathway involves urea carboxylase and allophanate hydrolase activity thought to be also involved in urea degradation (Hausinger, 2004; Kanamori et al., 2004, 2005). However, since this represents an ATP-dependent process and given the absence of obvious urea uptake mechanisms it may perhaps be more likely that this process is involved in a biosynthetic pathway (e.g., amino acid synthesis) in strain ES-1 rather than in urea utilization.

Assimilated nitrogen may subsequently be stored in form of cyanophycin *via* the action of two cyanophycin synthetases (CphA1, CphA2), both encoded next to each other (Supplementary Table 4B) and on three of the *Sideroxydans*-assigned contigs (contig000008, contig000020, contig000031). The fact that none of the metagenomic contigs encodes a cyanophycin degrading cyanophycinase appears less surprising given that cyanophycinase genes have so far not been detected in any of the available genomes of the *Betaproteobacteria* (Krehenbrink et al., 2002; Blast searches against the NCBI database were repeated on 23 August 2016 with the same result). Assuming that cyanophycin is synthesized in acidophilic *Sideroxydans* strains, this would point at the presence

of an alternative pathway to liberate nitrogen and carbon stored in cyanophycin in order to meet cellular requirements (Krehenbrink et al., 2002). The presumption that cyanophycin also serves as carbon storage molecule is based on the fact that the genetic basis for the metabolic capacity to store carbon in form of, for instance, polyhydroxybutyrate granules has so far not been detected among the *Sideroxydans*-assigned metagenomic contigs. As is the case for urease activity, cyanophycin synthesis is not encoded by the neutrophilic strain ES-1, though the presence of cyanophycin synthetase genes (*cphA1*, *cphA2*) in the genome of *G. capsiferriformans* strain ES-2 may indicate that genome analysis of further neutrophilic *Sideroxydans* strains may reveal their presence also in neutrophilic strains. The ability to use cyanophycin as nitrogen storage is also encoded in the genomes of other genera comprised of both neutrophilic (e.g., *Desulfosporosinus orientis*, *D. youngiae*, *D. meridiei*: Pester et al., 2012) and acidophilic (e.g., *D. acididurans* M1: Petzsch et al., 2015, *D. acidiphilus*: Pester et al., 2012) species.

Based on the metagenomic datset it appears that sulfate, which is present in surplus in AMD, represents the sole source of sulfur taken up by a specific sulfate ABC transporter or a sulfate permease (Supplementary Table 4C). Sulfate is predicted to be subsequently assimilated *via* the adenosine phosphosulfate (APS) pathway. This involves sulfate activation by a sulfate adenylyltransferase to adenosine-phosphosulfate (APS) and subsequent reduction to sulfite and sulfide. The latter reaction is, similar to that predicted for the neutrophilic iron oxidizers *S. lithotrophicus* strain ES-1 and *G. capsiferriformans* ES-2, catalyzed by a ferredoxin-dependent sulfite reductase rather than a NADH-dependent sulfite reductase (Supplementary Table 4C).

Similar to the neutrophilic strain ES-1 carbon acquisition seems to be achieved *via* the Calvin-Benson-Bassham cycle with form I and form II of the ribulose-1,5-bisphosphate carboxylase/oxygenase (RuBisCO). Carbon dioxide fixation also relates to the fact that culture ADE-12-1 had been enriched under autotrophic conditions. RuBisCO form I is encoded on three contigs (contig000009, contig_000020, contig_000030: Supplementary Table 4D). Both small (CbbS) and large (CbbL) subunit of RuBisCO are clustered together in each of these cases. Addition of the CbbL amino acid sequences to the corresponding alignment produced by Badger and Bek (2008) and subsequent phylogenetic analysis indicates that all copies belong to RuBisCO form IAq (Supplementary Figure 1). Moreover, each of these three RuBisCO gene clusters also harbor genes for the RuBisCO-activating enzymes CbbQ and CbbO downstream of *cbbL/S*, but lacks any carboxysome encoding genes which is, again, characteristic for form 1Aq (Badger and Bek, 2008). RuBisCO form II (CbbM) is also encoded on three metagenomic contigs (contig000006, contig000023, contig000025) assigned to acidophilic *Sideroxydans* strains. These are within a cluster comprised of seven genes including the RuBisCO-activating proteins CbbQ and CbbO and a carbonic anhydrase, though, as mentioned above, no carboxysome encoding genes were detected in any of the *Sideroxydans*-assigned metagenomic contigs. The presence of both forms of RuBisCO is likely to provide higher tolerance to fluctuating O_2 levels (Badger and Bek, 2008; Emerson et al., 2013) and even enable high CO_2 fixation rates under anaerobic growth conditions. For example, in *A. ferrooxidans* ATCC 23270 (Appia-Ayme et al., 2006) and *T. denitrificans* ATCC 25259 (Beller et al., 2006) the two isoforms were found to be differentially expressed depending on the oxygen conditions and the electron donor (ferrous iron or reduced sulfur compounds) suggesting that RuBisCO form II is only produced under anaerobic conditions. However, the lack of completely reconstructed genomes from the metagenomic dataset means again that the question regarding the presence of RuBisCO form I and II genes in the same acidophilic *Sideroxydans* strain remains unresolved.

The product of carbon fixation *via* the CBB cycle is 3-phosphoglycerate which is likely to be further metabolized in the pathways of the central carbon metabolism in order to generate precursors of bacterial biomass polymers. For example, although not found within an individual metagenomic contig, the genetic basis for all relevant activities required for a functional tricarboxylic acid (TCA) cycle are present in the *Sideroxydans*-assigned metagenomic contigs. Again, the lack of completely reconstructed genomes from the metagenome does not allow to unambigously determine whether all of the acidophilic *Sideroxydans* strains within enrichment culture ADE-12-1 encode the complete rather than the incomplete TCA cycle, which had been thought to be typical for obligate chemolithoautotrophic prokaryotes (Wood et al., 2004). This "horseshoe" type TCA cycle (Wood et al., 2004) lacks the enzyme 2-oxoglutarate dehydrogenase. However, a complete TCA cycle is also present in the neutrophilic *Sideroxydans* strain ES-1 and has recently been detected in strains belonging to the proposed genus "*Ferrovum*" (Moya-Beltrán et al., 2014; Ullrich et al., 2016a,b). The two subunits (E1, E2) that encode the 2-oxoglutarate dehydrogenase (E1) and the dihydrolipoamide succinyltransferase (E2) activity, are located next to each other. The third subunit (E3) encoding the dihydrolipoamide dehydrogenase activity of the 2-oxoglutarate dehydrogenase enzyme complex is known to be often shared with the E1-E2 subunit sets of pyruvate dehydrogenase and of branched-chain α-keto acid dehydrogenases (Berg and de Kok, 1997; McCartney et al., 1998). Therefore, it appears little as surprise that subunit E3 does not cluster with the first two components of the 2-oxoglutarate dehydrogenase enzyme complex.

The presence of a complete TCA cycle has generally been regarded as a sign of a heterotrophic life style and, therefore, raises the question as to the possibility that iron-oxidizing *Betaproteobacteria*, so far thought to be obligate autotrophs, might be able to also assimilate and utilize organic compounds for growth. However, based on their genome sequences the *Proteobacteria Nitrosomonas europea* and *Rhodobacter capsulatus* seem to encode 2-oxoglutarate dehydrogenase, but are apparently not able to achieve heterotrophic growth (Wood et al., 2004). Thus, although, as mentioned above, both neutrophilic and acidophilic *Sideroxydans* strains seem to encode the complete TCA cycle, this may not confer heterotrophic growth (see Wood et al., 2004 for a discussion on possible reasons).

Energy Metabolism

It is now widely accepted that iron oxidation pathways among ferrous iron-oxidizing bacteria are varied (e.g., Bonnefoy and Holmes, 2012; Ullrich et al., 2016a). However, it appears that the acidophilic *Sideroxydans* strains use the same pathway for energy production thought to be present in the neutrophilic strain ES-1 (Emerson et al., 2013). Automated annotation of the metagenomic sequence data did not indicate the presence of any genes related to iron oxidation. However, using psi-Blastp searches with those gene products as query that were found to be likely candidates for iron oxidation in *S. lithotrophicus* ES-1, revealed two metagenomic contigs (contig_000001, contig_000139) which encode gene clusters consisting of four genes each (Gall_all_14490 - Gall_all_14520 and Gall_all_209710 - Gall_all_209740, respectively) with high sequence similarity to the corresponding gene cluster in strain ES-1 (**Table 3**, Supplementary Table 4E). These genes represent homologs to the genes encoding MtrA/B in *Shewanella oneidensis* MR-1 and PioA/B genes in *Rhodopseudomonas palustris* TIE-1 which are involved in iron reduction and photoferrotrophy, respectively (Liu et al., 2012; Emerson et al., 2013). Moreover, MtoA, the gene product of the *mtrA* homolog from *S. lithotrophicus* ES-1, has experimentally been verified to be a decaheme cytochrome with Fe(II) oxidizing activity in *in vitro* assays (Liu et al., 2012). The model formulated based on these findings (Liu et al., 2012; Emerson et al., 2013) suggests that MtoA (Slit_2497/ Gall_all_14490) together with MtoB (Slit_2496/ Gall_all_14500) and the CymA (Slit_2495/ Gall_all_14510) homolog represent the Fe-oxidizing complex (in *S. lithotrophicus* ES-1/acidophilic *Sideroxydans* strains, Emerson et al., 2013). Additionally, both gene clusters on the two metagenomic contigs (contig_000001, contig_000139) also encode the cytochrome c-type protein upstream of *mtoA*, but lack a homolog of the hypothetical protein found to be present downstream of *cymA* in *S. lithotrophicus* ES-1 (Emerson et al., 2013).

The metagenomic contigs assigned to *Sideroxydans* strains further encode, in addition to cytochrome *bc*, the alternative complex (AC) III (ACIII, Supplementary Table 4E) that is also present in *S. lithotrophicus* ES-1 (Emerson et al., 2013). However, the precise pathway of the electrons from the outer membrane across the periplasm to these proteins at the cytoplasmic membrane remains unresolved within all *Gallionellaceae*. That is, homologs to neither rusticyanin nor to the soluble cytochromes Cyc1 and CycA-1 of *A. ferrooxidans* ATCC23270 were detected on the metagenomic contigs assigned to acidophilic *Sideroxydans* strains. A similar scenario has been reported previously following a detailed analysis of the genomes of *S. lithotrophicus* ES-1 and *G. capsiferriformans* ES-2 (Emerson et al., 2013). Additional analyses using the amino acid sequence of the c-type cytochrome of "*Ferrovum*" sp. strain JA12 (Ferro_ 02680), that was found to have sequence similarity to Cyc1 (AFE_3152) of *A. ferrooxidans* ATCC23270 (Ullrich et al., 2016a), as template for a psi-Blastp search against the metagenomic *Sideroxydans* contigs revealed a potential homolog (Gall_all_02140, Gall_all_16150, Gall_all_65820) on three contigs (contig000001, contig000003, contig000019, respectively). These proteins, thought to be *c4*-type cytochromes, seem to be soluble based on the prediction obtained from the structural analysis using the TMHMM tool (Möller et al., 2001, Supplementary Figures 2A–C). Moreover, a further *c*-type cytochrome (Gall_all_02130, Gall_all_16160, Gall_all_65830) was found to be encoded next to each of these soluble cytochromes, though no homologs to the CycA-1-like proteins in "*Ferrovum*" sp. strain JA12 were detected in the *Sideroxydans*-assigned contigs. TMHMM-based predictions (Möller et al., 2001) indicate that these further *c*-type cytochromes are soluble, but anchored to a membrane at their N-terminal end (Supplementary Figures 2E–G). Should these two cytochromes (i.e., the soluble *c4*-type and the anchored *c*-type cytochrome) indeed accomplish the electron transport from MtoA across the periplasm to the cytochrome *bc* complex at the cytoplasmic membrane, then the following scenario might represent the electron transfer path: the *c*-type cytochrome is anchored at the outer membrane where it receives the electrons from the extracellular MtoA. The soluble Cyc1-like *c4*-type cytochrome would then shuttle the electrons to the cytoplasmic membrane where it transfers them directly or *via* cytochrome *bc* to the ubiquinol pool. Finally, the electrons are subsequently directed either upstream for the reduction of oxidized $NAD(P)^+$ or downstream for the formation of a proton motive force.

As for the latter, five of the *Sideroxydans*-assigned contigs (contigs000003, contig000006, contig000019, contig000021, contig000215) encode F_0F_1-type ATPases, while one contig (contig000021) encodes a V-type ATPase (Supplementary Table 4E). In each of these cases, the genes encoding the various subunits of the ATP synthetases are organized within a gene cluster.

Apart from ferrous iron oxidation, the *Sideroxydans* metagenomic dataset also harbors three contigs (contig000005, contig000007, contig000011) with a cluster comprised of 12 genes that seem to encode proteins involved in dissimilatory sulfur oxidation (Supplementary Table 4E), including *dsr* genes. These Dsr enzymes have been shown to function in reversible (i.e., oxidative) manner to those found in sulfate reducing bacteria (Friedrich et al., 2005; Ghosh and Dam, 2009; Watanabe et al., 2014). This together with a contig (contig000067) encoding a gene cluster that harbors SoxXYZAB (**Figure 3**, Supplementary Table 4E) indicates that oxidation of reduced sulfur compounds may provide an additional path to gain energy for metabolic activities. Additional and more detailed analyses are likely to reveal further genes involved in the dissimilatory oxidation of sulfur compounds.

The *Sideroxydans*-assigned metagenomic contigs also encode enzymes for other redox reactions connected to the quinol pool. Among those are a predicted succinate dehydrogenase, an electron transfer flavoprotein (ETF) and a predicted flavoprotein dehydrogenase (ETF ubiquinone oxidoreductase) (**Figure 3**, Supplementary Table 4E).

Additionally, two (contig000035, contig000112) of the metagenomic contigs assigned to *Sideroxydans* also harbor a cluster comprised of five genes (*pdhR, lutABC, lutP*) that have sequence similarity to a GntR-type transcriptional repressor (PdhR, predicted to be involved in pyruvate metabolism), the lactate utilization proteins A, B and C and a lactate permease, respectively (Supplementary Table 4E). The lactate utilization

TABLE 3 | Result from psi-Blastp comparison of gene products encoded by a gene cluster in the genome of *S. lithotrophicus* ES-1 that is thought to be involved in iron oxidation, with gene products assigned to acidophilic *Sideroxydans* strains.

	Contig		CytC	MtoA	MtoB	CymA	
S. lithotrophicus ES-1	[a]		Slit_2498	Slit_2497	Slit_2496	Slit_2495	Slit_2494
ADE-12-1	000003		–	Gall_all_14490	Gall_all_14500	Gall_all_14510	Gall_all_14520
		score[b]		$383/4e^{-136}$	671/0.0	517/0.0	$182/e^{-59}$
		annotated as[c]		denitrification system component NirT	hypothetical protein	cytochrome c nitrite reductase pentaheme subunit	cytochrome c2
	000139		–	Gall_all_209740	Gall_all_209730	Gall_all_209720	Gall_all_209710
		score[b]		$384/e^{-136}$	653/0.0	521/0.0	$190/e^{-62}$
		annotated as[c]		denitrification system component NirT	hypothetical protein	cytochrome c nitrite reductase pentaheme subunit	cytochrome c551 subunit

[a] *closed genome.*
[b] *shown is score/E value from psi-Blastp with five iterations.*
[c] *result from automated annotation.*

complex ABC has been shown to be essential for growth of *Bacillus subtilis* on lactate as sole carbon source, while a *B. subtilis* mutant lacking the lactate permease only grew at a very slow rate (Chai et al., 2009). A low-level uptake of L-lactate *via* Na^+ or K^+ symporters has been discussed as possible reason for growth despite the absence of a functional lactate permease (Chai et al., 2009). Such a low-level lactate uptake may also be relevant for *S. lithotrophicus* strain ES-1 since its genome likewise encodes the lactate utilization complex LutABC and the GntR-type transcriptional repressor, but lacks a lactate permease. However, in contrast to *B. subtilis* neither the genome of *S. lithotrophicus* strain ES-1 nor the metagenomic contigs assigned to acidophilic *Sideroxydans* strains seem to encode a lactate dehydrogenase required for channeling the organic carbon into biosynthetic pathways or to make it available for a fermentative metabolism during anaerobic growth. This together with the fact that each of the three components of the lactate utilization complex in strain ES-1 or on the metagenomic contigs was inferred to contain an iron-sulfur cluster indicates that a cytochrome electron transfer is associated to lactate oxidation (i.e., respiration) rather than a biosynthetic pathway (i.e., heterotrophic growth) or NAD^+ recycling (Chai et al., 2009).

However, apart from the question regarding availability of lactate in typical AMD environments, growth of acidophilic strains under acidic conditions on organic acids also appears unusual as this is likely to damage the proton gradient across the cytoplasmic membrane and, hence, the proton motive force required for ATP synthesis. Organic acids like lactate are protonated under acidic pH conditions (e.g., in AMD), but release a proton upon entering the cytoplasm which is thought to have circumneutral pH and, thus, result in an import of protons (Alexander et al., 1987; Kishimoto et al., 1990; Ciaramella et al., 2005). A solution to this issue may be provided by a scenario in which the lactate utilizing enzyme complex is located at the periplasmic site of the inner membrane, while the lactate permease permits lactate entry into the periplasm.

The homologous gene cluster in *B. subtilis* also encodes a GntR-type transcriptional repressor (LutR), though this has only low sequence similarity to the GntR-type transcriptional repressor (PdhR) in contig000035 and contig000112. Lactate utilization in *B. subtilis* is under the dual control of LutR and the master regulator for biofilm formation SinR, and is induced in response to L-lactate availability (Chai et al., 2009). No SinR homolog was found in any of the *Sideroxydans*-assigned metagenomic contigs, indicating that the lactate utilization complex in the host cells of contig000035 and contig000112 transfers metabolic ability for energy production *via* lactate-utilization, but does not play a role in biofilm formation.

Sideroxydans strains as well as other microaerophilic species may encounter anoxic periods during which respiration with oxygen as terminal electron acceptor is no longer possible. Based on the metagenomic dataset acidophilic *Sideroxydans* strains seem to be able to produce energy during anaerobic growth *via* at least one respirative path. The presence of a gene cluster (GALL_all_03470 - GALL_all_03520: Supplementary Table 4E) encoding the formate hydrogenlyase (FHL) complex indicates that acidophilic *Sideroxydans* strains may utilize formate oxidation during anoxic episodes to subsequently channel electrons *via* NADH ubiquinone oxidoreductases in the respiratory system to protons. The fact that the FHL gene cluster also encodes the subunits of a group 4 hydrogenase (Vignais et al., 2001) further corroborates the notion that formate oxidation coupled to the reduction of protons plays a role in energy conservation under oxygen-limiting conditions. Since the overall driving force for formate oxidation is rather low (18 mV at pH 7 and equal partial gas pressure of CO_2 and H_2), the acidic environment of acidophilic *Sideroxydans* strains means that it increases by 30 mV for each drop in pH unit (McDowall et al., 2014). Should this process still not yield any energy, then it may at least represent another means of reducing the intracellular proton load by proton reduction to volatile H_2. However, more detailed analyses of all hydrogenases present in the metagenomic

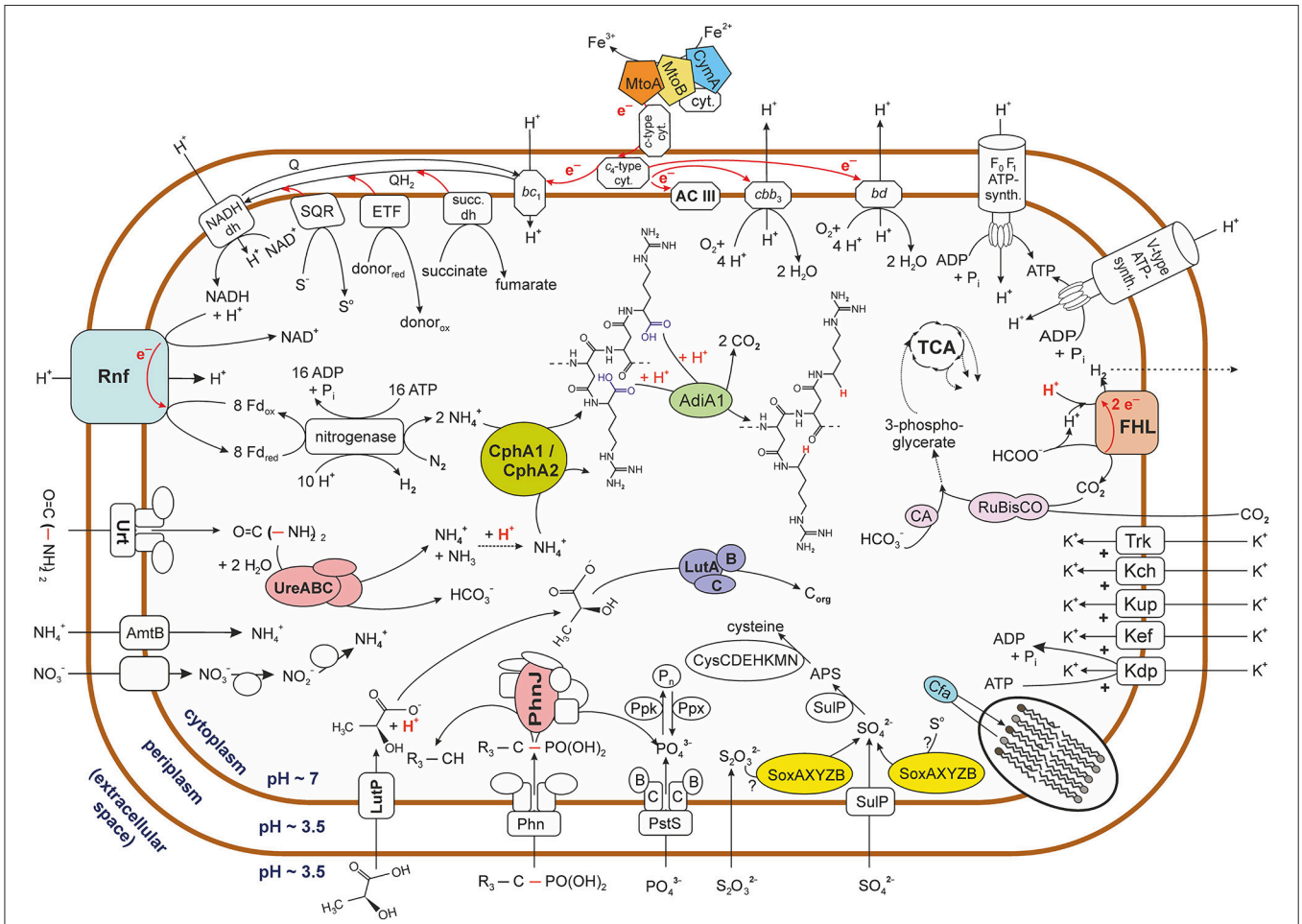

FIGURE 3 | Graphical representation of potential metabolic activities of acidophilic *Sideroxydans* strains. The figure represents the pool of metabolic pathways that were reconstructed from the metagenomic sequence data of contigs assigned to strains of the genus *Sideroxydans*. It therefore does not express the co-occurrence of various pathways within the same strain. Biochemical reactions do not reflect real stoichiometry with the exception of cases were it was judged to be of relevance. Question marks indicate that it is unknown which sulfur compound is oxidized *via* the Sox enzyme system. Based on its pKa (3.86) lactate is depicted in its acid form outside the cell, though the narrow difference to the external pH (3.5) means that only a small fraction of molecules will be protonated. Please also note in this context that, no lactate was added to the culture medium. Dotted arrows indicate that no details are provided on the multiple enzymes involved in the pathway while dashed lines indicate the potential path of a volatile compound (i.e., H_2). For reasons of clarity no details are provided on the tricarboxylic acid (TCA) cycle. Arrows deviating from the the TCA cycle indicate its relevance as a central carbon metabolic pathway, though this line of metabolic function was not further investigated in this study. Carbon dioxide appears to be reduced to 3-phosphoglycerate *via* the Calvin-Benson-Bassham cycle indicated by its key enzyme ribulose-1,5-bisphosphate carboxylase/oxygenase (RuBisCO). Names for the nitrate transporter and nitrate and nitrite reductases are not indicated due to contradicting nomenclature in the databases. FHL, formate hydrogenlyase; AC III, alternative complex III; ETF, electron transfer flavoprotein oxidoreductase; SDH, succinate dehydrogenase; SQR, sulfide quinone oxidoreductase; CA, carbonic anhydrase; NADH dh, NADH dehydrogenase; Phn, phosphonate uptake system. Enzymes involved in metabolic pathways are abbreviated by their acronyms. For details see Supplementary Table 4.

dataset might reveal further insights into electron transfer pathways and whether these have energy conserving potential. While the genome of *G. capsiferriformans* ES-2 encodes a pyruvate formate lyase (Galf_0602) for the conversion of pyruvate to acetyl-CoA and formate under anoxic conditions, a corresponding gene was neither detected in any of the *Sideroxydans*-assigned metagenomic contigs nor in the genome of the neutrophilic *Sideroxydans* strain ES-1. It remains speculative whether the pyruvate formate lyase is encoded on genomic fragments not covered by this metagenomic sequencing approach.

Strategies to Adapt to Life at Low pH

Analyses of the metagenomic sequence information of *Sideroxydans*-derived contigs indicate a repertoire of strategies to deal with the acidic environment. Several of those mechanisms are also encoded on the genome of the neutrophilic *S. lithotrophicus* strain ES-1. An example of those is the cyclopropane-fatty-acyl-phospholipid synthase (Supplementary Table 4F) which enables the cell to produce and subsequently incorporate cyclopropane fatty acids into its cell membrane, thus protecting against proton influx (Grogan and Cronan, 1997; Chang and Cronan, 1999; Mangold et al., 2013). In

addition to its potential to produce energy, the above mentioned formate hydrogenlyase activity also consumes one proton per molecule formate and may, thus, provide a means of buffering against high intracellular proton concentrations. Furthermore, creating a reversed, that is inside positive, membrane potential resembles a well-known strategy in pH homeostasis (Baker-Austin and Dopson, 2007). Both neutrophilic strain ES-1 and the *Sideroxydans*-assigned metagenomic contigs encode four uptake systems for potassium (the low affinity potassium transport system protein Kup, the voltage-gated potassium channel Kch, the Trk potassium uptake system and the Kef-type K^+ transport system, see Supplementary Table 4F) which is considered an effective agent in achieving reversal of the membrane potential.

However, detailed analysis of the metagenomic data also revealed the presence of genes encoding three putative cellular functions that seem to be unique to the acidophilic representatives of *Sideroxydans*. Firstly, the aforementioned potassium uptake systems achieve potassium transfer into the cytoplasm only at high extracellular potassium concentrations (e.g., Damnjanovic et al., 2013). In contrast to this, three metagenomic contigs (contigs000001, contig000049, contig000055) encode an additional Kdp-type K^+ uptake ATPase. This high-affinity potassium uptake system confers K^+ uptake into the bacterial cytoplasm even under low environmental K^+ concentrations (i.e., $[K^+]out < 100\,\mu M$), and, thus, maintains the cytoplasmic concentrations needed for, among other functions, pH homeostasis (Laimins et al., 1978; Epstein, 1985). In this ion pump, coupling of ATP hydrolysis to ion transport leads to a high-affinity uptake of potassium, though only at moderate transport rates and at the cost of ATP hydrolysis (Rhoads et al., 1976). Such a high-affinity potassium uptake system was not detected in the genome of *S. lithotrophicus* strain ES-1.

Secondly, and again in contrast to the genome of the neutrophilic strain ES-1, a gene cluster of 13 genes within contig000112 (Supplementary Table 4B) encodes both a urease and its accessory proteins as well as an ABC transporter for urea. Apart from providing the ability to utilize an alternative nitrogen source, urease activity has been known for some time to enable human pathogens, such as *Helicobacter pylori* (Eaton et al., 1991) and *Yersinia enterocolitica* and *Morganella morganii* (Young et al., 1996), to buffer against a high intracellular proton load. This buffering capacity is achieved through the urease catalyzed hydrolysis of urea which results in bicarbonate and ammonia (Mobley and Hausinger, 1989) and has recently also been proposed for "*Ferrovum*" group 2 strains JA12 and PN-J185 (Ullrich et al., 2016a,b). Since the gene cluster also encodes an ABC transporter for urea, it should further be mentioned that degradative processes of fossil organic matter within lignite similar to those processes reported for bioweathering of organics within copper shale (Matlakowska and Skłodowska, 2011; Matlakowska et al., 2012) may provide (traces of) urea in AMD.

The third feature which—based on the currently available genome data—seems to be unique to acidophilic *Sideroxydans* strains is related to the presence of two genes encoding the cyanophycin synthetases CphA1 and CphA2. Cyanophycin synthetase activity results in the non-ribosomal synthesis of the branched polypeptide cyanophycin which consists of aspartic acid in the backbone and an approximately equimolar amount of arginine in the side chain (Simon and Weathers, 1976). These genes are clustered together and found on three contigs (Supplementary Table 4B). Although, the presence of cyanophycin has been known for some time to occur in bacteria other than cyanobacteria (Krehenbrink et al., 2002), its potential role in pH homeostasis has not yet been discussed. The hypothesis put forward here is built on the facts that decarboxylation of amino acids is a well-known strategy in pH homeostasis (Baker-Austin and Dopson, 2007) and that the pKa values of the alpha-carboxy groups of the arginine residues is much lower (2.17, Campbell and Farrell, 2009) than the pH of the cytoplasms which is thought to be circumneutral. Decarboxylation of the deprotonated alpha-carboxy groups of arginine side chains in cyanophycin would then buffer against acidity. The presence of a biodegradative arginine decarboxylase (encoded by *adiA1* on contig001871) provides further support for this hypothesis. A contig (contig09308) encoding a cyanophycin synthetase and three contigs (contig01791, contig01794, contig04721) encoding degradative arginine decarboxylases were also detected in the metagenome constructed from a planktonic cell fraction of samples collected at an acid mine drainage (pH 2.5–2.7) stream biofilm situated 250 m below ground in the low-temperature (6–10°C) Kristineberg mine in northern Sweden (Liljeqvist et al., 2015). Moreover, since nitrogen does, in contrast to phosphate, not seem to be limiting in AMD, acidophiles may be able to accumulate large reservoirs of cyanophycin which may, in turn, not only represent a massive nitrogen and carbon reserve, but also an extensive buffer capacity against protons. Although, cyanophycin is widely known to occur in granular form in cyanobacteria, more recent research has shown that alterations to the side chains, such as incorporation of 5% lysine, results in a form soluble in an aqueous milieu (Frommeyer and Steinbüchel, 2013). Soluble cyanophycin is likely to be particularly accessible for enzymatic decarboxylation and, hence, might enable an almost instant response to high proton influx.

CONCLUDING REMARKS

Although, no pure culture or one that, similar to previous genomic studies on "*Ferrovum*" (Ullrich et al., 2016a,b), is composed of only the target microorganisms and a single contaminant, the availability of approx. 10 Mb of metagenomic sequence information derived from *Sideroxydans* strains provides a basis for the reconstruction of metabolic features present in acidophilic representatives of this genus. However, it must be reiterated in this context that the conclusions drawn from the analysis of the metagenomic data is limited by the lack of completely assembled genomes. Consequently, it remains unresolved which of these features are encoded by the same genome and to what extent the metagenomic assembly reflects genomic and, hence, metabolic variation of individual strains represented by the sequence data. While the

latter might indicate niche partitioning by various ecotypes within the genus *Sideroxydans*, the presence of redundancy within a strain (e.g., different metabolic pathways for energy production) seems to be a useful means to survive in a changing environment. Overall, the results from this analysis demonstrate genetic differences to the neutrophilic *Sideroxydans* strain ES-1 that relate to interactions of acidophilic *Sideroxydans* strains with the prevailing environmental conditions of their specific habitats. The findings from this study therefore suggest an evolutionary process driven by the adaptation to distinct environmental niches, which presumably results in ecological speciation. Whether acidophily or neutrophily is the more evolved life style is, however, still open to discussion.

Clearly, this report has not covered all information on acidophilic *Sideroxydans* strains available within the metagenomic sequence data, most likely not even all of that relevant for nutrient utilization, energy production and pH homeostasis. Moreover, life in a typical AMD environment also means increased cellular damage caused by, for instance, higher rates of oxygen radical formation due to the high concentrations of redox active metals (in particular iron). Therefore, the genomes of acidophiles typically encode numerous mechanisms for the detoxification of reactive oxygen species (ROS, see Ferrer et al., 2016) and the repair of damaged biomolecules (e.g., genomic DNA itself). However, a detailed analysis of these aspects was seen as beyond the remit of this article, though an initial screening of the metagenomic sequence information indicates that the acidophilic *Sideroxydans* strains also encode the genetic potential for ROS detoxification and DNA repair.

Finally, sequence information on other members present in enrichment culture ADE-12-1 has also not yet been challenged and their role, therefore, remains likewise unresolved. Detailed analysis of—at least—the other two abundant groups (*Opitutus*, *Telmatospirillum*) may elucidate some of the reasons for their enrichment under the microaerophilic conditions within the gradient tubes. Preliminary analysis of the metagenomic contigs assigned to *Opitutus* and *Telmatospirillum* strains indicate that similar life styles to those known for characterized representative strains of these genera are also encoded by the strains within enrichment culture ADE-12-1 (e.g., methylotrophy: Chin et al., 2001; Sizova et al., 2007). However, more detailed analyses of the metagenomic data along these lines of investigation were again beyond the scope of this article.

AUTHOR CONTRIBUTIONS

The study was proposed and designed by MM. AS produced enrichment culture ADE-12-1 and isolated the total metagenomic DNA. AP and RD planned metagenome sequencing. AP conducted sequence analyses including assembly and automated annotation of the genome reads. MV and MM analyzed the microbial diversity within enrichment culture ADE-12-1. MM analyzed the annotated metagenome data and wrote the manuscript. MS, RD, and AP contributed to the final manuscript by critical revision. All authors read and approved the manuscript and declare that the research was conducted in the absence of any commercial or financial relationships that could be construed as a potential conflict of interest.

ACKNOWLEDGMENTS

We are indebted to Vattenfall Europe Mining & Generation AG and G.E.O.S. Freiberg Ingenieurgesellschaft m.b.H. for access to samples from the treatment plant Tzschelln. Enrichment of microaerophilic strains and metagenome sequencing was funded by the European Social Fund (ESF) as part of the junior research group GETGEOWEB (project nr. 100101363). Dr. Andrea Thürmer, Janosch Gröning, and Beate Erler are thanked for 16S-tag Illumina sequencing and Dr. Bernd Wemheuer for the processing and analysis of the 16S-tag sequence reads.

SUPPLEMENTARY MATERIAL

The Supplementary Material for this article can be found online at: http://journal.frontiersin.org/article/10.3389/fmicb.2016.02082/full#supplementary-material

REFERENCES

Alexander, B., Leach, S., and Ingledew, W. J. (1987). The relationship between chemiosmotic parameters and sensitivity to anions and organic acids in the acidophile Thiobacillus ferrooxidans. *J. Gen. Microbiol.* 133, 1171–1179. doi: 10.1099/00221287-133-5-1171

Appia-Ayme, C., Quatrini, R., Denis, Y., Denizot, F., Silver, S., Roberto, F., et al. (2006). Microarray and bioinformatic analyses suggest models for carbon metabolism in the autotroph *Acidithiobacillus ferrooxidans*. *Hydrometallurgy* 83, 273–280. doi: 10.1016/j.hydromet.2006.03.029

Badger, M. R., and Bek, E. J. (2008). Multiple Rubisco forms in proteobacteria: their functional significance in relation to CO2 acquisition by the CBB cycle. *J. Exp. Bot.* 59, 1525–1541. doi: 10.1093/jxb/erm297

Baker-Austin, C., and Dopson, M. (2007). Life in acid: pH homeostasis in acidophiles. *Trends Microbiol.* 15, 165–171. doi: 10.1016/j.tim.2007.02.005

Bankevich, A., Nurk, S., Antipov, D., Gurevich, A. A., Dvorkin, M., and Kulikov, A. S. (2012). SPAdes: a new genome assembly algorithm and its applications to single-cell sequencing. *J. Comput. Biol.* 19, 455–477. doi: 10.1089/cmb.2012.0021

Beller, H. R., Chain, P. S., Letain, T. E., Chakicherla, A., Larimer, F. W., Richardson, P. M., et al. (2006). The genome sequence of the obligately chemolithoautotrophic, facultatively anaerobic bacterium Thiobacillus denitrificans. *J. Bacteriol.* 188, 1473–1488. doi: 10.1128/JB.188.4.1473-1488.2006

Berg, A., and de Kok, A. (1997). 2-Oxo acid dehydrogenase multienzyme complexes. The central role of the lipoyl domain. *Biol. Chem.* 378, 617–634.

Biegel, E., and Müller, V. (2010). Bacterial Na+-translocating ferredoxin: NAD+ oxidoreductase. *Proc. Nat. Acad. Sci. U.S.A.* 107, 18138–18142. doi: 10.1073/pnas.1010318107

Bigham, J. M., Schwertmann, U., Traina, S. J., Winland, R. L., and Wolf, M. (1996). Schwertmannite and the chemical modeling of iron in acid sulfate waters. *Geochim. Cosmochim. Acta* 60, 2111–2121. doi: 10.1016/0016-7037(96)00091-9

Bolger, A. M., Lohse, M., and Usadel, B. (2014). Trimmomatic: a flexible trimmer for Illumina sequence data. *Bioinformatics* 30, 2114–2120. doi: 10.1093/bioinformatics/btu170

Bonnefoy, V., and Holmes, D. S. (2012). Genomic insights into microbial iron oxidation and iron uptake strategies in extremely acidic environments. *Environ. Microbiol.* 14, 1597–1611. doi: 10.1111/j.1462-2920.2011.02626.x

Campbell, M. K., and Farrell, S. O. (2009). *Biochemistry*. Belmont, CA: Thomson Higher Education.

Chai, Y., Kolter, R., and Losick, R. (2009). A widely conserved gene cluster required for lactate utilization in *Bacillus subtilis* and its involvement in biofilm formation. *J. Bacteriol.* 191, 2423–2430. doi: 10.1128/JB.01464-08

Chang, Y. Y., and Cronan, J. E. (1999). Membrane cyclopropane fatty acid content is a major factor in acid resistance of *Escherichia coli*. *Mol. Microbiol.* 33, 249–259. doi: 10.1046/j.1365-2958.1999.01456.x

Chin, K. J., Liesack, W., and Janssen, P. H. (2001). Opitutus terrae gen. nov., sp. nov., to accommodate novel strains of the division '*Verrucomicrobia*' isolated from rice paddy soil. *Int. J. Syst. Evol. Microbiol.* 51, 1965–1968. doi: 10.1099/00207713-51-6-1965

Ciaramella, M., Napoli, A., and Rossi, M. (2005). Another extreme genome: how to live at pH 0. *Trends Microbiol.* 13, 49–51. doi: 10.1016/j.tim.2004.12.001

Cole, J. R., Wang, Q., Cardenas, E., Fish, J., Chai, B., Farris, R. J., et al. (2009). The ribosomal database project: improved alignments and new tools for rRNA analysis. *Nucleic Acids Res.* 37, D141–D145. doi: 10.1093/nar/gkn879

Damnjanovic, B., Weber, A., Potschies, M., Greie, J. C., and Apell, H. J. (2013). Mechanistic analysis of the pump cycle of the KdpFABC P-type ATPase. *Biochemistry* 52, 5563–5576. doi: 10.1021/bi400729e

Eaton, K. A., Brooks, C. L., Morgan, D. R., and Krakowka, S. (1991). Essential role of urease in pathogenesis of gastritis induced by *Helicobacter pylori* in gnotobiotic piglets. *Infect. Immun.* 59, 2470–2475.

Edgar, R. C. (2010). Search and clustering orders of magnitude faster than BLAST. *Bioinformatics* 26, 2460–2461. doi: 10.1093/bioinformatics/btq461

Emerson, D., Field, E. K., Chertkov, O., Davenport, K. W., Goodwin, L., Munk, C., et al. (2013). Comparative genomics of freshwater Fe-oxidizing bacteria: implications for physiology, ecology, and systematics. *Front. Microbiol.* 4:254. doi: 10.3389/fmicb.2013.00254

Emerson, D., and Floyd, M. M. (2005). Enrichment and isolation of iron-oxidizing bacteria at neutral pH. *Methods Enzymol.* 397, 112–123. doi: 10.1016/S0076-6879(05)97006-7

Engel, H., and Hanert, H. (1967). Isolierung von *Gallionella ferruginea* Ehrenberg. *Naturwissenschaften* 54, 147–148. doi: 10.1007/BF00625126

Epstein, W. (1985). The Kdp system: a bacterial K+ transport ATPase. *Curr. Top. Membr. Transp.* 23, 153–175.

Felsenstein, J. (2004). *Inferring Phylogenies*. Sunderland, MA: Sinauer Associates.

Ferrer, A., Orellana, O., and Levicán, G. (2016). "Oxidative stress and metal tolerance in extreme acidophiles," in *Acidophiles – Life in Extremely Acidic Environments,* eds R. Quatrini and D. B. Johnson (Norfolk, VA: Caister Academic Press), 63–76.

Friedrich, C. G., Bardischewsky, F., Rother, D., Quentmeier, A., and Fischer, J. (2005). Prokaryotic sulfur oxidation. *Curr. Opin. Microbiol.* 8, 253–259. doi: 10.1016/j.mib.2005.04.005

Frommeyer, M., and Steinbüchel, A. (2013). Increased lysine content is the main characteristic of the soluble form of the polyamide cyanophycin synthesized by recombinant *Escherichia coli*. *Appl. Environ. Microbiol.* 79, 4474–4483. doi: 10.1128/AEM.00986-13

García-Alcalde, F., Okonechnikov, K., Carbonell, J., Cruz, L. M., Götz, S., Tarazona, S., et al. (2012). Qualimap: evaluating next-generation sequencing alignment data. *Bioinformatics* 28, 2678–2679. doi: 10.1093/bioinformatics/bts503

Gelhaar, N. (2012). *Untersuchungen zu Kultivierungsbedingungen zur Isolierung von "Ferrovum" spp*. Diploma thesis, Freiberg, Germany: TU Bergakademie Freiberg.

Ghosh, W., and Dam, B. (2009). Biochemistry and molecular biology of lithotrophic sulfur oxidation by taxonomically and ecologically diverse bacteria and archaea. *FEMS Microbiol. Rev.* 33, 999–1043. doi: 10.1111/j.1574-6976.2009.00187.x

Grogan, D. W., and Cronan, J. E. (1997). Cyclopropane ring formation in membrane lipids of bacteria. *Microbiol. Mol. Biol. Rev.* 61, 429–441.

Hallbeck, L., Ståhl, F., and Pedersen, K. (1993). Phylogeny and phenotypic characterization of the stalk-forming and iron-oxidizing bacterium *Gallionella ferruginea*. *J. Gen. Microbiol.* 139, 1531–1535. doi: 10.1099/00221287-139-7-1531

Hallberg, K. B., Coupland, K., Kimura, S., and Johnson, D. B. (2006). Macroscopic streamer growths in acidic, metal-rich mine waters in North Wales consist of novel and remarkably simple bacterial communities. *Appl. Environ. Microbiol.* 72, 2022–2030. doi: 10.1128/AEM.72.3.2022-2030.2006

Hanert, H. (1968). Untersuchungen zur Isolierung, Stoffwechselphysiologie und Morphologie von *Gallionella ferruginea* Ehrenberg. *Arch. Mikrobiol.* 60, 348–376. doi: 10.1007/BF00408555

Hausinger, R. P. (2004). Metabolic versatility of prokaryotes for urea decomposition. *J. Bacteriol.* 186, 2520–2522. doi: 10.1128/JB.186.9.2520-2522.2004

Heinzel, E., Hedrich, S., Janneck, E., Glombitza, F., Seifert, J., and Schlömann, M. (2009a). Bacterial diversity in a mine water treatment plant. *Appl. Environ. Microbiol.* 75, 858–861 doi: 10.1128/AEM.01045-08

Heinzel, E., Janneck, E., Glombitza, F., Schlömann, M., and Seifert, J. (2009b). Population dynamics of iron-oxidizing communities in pilot plants for the treatment of acid mine waters. *Environ. Sci. Technol.* 43, 6138–6144. doi: 10.1021/es900067d

Janneck, E., Arnold, I., Koch, T., Meyer, J., Burghardt, D., and Ehinger, S. (2010). "Microbial synthesis of schwertmannite from lignite mine water and its utilisation for removal of arsenic from mine waters and for production of iron pigments," in *Mine Water and Innovative Thinking. Proceedings of the International Mine Water Association Symposium 2010,* eds C. Wolkersdorfer and A. Freund (Sydney, NSW: Cape Breton University Press), 131–134.

Johnson, D. B., and Hallberg, K. B. (2007). "Techniques for detecting and identifying acidophilic mineral-oxidizing microorganisms," in *Biomining,* eds D. E. Rawlings and D. B. Johnson (Berlin: S*pringer)*, 237–261.

Johnson, D. B., Hallberg, K. B., and Hedrich, S. (2014). Uncovering a microbial enigma: isolation and characterization of the streamer-generating, iron-oxidizing, acidophilic bacterium "*Ferrovum myxofaciens*". *Appl. Environ. Microbiol.* 80, 672–680. doi: 10.1128/AEM.03230-13

Johnson, D. B., and McGinness, S. (1991). A highly efficient and universal solid medium for growing mesophilic and moderately thermophilic, iron-oxidizing, acidophilic bacteria. *J. Microbiol. Methods* 13, 113–122. doi: 10.1016/0167-7012(91)90011-E

Kanamori, T., Kanou, N., Atomi, H., and Imanaka, T. (2004). Enzymatic characterization of a prokaryotic urea carboxylase. *J. Bacteriol.* 186, 2532–2539. doi: 10.1128/JB.186.9.2532-2539.2004

Kanamori, T., Kanou, N., Kusakabe, S., Atomi, H., and Imanaka, T. (2005). Allophanate hydrolase of Oleomonas sagaranensis involved in an ATP-dependent degradation pathway specific to urea. *FEMS Microbiol. Lett.* 245, 61–65. doi: 10.1016/j.femsle.2005.02.023

Kishimoto, N., Inagaki, K., Sugio, T., and Tano, T. (1990). Growth-inhibition of *Acidiphilium* species by organic-acids contained in yeast extract. *J. Ferment. Bioengin.* 70, 7–10. doi: 10.1016/0922-338X(90)90021-N

Klindworth, A., Pruesse, E., Schweer, T., Peplies, J., Quast, C., Horn, M., et al. (2013). Evaluation of general 16S ribosomal RNA gene PCR primers for classical and next-generation sequencing-based diversity studies. *Nucleic Acids Res.* 41:e1. doi: 10.1093/nar/gks808

Krehenbrink, M., Oppermann-Sanio, F. B., and Steinbüchel, A. (2002). Evaluation of non-cyanobacterial genome sequences for occurrence of genes encoding proteins homologous to cyanophycin synthetase and cloning of an active cyanophycin synthetase from Acinetobacter sp. strain DSM 587. *Arch. Microbiol.* 177, 371–380. doi: 10.1007/s00203-001-0396-9

Kucera, S., and Wolfe, R. S. (1957). A selective enrichment method for *Gallionella ferruginea*. *J. Bacteriol.* 74, 344–349.

Laimins, L. A., Rhoads, D. B., Altendorf, K., and Epstein, W. (1978). Identification of the structural proteins of an ATP-driven potassium transport system in *Escherichia coli*. *Proc. Natl. Acad. Sci. U.S.A.* 75, 3216–3219. doi: 10.1073/pnas.75.7.3216

Liljeqvist, M., Ossandon, F. J., González, C., Rajan, S., Stell, A., Valdes, J., et al. (2015). Metagenomic analysis reveals adaptations to a cold-adapted lifestyle in a low-temperature acid mine drainage stream. *FEMS Microbiol. Ecol.* 91:fiv011. doi: 10.1093/femsec/fiv011

Liu, J., Wang, Z., Belchik, S. M., Edwards, M. J., Liu, C., Kennedy, D. W., et al. (2012). Identification and characterization of MtoA: a decaheme c-type cytochrome of the neutrophilic Fe(II)-oxidizing bacterium *Sideroxydans lithotrophicus* ES-1. *Front. Microbiol.* 3:37. doi: 10.3389/fmicb.2012.00037

Ludwig, W., Strunk, O., Westram, R., Richter, L., and Meier, H., Yadhukumar, et al. (2004). ARB: a software environment for sequence data. *Nucleic Acids Res.* 32, 1363–1371. doi: 10.1093/nar/gkh293

Mangold, S., Rao Jonna, V., and Dopson, M. (2013). Response of *Acidithiobacillus caldus* toward suboptimal pH conditions. *Extremophiles* 17, 689–696. doi: 10.1007/s00792-013-0553-5

Matlakowska, R., and Skłodowska, A. (2011). Biodegradation of Kupferschiefer black shale organic matter (Fore-Sudetic Monocline, Poland) by indigenous microorganisms. *Chemosphere* 83, 1255–1261. doi: 10.1016/j.chemosphere.2011.03.003

Matlakowska, R., Skłodowska, A., and Nejbert, K. (2012). Bioweathering of Kupferschiefer black shale (Fore-Sudetic Monocline, SW Poland) by indigenous bacteria: implication for dissolution and precipitation of minerals in deep underground mine. *FEMS Microbiol. Ecol.* 81, 99–110. doi: 10.1111/j.1574-6941.2012.01326.x

McCartney, R. G., Rice, J. E., Sanderson, S. J., Bunik, V., Lindsay, H., and Lindsay, J. G. (1998). Subunit interactions in the mammalian α-ketoglutarate dehydrogenase complex. Evidence for direct association of the α-*ketoglutarate dehydrogenase and dihydrolipoamide dehydrogenase components. J. Biol. Chem.* 273, 24158–24164. doi: 10.1074/jbc.273.37.24158

McDowall, J. S., Murphy, B. J., Haumann, M., Palmer, T., Armstrong, F. A., and Sargent, F. (2014). Bacterial formate hydrogenlyase complex. *Proc. Natl. Acad. Sci. U.S.A.* 111, E3948–E3956. doi: 10.1073/pnas.1407927111

Mobley, H. L., and Hausinger, R. P. (1989). Microbial ureases: significance, regulation, and molecular characterization. *Microbiol. Rev.* 53, 85–108.

Möller, S., Croning, M. D., and Apweiler, R. (2001). Evaluation of methods for the prediction of membrane spanning regions. *Bioinformatics* 17, 646–653. doi: 10.1093/bioinformatics/17.7.646

Mosler, S., Poehlein, A., Voget, S., Daniel, R., Kipry, J., Schlömann, M., et al. (2013). Predicting the metabolic potential of the novel iron-oxidizing bacterium "*Ferrovum*" sp. JA12 using comparative genomics. *Adv. Materials Res.* 825, 153–156. doi: 10.4028/www.scientific.net/AMR.825.153

Moya-Beltrán, A., Cárdenas, J. P., Covarrubias, P. C., Issotta, F., Ossandon, F. J., Grail, B. M., et al. (2014). Draft genome sequence of the nominated type strain of "*Ferrovum myxofaciens*," an acidophilic, iron-oxidizing betaproteobacterium. *Genome Announc.* 2, e00834–e00814. doi: 10.1128/genomeA.00834-14

Pester, M., Brambilla, E., Alazard, D., Rattei, T., Weinmaier, T., Han, J., et al. (2012). Complete genome sequences of *Desulfosporosinus orientis* DSM765T, *Desulfosporosinus youngiae* DSM17734T, *Desulfosporosinus meridiei* DSM13257T, and *Desulfosporosinus acidiphilus* DSM22704T. *J. Bacteriol.* 194, 6300–6301. doi: 10.1128/JB.01392-12

Petzsch, P., Poehlein, A., Johnson, D. B., Daniel, R., Schlömann, M., and Mühling, M. (2015). Genome of the moderately acidophilic sulfate reducing Firmicute *Desulfosporosinus acididurans* (Strain M1T) *Genome Announc.* 3, e00881–e00815. doi: 10.1128/genomeA.00881-15

Pruesse, E., Quast, C., Knittel, K., Fuchs, B. M., Ludwig, W. G., Peplies, J., et al. (2007). SILVA: a comprehensive online resource for quality checked and aligned ribosomal RNA sequence data compatible with ARB. *Nucleic Acids Res.* 35, 7188–7196. doi: 10.1093/nar/gkm864

Quast, C., Pruesse, E., Yilmaz, P., Gerken, J., Schweer, T., Yarza, P., et al. (2013). The SILVA ribosomal RNA gene database project: improved data processing and web-based tools. Opens external link in new window. *Nucleic Acids Res.* 41, D590–D596. doi: 10.1093/nar/gks1219

Rhoads, D. B., Waters, F. B., and Epstein, W. (1976). Cation transport in *Escherichia coli*. VIII. Potassium transport mutants. *J. Gen. Physiol.* 67, 325–341. doi: 10.1085/jgp.67.3.325

Saitou, N., and Nei, M. (1987). The neighbor-joining method: a new method for reconstructing phylogenetic trees. *Mol. Biol. Evol.* 4, 406–425.

Seemann, T. (2014). Prokka: rapid prokaryotic genome annotation. *Bioinformatics* 30, 2068–2069. doi: 10.1093/bioinformatics/btu153

Simon, R. D., and Weathers, P. (1976). Determination of the structure of the novel polypeptide containing aspartic acid and arginine which is found in cyanobacteria. *Biochim. Biophys. Acta* 420, 165–176. doi: 10.1016/0005-2795(76)90355-X

Sizova, M. V., Panikov, N. S., Spiridonova, E. M., Slobodova, N. V., and Tourova, T. P. (2007). Novel facultative anaerobic acidotolerant *Telmatospirillum siberiense* gen. nov. sp. nov. isolated from mesotrophic fen. *Syst. Appl. Microbiol.* 30, 213–220. doi: 10.1016/j.syapm.2006.06.003

Tamura, K., Stecher, G., Peterson, D., Filipski, A., and Kumar, S. (2013). MEGA6: molecular evolutionary genetics analysis version 6.0. *Mol. Biol. Evol.* 30, 2725–2729. doi: 10.1093/molbev/mst197

Tischler, J. S., Jwair, R. J., Gelhaar, N., Drechsel, A., Skirl, A. M., Wiacek, C., et al. (2013). New cultivation medium for "*Ferrovum*" and Gallionella-related strains. *J. Microbiol. Methods* 95, 138–144. doi: 10.1016/j.mimet.2013.07.027

Ullrich, S. R., González, C., Poehlein, A., Tischler, J. S., Daniel, R., Schlömann, M., et al. (2016b). Gene loss and horizontal gene transfer contributed to the genome evolution of the extreme acidophile "*Ferrovum.*" *Front. Microbiol.* 7:797. doi: 10.3389/fmicb.2016.00797

Ullrich, S. R., Poehlein, A., Tischler, J. S., González, C., Ossandon, F. J., Daniel, R., et al. (2016a). Genome analysis of the biotechnologically relevant acidophilic iron-oxidizing strain JA12 indicates phylogenetic and metabolic diversity within the novel genus "*Ferrovum.*" *PLoS ONE* 11:e0146832. doi: 10.1371/journal.pone.0146832

Ullrich, S. R., Poehlein, A., Voget, S., Hoppert, M., Daniel, R., Leimbach, A., et al. (2015). Permanent draft genome sequence of *Acidiphilium* sp. JA12-A1. *Stand. Genomic Sci.* 10:56. doi: 10.1186/s40793-015-0040-y

Vignais, P. M., Billoud, B., and Meyer, J. (2001). Classification and phylogeny of hydrogenases. *FEMS Microbiol. Rev.* 25, 455–501. doi: 10.1111/j.1574-6976.2001.tb00587.x

Wang, H., and Norén, A. (2006). Metabolic regulation of nitrogen fixation in *Rhodospirillum rubrum*. *Biochem Soc. Trans.* 34, 160–161. doi: 10.1042/BST0340160

Watanabe, T., Kojima, H., and Fukui, M. (2014). Complete genomes of freshwater sulfur oxidizers *Sulfuricella denitrificans* skB26 and *Sulfuritalea hydrogenivorans* sk43H: genetic insights into the sulfur oxidation pathway of betaproteobacteria. *Syst. Appl. Microbiol.* 37, 387–395. doi: 10.1016/j.syapm.2014.05.010

Wood, A. P., Aurikko, J. P., and Kelly, D. P. (2004). A challenge for 21st century molecular biology and biochemistry: what are the causes of obligate autotrophy and methanotrophy? *FEMS Microbiol. Rev.* 28, 335–352. doi: 10.1016/j.femsre.2003.12.001

Young, G. M., Amid, D., and Miller, V. L. (1996). A bifunctional urease enhances survival of pathogenic *Yersinia enterocolitica* and *Morganella morganii* at low pH. *J. Bacteriol.* 178, 6487–6495. doi: 10.1128/jb.178.22.6487-6495.1996

Conflict of Interest Statement: The authors declare that the research was conducted in the absence of any commercial or financial relationships that could be construed as a potential conflict of interest.

frontiers in Microbiology

ORIGINAL RESEARCH
published: 20 February 2017
doi: 10.3389/fmicb.2017.00222

Genome Sequence of *Desulfurella amilsii* Strain TR1 and Comparative Genomics of *Desulfurellaceae* Family

*Anna P. Florentino[1,2], Alfons J. M. Stams[1,3] and Irene Sánchez-Andrea[1]**

[1] Laboratory of Microbiology, Wageningen University, Wageningen, Netherlands, [2] Sub-department of Environmental Technology, Wageningen University, Wageningen, Netherlands, [3] Centre of Biological Engineering, University of Minho, Braga, Portugal

The acidotolerant sulfur reducer *Desulfurella amilsii* was isolated from sediments of Tinto River, an extremely acidic environment. Its ability to grow in a broad range of pH and to tolerate certain heavy metals offers potential for metal recovery processes. Here we report its high-quality draft genome sequence and compare it to the available genome sequences of other members of *Desulfurellaceae* family: *D. acetivorans*, *D. multipotens, Hippea maritima*, *H. alviniae, H. medeae,* and *H. jasoniae*. For most species, pairwise comparisons for average nucleotide identity (ANI) and *in silico* DNA–DNA hybridization (DDH) revealed ANI values from 67.5 to 80% and DDH values from 12.9 to 24.2%. *D. acetivorans* and *D. multipotens,* however, surpassed the estimated thresholds of species definition for both DDH (98.6%) and ANI (88.1%). Therefore, they should be merged to a single species. Comparative analysis of *Desulfurellaceae* genomes revealed different gene content for sulfur respiration between *Desulfurella* and *Hippea* species. Sulfur reductase is only encoded in *D. amilsii*, in which it is suggested to play a role in sulfur respiration, especially at low pH. Polysulfide reductase is only encoded in *Hippea* species; it is likely that this genus uses polysulfide as electron acceptor. Genes encoding thiosulfate reductase are present in all the genomes, but dissimilatory sulfite reductase is only present in *Desulfurella* species. Thus, thiosulfate respiration via sulfite is only likely in this genus. Although sulfur disproportionation occurs in *Desulfurella* species, the molecular mechanism behind this process is not yet understood, hampering a genome prediction. The metabolism of acetate in *Desulfurella* species can occur via the acetyl-CoA synthetase or via acetate kinase in combination with phosphate acetyltransferase, while in *Hippea* species, it might occur via the acetate kinase. Large differences in gene sets involved in resistance to acidic conditions were not detected among the genomes. Therefore, the regulation of those genes, or a mechanism not yet known, might be responsible for the unique ability of *D. amilsii*. This is the first report on comparative genomics of sulfur-reducing bacteria, which is valuable to give insight into this poorly understood metabolism, but of great potential for biotechnological purposes and of environmental significance.

Keywords: comparative genomics, *Desulfurellaceae*, sulfur reducers, acidophiles, metabolism

OPEN ACCESS

Edited by:
Axel Schippers, Federal Institute for Geosciences and Natural Resources, Germany

Reviewed by:
Mario A. Vera, Pontifical Catholic University of Chile, Chile
Mark Dopson, Linnaeus University, Sweden
Raquel Quatrini, Fundación Ciencia and Vida, Chile

****Correspondence:***
Irene Sánchez-Andrea
irene.sanchezandrea@wur.nl

Specialty section:
This article was submitted to Extreme Microbiology, a section of the journal Frontiers in Microbiology

Received: *29 September 2016*
Accepted: *31 January 2017*
Published: *20 February 2017*

Citation:
Florentino AP, Stams AJM and Sánchez-Andrea I (2017) Genome Sequence of Desulfurella amilsii Strain TR1 and Comparative Genomics of Desulfurellaceae Family. Front. Microbiol. 8:222. doi: 10.3389/fmicb.2017.00222

The prefix of the locus tags for the analyzed species are *D. amilsii* – DESAMIL20_, *D. acetivorans* – Desace_, *H. maritima* – Hipma_, *H. jasoniae* – EK17DRAFT, *H. alviniae* – G415DRAFT_, and *H. medeae* – D891DRAFT_.

INTRODUCTION

Elemental sulfur reduction is a respiratory-chain dependent redox process that yields ATP by utilizing sulfur as an oxidizing agent. This metabolism is of great importance for the biogeochemical cycle of sulfur in extreme environments, from where sulfur reducers have most frequently been isolated (Bonch-Osmolovskaya et al., 1990; Stetter, 1996; Alain et al., 2009; Birrien et al., 2011). Sulfur reduction leads to the formation of sulfide, a compound that, despite its corrosive properties, has an important role in biotechnological applications, such as metal precipitation (Johnson and Hallberg, 2005). Early assumptions considered sulfur reduction to be of low physiological importance as reviewed by Rabus et al. (2006). However, it is now known that this metabolism can yield energy for growth coupled to the utilization of several electron donors, such as alcohols, organic acids, and sugars (Bonch-Osmolovskaya et al., 1990; Finster et al., 1997; Dirmeier et al., 1998; Boyd et al., 2007; Florentino et al., 2016b); and the majority of sulfur-reducing microorganisms are able to grow chemolithotrophically (Segerer et al., 1986; Bonch-Osmolovskaya et al., 1990; Caccavo et al., 1994; Stetter, 1996; Miroshnichenko et al., 1999). Although sulfur-reducing microorganisms have a versatile metabolism (Dirmeier et al., 1998; Boyd et al., 2007), little attention has been paid to its genomic features beyond the biochemistry and bioenergetics of the process.

From current observations, microorganisms able to reduce elemental sulfur are spread over more than a 100 genera in the tree of life (Florentino et al., 2016a). In the *Bacteria* domain, the majority of the sulfur-reducing species align within the *Proteobacteria* phylum. In this group, the *Desulfurellaceae* family comprises the genera *Desulfurella* and *Hippea*, inhabiting terrestrial environments and submarine hot vents, respectively (Blumentals et al., 1990; Greene, 2014). Although the genomes of several members of the *Desulfurellaceae* family are sequenced, *Hippea maritima* is the only species with its genome description reported.

Desulfurella amilsii, an acidotolerant sulfur reducer, was recently isolated from sediments of the Tinto River, an extreme acidic environment (Florentino et al., 2015). The phenotypic characterization of *D. amilsii* revealed its ability to utilize not only sulfur but also thiosulfate as an electron acceptor (as was reported for *D. propionica*) and to ferment pyruvate (as also reported for *D. acetivorans*). Unlike other members in the *Desulfurellaceae* family, *D. amilsii* utilizes formate as an electron donor and thrives at pH as low as 3 (Florentino et al., 2016a). The utilization of acetate is common among the species. However, the ability of *D. amilsii* to metabolize it at low pH is peculiar, since at acidic conditions, acetate is protonated and become acetic acid, a toxic compound for most prokaryotic species (Holyoak et al., 1996).

The respiration of elemental sulfur is thought to be coupled to ADP phosphorylation, in which hydrogenases or dehydrogenases transfer electrons to sulfur-reducing enzymes via electron carriers, such as menaquinones or cytochromes (Rabus et al., 2006) together with proton translocation. The biochemical mechanisms via which microorganisms reduce elemental sulfur to H_2S and the nature of the enzymes involved in the process are not yet completely understood, especially at low pH. The low solubility of elemental sulfur in aqueous medium (5 $\mu g\ L^{-1}$ at 20°C) and the chemical transformation of sulfur compounds, that is dependent on pH, hamper a broad understanding of sulfidogenic processes (Schauder and Müller, 1993; Florentino et al., 2016b). Some microorganisms, as for example *Wolinella succinogenes* (Macy et al., 1986) can overcome the low solubility of elemental sulfur by utilizing more hydrophilic forms of the compound, such as polysulfides. In aqueous solution containing nucleophiles, such as sulfide or cysteine, elemental sulfur can be readily converted to polysulfide (Blumentals et al., 1990; Schauder and Müller, 1993), particularly at neutral and high pH levels. The most studied sulfur reducers are neutrophiles where the enzymes that have been suggested to use polysulfide as a substrate -sulfhydrogenase (SH) and polysulfide reductase (PSR) – are targeted (Macy et al., 1986). However, the instability of polysulfide at low pH, makes it an unlikely substrate for acidophiles.

A sulfur reductase (SRE) was purified from the membrane fraction of *Acidianus ambivalens,* which respires elemental sulfur in a range of pH from 1 to 3.5 (Laska et al., 2003). This enzyme uses elemental sulfur as a substrate and seems to be responsible for sulfur respiration at low pH values, where the formation of soluble intermediates, such as polysulfide is unlikely. Therefore, direct contact is hypothesized to be essential for elemental sulfur reduction at low pH (Stetter and Gaag, 1983; Pihl et al., 1989; Finster et al., 1998; Laska et al., 2003). The mechanisms by which sulfur reducers get access to insoluble sulfur, however, are still unclear.

Although the optimum pH for growth of *Desulfurellaceae* members is approximately neutral (6.0–7.0), *D. acetivorans* withstands pH as low as 4.3 for its growth. However, the ability of *D. amilsii* to thrive at very acidic conditions, pH as low as 3, is unique in the *Desulfurellaceae* family, which makes it a potential catalyst for biotechnological processes, such as metal precipitation from acidic waste streams. To get insights into the encoded pathways for sulfur reduction by this strain, we analyzed the genome of *D. amilsii* and compared it with available genome sequences of other members within the *Desulfurellaceae* family. To the best of our knowledge, there is no reported study on comparative genomics of acidophilic sulfur-reducing microorganisms adapted to different conditions.

MATERIALS AND METHODS

Cultivation, Genome Sequencing and Assembly

For genome sequencing, a 500-mL culture of *D. amilsii* was grown on acetate and sulfur as described elsewhere (Florentino et al., 2015). Cells were harvested at the early stationary phase, when the sulfide production in the culture reached 10 mM, by centrifuging at 19000 × *g* for 20 min. Genomic DNA was extracted using the MasterPure^{TM} Gram Positive DNA Purification Kit (Epicentre, Madison, WI, USA), following the instructions of the manufacturer. The genome was sequenced using the Illumina HiSeq2000 paired-end sequencing platform

of GATC Biotech (Konstanz, Germany). Sequence assembly was performed using two independent assemblers: the OLC-assembler Edena (Hernandez et al., 2008) and the de-Bruijn-Graph-assembler Ray (Boisvert et al., 2010). Sets of overlapping sequences were identified from both assembling procedures and further merged into a more contiguous and consistent assembly, using the hybrid sequencing technology assembler Zorro (Argueso et al., 2009). The obtained sequences were further improved by scaffolding with Opera and by gap-closing with GapFiller (Boetzer and Pirovano, 2012). The closed gaps were manually verified.

Genome Annotation

Automated annotation was performed using the RAST annotation server (Aziz et al., 2008), followed by manual curation. Additional gene prediction analysis and functional annotation were done within the Integrated Microbial Genomes – Expert Review from the DOE – Joint Genome Institute pipeline (Markowitz et al., 2014). The predicted coding sequences (CDSs) were translated into amino acid sequences and used in homology searches in the National Center for Biotechnology Information (NCBI) non-redundant database and the Uniprot, TIGRFam, Pfam, SMART, PRIAM, KEGG, COG, and Interpro databases. These data sources were combined to assign a product description for each predicted protein. Clusters of regularly interspaced repeats (CRISPR) were identified via the web available tools CRISPRFinder (Grissa et al., 2007) and CRISPRTarget (Biswas et al., 2013). The N-terminal twin arginine translocation (Tat) signal peptides and the transmembrane helices were predicted using the online tools from TMHMM server v. 2.03[1] and PROTTER v. 1.0[2].

The Whole Genome Shotgun project of *Desulfurella amilsii* has been deposited at DDBJ/ENA/GenBank under the accession MDSU00000000. The version described in this paper is version MDSU01000000. The genome ID in the integrated microbial genomes-expert review (IMG) database is 2693429826.

Comparative Genomics

The genome sequences used for the comparative study (and their accession numbers) were: *D. acetivorans* strain A63 (CP007051), *D. multipotens* strain RH-8 (SAMN05660835), *H. maritima* strain MH2 (CP002606), *H. alviniae* strain EP5-r (ATUV00000000), *H. medeae* strain KM1 (JAFP00000000), and *H. jasoniae* strain Mar08-272r (JQLX00000000).

The average nucleotide identity analysis (ANI) between the genome dataset pairs was performed using the online tool ANI calculator, available at http://enve-omics.ce.gatech.edu/ani/index. The best hits (one-way ANI) and the reciprocal best hits (two-way ANI) were considered, as calculated by Goris et al. (2007). *In silico* DNA–DNA hybridization (DDH) values were determined using the recommended settings of the Genome-to-Genome Distance Calculator (GGDC) web server version 2.0 (Meier-Kolthoff et al., 2013).

The number of genes shared between *Desulfurella* and *Hippea* species was assessed by OrthoMCL tool (Wang et al., 2015) and a Venn diagram was built using the web-based tool InteractiVenn (Heberle et al., 2015). Orthology between two genes was defined as best bidirectional hits, which were required to have at least 30% identity over at least 80% coverage of both sequences (Chen et al., 2006). All analyzed genes and predicted proteins from the *Desulfurellaceae* members' genomes were compared using BLAST (Altschul et al., 1990).

The genomes were compared in terms of gene content using the 'Phylogenetic Profiler for Single Genes' of JGI-IMG website[3] to identify genes in the query genome that have homologs present or absent in other genomes. The 'Phylogenetic Profiler for Gene Cassettes' tool of the same website was also used to find part of a gene cassette in a query genome, as well as conserved part of gene cassettes in other genomes. In terms of functional capabilities, comparisons of relative abundance of protein families (COGs, Pfams, TIGRfams) across selected genomes were performed with the 'Abundance Profile Overview' and 'Function Profile' tools. The potential metabolic capabilities of genomes were compared in the context of KEGG pathways.

RESULTS AND DISCUSSION

General Characteristics of the *D. amilsii* Genome

The *D. amilsii* genome consists of 2.010.635 bp with a G + C content of 33.98% mol/mol. The initial sequencing resulted in 2.287.922 paired-end reads with a length of 301 bases, which were assembled into 20 contigs with a 687 fold coverage and a completeness of 99.9%. The largest scaffold consisted of 1,269,579 bp and the second and third largest scaffolds together consisted of 400,000 bp, covering more than 85% of the genome.

From the 2137 genes predicted by automated annotation in the genome, 49 were tRNA and rRNA genes, and 2088 protein coding genes (CDS). Two identical copies of the 16S rRNA gene (100% similarity) were identified. From the 2088 CDS (Supplementary Table S1), 1625 were predicted to have assigned COGs function, whilst 680 could not be assigned to any function in the database, and therefore were annotated as hypothetical proteins or proteins of unknown function. No pseudo genes were detected in the genome of *D. amilsii*, which is a unique characteristic in the *Desulfurellaceae* family. Two CRISPR regions were identified in the genome of 684 bp length with 10 spacers, and 291 bp length with 4 spacers, respectively. The spacers' sequences from the first locus match viral DNA sequences found in several species in a BLAST based search, including *Bacillus* sp., *Ralstonia* sp., *Shewanella* sp., *Acinetobacter* sp., *Propionibacterium* sp., *Campylobacter* sp., *Escherichia* sp., *Staphylococcus* sp., *Sphingomonas* sp., and *Moraxella* sp. The spacer's sequences related to the second locus match sequences of viral DNA also detected in *Edwardsiella hoshinae*, *Owenweeksia hongkongensis*, *Parascaris equorum,* and *Ovis canadensis* species.

[1] http://www.cbs.dtu.dk/services/TMHMM/

[2] http://wlab.ethz.ch/protter/start/

[3] https://img.jgi.doe.gov/

The genome encodes a complete tricarboxylic acid (TCA) cycle pathway (Supplementary Table S2). Besides, routes for pyruvate fermentation are encoded, and physiological tests revealed acetate, hydrogen and CO_2 as the end products (Florentino et al., 2016a). *D. amilsii* is able to grow chemolithotrophically; the CO_2 fixation could be possible via the reductive TCA cycle for which all the genes are encoded (Supplementary Table S3). The genome encodes Ni–Fe, Ni–Fe–Se, and Fe–S hydrogenases, an intracellular formate dehydrogenase (FDH) and a formate-hydrogen lyase. Genes encoding for dinitrogenase iron-molybdenum cofactor, nitrogen fixation protein NifU and glutamine synthetase type I are present in the genome and might be involved in nitrogen fixation by *D. amilsii*. Sulfur and thiosulfate were reported to serve as electron acceptors for this microorganism (Florentino et al., 2015, 2016a) and genes essential for sulfur and thiosulfate reduction are encoded (Supplementary Table S3). Moreover, the importance of electron transport in this microorganism is highlighted by a high number of electron transport related genes (159). Genes encoding resistance to acidic conditions (Supplementary Table S4), oxygen stress tolerance (Supplementary Table S5), and metals resistance (Supplementary Table S6) are also identified, which is in line with the reported ability of the microorganism to grow at pH as low as 3 (Florentino et al., 2016a) and in the presence of heavy metals in solution (Florentino et al., 2015).

Comparative Genomics

ANI and *In silico* DDH Analysis

Average nucleotide identity and *in silico* DDH values obtained from pairwise comparison of the available genome sequences of *Desulfurellaceae* family members are shown in **Table 1**. ANI values in the range of ≥95–96% correspond to ≥70% DDH standard for species definition (Goris et al., 2007). In general, the values are consistent with their phylogenetic relationships. While the taxonomic status of *D. amilsii* is well supported by the genomic signatures analysis, ANI and DDH values of *D. multipotens* and *D. acetivorans* were 98.6 and 88.1% respectively, surpassing the thresholds for species definition. The wet laboratory DNA–DNA hybridization experiment reported a borderline value of 69 ± 2% (Miroshnichenko et al., 1994) and the phylogenetic reconstruction of the *Desulfurella* genus shown by Florentino et al. (2016a) revealed more than 99.9% shared identity of 16S rRNA sequences for the two strains, while all the other members of the *Desulfurellaceae* family shared 92.1–97.7% identity (Supplementary Table S7).

The physiological characterization of these two strains revealed different abilities to utilize butyrate and H_2 as electron donors, which are oxidized by *D. multipotens* (Miroshnichenko et al., 1994) but not by *D. acetivorans* (Bonch-Osmolovskaya et al., 1990). Furthermore, the generation time was shown to be 2 h for *D. acetivorans*, while it was 5 h for *D. multipotens*, although generation time can generally vary with the growth conditions. The optimum range of temperature for growth ranged from 52–55°C in *D. acetivorans* (Bonch-Osmolovskaya et al., 1990) to 58–60°C in *D. multipotens* (Miroshnichenko et al., 1994). No chemotaxonomic information is provided in the characterization manuscripts of the mentioned strains. Although the characterization studies showed a G + C content of 31.4% mol/mol for *D. acetivorans* (Bonch-Osmolovskaya et al., 1990) and 33.5% mol/mol for *D. multipotens* (Miroshnichenko et al., 1994), the G + C content calculation based on the genome sequences shows no difference between them, with 32% mol/mol of G + C content. Despite the mentioned different physiological characteristics mentioned, the ANI values combined with an *in silico* DDH evaluation and a phylogenetic analysis of the 16S rRNA sequences support the similarity of both strains. Therefore, *D. multipotens* and *D. acetivorans* might belong to the same species and should be reclassified. Due to this finding, the comparative genomics described in this manuscript was performed with *D. acetivorans* as representative of *D. multipotens*, as it was the first species described and so represents the type strain of the genus.

In general, members of the *Desulfurellaceae* family possess a small genome, ranging from 1.7 to 2.0 Mbp of which more than 93% represent DNA coding regions, 80% of proteins with a predicted function and 70% of clusters of orthologous groups of proteins (COGs). General features of the genomes are compared in **Table 2**. In total, 2738 clusters of orthologous groups with functional prediction were found within the six members studied as shown in a Venn-diagram (**Figure 1**). The core genome consisted of 1073 shared sequences, 411 sequences shared by both *Desulfurella* genomes and 250 shared within the *Hippea* genus. *D. amilsii* showed the biggest genome size in the family and the biggest number of unique genes encoded, 283 (Supplementary Table S8), from which 62% are related to hypothetical proteins. Divergences in unique and shared gene sets might also explain other differences that have been found when conducting comparative studies on metabolism among the species, especially with respect to enzymes involved in sulfur reduction, sulfur disproportionation, pyruvate fermentation, and formate utilization.

Sulfur Reduction and Energy Conservation

The electron transport chain in sulfur reducers normally links hydrogenases or dehydrogenases to membrane bound or cytoplasmic sulfur/polysulfide reductases (Laska et al., 2003; Fauque and Barton, 2012; Florentino et al., 2016b). However, the electron-transfer pathways in the microorganisms analyzed here are not yet fully understood.

Sulfur metabolism in *Desulfurellaceae* members is quite diverse, as genes encoding for at least three enzymes involved in sulfur reduction are present in the group. Sulfur, sulfide and polysulfide are present in solution in a pH-dependent equilibrium ($HS^- + \frac{x-1}{8}S_8 \leftrightarrow S_n^{2-} + H^+$). At higher pH values, polysulfide is present as the dominant form, while at low pH values elemental sulfur prevails (Kleinjan et al., 2005).

Hippea species genomes possess genes encoding for the membrane bound PSR, an integral membrane protein complex responsible for quinone oxidation coupled to polysulfide reduction, and the cytoplasmic sulfide dehydrogenase (SUDH), reported to catalyze the reduction of polysulfide to hydrogen

TABLE 1 | Average nucleotide identity and *in silico* DNA–DNA hybridization pairwise comparison of the available genomes sequences of *Desulfurellaceae* family.

	Average nucleotide identity (ANI)						
	Dam	***Dac***	***Dmu***	***Hma***	***Hme***	***Hal***	***Hja***
1		80.0	80.0	68.4	67.5	68.7 (±0.1)	68.4
2	21.9 (±2.4)		**98.6**	68.9 (±0.1)	69.1 (±0.2)	69.8	69.1
3	21.8 (±2.4)	**88.1 (±2.3)**		68.8	67.8	69.4	69.0
4	24.2 (±2.4)	23.7 (±2.4)	23.2 (±2.4)		78.7	74.0 (±0.1)	72.9
5	27.2 (±2.4)	23.9 (±2.4)	24.1 (±2.4)	20.7 (±2.3)		73.4	72.6
6	21.6 (±2.4)	17.4 (±2.2)	17.0 (±2.2)	16.9 (±2.2)	12.9 (±2.5)		73.1
7	16.5 (±6.4)	14.9 (±3.5)	14.9 (±3.5)	16.1 (±1.0)	15.8 (±1.4)	16.3 (±0.7)	
	DNA–DNA hybridization (DDH)						

Dam, D. amilsii; Dac, D. acetivorans; Dmu, D. multipotens; Hma, H. Maritima; Hme, H. medeae; Hal, H. alviniae; Hja, H. jasoniae. The table is split by the empty diagonal cells; the ANI values are shown on the upper side and the in silico DDH values are shown on the lower side. Standard deviation values derived from bi-directional calculation are shown in brackets when they differed from 0. Values in bold highlight the off-limit comparison between D. acetivorans and D. multipotens.

TABLE 2 | General genome features of *Desulfurellaceae* members.

Features	***D. amilsii***	***D. acetivorans***	***H. maritima***	***H. alviniae***	***H. medeae***	***H. jasoniae***
Strain	TR1	A63	MH2	EP5-r	KM1	Mar08-272r
DSM number	29984	5264	10411	24586	–	24585
Genome size (Mbp)	2.0	1.8	1.7	1.7	1.7	1.7
Completeness (%)	99.9	100	99.1	72.6	99.1	100
DNA coding	1877485	1731246	1624527	1672554	1669463	1655666
G+C (%)	33.98	32.08	37.47	37.03	42.85	37.00
Scaffolds	20	2	1	4	1	18
Total genes	2135	1875	1780	1814	1776	1768
CDS	2086	1819	1723	1757	1719	1710
RNA genes	49	56	57	57	57	58
tRNA genes	45	48	48	46	48	46
Pseudo genes	–	53	46	39	23	11
Function prediction	1723	1586	1498	1477	1499	1495
COGs	1456	1402	1287	1327	1320	1306
Pfam domains	1719	1633	1529	1535	1541	1536
CRISPR counts	2	3	–	1	4	–

sulfide with NADPH as the electron donor (Macy et al., 1986; Ma et al., 2000). The domains 4Fe-4S, 4Fe-S Mo-bis of the catalytic subunit and Nfr of the membrane-bound subunit with nine transmembrane helices of the PSR are conserved in all the *Hippea* species. The pH range for growth of *Hippea* species (Miroshnichenko et al., 1999; Flores et al., 2012) supports the hypothesis of sulfur reduction through polysulfide in these microorganisms.

The alpha and beta subunits of the SUDH encoded in all genomes of the *Desulfurellaceae* family show domains conserved in all the microorganisms: NAD-binding and iron-sulfur clusters (3Fe-4S and 4Fe-4S) domains in the subunit SudhA and FAD-binding and iron-sulfur cluster 2Fe-2S domains in the subunit SudhB. In *D. acetivorans*, only SUDH-coding genes are present (Desace_0075-0076), which would suggest that polysulfide is the terminal electron acceptor in its respiration process. *D. amilsii* is unique as, in addition to SUDH (DESAMIL20_1852-1853), SRE is encoded (DESAMIL20_1357-1361). A SRE was isolated from the acidophile *Acidianus ambivalens*, and its subunits were partially characterized and compared to their homologous in the PSR isolated from *Wolinella succinogenes* (Laska et al., 2003). SRE is reported to be involved in direct reduction of elemental sulfur, with the electrons being donated by hydrogenase, quinones and cytochrome *c*. SRE also uses NADPH as an electron donor, but at low activity (Laska et al., 2003). The SRE encoded in the *D. amilsii* genome presents, in general, conserved domains for four of its subunits. The membrane anchor subunit (SreC), with nine transmembrane helices, has a PSR domain (**Figure 2**) similar to the one encoded in *A. ambivalens,* which was shown by Laska et al. (2003) to be phylogenetically unrelated to the analogous *W. succinogenes* protein. The catalytic subunit (SreA) contains the conserved molybdopterin domain, predicted to be functional with respect to oxidoreductase activity. The sequence, however, does not present a twin-arginine motif and so, in contrary to the SRE from *A. ambivalens*, it might be cytoplasm oriented. The subunit SreB also presents the 4Fe-4S domain

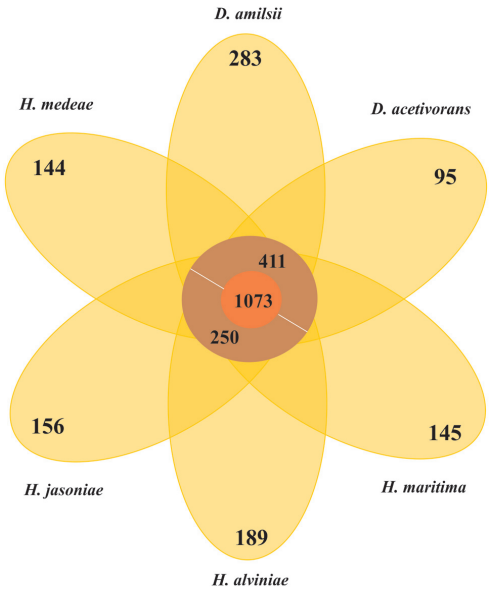

FIGURE 1 | Venn-diagram of the orthologous clusters of genes for *Desulfurellaceae* family members.

conserved, which has a high degree of sequence similarity to Mo-FeS enzymes of the DMSO reductase family. The subunit SreD in *D. amilsii* does not contain the conserved 4Fe-4S domain; but its function in sulfur respiration is not yet clears (Laska et al., 2003). The *sreE* gene encodes a protein of 209 aa length with similarity to reductase assembly proteins required either for the assembly of the Mo-containing large subunit of DMSO reductase or nitrate reductase (Blasco et al., 1998; Ray et al., 2003).

Since the reduction of elemental sulfur through polysulfide is unlikely at low pH, the SRE encoded in *D. amilsii* might play a role when this microorganism grows in acidic conditions. Moreover, several thiosulfate sulfurtransferases with rhodanese domains are exclusively encoded in *Desulfurella* species.

The enzyme SUDH isolated from *Pyrococcus furiosus* was reported to show SRE activity *in vitro*. However, the expression of its coding-genes also correlated to the carbon source rather than to elemental sulfur/polysulfide, especially when its intracellular concentration is below 1.25 mM (Ma and Adams, 2001). It is likely that this enzyme acts *in vivo* as a ferredoxin:NADPH oxidoreductase (NfnAB). In this case, in *Hippea* species, the sulfur reduction process might be carried out by the PSR, while in *Desulfurella* species the rhodanese-like thiosulfate sulfurtransferases might play an essential role. In **Figure 2**, a metabolic reconstruction of the possible sulfur reduction pathways in *D. amilsii* is depicted.

Desulfurella amilsii is able to use thiosulfate as a terminal electron acceptor in a range of pH from 5 to 7, an ability not reported for any of the other analyzed genomes of the members of *Desulfurellaceae*. Although *D. propionica* was also shown *in vivo* to utilize thiosulfate as an electron acceptor, its genome sequence is not yet available. The known pathway of thiosulfate reduction refers to a two-step process, involving the enzymes thiosulfate reductase and the dissimilatory sulfite reductase (Stoffels et al., 2012). The first is reported to be involved in the conversion of thiosulfate into sulfide and sulfite, which can be toxic for most microorganisms. The dissimilatory reductase converts the generated sulfite into sulfide, eliminating the toxicity of sulfite from the medium. In *D. amilsii*, it is likely that thiosulfate respiration occurs via this pathway, as the thiosulfate reductase, the dissimilatory sulfite reductase (DsrAB), the DsrC protein and the subunits DsrM and DsrK of the Dsr MKJOP complex are encoded in the genome. The genome of *D. acetivorans* encodes a thiosulfate reductase and the dissimilatory sulfite reductase, but subunits of the Dsr MKJOP transmembrane complex and the DsrC protein are not encoded. Therefore, the absence of subunits of Dsr MKJOP and DsrC might explain the inability of *D. acetivorans* to respire thiosulfate. **Table 3** summarizes the enzymes involved in sulfur and thiosulfate respiration, with their respective reactions and the orthologs genes.

Desulfurella species grow and produce sulfide and sulfate from sulfur in the absence of an organic electron donor (Florentino et al., 2016a), in a specific redox reaction that undergoes oxidation and reduction, also called disproportionation. Sulfur could be converted into sulfide via a sulfur-reducing enzyme (e.g., SRE/SUDH) and to sulfite by an unidentified enzyme. In general, the sulfite could be oxidized to sulfate by sulfite oxidoreductase (SUOR) or adenosine-5′-phosphosulfate (APS) reductase, with ATP sulfurylase or adenylylsulfate:phosphate adenylyltransferase (APAT) being involved (Finster et al., 1998; Frederiksen and Finster, 2003; Hardisty et al., 2013). Although the enzyme responsible for the conversion of sulfur into sulfite is not known, SUDH/SRE and DSR coding genes were detected in both *Desulfurella* members' genomes, suggesting that these bacteria might disproportionate elemental sulfur using this pathway. APS reductase was not detected in any species, which supports the inability of this group to use sulfate as electron acceptor or to disproportionate elemental sulfur via the reverse pathway from sulfite to APS and then to sulfate.

Sulfur metabolism in *Desulfurellaceae* family members is quite diverse. The presence of unique proteins in *D. amilsii* might explain its ability to respire elemental sulfur at low pH, where polysulfide is not available. The ability of *D. amilsii* to respire thiosulfate in a two-step process is also unique among the analyzed members of the family. Besides, disproportionation appears as a feature only shared by members of *Desulfurella* genus, and so this genus, with a more versatile metabolism, offers more possibilities for biotechnological application based on sulfidogenesis.

Other Aspects of *Desulfurellaceae* Members' Metabolism

Enzymes involved in the central carbon metabolism of *Desulfurellaceae* members are listed in Supplementary Table S2 and the ones involved in energy metabolism and conservation are listed in Supplementary Table S3. The general metabolic reconstruction of *D. amilsii* is depicted in **Figure 3**, in which

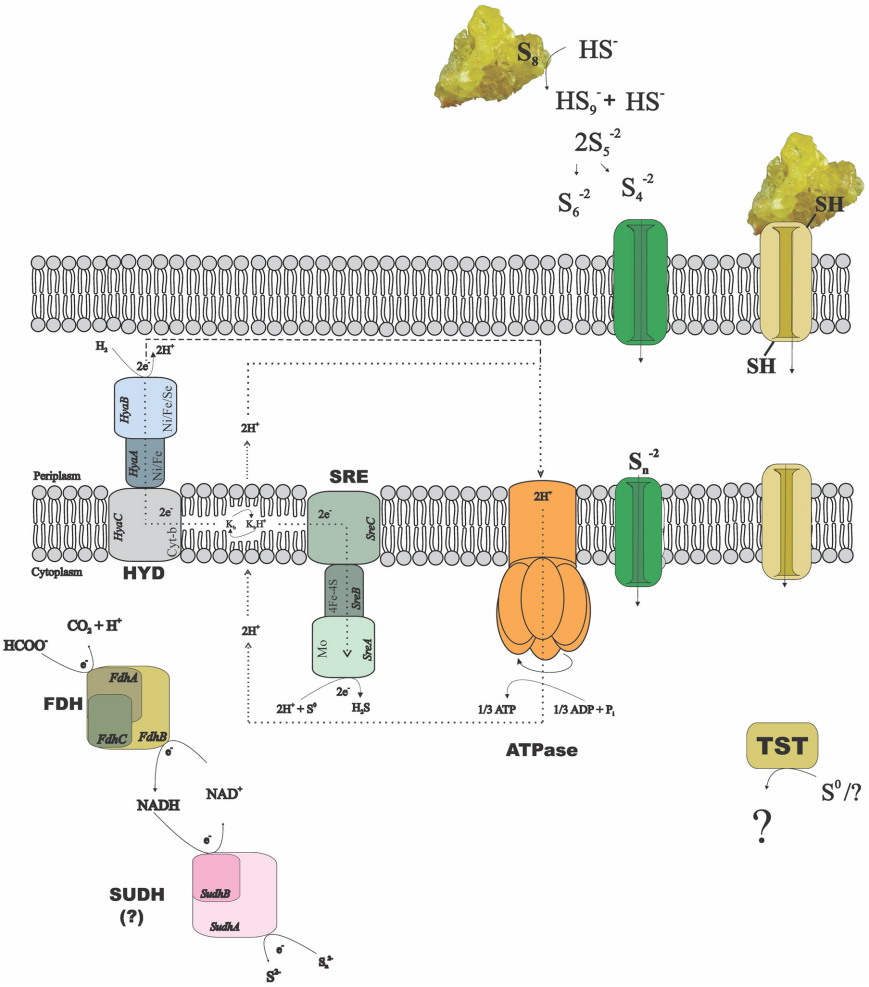

FIGURE 2 | Possible mechanisms of sulfur/polysulfide respiration in *Desulfurella amilsii*. During chemolithotrophic growth, hydrogenases (HYD) might transfer electrons to sulfur reductase (SRE) via menaquinones (K) encoded in the genome, and protons to an encoded ATPase, creating a proton motive force. If sulfide dehydrogenase (SUDH) plays a role in sulfur respiration, its cytoplasmic nature hampers the generation of proton motive force by any conventional mechanisms and therefore, it is likely that the membrane-bound hydrogenases pump protons out of the cell to generate a gradient. In case of formate used as electron donor, the intracellular formate dehydrogenase (FDH) encoded might transfer electrons to SUDH, with NAD^+/NADH as intermediates. Moreover, rhodanese-like proteins (TST) encoded in the genome might have a role in the process, but its performance in sulfur-respiring microorganisms is not yet clearly understood.

the differential central carbon metabolism for *Desulfurellaceae* members can also be seen. Proteins for complete Embden-Meyerhof-Parnas and oxidative TCA cycle pathways are encoded in all the genomes of the *Desulfurellaceae* members, as well as decarboxylating malate dehydrogenase (ME), which can catalyze the reversible conversion of malate to pyruvate. Although the malate dehydrogenase is present, malate transporters are not encoded in the genome of the analyzed *Desulfurella* genus members, which might explain their inability to use malate as an electron donor for growth.

Besides the conversion of phosphoenolpyruvate to pyruvate via pyruvate kinase (PYK) and the irreversible carboxylation of pyruvate to form oxaloacetate via pyruvate carboxylase (PYC) common for all *Desulfurellaceae* members, *Desulfurella* and *H. jasoniae* genomes also encode the phosphoenolpyruvate carboxylase (PCK). Pyruvate:ferredoxin oxidoreductase (PFOR) and related 2-oxoacid:ferredoxin oxidoreductases are encoded in all the genomes in the group, where pyruvate oxidation is a main intermediate metabolic reaction. Moreover, all the genomes possess the gene encoding pyruvate:formate lyase (PFL), involved in pyruvate metabolism and leading to the production of acetyl-CoA and formate. *D. amilsii* and *D. acetivorans* were shown to ferment pyruvate in laboratorial analyses, but formate could only be used as an electron donor by *D. amilsii* (Florentino et al., 2016a), despite the subunits FdoG, FdoH and FdoI of a FDH being encoded in *D. acetivorans* genome.

All members of the *Desulfurellaceae* family can utilize acetate (Florentino et al., 2016a). The metabolism of acetate starts with its activation to acetyl-CoA, an essential intermediate of

TABLE 3 | Enzymes, reactions and occurrence of orthologous genes involved in elemental sulfur and thiosulfate respiration in *Desulfurellaceae* family.

Enzyme	Reaction	Occurrence of orthologous genes						
		Subunits	*Dam*	*Dac*	*Hma*	*Hja*	*Hal*	*Hme*
Polysulfide reductase	$S_n^{2-} \rightarrow S^{2-} + S_{n-1}^{2-}$	PsrA	–	–	0433	1370	0846	0560
		PsrB	–	–	0434	1371	0847	0561
		PsrC	–	–	0435	1372	0848	0562
Sulfide dehydrogenase*	$S_n^{2-} \rightarrow S^{2-} + S_{n-1}^{2-}$	SudhA	1853	0076	0231	1601	1361	1618
		SudhB	1852	0075	0230	1600	1360	1617
Sulfur reductase	$S^0 \rightarrow S^{2-}$	SreA	1359	–	–	–	–	–
		SreB	1357	–	–	–	–	–
		SreC	1358	–	–	–	–	–
		SreD	1360	–	–	–	–	–
		SreE	1361	–	–	–	–	–
Thiosulfate reductase	$S_2O_3^{2-} \rightarrow S^{2-} + SO_3^{2-}$	PhsA	9	1254	0433	1171	1675	0227
		PhsB	8	1253	–	–	–	–
		PhsC	10	1255	–	1172	1676	0228
Sulfite reductase DsrC Complex Dsr MK	$SO_3^{2-} \rightarrow S^{2-}$	DsrA	1435	1402	–	–	–	–
		DsrB	1434	1401	–	–	–	–
		DsrC	1431, 2056	–	–	–	–	–
		DsrM	1430	–	–	–	–	–
		DsrK	1429	–	–	–	–	–

*Dam, D. amilsii; Dac, D. acetivorans; Hma, H. maritima; Hja, H. Jasoniae; Hal, H. alviniae; Hme, H. medeae. The prefix of the locus tags for the analyzed species are DESAMIL20_ (D. amilsii); Desace_ (D. acetivorans); Hipma_ (H. maritima); EK17DRAFT_ (H. jasoniae); G415DRAFT_ (H. alviniae) and D891DRAFT_ (H. medeae). To avoid repetition of the prefix in the table, all the locus tags are represented only by the specific identifier. *Possibly functioning as bifurcating/confurcating enzyme.*

various anabolic and catabolic pathways in all forms of life (Ingram-Smith et al., 2006). Acetate activation involves either the enzymes acetyl-CoA synthetase (ACS), acetate kinase (ACK) in combination with phosphate acetyltransferase (PTA), or the enzyme succinyl-CoA: acetate CoA-transferase (SCACT). All *Desulfurellaceae* species have the enzyme ACS encoded in their genome. In *Desulfurella* species, however, acetyl-CoA could also be generated from acetate via acetylphosphate involving ACK and PTA. The genome analysis shows both pathways for acetate oxidation are encoded in *Desulfurella* species. However, experimental studies performed by Schmitz et al. (1990) showed that cell extracts of *D. acetivorans* had high specific activities of ACK (5 U/mg) and PTA (14 U/mg), but no activity of the alternative ACS nor the SCACT. Although Goevert and Conrad (2010) demonstrated acetate activation via ACK and its metabolization via the TCA cycle in *H. maritima*, genes encoding ACK are not found in any *Hippea* members' genome.

Chemolithotrophic growth of *Desulfurellaceae* members with H_2 as electron donor and S^0 as electron acceptor requires at least two enzymes in a short electron transport chain composed by a hydrogenase, an electron carrier, and a sulfur/polysulfide reductase. Only one Ni-Fe type hydrogenase (HybABC), which catalyzes reversible hydrogen production/consumption, is encoded in *Desulfurellaceae* members together with its maturation protein HypABCDEF (Supplementary Table S3). The subunit HybB is embedded in the membrane and the subunit HybA possess a tat signal, therefore the hydrogenase is membrane-bound facing periplasm. The hydrogen is converted into protons, creating proton motive force and electrons which are transferred via intramembrane electron carriers, such as the encoded menaquinone, to the membrane bound SRE or PSR, or to the cytoplasmic SUDH.

Although physiological tests revealed some differences among the studied species, the comparative genomic analysis on the general metabolism of *Desulfurellaceae* members does not show great divergence in gene sets involved in chemolithotrophic growth, TCA cycle and pyruvate fermentation. However, the utilization of acetate might have different routes of metabolization by the two analyzed genera.

Resistance Mechanisms at Low pH

Acidophiles and acidotolerant microorganisms can have a broad range of adaptation mechanisms to thrive at acidic environments, while ensuring higher cytoplasmic pH values than the surrounding environment (Baker-Austin and Dopson, 2007).

It is predicted that *Desulfurella* species can synthesize degradative arginine decarboxylase to consume intracellular protons via the amino acid decarboxylation reaction and, consequently, neutralize the medium. Moreover, the analyzed *Desulfurella* species encode the K^+-transporting ATPase and a putative regulating histidine kinase, involved in the generation of positive internal membrane potential by influx of potassium ions in order to inhibit the flux of protons in extreme acidophiles (Dopson and Johnson, 2012). ABC phosphate

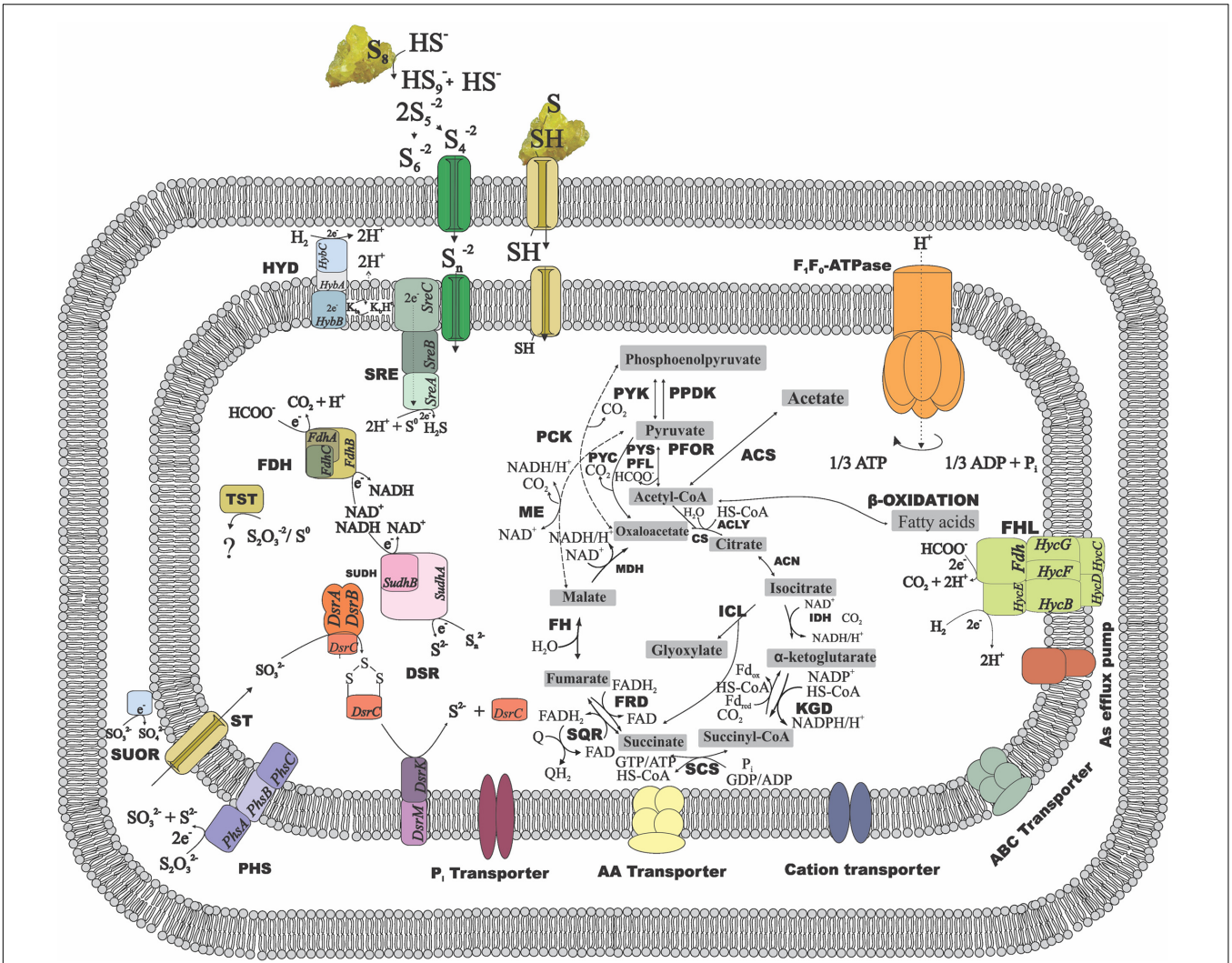

FIGURE 3 | Metabolic reconstruction of *D. amilsii*. Acetate, hydrogen or formate are possible electron donors for the given scheme while sulfur or thiosulfate are reflected as electron acceptors. The amino acids, cations and phosphate transporters encoded in the genome and likely involved in resistance to stress conditions are also depicted. ACK, acetate kinase; ACLY, ATP citrate lyase; ACS, acetyl-CoA synthetase; CS, citrate synthase; DSR, Dissimilatory sulfite reductase; FDH, formate dehydrogenase; FH, fumarate hydratase; FHL, formate hydrogen lyase; FRD, fumarate reductase; HYD, hydrogenase; ICL, Isocitrate lyase; IDH, Isocitrate dehydrogenase; KGD, α-ketoglutarate dehydrogenase; MDH, malate dehydrogenase; ME, malic enzymes; MK, menaquinone; PCK, phosphoenolpyruvate carboxinase; PFL, pyruvate:formate lyase; PFOR, pyruvate:ferredoxin oxidoreductase; PHS, thiosulfate reductase; PPDK, pyruvate phosphate dikinase; PTA, phosphotransacetylase; PYC, pyruvate carboxylase; PYK, pyruvate kinase; PYS, Pyruvate synthase; SCS, Succinyl-CoA synthetase; SQR, succinate-coenzyme Q reductase; SRE, sulfur reductase; SUDH, sulfide dehydrogenase; SUOR, sulfite oxidoreductase; TST, thiosulfate sulfurtransferase. The central carbon metabolism in the figure can be extended to all the members of Desulfurellaceae family, as most of the features are conserved among the species. The dashed lines represent exclusive possible conversions for Desulfurella species and the solid lines represent possible conversions common to all members of the studied family.

transporters, sodium-coupled antiporters and amino acid antiporters that are pH dependent (Kanjee and Houry, 2013) and related to acid resistance are also encoded in the referred genomes (Supplementary Table S4). The genomic components potentially involved in stress response to acidic environments in *Desulfurellaceae* members are listed in Supplementary Table S4.

The ability of *Desulfurella* species to thrive at low pH using acetate as an electron donor requires resistance mechanisms. When the pH of the medium is lower than the pKa value of acetic acid (4.75), the weak organic acid prevails in its protonated form, which crosses the cytoplasmic membrane by diffusion. At neutral cytoplasmic pH, the acid dissociates, leading to the release of protons and respective anions, resulting in the acidification of the cytoplasm (Holyoak et al., 1996). *Desulfurella* species genomes encode the ATP-binding cassette transporter (AatA) reported to be involved in acetic acid resistance in acetic acid bacteria (Nakano et al., 2006). This putative ABC transporter contains two ABC motifs in tandem on a single polypeptide, which possibly serves as an exporter of acetic acid, maintaining a low level of intracellular acetic acid concentration (Nakano et al., 2006).

The genes encoded in *Desulfurellaceae* family members possibly involved in resistance to low pH do not vary. However

physiological tests showed the ability of *Desulfurella* species to grow at more acidic environments, with *D. amilsii* being able to grow at pH as low as 3 (Florentino et al., 2016a) and *D. acetivorans* at pH 4.3 (Bonch-Osmolovskaya et al., 1990). Different regulation of those genes, or a completely unknown mechanism encoded in those microorganisms, might be key to explain the differences in resistance of high proton concentrations.

Response to Oxidative Stress

Survival of strict anaerobic microorganisms, such as the members of the *Desulfurellaceae* family, in environments exposed to high redox potential would include antioxidant strategies. Furthermore, the acidotolerant *D. amilsii* was isolated from acidic sediments from the Tinto River which possess zones with very high redox conditions (up to +400mV) and high concentrations of soluble metals, such as copper, iron, and zinc (Florentino et al., 2015). The excess of metals contributes to redox-active metals toxicity, generating reactive oxygen species (ROS) via the slow Fenton and Haber–Weiss reactions. When the oxidation states of the metal ions switches, reactive species, such as hydrogen peroxide (H_2O_2) and superoxide ($\bullet O^{2-}$) are activated to the hydroxyl radical ($\bullet$OH), resulting in a highly reactive form (Flora et al., 2008). Therefore, the presence of genes encoding oxidative stress related enzymes is of great importance for the survival of this species in its original habitat.

Superoxide reductase desulfoferrodoxin is encoded in all *Desulfurellaceae* members' species, as well as rubredoxin, that can transfer electrons and reduce the superoxide dismutase (Supplementary Table S5) (Sheng et al., 2014). Reduction of peroxides is performed by enzymes such as glutathione peroxidase, peroxirredoxin, rubrerythrins, alkylhydroperoxidases and catalases. Rubrerythrin is encoded in all the genomes; in *Desulfurella* species, *H. alviniae* and *H. jasoniae* the rubrerythrin-coding gene is flanked by a peroxiredoxin, while in *H. maritima* and *H. medea* it is flanked by a DNA repair mechanism involved in gene spore photoproduct lyase. Peroxiredoxins and thioredoxins-coding genes are present in all *Desulfurellaceae* genomes studied. Together with rubrerythrin and the ferric uptake regulator (Fur) family, the peroxiredoxins and thioredoxins are well-represented in acidophiles and acidotolerant microorganisms (Cárdenas et al., 2016). The rubrerythrin and the Fur family replace activities of catalase and oxidative stress response regulators in neutrophiles, while peroxiredoxins and thioredoxins remove organic peroxides originated when ROS attack organic molecules (Cárdenas et al., 2012).

Oxidizing agents normally modify the DNA in complex patterns, leading to mutagenic effects. Three different DNA repair pathways are involved in the removal of the oxidized bases in DNA and their mismatches: base excision repair (BER), nucleotide excision repair (NER) and mismatch repair (MMR). The genomes of the *Desulfurella* species encode DNA repair mechanisms, including the protein RecA, the excinuclease UvrABC and the GroEL protein (Supplementary Table S4). All bacterial genomes analyzed contained genes for the detection and removal of modified purine and pyrimidine bases (BER pathway), including orthologs of the uracyl-DNA glycosylase gene. The UvrABC repair system for NER pathway, which operates on the removal of bulky lesions from the DNA duplex, was present in the genome of all species. Additionally, genes responsible for the SOS response to DNA damage, RecA/RadA were found in all organisms; LexA, however, is only present in *D. acetivorans*. Genes encoding the Dps protein, endonucleases and the minimal essential complex for mismatched base repair were not detected in any of the analyzed genomes.

Despite the different isolation sources of the *Desulfurellaceae* members and a lack of physiological data from *Hippea* species and *D. acetivorans*, differences in genes encoding resistance to oxidative stress were not detected in the genome, and so regulatory processes might be responsible for them to tackle the harsh conditions.

Metals Resistance

Several prokaryotes show specific genetic mechanisms of resistance to toxic concentrations of metals in the environment, which include their oxidation or reduction to less toxic valence states, incorporation or precipitation of heavy metals as metal sulfides complexes, and the direct transport of metals out of the membrane (Ji and Silver, 1995). Generally, the mechanisms for uptake of metals can be ATP-independent and driven by chemosmotic gradients across the membrane or is dependent on the energy released from ATP hydrolysis in a substrate-specific manner (Ahemad, 2012).

One of the ATP-based mechanisms proposed for metals resistance in bacteria is the synthesis of polyphosphates via the enzyme polyphosphate kinase, which can interact with metal ions due to its polyanion nature (Pan-Hou et al., 2002). Genes encoding the polyphosphate kinase are present in *Desulfurella* species and in *H. maritima*. *D. amilsii* was shown to be resistant to relatively high concentrations of copper and nickel (Florentino et al., 2015). The resistance to copper can also be related to the presence of genes encoding the copper-exporting P-type ATPase, present in all species.

Desulfurella species and *H. maritima* genomes encode the Co/Zn/Cd efflux system, components of inorganic ion transport and metabolism. *Desulfurella* species and *H. alviniae* encode some cation transporters (Supplementary Table S6), that are unspecific and chemiosmotic gradient driven across their cytoplasmic membrane.

Although genes encoding resistance to heavy metals are in all the analyzed species, the isolation source of *D. amilsii* is a metal rich environment, and, as many metals are more soluble at acidic pH, this microorganism is more exposed to the high metal concentrations than the other members of *Desulfurellaceae* family isolated from neutrophilic environments (Bonch-Osmolovskaya et al., 1990; Miroshnichenko et al., 1999; Flores et al., 2012). Besides, as described by Dopson et al. (2014), high concentrations of sulfate are also normally present in acidic environments, which can complex metal cations and lower the concentration of free metals that can enter the microbial cell cytoplasm. Therefore, it is likely that such abiotic factor, in combination with other factors, such as the competition with protons for binding sites, might contribute to the increased tolerance to metals in solution by *D. amilsii* in comparison to its neutrophilic relatives.

CONCLUSION

Analysis of available genomes of the *Desulfurellaceae* family provided insight into their members' energy and carbon metabolism, helping in the elucidation of the genomic diversity in this group of microbes. Comparative genome analysis revealed that the gene content for sulfur respiration differs between genera and within the *Desulfurella* genus. PSR might be the responsible enzyme for indirect sulfur reduction in *Hippea*. SRE is suggested to play a role in sulfur reduction by *D. amilsii,* especially when it grows at low pH. Since the enzyme annotated as SUDH might act as a bifurcating enzyme, respiration of elemental sulfur by *Desulfurella* spp. possibly occurs via other enzymes, such as the encoded rhodanese-like sulfurtransferases. Gene prediction supported by experimental analysis in *Desulfurella* species indicate a more versatile metabolism in this group. Although the ability to grow at extreme acidic environments is only confirmed in *D. amilsii*, great differences in the gene sets involved in the resistance to low pH conditions could not be detected in a comparative genome analysis. Therefore, the regulation of those genes in *D. amilsii*, or a resistance mechanism not yet known, might be responsible for the unique ability of this microorganism to survive in acidic conditions. This is the first report on comparative genomics of sulfur-reducing microorganisms able to grow at different conditions, which might help follow up analyses to broaden the knowledge on this poorly understood group of prokaryotes. Further studies need to be performed to address remaining questions about the active pathways and how environmental conditions interfere with them.

AUTHOR CONTRIBUTIONS

AF: Drafting the manuscript; acquisition and analysis of the data; AF and IS-A: Giving substantial contributions to the conception or design of the work; interpretation of data for the article; AF, IS-A, and AS: Agreement to be accountable for all aspects of the work; ensuring that questions related to the accuracy or integrity of any part of the work was properly investigated; IS-A and AS: Revising the manuscript critically for important intellectual content and final approval of the version to be published.

ACKNOWLEDGMENTS

The authors thank CNPq (Conselho Nacional de Desenvolvimento Cientifiìco e Tecnoloìgico), organization of the Brazilian Government for supporting the doctoral study program for the development of Science and Technology. Research of IS-A and AM Stams is financed by ERC grant project 323009, and Gravitation grant project 024.002.002 from The Netherlands Ministry of Education, Culture and Science. Thanks to Bastian Hornung for the bioinformatics support and to Robert Smith for the English revision.

SUPPLEMENTARY MATERIAL

The Supplementary Material for this article can be found online at: http://journal.frontiersin.org/article/10.3389/fmicb.2017.00222/full#supplementary-material

REFERENCES

Ahemad, M. (2012). Implication of bacterial resistance against heavy metals in bioremediation: a review. *Inst. Integr. Omics Appl. Biotechnol. J.* 3, 39–46.

Alain, K., Callac, N., Guégan, M., Lesongeur, F., Crassous, P., Cambon-Bonavita, M. A., et al. (2009). *Nautilia abyssi* sp. nov., a thermophilic, chemolithoautotrophic, sulfur-reducing bacterium isolated from an East Pacific Rise hydrothermal vent. *Int. J. Syst. Evol. Microbiol.* 59, 1310–1315. doi: 10.1099/ijs.0.005454-0

Altschul, S. F., Gish, W., Miller, W., Myers, E. W., and Lipman, D. J. (1990). Basic local alignment search tool. *J. Mol. Biol.* 215, 403–410.

Argueso, J. L., Carazzolle, M. F., Mieczkowski, P. A., Duarte, F. M., Netto, O. V. C., Missawa, S. K., et al. (2009). Genome structure of a *Saccharomyces cerevisiae* strain widely used in bioethanol production. *Genome Res.* 19, 2258–2270. doi: 10.1101/gr.091777.109

Aziz, R. K., Bartels, D., Best, A. A., Dejongh, M., Disz, T., Edwards, R. A., et al. (2008). The RAST server: rapid annotations using subsystems technology. *BMC Genomics* 9:75. doi: 10.1186/1471-2164-9-75

Baker-Austin, C., and Dopson, M. (2007). Life in acid: pH homeostasis in acidophiles. *Trends Microbiol.* 15, 165–171.

Birrien, J. L., Zeng, X., Jebbar, M., Cambon-Bonavita, M. A., Quérellou, J., Oger, P., et al. (2011). *Pyrococcus yayanosii* sp. nov., an obligate piezophilic hyperthermophilic archaeon isolated from a deep-sea hydrothermal vent. *Int. J. Syst. Evol. Microbiol.* 61, 2827–2881. doi: 10.1099/ijs.0.024653-0

Biswas, A., Gagnon, J. N., Brouns, S. J., Fineran, P. C., and Brown, C. M. (2013). CRISPRTarget: bioinformatic prediction and analysis of crRNA targets. *RNA Biol.* 10, 817–827. doi: 10.4161/rna.24046

Blasco, F., Dos Santos, J. P., Magalon, A., Frixon, C., Guigliarelli, B., Santini, C. L., et al. (1998). NarJ is a specific chaperone required for molybdenum cofactor assembly in nitrate reductase A of *Escherichia coli*. *Mol. Microbiol.* 28, 435–447.

Blumentals, I., Itoh, M., Kelly, R. M., and Olson, G. J. (1990). Role of polysulfides in reduction of elemental sulfur by the hyperthermophilic archaebacterium *Pyrococcus furiosus*. *Appl. Environ. Microbiol.* 56, 1255–1262.

Boetzer, M., and Pirovano, W. (2012). Toward almost closed genomes with GapFiller. *Genome Biol.* 13, 1–9. doi: 10.1186/gb-2012-13-6-r56

Boisvert, S., Laviolette, F., and Corbeil, J. (2010). Ray: simultaneous assembly of reads from a mix of high-throughput sequencing technologies. *J. Comput. Biol.* 17, 1519–1533. doi: 10.1089/cmb.2009.0238

Bonch-Osmolovskaya, E. A., Sokolova, T. G., Kostrikina, N. A., and Zavarzin, G. A. (1990). *Desulfurella acetivorans* gen. nov. and sp. nov. - a new thermophilic sulfur-reducing eubacterium. *Arch. Microbiol.* 153, 151–155.

Boyd, E. S., Jackson, R. A., Encarnacion, G., Zahn, J. A., Beard, T., Leavitt, W. D., et al. (2007). Isolation, characterization, and ecology of sulfur-respiring crenarchaea inhabiting acid-sulfate-chloride-containing geothermal springs in Yellowstone National Park. *Appl. Environ. Microbiol.* 73, 6669–6677.

Caccavo, F. Jr., Lonergan, D. J., Lovley, D. R., Davis, M., Stolz, J. F., and McInerney, M. J. (1994). *Geobacter sulfurreducens* sp. nov., a hydrogen- and acetate-oxidizing dissimilatory metal-reducing microorganism. *Appl. Environ. Microbiol.* 60, 3752–3759.

Cárdenas, J. P., Moya, F., Covarrubias, P., Shmaryahu, A., Levicán, G., Holmes, D. S., et al. (2012). Comparative genomics of the oxidative stress response in bioleaching microorganisms. *Hydrometallurgy* 12, 162–167.

Cárdenas, J. P., Quatrini, R., and Holmes, D. S. (2016). Aerobic lineage of the oxidative stress response protein rubrerythrin emerged in an ancient microaerobic, (hyper)thermophilic environment. *Front. Microbiol.* 7:1822. doi: 10.3389/fmicb.2016.01822

Chen, F., Mackey, A. J., Stoeckert, C. J., and Roos, D. S. (2006). OrthoMCL-DB: querying a comprehensive multi-species collection of ortholog groups. *Nucleic Acids Res.* 34, 363–368.

Dirmeier, R., Keller, J., Hafenbradl, D., Braun, F. J., Rachel, R., Burggraf, S., et al. (1998). *Thermococcus acidaminovorans* sp. nov., a new hyperthermophilic alkalophilic arcaheon growing on amino acids. *Extremophiles* 2, 109–114.

Dopson, M., and Johnson, D. B. (2012). Biodiversity, metabolism and applications of acidophilic sulfur-metabolizing microorganisms. *Environ. Microbiol.* 14, 2620–2631. doi: 10.1111/j.1462-2920.2012.02749.x

Dopson, M., Ossandon, F. J., Lövgren, L., and Holmes, D. S. (2014). Metal resistance or tolerance? Acidophiles confront high metal loads via both abiotic and biotic mechanisms. *Front. Microbiol.* 5:157. doi: 10.3389/fmicb.2014.00157

Fauque, G. D., and Barton, L. L. (2012). Hemoproteins in dissimilatory sulfate- and sulfur-reducing prokaryotes. *Adv. Microb. Physiol.* 60, 1–90. doi: 10.1016/B978-0-12-398264-3.00001-2

Finster, K., Coates, J. D., Liesack, W., and Pfennig, N. (1997). *Desulfuromonas thiophila* sp. nov., a new obligately sulfur-reducing bacterium from anoxic freshwater sediment. *Int. J. Syst. Bacteriol.* 47, 754–758.

Finster, K., Leiesack, W., and Thamdrup, B. O. (1998). Elemental sulfur and thiosulfate disproportionation by *Desulfocapsa sulfoexigens* sp. nov., a new anaerobic bacterium isolated from marine surface sediment. *Appl. Environ. Microbiol.* 64, 119–125.

Flora, S. J., Mittal, M., and Mehta, A. (2008). Heavy metal induced oxidative stress & its possible reversal by chelation therapy. *Indian J. Med. Res.* 128, 501–523.

Florentino, A. P., Brienza, C., Stams, A. J., and Sanchez-Andrea, I. (2016a). *Desulfurella amilsii* sp. nov., a novel acidotolerant sulfur-respiring bacterium isolated from acidic river sediments. *Int. J. Syst. Evol. Microbiol.* 66, 1249–1253. doi: 10.1099/ijsem.0.000866

Florentino, A. P., Weijma, J., Stams, A. J., and Sanchez-Andrea, I. (2015). Sulfur reduction in acid rock drainage environments. *Environ. Sci. Technol.* 49, 11746–11755. doi: 10.1021/acs.est.5b03346

Florentino, A. P., Weijma, J., Stams, A. J. M., and Sánchez-Andrea, I. (2016b). "Ecophysiology and application of acidophilic sulfur-reducing microorganisms," in *Biotechnology of Extremophiles: Advances and Challenges*, ed. H. P. Rampelotto (Cham: Springer International Publishing), 141–175.

Flores, G. E., Hunter, R. C., Liu, Y., Mets, A., Schouten, S., and Reysenbach, A. L. (2012). *Hippea jasoniae* sp. nov. and *Hippea alviniae* sp. nov., thermoacidophilic members of the class Deltaproteobacteria isolated from deep-sea hydrothermal vent deposits. *Int. J. Syst. Evol. Microbiol.* 62, 1252–1258. doi: 10.1099/ijs.0.033001-0

Frederiksen, T.-M., and Finster, K. (2003). Sulfite-oxido-reductase is involved in the oxidation of sulfite in *Desulfocapsa sulfoexigens* during disproportionation of thiosulfate and elemental sulfur. *Biodegradation* 14, 189–198.

Goevert, D., and Conrad, R. (2010). Stable carbon isotope fractionation by acetotrophic sulfur-reducing bacteria. *FEMS Microbiol. Ecol.* 71, 218–225. doi: 10.1111/j.1574-6941.2009.00811.x

Goris, J., Konstantinidis, K., Klappenbach, J., Coenye, T., Vandamme, P., and Tiedje, J. (2007). DNA-DNA hybridization values and their relationship to whole-genome sequence similarities. *Int. J. Syst. Evol. Microbiol.* 57, 81–91.

Greene, A. C. (2014). "The family desulfurellaceae," in *The Prokaryotes: Deltaproteobacteria and Epsilonproteobacteria*, eds E. Rosenberg, E. F. Delong, S. Lory, E. Stackebrandt, and F. Thompson (Berlin: Springer), 135–142.

Grissa, I., Vergnaud, G., and Pourcel, C. (2007). CRISPRFinder: a web tool to identify clustered regularly interspaced short palindromic repeats. *Nucleic Acids Res.* 35, W52–W57.

Hardisty, D. S., Olyphant, G. A., Bell, J. B., Johnson, A. P., and Pratt, L. M. (2013). Acidophilic sulfur disproportionation. *Geochim. Cosmochim. Acta* 113, 136–151.

Heberle, H., Meirelles, G. V., Da Silva, F. R., Telles, G. P., and Minghim, R. (2015). InteractiVenn: a web-based tool for the analysis of sets through Venn diagrams. *BMC Bioinformatics* 16:169. doi: 10.1186/s12859-015-0611-3

Hernandez, D., Francois, P., Farinelli, L., Osteras, M., and Schrenzel, J. (2008). De novo bacterial genome sequencing: millions of very short reads assembled on a desktop computer. *Genome Res.* 18, 802–809. doi: 10.1101/gr.072033.107

Holyoak, C. D., Stratford, M., Mcmullin, Z., Cole, M. B., Crimmins, K., Brown, A. J., et al. (1996). Activity of the plasma membrane H+-ATPase and optimal glycolytic flux are required for rapid adaptation and growth of *Saccharomyces cerevisiae* in the presence of the weak-acid preservative sorbic acid. *Appl. Environ. Microbiol.* 62, 3158–3164.

Ingram-Smith, C., Martin, S. R., and Smith, K. S. (2006). Acetate kinase: not just a bacterial enzyme. *Trends Microbiol.* 14, 249–253.

Ji, G., and Silver, S. (1995). Bacterial resistance mechanisms for heavy metals of environmental concern. *J. Ind. Microbiol.* 14, 61–75.

Johnson, D. B., and Hallberg, K. B. (2005). Acid mine drainage remediation options: a review. *Sci. Total Environ.* 338, 3–14.

Kanjee, U., and Houry, W. A. (2013). Mechanisms of acid resistance in *Escherichia coli*. *Annu. Rev. Microbiol.* 67, 65–81. doi: 10.1146/annurev-micro-092412-155708

Kleinjan, W. E., De Keizer, A., and Janssen, A. J. H. (2005). Equilibrium of the reaction between dissolved sodium sulfide and biologically produced sulfur. *Colloids Surf. B Biointerfaces* 43, 228–237.

Laska, S., Lottspeich, F., and Kletzin, A. (2003). Membrane-bound hydrogenase and sulfur reductase of the hyperthermophilic and acidophilic archaeon *Acidianus ambivalens*. *Microbiology* 149, 2357–2371.

Ma, K., and Adams, M. W. W. (2001). Ferredoxin:NADP oxidoreductase from *Pyrococcus furiosus*. *Methods Enzymol.* 334, 40–45.

Ma, K., Weiss, R., and Adams, M. W. W. (2000). Characterization of hydrogenase II from the hyperthermophilic archaeon *Pyrococcus furiosus* and assessment of its role in sulfur reduction. *J. Bacteriol.* 182, 1864–1871.

Macy, J., Schröder, I., Thauer, R., and Kröger, A. (1986). Growth the *Wolinella succinogenes* on H2S plus fumarate and on formate plus sulfur as energy sources. *Arch. Microbiol.* 144, 147–150.

Markowitz, V. M., Chen, I.-M. A., Palaniappan, K., Chu, K., Szeto, E., Pillay, M., et al. (2014). IMG 4 version of the integrated microbial genomes comparative analysis system. *Nucleic Acids Res.* 42, D560–D567. doi: 10.1093/nar/gkt963

Meier-Kolthoff, J. P., Auch, A. F., Klenk, H. P., and Göker, M. (2013). "GBDP on the grid: a genome-based approach for species delimitation adjusted for an automated and highly parallel processing of large data sets," in *Hochleistungsrechnen in Baden-Württemberg – Ausgewählte Aktivitäten im bwGRiD 2012*, eds J. Schulz and S. Hermann (Karlsruhe: KIT Scientific Publishing).

Miroshnichenko, M. L., Gongadze, G. A., Lysenko, A. M., and Bonch-Osmolovskaya, E. A. (1994). Desulfurella multipotens sp. nov., a new sulfur-respiring thermophilic eubacterium from Raoul Island (Kermadec archipelago, New Zealand). *Arch. Microbiol.* 161, 88–93.

Miroshnichenko, M. L., Rainey, F. A., Rhode, M., and Bonch-Osmolovskaya, E. A. (1999). *Hippea maritima* gen. nov., sp. nov., a new genus of thermophilic, sulfur-reducing bacterium from submarine hot vents. *Int. J. Syst. Bacteriol.* 49(Pt 3), 1033–8.

Nakano, S., Fukaya, M., and Horinouchi, S. (2006). Putative ABC transporter responsible for acetic acid resistance in *Acetobacter aceti*. *Appl. Environ. Microbiol.* 72, 497–505.

Pan-Hou, H., Kiyono, M., Omura, H., Omura, T., and Endo, G. (2002). Polyphosphate produced in recombinant *Escherichia coli* confers mercury resistance. *FEMS Microbiol. Lett.* 207, 159–164.

Pihl, T. D., Schicho, R. N., Kelly, R. M., and Maier, R. J. (1989). Characterization of hydrogen-uptake activity in the hyperthermophile *Pyrodictium brockii*. *Proc. Natl. Acad. Sci. U.S.A.* 86, 138–141.

Rabus, R., Hansen, T. A., and Widdel, F. (2006). "Dissimilatory sulfate- and sulfur-reducing prokaryotes," in *Prokaryotes*, Vol. 2, eds M. Dworkin, S. Falkow, E. Rosenberg, K.-H. Schleifer, and E. Stackebrandt (New York, NY: Springer), 659–768. doi: 10.1016/B978-0-12-398264-3.00001-2

Ray, N., Oates, J., Turner, R. J., and Robinson, C. (2003). DmsD is required for the biogenesis of DMSO reductase in *Escherichia coli* but not for the interaction of the DmsA signal peptide with the Tat apparatus. *FEBS Lett.* 534, 156–160.

Schauder, R., and Müller, E. (1993). Polysulfide as a possible substrate for sulfur-reducing bacteria. *Arch. Microbiol.* 160, 377–382.

Schmitz, R. A., Bonch-Osmolovskaya, E. A., and Thauer, R. K. (1990). Different mechanisms of acetate activation in *Desulfurella acetivorans* and *Desulfuromonas acetoxidans*. *Arch. Microbiol.* 154, 274–279. doi: 10.1111/j.1574-6941.2009.00811.x

Segerer, A., Neuner, A., Kristjansson, J. K., and Stetter, K. O. (1986). *Acidianus infernus* gen. nov., sp. nov., and *Acidianus brierleyi* Comb. nov.: facultatively aerobic, extremely acidophilic thermophilic sulfur-metabolizing archaebacteria. *Int. J. Syst. Bacteriol.* 36, 559–564.

Sheng, Y., Abreu, I. A., Cabelli, D. E., Maroney, M. J., Miller, A.-F., Teixeira, M., et al. (2014). Superoxide dismutases and superoxide reductases. *Chem. Rev.* 114, 3854–3918.

Stetter, K. O. (1996). Hyperthermophilic prokaryotes. *FEMS Microbiol. Rev.* 18, 149–158.

Stetter, K. O., and Gaag, G. (1983). Reduction of molecular sulphur by methanogenic bacteria. *Nature* 305, 309–311.

Stoffels, L., Krehenbrink, M., Berks, B. C., and Unden, G. (2012). Thiosulfate reduction in *Salmonella enterica* is driven by the proton motive force. *J. Bacteriol.* 194, 475–485. doi: 10.1128/JB.06014-11

Wang, Y., Coleman-Derr, D., Chen, G., and Gu, Y. Q. (2015). OrthoVenn: a web server for genome wide comparison and annotation of orthologous clusters across multiple species. *Nucleic Acids Res.* 43, 78–84. doi: 10.1093/nar/gkv487

Conflict of Interest Statement: The authors declare that the research was conducted in the absence of any commercial or financial relationships that could be construed as a potential conflict of interest.

frontiers in Microbiology

ORIGINAL RESEARCH
published: 08 December 2016
doi: 10.3389/fmicb.2016.01963

In situ Spectroscopy Reveals that Microorganisms in Different Phyla Use Different Electron Transfer Biomolecules to Respire Aerobically on Soluble Iron

Robert C. Blake II[1], Micah D. Anthony[1], Jordan D. Bates[1], Theresa Hudson[2], Kamilya M. Hunter[2], Brionna J. King[2], Bria L. Landry[2], Megan L. Lewis[2] and Richard G. Painter[1]*

[1] College of Pharmacy, Xavier University of Louisiana, New Orleans, LA, USA, [2] Department of Biology, Xavier University of Louisiana, New Orleans, LA, USA

Absorbance spectra were collected on 12 different live microorganisms, representing six phyla, as they respired aerobically on soluble iron at pH 1.5. A novel integrating cavity absorption meter was employed that permitted accurate absorbance measurements in turbid suspensions that scattered light. Illumination of each microorganism yielded a characteristic spectrum of electrochemically reduced colored prosthetic groups. A total of six different patterns of reduced-minus-oxidized difference spectra were observed. Three different spectra were obtained with members of the Gram-negative eubacteria. *Acidithiobacillus*, representing Proteobacteria, yielded a spectrum in which cytochromes *a* and *c* and a blue copper protein were all prominent. *Acidihalobacter*, also representing the Proteobacteria, yielded a spectrum in which both cytochrome *b* and a long-wavelength cytochrome *a* were clearly visible. Two species of *Leptospirillum*, representing the Nitrospirae, both yielded spectra that were dominated by a cytochrome with a reduced peak at 579 nm. *Sulfobacillus* and *Alicyclobacillus*, representing the Gram-positive Firmicutes, both yielded spectra dominated by *a*-type cytochromes. *Acidimicrobium* and *Ferrimicrobium*, representing the Gram-positive Actinobacteria, also yielded spectra dominated by *a*-type cytochromes. *Acidiplasma* and *Ferroplasma*, representing the Euryarchaeota, both yielded spectra dominated by a ba_3-type of cytochrome. *Metallosphaera* and *Sulfolobus*, representing the Crenarchaeota, both yielded spectra dominated by the same novel cytochrome as that observed in the Nitrospirae and a new, heretofore unrecognized redox-active prosthetic group with a reduced peak at around 485 nm. These observations are consistent with the hypothesis that individual acidophilic microorganisms that respire aerobically on iron utilize one of at least six different types of electron transfer pathways that are characterized by different redox-active prosthetic groups. *In situ* absorbance spectroscopy is shown to be a useful complement to existing means of investigating the details of energy conservation in intact microorganisms under physiological conditions.

Keywords: *in situ* spectroscopy, aerobic respiration on iron, electron transport chains, cytochromes, chemolithotrophic bacteria

OPEN ACCESS

Edited by:
David Barrie Johnson, Bangor University, UK

Reviewed by:
Violaine Bonnefoy, Centre National de la Recherche Scientifique, France
Gloria Paz Levicán, University of Santiago, Chile, Chile

****Correspondence:***
Robert C. Blake II
rblake@xula.edu

Specialty section:
This article was submitted to Extreme Microbiology, a section of the journal Frontiers in Microbiology

Received: *30 August 2016*
Accepted: *23 November 2016*
Published: *08 December 2016*

Citation:
Blake II RC, Anthony MD, Bates JD, Hudson T, Hunter KM, King BJ, Landry BL, Lewis ML and Painter RG (2016) In situ Spectroscopy Reveals that Microorganisms in Different Phyla Use Different Electron Transfer Biomolecules to Respire Aerobically on Soluble Iron. Front. Microbiol. 7:1963. doi: 10.3389/fmicb.2016.01963

INTRODUCTION

The capacity to respire aerobically on soluble ferrous ions under strongly acidic conditions (pH < 3) is currently thought to be expressed in 42 species distributed among 19 genera in six phyla (Bonnefoy and Holmes, 2012; Johnson et al., 2012). It is generally accepted that the electron donor, soluble iron, does not enter the cytoplasm in appreciable quantities in any of these microorganisms. Consequently, microorganisms must express appropriate electron transfer biomolecules to conduct respiratory electrons from the extracellular iron to the intracellular molecular oxygen that serves as the terminal electron acceptor. A variety of different electron transfer proteins and redox-active prosthetic groups have been posited by many laboratories to participate in aerobic respiration on iron. These reports include studies using purified proteins and protein complexes (Cox and Boxer, 1978; Kai et al., 1992; Blake and Shute, 1997; Castelle et al., 2008; Singer et al., 2008; Bandeiras et al., 2009), spectroscopic studies on cell-free extracts (Hart et al., 1991; Blake et al., 1993; Yarzabal et al., 2002; Brasseur et al., 2004; Kappler et al., 2005; Bathe and Norris, 2007; Dinarieva et al., 2010), inventories of putative respiratory proteins deduced from whole-cell genomic sequencing activities (reviewed in Auernik and Kelly, 2008; Kozubal et al., 2011; Ilbert and Bonnefoy, 2013), and lists of likely respiratory proteins identified in transcriptomic (Auernik and Kelly, 2008; Quatrini et al., 2009) and proteomic (Dopson et al., 2005; Ram et al., 2005; Bouchal et al., 2006; Valenzuela et al., 2006) studies of cells cultured in the presence of soluble iron.

This laboratory initiated a new systems approach to study respiratory electron transfer in intact cells using a novel integrating cavity absorption meter (ICAM) that permitted the acquisition of accurate absorbance data in suspensions of cells that scattered light (Blake and Griff, 2012; Li et al., 2015). The observation chamber of this spectrophotometer comprised a reflecting cavity that was completely filled with the colored suspension of intact microorganisms. This physical arrangement permitted the suspensions of live bacteria to be irradiated in an isotropic homogeneous field of incident measuring light where the absorbed radiant power was expected to be independent of scattering effects (Elterman, 1970; Fry et al., 1992; Javorfi et al., 2006; Hodgkinson et al., 2009). When intact cells of either *Leptospirillum ferrooxidans* or *Acidithiobacillus ferrooxidans* were exposed to soluble ferrous ions under physiological solution conditions, the reduced forms of selected redox-active cellular prosthetic groups were immediately apparent in the absorbance spectrum of each organism. When the electron-accepting capability of the soluble molecular oxygen (4 × 236 μM at 30°C) exceeded that of the electron-donating capacity of the soluble ferrous ions (≤500 μM), the spectrum of each iron-reduced organism returned to that of the resting air-oxidized organism.

In this study, the same ICAM was exploited to test the hypothesis that different types of redox-active prosthetic groups and electron transfer biomolecules were expressed by microorganisms from each of the six phyla that contain acidophilic members that respire aerobically on iron. This hypothesis was consistent with the observations that (i) *L. ferrooxidans* and *A. ferrooxidans*, which represent the phyla Nitrospirae and Proteobacteria, respectively, produced completely different spectral changes when their intact cells were exposed to iron (Blake and Griff, 2012; Li et al., 2015) and (ii) a number of other different redox-active biomolecules have been implicated in iron-oxidizing acidophiles that are currently assigned to other phyla. We tested this hypothesis by characterizing the cellular absorbance changes that occurred when soluble iron was mixed with cells of two different organisms derived from each of the six phyla that contain members that respire aerobically on iron. A total of six different patterns of iron-dependent absorbance changes were observed: three in the Gram-negative eubacteria; two in the archaea; and one in the Gram-positive eubacteria. We conclude that there are as many as six different sets of prosthetic groups and biomolecules that can accomplish aerobic respiration on soluble iron.

MATERIALS AND METHODS

Cell Culture

Acidithiobacillus ferrooxidans ATCC 23270^T, *L. ferrooxidans* DSM 2705^T, and *L. ferriphilum* DSM 14647^T were cultured autotrophically on soluble ferrous ions at 30°C in the medium described elsewhere (Tuovinen and Kelly, 1973), adjusted to 158 mM $FeSO_4 \cdot 7H_2O$ and pH 1.5. *Acidihalobacter ferrooxidans* 14175, *Sulfobacillus thermosulfidooxidans* 9293^T, *Alicyclobacillus ferrooxydans* 22381^T, *Acidimicrobium ferrooxidans* 10331^T, *Ferrimicrobium acidiphilum*, 19497^T, *Acidiplasma aeolicum* 18409^T, *Ferroplasma acidiphilum* 12658^T, *Metallosphaera sedula* 5348^T, and *Sulfolobus metallicus* 6482^T were all obtained from the DSM. Each organism was cultured on 20 mM ferrous sulfate at pH 1.5 using the relevant mixotrophic medium and growth temperature recommended for each microorganism in the DSM media guide. Cells grown to late stationary phase were harvested by centrifugation, washed twice with 0.02 M H_2SO_4, and resuspended in sufficient 0.02 M H_2SO_4 to achieve a stock suspension of approximately 1×10^{10} cells/ml. Each stock suspension was stored at 4°C for no longer than a week while spectroscopic experiments were conducted on aliquots of the cells.

Quantification of Microorganisms

Absolute numbers of microorganisms were determined by electrical impedance measurements in a Multisizer 4 particle counter (Beckman Coulter, Inc., Brea, CA, USA) fitted with a 30-μm aperture (Blake and Griff, 2012; Li et al., 2015). The instrument was programmed to siphon 50 μl of sample that contained Isoton II as the electrolyte. The current applied across the aperture was 600 μA. Voltage spikes attendant with impedance changes as microorganisms passed through the aperture were monitored with an instrument gain of four.

Absorbance Measurements with Cell Suspensions

Absorbance measurements on intact cells in suspension were conducted in an OLIS CLARiTY 1000A spectrophotometer (On Line Instrument Systems, Inc., Bogart, GA, USA) as described previously (Blake and Griff, 2012; Li et al., 2015). In a typical experiment, identical 8-ml solutions of 0.02 M sulfuric acid, pH 1.5, were added to both the sample and reference observation cavities of the spectrophotometer. A volume was withdrawn from the sample cavity and replaced with an equal volume of suspended cells. The contents of both observation cavities were maintained at the respective growth temperature of each organism using a model TC-1 Peltier temperature control element from Quantum Northwest (Liberty Lake, WA, USA). After recording a stable baseline, 40 μl of a 200 mM solution of ferrous sulfate, pH 1.5, were added to the sample observation chamber to create a 1.0 mM solution in reduced iron. This concentration of the ferrous ion electron donor was always in excess to the electron accepting capacity of the molecular oxygen electron acceptor in the reaction mixtures, which ranged from 236 to 150 μM in the mixtures at temperatures from 30 to 65°C, respectively. Raw absorbance spectra were subsequently collected at a rate of 6.2/s for several minutes. Iron-dependent absorbance changes in the suspensions of cells were complete in the time that it took to add the electron donor, close the chamber, and initiate the data collection. The resulting absorbance changes were stable for the entire time that raw data were collected. These raw absorbance values were subsequently converted to equivalent absorbance values per cm using Fry's method (Fry et al., 2010) with analysis software provided by OLIS, Inc.

RESULTS

Integrating Cavity Absorption Meter

The principal features of the ICAM employed herein to conduct absorbance measurements on intact cells in turbid suspensions were described earlier (Blake and Griff, 2012; Li et al., 2015). This novel design for a spectrophotometer imposes two consequences. First, the multiple transversals around the interior of the observation cavity means that the incident exciting light experiences a much longer effective path length than it would in an equivalent linear spectrophotometer where the transmitted light experiences only one pass through a filled cuvette. Consequently, absorbance measurements in this ICAM result in a much greater sensitivity than would equivalent measurements in a standard linear spectrophotometer. Second, to the extent that the exciting incident light can be made to be totally diffuse, there are no longer deleterious consequences to absorbance measurements from turbid suspensions that scatter light. If the exciting light is already randomly scattered to a maximum extent, then additional light scattering by the turbid sample will have no immediate consequences on the integrity of the absorbance measurement. Thus it is possible to conduct absorbance measurements *in situ* in whole cells under physiological solution conditions.

Gram-Negative Eubacteria

The Proteobacteria and the Nitrospirae are the two phyla of Gram-negative eubacteria that contain obligately acidophilic members that respire aerobically on soluble iron (Bonnefoy and Holmes, 2012). These bacteria are distributed among at least four genera in the Proteobacteria: *Acidithiobacillus, Acidiferrobacter, Acidihalobacter* and *Ferrovum*. There are four species recognized within the genus *Acidithiobacillus* that oxidize iron, while there are at least two species within the genus *Acidihalobacter* that also do so. We chose *Ah. ferrooxidans* and *At. ferrooxidans* to represent the Proteobacteria phylum in the *in situ* spectroscopic studies reported herein.

Figure 1 shows the reduced minus oxidized difference spectrum that was observed when intact cells of air-oxidized *Ah. ferrooxidans* were exposed to excess ferrous ions at 35°C and pH 1.5. This difference spectrum was different from that obtained previously with *At. ferrooxidans* (Li et al., 2015) in a number of ways. First, the difference spectrum in **Figure 1** exhibited no evidence of typical reduced cytochrome *c*-dependent absorbance changes around 417 or 550 nm. In contrast, the participation of *c*-type cytochromes in the comparable difference spectrum obtained previously with *At. ferrooxidans* was indicated by prominent peaks at 417, 520, and 551 nm. Second, the reduced peak at 565 nm in **Figure 1** was clearly in the spectral region normally attributed to the reduced peaks of *b*-type cytochromes, a feature that was absent in the spectrum obtained using intact *At. ferrooxidans*. Third, the first α peak encountered in the difference spectrum of *Ah. ferrooxidans* had a reduced peak at 608 nm, some 10 nm red-shifted from the equivalent peak seen in *At. ferrooxidans* at 598 nm. Finally, there was no evidence of a broad trough of negative absorbance in the spectrum in **Figure 1** that one could attribute to the iron-dependent reduction of a

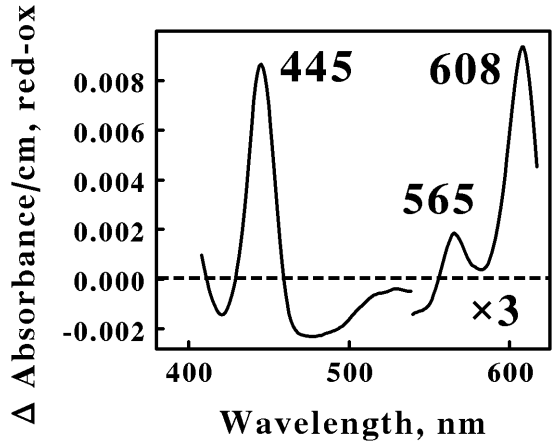

FIGURE 1 | Reduced minus oxidized difference spectra obtained when excess ferrous sulfate was mixed with intact cells of *Acidihalobacter ferrooxidans*, representing the Proteobacteria. The number of cells present in 8 ml were 2.7×10^9. The bold numbers identify the wavelengths where each peak exhibited its maximum value. The absorbance values in the α β regions of the spectrum were multiplied by 3 to aid in the clarity of presentation.

rusticyanin-like molecule. In contrast, iron-reduced intact *At. ferrooxidans* exhibited a broad trough of negative absorbance in the difference spectrum from 500 to 650 nm which was consistent with the hypothesis that concentrated amounts of the blue copper protein rusticyanin were reduced by soluble iron.

Spectral properties similar to those shown in **Figure 1** have been reported for terminal oxidases expressed by two other Gram-negative eubacteria: *Thermus thermophilus*, a thermophile that grows at 70°C (Zimmerman et al., 1988); and *Rhodothermus marinus*, a thermohalophilic bacterium (Verissimo et al., 2007). The positions of the reduced α and β peaks varied between these two bacteria from 600 to 613 nm and from 577 to 562 nm, respectively. These absorbance properties were attributed to a cytochrome ba_3 terminal oxidase expressed by these two extremophilic eubacteria. A working hypothesis is that the absorbance properties shown in **Figure 1** represent a cytochrome ba_3-type terminal oxidase that participates in the aerobic iron respiratory chain of the obligately halophilic and acidophilic *Ah. ferrooxidans*. In any case, it is evident that *At*. and *Ah. ferrooxidans* utilize different prominent redox-active prosthetic groups and biomolecules for respiratory electron transfer when they respire aerobically on soluble iron.

Leptospirillum is the only genus within the Nitrospirae that is known to contain acidophilic members that respire aerobically on iron. The reduced minus oxidized difference spectra contrasted above were quite different from that observed when intact cells of *L. ferrooxidans* were mixed with excess ferrous ions at 30°C and pH 1.5 (Blake and Griff, 2012).

The difference spectrum obtained with *L. ferrooxidans* had a reduced α peak at the unusual position of 579 nm and represents a unique iron-responsive cytochrome that has not been reported for members of the Proteobacteria (Singer et al., 2008). Spectral changes attributable to blue copper proteins or typical cytochromes *a*, *b*, or *c* have not been reported in the genus *Leptospirillum* and were not visible in the ICAM spectra reported earlier (Blake and Griff, 2012). A working hypothesis is that members of the Nitrospirae and the Proteobacteria express and utilize different redox-active biomolecules to conduct aerobic respiration on iron.

Gram-Positive Eubacteria

The Firmicutes and the Actinobacteria are the two phyla of Gram-positive eubacteria that contain obligatory acidophilic members that respire aerobically on soluble iron (Bonnefoy and Holmes, 2012). These acidophilic bacteria are distributed among at least three genera in the Firmicutes: *Sulfobacillus, Alicyclobacillus*, and *Acidibacillus*. *Sulfobacillus* and *Alicyclobacillus* contain at least five and four separate species, respectively, that respire on iron. We chose *S. thermosulfidooxidans* and *Alb. ferrooxydans* to represent the Firmicutes phylum in the *in situ* spectroscopic studies reported herein.

Figure 2 shows the reduced minus oxidized difference spectra that were observed when intact cells of *S. thermosulfidooxidans* and *Alb. ferrooxydans* were mixed with excess ferrous ions at pH 1.5 and 50 and 30°C, respectively. Although the two difference spectra differed by several nanometers in both their reduced Soret and α peaks, we judged the two spectra to be sufficiently similar so as to represent the same type of heme prosthetic group embedded in slightly different protein environments. Because the positions of both reduced α peaks were greater than 600 nm, our hypothesis is that the spectra in **Figure 2** represent the respective terminal oxidases in the aerobic iron respiratory chains of these two Firmicutes.

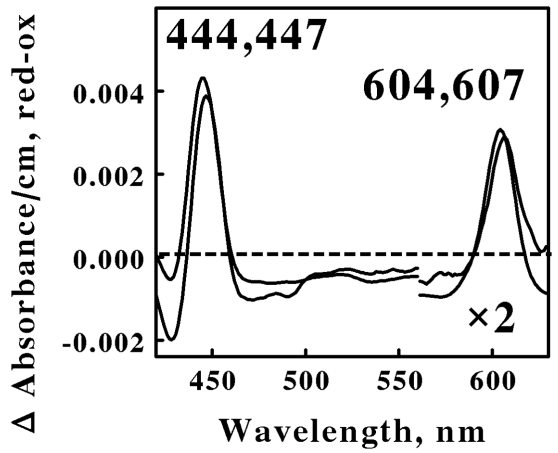

FIGURE 2 | Reduced minus oxidized difference spectra obtained when excess ferrous sulfate was mixed with intact cells of *Sulfobacillus thermosulfidooxidans* (lower wavelengths) and *Alicyclobacillus ferrooxydans* (higher wavelengths), representing the Firmicutes. The number of cells present in 8 ml were 6.8×10^{10} and 4.4×10^{10} for *S. thermosulfidooxidans* and *A. ferrooxydans*, respectively. The absorbance values in the α regions of both spectra were multiplied by 2 to aid in the clarity of presentation.

Acidophilic bacteria that respire aerobically on soluble iron are distributed among as least five genera in the phylum Actinobacteria: *Acidimicrobium, Ferrimicrobium, Ferrithrix, Acidithrix,* and perhaps *Acidithiomicrobium*. We chose *Am. ferrooxidans* and *Fm. acidiphilum* to represent the Actinobacteria phylum in the *in situ* spectroscopic studies reported herein. **Figure 3** shows the reduced minus oxidized difference spectra that were observed when intact cells of *Am. ferrooxidans* and *Fm. acidiphilum* were mixed with excess ferrous ions at pH 1.5 and 45° and 32°C, respectively. As was the case with the two spectra shown in **Figure 2**, the two difference spectra shown in **Figure 3** differed by only a few nanometers in both their reduced Soret and α peaks. Once again, we judged the two spectra in **Figure 3** to be sufficiently similar so as to represent the same type of heme prosthetic group embedded in slightly different protein environments.

All four of the difference spectra shown in **Figures 2** and **3** are highly similar. The wavelengths of maximum absorbance of the reduced Sorets and α peaks in all four difference spectra support the hypothesis that each spectrum represents an *a*-type heme that is part of the terminal oxidase in its respective microorganism. The slight differences among the four spectra are presumed to be due to subtle structural differences among the respective globins that bind and function using the same *a*-type porphyrins.

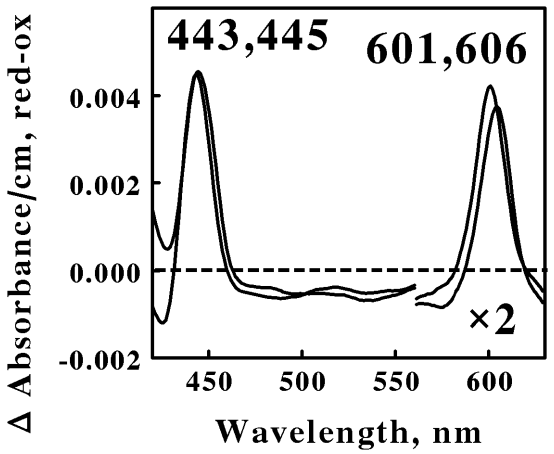

FIGURE 3 | Reduced minus oxidized difference spectra obtained when excess ferrous sulfate was mixed with intact cells of *Ferrimicrobium acidiphilum* (lower wavelengths) and *Acidimicrobium ferrooxidans* (higher wavelengths), representing the Actinobacteria. The number of cells present in 8 ml were 3.7×10^{10} and 3.1×10^{10} for *F. acidiphilum* and *A. ferrooxidans*, respectively. The absorbance values in the α regions of both spectra were multiplied by 2 to aid in the clarity of presentation.

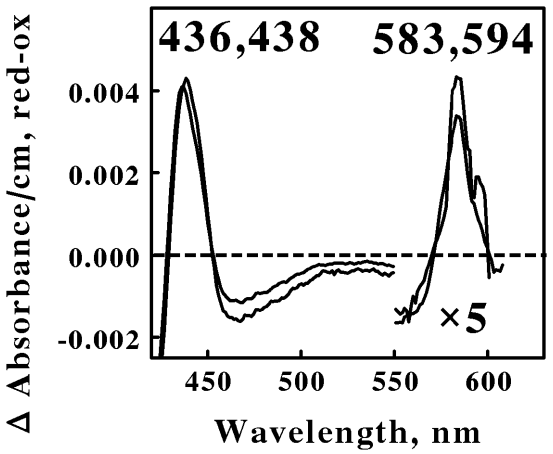

FIGURE 4 | Reduced minus oxidized difference spectra obtained when excess ferrous sulfate was mixed with intact cells of *Acidiplasma aeolicum* (lower wavelengths) and *Ferroplasma acidiphilum* (higher wavelengths), representing the Euryarchaeota. The number of cells present in 8 ml were 8.8×10^{10} and 9.5×10^{10} for *A. aeolicum* and *F. acidiphilum*, respectively. The absorbance values in the α β regions of both spectra were multiplied by 5 to aid in the clarity of presentation.

Thus Gram-positive eubacteria that respire aerobically on iron do so using basically the same principal redox-active prosthetic group in their respective terminal oxidases, regardless of the phylum or genus into which the bacterium is assigned on the basis of the sequence of its 16S ribosomal RNA. We posit that the Gram-positive eubacteria express a unique type of electron transfer pathway and strategy to accomplish aerobic respiration on soluble iron.

Archaea

The Crenarchaeota and Euryarchaeota are the two phyla of Archaea that contain obligately acidiphilic members that respire aerobically on soluble iron (Bonnefoy and Holmes, 2012). These Archaea are distributed among two genera in the acidophilic Euryarchaeota: *Acidiplasma* and *Ferroplasma*. *Acidiplasma* and *Ferroplasma* contain at least two and three separate species, respectively, that respire aerobically on soluble iron. We chose *Ap. aeolicum* and *Fp. acidiphilum* to represent the Crenarchaeota phylum in the *in situ* spectroscopic studies reported herein.

Figure 4 shows the reduced minus oxidized difference spectra that were observed when intact cells of *Ap. aeolicum* and *Fp. acidiphilum* were mixed with excess ferrous ions at pH 1.5 and 40° and 35°C, respectively. The absorbance of the reduced α peak observed with *Ap. aeolicum* had a maximum value at 583 nm, but there was also a discernible shoulder at longer wavelengths. The corresponding α peak observed with iron-reduced *Fp. acidiphilum* exhibited two distinct peaks of absorbance, a more intense peak at 583 nm and a less intense peak at 594 nm. Others have reported the existence of an $a_{583}aa_3$-type of terminal oxidase in *S. tokodaii*, a member of the phylum Euryarchaeota (Iwasaki et al., 1995; Schafer, 1996; Schafer et al., 1996). The a_{583} component in the latter organism is also represented as heme A_S, an *a*-type heme with a formyl group on ring 1 and a hydroxyethylgeranylgeranyl side chain on ring 2 of the *a*-heme frame (Lubben and Morand, 1994). The accompanying aa_3 component of the terminal oxidase in *S. tokodaii* had a reduced α peak at 603 nm. Because the existence of a reduced α peak at 583 nm is rare, we hypothesize that the terminal oxidases expressed by these two members of the Crenarchaeota represent a novel $a_{583}aa_3$-type of terminal oxidase where the aa_3 component differs slightly from that expressed in *S. tokodaii*.

Acidophilic bacteria that respire aerobically on soluble iron are distributed among four genera in the phylum Euryarchaeota: *Metallosphaera, Sulfolobus*, *Acidianus*, and *Sulfurococcus*. We chose *M. sedula* and *S. metallicus* to represent the Euryarchaeota phylum in the *in situ* spectroscopic studies reported herein. **Figure 5** shows the reduced minus oxidized difference spectra that were observed when intact cells of each Archaea were mixed with excess ferrous ions at pH 1.5 and 60°C. Although the two difference spectra differed by several nanometers in all three peaks, we judged the two spectra to be sufficiently similar so as to represent the same prosthetic groups embedded in slightly different protein environments.

The first observation was that the reduced Soret and α peaks at around 422/423 and 578/579 nm, respectively, were remarkably similar to those reported for *L. ferrooxidans* (Singer et al., 2008; Blake and Griff, 2012). Thus one can hypothesize that the same heme prosthetic group is expressed and utilized for aerobic respiration on soluble iron by members of both the eubacterial Nitrospirae and the archaeal Euryarchaeota phyla. Interestingly, there is no evidence for genes in *M. sedula* 5348^T, *M. cuprina* Ar-4, or *S. metallicus* 6482^T that encode a protein similar to the cytochrome 579 that is expressed in *L. ferrooxidans* 2705^T.

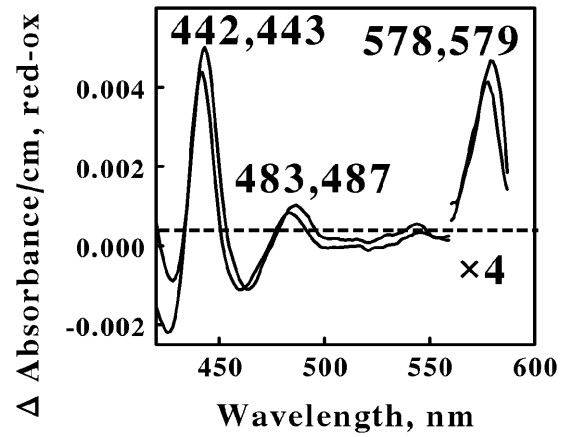

FIGURE 5 | Reduced minus oxidized difference spectra obtained when excess ferrous sulfate was mixed with intact cells of *Metallosphaera sedula* (lower wavelengths) and *Sulfolobus metallicus* (higher wavelengths), representing the Crenarchaeota. The number of cells present in 8 ml were 7.3×10^{10} and 1.2×10^{11} for *M. sedula* and *S. metallicus*, respectively. The absorbance values in the α regions of both spectra were multiplied by 4 to aid in the clarity of presentation.

The second observation was that no spectral evidence was obtained for the participation of an $a_{583}aa_3$-type of terminal oxidase in either of these two representatives of Euryarchaeota, despite its existence in *S. tokodaii* (another member of the Euryarchaeota) and the participation of this latter terminal oxidase during respiration in the Crenarchaeota. The third observation was that a novel spectral species with a reduced peak at around 485 nm was observed when both Euryarchaeota were mixed with an excess of soluble ferrous ions. No evidence for a similar spectral peak was evident from the data reported for *Leptospirillum*. We know of no redox-active prosthetic group that exhibits a reduced peak in the vicinity of 485 nm. We hypothesize that this unexpected spectral intermediate represents a heretofore unknown and uncharacterized prosthetic group that is expressed and exploited by these Euryarchaeota as they respire aerobically on soluble iron.

DISCUSSION

Our absorbance measurements using a novel integrating observation cell to negate deleterious light-scattering effects in turbid suspensions enabled us to observe those redox-active colored prosthetic groups that were reduced when live cells were exposed to soluble iron under physiological conditions. Any reduced prosthetic group that is observed under these conditions must necessarily play a part in the respiratory electron transfer pathway of that microorganism that conducts electrons from extracellular iron to either intracellular oxygen or onto pyridine nucleotides to generate reducing power within the cell. Further, the actual observance of the reduced form implies that the subsequent oxidation of the prosthetic group in question must be slower than its prior reduction, otherwise the transient reduced form might not achieve a sufficient concentration to be detected using absorbance measurements. This type of situation may account for our inability to detect cytochrome *b* using the ICAM in intact *At. ferrooxidans* and other eubacteria and archaea, where a *b*-type cytochromes have been implicated in the electron transfer pathways required to reconstitute the reducing pool necessary for anabolic processes. We observed a number of different colored prosthetic groups in the observations reported above: *b*- and *c*-type cytochromes; numerous *a*-type cytochromes with reduced peaks from 583 to 608 nm; a blue copper protein, a cytochrome with a reduced peak at 579 nm; and an unknown prosthetic group with a reduced peak at around 485 nm. There are simply too many different prosthetic groups in the cornucopia of colored proteins documented above for all of them to represent different rate-limiting steps in a generic respiratory chain that contains all of these components. It is evident that multiple types of respiratory chains must exist among different microorganisms.

We propose that the data summarized herein are consistent with the hypothesis that at least six different strategies exist in acidophilic microorganisms to conduct aerobic respiration on soluble iron. Each stratagem is characterized by a different set of redox-active prosthetic groups. At least three electron transfer strategies were evident in the Gram-negative eubacteria, which must conduct electrons across a periplasmic space. Still further differences may exist within the four highly related taxa of iron-oxidizing acidithiobacilli, where at least two different pathways for iron oxidation have been proposed to reconcile models that had previously been considered to be conflicting (Amouric et al., 2011). At least two electron transfer strategies were evident in the Archaea, which have only a single plasma membrane to cross. Given the apparent diversity of electron transfer pathways expressed by members in these latter four phyla, it is perhaps surprising that only a single electron transfer strategy may exist in members contained within the two phyla of Gram-positive eubacteria. In any event, the simple picture of a highly conserved universal mechanism for respiratory iron oxidation is clearly inaccurate. It is likely that we do not yet possess a complete inventory of all the redox-active prosthetic groups nor all the microorganisms that participate in respiratory iron oxidation in acidic environments. One should perhaps consider these *in situ* spectroscopic analyses of the most conspicuous components of each respiratory chain as a first step in a more detailed investigation of each unique type of respiratory chain.

The cell wall architectural features of the Gram-negative, Gram-positive and archaea microorganisms are so structurally different that it is difficult to imagine how all three types of organisms could express the identical biomolecules to conduct electrons from the exterior of the cell to their interior to accomplish oxidative phosphorylation. Gram negative eubacteria contain a relatively thin peptidoglycan layer adjacent to their plasma membrane. This is responsible for the cell wall's inability to retain the crystal violet stain upon decolorization with ethanol-acetic acid during Gram staining. In addition to their thin peptidoglycan layer, the Gram negative bacteria also contain an outer membrane comprised of phospholipids and lipopolysaccharides (Beveridge, 1999). Gram positive eubacteria generally contain a single relatively thick layer of peptidoglycan

that comprises a rigid cell wall around the outside of their plasma membrane. Most archaea possess a plasma membrane and an outer cell wall that is assembled from surface-layer proteins, which form a so-called S-layer (Sara and Sleytr, 2000). An S-layer is typically a rigid array of protein molecules that cover the outside of the archaeal cell like chain mail (Engelhardt and Peters, 1998); S-layers have been reported for the *Sulfolobus* and *Metallosphaera* genera (Veith et al., 2009). Notable exceptions to this general structural motif among archaea are that the three known species of *Ferroplasma* exhibit no S-layer and are simply bounded by a mere plasma membrane (Golyshina et al., 2000).

When considering the structural features that might be of greatest relevance to the initial electron transfer reactions that occur between bulk extracellular ferrous ions and cellular electron acceptors, the most immediate differences among these three cell types are the natures of the corresponding periplasmic spaces. The periplasm is the space bordered by the inner and outer membranes in Gram negative bacteria. Strictly speaking, there is no periplasmic space in Gram positive bacteria because there is only one biological membrane, the plasma membrane. However, a region termed the 'inner wall zone' has been observed between the plasma membrane and the mature peptidoglycan cell wall (Matias and Beveridge, 2005; Zuber et al., 2006). Similarly, a region termed a 'quasi-periplasmic space' has been observed in TEM images between the plasma membrane and the S-layer in archaea (Baumeister and Lembcke, 1992).

Given the significant differences in the outer architectural features of these phylogenetically diverse microorganisms, the hypothesis that was tested in the comparative results presented above is that microorganisms with different types of cell walls will express different electron transfer proteins to respire aerobically on extracellular ferrous ions. Because one might expect different electron transfer proteins to conduct electron transfer reactions at different rates, the next working hypothesis is that different genera of iron-oxidizing bacteria will catalyze the oxidation of iron or the reduction of molecular oxygen at different rates. The test of this hypothesis would be to carefully quantify and compare the kinetic properties of aerobic respiration on iron by each of the intact microorganisms whose *in situ* spectral changes are reported herein. In so doing, one should focus on quantifying both the oxidation of ferrous ions (and/or the appearance of ferric ions) and the consumption of molecular oxygen. In this way, one could achieve a good estimate of the partition of respiratory electrons between oxygen reduction and the reduction of pyridine nucleotides. Such kinetic studies might also reveal any competitive advantages that particular types of respiratory chains might enjoy in terms of catalytic efficiency (turnover number) or affinities for iron or oxygen. Cell wall structural features aside, the evident question is why microorganisms apparently use so many different strategies to conduct aerobic respiration on iron.

AUTHOR CONTRIBUTIONS

RB wrote the manuscript and directed the project; he also collected and interpreted data for *Acidithiobacillus ferrooxidans*, *Alicyclobacillus ferrooxydans*, and both *Leptospirillum ferrooxidans* and *L. ferriphilum*. MA collected and interpreted data for *Ferrimicrobium acidiphilum*. JB collected and interpreted data for *Acidimicrobium ferrooxidans*. TH and BK collected and interpreted data for *Ferroplasma acidiphilum*. KH and BL collected and interpreted data for *Acidiplasma aeolicum*. ML and RP collected and interpreted data for *Sulfobacillus thermosulfidooxidans*. RP also collected and interpreted data for *Metallosphaera sedula* and *Sulfolobus metallicus*.

FUNDING

Research reported in this publication was supported in part by the National Institute of General Medical Sciences of the National Institutes of Health under Award Number TL4GM118968. Support was also provided in part by grant number 2G12MD7595 from the National Institute on Minority Health and Health Disparities (NIMHD), National Institutes of Health (NIH), and the Department of Health and Human Services (DHHS). In both cases, the contents of this publication are solely the responsibility of the authors and do not necessarily represent the official views of NIMHD, NIGMS, or NIH

ACKNOWLEDGMENT

The authors thank a reviewer of this manuscript for generously contributing the information that genomic evidence for the *Leptospirillum* cytochrome 579 is not present the selected archaea that respire aerobically on iron.

REFERENCES

Amouric, A., Brochier-Armanet, C., Johnson, D. B., Bonnefoy, V., and Hallberg, K. B. (2011). Phylogenetic and genetic variation among Fe(II)-oxidizing acidithiobacilli supports the view that these comprise multiple species with different ferrous iron oxidation pathways. *Microbiology* 157, 111–122. doi: 10.1099/mic.0.044537-0

Auernik, K. S., and Kelly, R. M. (2008). Identification of components of electron transport chains in the extremely thermoacidophilic Crenarchaeon *Metallosphaera sedula* through iron and sulfur compound oxidation transcriptomes. *App. Environ. Microbiol.* 74, 7723–7732. doi: 10.1128/AEM.01545-08

Bandeiras, T. M., Refojo, P. N., Todorovic, S., Murgida, D. H., Hildebrandt, P., Bauer, C., et al. (2009). The cytochrome ba complex from the thermoacidophilic crenarchaeote *Acidianus ambivalens* is an analog of bc1 complexes. *Biochim. Biophys. Acta* 1787, 37–45. doi: 10.1016/j.bbabio.2008.09.009

Bathe, S., and Norris, P. R. (2007). Ferrous iron–and sulfur-induced genes in *Sulfolobus metallicus*. *Appl. Environ. Microbiol.* 73, 2491–2497. doi: 10.1128/AEM.02589-06

Baumeister, W., and Lembcke, G. (1992). Structural features of archaebacterial cell envelopes. *J. Bioenerg. Biomembr.* 24, 567–575. doi: 10.1007/BF00762349

Beveridge, T. J. (1999). Structures of Gram-negative cell walls and their derived membrane vesicles. *J. Bacteriol.* 181, 4725–4733.

Blake, R. C. II, and Griff, M. N. (2012). In situ spectroscopy on intact *Leptospirillum ferrooxidans* reveals that reduced cytochrome 579 is an obligatory intermediate in the aerobic iron respiratory chain. *Front. Microbiol.* 3:136. doi: 10.3389/fmicb.2012.00136

Blake, R. C. II, and Shute, E. A. (1997). "Purification and characterization of a novel cytochrome from *Leptospirillum ferrooxidans*," in *Proceedings of the International Biohydrometallurgy Symposium 97–BIOMINE97*, (Glenside, PA: Australian Mineral Foundation), 1–3.

Blake, R. C. II, Schute, E. A., Greenwood, M. M., Spencer, G. M., and Ingledew, W. J. (1993). Enzymes of aerobic respiration on iron. *FEMS Microbiol. Rev.* 11, 9–18. doi: 10.1111/j.1574-6976.1993.tb00261.x

Bonnefoy, V., and Holmes, D. S. (2012). Genomic insights into microbial iron oxidation and iron uptake strategies in extremely acidic environments. *Environ. Microbiol.* 14, 1597–1611. doi: 10.1111/j.1462-2920.2011.02626.x

Bouchal, P., Zdrahal, Z., Helanova, S., Janiczek, O., Hallberg, K. B., and Mandl, M. (2006). Proteomic and bioinformatic analysis of iron- and sulfur-oxidizing *Acidithiobacillus ferrooxidans* using immobilized pH gradients and mass spectrometry. *Proteomics* 6, 4278–4285.

Brasseur, G., Levican, G., Bonnefoy, V., Holmes, D., Jedlicki, E., and Lemesle-Meunier, D. (2004). Apparent redundancy of electron transfer pathways via bc(1) complexes and terminal oxidases in the extremophilic chemolithoauthtrophic *Acidithiobacillus ferrooxidans*. *Biochem. Biophys. Acta* 1656, 114–126.

Castelle, C., Guiral, M., Malarte, G., Ledgham, F., Leroy, G., Brugna, M., et al. (2008). A new iron-oxidizing/O2-reducing supercomplex spanning both inner and outer membranes, isolated from the extreme acidophile *Acidithiobacillus ferrooxidans*. *J. Biol. Chem.* 283, 25803–25811. doi: 10.1074/jbc.M802496200

Castelle, C. J., Roger, M., Bauzan, M., Brugna, M., Lignon, S., Nimtz, M., et al. (2015). The aerobic respiratory chain of the acidophilic archaeon *Ferroplasma acidiphilum*: a membrane-bound complex oxidizing ferrous iron. *Biochim. Biophys. Acta* 1847, 717–728. doi: 10.1016/j.bbabio.2015.04.006

Cox, J. C., and Boxer, D. H. (1978). The purification and some properties of rusticyanin, a blue copper protein involved in iron (II) oxidation from *Thiobacillus ferroxidans*. *Biochem. J.* 174, 497–502. doi: 10.1042/bj1740497

Dinarieva, T. Y., Zhuravleva, A. E., Pavlenko, O. A., Tsaplina, I. A., and Netrusov, A. I. (2010). Ferrous iron oxidation in moderately thermophilic acidophile *Sulfobacillus sibiricus* N1T. *Can. J. Microbiol.* 56, 803–808. doi: 10.1139/w10-063

Dopson, M., Baker-Austin, C., and Bond, P. L. (2005). Analysis of differential protein expression during growth states of *Ferroplasma* strains and insights into electron transport for iron oxidation. *Microbiology* 151, 4127–4137. doi: 10.1099/mic.0.28362-0

Elterman, P. (1970). Integrating cavity spectroscopy. *Appl. Opt.* 9, 2140–2142. doi: 10.1364/AO.9.002140

Engelhardt, H., and Peters, J. (1998). Structural research on surface layers: a focus on stability, surface layer homology domains, and surface layer-cell wall interactions. *J. Struct. Biol.* 124, 276–302. doi: 10.1006/jsbi.1998.4070

Fry, E. S., Kattawar, G. W., and Pope, R. M. (1992). Integrating cavity absorption meter. *Appl. Opt.* 31, 2055–2065. doi: 10.1364/AO.31.002055

Fry, E. S., Kattawar, G. W., Strycker, B. D., and Zhai, P. W. (2010). Equivalent path lengths in an integrating cavity: comment. *Appl. Opt.* 49, 575–577. doi: 10.1364/AO.49.000575

Golyshina, O. V., Pivovarova, T. A., Karavaiko, G. I., Kondrateva, T. F., Moore, E. R., Abraham, W. R., et al. (2000). *Ferroplasma acidiphilum* gen. nov., sp. nov., an acidophilic, autotrophic, ferrous-iron-oxidizing, cell-wall-lacking, mesopilic member of the Ferroplasmaceae fam. nov., comprising a distinct linage of the Archaea. *Int. J. Syst. Evol. Microbiol.* 50, 997–1006. doi: 10.1099/00207713-50-3-997

Hart, A. J., Murrell, J. C., Poole, R. K., and Norris, P. R. (1991). An acid-stable cytochrome in iron-oxidizing *Leptospirillum ferrooxidans*. *FEMS Microbiol. Lett.* 81, 89–94. doi: 10.1111/j.1574-6968.1991.tb04718.x

Hodgkinson, J., Masiyano, D., and Tatam, R. P. (2009). Using integrating spheres as absorption cells: path-length distribution and application of Beer's law. *Appl. Opt.* 48, 5748–5758. doi: 10.1364/AO.48.005748

Ilbert, M., and Bonnefoy, V. (2013). Insight into the evolution of iron oxidation pathways. *Biochim. Biophys. Acta* 1827, 161–175. doi: 10.1016/j.bbabio.2012.10.001

Iwasaki, T., Wakagi, T., Isogai, Y., Iizuka, T., and Oshima, T. (1995). Resolution of the aerobic respiratory system of the thermoacidophilic archaeon, *Sulfolobus* sp. *strain* 7. *J. Biol. Chem.* 270, 30893–30901. doi: 10.1074/jbc.270.52.30893

Javorfi, T., Erostyak, J., Gal, J., Buzady, A., Menczel, L., Grab, G., et al. (2006). Quantitative spectrophotometry using integrating cavities. *J. Photochem. Photobiol. B Biol.* 82, 127–131. doi: 10.1016/j.jphotobiol.2005.10.002

Johnson, D. B., Kanao, T., and Hedrich, S. (2012). Redox transformations of iron at extremely low pH: fundamental and applied aspects. *Front. Microbiol.* 3:96. doi: 10.3389/fmicb.2012.00096

Kai, M., Yano, T., Tamegai, H., Fukumori, Y., and Yamanaka, T. (1992). *Thiobacillus ferrooxidans* cytochrome c oxidase: purification and molecular and enzymatic features. *Biochem. J.* 44, 6471–6481.

Kappler, U., Sly, L. I., and McEwan, A. G. (2005). Respiratory gene clusters of *Metallosphaera sedula*–differential expression and transcriptional organization. *Microbiology* 151, 35–43. doi: 10.1099/mic.0.27515-0

Kozubal, M. A., Dlakic, M., Macur, R. E., and Inskeep, W. P. (2011). Terminal oxidase diversity and function in "*Metallosphaera yellowstonensis*": gene expression and protein modeling suggest mechanisms of Fe(II) oxidation in the Sulfolobales. *Appl. Environ. Microbiol.* 77, 1844–1853. doi: 10.1128/AEM.01646-10

Li, T. F., Painter, R. G., Ban, B., and Blake, I. I. R. C. (2015). The multi-center aerobic iron respiratory chain of *Acidithiobacillus ferrooxidans* functions as an ensemble with a single macroscopic rate constant. *J. Biol. Chem.* 290, 18293–18303. doi: 10.1074/jbc.M115.657551

Lubben, M., and Morand, K. (1994). Novel prenylated hemes as cofactors of cytochrome oxidases. *J. Biol. Chem.* 269, 21473–21479.

Matias, V. R., and Beveridge, T. J. (2005). Cryo-electron microscopy reveals native polymeric cell wall structure in Bacillus subtilis 168 and the existence of a periplasmic space. *Mol. Microbiol.* 56, 240–251. doi: 10.1111/j.1365-2958.2005.04535.x

Quatrini, R., Appia-Ayme, C., Denis, Y., Jedlicki, E., Holmes, D. S., and Bonnefoy, V. (2009). Extending the models for iron and sulfur oxidation in the extreme acidophile *Acidithiobacillus ferrooxidans*. *BMC Genomics* 10:394. doi: 10.1186/1471-2164-10-394

Ram, R. J., VerBerkmoes, N., Thelen, M. P., Tyson, G. W., Baker, B. J., Blake, R. C. II, et al. (2005). Community proteomics of a natural microbial biofilm. *Science* 308, 1915–1920. doi: 10.1126/science.%201109070

Sara, M., and Sleytr, U. B. (2000). S-layer proteins. *J. Bacteriol.* 182, 859–868. doi: 10.1128/JB.182.4.859-868.2000

Schafer, G. (1996). Bioenergetics of the archaebacterium *Sulfolobus*. *Biochim. Biophys. Acta* 1277, 163–200. doi: 10.1016/S0005-2728(96)00104-1

Schafer, G., Purschkee, W., and Schmidt, C. L. (1996). On the origin of respiration: electron transport proteins from archaea to man. *FEMS Microbiol. Rev.* 18, 173–188. doi: 10.1111/j.1574-6976.1996.tb00235.x

Singer, S. W., Chan, C. S., Zemla, A., VerBerkmoes, N. C., Hwang, M., Hettlich, R. L., et al. (2008). Characterization of cytochrome 579, an unusual cytochrome isolated from an iron-oxidizing microbial community. *Appl. Environ. Microbiol.* 74, 4454–4462. doi: 10.1128/AEM.02799-07

Tuovinen, O. H., and Kelly, D. P. (1973). Studies on the growth of *Thiobacillus ferrooxidans*. I. Use of membrane filters and ferrous iron agar to determine viable numbers, and comparison with 14CO2-fixation and iron oxidation as measures of growth. *Arch. Microbiol.* 22, 285–296.

Valenzuela, L., Chi, A., Beard, S., Orell, A., Guiliani, N., Shabanowitz, J., et al. (2006). Genomics, metagenomics and proteomics in biomining microorgansisms. *Biotechnol. Adv.* 24, 197–211. doi: 10.1016/j.biotechadv.2005.09.004

Veith, A., Klingl, A., Zolghadr, B., Lauber, K., Mentele, R., Lottspeich, F., et al. (2009). Acidianus, *Sulfolobus* and *Metallosphaera* surface layers: structure, composition and gene expression. *Mol. Microbiol.* 73, 58–72. doi: 10.1111/j.1365-2958.2009.06746.x

Verissimo, A. F., Pereira, M. M., Melo, A. M. P., Hreggvidssson, G. O., Kristjansson, J. K., and Teixeira, M. (2007). A ba3 oxygen reductase from the thermohalophilic bacterium *Rhodothermus marinus*. *FEMS Microbiol. Lett.* 269, 41–47. doi: 10.1111/j.1574-6968.2006.00598.x

Yarzabal, A., Brasseur, G., and Bonnefoy, V. (2002). Cytochromes c of *Acidithiobacillus ferrooxidans*. *FEMS Microbiol. Lett.* 209, 189–195. doi: 10.1016/S0378-1097(02)00514-1

Zimmerman, B. H., Nitsche, C. I., Fee, J. A., Rusnak, F., and Munck, E. (1988). Properties of a copper-containing cytochrome ba3: a second terminal oxidase from the extreme thermophile *Thermus thermophilus*. *Proc. Natl. Acad. Sci. USA* 85, 5779–5783. doi: 10.1073/pnas.85.16.5779

Zuber, B., Haenni, M., Ribeiro, T., Minnig, K., Lopes, F., Moreillon, P., et al. (2006). Granular layer in the periplasmic space of Gram-positive bacteria and fine structures of *Enterococcus gallinarum* and *Streptococcus gordonii* septa revealed by cryoelectron microscopy of vitreous sections. *J. Bacteriol.* 188, 6652–6660. doi: 10.1128/JB.00391-06

Conflict of Interest Statement: The authors declare that the research was conducted in the absence of any commercial or financial relationships that could be construed as a potential conflict of interest.

frontiers in Microbiology

ORIGINAL RESEARCH
published: 03 November 2016
doi: 10.3389/fmicb.2016.01755

The Two-Component System RsrS-RsrR Regulates the Tetrathionate Intermediate Pathway for Thiosulfate Oxidation in *Acidithiobacillus caldus*

Zhao-Bao Wang[1], Ya-Qing Li[1], Jian-Qun Lin[1], Xin Pang[1], Xiang-Mei Liu[1], Bing-Qiang Liu[2], Rui Wang[1], Cheng-Jia Zhang[1], Yan Wu[1], Jian-Qiang Lin[1] and Lin-Xu Chen[1]**

[1] State Key Laboratory of Microbial Technology, Shandong University, Jinan, China, [2] School of Mathematics, Shandong University, Jinan, China

OPEN ACCESS

Edited by:
Axel Schippers, Federal Institute for Geosciences and Natural Resources, Germany

Reviewed by:
Jeremy Dodsworth, California State University, San Bernardino, USA
Mark Dopson, Linnaeus University, Sweden

***Correspondence:**
Jian-Qiang Lin
jianqianglin@sdu.edu.cn
Lin-Xu Chen
linxuchen@sdu.edu.cn

Specialty section:
This article was submitted to Extreme Microbiology, a section of the journal Frontiers in Microbiology

Received: *17 June 2016*
Accepted: *19 October 2016*
Published: *03 November 2016*

Citation:
Wang Z-B, Li Y-Q, Lin J-Q, Pang X, Liu X-M, Liu B-Q, Wang R, Zhang C-J, Wu Y, Lin J-Q and Chen L-X (2016) The Two-Component System RsrS-RsrR Regulates the Tetrathionate Intermediate Pathway for Thiosulfate Oxidation in Acidithiobacillus caldus. Front. Microbiol. 7:1755. doi: 10.3389/fmicb.2016.01755

Acidithiobacillus caldus (*A. caldus*) is a common bioleaching bacterium that possesses a sophisticated and highly efficient inorganic sulfur compound metabolism network. Thiosulfate, a central intermediate in the sulfur metabolism network of *A. caldus* and other sulfur-oxidizing microorganisms, can be metabolized via the tetrathionate intermediate (S_4I) pathway catalyzed by thiosulfate:quinol oxidoreductase (Tqo or DoxDA) and tetrathionate hydrolase (TetH). In *A. caldus*, there is an additional two-component system called RsrS-RsrR. Since *rsrS* and *rsrR* are arranged as an operon with *doxDA* and *tetH* in the genome, we suggest that the regulation of the S_4I pathway may occur via the RsrS-RsrR system. To examine the regulatory role of the two-component system RsrS-RsrR on the S_4I pathway, Δ*rsrR* and Δ*rsrS* strains were constructed in *A. caldus* using a newly developed markerless gene knockout method. Transcriptional analysis of the *tetH* cluster in the wild type and mutant strains revealed positive regulation of the S_4I pathway by the RsrS-RsrR system. A 19 bp inverted repeat sequence (IRS, AACACCTGTTACACCTGTT) located upstream of the *tetH* promoter was identified as the binding site for RsrR by using electrophoretic mobility shift assays (EMSAs) *in vitro* and promoter-probe vectors *in vivo*. In addition, Δ*rsrR*, and Δ*rsrS* strains cultivated in $K_2S_4O_6$-medium exhibited significant growth differences when compared with the wild type. Transcriptional analysis indicated that the absence of *rsrS* or *rsrR* had different effects on the expression of genes involved in sulfur metabolism and signaling systems. Finally, a model of tetrathionate sensing by RsrS, signal transduction via RsrR, and transcriptional activation of *tetH-doxDA* was proposed to provide insights toward the understanding of sulfur metabolism in *A. caldus*. This study also provided a powerful genetic tool for studies in *A. caldus*.

Keywords: RsrS-RsrR, two-component system, *Acidithiobacillus caldus*, sulfur metabolism, thiosulfate oxidation, S_4I pathway, transcriptional regulation, *cis* regulatory element

INTRODUCTION

Sulfur oxidizing microorganisms, widely distributed within the chemoautotrophic bacteria and archaea (Goebel and Stackebrandt, 1994; Friedrich, 1997; Suzuki, 1999; Kletzin et al., 2004; Friedrich et al., 2005; Frigaard and Dahl, 2008; Ghosh and Dam, 2009), have evolved a variety of sulfur redox enzymes to metabolize elemental sulfur and various reduced inorganic sulfur compounds (RISCs). Thiosulfate, a central intermediate, plays a key role in inorganic sulfur metabolism in these sulfur oxidizers (Friedrich et al., 2005; Ghosh and Dam, 2009). It is metabolized mainly through the sulfur oxidizing (Sox) enzyme system and the tetrathionate intermediate (S_4I) pathway. The Sox system, composed of SoxYZ, SoxAX, SoxB, and $Sox(CD)_2$ (Friedrich et al., 2000, 2005), completely decomposes thiosulfate to sulfate without generating any sulfur intermediates. Many acidophiles (Friedrich et al., 2005; Ghosh and Dam, 2009; Williams and Kelly, 2013) have a truncated Sox system without $Sox(CD)_2$ (Dahl and Prange, 2006). The alternate S_4I pathway is widely found in chemoautotrophic genera including *Acidithiobacillus*, *Thermithiobacillus*, *Halothiobacillus*, and *Tetrathiobacter* (Dam et al., 2007; Ghosh and Dam, 2009). This pathway is made up of a thiosulfate:quinol oxidoreductase (Tqo or DoxDA) and a tetrathionate hydrolase (TetH). DoxDA oxidizes thiosulfate to tetrathionate, while TetH hydrolyzes tetrathionate to thiosulfate and other products (Hallberg et al., 1996; Ghosh and Dam, 2009). Thus, the Sox and S_4I pathways play important roles in the metabolism of RISCs in sulfur-oxidizing microorganisms.

Acidithiobacillus caldus (*A. caldus*) is an obligate chemoautotrophic sulfur-oxidizing bacterium and one of the most abundant microorganisms in industrial bioleaching systems (Hallberg and Lindström, 1994, 1996; Rawlings, 1998; Dopson and Lindström, 1999). *A. caldus* possesses a truncated Sox system encoded by two *sox* clusters (*sox*-I and *sox*-II) and also has a typical S_4I pathway encoded by a *tetH* cluster (Valdés et al., 2008, 2009; Chen et al., 2012). Furthermore, sulfur metabolism also occurs by other enzymes in this organism. A sulfur quinone oxidoreductase enzyme (SQR) is responsible for oxidation of hydrogen sulfide (Wakai et al., 2004). A sulfur oxygenase reductase (SOR) catalyzes the disproportionation of elemental sulfur to produce sulfite, thiosulfate, and sulfide (Kletzin, 1989, 1992). A sulfur dioxygenase (SDO) can oxidize the thiol-bound sulfane sulfur atoms (R-S-SH) which is activated from S_8 (Rohwerder and Sand, 2003, 2007). It was proposed that the disulfide reductase complex (HdrABC) could catalyze sulfane sulfate (RSSH) to produce sulfite and regenerate RSH, following donation of electrons to the quinone pool (Quatrini et al., 2009). The Rhodanese (RHD) enzyme can transfer a sulfur atom from thiosulfate to sulfur acceptors such as cyanide and thiol compounds (Schlesinger and Westley, 1974; Gardner and Rawlings, 2000). Furthermore, two thiosulfate-transferring proteins, DsrE and TusA, react with tetrathionate to yield protein Cys-S-thiosulfonates, and trigger an irreversible transfer of thiosulfate from DsrE to TusA. This indicates that both these proteins are important players in the dissimilatory sulfur and tetrathionate metabolism (Liu et al., 2014). The *tetH* cluster of *A. caldus* includes *ISAc*1, *rsrR*, *rsrS*, *tetH*, and *doxD*, which encode a transposase, a RsrS-RsrR two-component system (TCS), a tetrathionate hydrolase and a thiosulfate:quinol oxidoreduetase subunit, respectively (Rzhepishevska et al., 2007). The differences in the expression of TetH with different sulfur substrates and the location of the RsrS-RsrR system upstream of the *tetH* gene imply that a regulatory mechanism exists at the transcriptional level (Bugaytsova and Lindström, 2004; Rzhepishevska et al., 2007). However, up to now nothing is known about this potential mechanism. Additionally, we also found a σ^{54}-dependent two-component system (named TspS-TspR), upstream of the *sox*-I cluster of *A. caldus* (unpublished data). The discoveries of TCSs in *tetH* and *sox* clusters of *A. caldus* indicated that TCSs are potentially involved in signal transduction from substrate sensing to subsequent transcriptional regulation of the sulfur-oxidizing genes. These TCS-dependent regulatory systems possibly allow *A. caldus* to adapt to a variety of sulfur energy sources in different growth environments.

TCSs are predominant signal transduction components used by prokaryotic microorganisms to convert rapid environmental changes into specific adaptive responses (Bourret and Silversmith, 2010; Capra and Laub, 2012; Lehman et al., 2015). They typically consist of a membrane-bound sensor histidine kinase (HK), which senses a specific environmental stimulus and undergoes autophosphorylation, and a cognate response regulator (RR), which receives the phosphoryl group via various phosphotransfer pathways and modulates gene transcription by binding to *cis* regulatory elements in the promoter region (Forst et al., 1989; Huang et al., 1997; Bilwes et al., 1999; Stock et al., 2000; Bourret and Silversmith, 2010).

The most effective way to study gene function *in vivo* is mutagenesis of the gene of interest. Gene transfer methods, conjugation, and electroporation, have been developed for *A. caldus*, and mutants were constructed by a marker replacement knockout method (Liu et al., 2007; Zyl et al., 2008; Chen et al., 2010, 2012). However, previously reported gene knockout methods are extremely difficult and not reproducible. Moreover, the antibiotic marker gene introduced into the mutants makes it difficult for creating multiple mutations and may lead to polar effects on downstream genes as well as cause potential biological safety issues in industrial applications. Therefore, the development of a reliable and markerless gene knockout method is of great significance for performing molecular biology research and genetic engineering in *A. caldus*.

In order to detect the regulatory mechanism of the S_4I pathway, we analyzed the *tetH* cluster of the sulfur oxidation system in *A. caldus*. We developed an efficient markerless gene knockout system for *A. caldus* and successfully obtained knockout mutants of *rsrR* and *rsrS*. Physiological and transcriptional analyses of the mutants were carried out to uncover the regulatory mechanism of RsrS-RsrR on the S_4I pathway.

MATERIALS AND METHODS

Bacterial Strains and Growth Conditions

The bacterial strains and plasmids used in this study are listed in **Table 1**. The strain *A. caldus* MTH-04 has been deposited

TABLE 1 | Strains and plasmids used in the study.

Strains or plasmids	Genotype or description	Source or references
STRAINS		
A. caldus MTH-04	Isolated from Tengchong area, Yunnan province, China	Our lab
A. caldus MTH-04 Δ*rsrR* mutant	Δ*rsrR*	This study
A. caldus MTH-04 Δ*rsrS* mutant	Δ*rsrS*	This study
Escherichia coli DH5α	F^-_Φ80d *lacZ*ΔM15Δ*(lacZYA-argF)* U169 *end A1 recA*1 *hsdR*17*(rk$^-$,mk$^+$)* *supE*44λ*-thi-1 gyr*96 *rel*A1 *phoA*	TransGen Biotech Corp. China
Escherichia coli SM10	*Thr leu hsd recA* Km^{r}RP4-2-Tc::Mu	Simon et al., 1983
Escherichia coli BL21 (DE3)	F$^-$*ompT hdsSB*(Rb$^-$mB$^-$) *gal dgmmet*(DE3)	TransGen Biotech Corp. China
PLASMIDS		
pMD19-T	Ap^r, ColE1 replicon	TaKaRa Cor.
pSDUDI	suicide plasmid; Ap^r; Km^r; oriTRP4; multi-cloning sites	This study
pSDUDI::rsrR(UHA + DHA)	suicide plasmid for *rsrR* deletion	This study
pSDUDI::rsrS(UHA + DHA)	suicide plasmid for *rsrS* deletion	This study
pSDU1-tac	Cm^r; IncQ, mob$^+$, tac promoter	Our lab
pSDU1-I-SceI	Cm^r; mob$^+$; Ptac; containing I-*Sce*I gene	This study
pET-22b	Amp^r	Novagen Cor.
pJRD215	Sm^r, Km^r; IncQ, Mob$^+$	Davison et al., 1987
pJRD-P360IRS	Sm^r, Km^r; IncQ, Mob$^+$; PtetH(360 bp); *gusA*	This study
pJRD-P148IRS	Sm^r, Km^r; IncQ, Mob$^+$; PtetH(148 bp); *gusA*	This study
pJRD-P90	Sm^r, Km^r; IncQ, Mob$^+$; PtetH(90 bp); *gusA*	This study
RP4	Ap^r, Tc^r, Km^r; IncP, tra$^+$	Datta et al., 1971
pACBSR	Cm^r; I-*Sce* I, λ-Red recombination system	Herring et al., 2003

in the China General Microbiological Culture Collection Center (CGMCC) with the accession number CGMCC 1.15711. Liquid Starkey-S^0 and -$K_2S_4O_6$ inorganic media and solid Starkey-$Na_2S_2O_3$ plates for *A. caldus* MTH-04 culture were prepared as reported previously (Jin et al., 1992). Elemental sulfur (S^0; boiling sterilized, 8g/L) or $K_2S_4O_6$ (membrane filtration, 3 g/L) were added prior to inoculation. Chloromycetin, kanamycin, and streptomycin were added to a final concentration of 34, 100, and 100 μg/mL in LB media, and at 60, 100, and 100 μg/mL in liquid and solid Starkey media. The culture conditions were 37°C, 200 r/min for *Escherichia coli* (*E. coli*), and 40°C, 150 r/min for *A. caldus* MTH-04 (Chen et al., 2012).

The wild type and mutant strains of *A. caldus* were initially grown on a solid Starkey-$Na_2S_2O_3$ plate. One colony from each plate was inoculated into 10 mL Starkey-S^0 liquid medium and grown to stationary phase. The saturated 10 mL culture was then transferred to 150 mL Starkey-S^0 liquid medium and allowed to grow to stationary phase. Finally, cells in the 150 mL culture were collected by centrifugation at 12000 × g for 5 min and diluted with Starkey liquid medium to a final concentration of OD_{600} = 1.0. In order to measure growth or extract RNA, 1 mL of this culture was inoculated into 150 mL Starkey-S^0 or -$K_2S_4O_6$ liquid medium. Cell growth in Starkey-S^0 medium was measured at OD_{600} after removal of elemental sulfur in the sample by low-speed centrifugation at 400 × g for 5 min (Yu et al., 2014). Only a small amount of cells (<1.5 %) were found attached to the sulfur particles, which were neglected in the cell growth measurement. All experiments were performed in triplicate.

Construction of Plasmids pSDUDI and pSDU1-I-Sce I

To construct the basic suicide plasmid vector pSDUDI, the *ori*T region was initially amplified from the plasmid RP4 using primers oriT EcoR sen and oriT Sal ant and digested with *Eco*R I/*Sal* I. A ColE1-AmpR fragment was amplified by PCR from pMD19-T vector using primers pMD19 Sal sen and pMD19 EcoR ant and digested with *Eco*R I/*Sal* I. The two PCR products were ligated together to generate plasmid pMD-oriT. The plasmid pMD-oriT was then amplified by PCR using primers pMD19 Nde sen and oriT Apa ant to generate a linearized plasmid. This was digested with *Nde* I/*Apa* I, and ligated to *Nde* I/*Apa* I digested Km resistant gene amplified from plasmid pJRD215 using primers Km Apa sen and Km Nde ant. The resulting plasmid was the basic suicide plasmid pSDUDI. An I-*Sce* I recognition site (5′-TAGGGATAACAGGGTAAT-3′) and multiple cloning sites (MCS) were introduced into pSDUDI by PCR using primers Km Apa sen and pMD19 Nde sen/Km Nde ant, respectively. All primers used are listed in **Table 2**.

The I-Sce I-expressing plasmid pSDU1-I-Sce I was constructed by generating a linearized form of the vector pSUD1-tac by PCR amplification with pSDU1 Xba sen and tac Bam ant. The I-Sce I gene was then amplified from plasmid pACBSR using primers I-Sce Bam sen and I-Sce Xba ant, digested with *Bam*H I and *Xba* I, and ligated into the *Bam*H I/*Xba* I treated linearized vector pSUD1-tac. The resulting plasmid was designated as pSDU1-I-Sce I.

TABLE 2 | Primers used in construction of suicide plasmid and I-Sce I-expressing plasmid.

Primer name	Primer Sequence (5′ →3′)
oriT EcoR sen	ATTCCGGAATTCGCTCGTCCTGCTTCTCTTCG
oriT Sal ant	TCACGCGTCGACCGGGATTCAACCCACTCG
pMD19 Sal sen	TCACGCGTCGACGCGGTAATACGGTTATCCACAG
pMD19 EcoR ant	ATTCCGGAATTCAATGGTTTCTTAGACGTCAGGT
pMD19 Nde sen	TTATCATATGCAATTGAAGCTTGGTACCGCGGCTAGCGG CCGCGCGGTAATACGGTTATCCACAG
oriT Apa ant	TATAGGGCCCCGACCGGGATTCAACCCA
Km Apa sen	GTGAGGGCCCATAGGGATAACAGGGTAATAT GAATGTCA GCTACTGG
Km Nde ant	TTATCATATGACGCGTGGATCCGAGCTCTAGACTAG TCGACAATCGAAATCTCGTGATGG
pSDU1 Xba sen	CTTCATGCATTCTAGATCATGTTTGACAGCTTATC
tac Bam ant	TCGCGGATCCTCCTGCAGTGTTTCCTGTGTGAAATTG
I-Sce Bam sen	TTACGCGGATCCAGGAGGGTACCTATATGCATATGAAAAA CATCAAAAAAAACC
I-Sce Xba ant	TTCTTCTCTAGAACGTCGGGCCCTTATTTCAGGAAAGTTT CGGAGGAG

Restriction sites were indicated with underline.

Generation of Knockout Mutants

To generate the suicide plasmid for *rsrR*, the upstream and downstream homologous arms (UHA and DHA) of this gene were amplified using the primer pairs R1F/R1R and R2F/R2R, respectively. The two homologous arms were then linked using fusion PCR (Yon and Fried, 1989). Finally, the fused fragments were digested with *Spe* I and *Not* I, and ligated to Spe I/Not I digested plasmid pSDUDI, thus generating the suicide plasmid pSDUDI::rsrR (UHA + DHA).

The suicide plasmid for *rsrS* was constructed in a similar manner by amplifying the two homologous arms (UHA and DHA) of *rsrS* using S1F/S1R and S2F/S2R. The UHA, DHA, and plasmid pSDUDI were then digested with *Spe* I/*Hin*d III, *Hin*d III/*Kpn* I, and *Spe* I/*Kpn* I, respectively. The three digested fragments were finally ligated to each other, and transformed into *E. coli* DH5α and screened for the suicide plasmid pSDUDI::rsrS (UHA + DHA).

The suicide plasmids for both genes were verified by restriction enzyme digestion and sequencing.

The suicide plasmids were transformed into *E. coli* SM10, and the transformed *E. coli* SM10 were conjugated with *A. caldus* as described earlier (Liu et al., 2007). After the first homologous recombination, the single crossover mutants were selected for kanamycin resistance on Starkey-$Na_2S_2O_3$ solid plates. Single recombination events were rapidly identified by PCR using R4F/R and S4F/R primers for *rsrR* and *rsrS*, respectively. The I-*Sce* I-expressing plasmid (pSDU1-I-Sce I) was then transferred into the single crossover mutants to induce a second homologous recombination, thereby generating the target mutants. The Δ*rsrR* and Δ*rsrS* strains were identified by PCR based screening using R4F/R and S4F/R primers. Finally, the PCR fragments amplified from Δ*rsrR* and Δ*rsrS* were sequenced using primers R5F/R and S5F/R, respectively to confirm their identity. All primers used in this section are listed in **Table S1**.

Elimination of the I-*Sce* I expression plasmid was achieved by spontaneous loss. The mutant containing I-*Sce* I expression plasmid was inoculated into the non-selective liquid Starkey-S^0 medium and grown to stationary phase. An aliquot from the culture was diluted and plated on non-selective solid Starkey-$Na_2S_2O_3$ medium. Colony PCR was carried out to screen for loss of the plasmid using the primers RepA sen and RepC, which are also listed in **Table S1**. About 3–5 consecutive transfers were carried out to obtain the Δ*rsrR* and Δ*rsrS* mutants without the I-*Sce* I expression plasmid.

Real-Time Quantitative PCR

For RNA isolation, the culture was filtered through filter papers with a pore size of 15–20 μm to remove the sulfur powder, after which the cells were harvested by centrifugation at 12000 × g under refrigerated conditions. RNAprotect Bacteria Reagent (Qiagen Cor.) was added to resuspend the cells and inhibit changes to RNA transcripts. The suspension was mixed immediately by vortexing for 5 s, incubated for 5 min at room temperature, and centrifuged for 10 min at 5000 × g. The supernatant was discarded and the harvested cells were stored at −70°C. The RNAs were extracted by using RNAiso Plus kit (TaKaRa Cor.) according to the manufacturer's instructions. Reverse transcription was performed using the PrimeScript™ RT reagent Kit with gDNA Eraser (Perfect Real Time) (TaKaRa Cor.). One microgram of total RNA was used for every 20 μL reverse transcription reaction system to obtain cDNA under the following reaction conditions: 42°C for 2 min, 37°C for 15 min, and 85°C for 5 s. The cDNAs from various cultures were used with SYBR® *Premix Ex Taq*™ (TliRNaseH Plus; TaKaRa Cor.) for real-time quantitative PCR reactions, which were performed using LightCycler® 480 (Roche). Two-hundred nanograms of cDNA was used in a 20 μL RT-qPCR reaction. The conditions for qPCR were as follows: 95°C for 30 s followed by 40 cycles at 95°C for 5 s and 60°C for 30 s, and a final cycle at 95°C for 5 s, 60°C for 1 min and 95°C with continuous mode. The data and fold change were calculated using the LightCycler® 480 software. The primers used in this assay were designed using PRIMER PREMIER 5 software (PREMIER Biosoft Int., Palo Alto, CA, USA) and are listed in **Table S2**. The *gapdH* gene of *A. caldus*, encoding glyceraldehyde-3-phosphate dehydrogenase, was used as the reference gene for normalization (Livak and Schmittgen, 2001). Relative expression was calculated using the comparative $\Delta\Delta C_T$ method, and the values were expressed as $2^{-\Delta\Delta CT}$ (Livak and Schmittgen, 2001). Three independent replicates were performed for each experiment. The values shown in this study are the means of three independent replicates showing fold changes (FC). FC $\geq$ 2, $P \leq 0.05$ and FC $\leq$ 0.5, $P \leq 0.05$ were regarded as significant changes, designated as up-regulation and down-regulation, respectively. No significant change was inferred when $0.5 \leq FC \leq 2$, $P \geq 0.05$. The *SD*-value was calculated using Origin software with "descriptive statistics," and the *P*-value was calculated by using GraphPad Prism software with "unpaired *t*-test."

EMSA Assays

The expression and purification of RsrR was performed as described. The *rsrR* gene of *A. caldus* MTH-04 was amplified by PCR using primers rsrR-F and rsrR-R listed in **Table S3**. The PCR product was cloned into plasmid pET-22b, generating the expression plasmid pET-22b-rsrR. A positive clone was verified by sequencing, and transformed into *E. coli* BL21 (DE3). RsrR was purified using HisTrap HP column (GE Healthcare), and the concentration of the purified protein was determined using the Bradford assay.

DNA fragments were obtained by PCR amplification using different sets of primers listed in **Table S3**. The G360, T360, T148, and T90 fragments were obtained using primer-pairs G360-F and G360-R, T360-F and T360/148/90-R, T148-F and T360/148/90-R, and T90-F and T360/148/90-R, respectively. The G360+58IRS fragment was obtained after two rounds of PCR. The first round of PCR was performed with G360 fragment as the template using the primer-pair G360-F and G360+58IRS–R1. In the second round of PCR, the PCR product from the first round was used as the template with the primer-pair G360-F and G360+58IRS–R2, to generate the G360+58IRS fragment. The T360Δ19 fragment was obtained by fusion PCR. Two fragments were generated by PCR from the T360 fragment using the primer-pairs T360-F and T360Δ19-R, and T360Δ19-F1 and T360/148/90-R. Fusion PCR was then performed using the two generated fragments as templates with the primer pair T360-F and T360/148/90-R to obtain the T360Δ19 fragment without the 19 bp IRS. After PCR amplification, the amplified fragments were purified using QIAquick Gel Extraction Kit (Qiagen Corp.), desalted, and concentrated using ultrafiltration. Ultrafiltration was carried out using Amicon Ultra-15 mL, 3 kDa Centrifugal Filter Unit (Millipore Corp.) at 5000 × g in a refrigerated centrifuge.

EMSA assays were performed as described in Pardo and Orejas (2014). Initially, a 15 μL reaction mixture containing 1.5 μL 10× Binding Buffer, 1 μg of salmon sperm DNA, and 1 μg RsrR was mixed and used as the reaction solution. Reaction solution containing PBS (phosphate buffer saline) instead of RsrR was used as a negative control. Both solutions were prepared and incubated at room temperature for 20 min. Two-hundred nanogram of DNA fragments were then added to both mixtures and incubated at room temperature for another 20 min. The DNA-protein complexes in both reactions were separated on 6.5% nondenaturing polyacrylamide gels in 0.25× TBE (22.25 mM Tris-Boric acid, 0.5 mM EDTA) on ice (150 volts for 1.5 h). Visualization of the bands was done using ethidium bromide staining as described earlier (Bidart et al., 2014).

The primers used for constructing the three IRS-probe vectors and the primers that were used to verify the function of the 19bp-IRS *in vivo* are listed in **Table S4**.

Gene Sequences

The nucleotide sequences of *rsrR* and *rsrS* have been deposited with GenBank accession numbers KX161704 and KX161705, respectively. This Whole Genome Shotgun project for *A.caldus* MTH-04 has been deposited at DDBJ/ENA/GenBank under the accession LXQG00000000.

RESULTS

Analysis of *tetH* Clusters in *A. caldus* and Other Sulfur Oxidizers

The *tet*H clusters in various bacteria and archaea were compared for analysis. As shown in **Figure 1**, the two functional genes (*tetH* and *doxDA*) of the S_4I pathway were distributed in chemoautotrophic sulfur oxidizers including bacteria and archaea of the genera *Acidithiobacillus* and *Acidianus*, respectively. However, only *A. caldus* and *Acidithiobacillus ferrooxidans* have a specific two-component system (TCS) upstream the *tetH* gene. The cluster of *A. caldus* MTH-04 was identical to that of *A. caldus* SM-1 and shared 99% identity with that of *A. caldus* ATCC 51756. Furthermore, the *tetH* cluster in *Acidithiobacillus* sp. GGI-221 has certain components including *tetH* and *doxDA* with 61 and 59% identity, respectively. The 16S rRNA gene sequence of *Acidithiobacillus* sp. GGI-221 shows 99.7% identity to *Acidithiobacillus ferrooxidans* indicating that this is a strain of *Acidithiobacillus ferrooxidans* (Williams and Kelly, 2013). However, the TCS of *A. ferrooxidans* is σ^{54}-dependent and has a different order from *tcsS* to *tcsR* encoding the sensor histidine kinase and the cognate response regulator when compared to *A. caldus*. The *tetH* and *doxDA* genes are arranged in a cluster in *A. caldus* and *Acidithiobacillus thiooxidans*, while they were separately distributed in the genomes of *Acidianus* and other *Acidithiobacillus* spp. Two copies of *doxDA* genes are located separately in the genomes of *A. ferrooxidans* and *Acidianus hospitalis* W1, while in *Acidianus ambivalens* DSM 3772 there are two copies of *tetH*. Moreover, *doxDA* in *Acidithiobacillus* spp. encodes a protein with two domains DoxD and DoxA, but DoxD and DoxA in *Acidianus hospitalis* W1 and *Acidianus ambivalens* DSM 3772 are two individual subunits encoded by two separate genes, *doxD* and *doxA* (Müller et al., 2004; Valenzuela et al., 2008; Valdés et al., 2009; Mangold et al., 2011). BLAST and multiple alignment (**Figure S1**) results demonstrated that the two subunits DoxD and DoxA are fused as one protein in the three *A. caldus* strains, MTH-04, SM-1, and ATCC 51756, indicating that the *doxD* gene in this *tetH* cluster encodes a protein that has two domains corresponding to DoxD and DoxA (Müller et al., 2004). Thus, we renamed the *doxD* gene in these strains as *doxDA* or *tqo*.

Development of a Markerless Gene Knockout System to Construct Δ*RsrS* and Δ*RsrR*

A mobile suicide vector (pSDUDI, **Figure 2A**) was employed to introduce homologous sequences of the target genes into *A. caldus* cells, and to integrate these homologous sequences into the genome by homologous recombination, thus generating cointegrates (**Figure 2C**). The backbone of the suicide plasmid was derived from pUC19 and therefore cannot replicate in *A. caldus*. Second, the origin of transfer (*ori*T) of plasmid RP4 was cloned into this plasmid, which allows it to be mobilized

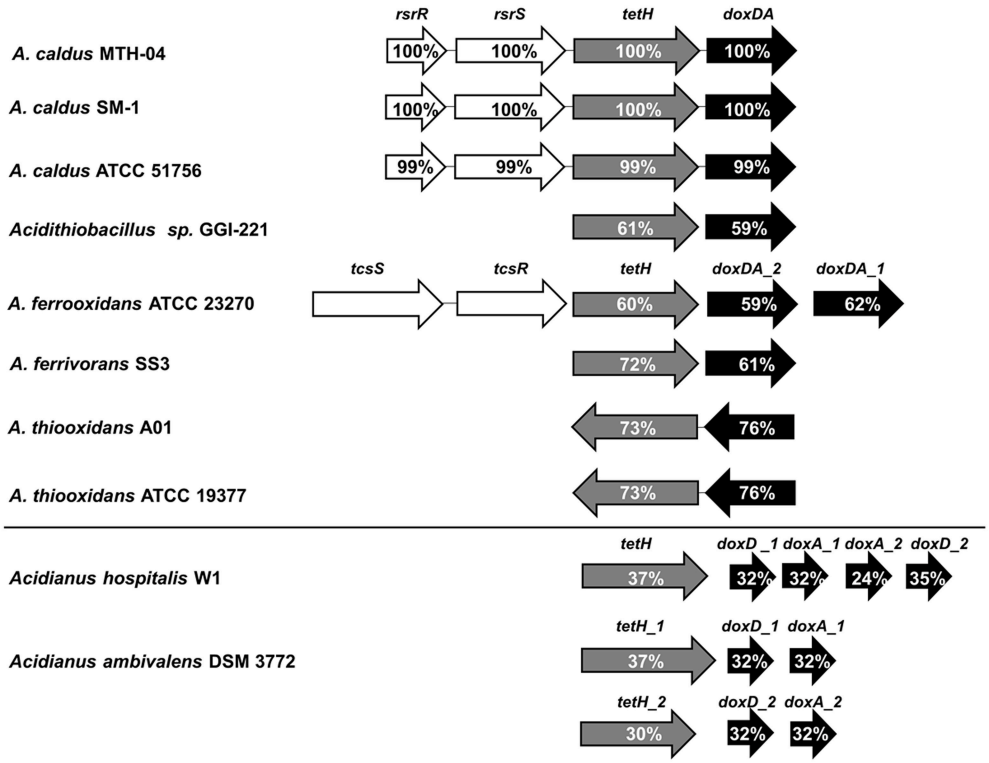

FIGURE 1 | Comparison of *tetH* clusters in various bacteria and archaea. *rsrR* and *tcsR*, response regulators of TCSs (two-component systems); *rsrS* and *tcsS*, histidine kinases of TCSs; *tetH*, tetrathionate hydrolase; *doxDA*, thiosulfate:quinone oxidoreductase. The percentages of amino acid similarity between proteins and their homologs are indicated. The database of National Center for Biotechnology Information (NCBI), http://www.ncbi.nlm.nih.gov/ was used in this study. NCBI Taxonomy IDs for *Acidithiobacillus caldus* SM-1, *Acidithiobacillus caldus* ATCC 51756, *Acidithiobacillus* sp. GGI-221, *Acidithiobacillus ferrooxidans* ATCC 23270, *Acidithiobacillus ferrooxidans* SS3, *Acidithiobacillus thiooxidans* A01, *Acidithiobacillus thiooxidans* ATCC 19377, *Acidianus hospitalis* W1, and *Acidianus ambivalens* DSM 3772 are 990288, 637389, 872330, 243159, 743299, 1432062,637390, 933801, and 2283, respectively. Accession numbers (GenBank) for these proteins are: *A. caldus* MTH-04, RsrR (ANJ65973.1), RsrS (ANJ65974.1), TetH (OAN03451.1), DoxDA (OAN03452.1); *A. caldus* SM-1, RsrR (AEK59530.1), RsrS (AEK58242.1), TetH (AEK58243.1), DoxDA (AEK58244.1); *A. caldus* ATCC 51756, RsrR (ABP38227.1), RsrS (ABP38226.1), TetH (ABP38225.1), DoxDA (ABP38224.1); *Acidithiobacillus sp.* GGI-221, TetH (EGQ60847.1), DoxDA (EGQ62792.1); *A. ferrooxidans* ATCC 23270, TcsS (WP_041646693.1), TcsR (WP_012535753.1), TetH (ACK80599.1), DoxDA_2 (ACK79881.1), DoxDA_1 (ACK78481.1); *A. ferrooxidans* SS3, TetH (AEM46280.1), DoxDA (AEM47534.1); *A. thiooxidans* A01, TetH (WP_024894935.1), DoxDA (WP_024894934.1); *A. thiooxidans* ATCC 19377, TetH (WP_029316048.1), DoxDA (WP_010638552.1); *Acidianus hospitalis* W1, TetH (AEE94548.1), DoxD_1 (AEE93006.1), DoxA_1 (AEE93005.1), DoxA_2 (AEE93131.1), DoxD_2 (AEE93130.1); *Acidianus ambivalens* DSM 3772, TetH_1 (CBY66038.1), DoxD_1 (CAA69986.1), DoxA_1 (CAA69987.1), TetH_2 (CBY66040.1), DoxD_2 (CAA70827.1), DoxA_2 (CAA70828.1).

into *A. caldus* with high efficiency. Third, an 18 bp I-*Sce* I endonuclease recognition site (5′-TAGGGATAACAGGGTAAT-3′) was also introduced into this plasmid to facilitate cleavage of the cointegrate by I-Sce I endonuclease.

The I-*Sce* I-expressing plasmid (pSDU1-I-Sce I) shown in **Figure 2B** was derived from pJRD215, which can replicate and remain stable in *A. caldus*. The Ptac promoter was introduced into this plasmid to express I-*Sce* I in *A. caldus*. Mobilization of pSDU1-I-Sce I into the cointegrate of *A. caldus* would lead to the generation of double-stranded breaks (DSBs) at the I-*Sce* I site. The subsequent second homologous recombination event, would ultimately lead to generation of the mutant or wild type strains (**Figure 2C**).

Verification of the Δ*rsrR* and Δ*rsrS* strains is shown in **Figure 3**. Smaller fragments were amplified from Δ*rsrR* and Δ*rsrS* strains compared to the wild type using primers R4F/R and S4F/R (lane 1, 5.1 kb; lane 2, 4.6 kb; lane 3, 1.0 kb, and lane 4, 551 bp), and R5F/R and S5F/R (lane 1, 5.0 kb; lane 2, 3.9 kb; lane 3, 2.1 kb, and lane 4, 910 bp; **Figures 3C,D** lanes 1–4). No band could be amplified from *rsrR* and *rsrS* knockout strains using primers R3F/R and S3F/R (**Figures 3C,D** lanes 6), while there were 413 and 850 bp bands for *rsrR* and *rsrS* genes, respectively in the wild type as shown in **Figures 3C,D** lanes 5. The sizes of the observed PCR bands were as expected in different strains. The precise sequences of the two mutants were confirmed by sequencing the PCR fragments (**Figures 3C,D** lane 2) derived from Δ*rsrR* and Δ*rsrS*.

Transcriptional Changes of the *tetH* Cluster

To verify the influence of the lack of RsrR or RsrS on the S_4I pathway, relative RNA transcript levels of genes in the *tetH* cluster of Δ*rsrR*, Δ*rsrS*, and the wild type strains were tested by RT-qPCR. Strains were grown to mid-log phase in S^0-medium (at the 4th day), followed by addition of equal volumes of

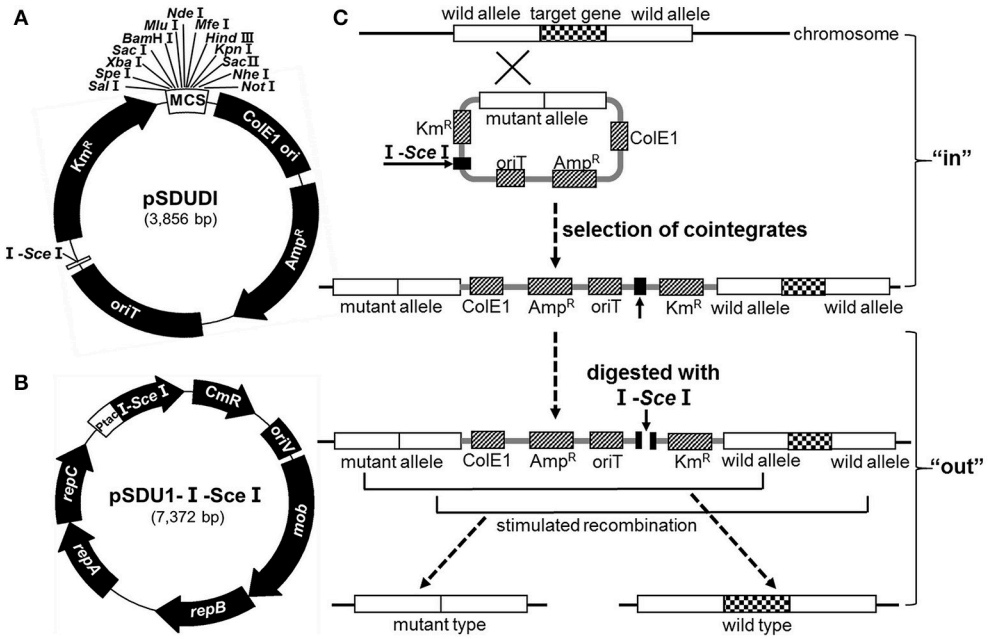

FIGURE 2 | The markerless gene knockout strategy in *A. caldus*. (A) Map of the suicide plasmid pSDUDI. ColE1, the replication origin; *ori*T, the origin of transfer; I-SceI, endonuclease recognition site. **(B)** Plasmid pSDU1-I-Sce I. I-Sce I endonuclease gene was under the control of Ptac promoter. **(C)** General scheme of the markerless gene knockout method. At the "in" step, the suicide plasmid carrying homologous sequences specific to the targeted gene was conjugated into *A. caldus*, and integrated into the chromosome with the help of Rec homologous recombination system in *A. caldus*. At the "out" step, the I-Sce I endonuclease encoded by plasmid pSDU1-I-Sce I created the double-stranded breaks (DSBs) on the chromosome, which acted as the signal to stimulate a second recombination event, generating either a wild type or a mutant type.

either $K_2S_4O_6$ or H_2O to the stimulation and control groups, respectively. Cells at the 4th and 4.5th days were collected to purify total RNA for transcriptional analysis. The ratio of relative RNA transcripts levels of the genes at the two time points were calculated and are shown in **Figure 4**. After stimulation with exogenous $K_2S_4O_6$ at a final concentration of 3 g/L, the relative RNA transcript levels of *rsrS*, *rsrR*, *tetH*, and *doxDA* in the wild type increased by about 5, 20, 60, and 80 fold, respectively (**Figure 4A**). However, the relative transcript levels of these genes in the two mutants did not show any obvious increase ($0.5 \leq$ ratio ≤ 2.0; **Figure 4A**). In the control group, addition of water did not result in a significant change in expression of any of the four genes in the three strains ($0.5 \leq$ ratio ≤ 2.0; **Figure 4B**). This result supported the notion that there is a $K_2S_4O_6$-dependent positive regulation of RsrS-RsrR on *tetH-doxDA*.

Determination of the *Cis*-Regulatory Element of RsrR

Positive control of the cotranscription of *tetH* and *doxDA* (Rzhepishevska et al., 2007) is likely achieved by binding of RsrR to a *cis*-regulatory element at the promoter region of *tetH*. To confirm the above hypothesis, three fragments about 360, 148, and 90 bp upstream of the "ATG" of *tetH* were amplified to test for their interaction with RsrR by electrophoretic mobility shift assays (EMSAs) (**Figure 5A**). A 360 bp fragment amplified from the *gapdH* gene of *A. caldus* was used as a negative control. The results showed that the binding region is located in a 58 bp region between 90 and 148 bp upstream of "ATG" (**Figure 5B**). When the 58 bp region was fused with the 360 bp *gapdH* fragment, the fusion could bind to RsrR (**Figure 5C**), indicating that this *cis*-regulatory element was located in the 58 bp region. To further narrow down the binding region of RsrR, the software package Repeat Around-2.1 was used to analyze this region and a 19 bp (AACACCTGTTACACCTGTT) inverted repeat sequence (IRS) within the 58 bp region was predicted to be the binding sequence (**Figure 5A**). Upon removal of the 19 bp-IRS from the 360 bp-fragment upstream of *tetH*, binding of RsrR could not be observed (**Figure 5D**), which suggested that the 19 bp-IRS was the key binding site of RsrR.

To verify the function of the 19 bp-IRS on the transcription of *tetH* and *doxDA in vivo*, the 360, 148, and 90 bp fragments upstream of the "ATG" of *tetH* were fused to the reporter gene *gusA* to generate three IRS-probe vectors, as shown in **Figure 5E**. The resulting plasmids were designated as pJRD-P360IRS, pJRD-P148IRS, and pJRD-P90, respectively and were mobilized into wild type and Δ*rsrR* strains. All strains were grown in S^0-medium, and the relative RNA transcript levels of *gusA* in each strain were measured after stimulation with $K_2S_4O_6$. As shown in **Figure 5F**, a significantly low level of *gusA* transcript was observed in the wild type strain harvesting plasmid pJRD-P90 when compared with that with pJRD-P360IRS and pJRD-P148IRS, indicating that the 19 bp-IRS had a positive effect on the transcription of *tetH* promoter. The relative *gusA* RNA transcript levels from plasmids pJRD-P360IRS and pJRD-P148IRS in Δ*rsrR*

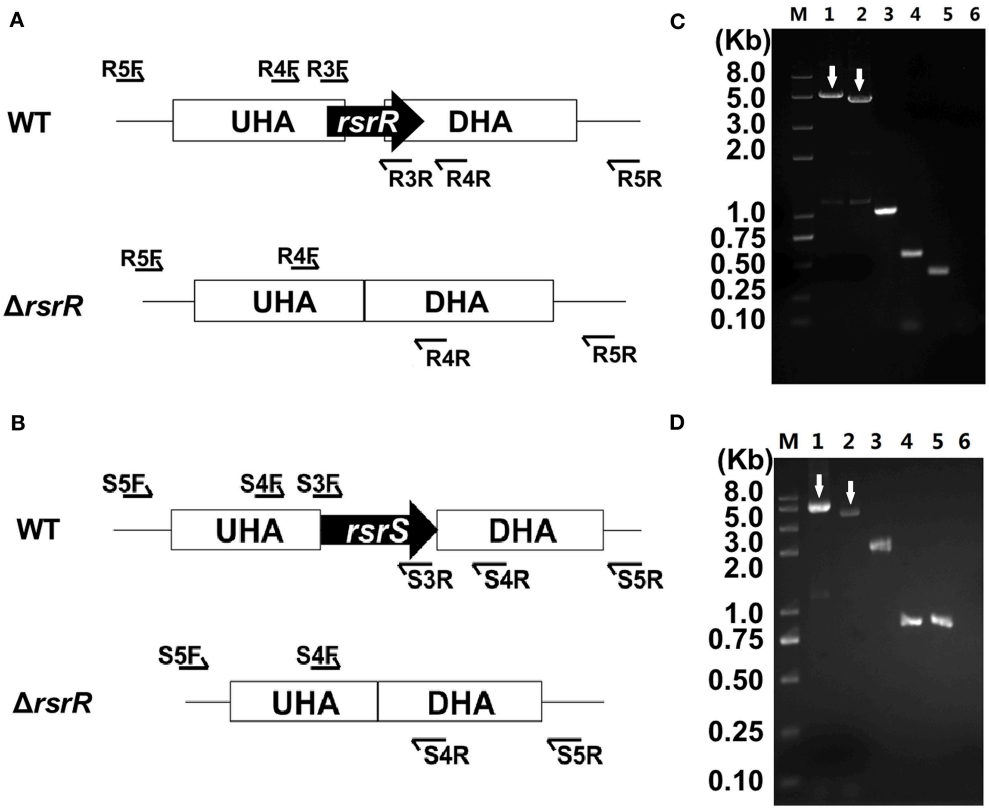

FIGURE 3 | Confirmation of *rsrR* and *rsrS* mutants by PCR analyses. (A,B) Diagram of three sets of primers specific to target genes (*rsrR* and *rsrS*), the upstream and downstream homologous arms (UHA and DHA) and the sequences outside of homologous arms, respectively. **(C,D)** PCR analyses of the chromosomes of Δ*rsrR* and Δ*rsrS*. Lane 1 and 2, PCR amplifications from wild type and mutants using primers R5F/R or S5F/R, respectively; lane 3 and 4, PCR amplifications from wild type and mutants using primers R4F/R or S4F/R, respectively; lane 5 and 6, PCR amplifications from wild type and mutants using primers R3F/R or S3F/R, respectively. In **(C,D)**, the arrows are added to indicate the target bands.

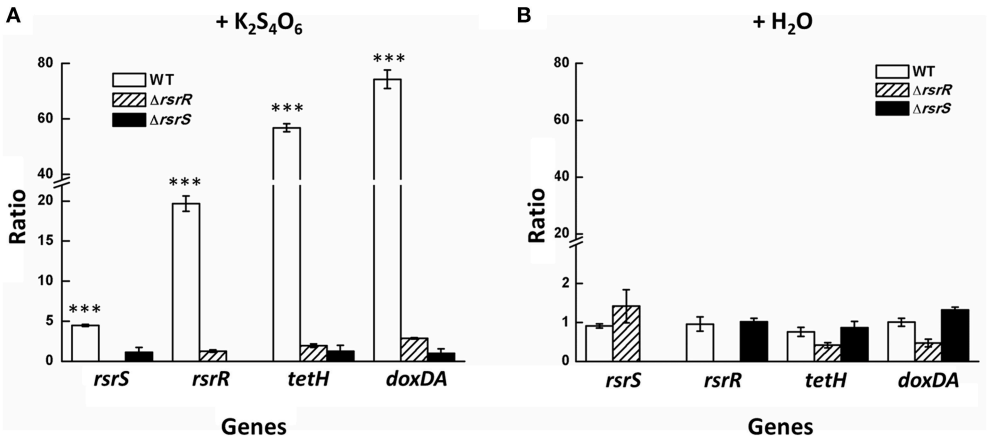

FIGURE 4 | Relative RNA transcripts level changes of *tetH* cluster in Δ*rsrR*, Δ*rsrS*, and the wild type in S^0-medium with the addition of $K_2S_4O_6$ (A) and H_2O (B). The addition of the same volume H_2O was set as the control group. Asterisks denote statistically significant changes (***$P \leq 0.001$).

were much lower than those in the wild type strain, indicating that IRS is needed for the positive effect of RsrR.

Structural simulation and protein sequence alignment between RsrS-RsrR and EnvZ-OmpR were also carried out in order to help understand the mechanism of regulation of the *tetH* cluster by RsrS-RsrR, which showed that the two TCSs are highly identical at the protein level (**Figure S2**).

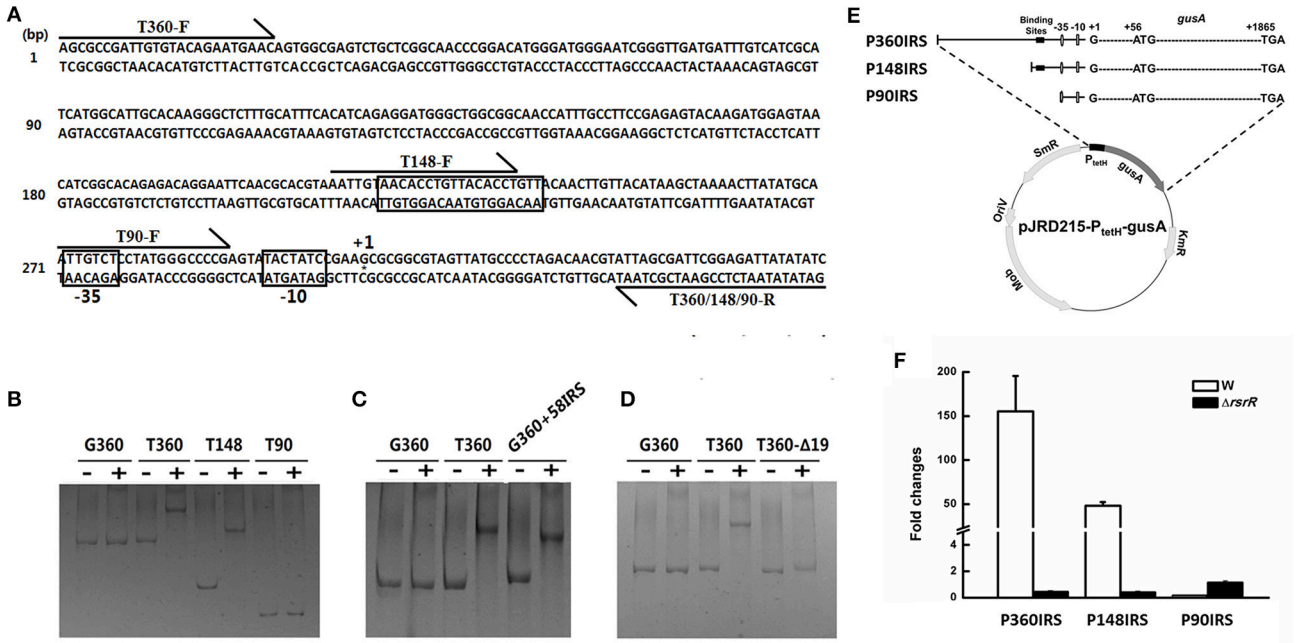

FIGURE 5 | The functional identification of a 19-bp inverted repeat sequence (IRS) upstream the *tetH* promoter. (A) The loci of IRS, −10/−35 regions, the transcriptional start site and primers on the sequence upstream *tetH* gene. **(B–D)** The results of EMSAs to determine the binding ability of RsrR to the regulatory sequence. −, the group containing the nucleotide fragments without RsrR; +, the group containing both the different nucleotide fragments and RsrR. G360, a 360 bp-fragment from the *gapdH* gene used as a control; T360, T148 and T90, a 360 bp-, 148 bp-, or 90 bp-fragment amplified from upstream region of *tetH*; G360+58IRS, a 58 bp sequence containing the IRS fused with the 360 bp-fragment from *gapdH*; T360Δ19: the T360 fragment with IRS removed. **(E)** Diagram of series of IRS-probe vectors containing various versions of the upstream region of *tetH*. **(F)** Transcriptional analysis of *gusA* on the IRS-probe vectors in Δ*rsrR* and the wild type.

Growth Analyses of the Mutants in Different Sulfur-Substrate Media

As shown in **Figure 6**, the growth rates of the *rsrR* or *rsrS* knockout mutants were not similar to the wild type. When grown in S^0-medium, both Δ*rsrR* and Δ*rsrS* had a slight growth advantage over the wild type strain from the 5th to the 11th day, which corresponds to the logarithmic growth phase prior to entering into the stationary phase. In contrast, the wild type strain grew slightly better than the mutants after the 15th day (**Figure 6A**). When $K_2S_4O_6$ was used as the sole sulfur substrate, the three strains showed very slow overall growth (up to 0.06) compared to S^0-medium due to differences in RISCs metabolism for different substrates (Zyl et al., 2008; Chen et al., 2012; Zhang et al., 2014). In $K_2S_4O_6$-medium, Δ*rsrR* and Δ*rsrS* had a 2 and 4 day growth delay in lag phase, respectively when compared to the wild type. However, the three tested strains reached approximately the same growth when they reached stationary phase (**Figure 6B**). In addition, complementation of the mutations with wild type alleles resulted in a growth pattern similar to the wild type in both media (**Figures 6C,D**). Therefore, the recovery of growth of the mutants in $K_2S_4O_6$-medium after a delay of several days suggested that RsrS-RsrR might be the primary, but not the sole signal transduction pathway that regulates the metabolism of tetrathionate.

Influence of *RsrR* and *RsrS* on Sulfur Metabolism and Signaling Systems

In *A. caldus*, the sulfur-oxidizing mechanisms include the periplasmic Sox system, the S_4I pathway, and the RISCs oxidation enzymes such as SOR, SDO, SQR, HDR, RHD, DsrE, and TusA (mentioned in the Introduction Section). To investigate the effect of the absence of RsrS and RsrR on the S_4I pathway, we analyzed the relative RNA transcript levels of genes attributed to play a role in the *A. caldus* RISCs metabolism. Cross-talk often occurs between a sensor kinase and a non-cognate response regulator in the TCSs (Procaccini et al., 2011), so genes encoding single- and two-component systems (SCSs and TCSs) were also analyzed for their relative RNA transcript levels. The transcriptional analysis of these sulfur-oxidizing and regulatory genes during cultivation on S^0 was carried out by RT-qPCR. All data were calculated and the statistically valid data were showed as the mean value of three independent replicates in **Figure 7** (original data with values for standard deviation and *P*-value are listed in **Supplementary Text S1**). As shown, several genes in the mutants had significant changes in expression (FC $\geq$ 2, $P \leq 0.05$, up-regulation; FC $\leq$ 0.5, $P \leq 0.05$, down-regulation) when compared with the wild type. The deletion of *rsrR* resulted in a sharp up-regulation (FC $\geq$ 6, $P \leq 0.05$) of *tetH-dox*DA, *sox* operon I, *sdo*-1, and *sdo*-2, clear down-regulation (FC $\leq$ 0.01, $P \leq 0.05$) of *tusA*, and weak

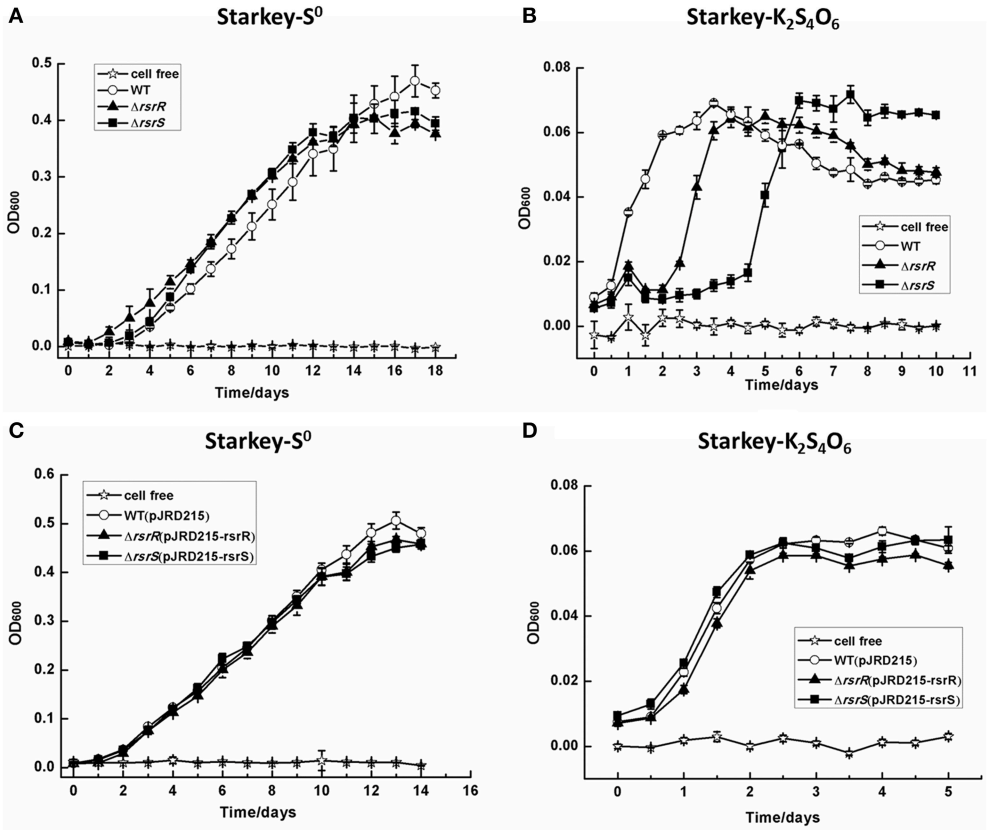

FIGURE 6 | The growth curves of the wild type, Δ*rsrR*, and Δ*rsrS* mutants, and complemented strains of *A. caldus* MTH-04 grown in Starkey medium to which were added different energy sources. All the measurements were performed in triplicate. The values for OD600 are the mean of the three independent replicates. The *SD*-values are shown in the figure with short bars on the top of the columns, and they were calculated by using the Origin software with "descriptive statistics." **(A,C)** Growth in Starkey-S^0 medium; **(B,D)** Growth in Starkey-$K_2S_4O_6$ medium. WT, Δ*rsrR*, and Δ*rsrS*, WT(pJRD215), Δ*rsrR*(pJRD215-rsrR), and Δ*rsrS*(pJRD215-rsrS) represent the wild type, mutants, wild type carrying plasmid pJRD215, and complemented strains of *A. caldus* MTH-04, respectively.

transcriptional changes ($2 \leq FC \leq 6$, $P \leq 0.05$) in *sox* operon II, *sqr*, and *rhd*. The absence of *rsrR* also resulted in significant up-regulation ($FC \geq 2$, $P \leq 0.05$) of a majority of regulator genes in TCSs including *ompR* (A5904_2590), *phoB* (A5904_0374), *cheY* (A5904_1450), *tspR* (A5904_2485), A5904_0219, A5904_0936, A5904_1207, A5904_1342 and A5904_1480, and in SCSs including A5904_0420, A5904_0789 and A5904_1113. The sensor histidine kinase (HK) genes *rsrS* and *envZ* in TCSs are up-regulated significantly in the *rsrR* knockout strain. However, the HK genes *phoR* (A5904_0373), *cheA* (A5904_1448), *tspS* (A5904_2484), *kdpD* (A5904_1340), *fleS* (A5904_1479), A5904_0218 and A5904_0934 had no obvious transcriptional changes in this mutant. In the Δ*rsrS* strain, the genes of the Sox operon (except *soxYZ* in operon II), *tetH*, and *doxDA* showed significant changes in expression when compared to the wild type. The expression of *soxYZ* in operon II was reduced to almost undetectable levels. Almost all the other genes involved in the sulfur oxidation system, TCSs, and SCSs did not show significant changes. However, *tspS* showed a significant change ($2 \leq FC \leq 7$, $P \leq 0.05$) in the Δ*rsrS* strain.

DISCUSSION

The lack of a reliable gene knockout method for *A. caldus* has been a significant obstacle in the progress of uncovering the sulfur oxidation mechanism and other important physiological functions in this organism (Valdés et al., 2009; You et al., 2011; Chen et al., 2012). In this study, we developed a markerless gene knockout technique using a suicide plasmid and an I-*Sce* I-expressing plasmid. There are two advantages of our markerless gene knockout technique. The first is that we used an endogenous Rec (RecA and RecBCD) system of *A. caldus*, rather than an exogenous λ-Red or RecET system, for homologous recombination to avoid the incompatibility of an exogenous recombination system. The second advantage is that we used conjugation as our gene transfer method, which is the optimal way to incorporate plasmids into cells because conjugation facilitates homologous recombination between the suicide plasmid and the host chromosome (Dillingham and Kowalczykowski, 2008). Furthermore, this knockout technique can be further optimized to integrate genes or other sequences into *A. caldus*.

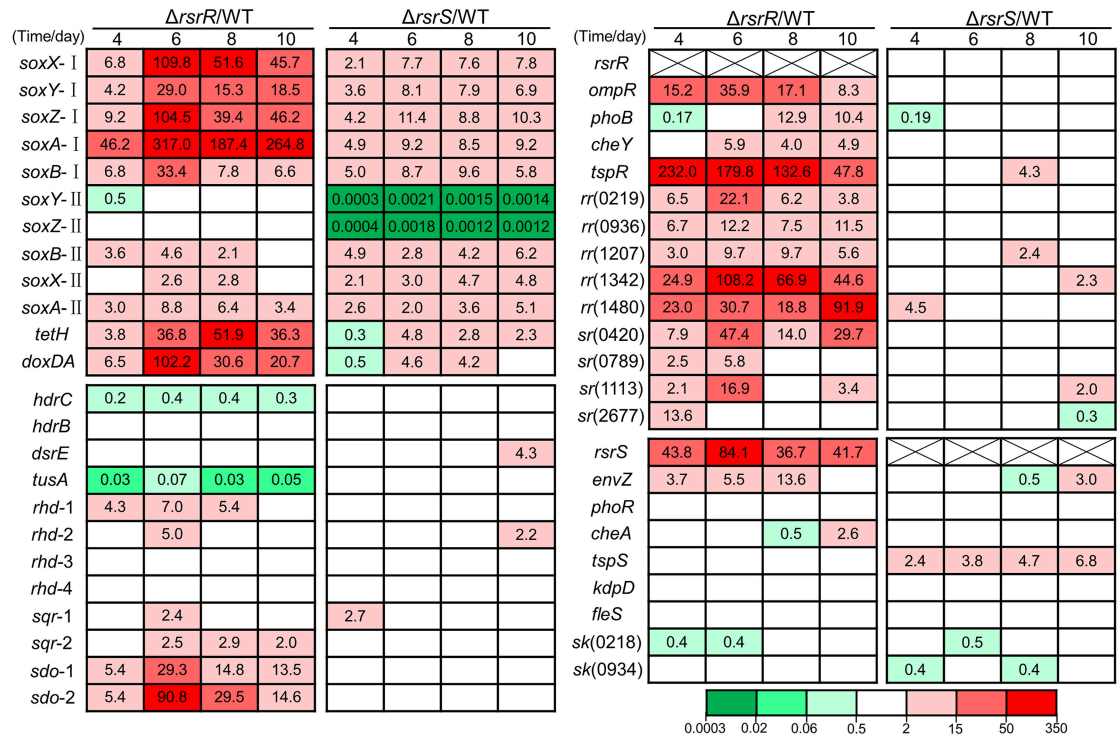

FIGURE 7 | The relative transcription levels of genes involved in sulfur metabolism and signaling systems during the S^0-cultivating process. This is the valid mean value of three independent replicates showing fold changes (FC) determined by RT-qPCR analyses of the mutant against the wild-type. FC $\geq$ 2, $P \leq 0.05$ and FC $\leq$ 0.5, $P \leq 0.05$ were regarded as the significant changes. FC $\geq$ 2, $P \leq 0.05$, up-regulation; FC $\leq$ 0.5, $P \leq 0.05$, down-regulation; 0.5 $\leq$ FC $\leq$ 2, $P \geq 0.05$, no change (data are not shown in the figure). FC-values are represented with different colors as indicated in the color bar. The data of standard deviation (*SD*) and *P*-value were shown in **Supplementary Text S1**. The *SD*-value was calculated by using the Origin software with "descriptive statistics." The *P*-value was calculated by using the GraphPad Prism software with "unpaired *t*-test." The original data with the values for standard deviation and *P*-value are listed in **Supplementary Text S1**. The putative function of proteins encoded by these genes: *soxX*-I (A5904_2486), *soxX*-II (A5904_2525), cytochrome c class I; *soxY*-I (A5904_2487), *soxY*-II (A5904_2520), sulfur covalently binding protein; *soxZ*-I (A5904_2488), *soxZ*-II (A5904_2521), sulfur compound chelating protein; *soxA*-I (A5904_2489), *soxA*-II (A5904_2526), cytochrome c (diheme); *soxB*-I (A5904_2491), *soxB*-II (A5904_2522), sulfate thiol esterase; *hdrC* (A5904_1042), *hdrB* (A5904_1043), heterodisulfide reductase subunit C and B; *dsrE* (A5904_2473), *tusA* (A5904_2474), sulfur transferase; *rhd-1* (A5904_0894), *rhd-2* (A5904_1407), *rhd-3* (A5904_2860), *rhd-4* (A5904_2475), rhodanese (sulfur transferase); *sqr-1* (A5904_1436), *sqr-2* (A5904_2678), sulfide quinone reductase; *sdo-1* (A5904_0421), *sdo-2* (A5904_0790), sulfur dioxygenase; *envZ* (A5904_2589), *ompR* (A5904_2590), osmolarity regulation; *phoB* (A5904_0374), *phoR* (A5904_0373), phosphate regulon; *cheY* (A5904_1450), *cheA* (A5904_1448), chemotaxis; *tspR* (A5904_2485), *tspS* (A5904_2484), regulation for Sox pathway; *kdpD* (A5904_1340), unknown; *fleS* (A5904_1479), flagellum associated; *rr* (A5904_0219, A5904_0936, A5904_1207, A5904_1342, A5904_1480), putative response regulators in TCSs; *hk* (A5904_0218, A5904_0934), putative sensor histidine kinases in TCSs; *sr* (A5904_0420, A5904_0789, A5904_1113, A5904_2677), putative regulators in SCSs.

A. caldus has a complex sulfur oxidation system that includes periplasmic sulfur-oxidizing pathways (Sox and S_4I) and cytoplasmic sulfur-oxidizing enzymes (SDO, SOR, HDR etc.) (Chen et al., 2012). The *sor* gene in the wild type and both mutants of *A. caldus* MTH-04 was lost during the long period of subcultivation in S^0-medium under the laboratory conditions (as confirmed by sequence analysis of PCR products). The loss of *sor* is probably caused by transposition of the transposon as has been reported for the strain *A. caldus* SM-1 (You et al., 2011). The sulfur oxidation pathways in the two cellular compartments are probably connected by tetrathionate, which can enter the cytoplasm and react with DsrE or TusA to generate protein Cys-S-thiosulfonates, thus initiating sulfur metabolism in the cytoplasm (Liu et al., 2014). Comparative analysis of the S_4I pathway genes *tetH* and *doxDA* in *Acidithiobacillus* spp. and the archaea *Acidianus hospitalis* and *Acidianus ambivalens,* indicated that only *A. caldus* evolved an *rsrRS-tetH-doxDA*-like cluster (**Figure 1**). The combination of two functional genes (*tetH* and *doxDA*) and the TCS regulatory genes (*rsrR* and *rsrS*) in this cluster potentially allows *A. caldus* to regulate its S_4I pathway via the RsrS-RsrR system. Thus, *A. caldus* can efficiently maintain the balance between thiosulfate and tetrathionate in the periplasm and modulate the periplasmic and cytoplasmic sulfur-oxidizing pathways.

The positive regulatory role of RsrS-RsrR on the S_4I pathway was inferred from the transcriptional analysis of the *tetH* cluster in the *rsrR* and *rsrS* knockout mutants and the wild type upon stimulation with $K_2S_4O_6$. The relative transcriptional levels of genes in the *tetH* cluster in the *rsrR* or *rsrS* knockouts were much lower as compared to that in the wild type when stimulated with $K_2S_4O_6$ (**Figure 4A**), indicating a positive effect of RsrS-RsrR on the transcriptional regulation of *tetH* and *doxDA*.

Thus, RsrS-RsrR linked the signal from tetrathionate to the transcription of *tetH* and *doxDA*, which allowed adjustment of the S_4I pathway in *A. caldus* to utilize tetrathionate in the growth environment.

The determination of the positive regulation of RsrS-RsrR for S_4I pathway, combined with simultaneous transcription of *tetH-doxDA* and the P1 promoter upstream of *tetH* (Rzhepishevska et al., 2007), indicated the existence of a *cis*-regulatory element in *A. caldus*. The data from the EMSA assays *in vitro* and the promoter-probe vector analysis *in vivo* revealed direct interaction between RsrR and the IRS upstream of the *tetH* promoter, along with the effects of the IRS on the transcriptional activity of the promoter. The 19 bp-IRS (AACACCTGTTACACCTGTT) is composed of two 9 bp complementary inverted half-sites (AACACCTGT and ACACCTGTT) with a 1-bp interval (T). The RsrS-RsrR in *A. caldus* is an EnvZ-OmpR like TCS (Rzhepishevska et al., 2007), in which the response regulators (RsrR and OmpR) share 42% identity and the sensor histidine kinases (RsrS and EnvZ) share 30% identity at the amino acid level. The high level of identity in the structures and protein sequences between RsrS-RsrR and EnvZ-OmpR indicate that RsrR is a typical regulator with a winged helix-turn-helix (HTH) DNA-binding domain, allowing the RsrR dimer to interact with the 19 bp IRS through the binding of two HTH domains to the two 9 bp half-sites of the IRS. RsrS has a predicted unique sensor domain, suggesting that it has the ability to detect the signal from tetrathionate. These results are consistent with the previously reported mechanism of TCS in translating environmental stimuli to specific adaptive responses (Martínez-Hackert and Stock, 1997; Mattison and Kenney, 2002; Wang, 2012). Therefore, we propose a tetrathionate-dependent transcriptional regulation model of the S_4I pathway by RsrS-RsrR in *A. caldus*. As shown in **Figure 8**, the membrane-bound sensor of histidine kinase RsrS might sense the signal from tetrathionate in the periplasm, which may then autophosphorylate the conserved His site, and transfer the phosphoryl group to the conserved Asp site of RsrR, thus generating an active dimer. The RsrR dimer might recognize and bind to the 19 bp IRS with its HTH domains to promote the transcriptional activity of the *tetH* promoter by assisting the recruitment of the RNA polymerase or by strengthening the binding between the RNA polymerase and the DNA sequence (Hochschild and Dove, 1998; Kenney, 2002).

Blocking of the signaling pathway from tetrathionate to S_4I pathway caused changes in growth and transcription patterns. The absence of RsrS or RsrR led to several days delay of growth in $K_2S_4O_6$-medium. The survival of mutants in $K_2S_4O_6$-medium indicated that the RsrS-RsrR mediated signal pathway is redundant with other pathways in promoting the transcription of *tetH-doxDA* and decomposition of tetrathionate. Transcriptional analysis revealed that the knockout of *rsrR* had a much stronger impact on the transcription of these genes than that of *rsrS*, both in terms of the number of genes being affected and in the magnitude of changes in transcription levels. The relative change in the RNA transcript levels in the mutants during growth in S^0-medium revealed that the knockout of either *rsrS* or *rsrR* not only caused significant up- or down-regulation of the majority of sulfur-oxidizing genes, but also resulted in significant changes in transcription of most regulatory genes. The RsrS-RsrR and EnvZ-OmpR like two-component systems share significant homology owing to their evolutionary relationship (Rzhepishevska et al., 2007). The high level of sequence similarity and close homologous relation between some TCSs raises the possibility of undesired cross-talk between a sensor kinase and a non-cognate response regulator (Howell et al., 2003; Siryaporn and Goulian, 2008; Procaccini et al., 2011; Guckes et al., 2013; Bielecki et al., 2015; Nguyen et al., 2015). The transcriptional changes of these genes of TCSs in Δ*rsrS* and Δ*rsrR* implied that cross-talk potentially occurs between RsrS-RsrR and other TCSs. Therefore, we propose that the absence of RsrS or RsrR in *A. caldus* might result in the remodulation of the signal transduction pathways and changes in the transcriptional regulatory mechanisms, and certain sulfur-oxidizing pathways may be adjusted to complete the sulfur metabolism. This may be a reasonable explanation for the differences in growth between

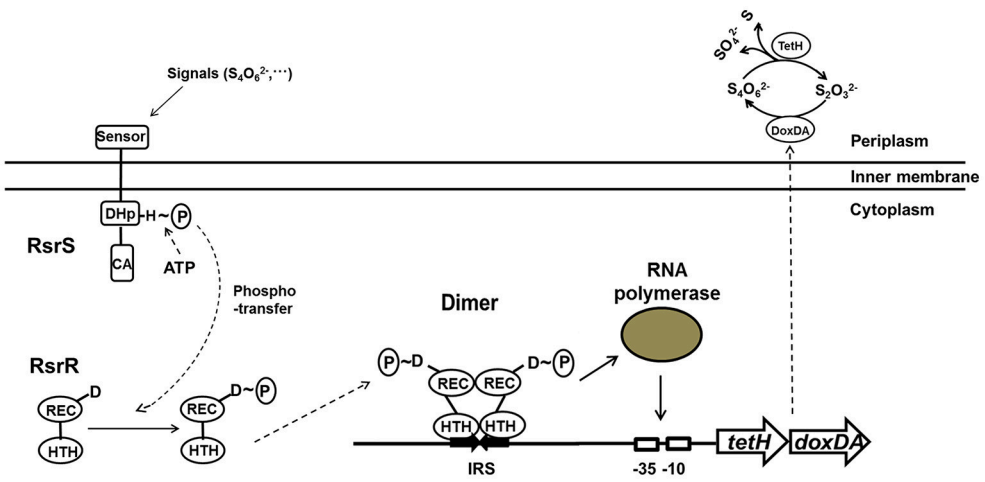

FIGURE 8 | The signal transduction and transcriptional regulation model of RsrS-RsrR on the S_4I pathway in *A. caldus*.

the mutants and the wild type in S^0-medium and the ability of Δ*rsrS* and Δ*rsrR* mutants to grow in $K_2S_4O_6$-medium. In addition, sequences homologous to the 19-bp IRS were not found at any other loci across the whole genomes of three *A. caldus* strains MTH-04, SM-1 and ATCC51756 by using bioinformatics tools (BBS, MP3 and Fimo; Grant et al., 2011; Ma et al., 2013), implying that RsrS-RsrR was specific for regulation of the S_4I pathway. The discovery of this sequence indicates an important role of the signaling and regulatory systems in efficient metabolism of various RISCs in *A. caldus*. Further, exploration of the two-component and other regulatory systems would provide novel insights to better understand the sulfur metabolism and regulation network in *A. caldus*.

CONCLUSION

In this study, we developed a reliable markerless gene knockout method for *A. caldus* and constructed RsrS-RsrR two-component system mutants. We illustrated the regulatory role of RsrS-RsrR on the S_4I pathway and proposed a tetrathionate-dependent transcriptional regulation model for the two-component system in the S_4I pathway. Our markerless gene knockout system has many potential applications both in investigations of molecular mechanisms as well as genetic engineering. The elucidation of the mechanism of regulation of the S_4I pathway by the RsrS-RsrR system helps improve our understanding of molecular mechanisms in the regulation of sulfur metabolism network in *A. caldus*.

AUTHOR CONTRIBUTIONS

ZW, JQiL, and LC designed, conducted and composed the paper. ZW, YL, CZ, and YW conducted the experiments. BL and RW performed bioinformatics analysis. JQuL, XP, XL, BL, and RW analyzed the data and revised the paper.

FUNDING

This work was supported by grants from the Natural Science Foundation (Grant No. 31370138, 31570036), the National Basic Research Program (2010CB630902), the Natural Science Foundation (Grant No. 31400093, 31370084, 30800011), the China Postdoctoral Science Foundation (Grant No. 2015M580585) and the State Key Laboratory of Microbial Technology Foundation (M2015-03), People's Republic of China.

ACKNOWLEDGMENTS

We are grateful to Prof. Qingsheng Qi and Prof. Lushan Wang from Shandong University for providing plasmid pACBSR and assisting protein homology modeling.

SUPPLEMENTARY MATERIAL

The Supplementary Material for this article can be found online at: http://journal.frontiersin.org/article/10.3389/fmicb.2016.01755/full#supplementary-material

Figure S1 | Multiple alignment of the combined DoxD and DoxA amino acid sequences with homologs. Conserved residues are shown with black shadow. Accession numbers (GenBank): *Acidithiobacillus caldus* SM-1, DoxD (fused DoxDA), AEK58244; *Acidithiobacillus caldus* MTH-04, fused DoxDA, OAN03452; *Acidithiobacillus caldus* ATCC 51756, DoxD (fused DoxDA), ABP38224; *Acidithiobacillus thiooxidans*, fused DoxDA, WP_024894934; *Acidithiobacillus ferrooxidans*, fused DoxDA, CDQ09967; *Sulfolobus tokodaii*, DoxD and DoxA, NP_377837 and NP_377838; *Sulfolobus solfataricus*, DoxD and DoxA, NP_343149 and NP_343148; *Acidianus ambivalens*, DoxD and DoxA, CAA70827 and CAA70828; *Acidianus ambivalens*, DoxD2 and DoxA2, CAC86936 and CAC86935; *Bacteroides thetaiotaomicron*, fused DoxDA, NP_809428.

Figure S2 | Amino acid sequence and protein structure analysis of RsrR and RsrS. Every domain is shown in the figure. **(A)** Amino acid sequence alignment between RsrR and OmpR; **(B)** Amino acid sequence alignment between RsrS and EnvZ; **(C)** Protein structure fitting of RsrR and OmpR (blue for RsrR, red for OmpR); **(D)** Protein structure fitting of RsrS and EnvZ (gray for RsrS, red for EnvZ).

Table S1 | Primers used for constructing Δ*rsrR* and Δ*rsrS*.

Table S2 | Primers used for RT-qPCR.

Table S3 | Primers used for EMSA assays.

Table S4 | Primers used for constructing IRS-probe vectors.

Supplementary Text S1 | The original data for the relative transcription levels of genes involved in sulfur metabolism and signaling systems during the S0-cultivating process.

REFERENCES

Bidart, G. N., Rodríguez-Díaz, J., Monedero, V., and Yebra, M. J. (2014). A unique gene cluster for the utilization of the mucosal and human milk-associated glycans galacto-*N*-biose and lacto-*N*-biose in *Lactobacillus casei*. *Mol. Microbiol.* 93, 521–538. doi: 10.1111/mmi.12678

Bielecki, P., Jensen, V., Schulze, W., Gödeke, J., Strehmel, J., Eckweiler, D., et al. (2015). Cross talk between the response regulators PhoB and TctD allows for the integration of diverse environmental signals in *Pseudomonas aeruginosa*. *Nucleic Acids Res.* 43, 6413–6425. doi: 10.1093/nar/gkv599

Bilwes, A. M., Alex, L. A., Crane, B. R., and Simon, M. I. (1999). Structure of CheA, a signal-transducing histidine kinase. *Cell* 96, 131–141.

Bourret, R. B., and Silversmith, R. E. (2010). Two-component signal transduction. *Curr. Opin. Microbiol.* 13, 113–115. doi: 10.1016/j.mib.2010.02.003

Bugaytsova, Z., and Lindström, E. B. (2004). Localization, purification and properties of a tetrathionate hydrolase from *Acidithiobacillus caldus*. *Eur. J. Biochem.* 271, 272–280. doi: 10.1046/j.1432-1033.2003.03926.x

Capra, E. J., and Laub, M. T. (2012). The evolution of two-component signal transduction systems. *Annu. Rev. Microbiol.* 66, 325–347. doi: 10.1146/annurev-micro-092611-150039

Chen, L., Lin, J., Li, B., Lin, J., and Liu, X. (2010). Method development for electrotransformation of *Acidithiobacillus caldus*. *J. Microbiol. Biotechnol.* 20, 39–44. doi: 10.4014/jmb.0905.05023

Chen, L., Ren, Y., Lin, J., Liu, X., Pang, X., and Lin, J. (2012). *Acidithiobacillus caldus* sulfur oxidation model based on transcriptome analysis between the wild type and sulfur oxygenase reductase defective mutant. *PLoS ONE* 7:e39470. doi: 10.1371/journal.pone.0039470

Dahl, C., and Prange, A. (2006). "Bacterial sulfur globules: occurrence, structure and metabolism" in *Inclusions in Prokaryotes*, ed J. M. Shively (Heidelberg: Springer), 21–51.

Dam, B., Mandal, S., Ghosh, W., Das Gupta, S. K., and Roy, P. (2007). The S4-intermediate pathway for the oxidation of thiosulfate by the chemolithoautotroph *Tetrathiobacter kashmirensis* and inhibition of tetrathionate oxidation by sulfite. *Res. Microbiol.* 158, 330–338. doi: 10.1016/j.resmic.2006.12.013

Datta, N., Hedges, R. W., Shaw, E. J., Sykes, R. B., and Richmond, M. H. (1971). Properties of an R factor from *Pseudomonas aeruginosa*. *J. Bacteriol.* 108, 1244–1249.

Davison, J., Heusterspreute, M., Chevalier, N., Ha-Thi, V., and Brunei, F. (1987). Vectors with restriction site banks V. pJRD215, a wide-host-range cosmid vector with multiple cloning sites. *Gene* 51, 275–280. doi: 10.1016/0378-1119(87)90316-7

Dillingham, M. S., and Kowalczykowski, S. C. (2008). RecBCD enzyme and the repair of double-stranded DNA breaks. *Microbiol. Mol. Biol. Rev.* 72, 642–671. doi: 10.1128/MMBR.00020-08

Dopson, M., and Lindström, E. B. (1999). Potential role of *Thiobacillus caldus* in arsenopyrite bioleaching. *Appl. Environ. Microbiol.* 65, 36–40.

Forst, S., Delgado, J., and Inouye, M. (1989). Phosphorylation of OmpR by the osmosensor EnvZ modulates expression of the *ompF* and *ompC* genes in *Escherichia coli*. *Proc. Natl. Acad. Sci. U.S.A.* 86, 6052–6056.

Friedrich, C. G. (1997). Physiology and genetics of sulfur-oxidizing bacteria. *Adv. Microb. Physiol.* 39, 235–289. doi: 10.1016/S0065-2911(08)60018-1

Friedrich, C. G., Bardischewsky, F., Rother, D., Quentmeier, A., and Fischer, J. (2005). Prokaryotic sulfur oxidation. *Curr. Opin. Microbiol.* 8, 253–259. doi: 10.1016/j.mib.2005.04.005

Friedrich, C. G., Quentmeier, A., Bardischewsky, F., Rother, D., Kraft, R., Kostka, S., et al. (2000). Novel genes coding for lithotrophic sulfur oxidation of *Paracoccus pantotrophus* GB17. *J. Bacteriol.* 182, 4677–4687. doi: 10.1128/JB.182.17.4677-4687.2000

Frigaard, N. U., and Dahl, C. (2008). Sulfur metabolism in phototrophic sulfur bacteria. *Adv. Microb. Physiol.* 54, 103–200. doi: 10.1016/S0065-2911(08)00002-7

Gardner, M. N., and Rawlings, D. E. (2000). Production of rhodanese by bacteria present in bio-oxidation plants used to recover gold from arsenopyrite concentrates. *J. Appl. Microbiol.* 89, 185–190. doi: 10.1046/j.1365-2672.2000.01117.x

Ghosh, W., and Dam, B. (2009). Biochemistry and molecular biology of lithotrophic sulfur oxidation by taxonomically and ecologically diverse bacteria and archaea. *FEMS Microbiol. Rev.* 33, 999–1043. doi: 10.1111/j.1574-6976.2009.00187.x

Goebel, B. M., and Stackebrandt, E. (1994). Cultural and phylogenetic analysis of mixed microbial populations found in natural and commercial bioleaching environments. *Appl. Environ. Microbiol.* 60, 1614–1621.

Grant, C. E., Bailey, T. L., and Noble, W. S. (2011). FIMO: scanning for occurrences of a given motif. *Bioinformatics* 27, 1017–1018. doi: 10.1093/bioinformatics/btr064

Guckes, K. R., Kostakioti, M., Breland, E. J., Gu, A. P., Shaffer, C. L., and Charles, R., et al. (2013). Strong cross-system interactions drive the activation of the QseB response regulator in the absence of its cognate sensor. *Proc. Natl. Acad. Sci. U.S.A.* 110, 16592–16597. doi: 10.1073/pnas.1315320110

Hallberg, K. B., Dopson, M., and Lindström, E. B. (1996). Reduced sulfur compound oxidation by *Thiobacillus caldus*. *J. Bacteriol.* 178, 6–11.

Hallberg, K. B., and Lindström, E. B. (1994). Characterization of *Thiobacillus caldus* sp. nov., a moderately thermophilic acidophile. *Microbiology* 140, 3451–3456.

Hallberg, K. B., and Lindström, E. B. (1996). Multiple serotypes of the moderate thermophile *Thiobacillus caldus*, a limitation of immunological assays for biomining microorganisms. *Appl. Environ. Microbiol.* 62, 4243–4246.

Herring, C. D., Glasner, J. D., and Blattner, F. R. (2003). Gene replacement without selection: regulated suppression of amber mutations in *Escherichia coli*. *Gene* 311, 153–163. doi: 10.1016/S0378-1119(03)00585-7

Hochschild, A., and Dove, S. L. (1998). Protein-protein contacts that activate and repress prokaryotic transcription. *Cell* 92, 597–600. doi: 10.1016/S0092-8674(00)81126-5

Howell, A., Dubrac, S., Andersen, K. K., Noone, D., Fert, J., Msadek, T., et al. (2003). Genes controlled by the essential YycG/YycF two-component system of *Bacillus subtilis* revealed through a novel hybrid regulator approach. *Mol. Microbiol.* 49, 1639–1655. doi: 10.1046/j.1365-2958.2003.03661.x

Huang, K.-J., Lan, C.-Y., and Igo, M. M. (1997). Phosphorylation stimulates the cooperative DNA-binding properties of the transcription factor OmpR. *Proc. Natl. Acad. Sci. U.S.A.* 94, 2828–2832.

Jin, S., Yan, W., and Wang, Z. (1992). Transfer of IncP plasmids to extremely acidophilic *Thiobacillus thiooxidans*. *Appl. Environ. Microbiol.* 58, 429–430.

Kenney, L. J. (2002). Structure/function relationships in OmpR and other winged-helix transcription factors. *Curr. Opin. Microbiol.* 5, 135–141. doi: 10.1016/S1369-5274(02)00310-7

Kletzin, A. (1989). Coupled enzymatic production of sulfite, thiosulfate, and hydrogen sulfide from sulfur: purification and properties of a sulfur oxygenase reductase from the facultatively anaerobic archaebacterium *Desulfurolobus ambivalens*. *J. Bacteriol.* 171, 1638–1643.

Kletzin, A. (1992). Molecular characterization of the *sor* gene, which encodes the sulfur oxygenase/reductase of the thermoacidophilic Archaeum *Desulfurolobus ambivalens*. *J. Bacteriol.* 174, 5854–5859.

Kletzin, A., Urich, T., Müller, F., Bandeiras, T. M., and Gomes, C. M. (2004). Dissimilatory oxidation and reduction of elemental sulfur in thermophilic archaea. *J. Bioenerg. Biomembr.* 36, 77–91. doi: 10.1023/B:JOBB.0000019600.36757.8c

Lehman, M. K., Bose, J. L., Sharma-Kuinkel, B. K., Moormeier, D. E., Endres, J. L., Sadykov, M. R., et al. (2015). Identification of the amino acids essential for LytSR-mediated signal transduction in *Staphylococcus aureus* and their roles in biofilm-specific gene expression. *Mol. Microbiol.* 95, 723–737. doi: 10.1111/mmi.12902

Liu, L., Stockdreher, Y., Koch, T., Sun, S., Fan, Z., Josten, M., et al. (2014). Thiosulfate transfer mediated by DsrE/TusA homologs from acidothermophilic sulfur-oxidizing archaeon *Metallosphaera cuprina*. *J. Biol. Chem.* 289, 26949–26959. doi: 10.1074/jbc.M114.591669

Liu, X., Lin, J., Zhang, Z., Bian, J., Zhao, Q., and Liu, Y. (2007). Construction of conjugative gene transfer system between *E. coli* and moderately thermophilic, extremely acidophilic *Acidithiobacillus caldus* MTH-04. *J. Microbiol. Biotechnol.* 17, 162–167.

Livak, K. J., and Schmittgen, T. D. (2001). Analysis of relative gene expression data using real-time quantitative PCR and the $2^{-\Delta\Delta CT}$ method. *Methods* 25, 402–408. doi: 10.1006/meth.2001.1262

Ma, Q., Liu, B., Zhou, C., Yin, Y., Li, G., and Xu, Y. (2013). An integrated toolkit for accurate prediction and analysis of *cis*-regulatory motifs at a genome scale. *Bioinformatics* 29, 2261–2268. doi: 10.1093/bioinformatics/btt397

Mangold, S., Valdés, J., Holmes, D. S., and Dopson, M. (2011). Sulfur metabolism in the extreme acidophile *Acidithiobacillus caldus*. *Front. Microbio.* 2:17. doi: 10.3389/fmicb.2011.00017

Martínez-Hackert, E., and Stock, A. M. (1997). The DNA-binding domain of OmpR: crystal structures of a winged helix transcription factor. *Structure* 5, 109–124. doi: 10.1016/S0969-2126(97)00170-6

Mattison, K., and Kenney, L. J. (2002). Phosphorylation alters the interaction of the response regulator OmpR with its sensor kinase EnvZ. *J. Biol. Chem.* 277, 11143–11148. doi: 10.1074/jbc.M111128200

Müller, F. H., Bandeiras, T. M., Urich, T., Teixeira, M., Gomes, C. M., and Kletzin, A. (2004). Coupling of the pathway of sulphur oxidation to dioxygen reduction: characterization of a novel membrane-bound thiosulphate:quinone oxidoreductase. *Mol. Microbiol.* 53, 1147–1160. doi: 10.1111/j.1365-2958.2004.04193.x

Nguyen, M. P., Yoon, J. M., Cho, M. H., and Lee, S. W. (2015). Prokaryotic 2-component systems and the OmpR/PhoB superfamily. *Can. J. Microbiol.* 61, 799–810. doi: 10.1139/cjm-2015-0345

Pardo, E., and Orejas, M. (2014). The *Aspergillus nidulans* $Zn(II)_2Cys_6$ transcription factor AN5673/RhaR mediates L-rhamnose utilization and the production of α-L-rhamnosidases. *Microb. Cell Fact.* 13:161. doi: 10.1186/s12934-014-0161-9

Procaccini, A., Lunt, B., Szurmant, H., Hwa, T., and Weigt, M. (2011). Dissecting the specificity of protein-protein interaction in bacterial two-component signaling: Orphans and crosstalks. *PLoS ONE* 6:e19729. doi: 10.1371/journal.pone.0019729

Quatrini, R., Appia-Ayme, C., Denis, Y., Jedlicki, E., Holmes, D., and Bonnefoy, V. (2009). Extending the models for iron and sulfur oxidation in the

extreme acidophile *Acidithiobacillus ferrooxidans*. *BMC Genomics* 10:394. doi: 10.1186/1471-2164-10-394

Rawlings, D. E. (1998). Industrial practice and the biology of leaching of metals from ores. *J. Ind. Microbiol. Biotechnol.* 20, 268–274.

Rohwerder, T., and Sand, W. (2003). The sulfane sulfur of persulfides is the actual substrate of the sulfur-oxidizing enzymes from *Acidithiobacillus* and *Acidiphilium* spp. *Microbiology* 149, 1699–1709. doi: 10.1099/mic.0.26212-0

Rohwerder, T., and Sand, W. (2007). Oxidation of inorganic sulfur compounds in acidophilic prokaryotes. *Eng. Life Sci.* 7, 301–309. doi: 10.1002/elsc.200720204

Rzhepishevska, O. I., Valdés, J., Marcinkeviciene, L., Gallardo, C. A., Meskys, R., Bonnefoy, V., et al. (2007). Regulation of a novel *Acidithiobacillus caldus* gene cluster involved in metabolism of reduced inorganic sulfur compounds. *Appl. Environ. Microbiol.* 73, 7367–7372. doi: 10.1128/AEM.01497-07

Schlesinger, P., and Westley, J. (1974). An expanded mechanism for rhodanese catalysis. *J. Biol. Chem.* 249, 780–788.

Simon, R., Priefer, U., and Pühler, A. (1983). A broad host range mobilization system for *in vitro* genetic engineering: transposon mutagenesis in gram-negative bacteria. *Biotechology* 1, 784–790.

Siryaporn, A., and Goulian, M. (2008). Cross-talk suppression between the CpxA-CpxR and EnvZ-OmpR two-component systems in *E. coli*. *Mol. Microbiol.* 70, 494–506. doi: 10.1111/j.1365-2958.2008.06426.x

Stock, A. M., Robinson, V. L., and Goudreau, P. N. (2000). Two-component signal transduction. *Annu. Rev. Biochem.* 69, 183–215. doi: 10.1146/annurev.biochem.69.1.183

Suzuki, I. (1999). Oxidation of inorganic sulfur compounds: chemical and enzymatic reactions. *Can. J. Microbiol.* 45, 97–105.

Valdés, J., Pedroso, I., Quatrini, R., and Holmes, D. S. (2008). Comparative genome analysis of *Acidithiobacillus ferrooxidans*, *A. thiooxidans and A. caldus:* insights into their metabolism and ecophysiology. *Hydrometallurgy* 94, 180–184. doi: 10.1016/j.hydromet.2008.05.039

Valdés, J., Quatrini, R., Hallberg, K., Dopson, M., Valenzuela, P., and Holmes, D. S. (2009). Genome announcement: draft genome sequence of the extremely acidophilic bacterium *Acidithiobacillus caldus* ATCC 51756 reveals metabolic versatility in the genus *Acidithiobacillus*. *J. Bacteriol.* 191, 5877–5878. doi: 10.1128/JB.00843-09

Valenzuela, L., Chi, A., Beard, S., Shabanowitz, J., Hunt, D. F., and Jerez, C. A. (2008). "Differential-expression proteomics for the study of sulfur metabolism in the chemolithoautotrophic *Acidithiobacillus ferrooxidans*," in *Microbial Sulfur Metabolism*, eds C. Dahl and C. G. Friedrich (Berlin: Springer), 77–86.

Zyl, L. J. V., Munster, J. M. V., and Rawlings, D. E. (2008). Construction of *arsB* and *tetH* mutants of the sulfur-oxidizing bacterium *Acidithiobacillus caldus* by marker exchange. *Appl. Environ. Microbiol.* 74, 5686–5694. doi: 10.1128/AEM.01235-08

Wakai, S., Kikumoto, M., Kanao, T., and Kamimura, K. (2004). Involvement of sulfide:quinone oxidoreductase in sulfur oxidation of an acidophilic iron-oxidizing bacterium *Acidithiobacillus ferrooxidans* NASF-1. *Biosci. Biotechnol. Biochem.* 68, 2519–2528. doi: 10.1271/bbb.68.2519

Wang, S. (2012). "Bacterial two-component systems: structures and signaling mechanisms," in *Protein Phosphorylation in Human Health*, ed C. Huang (Rijeka: InTech Press), 439–466.

Williams, K. P., and Kelly, D. P. (2013). Proposal for a new class within the phylum *Proteobacteria*, *Acidithiobacillia* classis nov., with the type order *Acidithiobacillales*, and emended description of the class *Gammaproteobacteria*. *Int. J. Syst. Evol Microbiol* 63, 2901–2906. doi: 10.1099/ijs.0.049270-0

Yon, J., and Fried, M. (1989). Precise gene fusion by PCR. *Nucleic Acids Res.* 17, 4895.

You, X., Guo, X., Zheng, H., Zhang, M., Liu, L., Zhu, Y., et al. (2011). Unraveling the *Acidithiobacillus caldus* complete genome and its central metabolisms for carbon assimilation. *J. Genet. Genomics* 38, 243–252. doi: 10.1016/j.jgg.2011.04.006

Yu, Y., Liu, X., Wang, H., Li, X., and Lin, J. (2014). Construction and characterization of *tetH* overexpression and knockout strains of Acidithiobacillus ferrooxidans. *J. Bacteriol.* 196, 2255–2264. doi: 10.1128/JB.01472-13

Zhang, M., Jiang, C., You, X., and Liu, S. (2014). Construction and application of an expression vector from the new plasmid pLAtc1 of *Acidithiobacillus caldus*. *Appl. Microbiol. Biotechnol.* 98, 4083–4094. doi: 10.1007/s00253-014-5507-z

Conflict of Interest Statement: The authors declare that the research was conducted in the absence of any commercial or financial relationships that could be construed as a potential conflict of interest.

frontiers in Microbiology

ORIGINAL RESEARCH
published: 10 February 2017
doi: 10.3389/fmicb.2017.00211

Indirect Redox Transformations of Iron, Copper, and Chromium Catalyzed by Extremely Acidophilic Bacteria

D. Barrie Johnson[1], Sabrina Hedrich[2] and Eva Pakostova[1]*

[1] School of Biological Sciences, College of Natural Sciences, Bangor University, Bangor, UK, [2] Federal Institute for Geosciences and Natural Resources, Hannover, Germany

Experiments were carried out to examine redox transformations of copper and chromium by acidophilic bacteria (*Acidithiobacillus, Leptospirillum,* and *Acidiphilium*), and also of iron (III) reduction by *Acidithiobacillus* spp. under aerobic conditions. Reduction of iron (III) was found with all five species of *Acidithiobacillus* tested, grown aerobically on elemental sulfur. Cultures maintained at pH 1.0 for protracted periods displayed increasing propensity for aerobic iron (III) reduction, which was observed with cell-free culture liquors as well as those containing bacteria. *At. caldus* grown on hydrogen also reduced iron (III) under aerobic conditions, confirming that the unknown metabolite(s) responsible for iron (III) reduction were not (exclusively) sulfur intermediates. Reduction of copper (II) by aerobic cultures of sulfur-grown *Acidithiobacillus* spp. showed similar trends to iron (III) reduction in being more pronounced as culture pH declined, and occurring in both the presence and absence of cells. Cultures of *Acidithiobacillus* grown anaerobically on hydrogen only reduced copper (II) when iron (III) (which was also reduced) was also included; identical results were found with *Acidiphilium cryptum* grown micro-aerobically on glucose. Harvested biomass of hydrogen-grown *At. ferridurans* oxidized iron (II) but not copper (I), and copper (I) was only oxidized by growing cultures of *Acidithiobacillus* spp. when iron (II) was also included. The data confirmed that oxidation and reduction of copper were both mediated by acidophilic bacteria indirectly, via iron (II) and iron (III). No oxidation of chromium (III) by acidophilic bacteria was observed even when, in the case of *Leptospirillum* spp., the redox potential of oxidized cultures exceeded +900 mV. Cultures of *At. ferridurans* and *A. cryptum* reduced chromium (VI), though only when iron (III) was also present, confirming an indirect mechanism and contradicting an earlier report of direct chromium reduction by *A. cryptum*. Measurements of redox potentials of iron, copper and chromium couples in acidic, sulfate-containing liquors showed that these differed from situations where metals are not complexed by inorganic ligands, and supported the current observations of indirect copper oxido-reduction and chromium reduction mediated by acidophilic bacteria. The implications of these results for both industrial applications of acidophiles and for exobiology are discussed.

Keywords: acidophilic bacteria, chromium, copper, iron, oxido-reduction of metals, redox potentials

OPEN ACCESS

Edited by:
Robert Duran, University of Pau and Pays de l'Adour, France

Reviewed by:
Timothy Ferdelman, Max Planck Institute for Marine Microbiology, Germany
Andreas Teske, University of North Carolina at Chapel Hill, USA

****Correspondence:***
D. Barrie Johnson
d.b.johnson@bangor.ac.uk

Specialty section:
This article was submitted to Extreme Microbiology, a section of the journal Frontiers in Microbiology

Received: *23 September 2016*
Accepted: *30 January 2017*
Published: *10 February 2017*

Citation:
Johnson DB, Hedrich S and Pakostova E (2017) Indirect Redox Transformations of Iron, Copper, and Chromium Catalyzed by Extremely Acidophilic Bacteria. Front. Microbiol. 8:211. doi: 10.3389/fmicb.2017.00211

INTRODUCTION

Acidophilic prokaryotes, defined as those that grow optimally at or below pH 3.0, display a far greater propensity for chemolithotrophy than other groups of bacteria and archaea that have higher pH growth optima (Johnson and Aguilera, 2015; Dopson, 2016). This is due to a number of factors, the most important of which is that their natural habitats are often rich in reduced sulfur and iron, and sulfide minerals, but often contain relatively small concentrations of dissolved organic carbon. In addition, the extreme acidity means that the solubility and bioavailability of cationic metals is much greater than in circum-neutral pH environments.

The most well studied chemolithotrophic life-styles (amongst acidophiles) are those based on the oxidation of reduced iron (Fe^{2+}) by, for example, *Leptospirillum* spp. (Rawlings et al., 1999), and also of elemental sulfur and reduced inorganic sulfur compounds (RISCs) such as tetrathionate ($S_4O_6^{2-}$) by *Acidithiobacillus* spp. and others (Dopson and Johnson, 2012). More recently, hydrogen has also been shown to be an electron donor for many species of acidophilic bacteria (Hedrich and Johnson, 2013a). In contrast, the range of electron acceptors used by extreme acidophiles appears to be more restricted than those used by neutrophilic prokaryotes, though dissimilatory reduction of iron (III) has been reported for many chemolithotrophic and heterotrophic acidophiles (Johnson et al., 2012). Redox transformations of inorganic electron donors and acceptors are frequently coupled in acidophile metabolisms. For example, both *Acidithiobacillus* (*At.*) *ferrooxidans* and *At. ferridurans* can couple the oxidation of elemental sulfur, RISCs and hydrogen to the reduction of molecular oxygen or iron (III).

In both natural and anthropogenic acidic environments, indigenous microorganisms encounter soluble transition metals (and metalloids, such as arsenic) that can exist in variable redox states. While the most abundant of these is almost invariably iron, other metals such as copper can be present in very elevated (>10 g/L) concentrations in pregnant leach solutions (PLS) generated in biomining operations, and in lower concentrations in mine drainage waters. The dissimilatory oxidation of iron (II) by acidophilic bacteria has been recognized since the early 1950s (Colmer et al., 1950). Iron reduction at low pH was first reported by Brock and Gustafson (1976), though the fact that dissimilatory reduction of iron (III) could be used to support the growth of some acidophiles (*At. ferrooxidans* and *Acidiphilium*) was only confirmed much later (Pronk and Johnson, 1992). In contrast to *Acidithiobacillus* spp., *Acidiphilium* spp. require trace amounts of oxygen for growth on iron (III), though non-growing cells can reduce iron in the absence of molecular oxygen. *Acidithiobacillus* spp. that can oxidize both iron (II) and reduced sulfur have a far greater propensity for coupling the oxidation of iron (II) to the reduction of molecular oxygen than for coupling the oxidation of sulfur either to oxygen (Sandoval Ponce et al., 2012) or to iron (III). In a report that appeared to contradict this principle, Sand (1989) noted that sulfur-grown *At. ferrooxidans* cultures that developed extremely low pH values (<1.3) became net productive of iron (II), even under aerobic conditions.

There have also been occasional reports of acidophilic bacteria catalyzing redox transformations of transition metals other than iron. For example, Nielsen and Beck (1972) found that *At. ferrooxidans* could grow on "museum-grade" chalcocite (Cu_2S), and that Cu^{2+} was generated, while Lewis and Miller (1977) claimed that both Sn^{2+} and Cu^{+} could be oxidized by *At. ferrooxidans*, though neither could act as a sole energy source. Sugio et al. (1990) reported that an iron-oxidizing *Acidithiobacillus* sp. coupled the reduction of copper (II) to the oxidation of elemental sulfur, and suggested a direct (enzymatic) mechanism for the reaction with a pH optimum (5.0), which is well above pH optimum for growth of this acidophile. While there are no accounts of any acidophile being able to oxidize chromium (III), the reduction of chromium (VI) by three heterotrophic acidophiles, *Acidiphilium* (*A.*) *cryptum* (strain JF-5; Cummings et al., 2007) and *Acidocella aromatica*^{T} (Masaki et al., 2015), which are both mesophilic bacteria, and by a thermo-acidophilic archaeon (*Sulfolobus*; Masaki et al., 2016), has been described. Other reports of redox transformations of metals mediated by acidophilic prokaryotes include reduction of manganese (Sugio et al., 1988a), oxidation (Sugio et al., 1992) and reduction (Sugio et al., 1988b) of molybdenum, reduction of vanadium (Briand et al., 1996; Okibe et al., 2016) and oxidation of uranium (DiSpirito and Tuovinen, 1982).

Here we report the indirect dissimilatory redox transformations of three transition metals (iron, copper, and chromium) mediated by different genera and species of extremely acidophilic bacteria, *Acidithiobacillus, Leptospirillum,* and *Acidiphilium.*

MATERIALS AND METHODS

Bacteria and Culture Conditions

Representative strains of five species of *Acidithiobacillus*, three of which (*At. ferrooxidans* (ATCC 23270^{T}), *At. ferridurans* (ATCC 33020^{T}) and *At. ferrivorans* (strain Peru6)) oxidize iron (II) as well as reduced sulfur, while two (*At. thiooxidans* DSM 14887^{T} and *At. caldus* DSM 8584^{T}) do not oxidize iron, were used in experimental work. The Peru6 strain was used as this is the only isolate of *At. ferrivorans* that is known (like *At. ferrooxidans, At. ferridurans,* and *At. caldus*) to grow autotrophically on hydrogen. The iron (II)-oxidizing autotrophs *Leptospirillum* (*L.*) *ferrooxidans* (DSM 2705^{T}) and *L. ferriphilum* (strain MT63), and the obligately heterotrophic iron (III)-reducer *A. cryptum* (strain SJH) were also used in some experiments. Physiological characteristics of the bacteria used are listed in **Table 1**.

Bacteria were grown in batch cultures in shake flasks and in pH- and temperature-controlled bioreactors (Electrolab, UK). Hydrogen-grown cultures were grown as described elsewhere (Hedrich and Johnson, 2013a) in sealed jars within which the atmosphere was enriched with both hydrogen and carbon dioxide. For anaerobic growth on hydrogen, oxygen was removed by including an AnaeroGen^{TM} sachet (Fisher, UK) in each sealed jar.

TABLE 1 | Some physiological characteristics of the acidophilic bacteria used in the present study.

Bacterium	Dissimilatory oxidation*			Dissimilatory reduction*	Temperature response#
	Fe(II)	S^0	H_2	Fe(III)	
At. ferrooxidans^T	+	+	+	+	M
At. ferridurans^T	+	+	+	+	M
At. ferrivorans Peru6	+	+	+	+	M
At. thiooxidans^T	−	+	−	−	M
At. caldus^T	−	+	+	−	MT
L. ferrooxidans^T	+	−	−	−	M
L. ferriphilum MT63	+	−	−	−	MT
A. cryptum SJH	−	−	−	+	M

*supporting bacterial growth; #M, mesophilic (T_{opt} 25–35°C); MT, moderately thermophilic (T_{opt} 40–50°C)

Aerobic Reduction of Iron (III) by *Acidithiobacillus* spp.

Bacteria were grown in shake flask cultures (100 mL in 250 mL conical flasks) containing 0.5% (w/v) elemental sulfur "flower" (VWR, UK), 5 mM iron (III) sulfate, basal salts and trace elements (Ňancucheo et al., 2016) and adjusted initially to pH 3.0. Cultures were incubated at 30°C (*At. ferrooxidans*, *At. ferridurans* and *At. thiooxidans*) or 40°C (*At. caldus*), and samples withdrawn at regular intervals to measure pH, redox potentials (as E_H values) and concentrations of iron (II).

Following this, *At. ferridurans* and *At. caldus* were grown aerobically with elemental sulfur as electron donor in bioreactors maintained at 30 and 40°C, respectively, under controlled pH (*via* automated addition of acid or alkali). The bioreactors were aerated (1 L sterile air/min) and stirred at 100 rpm, and the growth medium used was as described for shake flask cultures, except that 50 μM iron (II) sulfate was used in place of 5 mM iron (III). The pH of the bioreactors was maintained at 2.0 (by automated addition of 1 M NaOH) until numbers of planktonic cells had reached $\sim 10^9$/mL, and then lowered, stepwise (using 1 M H_2SO_4), and held at pre-determined values, again by automated addition of 1 M NaOH, ultimately to pH 1.0. Samples were withdrawn at regular intervals and their potential for reducing iron (III) assessed. This involved adding iron (III) sulfate (1 mM, final concentration) to 5 mL of culture (maintained aerobically), and determining concentrations of iron (II) after 5 min, and again after 2 and 5 h. During the period when the bioreactors were held at pH 1.0, iron (III) reduction was also assessed using cell-free culture liquor samples (obtained by centrifuging samples at 10,000 × *g* for 5 min) and values compared with those using samples that contained bacteria.

To determine whether the potential for iron (III) reduction was confined to cultures grown on sulfur, *At. caldus* was grown aerobically with hydrogen as sole electron donor in culture media adjusted (with sulfuric acid) to either pH 1.0 or 2.0. These were incubated for up to 20 days, and samples withdrawn periodically to measure culture optical densities (at 600 nm, as a measure of growth) and to determine the iron (III)-reducing potential of whole culture and cell-free samples, as described above.

Redox Transformations of Copper by Acidophilic Bacteria

Prior to testing cultures for their abilities to catalyze the dissimilatory reduction of copper (II) or oxidation of copper (I) (or both), minimum inhibitory concentrations (MICs) of copper (I) were determined for the various acidophile species used. For this, solutions of copper (II) sulfate (pH 2.0) were reduced by adding different volumes of 1 M hydroxylamine hydrochloride to the culture media. In each case, copper (II) was present in excess in order to ensure that there was no residual hydroxylamine which might otherwise have compromised the results obtained (hydroxylamine decomposes to nitrous oxide and water upon reaction with copper (II)). Cultures were set up with *At. ferrooxidans* and *At. ferridurans* (both pre-grown on hydrogen), *L. ferrooxidans* and *L. ferriphilum* (grown on iron, using iron (III)-free washed cell suspensions), and glucose-grown *A. cryptum*. Iron (II) or glucose was provided as electron donor, and growth was confirmed from cell counts and/or monitoring iron (II) oxidation.

Shake flask cultures, similar to those described for iron reduction except that iron (III) sulfate was replaced by 5 mM copper (II) sulfate and 100 μM iron (II) sulfate added to provide nutritional amounts of iron, were set up to examine whether copper (II) was reduced by *Acidithiobacillus* spp. when oxidizing elemental sulfur and incubated under aerobic conditions. In addition, samples of cultures of *At. caldus* and *At. ferridurans* grown aerobically on sulfur in pH-controlled bioreactors, as described above, were tested occasionally for their abilities to reduce copper (II).

Copper (II) reduction by autotrophic acidophiles was tested in cultures grown with hydrogen as electron donor, under anoxic conditions. This eliminated the possibility that changes in copper speciation was mediated by reduced sulfur compounds (e.g., copper (II) is well known to be reduced, and copper (I) to be complexed, by thiosulfate). *At. ferrooxidans* and *At. ferridurans* were grown in liquid media (pH 2.0) containing different concentrations of copper (II) sulfate and iron (III) sulfate (or 50 μM iron (II) sulfate, as control cultures) and incubated, anaerobically, under hydrogen-enriched atmospheres. Samples were removed at intervals to measure concentrations of copper (I) and iron (III). *A. cryptum* was grown (with glucose as electron

donor) under both micro-aerobic and anaerobic conditions in a liquid medium (pH 2.3), again containing varying concentrations of copper (II) sulfate and iron (III) sulfate and changes in copper and iron speciation and redox potentials recorded. Growth and reduction of copper (II) was also tested using *At. caldus* and *At. ferrivorans*, incubated anaerobically with hydrogen as sole electron acceptor.

The ability of resting cells of *At. ferridurans* to catalyze the dissimilatory oxidation of copper (I) was tested by first growing a culture aerobically (at pH 2.0) with hydrogen as sole electron donor, to a cell density of $\sim 10^9$/mL, harvesting and re-suspending cells in basal salts (pH 2.0). A copper (I) solution was prepared by reducing a solution of copper (II) sulfate with hydroxylamine hydrochloride (1 M), again ensuring an excess of copper (II) to avoid any carryover of non-oxidized hydroxylamine. The cell suspension and copper (I) solutions were mixed to give a concentration of about 3 mM copper (I), and incubated at 30°C for 2 h, during which time samples were removed at regular intervals to determine residual concentrations of copper (I). Two controls were run in parallel: (i) non-inoculated copper (I) + pH 2.0 basal salts; (ii) an inoculated control containing 5 mM iron (II) as well as copper (I), which was monitored for concentrations of reduced iron as well as copper (I).

To determine whether oxidation of copper (I) occurred in growing cultures of iron-oxidizing acidophiles, an experiment was set up using media containing copper (I), both with and without added iron (II). Copper (II) sulfate was added (to 5 mM) to basal salts/trace elements liquid medium (pH 2.0) and hydroxylamine hydrochloride (as a sterile 1 M solution) added to reduce ∼60% of the copper present to copper (I). Iron (II) sulfate was added to 50% of the cultures (to 5 mM) which were then inoculated with either *At. ferrooxidans* or *At. ferridurans,* both grown on hydrogen as electron donor. Flasks were incubated, shaken, at 30°C, and samples withdrawn at regular intervals to measure concentrations of copper (I) and iron (II), and redox potentials. To examine the stability of copper (I) in non-inoculated media, separate shake flasks [amended, or not, with 5 mM iron (II) sulfate] were incubated alongside those containing the acidithiobacilli.

Redox Transformations of Chromium by Acidophilic Bacteria

As with copper, the relative toxicities of both reduced (Cr^{3+}; supplied as $Cr_2(SO_4)_3$) and oxidized (CrO_4^{2-}; supplied as Na_2CrO_4) chromium were determined for cultures grown aerobically on hydrogen (*At. ferrooxidans*, *At. ferridurans,* and *At. ferrivorans*) at pH 2.0, or on glucose (*A. cryptum*) at pH 2.5, prior to testing for dissimilatory oxidation and reduction of the metal. The growth media used contained 50 μM iron (III) sulfate in order to avoid abiotic reduction of chromium (VI) by iron (II). The tolerance of *L. ferrooxidans* and *L. ferriphilum* was tested only for chromium (III), as both of these bacteria use only iron (II) as electron donor. Growth of cultures was confirmed from monitoring changes in cell numbers and (where appropriate) iron (II) oxidation.

Chromium (III) oxidation was tested (by iron-oxidizing acidophiles only) using both growing and resting cultures. For the former, liquid media containing 10 mM chromium (III) and either 0 or 10 mM iron (II) (pH 2.0) were inoculated with active cultures of *At. ferrooxidans*, *At. ferridurans*, *At. ferrivorans*, *L. ferrooxidans,* and *L. ferriphilum*, and changes in concentrations of iron (II) and chromium (VI) monitored for up to 18 days. Oxidation of chromium (III) by fully oxidized cultures of the same iron-oxidizing acidophiles was tested by growing cultures aerobically in a 20 mM iron (II) sulfate medium (initial pH 1.8) to completion of oxidation (determined by the maximum E_H values measured), adding 10 mM chromium (III) sulfate and measuring changes in E_H values and chromium (VI) concentrations after 5 min.

Reduction of chromium (VI) was also tested using both growing and resting cultures of *At. ferrooxidans, At. ferridurans,* and *At. ferrivorans*. Bacteria were grown anaerobically with hydrogen as electron donor in media containing iron (III) (125 μM or 5 mM) with or without 25 μM chromium (VI) and concentrations of iron (II) and chromium (VI) measured after 10 days. Chromium (VI) was added (to 200 μM) to chromium-free cultures of *At. ferridurans* grown anaerobically on hydrogen and iron (III), and residual concentrations of chromium (VI) and iron (II) measured after 5 min. To test chromium (VI) reduction by non-growing cultures, the same three *Acidithiobacillus* spp. were grown aerobically (again with hydrogen as electron donor) in chromium-free media. Cultures (containing $>10^9$ bacteria/mL) were harvested, washed and re-suspended in basal salts (pH 2.0). To aliquots of each of these was added either 25 μM chromium (VI), 1 mM iron (III), or 25 μM chromium (VI) + 1 mM iron (III). Cell suspensions were sparged (at 30°C) with either pure N_2 or H_2/N_2 for up to 2 h, and changes in concentrations of chromium (VI) and iron (II) recorded.

Chromium (VI) reduction by growing cultures and cell suspensions of *A. cryptum* was also tested. Chromium (VI) (100 μM – 1 mM) was added to cultures grown under micro-aerobic conditions in which all of the iron (III) present initially (4.6 mM) had been reduced to iron (II), and chromium (VI) concentrations measured after 5 min. Chromium (VI) reduction by harvested biomass of *A. cryptum* used a similar protocol to that described above for the *Acidithiobacillus* spp. except that biomass was grown aerobically at pH 2.5 with glucose as electron donor, and reduction by cell suspensions examined under both anaerobic (N_2-sparged) and "micro-aerobic" conditions (10 mL of suspension in non-gassed 25 mL bottles) both in the presence and absence of added glucose (1 mM), at 30°C.

Measurements of Standard Redox Potentials in Acidic, Sulfate-Containing Solutions

The standard redox potentials of the iron (II)/iron(III), copper (I)/copper(II), and chromium (III)/chromium (VI) couples were determined experimentally in defined acidic, sulfate-containing solutions. For the iron couple, equimolar (10 mM) solutions

of iron (II) and iron (III) (as sulfate salts) were prepared and redox potentials measured at between pH 0.495 and 2.25. The effect on redox potentials of adding 50 or 100 mM magnesium sulfate to the iron (II)/iron (III) solution at pH 2.25 was also recorded. For copper, a 5 mM copper (II) sulfate solution (pH 2.0) was partially reduced by adding different values of 1 M hydroxylamine hydrochloride, and copper (I) concentrations determined. The redox potentials of three solutions containing varying ratios of copper (I)/copper (II) were measured, and the $E_H{}^0$ determined in each case, using the Nernst equation. In the case of chromium, an acidic (pH 2.43) solution containing equimolar concentrations of chromium (III) sulfate and sodium chromate was prepared and the redox potential ($E_H{}^0$) measured. The solution was then progressively acidified (with H_2SO_4) to pH 1.78, and the response to this on solution $E_H{}^0$ values recorded.

Solubility and Stability of Copper (I) in Acidic Iron (II) Sulfate Solutions

The solubility of copper (I) chloride (Alfa Aesar, Ward Hill, MA, USA) in acidic (pH 2.0) water and in solutions of iron (II) sulfate (10 mM to 1 M, also at pH 2.0) was determined. The redox potentials of these solutions were also measured immediately after being prepared. The solutions were then left at room temperature (*ca.* 22°C) for up to 24 h, when they were visually inspected and tested for concentrations of copper (I) and copper (II), and redox potentials measured.

Analytical Techniques

Concentrations of iron (II) were determined using the Ferrozine colorimetric assay (Stookey, 1970). Total iron was measured using the same assay after reducing soluble iron (III) to iron (II) with ascorbic acid, and iron (III) concentrations from differences in total and iron (II) concentrations. Concentrations of copper (I) were determined using the bicinchoninic acid colorimetric assay (Anwar et al., 2000), total copper following reduction of copper (II) to copper (I) with hydroxylamine, and copper (II) determined from differences in total copper and copper (I) concentrations. Concentrations of chromium (VI) were measured by ion chromatography (Phesatcha et al., 2012), using a Dionex DX-320 ion chromatograph attached to an Ion Pac CS5A column and an AD25 absorbance detector (Dionex, Sunnyvale, CA, USA), and analyzed using Chromeleon software (version 6.40) (Ňancucheo and Johnson, 2012).

A pHase combination glass electrode (VWR International, UK) was used to measure pH values, and a combined platinum Pt sensing electrode and a Ag/AgCl reference electrode (Thermo Fisher Scientific Inc., USA) to measure redox potentials, which were adjusted to be relative to a standard hydrogen electrode (E_H values). The redox electrode was standardized against two reference solutions of known redox potentials (ZoBell's and Light's). Both electrodes were used in conjunction with an Accumet 50 pH/redox meter.

RESULTS

Aerobic Reduction of Iron (III) by *Acidithiobacillus* spp.

As shown in **Figure 1**, the pH of shake flask cultures of *Acidithiobacillus* spp. grown aerobically on elemental sulfur declined as incubation progressed, due to the production of sulfuric acid:

$$2\,S^0 + 2\,H_2O + 3\,O_2 \rightarrow 3\,H^+ + HSO_4^- + SO_4{}^{2-}.$$

The rates of acid production were similar in cultures of the three mesophilic species, but faster with those of the moderate thermophile *At. caldus*. Corresponding trends were also noted with iron (III) reduction and, consequentially, decreases in culture E_H values. Iron (III) was reduced to iron (II) in aerobic cultures of *At. caldus* from the start of the experiment, and was complete by day 12. In contrast, concentrations of iron (II) increased slowly in cultures of the three mesophilic species up to ∼day 25 (when pH values had fallen to ∼1.3) at which point the increases became much more rapid.

Figure 2 shows the potential of cultures of *At. caldus* and *At. ferridurans* to reduce iron (III), in samples removed from bioreactors at fixed pH values. Controlled acidification of the *At. caldus* bioreactor was carried out using fewer stages than for *At. ferridurans,* which is less tolerant of extremely low pH. While both *At. caldus* and *At. ferridurans* displayed some potential for reducing iron (III) in all samples removed from the bioreactors, this was far greater in those taken when the pH was 1.0 than at higher pH values. There was also a notable increase in iron (III) reduction potential during the 7 days period when the *At. caldus* bioreactor was maintained at pH 1.0. While numbers of planktonic cells of *At. caldus*, and, to a lesser extent, *At. ferridurans*, increased to some extent during the time course of this experiment, ensuring that these were $\sim 10^9$/mL at the start of the experiment minimized the impact of biomass size on the iron reduction data obtained. Comparison of iron (III) reduction by cell-free bioreactor samples and those containing bacteria (all from samples taken when both bioreactors were maintained at pH 1.0) showed little differences (**Figure 3**). All data shown in **Figures 2** and **3** are of iron (II) generated after 5 min incubation. Concentrations of iron (II) were usually significantly greater (about two-fold) after 2 h incubation but did not generally increase further with time, though again values were similar in both cell-free samples and those that contained bacteria with protracted incubation. No iron (III) reduction was observed in controls (i.e., basal salts/trace elements solutions adjusted to pH 1.0).

Cultures of *At. caldus* grown aerobically on hydrogen at pH 1.0 and 2.0 showed similar growth rates and growth yields (**Figure 4**). The pH of these cultures did not alter much during incubation, since, in contrast to growth on iron (II) or reduced sulfur, aerobic oxidation of hydrogen neither generates nor consumes protons. As with sulfur-grown *At. caldus*, both bacteria-containing and cell-free samples from aerobic cultures of *At. caldus* grown aerobically on hydrogen were able to reduce iron (III). In most cases, cell-free samples from cultures grown at pH 1.0 were

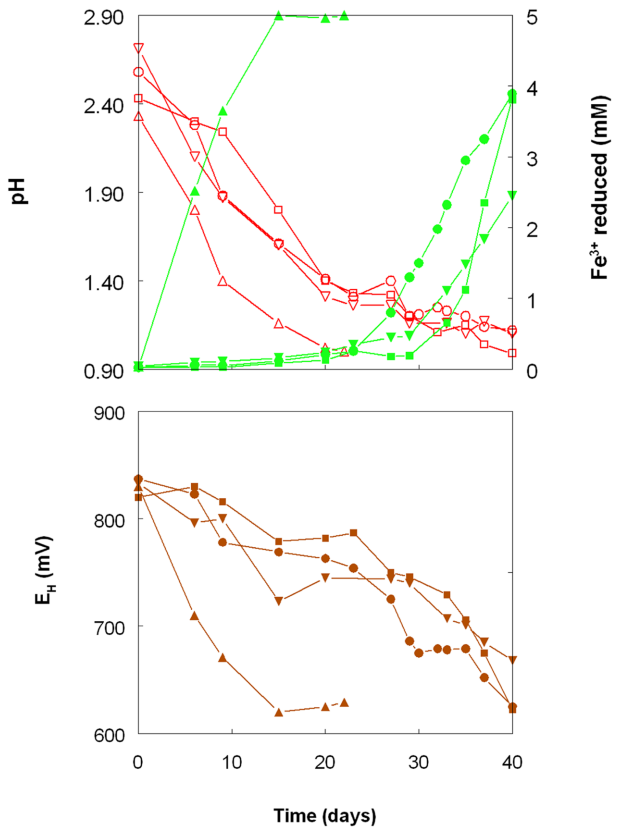

FIGURE 1 | Changes in pH values (red lines), amounts of iron (III) reduced (green lines) and redox potentials (E_H; brown lines) in shake flask cultures of *Acidithiobacillus* spp. grown aerobically on elemental sulfur in the presence of 5 mM ferric iron. Key: (●, ○) *Acidithiobacillus ferrooxidans*^{T}; (■, □) *At. ferridurans*^{T}; (▲, Δ) *At. caldus*^{T}; (▼, ∇); *At. thiooxidans*^{T}.

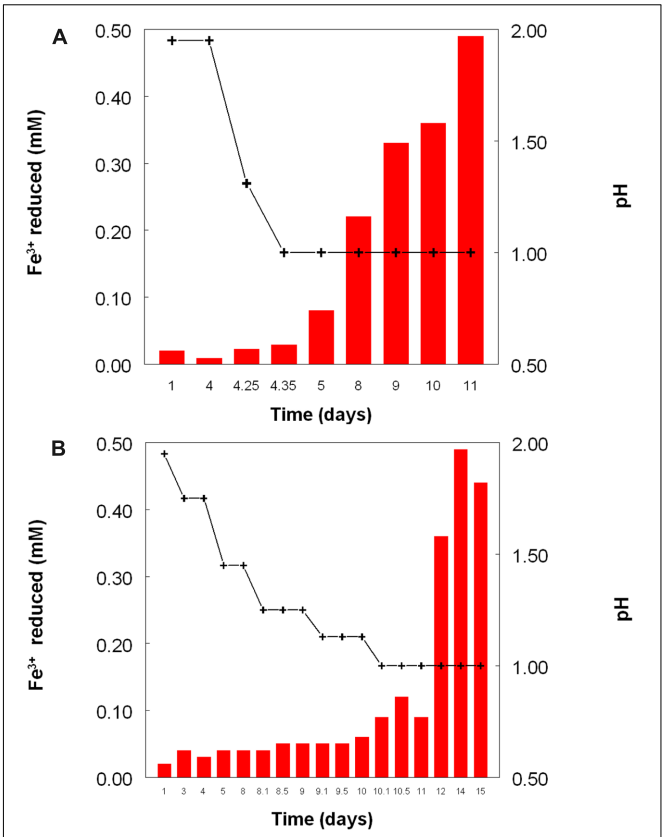

FIGURE 2 | Reduction of iron (III) (red bars) by samples of cultures of (A) *At. caldus*^{T}, and **(B)** *At. ferridurans*^{T} grown in bioreactors at varying pH. Stepwise decreases in bioreactor pH are depicted by the black line.

superior in this respect to those grown at pH 2.0, even though optical densities of these cultures were similar on each sampling occasion (**Figure 4**).

Redox Transformations of Copper by Acidophilic Bacteria

Preliminary tests carried out with several species of acidophilic bacteria showed that, in every case, growth was inhibited by much smaller concentrations of copper (I) than has been reported elsewhere (and confirmed in the present study) for copper (II). The acidophiles tested displayed varying sensitivities to copper (I) which tended to parallel those to copper (II), apart from being far more acute [e.g., *L. ferrooxidans* was far more sensitive to both copper (I) and copper (II) than *L. ferriphilum*; **Table 2**]. In all subsequent experiments, care was taken to ensure that copper (I) concentrations present in culture media were within the range which allowed growth of the different species of acidophilic bacteria tested.

Copper (I) accumulated in aerobic cultures of sulfur-grown *Acidithiobacillus* spp., though at slower rates and to lower final concentrations than those found with iron (III)-containing cultures (**Figure 5**). In contrast to cultures grown with iron, rates of sulfuric acid production were similar with all four *Acidithiobacillus* spp. tested, though more copper (I) was generated by *At. caldus* than by the other three species tested. Redox potentials in these cultures showed initial increases followed by continuous decreases in all cultures, and again the fluctuations in E_H values were more rapid in the case of *At. caldus* than with the other acidithiobacilli (**Figure 5**). Data in **Figure 6** show that samples taken from aerobic bioreactor cultures of *At. caldus* and *At. ferridurans* grown on elemental sulfur also reduced copper (II) to copper (I). In the case of *At. ferridurans*, copper (II) reduction potentials showed some degree of correlation to bioreactor pH values ($r^2 = 0.78$) though there were insufficient data to conclude whether this was also the case for *At. caldus*. As with iron (III), reduction of copper (II) to copper (I) was found to be similar in both cell-free and bacteria-containing bioreactor samples (data not shown).

When grown anaerobically on hydrogen with no iron (III) added, no growth or reduction of copper (II) to copper (I) was observed with all four *Acidithiobacillus* spp. (*At. ferrooxidans, At. ferridurans, At. ferrivorans,* and *At. caldus*) tested. However, when iron (III) was included in the medium, both it and copper (II) were reduced by *At. ferrooxidans* and *At. ferridurans*. **Figure 7A** shows that, in media containing initially 20 mM of

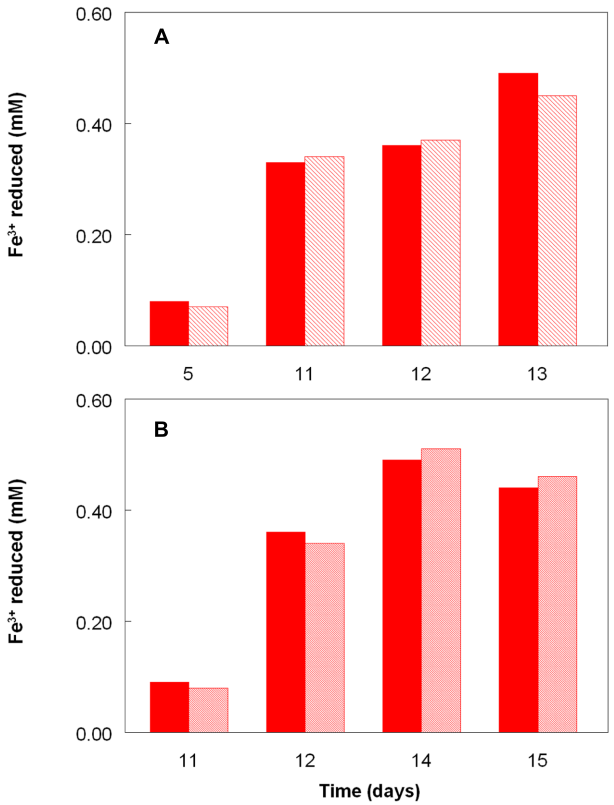

FIGURE 3 | Comparison of iron (III) reduction by bacteria-containing (solid bars) and cell-free culture liquors (hatched bars) of (A) *At. caldus*^{T} and **(B)** *At. ferridurans*^{T}, grown aerobically on elemental sulfur in bioreactors. The pH of both bioreactors at the times of sampling shown was 1.0.

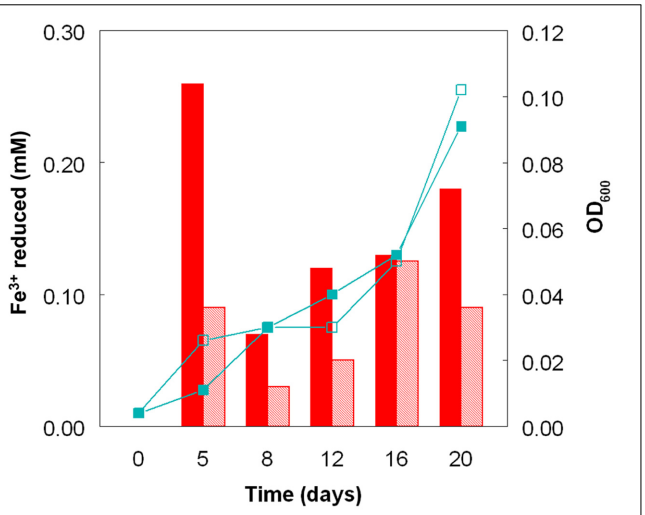

FIGURE 4 | Reduction of iron (III) by cell-free culture liquors of *At. caldus*^{T} grown aerobically on hydrogen at pH 1.0 (solid bars) and at pH 2.0 (hatched bars) to reduce iron (III). The line graphs depict corresponding changes in culture optical densities (■, pH 1.0; □, pH 2.0).

both metals in their oxidized forms, virtually all of the iron was reduced, but only ∼50% of the copper, after 4 days of incubation. An identical trend of copper reduction occurring only in cultures that were amended with iron (III) was also observed with *A. cryptum* (micro-aerobic cultures only; growth and reduction of iron and copper was not observed under strictly anoxic conditions) though, in this case, ∼90% of the copper (II) present was reduced to copper (I). In cultures of this heterotrophic acidophile, redox potentials decreased by ∼300 mV during incubation and displayed minor reversions (increases of ∼50 mV) toward the end of the incubation period (**Figure 7B**).

Harvested biomass of *At. ferridurans* grown on hydrogen did not oxidize copper (I), in contrast to iron (II) which was oxidized (**Figure 7A**). No detectable changes in copper (I) concentrations were observed in non-inoculated controls over the same time. Likewise copper (I) was not oxidized in cultures of *At. ferrooxidans* or *At. ferridurans* that did not contain iron (II); small decreases in copper (I) concentrations in inoculated cultures over time were similar to those observed in non-inoculated controls (data not shown). In contrast, when iron (II) was also included in the culture medium, both it and copper (I) were oxidized, and redox potentials increased by >250 mV after a lag period of about 4 days in cultures of both iron-oxidizing *Acidithiobacillus* spp. (**Figure 8**).

Redox Transformations of Chromium by Acidophilic Bacteria

Anionic chromium (VI) was shown to be far more toxic to the acidophilic bacteria tested than cationic chromium (III) (**Table 3**). No growth of any of the *Acidithiobacillus* spp. was observed in cultures (pH 2.0, with hydrogen as electron donor) to which chromium (VI) was added at 5 μM and above. In contrast, *A. cryptum* grew in the presence of 50 μM chromate at pH 2.5 (aerobically, with glucose as electron donor). In contrast, most of the iron-oxidizing autotrophic acidophiles grew in the presence of 50 mM chromium (III), though both *L. ferrooxidans* and the heterotroph *A. cryptum* were inhibited by this concentration of the metal but grew in the presence of 10 mM chromium (III) (**Table 3**).

No chromium (VI) was detected in chromium (III)-amended cultures of any of the five species of iron-oxidisers tested, irrespective of whether the growth media also initially contained iron (II). More positive redox potentials were recorded in (chromium-free) iron (II)-grown cultures of *Leptospirillum* spp. (+883 to +904 mV) than *Acidithiobacillus* spp. (+844 to +852 mV). However, while addition of chromium (III) caused the redox potential of oxidized *L. ferriphilum* cultures to fall by ∼30 mV, changes in E_H values were <10 mV in other cultures and, in all cases, no chromium (VI) was subsequently detected.

No growth or reduction of either chromium (VI) or iron (III) was found in cultures of the three *Acidithiobacillus* spp. incubated anaerobically with hydrogen as electron donor. However, all of the chromium (VI) added to anaerobic cultures of *At. ferridurans* in which the iron (III) present had been reduced to iron (II), was rapidly reduced to below detectable levels (∼10 μM).

TABLE 2 | Comparison of the relative toxicities of copper (I) and copper (II) to some species of acidophilic bacteria.

Bacterium	Copper (I)		Copper (II)	
	MGC	MIC	MGC	MIC
At. ferrooxidans^T	8.5	11.5	400[1]	500[1]
At. ferridurans^T	11.5	14	200[1]	300[1]
L. ferrooxidans^T	1	2	10[2]	20[2]
L. ferriphilum MT63	8.5	11.5	200[2]	300[2]
A. cryptum SJH	2.4	4.4	15[3]	20[3]

[1]*Hedrich and Johnson (2013b);* [2]*Galleguillos et al. (2009);* [3]*Johnson (unpublished). Copper concentrations are mmoles/L. MGC, maximum concentration recorded for growth; MIC minimum inhibitory concentration.*

Tests of metal reduction carried out with cell suspensions of acidithiobacilli showed that, while no reduction of iron (III) occurred when these were sparged with N_2, two of the three species (*At. ferridurans* and *At. ferrivorans*) reduced iron when hydrogen was provided. However, inclusion of 25 μM chromium (VI) to the cell suspensions completely inhibited reduction of iron (III), and no reduction of chromium was found to occur in iron-free cell suspensions.

Chromate reduction by *A. cryptum* showed some similarities but also some differences to results obtained with the acidithiobacilli. Concentrations of >25 μM chromium (VI) inhibited both growth and iron reduction under micro-aerobic conditions, even though cultures grew aerobically in the presence of 50 μM chromium (VI). All of the chromium (VI) added (up to 1 mM) to reduced (iron (II)-containing) cultures of *A. cryptum* was reduced, with concomitant generation of iron (III) (**Table 4**). Iron (III) was reduced by cell suspensions of *A. cryptum* maintained under micro-aerobic conditions only when glucose was added, while iron (III) reduction occurred in N_2-sparged cell suspensions in both the presence and absence of added glucose. No reduction of chromium (VI) was observed in both micro-aerobic and anaerobic cell suspensions when this metal was added alone, but when both iron (III) and chromium (VI) were added to cell suspensions, both metals were reduced, again under micro-aerobic and anaerobic conditions (**Figure 10**).

Redox Potentials of Iron, Copper, and Chromium in Acidic, Sulfate-Rich Liquors, and Solubility and Stability of Copper (I) in Acidic Iron (II) Solutions

The standard redox potentials ($E_H{}^0$ values) of acidic, sulfate-containing solutions containing iron, copper or chromium present in both oxidized and reduced forms produced values which were, in each case, significantly different from those published for solutions where the metals are non-complexed. In the case of iron, the $E_H{}^0$ recorded at pH 2.0 was +663 mV, and this increased as the pH was lowered and decreased as pH was increased, beyond pH 2.0 (**Figure 9**, which shows $E_H{}^0$ values of the iron (II)/iron (III) couple as functions of both pH and calculated proton (hydronium ion) concentrations). Addition of 50 and 100 mM magnesium sulfate to the 10 mM iron (II) sulfate solution (at pH 2.25) caused the measured $E_H{}^0$ to decrease by 3 and 5 mV, respectively. The $E_H{}^0$ values of copper (I)/copper (II) sulfate solutions at pH 2.0, calculated using the Nernst equation using solutions where the molar ratios of the two ions varied between 1.0:4.0 and 2.9:2.1, were 548 ± 3 mV. Addition of 5 mM copper (II) sulfate to a solution of 10 mM iron (II) sulfate (both at pH 2.0) only resulted in minor changes in E_H values (2 to 3 mV). However, colorimetric analysis showed that concentrations of iron (II) were lowered by ∼1 mM as a consequence, inferring that ∼1 mM copper (II) had been reduced.

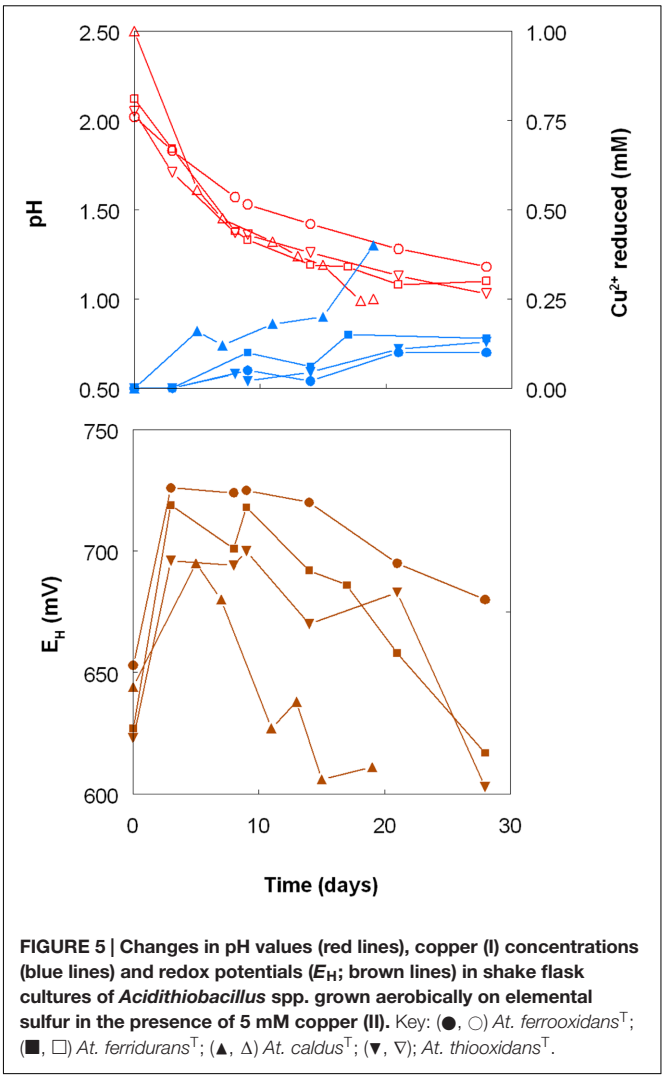

FIGURE 5 | Changes in pH values (red lines), copper (I) concentrations (blue lines) and redox potentials (E_H; brown lines) in shake flask cultures of *Acidithiobacillus* spp. grown aerobically on elemental sulfur in the presence of 5 mM copper (II). Key: (●, ○) *At. ferrooxidans*^{T}; (■, □) *At. ferridurans*^{T}; (▲, Δ) *At. caldus*^{T}; (▼, ▽); *At. thiooxidans*^{T}.

Solubility and stability tests carried out with copper (I) chloride showed that, not only was this metal salt far more soluble in acidic iron (II) sulfate than in pure water adjusted to the same pH [15.2 mM in 1 M iron (II) sulfate compared to 2.7 mM in acidic (pH 2.0) water], but that copper (I) did not disproportionate (to copper (II) and elemental copper) over 24 h in the presence of either 100 mM or 1 M iron (II) sulfate, though there was clear evidence of disproportionation in both iron-free acidic water and 10 mM iron (II) sulfate solutions, as evidenced from the presence of soluble copper (II) and accumulation of

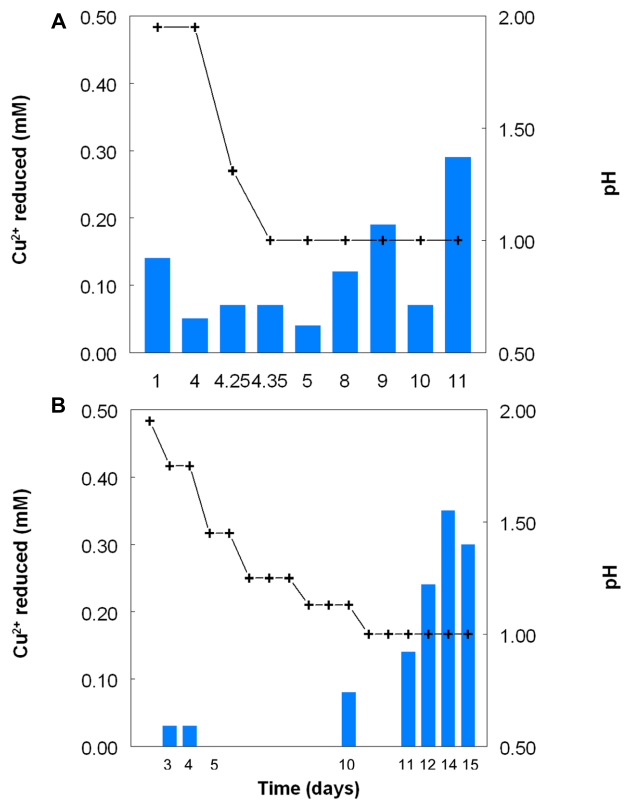

FIGURE 6 | Reduction of copper (II) (blue bars) by samples of cultures of (A) *At. caldus*^{T}, and **(B)** *At. ferridurans*^{T} grown in bioreactors at varying pH. Stepwise decreases in bioreactor pH are depicted by the black line.

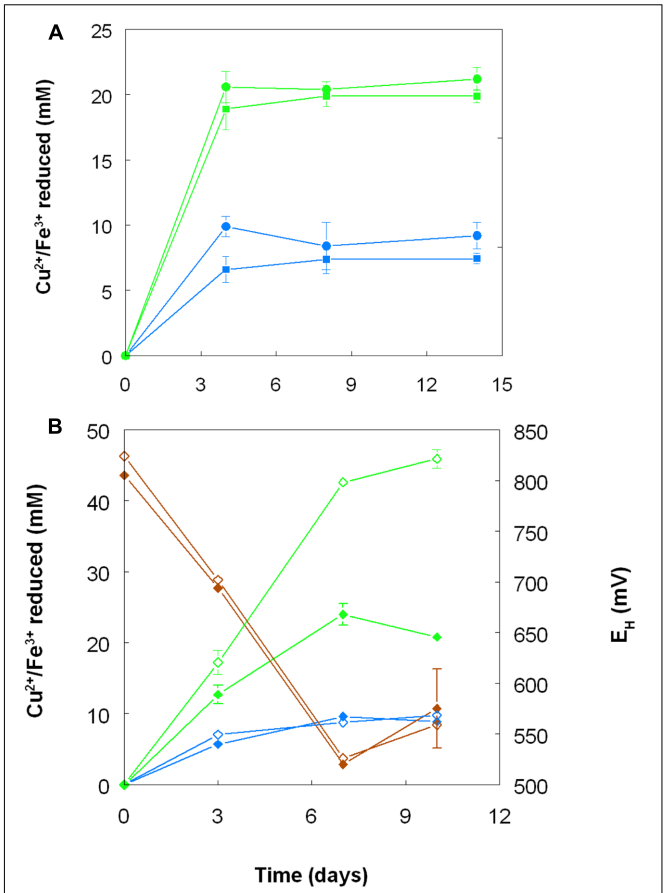

FIGURE 7 | Reduction of copper (II) (blue lines) and iron (III) (green lines), and changes in redox potentials (brown lines; data for *A. cryptum* only) in shake flask cultures of acidophilic bacteria grown under oxygen-limiting conditions. (A) *At. ferrooxidans* (●) and *At. ferridurans* (■) grown under anoxic conditions with hydrogen as electron donor in liquid medium containing 20 mM of both copper (II) sulfate and iron (III) sulfate. **(B)** *A. cryptum* grown under micro-aerobic conditions with glucose as electron donor in liquid media containing 10 mM copper (II) sulfate and either 20 mM (filled symbols) or 50 mM (hollow symbols) iron (III) sulfate. No reduction of copper (II) was observed in cultures of all three acidophiles that did not initially contain iron (III).

films of elemental copper on the surfaces of the solutions (data not shown).

The measured $E_H{}^0$ of the chromium (III)/ chromium (VI) (chromate) couple at pH 2.43 was +844 mV. This varied with pH, increasing to +877 mV at pH 1.97, and to +895 mV at pH 1.78.

DISCUSSION

Reduction of Iron (III) by *Acidithiobacillus* spp. in Aerobic Cultures

Shake flask experiments confirmed the observation by Sand (1989) that iron (III) could be reduced by *At. ferrooxidans,* grown aerobically on elemental sulfur at extremely low pH, but also showed that iron reduction also occurred in aerobic cultures of other *Acidithiobacillus* spp., including two that do not oxidise iron (II) (**Figures 1–4**). The pH at which rates of iron (III) reduction accelerated with both *At. ferrooxidans* and *At. ferridurans* (∼1.3) corresponded to the pH growth minima reported for both type strains (Hedrich and Johnson, 2013b). Since both species use iron (II) in preference to other electron donors (Yarzabal et al., 2004; Sandoval Ponce et al., 2012) it is likely that any iron (III) reduction that occurred within the growth pH range of these acidophiles would have been masked by re-oxidation of the iron (II) generated. This would not be the case with the moderate thermophile *At. caldus*, and it is interesting that iron (II) accumulated in cultures of this acidophile from close to the start of the experiment (**Figure 1**). A similar pattern was not, however, found with *At. thiooxidans*, a mesophilic species that also does not oxidize iron, where accumulation of iron (II) only became significant at and below pH 1.2.

The experiment carried out in pH-controlled bioreactors showed that the propensity of *At. caldus* to reduce iron (III) under aerobic conditions was also greatly affected by the pH of the growth medium (**Figure 2**). Samples taken from the bioreactor when maintained above pH 1.0, showed some, though relatively small, ability to reduce iron (III) rapidly, but this increased dramatically when the culture was held at pH 1.0. A similar scenario was observed with *At. ferridurans*. However,

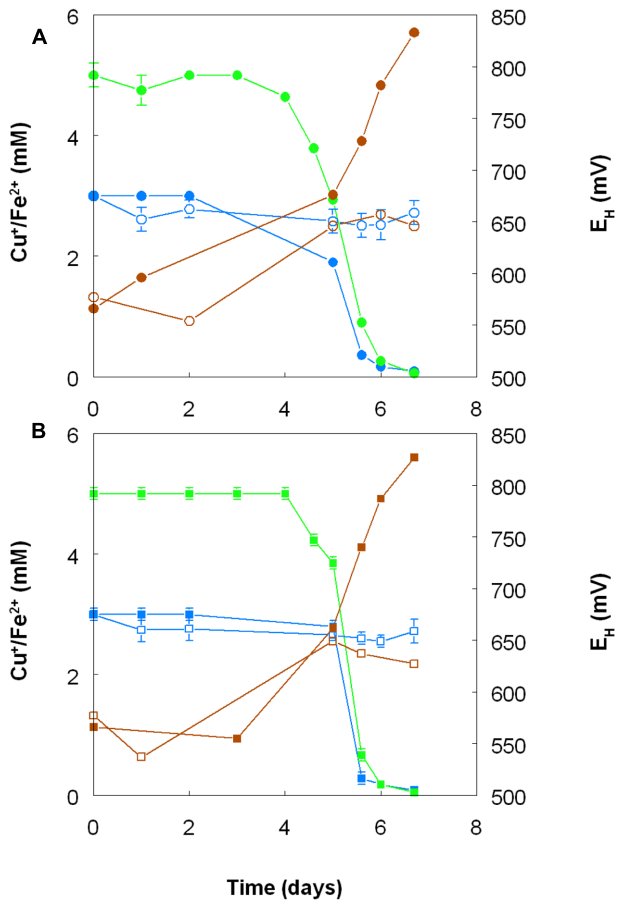

FIGURE 8 | Oxidation of copper (I) (blue lines) and iron (II) (green lines), and corresponding changes in redox potentials (brown lines) by cultures of (A) *At. ferrooxidans* and **(B)** *At. ferridurans*, grown aerobically in cultures containing either both metals (filled symbols) or only copper (I) (hollow symbols). Error bars depict data ranges of replicate cultures.

TABLE 3 | Comparison of the relative toxicities of chromium (III) and chromium (VI) to some species of acidophilic bacteria.

Bacterium	Chromium (III)		Chromium (VI)	
	MGC	MIC	MGC	MIC
At. ferrooxidans^T	50	100	0*	5*
At. ferridurans^T	100	>100	0*	5*
At. ferrivorans Peru6	100	>100	0*	5*
L. ferrooxidans^T	50	100	nd	nd
L. ferriphilum MT63	10	50	nd	nd
A. cryptum SJH	10	50	50**	100**

**at pH 2.0; **at pH 2.5. Chromium (III) concentrations are mmoles/L, and chromium (VI) concentrations are μmoles/L. MGC, maximum concentration recorded for growth; MIC minimum inhibitory concentration; nd, not determined.*

in both cases, bacterial cells did not have to be present for iron (III) reduction to occur (**Figure 3**), the implication being that the latter was mediated (for both species) by one or more soluble metabolites generated by the bacteria. Inorganic sulfur compounds, generated as waste products during growth on elemental sulfur (Steudel et al., 1987), have been implicated in mediating metal ion reduction by *Acidithiobacillus* spp. (Briand et al., 1996). However, hydrogen-grown *At. caldus* also displayed similar abilities to reduce iron, again irrespective of bacterial cells being present (**Figure 4**), confirming that sulfur intermediates were not solely (if at all) responsible for mediating aerobic iron (III) reduction by these acidophiles. It is also possible that redox-active biomolecules (e.g., cytochromes) are released into culture liquors during active growth or lysis of the acidophilic bacteria, and that these also mediate iron (III) reduction. Results from this work, showing that aerobic iron (III) reduction by *Acidithiobacillus* spp. appears not to be correlated with growth, support the observation by Hallberg et al. (2001) that species that do not oxidize iron (such as *At. caldus* and *At. thiooxidans*) cannot grow by respiring iron (III), unlike the iron-oxidizing acidithiobacilli.

TABLE 4 | Changes in concentrations of iron (II) and chromium (VI) following addition of different concentrations of sodium chromate to a culture of *A. cryptum* SJH grown under micro-aerobic conditions, where all of the iron (III) present initially had been reduced to iron (II).

Chromium (VI) added (μmoles/L)	Fe^{2+}(mmoles/L)	CrO_4^{2-} (μmoles/L)
0	4.6	0
100	3.28	0
200	2.20	0
500	<0.05	0
1000	<0.05	40

Reduction of Copper (II) and Toxicity of Copper (I) to Acidophilic Bacteria

Although tolerance of acidophilic bacteria to both iron (II) and iron (III) have been frequently reported in the literature, published copper tolerance data refer exclusively to copper (II). As found in the present study, copper (I) is much more toxic to these bacteria (**Table 2**), with MICs being generally an order of magnitude or more lower that those reported for copper (II). Copper occurs immediately above silver in the Periodic Table of elements, and it is interesting to note that monovalent silver (Ag^+) is highly toxic to acidophilic bacteria, inhibiting growth when present in micro-molar concentrations (Tuovinen et al., 1985). Copper (I) is, however, both relatively insoluble and highly unstable in most aqueous solutions, where it disproportionates to copper (II) and elemental copper ($2\ Cu^+ \rightarrow Cu^{2+} + Cu^0$). Results from the current work have shown that, not only is the solubility of copper (I) chloride far greater in 1 M iron (II) sulfate (pH 2) than in water acidified to the same pH value, but that the stability of copper (I) is greatly enhanced by the presence of iron (II). This has important implications for acidic copper-rich waters, such as some acid mine drainage (AMD) streams and PLS.

Acidithiobacillus spp. grown aerobically on elemental sulfur also reduced copper (II), though far less copper (I) than iron (II) accumulated in shake flask cultures (**Figure 5**). The amounts of iron and copper reduced by bioreactor cultures of *At. caldus*

and *At. ferridurans* tested off-line were more similar (**Figure 6**), and, as with iron, copper reduction was observed with cell-free culture liquors of both acidophiles, suggesting a common mechanism for iron and copper reduction by the acidithiobacilli grown under these conditions. When hydrogen (for autotrophic species) or glucose (for the heterotroph *A. cryptum*) was used as electron donor, the possibility that iron and copper reduction were both mediated by one or more sulfur metabolites was eliminated (**Figure 7**). While none of the *Acidithiobacillus* spp. tested, (*At. ferrooxidans, At. ferridurans, At. ferrivorans,* and *At. caldus*) were able to couple the oxidation of hydrogen to the dissimilatory reduction of copper (II) directly, at least two species (*At. ferrooxidans* and *At. ferridurans*) could do this indirectly using iron as an electron shuttle (**Figure 8**). A similar scenario was observed with *A. cryptum* grown under micro-aerobic conditions. The mechanism of copper (II) reduction therefore appeared to involve the reduction of iron (III) to iron (II) (which has been well documented in all three of these species), and the subsequent reduction of copper (II) by iron (II). This regenerates iron (III) which can again act as a direct electron acceptor for these acidophiles, allowing them to utilize copper (I) as an indirect electron acceptor (**Figure 11**).

The results of experiments carried out with both harvested biomass and active cultures of iron-oxidizing acidophiles showed that copper (I) did not act as a direct electron donor for these bacteria. However, it could act as an indirect donor in the presence of soluble iron, as demonstrated in cultures where iron (II) was included in the growth medium. Generation of iron (III) by the bacteria resulted in copper (I) being oxidized to copper (II), and the iron (II) so-formed being again oxidized to iron (III). This allowed the bacteria to harness the electron donor potential of copper (I) (**Figure 11**), even though they seemingly lack the enzymatic apparatus for oxidizing reduced copper directly.

Redox Potentials of Iron and Copper Couples in Acidic, Sulfate-Rich Solutions

The fact that iron can both oxidize and reduce copper (and *vice versa*) might appear to be thermodynamically untenable. However, consideration of redox potentials of the iron (II)/iron (III) and copper (I)/copper (II) couples in acidic, sulfate-rich solutions resolves this apparent conundrum (**Figure 9**). The frequently quoted standard redox potential ($E_H{}^0$) of the iron (II)/iron (III) couple is +770 mV, and that of the copper (I)/copper (II) couple is ∼ +160 mV. However, these values apply to situations where both metals are present as soluble and non-complexed ions, and it is known for example that, in the presence of organic chelating agents such as citrate or haem, the $E_H{}^0$ value of the iron couple is considerably less positive than +770 mV. Most extremely acidic environments contain relatively small concentrations of dissolved organic carbon (<10 mg/L) and therefore organic chelation of iron is usually negligible. However, in acidic, sulfate-rich waters, such as AMD and PLS, iron (III) is complexed by both hydroxyl and sulfate anions, forming a range or cationic and anionic complexes [$Fe(OH)^{2+}$, $Fe(OH)_2{}^+$, $Fe(SO_4)^+$, $Fe(SO_4)_2{}^-$), the relative proportions of which vary with pH and sulfate concentrations (Welham et al., 2000). As a consequence, the $E_H{}^0$ of the iron (II)/iron (III) couple is significantly less than +770 mV in these waters (Johnson et al., 2012). In the present study, the measured $E_H{}^0$ was between +657 mV (at pH 2.25) and +685 mV (at pH 0.5) at a molar ratio of 2 iron/2.5 sulfate. Increasing the molar ratio more in favor of sulfate depressed the $E_H{}^0$ value (at pH 2.25) presumably by increasing the relative proportion of the $Fe(SO_4)_2{}^-$ complex present, though the impact of sulfate did not appear to be as significant as that of solution pH. In contrast, the $E_H{}^0$ of the copper (I)/copper (II) couple in acidic, sulfate-rich solutions, calculated from measurements of E_H values of solutions containing known concentrations of both ions, was ∼400 mV more positive that the value commonly quoted. The consequence of the is that, although an iron (III)-rich liquor will always have a sufficiently positive redox potential to allow it to oxidize copper (I), an acidic iron (II) sulfate-rich solution can have a lower E_H value [+539 mV for a pH 2.0 solution containing 99% iron (II) and 1% iron (III) sulfate] than an acidic copper (II) sulfate-rich solution [+666 mV for a pH 2.0 solution containing 99% copper (II) and 1% copper (I) sulfate], values calculated using the Nernst equation and the $E_H{}^0$ values determined in the current experiments. Mixing the two solutions would therefore result in a partial reduction of copper (II) [and oxidation of iron (II)], as observed in the present work. Matocha et al. (2005) had previously reported that copper (II) could be reduced to copper (I) by iron (II) under abiotic conditions. The important difference between a static (chemical) situation and a dynamic (biological) scenario is that, in the latter, the continuous regeneration of iron (II) (as a consequence of dissimilatory iron reduction) would result in a much greater increase in copper (I) concentrations, as found in the experiments described herein.

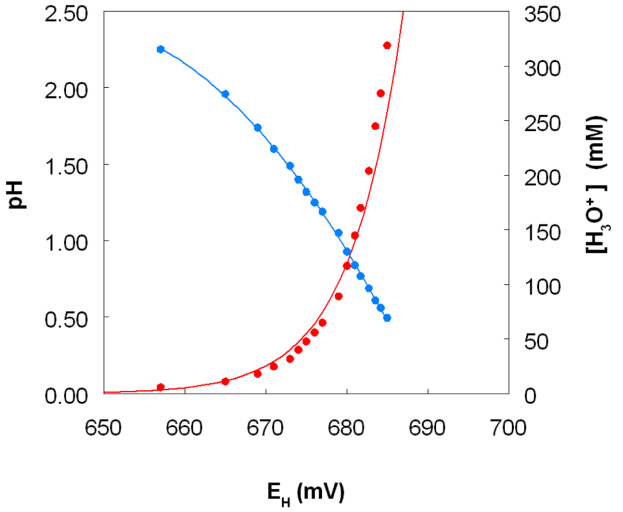

FIGURE 9 | Variation of the measured standard redox potential of the iron (II)/iron (III) couple measured in acidic sulfate-rich solutions as a function of pH (in blue) and as a function of calculated proton (hydronium ion) concentration (in red).

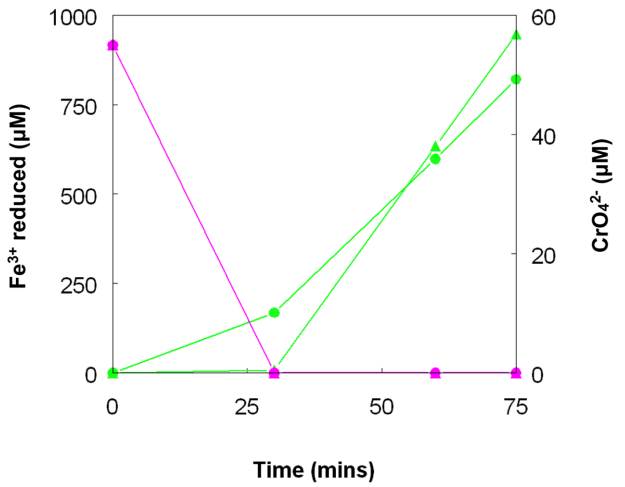

FIGURE 10 | Concomitant reduction of iron (III) (green lines) and chromium (VI) (magenta lines) by cell suspensions of *A. cryptum*. Key: (●, ●) anaerobic suspensions; (▲, ▲) "micro-aerobic" suspensions. No reduction of chromium (VI) was observed when iron (III) was not added to cell suspensions.

Toxicity and Redox Transformations of Chromium

Chromium (VI) was confirmed to be far more toxic to the extreme acidophiles examined than chromium (III) (**Table 3**). Metal oxyanions are known to be generally more toxic than metal cations to acidophilic bacteria due to the fact that, in contrast to neutrophiles, they have positive rather than negative membrane potentials (Norris and Ingledew, 1992). This could also help explain why *A. cryptum* was apparently more tolerant to chromium (VI) than the acidithiobacilli, as the former was grown at a higher pH than the latter which would result in its membrane potential being less positive.

The measured standard redox potential ($E_H{}^0$) of the chromium (III)/chromium (VI) couple was much more positive than either that of the iron or copper couples. This was not unexpected, though the values measured in the current work were less positive (+844 to +895 mV) than that generally quoted for the $Cr_2O_7{}^{2-}/Cr^{3+}$ couple (+1.33 V). Chromium (III), like iron (III), is readily complexed by inorganic anions, and the dominant form of the chromate anion varies with solution pH (existing mostly as $HCrO_4{}^-$ at pH 2.0, with undissociated H_2CrO_4 becoming increasingly relatively abundant as pH decreases; Tandon et al., 1984). There are no reports of direct biogenic oxidation of chromium (III) to chromium (VI), though this reaction can be mediated by manganese (III) or manganese (IV) minerals generated biologically (Lloyd et al., 2015). However, since the $E_H{}^0$ of the chromium (III)/chromium (VI) couple determined in acidic sulfate-containing liquors in the present study was actually slightly less positive than the maximum redox potentials of *Leptospirillum* spp. grown on iron (II), there was the possibility that some chromium (VI) may be generated indirectly by this iron-oxidiser. However, there was no evidence of chromium (VI) generation in these cultures either containing chromium (III) initially, or to which chromium (III) was added after iron oxidation had ceased. This was also the case with the *Acidithiobacillus* spp., though terminal E_H values of cultures of these iron-oxidisers were less positive, as recorded elsewhere (Rawlings et al., 1999), which is a reflection of their lower affinity for iron (II) and greater sensitivity to iron (III) than *Leptospirillum* spp. (Norris et al., 1988). The reason why no chromium (III) oxidation was observed even in cultures where E_H values exceeded +900 mV was possibly due to the amounts of chromium (VI) generated being below limits of detection, or because of the acute toxicity of chromium (VI) to iron-oxidizing acidophiles which would have limited the reaction.

As was the case with copper (II), there was no evidence to support the hypothesis that chromium (VI) can be reduced directly to chromium (III) by acidophilic bacteria, though

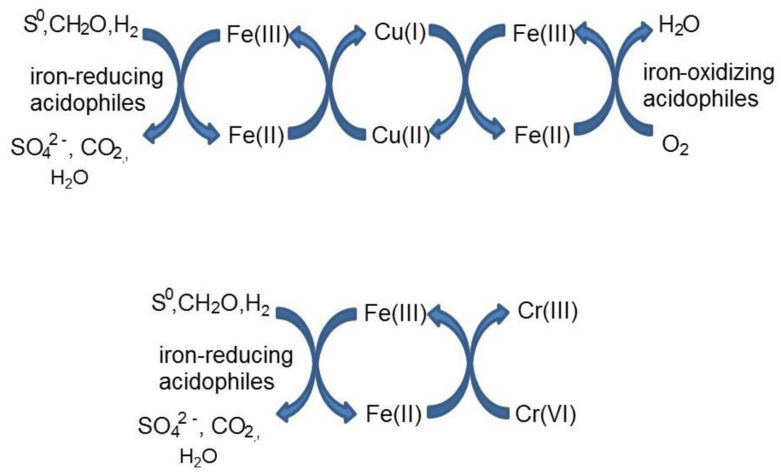

FIGURE 11 | Schematic representation of indirect redox transformation of copper and chromium mediated by acidophilic bacteria.

this may occur indirectly *via* iron (II) generated under either anaerobic (*Acidithiobacillus* spp.) or micro-aerobic (*A. cryptum*) conditions (**Table 4**; **Figure 10**). The fact that chromium (VI) was reduced rapidly by cultures of *At. ferridurans* and *A. cryptum* that had already reduced iron (III) to iron (II) was not unexpected, as chromium (VI) is well known to be reduced by iron (II) in acidic solutions:

$$CrO_4^{2-} + 3\,Fe^{2+} + 8\,H^+ \rightarrow Cr^{3+} + 3\,Fe^{3+} + 4\,H_2O.$$

Both metals were also reduced when they were added to cell suspensions in their oxidized forms, confirming that chromium (VI) and iron (III) reduction can be concurrent. This was demonstrated with *A. cryptum* only, as even 25 μM chromate was sufficient to totally inhibit iron reduction by the acidithiobacilli. The inability of *A. cryptum* to reduce chromium (VI) in the absence of iron contradicts the earlier findings of Cummings et al. (2007) who reported that cell suspensions of *A. cryptum* strain JF-5 could reduce chromium (VI) directly, whether or not an electron donor (glucose) was provided. They also suggested that the reaction was enzymatic. However, the rate of chromium (VI) reduction reported by Cummings et al. was very slow, requiring 10 h to reduce concentrations from 50 μM to about 10 μM (though this was greatly accelerated when iron was added), compared to near complete indirect reduction of 50 μM chromium (VI) within 30 min found in the present study. Possible reasons for the discrepancy in the results of the two studies include: (i) strain variation (though *A. cryptum* strains SJH and JF-5 share >99.5% similarity of their 16S rRNA genes); (ii) growth media and carry over of organic materials [Cummings et al. (2007) grew their strain on a tryptone soya broth/vitamins liquid medium and some complex organic compounds are known to reduce chromium (VI), while *A. cryptum* SJH was grown in glucose/minimal salts, which would have eliminated this possibility]; (iii) the presence of iron (II) or iron (III) (which would be reduced) in cell suspensions in the earlier study, as only trace amounts (micro-molar concentrations) of iron (II) are necessary to reduce equivalent concentrations of chromium (VI). Masaki et al. (2015) also included tryptone soya broth in the media they used to cultivate *Acidocella aromatica* (which was not necessary, as this acidophile cannot utilize the organic components present in this material) and, interestingly, found that chromium (VI) was reduced even in aerobic cultures. The results of the present study lead us to conclude that, while chromium (VI) can be reduced by acidophilic prokaryotes, this is mediated indirectly by species that reduce iron (III) to iron (II) (**Figure 11**), and that evidence for direct reduction requires re-evaluation and validation.

Implications for Biotechnology and the Biosphere

The results of the current study have widespread implications for established and emerging biotechnologies that utilize acidophilic microorganisms. For example, reductive dissolution has been proposed as a means of extracting base metals such as nickel and cobalt from oxidized ores, such as laterites (Johnson et al., 2013). The process was originally demonstrated using anaerobic bioreactors containing acidophilic bacteria that couple the oxidation of elemental sulfur to the reduction of iron (III), though more recently Marrero et al. (2015) reported that reductive dissolution of laterite tailings occurred in aerobic bioreactors containing *At. thiooxidans* and *At. ferrooxidans* at extremely low pH. Data from the current study, showing that iron (III) was reduced by several species of *Acidithiobacillus* at pH values where re-oxidation of the iron (II) produced by *At. ferrooxidans* does not occur, support their findings, though it is worth noting that iron (II) can be oxidized at pH < 1.0 by more acid-tolerant acidophiles (*Leptospirillum* and *Ferroplasma* spp.) which would obviate mineral dissolution *via* a reductive mechanism. The findings that not only copper (II) can be reduced indirectly by iron-reducing acidophiles but also that copper (I) is a far more toxic form of this metal to biomining bacteria, should be taken into account when managing PLS produced by heap bioleaching at copper mines, where mineral-oxidizing prokaryotes have a critical role in metal extraction. Finally, indirect reduction of highly bio-toxic chromium (VI) to the less harmful chromium (III) cation could be used to remediate Cr-contaminated wastewaters. The advantage of using acidophiles in this process is that the chromium (III) generated would be maintained in solution rather than precipitated within a bioreactor, thereby facilitating its downstream recovery.

Apart from the industrial connotations, indirect oxido-reduction of copper and, to a lesser extent, reduction of chromium (VI) has potential implications for lithotrophic life on our own planet, and possibly beyond. The implication is that copper (I) minerals, such as chalcocite (Cu_2S) could act as sources of energy, not only for acidophilic bacteria such as *Acidithiobacillus* spp. that can oxidize reduced sulfur (as reported by Nielsen and Beck, 1972), but also for iron-oxidisers, such as *Leptospirillum* spp. and *Ferrimicrobium acidiphilum*, that only oxidize iron (II), allowing them to exploit low pH environments that are rich in reduced copper but contain relatively little iron. The reverse reaction, whereby microbial growth could be supported by indirect dissimilatory reduction of copper (II), could also be significant in copper-rich environments. Both processes provide tantalizing scenarios of how lithotrophic prokaryotes might thrive in geological niches previously considered as both hostile and unimportant for life.

AUTHOR CONTRIBUTIONS

DBJ: experimental work, writing manuscript, preparing Figures and Tables. SH: conceptual discussions, editing of manuscript. EP: experimental work, editing of manuscript.

ACKNOWLEDGMENT

Part of this work was supported by the *European Union Horizon 2020* project "BioMOre" (Grant agreement # 642456).

REFERENCES

Anwar, M. A., Iqbal, M., Qamar, M. A., Rehman, M., and Khalid, A. M. (2000). Technical communication: determination of cuprous ions in bacterial leachates and for environmental monitoring. *World J. Microb. Biot.* 16, 135–138. doi: 10.1023/A:1008978501177

Briand, L., Thomas, H., and Donati, E. (1996). Vanadium (V) reduction in *Thiobacillus thiooxidans* cultures on elemental sulfur. *Biotechnol. Lett.* 18, 505–508. doi: 10.1007/BF00140192

Brock, T. D., and Gustafson, J. (1976). Ferric iron reduction by sulfur- and iron-oxidizing bacteria. *Appl. Environ. Microbiol.* 32, 567–571.

Colmer, A. R., Temple, K. L., and Hinkle, M. E. (1950). An iron-oxidizing bacterium from the acid drainage of some butiminous coal mines. *J. Bacteriol.* 59, 317–328.

Cummings, D. E., Fendorf, S., Singh, N., Sani, R. K., Peyton, B. M., and Magnuson, T. S. (2007). Reduction of Cr(VI) under acidic conditions by the facultative Fe(III)-reducing bacterium *Acidiphilium cryptum*. *Environ. Sci. Technol.* 41, 146–152. doi: 10.1021/es061333k

DiSpirito, A. A., and Tuovinen, O. H. (1982). Uranous ion oxidation and carbon dioxide fixation by *Thiobacillus ferrooxidans*. *Arch. Microbiol* 133, 33–37. doi: 10.1007/BF00943765

Dopson, M. (2016). "Physiological and phylogenetic diversity of acidophilic bacteria," in *Acidophiles: Life in Extremely Acidic Environments*, eds R. Quatrini and D. B. Johnson (Haverhill: Caistor Academic Press), 79–92.

Dopson, M., and Johnson, D. B. (2012). Biodiversity, metabolism and applications of acidophilic sulfur- metabolizing micro-organisms. *Environ. Microbiol.* 14, 2620–2631. doi: 10.1111/j.1462-2920.2012.02749

Galleguillos, P. A., Hallberg, K. B., and Johnson, D. B. (2009). Microbial diversity and genetic response to stress conditions of extremophilic bacteria isolated from the Escondida copper mine. *Adv. Mat. Res.* 71-73, 55–58.

Hallberg, K. B., Thompson, H. E. C., Boeselt, I., and Johnson, D. B. (2001). "Aerobic and anaerobic sulfur metabolism by acidophilic bacteria," in *Biohydrometallurgy: Fundamentals, Technology and Sustainable Development*, eds V. S. T. Ciminelli and O. Garcia Jr. (Amsterdam: Elsevier), 423–431.

Hedrich, S., and Johnson, D. B. (2013a). Aerobic and anaerobic oxidation of hydrogen by acidophilic bacteria. *FEMS Microbiol. Lett.* 349, 40–45.

Hedrich, S., and Johnson, D. B. (2013b). *Acidithiobacillus ferridurans*, sp. nov.; an acidophilic iron-, sulfur- and hydrogen-metabolizing chemolithotrophic *Gammaproteobacterium*. *Int. J. Syst. Evol. Microbiol.* 63, 4018–4025. doi: 10.1099/ijs.0.049759-0

Johnson, D. B., and Aguilera, A. (2015). "The microbiology of extremely acidic environments," in *Manual of environmental microbiology*, 4th Edn, eds M. V. Yates, H. Cindy, C. H. Nakatsu, R. V. Miller, and S. D. Pillai (New York, NY: ASM Press), doi: 10.1128/9781555818821.ch4.3.1

Johnson, D. B., Grail, B. M., and Hallberg, K. B. (2013). A new direction for biomining: extraction of metals by reductive dissolution of oxidized ores. *Minerals* 3, 49–58. doi: 10.3390/min3010049

Johnson, D. B., Kanao, T., and Hedrich, S. (2012). Redox transformations of iron at extremely low pH: fundamental and applied aspects. *Front. Microbiol.* 3:96. doi: 10.3389/fmicb.2012.00096

Lewis, A. J., and Miller, J. D. A. (1977). Stannous and cuprous ion oxidation by *Thiobacillus ferrooxidans*. *Can. J. Microbiol.* 23, 319–324. doi: 10.1139/m77-047

Lloyd, J. R., Coates, J. D., Williamson, A. J., and Watts, M. P. (2015). "Geomicrobial Interactions with Other Transition Metals (Chromium, Molybdenum, Vanadium, Technetium), Metalloids (Polonium), Actinides (Uranium, Neptunium, and Plutonium) and the Rare Earth Elements," in *Ehrlich's Geomicrobiology*, 6th Edn, eds H. L. Ehrlich, D. K. Newman, and A. Kappler (Boca Raton, FL: CRC Press), 452–476.

Marrero, J., Coto, O., Goldmann, S., Graupner, T., and Schippers, A. (2015). Recovery of nickel and cobalt from laterite tailings by reductive dissolution under aerobic conditions using *Acidithiobacillus* species. *Environ. Sci. Technol.* 9, 6674–6682. doi: 10.1021/acs.est.5b00944

Masaki, Y., Hirajima, T., Sasaki, K., and Okibe, N. (2015). Bioreduction and immobilization of hexavalent chromium by the extremely acidophilic Fe(III)-reducing bacterium *Acidocella aromatica* strain PFBC. *Extremophiles* 19, 495–503. doi: 10.1007/s00792-015-0733-6

Masaki, Y., Tsutsumi, K., Hirano, S., and Okibe, N. (2016). Microbial community profiling of the Chinoike Jigoku ("Blood Pond Hell") hot spring in Beppu, Japan: isolation and characterization of Fe(III)-reducing *Sulfolobus* sp. strain GA1. *Res. Microbiol.* 167, 595–603. doi: 10.1016/j.resmic.2016.04.011

Matocha, C. J., Karathanasis, A. D., Rakshit, S., and Wagner, K. M. (2005). Reduction of copper (II) by iron (II). *J. Environ. Qual.* 34, 1539–1546. doi: 10.2134/jeq2005.0002

Ňancucheo, I., and Johnson, D. B. (2012). Selective removal of transition metals from acidic mine waters by novel consortia of acidophilic sulfidogenic bacteria. *Microb. Biotechnol.* 5, 34–44. doi: 10.1111/j.1751-7915.2011.00285.x

Ňancucheo, I., Rowe, O. F., Hedrich, S., and Johnson, D. B. (2016). Solid and liquid media for isolating and cultivating acidophilic and acid-tolerant sulfate-reducing bacteria. *FEMS Microbiol. Lett.* 363, fnw083. doi: 10.1093/femsle/fnw083

Nielsen, A. M., and Beck, J. V. (1972). Chalcocite oxidation and coupled carbon dioxide fixation by *Thiobacillus ferrooxidans*. *Science* 175, 1124–1126. doi: 10.1126/science.175.4026.1124

Norris, P. R., Barr, D. W., and Hinson, D. (1988). "Iron and mineral oxidation by acidophilic bacteria: affinities for iron and attachment to pyrite," in *Biohydrometallurgy: Proceedings of the International Symposium, Warwick*, eds P. R. Norris and D. P. Kelly (Kew: Science and Technology Letters), 43–59.

Norris, P. R., and Ingledew, W. J. (1992). "Acidophilic bacteria: adaptations and applications," in *Molecular biology and biotechnology of extremophiles*, eds R. A. Herbert and R. J. Sharp (Glasgow: Blackie), 115–142.

Okibe, N., Maki, M., Nakayama, D., and Sasaki, K. (2016). Microbial recovery of vanadium by the acidophilic bacterium, *Acidocella aromatica*. *Biotechnol. Lett.* 38, 1475–1481. doi: 10.1007/s10529-016-2131-2

Phesatcha, T., Worawirunwong, W., and Rohrer, J. (2012). *Separation of chromium (III) and chromium (VI) by ion chromatography*. Waltham, MA: Thermo Fisher Scientific Inc.

Pronk, J. T., and Johnson, D. B. (1992). Oxidation and reduction of iron by acidophilic bacteria. *Geomicrobiol. J.* 10, 153–171. doi: 10.1080/01490459209377918

Rawlings, D. E., Tributsch, H., and Hansford, G. S. (1999). Reasons why '*Leptospirillum*'-like species rather than *Thiobacillus ferrooxidans* are the dominant iron-oxidizing bacteria in many commercial processes for the biooxidation of pyrite and related ores. *Microbiology* 145, 5–13. doi: 10.1099/13500872-145-1-5

Sand, W. (1989). Ferric iron reduction by *Thiobacillus ferrooxidans* at extremely low pH values. *Biogeochemistry* 7, 195–201. doi: 10.1007/BF00004217

Sandoval Ponce, J., Moinier, D., Byrne, D., Amouric, A., and Bonnefoy, V. (2012). *Acidithiobacillus ferrooxidans* oxidizes ferrous iron before sulfur likely through transcriptional regulation by the global redox responding RegBA signal transducing system. *Hydrometallurgy* 12, 187–194. doi: 10.1016/j.hydromet.2012.07.016

Steudel, R., Holdt, G., Göbel, T., and Hazeu, W. (1987). Chromatographic separation of higher polythionates SnO62- (n = 3. . .22) and their detection in cultures of *Thiobacillus ferrooxidans*; molecular composition of bacteria sulfur secretions. *Angewandte Chemie (English international edition)* 26, 151–153. doi: 10.1002/anie.198701511

Stookey, L. L. (1970). Ferrozine—a new spectrophotometric reagent for iron. *Anal. Chem.* 42, 779–781. doi: 10.1021/ac60289a016

Sugio, T., Hirayama, K., Inagaki, K., Tanaka, H., and Tano, T. (1992). Molybdenum oxidation by *Thiobacillus ferrooxidans*. *Appl. Environ. Microbiol.* 58, 1768–1771.

Sugio, T., Tsujita, Y., Hirayama, K., Inagaki, K., and Tano, T. (1988a). Mechanism of tetravalent manganese reduction with elemental sulfur by *Thiobacillus ferrooxidans*. *Agricult. Biol. Chem.* 52, 185–190. doi: 10.1271/bbb1961.52.185

Sugio, T., Tsujita, Y., Katagiri, T., Inagaki, K., and Tano, T. (1988b). Reduction of Mo^{6+} with elemental sulfur by *Thiobacillus ferrooxidans*. *J. Bacteriol.* 170, 5956–5959. doi: 10.1128/jb.170.12.5956-5959.1988

Sugio, T., Tsujita, Y., Inagaki, K., and Tano, T. (1990). Reduction of cupric ions with elemental sulphur by *Thiobacillus ferrooxidans*. *Appl. Environ. Microbiol.* 56, 693–696.

Tandon, R. K., Crisp, P. T., and Ellis, J. (1984). Effect of pH on chromium (VI) species in solution. *Talanta* 31, 227–228. doi: 10.1016/0039-9140(84)80059-4

Tuovinen, O. H., Puhakka, J., Hiltunen, P., and Dolan, K. M. (1985). Silver toxicity to ferrous iron and pyrite oxidation and its alleviation by yeast extract in

cultures of *Thiobacillus ferrooxidans*. *Biotechnol. Lett* 7, 389–394. doi: 10.1007/BF01166209

Welham, N. J., Malatt, K. A., and Vukcevic, S. (2000). The effect of solution speciation on iron-sulphur-arsenic-chloride systems at 298 K. *Hydrometallurgy* 57, 209–223. doi: 10.1039/c6dt04221j

Yarzabal, A., Appia-Ayme, C., Ratouchniak, J., and Bonnefoy, V. (2004). Regulation of the expression of the *Acidithiobacillus ferrooxidans* rus operon encoding two cytochromes c, a cytochrome oxidase and rusticyanin. *Microbiology* 150, 2113–2123. doi: 10.1099/mic.0.26966-0

Conflict of Interest Statement: The authors declare that the research was conducted in the absence of any commercial or financial relationships that could be construed as a potential conflict of interest.

frontiers in Microbiology

ORIGINAL RESEARCH
published: 20 December 2016
doi: 10.3389/fmicb.2016.02044

Quantitative Monitoring of Microbial Species during Bioleaching of a Copper Concentrate

Sabrina Hedrich[1], Anne-Gwenaëlle Guézennec[2], Mickaël Charron[2], Axel Schippers[1] and Catherine Joulian[2]*

[1] Resource Geochemistry, Federal Institute for Geosciences and Natural Resources, Hannover, Germany, [2] Bureau de Recherches Géologiques et Minières, Orléans, France

Monitoring of the microbial community in bioleaching processes is essential in order to control process parameters and enhance the leaching efficiency. Suitable methods are, however, limited as they are usually not adapted to bioleaching samples and often no taxon-specific assays are available in the literature for these types of consortia. Therefore, our study focused on the development of novel quantitative real-time PCR (qPCR) assays for the quantification of *Acidithiobacillus caldus, Leptospirillum ferriphilum, Sulfobacillus thermosulfidooxidans*, and *Sulfobacillus benefaciens* and comparison of the results with data from other common molecular monitoring methods in order to evaluate their accuracy and specificity. Stirred tank bioreactors for the leaching of copper concentrate, housing a consortium of acidophilic, moderately thermophilic bacteria, relevant in several bioleaching operations, served as a model system. The microbial community analysis via qPCR allowed a precise monitoring of the evolution of total biomass as well as abundance of specific species. Data achieved by the standard fingerprinting methods, terminal restriction fragment length polymorphism (T-RFLP) and capillary electrophoresis single strand conformation polymorphism (CE-SSCP) on the same samples followed the same trend as qPCR data. The main added value of qPCR was, however, to provide quantitative data for each species whereas only relative abundance could be deduced from T-RFLP and CE-SSCP profiles. Additional value was obtained by applying two further quantitative methods which do not require nucleic acid extraction, total cell counting after SYBR Green staining and metal sulfide oxidation activity measurements via microcalorimetry. Overall, these complementary methods allow for an efficient quantitative microbial community monitoring in various bioleaching operations.

Keywords: quantitative real-time PCR, bioleaching, community monitoring, *Acidithiobacillus*, *Leptospirillum*, *Sulfobacillus*

OPEN ACCESS

Edited by:
Thulani Peter Makhalanyane, University of Pretoria, South Africa

Reviewed by:
Jeannette Marrero-Coto, Leibniz University of Hanover, Germany
Mark Dopson, Linnaeus University, Sweden
William Nyasha Mavengere, Stellenbosch University, South Africa

****Correspondence:***
Sabrina Hedrich
sabrina.hedrich@bgr.de

Specialty section:
This article was submitted to Extreme Microbiology, a section of the journal Frontiers in Microbiology

Received: *30 September 2016*
Accepted: *05 December 2016*
Published: *20 December 2016*

Citation:
Hedrich S, Guézennec A-G, Charron M, Schippers A and Joulian C (2016) Quantitative Monitoring of Microbial Species during Bioleaching of a Copper Concentrate. Front. Microbiol. 7:2044. doi: 10.3389/fmicb.2016.02044

INTRODUCTION

Bioleaching, the extraction of metals by means of microorganisms, is nowadays a well-established process and an economic alternative to conventional roasting or pressure oxidation techniques for sulfidic low-grade ores. This environmental-friendly and low cost technology becomes especially important in the current context, where mineral resources are becoming more complex and

of lower grade. In order to enhance the application spectrum and improve the bioleaching performance, fundamental research is required to understand the process and optimize operating parameters.

Bioleaching performance is mainly driven by the colonization of the ore by adapted microbial species and their subsequent activity which is influenced by process parameters such as, e.g., agitation/aeration rates, nutrient medium composition and carbon dioxide enrichment. Accurate monitoring of the microbial bioleaching community is therefore essential for process control and to enhance the leaching efficiency, as well as to understand the microbiological aspects of the process as a key factor to design and operate a bioleaching system.

In recent years, rapid advances especially in tools for molecular microbial ecology have emerged and various techniques to monitor the microbial community in bioleaching processes are available (e.g., Johnson and Hallberg, 2007). They comprise culture-dependent (plating, MPN counts) and biomolecular approaches such as the genetic fingerprinting techniques, terminal restriction fragment length polymorphism (T-RLFP; Wakeman et al., 2008), capillary electrophoresis single-strand conformation polymorphism (CE-SSCP; Foucher et al., 2003), denaturating gradient gel electrophoresis (DGGE; Demergasso et al., 2005; Halinen et al., 2009), microscopic methods like fluorescence *in situ* hybridization (FISH and CARD-FISH, Schippers et al., 2008), microarray approaches (e.g., Garrido et al., 2008; Remonsellez et al., 2009), quantitative real-time PCR (qPCR; Liu et al., 2006; Zhang et al., 2009), and next generation sequencing techniques (e.g., Cardenas et al., 2016).

Depending on the process and nature of the samples, suitable methods are, however, limited as parameters such as low sample amount (combined with low cell numbers of, e.g., autotrophic leaching organisms), the presence of particles, low pH and high concentrations of metals often negatively influence adequate implementation of the analysis.

When applying molecular analysis, efficient nucleic acid extraction is key to subsequent quantification of all microorganisms in the sample. Also low pH and high metal content can inhibit nucleic acid extraction and downstream processing such as polymerase chain reaction (PCR) and often pre-treatment of the sample is required. Furthermore, detachment of cells from particles and disruption of biofilms are critical when extracting nucleic acids from bioleaching samples (e.g., Zammit et al., 2011).

Species-specific (semi-)quantification can be achieved by various molecular methods, e.g., T-RFLP, CE-SSCP, or qPCR. While T-RFLP and CE-SSCP represent semi-quantitative methods based on PCR, qPCR is currently the most common method for quantitative microbial community monitoring. Even so qPCR is widely used and numerous assays have been described in the literature for the quantification of total bacteria, archaea, and special groups of microorganisms, there is only a limited number of assays published for bioleaching organisms (e.g., Liu et al., 2006; Remonsellez et al., 2009; Zhang et al., 2009). When searching for appropriate assays to monitor a defined bioleaching community it was found that most of these assays do not target the desired species or are not specific enough for quantification on species-level.

Quantification of cell abundances can also be achieved by microscopy-based approaches such as fluorescence *in situ* hybridization (FISH), catalyzed-reporter-deposition FISH (CARD-FISH), and total cell counts by SYBR Green staining. These methods often suffer from issues such as low cell numbers, cell attachment to particles and auto-fluorescence of these particles. These methods are greatly affected by the acidic pH and elevated metal concentrations which influence the binding properties of the DNA stain and lower the fluorescence signal intensity. Therefore, it is often difficult to stain the cells properly and to differentiate between living organisms and particles.

This study aims to develop and evaluate a selection of molecular methods to monitor the microbial community in bioleaching operations in order to define specific, quick, and reliable methods to be applied in further monitoring studies. In particular, our investigations focus on the quantification of microorganisms at species level *via* qPCR and comparison with T-RFLP and CE-SSCP data. Further focus is on the application and improvement of total cell counting assays for the bioleaching samples. In addition, microcalorimetric bioleaching activity measurements (Rohwerder et al., 1998) are provided for comparison. The model system in our study is a bioreactor set up for the bioleaching of copper concentrate which has been applied in previous studies before and houses a specially adapted microbial consortium proven very efficient for the bioleaching of this material (Spolaore et al., 2011).

MATERIALS AND METHODS

Microorganisms, Media, and Growth Conditions

The bioleaching culture used was the KCC consortium successfully applied in previous Cu concentrate bioleaching experiments containing *Leptospirillum ferriphilum, Sulfobacillus benefaciens, Sulfobacillus thermosulfidooxidans,* and *Acidithiobacillus caldus* (Spolaore et al., 2011). The consortium was routinely kept on 3% Cu concentrate in basal salt medium pH 1.8 (Wakeman et al., 2008) at 42°C, which served as inoculum for this study.

Pure cultures of each strain were grown in shake flasks containing basal salts pH 1.8–2.0 supplemented with 10 mM ferrous sulfate (*L. ferriphilum*) or 1% sulfur (sulfobacilli and *A. caldus*). The ferrous sulfate solution was filter-sterilized (0.1 μm) and the sulfur used was sterilized by tyndallization.

Batch Bioleaching Reactor

Batch bioleaching reactors operated with the described acidophilic consortium served as model system for microbial monitoring studies. In order to adapt the microorganisms to the mineral and higher solid loads and to achieve maximum metal bioleaching, the experiments followed a 5-step adaptation protocol:

(1) cultivation in shake flasks with 3% solid load for about 2 weeks;
(2) transfer of this culture to a 2 L bioreactor with 5% solid load for one week;
(3) transfer to a 2 L bioreactor with 10% solid load;
(4) repeat step 3;
(5) final bioleaching step in three parallel 2 L bioreactors with 10% solid load.

The experiments of step 3−5 were terminated when copper dissolution reached a plateau approximately between day 6 and 8. At this point the cultures were immediately transferred to the next step to start a new bioreactor run.

Bioleaching experiments were conducted in 2 L temperature-controlled (42°C), stirred batch bioreactors (Electrolab, UK). The reactors were fully baffled and agitation was performed using a dual impeller system consisting of a standard 6-blade Rushton turbine in combination with a 6-blade 45° axial flow impeller with speed set at 400 rpm. Tests were carried out at 5−10% (w/v) solid load and an initial acidification of the pulp with sulfuric acid to about pH 2.0 (acid consumption of 182.3 g H_2SO_4/kg). Inoculation was performed by adding 200 mL of the above described culture at 0.5 days after initial acidification of the material. The bioreactors were sparged with air at 120 L/h. Each experiment was carried out in triplicate and copper dissolution and kinetics during bioleaching was followed. The material used was a copper concentrate originating from a black shale ore and was supplied by the company KGHM (Poland). The concentrate had a particle size of <90 μm and had the following main characteristics: 13.3% Cu, 9.4% Fe, 16.5% S, 1.1% total inorganic carbon and 9.1% total organic carbon.

Chemical Analysis

Daily pH (Blueline 18 pH electrode, Schott, Germany) and redox (BlueLine 31 Rx electrode, Schott, Germany) measurements on bioreactor runs were carried out directly in the pulp. The measured redox values were corrected to the standard hydrogen electrode and reported as E_h. Ferrous and ferric iron concentrations were measured in 0.45 μm-filtered samples using Ferrozine (Lovley and Phillips, 1987). Dissolved metals were regularly determined in filtered, acidified samples using ICP-OES or atomic absorption spectroscopy (Varian SpectrAA-300). At the end of bioleaching step 5, the residue was completely harvested from the three bioreactors, washed with acidified (pH 1.5) water and dried before performing digestion with nitric acid following analysis of the metals by ICP-OES or atomic absorption spectroscopy.

Nucleic Acid Extraction and Quantification

For DNA extraction, 2−5 mL of homogeneous slurry samples were regularly taken from the bioreactors and centrifuged for 20 min at 13,000 × *g*, and the pellet was washed twice with 10 mM Tris buffer, pH 8. DNA extraction was achieved by using the FastDNA Spin Kit for Soil (MP Biomedicals) according to a modified protocol (Webster et al., 2003). Concentration of DNA extracts, as well as of PCR products and plasmids, was determined by measuring absorbance at 260 nm in a FoodALYT photometer (Omnilab) equipped with a Hellma Tray cell (Hellma Anlytics) or in a Quantus fluorometer (Promega).

Quantitative Real-Time PCR

Primer Design

For the design of specific primers, full length 16S rRNA gene sequences of the target strains (NR_044352, AF356829, NR_040945, Z29975) and also 40 other sequences from various strains of each species and related organisms were downloaded from NCBI and aligned using Clustal X in Mega 6.0 (Tamura et al., 2013). Primers were selected by manual search for variable regions in the 16S rRNA gene sequence of each species which was most likely different from the other species in the alignment. Selected primers (**Table 1**) were finally checked *via in silico* PCR using AmplifX (version 1.7.0; Jullien, 2013).

qPCR Quantification and Thermocycling

Quantitative real-time-PCR was applied in two laboratories (BGR, Hannover, Germany and BRGM, Orleans, France) to quantify total bacteria (Nadkarni et al., 2000) and specific bioleaching species (**Table 1**) by targeting their 16S rRNA genes. Extracted DNA was amplified by qPCR using the devices StepOne™ (Applied Biosystems) or CFX Connect (BioRad). Master mixes from the companies Applied Biosystems™ (for SYBR green assays at BGR), Quanta Biosciences Inc. (TaqMan® assays at BGR), or BioRad (SYBR assays at BRGM) were used. Reactions were performed in a total volume of 10 μL containing 1X master mix, 0.5 μM each primer and different concentrations of DNA. Each DNA extract was measured in duplicate or

TABLE 1 | Designed primers for the quantification by qPCR of bacterial species of the KCC consortium.

Target	Name	Sequence (5′→3′)	Product size (bp)
Acidithiobacillus caldus	Acaldus_F	CGGATCCGAATACGGTCTG	396
	Acaldus_PC1_RC*	TCAGCACCTAAGGCGCCAA	
Leptospirillum ferriphilum	Lfp392F	GAAGGCTTTCGGGTTGTAAACCAC	210
	Lfp601R	TTAAGCCACGGCCTTTCACCAA	
Sulfobacillus thermosulfidooxidans	St_F	TGTCGTGAGATGTTGGGTTAG	225
	St_R	AGATCCCGTTTGAAGGATTGG	
Sulfobacillus benefaciens	Sb1030F	CAGCTCGTGTCGTGAGATGT	236
	Sb1265R	ACTGAGGATCCGTTTGCGG	

*Modified from Liu et al. (2006).

triplicate in at least two 10-fold dilutions to check for PCR inhibition. Purified 16S rRNA gene PCR products of pure strains or linearized plasmids carrying a target 16S rRNA gene were used as standards for qPCR. A seven-point serial decimal dilution of the respective standard was run in duplicate or triplicate with each set of reactions to generate the standard curve of C_t (threshold cycle) versus the number of gene copies.

A temperature gradient was applied to determine the optimal annealing temperature for each primer pair. Final cycling conditions were an initial denaturation at 95°C for 10 min, 30 or 40 cycles of denaturation at 95°C for 15 s and annealing/elongation for 30 s at 60°C. Melt curves were constructed after each qPCR run with the following parameters: one cycle of 95°C for 15 s and 60°C for 1 min followed by temperature ramping up to 95°C in increments of 0.3°C.

Assay Validation and Specificity Test

The specificity of each primer pair for the target species was evaluated from the efficiency and melt curves of the qPCR assays. The amplification products were furthermore analyzed on an agarose gel to confirm the absence of unspecific products. Species specificity of primers was checked by using genomic and plasmid DNA of *S. benefaciens*, *S. thermsosulfidooxidans*, *S. acidophilus, L. ferriphilum, L. ferrooxidans, A. caldus, A. thiooxidans, A. ferridurans, A. ferrivorans, A. ferriphilus*, and *A. ferrooxidans* as template with each primer set to ensure that there was no cross-reactivity. If no signal and amplification product was detected in the qPCR curves and on the agarose gel for the other species the assay was classified as specific for the target species. The assays were then tested on various bioreactor samples which had previously been analyzed with other quantitative methods.

T-RFLP Monitoring

Amplification of a 900 bp fragment of the 16S rRNA gene for T-RFLP analysis from DNA extracts was achieved using DreamTaq PCR Master Mix (Thermo Fisher) and a Cy5-labeled 8F forward primer (Frank et al., 2007) and 907R (Muyzer et al., 1995) as described previously (Okibe et al., 2003). Up to 4 μL of PCR product were digested in a 10 μL reaction with 1 U of the restriction endonuclease HaeIII (Thermo Scientific) and 1 μL appropriate buffer. The reactions were incubated at 37°C for 2-3 h. Terminal restriction fragments (T-RFs) were analyzed on a capillary sequencer (Beckman Coulter, GenomeLab GeXP Genetic Analysis System) using a 600 bp size standard and identified by reference to the databank of acidophilic microorganisms held at BGR (including the T-RFs of the species within the bioleaching consortium). Relative abundances of T-RFs were calculated on the basis of peak areas.

CE-SSCP Monitoring

Amplification of a 200 bp fragment of the 16S rRNA gene for CE-SSCP analysis from DNA extracts was achieved using GoTaq polymerase PCR mix (Promega) and the w49 forward primer and the 5′-end FAM-labeled w34 primer (Foucher et al., 2003). One microliter of 10- to 50-fold diluted PCR product and 0.2 μL of Genescan-600 LIZ internal standard (Applied Biosystems) were heat denatured in deionized formamide (Applied Biosystems), and immediately cooled on ice. Fragment analyses were performed on an ABI Prism 310 genetic analyser using the non-denaturing CAP polymer (Applied Biosystems). Raw data analyses and assignment of peak position were done with the software GeneScan (Applied Biosystems) and relative abundances were calculated on the basis of peak areas.

SYBR Green Staining of Slurry Samples from Bioleaching Reactors

Slurry samples from the bioreactors were either processed directly or fixed in 4% formaldehyde and stored at 4°C until further processing. SYBR Green staining for total cell numbers was carried out according to Lunau et al. (2005) following homogenization of the samples by ultrasonic treatment (20 s, 20 cycles, 20% intensity). After appropriate dilution, the sample was applied onto a membrane filter (Whatman Nucleopore, $d = 25$ mm, 0.2 μm pore size). To enhance the visibility of the cells and avoid interactions with the metals and particles the following treatments were tested:

(i) Washing with acidified (pH 1.8) basal salts medium to remove metals and remaining iron to avoid precipitation of ferric iron during TE buffer treatment (higher pH)
(ii) Treatment with 0.05% Triton X to detach cells and allow homogenous distribution of the sample on the filter
(iii) Treatment with 0.1% Tween 20 to detach cells and allow homogenous distribution of the sample on the filter

Each pre-treatment step was followed by rinsing with TE buffer in order to reach the appropriate neutral pH again for SYBR Green staining. Afterward the filter was put onto a microscopic slide and covered with 20 μL staining solution (6% SYBR Green, 7% Mowiol, 1% ascorbic acid) before counting cells under the microscope.

All treatment methods were performed in triplicate on at least three independent bioleaching samples to validate the method. Cell numbers were determined for each sample by counting across the whole filter area and at least 50 fields of view.

Microcalorimetry

Microcalorimetric measurements were carried out at the beginning and end of each experiment in order to determine the activity of the cultures on the concentrate (Schippers and Bosecker, 2005). Therefore 1 mL of the pulp was put into a 4 mL glass ampoule and the supernatant was removed after 5 min of settling. The ampoule was sealed and the heat output measured in a TAM III microcalorimeter (TA Instruments) at 42°C. Samples were measured in triplicate for about 12 h. The weight of the residue before the experiment and the dry weight afterward were determined in order to calculate the heat output per gram solids. Chemical control experiments were conducted with the same set up.

Statistical Analysis

Statistical analyses were run to compare for one species the ratio determined by qPCR and the ratio determined by CE-SSCP or T-RFLP. Differences were determined with a nonparametric Kruskal−Wallis test with $\alpha = 0.05$, using the XLSTAT software.

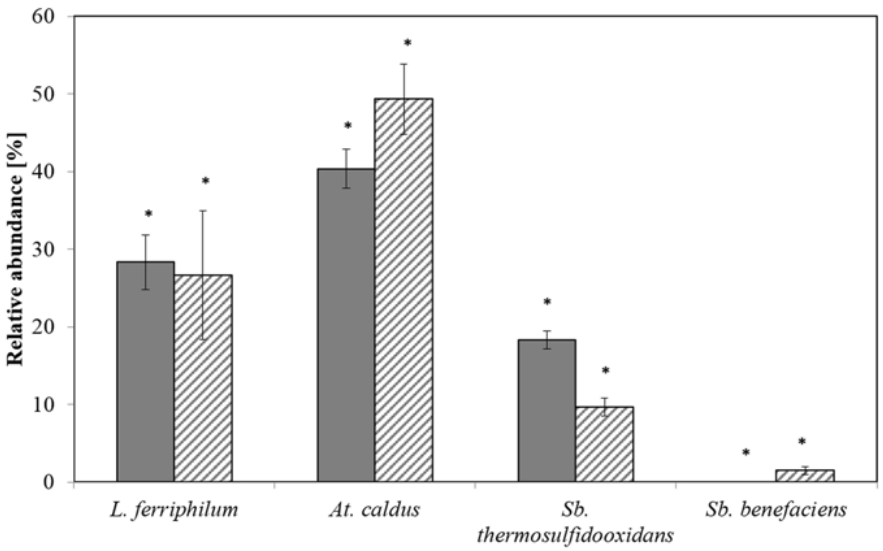

FIGURE 1 | Relative abundances of the dominant bioleaching species at step 5 as determined by T-RFLP (plain) and qPCR (hatched). Data are mean values of triplicates ±SD. Asterisk above the plots indicate no significant difference between T-RFLP and qPCR results (Kruskal–Wallis-Test, $p < 0.005$).

RESULTS

Development of Quantitative Real-Time PCR Assays

Novel qPCR assays targeting the four species relevant in our bioleaching experiments (*A. caldus, L. ferriphilum, S. thermosulfidooxidans, S. benefaciens*) were especially designed for this study. Melt curve analysis proved the specificity of the designed assays for the target species. Only the *L. ferriphilium* assay yielded an amplification product with *L. ferrooxidans* DNA but all of the other assays were clearly species-specific, as also confirmed by gel electrophoresis. Different concentrations of DNA were tested to establish the detection limit with linear calibration curves being obtained over seven orders of magnitudes ranging from 10^3-10^9 16S rRNA gene copies. All four designed qPCR assays reached appropriate amplification efficiencies (≧94%) and r^2 values of 0.99. The precision of the assays was measured by calculating the variation in C_t values across three replicate samples, and an average standard deviation of less than 0.16 units proved the reproducibility of the real-time PCR assays. Successful application of the novel qPCR assays was confirmed at BGR and BRGM by using different qPCR machines, master mixes, and application to various DNA extracts of bioleaching samples.

Comparison of Different Molecular Monitoring Methods

T-RFLP and CE-SSCP fingerprinting analyses were performed on the same DNA extracts as used for qPCR and the quantitative data gained, expressed as relative abundance of a defined species in the total bacterial community, were compared to evaluate the most accurate and efficient method. All three methods gave the same trend for the relative abundance of the different species.

Relative abundances measured by qPCR and T-RFLP yielded to similar results for each of the species *L. ferriphilum*, *A. caldus*, and *S. thermosulfidooxidans*, with no significant differences detected by a Kruskal-Wallis test ($p < 0.005$; **Figure 1**). The abundance of *S. benefaciens* was usually below the detection limit for T-RFLP analysis (**Figure 1**), while qPCR succeeded to detect this species even if only present in minor amounts (<8%); again, differences were not significant (Kruskal–Wallis test $p < 0.005$; **Figure 1**).

CE-SSCP allowed the detection of all the four target species, and a reasonable correlation between CE-SSCP and qPCR was found (**Figure 2**). But species-specific qPCR showed usually slightly lower relative abundances than the ones deduced from CE-SSCP profiles. However, as obtained for T-RFLP and qPCR results, differences were not found to be significant (Kruskal–Wallis test $p < 0.005$).

Total Bacterial Counts Using SYBR Green Staining

When using the standard SYBR Green staining protocol as described by Lunau et al. (2005) for monitoring total cell numbers during bioleaching, we found an inhomogeneous distribution of the cells which was mostly due to cell attachment to particles and formation of clusters on the filter. The cells were visible in two levels of focusing as some were overlapping. Also a very fast fading of the fluorescent signal made it almost impossible to count the cells. Therefore, we tested three different pre-treatment methods with the aim to improve the fluorescent signal as well as the distribution of the cells on the filter.

While washing the samples with acidified basal salt medium did not improve the SYBR Green staining method, pre-treatment with detergents made a change. Treatment with 0.05% Triton X

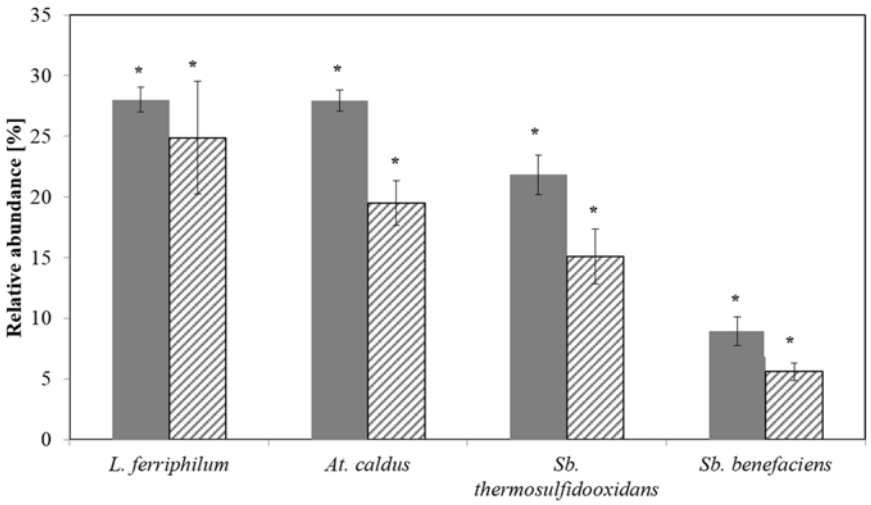

FIGURE 2 | Relative abundances of the dominant bioleaching species at step 5 as determined by CE-SSCP (plain) and qPCR (hatched). Data are mean values of triplicates ±SD. Asterisk above the plots indicate no significant difference between CE-SSCP and qPCR results (Kruskal–Wallis-Test, $p < 0.005$).

led to a much better microscopic image, the sample distribution was more homogeneous, and cells did not overlap and were better visible. One disadvantage was that the fluorescence signal was very strong and the background too, however, the contrast improved after a few minutes under the microscope. Also the cells and particles seemed somehow swollen, lower concentrations of Triton X did not overcome this side effect.

The pre-treatment with Tween 20 resulted in a better microscopic observation with a homogeneous distribution of the cells on the filter which allowed more accurate cell counting. Cell numbers were equal to the pre-treatment with Triton X but no side effects were visible when using Tween 20. Thus, for further SYBR Green staining and total cell counts of such bioleaching samples the Tween 20 pre-treatment was selected.

Monitoring of Bioleaching Reactors

Batch bioreactors housing the KCC consortium of moderately thermophilic and acidophilic bacteria utilized for bioleaching of a copper concentrate served as model system for microbial monitoring studies with the aim of evaluating the selected monitoring methods. Several experiments with the same set up were conducted in order to generate various samples for comparative microbial community studies. Besides detailed molecular monitoring only the chemical results of one standard experiment are reported.

Physico-Chemical Parameters

Each bioleaching experiment was started by adding sulfuric acid to the medium after adding the ore and before inoculation. The acid neutralized most of the carbonates and kept the pH below 2.0 instead of the initial pH 4.1 to avoid inhibition of the acidophilic bacteria. This already caused some copper and iron dissolution (**Figure 3A**). Solution pH dropped from 2.0 to 1.3 under biological leaching conditions. The redox potential increased from initial 545 mV to about 903 mV during the course of the bioleaching experiment (**Figure 3B**) whereas it remains rather constant in the chemical control experiment.

The kinetics of metal release improved constantly from bioleaching adaptation step 2 to 5 as shown in **Table 2**. The increase in bioleaching activity due to the adaptation procedure could also be noted by a decrease in solution pH and increase in redox potential (data not shown).

The dissolved copper concentration in the medium of bioleaching step 5 strongly increased until day 4 and only increased slightly in the following days to about 14440 mg/L Cu after 10 days (**Figure 3A**). Similar kinetics were observed for iron dissolution with a maximum of 4180 mg/L Fe on day 4 of the bioleaching.

Final copper recovery from the copper concentrate during bioleaching under standard conditions in step 5 was about 94% compared to 53% in chemical control experiments (data not shown). The overall Fe and total S extraction (54 and 62%, respectively) was lower than sulfide (88%) and Cu recovery (94%). In this kind of system Fe and S leaching yields are usually underestimated because of the formation of precipitates (e.g., jarosite, gypsum).

Microbial Community Monitoring Using qPCR

The microbial community in the bioleaching reactors was represented by *L. ferriphilum, A. caldus, S. thermosulfidooxidans*, and *S. benefaciens*. The species *A. caldus and S. thermosulfidooxidans* were dominant at the end of bioleaching steps 2 and 3 and still comprised a major part of the community at steps 4 and 5 (**Figure 4**). The relative abundance of *L. ferriphilum* in the microbial community increased in step 4 and 5 of the experiment making it the key player in these two steps besides *A. caldus* and *S. thermosulfidooxidans*. *S. benefaciens* only represented a minor proportion of the leaching community throughout all bioleaching steps. In some experiments, *S. benefaciens* was even under the detection limit for qPCR

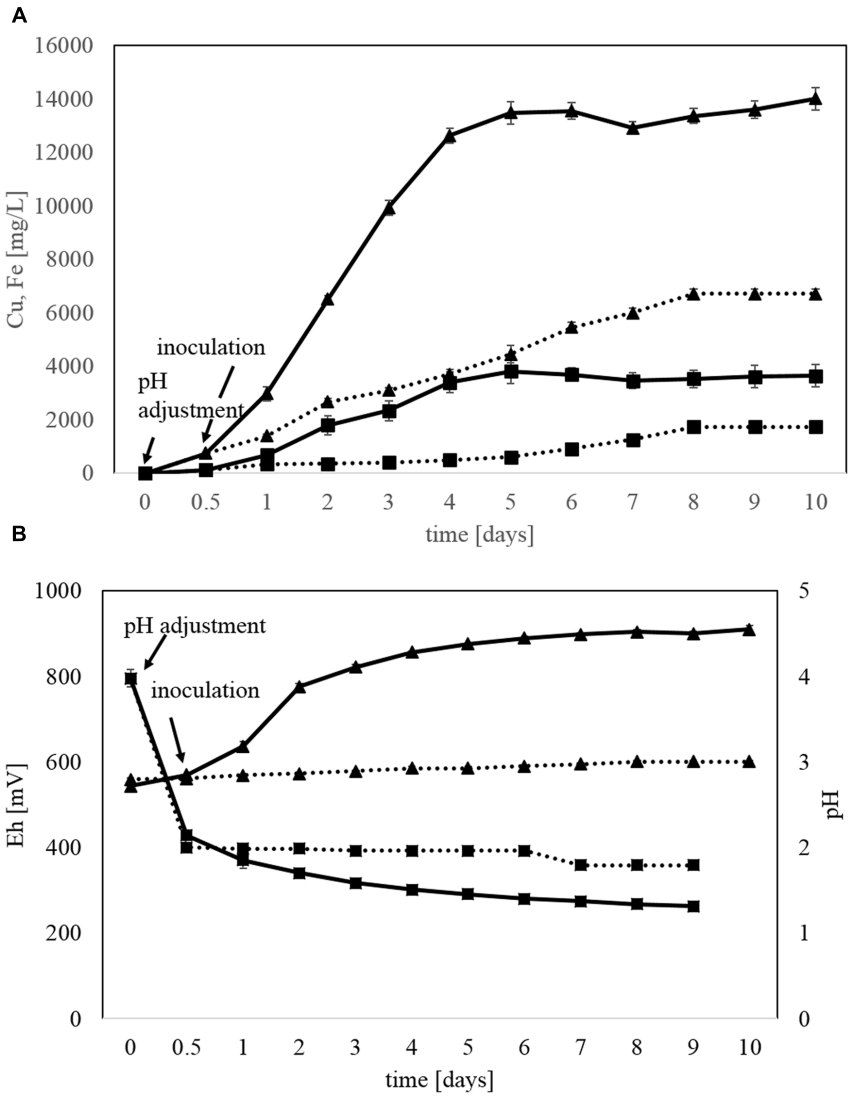

FIGURE 3 | Kinetics of batch bioleaching step 5 in stirred bioreactors with copper concentrate and the acidophilic, moderately thermophilic bioleaching KCC consortium. (A) Copper (triangles) and iron (squares) dissolution in bioleaching (solid line) and chemical (dotted line) experiments. **(B)** pH (squares) and E_h (triangles) in bioleaching (solid line) and chemical (dotted line) experiments. Data are mean values of triplicates ±SD.

TABLE 2 | Improvement of Cu release kinetics between steps 2 and 5 of the adaptation procedure.

Cu leaching rate (mgCu/L/h)			
Step 2	**Step 3**	**Step 4**	**Step 5**
81.2	107.9	116.6	120.2

but could be detected again in later bioleaching steps from the same inoculum (data not shown). There was no pronounced change in community composition between adaptation steps 4 and 5.

Figure 5 shows the monitoring of the microbial community through the course of the experiment in step 5. The iron-oxidizer *L. ferriphilum* dominated the experiment at the beginning and end and was strongly accompanied by the sulfur-oxidizers *A. caldus* and *S. thermosulfidooxidans*. *S. benefaciens* was only present in very low numbers during the whole experiment.

Figure 6 shows the total cell numbers for step 5 using SYBR Green staining in comparison with total cell numbers deduced from bacterial 16S rRNA gene copy numbers determined by qPCR. The later were transferred into cell numbers by taking into account the specific 16S rRNA gene copies of the strains in the KCC consortium. It confirmed an increase in cell numbers over time of the bioleaching experiment from about 10^6 to 10^9 cells/mL. There was no difference between the analyses of samples fixed in formaldehyde and stored at −20°C or samples which were directly processed without formaldehyde fixation. Total cell numbers determined

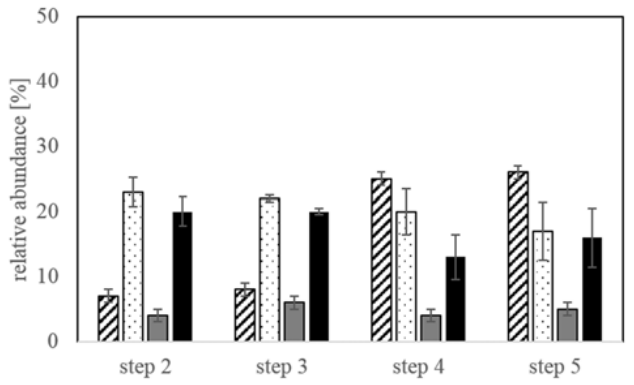

FIGURE 4 | Relative abundance of the four different species (*Leptospirillum ferriphilum*-hatched bars, *Acidithiobacillus caldus*-dotted bars, *Sulfobacillus benefaciens*-gray bars, *Sulfobacillus thermosulfidooxidans*-black bars) in the bioleaching reactors at the end of each bioleaching experiment determined by qPCR. Data are mean values of triplicates ±SD.

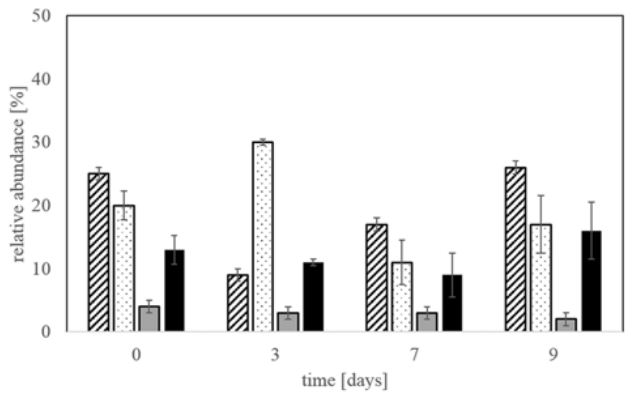

FIGURE 5 | Monitoring of the microbial community in step 5 of triplicate bioleaching experiments using qPCR. *L. ferriphilum*-hatched bars, *A. caldus*- dotted bars, *S. benefaciens*-gray bars, *S. thermosulfidooxidans*-black bars. Data are mean values of triplicates ±SD.

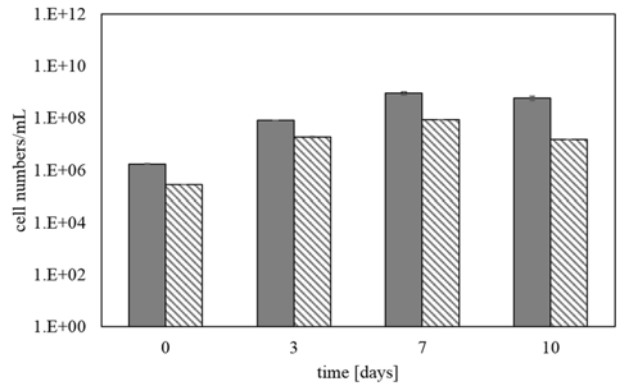

FIGURE 6 | Total cell numbers determined by SYBR Green staining (gray bars) and qPCR (hatched bars) during step 5 of the copper concentrate bioleaching. Error bars represent data from three identical bioreactor runs and triplicate measurements of each.

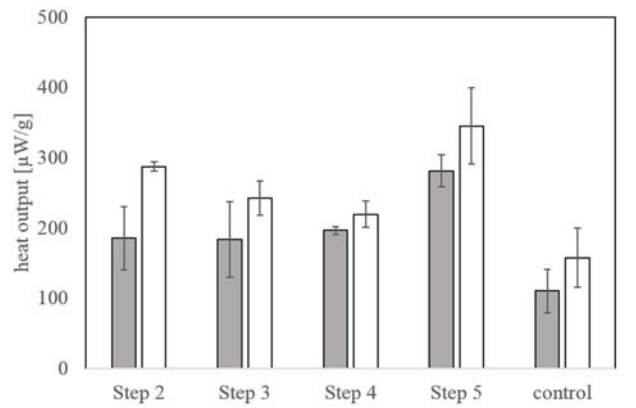

FIGURE 7 | Biological activity as determined by microcalorimetry at the start and end of each bioleaching step at 42°C. The chemical control measurements were conducted with the same set up. Error bars represent 2−3 identical bioleaching tests with triplicate measurements in the microcalorimeter.

by SYBR Green staining and total bacteria via qPCR in **Figure 6** show a strong correlation between the two monitoring methods.

Microcalorimetric Activity Measurements

The biological activity at the beginning of bioleaching steps 2−4 was very similar at about 190 µW/g and increased toward the end of the experiment (**Figure 7**). While the final heat output in step 2 was higher compared to steps 3 and 4, the biological activity reached a maximum in bioleaching step 5 off around 345 µW/g. Overall, the bioleaching activity progressively increased between the bioleaching steps. Heat output measured in the chemical control (**Figure 7**) also increased during the experiment but was always below that of the biological setups.

DISCUSSION

The aim of this study was to develop and evaluate various methods for monitoring bioleaching microbial communities and investigate changes in the microbial community composition and its performance during bioleaching applications. Bioleaching experiments with copper concentrate and the acidophilic, moderately thermophilic KCC consortium in 2 L stirred tank bioreactors following a 5-step adaptation protocol served as a model system for biomining operations in this study.

According to the main aim of this study, we focused on the quantitative monitoring of the microbial community during the bioleaching process. The bioreactor system was inoculated with the mixed KCC culture of the iron-oxidizer *L. ferriphilum*, the sulfur oxidizer *A. caldus* and the iron−sulfur-oxidizing *S. thermosulfidooxidans* and *S. benefaciens*. These organisms are

commonly found in stirred tank operations (Olson et al., 2003; Schippers, 2007; d'Hugues et al., 2008; Spolaore et al., 2011) where they combine autotrophic and mixotrophic growth as well as iron- and sulfur-oxidizing abilities to efficiently carry out bioleaching of sulfide ores. In order to better understand the behavior and role of these organisms in the bioleaching process, a quantitative and species-specific monitoring of each member of the community during the bioleaching process is essential.

We chose to focus on qPCR as it is currently the most common method for quantitative microbial community monitoring. We tested qPCR assays reported in the literature to target *Acidithiobacillus*, *Leptospirillum* and *Sulfobacillus* species (e.g., Liu et al., 2006; Remonsellez et al., 2009; Zhang et al., 2009) and found that most of them were only specific on genus-level or not specific for the desired species (results not shown). Thus we designed new qPCR assays targeting the species of the KCC consortium. The assays were confirmed to be specific for *A. caldus, S. thermosulfidooxidans* and *S. benefaciens* and *L. ferrooxidans/ferriphilum* by carrying out various cross-checks with closely related species and strains. The novel assays were successfully applied to monitor the microbial community during bioleaching in stirred-tank reactors.

The qPCR results were also compared with data from the commonly used molecular fingerprinting methods T-RFLP and CE-SSCP. Both methods are classified as semi-quantitative since they are based on end-point PCR, while qPCR gives accurate quantification and absolute gene copy numbers. Indeed, the very beginning of the amplification is monitored online when the fluorescence intensity is proportional to the copy number of the target gene initially present in the DNA extract (Heid et al., 1996; Wittwer et al., 1997). T-RFLP and CE-SSCP allow relative quantification of all species present in one sample at the same time, since they are based on the amplification of the 16S rRNA gene of the total community, and therefore also allow the detection of previously unexpected species in the community. qPCR requires separate amplification of each taxon using species-specific primers and allows only the quantification of the abundance of the target species or comparison of their relative abundance with the number of total bacteria determined by another assay, but will not detect other unexpected species in a sample. Fingerprinting and qPCR are thus complementary monitoring methods. Even though qPCR is more expensive and time consuming, species-specific quantification is often more accurate and, if the number of gene copies on the genome of the target strain is known, cell numbers can be deduced from a standard reporting known gene copy numbers.

Statistical analysis confirmed that there are no significant differences between the relative abundances of the various species determined by species-specific qPCR and TRFLP or CE-SSCP molecular fingerprints. The data lead to comparable results and trends appeared suitable to monitor bioleaching species abundances in the studied bioleaching reactors. Contrary to molecular fingerprint, qPCR gives also absolute cell numbers, expressed, e.g., as cells per mL of culture, thus data on the multiplication or decline of the number of each species in a reactor. Molecular fingerprinting, however, as it uses universal bacterial primers, may allow the detection of other taxa developing in a reactor, initially not inoculated but introduced by the ore. The specific characteristics of each technique make them complementary and suitable for monitoring bacterial communities in bioleaching processes.

All PCR-based molecular monitoring methods require the extraction of nucleic acids and, as in the presented study when DNA is used, active as well as inactive cells are detected, and therefore no information about the activity status of the microorganisms is determined. However, quantitative monitoring on active cells using the described methods could be achieved by targeting RNA rather than DNA. When running reactors in continuous mode for large-scale bioleaching operation, DNA-based monitoring should also be informative on active cells because of the wash-out of inactive ones.

In complement, we also applied two methods, SYBR Green staining for total cell counting and microcalorimetry, which target whole cells and do not require any extraction of nucleic acids, proteins or lipids. Both methods can be directly applied to the pulp samples and allow a quick and easy monitoring of cell abundance.

For SYBR Green staining of bioleaching pulp samples, a special pre-treatment protocol was established, which greatly improved the quality of the microscopic observation in terms of both the fluorescence intensity and the distribution of the cells on the filter. A constant increase in cell numbers over the experimental time was shown confirming that the cells grew during bioleaching by the oxidation of reduced sulfur compounds and ferrous iron. SYBR Green staining, according to the newly adapted protocol, is therefore a quick and reliable method to monitor and detect changes in the total cell number and therefore indirectly overall bioleaching activity as it has already been routinely used in several other studies (e.g., Schippers et al., 2008). The strong correlation of cell counts determined by SYBR Green staining and those deduced from the total bacteria qPCR assay clearly shows the power and reliability of these two complementary methods for the determination of total cells in bioleaching experiments.

Isothermal microcalorimetry determines the heat output from exothermic chemical reactions and is therefore a tool for microbial activity measurements if the chemical reactions are catalyzed by microorganisms (Braissant et al., 2010). This has shown to be the case for bioleaching, e.g., metal sulfide oxidation by acidophhilic bacteria, and a correlation between heat output and the metal sulfide dissolution rate as well as cell numbers of acidophiles was found for laboratory and environmental samples (Schippers et al., 1995; Rohwerder et al., 1998). In a few cases, microcalorimetry was used for the monitoring of bioleaching operations (Sand et al., 1993) or field experiments for the inhibition of biological metal sulfide oxidation for acid mine drainage prevention (Sand et al., 2007). When determining the biological activity at the beginning (low cell abundance) and end (high cell abundance) of the last bioleaching step in our experiments, the heat output data confirmed that the activity increased during the experiment. Furthermore, an increase of

the activity of the cells between the five bioleaching steps was confirmed, which correlates with the increase in SYBR Green counts as well as in copper dissolution and iron oxidation rate. The heat output measured in the chemical control was most likely due to the acid dissolution of some mineral phases as also confirmed by the copper and iron dissolution data of the chemical control.

Following copper and iron dissolution from the copper concentrate over time confirmed that bacteria strongly catalyzed the bioleaching of the concentrate with a maximum copper dissolution of 94%. Metal bioleaching was enhanced by applying the 5-step adaptation protocol since the bacteria were adapted to the ore and the physico-chemical conditions and were therefore able to achieve maximum performance. Final copper recovery was achieved after about 6−7 days, afterward there was no significant change in soluble metal concentration and pH. Solution pH dropped from about 2.0 at the beginning to 1.3 under biological leaching conditions due to the oxidation of sulfides and formation of sulfuric acid by bacteria. The redox potential increased from initial 545 mV to about 903 mV, mainly caused by the dissolution of ferrous iron and oxidation to ferric iron. The overall Fe (54%) and total S (62%) extraction was lower compared to sulfide (88.3%) and Cu recovery (94%), which is probably due to Fe and sulfate precipitation as jarosite.

The achieved results correlate with earlier reports on this system (Spolaore et al., 2011) where a maximum copper recovery of 95% was achieved after 6.25 days with a similar concentrate and the same laboratory setup. In this work the authors showed that incomplete copper dissolution was mainly due to remaining chalcopyrite in the concentrate which is more recalcitrant to bioleaching than the other copper sulfides.

S. benefaciens was only detected in lower numbers throughout the course of the experiment, but its presence clearly showed that there must be a direct role in the bioleaching process. This example perfectly shows how the bioleaching consortium works together by the sulfur-oxidizer initiating the pH decrease and thereby the bioleaching of metals including copper and ferrous iron and the iron oxidizers later contributing to the bioleaching process by converting ferrous to ferric iron.

Microbial community analysis at the end of each bioleaching step confirmed that *A. caldus* and *S. thermosulfidooxidans* dominated in step 2 and 3 but were overtaken by *L. ferriphilum* in step 4 and 5 of the adaptation procedure. *A. caldus* and *S. thermosulfidooxidans* both oxidize reduced sulfur compounds and thereby generate acidity which was clearly detected as the initial dominant phase in the bioleaching reactors whereas enhanced iron release and oxidation took place after 2–3 days and was more enhanced in later adaptation steps. Therefore, this could be an explanation for the dominance of *L. ferriphilum* in step 4 and 5 of the bioleaching compared to earlier adaptation steps together with the ability of *L. ferriphilum* to thrive at very low pH values and high redox potentials. This again clearly shows that it is necessary to adapt the microorganisms to the ore and increasing solid load to achieve most efficient bioleaching of relevant metals.

This study has enhanced our knowledge and the "toolbox" for the quantitative monitoring of bioleaching operations, by successfully applying four novel qPCR assays for measuring the abundance of common bioleaching species. It confirmed that standard fingerprinting methods and qPCR give similar results, but only when expressed as a relative measure of the abundance as fingerprinting methods cannot determine cell numbers. The additional application of two quick and convenient whole cell methods, SYBR Green staining and microcalorimetry helped to follow changes in cell number and activity during the bioleaching experiment. Altogether, the applied methods are well suited for microbial community monitoring and will help to understand the bioleaching process and react to optimize bioleaching performance.

AUTHOR CONTRIBUTIONS

SH designed the study, conducted, and supervised the experiments at BGR, analyzed the data and wrote the manuscript. A-GG designed and supervised bioleaching experiments and analyzed the data at BRGM and contributed to the manuscript. MC conducted molecular experiments and analysis at BRGM. AS discussed data at BGR and contributed to th manuscript. CJ conducted and analyzed molecular experiments at BRGM and wrote the manuscript together with SH.

FUNDING

This work is part of the collaborative bilateral research project Ecometals co-funded by the German Federal Ministry of Education and Research (BMBF under the grant ID 033RF001) and the French National Research Agency (ANR-13-RMNP-0006).

ACKNOWLEDGMENTS

We thank I. Kruckemeyer and J. Jacob for help in conducting bioleaching experiments, I. Kruckemeyer and D. Frohloff for DNA extraction, qPCR analysis and help with SYBR Green staining. J. Hellal is kindly acknowledged for her expertise on statistical analyses. We also thank F. Bodenan for project coordination at BRGM and KGHM for providing the copper concentrate samples.

REFERENCES

Braissant, O., Wirz, D., Göpfert, B., and Daniels, A. U. (2010). Use of isothermal microcalorimetry to monitor microbial activities. *FEMS Microbiol. Lett.* 303, 1–8. doi: 10.1111/j.1574-6968.2009.01819.x

Cardenas, J. P., Quatrini, R., and Holmes, D. S. (2016). Genomic and metagenomic challenges and opportunities for bioleaching: a mini-review. *Res. Microbiol.* 167, 529–538. doi: 10.1016/j.resmic.2016.06.007

Demergasso, C. S., Galleguillos, P. A., Escudero, L. V., Zepeda, V. J., Castillo, D., and Casamayor, E. O. (2005). Molecular characterization of microbial populations in a low-grade copper ore bioleaching test heap. *Hydrometallurgy* 80, 241–253. doi: 10.1016/j.hydromet.2005.07.013

d'Hugues, P., Joulian, C., Spolaore, P., Michel, C., Garrido, F., and Morin, D. (2008). Continuous bioleaching of a cobaltiferous pyrite in stirred reactors: population dynamics and EPS production vs. bioleaching performances. *Hydrometallurgy* 94, 34–41. doi: 10.1016/j.hydromet.2008.05.045

Foucher, S., Battaglia-Brunet, F., d'Hugues, P., Clarens, M., Godon, J. J., and Morin, D. (2003). Evolution of the bacterial population during the batch bioleaching of a cobaltiferous pyrite in a suspended-solids bubble column and comparison with a mechanically agitated reactor. *Hydrometallurgy* 71, 5–12. doi: 10.1016/S0304-386X(03)00142-7

Frank, D. N., Amand, A. L. S., Feldman, R. A., Boedeker, E. C., Harpaz, N., and Pace, N. R. (2007). Molecular phylogenetic characterization of microbial community imbalances in human inflammatory bowel diseases. *Proc. Natl. Acad. Sci. U.S.A.* 104, 13780–13785. doi: 10.1073/pnas.0706625104

Garrido, P., González-Toril, E., García-Moyano, A., Moreno-Paz, M., Amils, R., and Parro, V. (2008). An oligonucleotide prokaryotic acidophile microarray (PAM): its validation and its use to monitor seasonal variations in extreme acidic environments with total environmental RNA. *Environ. Microbiol.* 10, 836–850. doi: 10.1111/j.1462-2920.2008.01477.x

Halinen, A. K., Rahunen, N., Kaksonen, A. H., and Puhakka, A. (2009). Heap bioleaching of a complex sulfide ore. Part I: effect of pH on metal extraction and microbial composition in pH controlled columns. *Hydrometallurgy* 98, 92–100. doi: 10.1016/j.hydromet.2009.04.005

Heid, C. A., Stevens, J., Livak, K. J., and Williams, P. M. (1996). Real time quantitative PCR. *Genome Res.* 6, 986–994. doi: 10.1101/gr.6.10.986

Johnson, D. B., and Hallberg, K. B. (2007). "Techniques for detecting and identifying acidophilic mineral-oxidizing microorganisms," in *Biomining*, eds D. E. Rawlings and D. B. Johnson (Berlin: Springer-Verlag), 237–261.

Jullien, N. (2013). *AmplifX 1.7.0*. Marseille: CNRS, Aix-Marseille Université.

Liu, C.-G., Plumb, J., and Hendry, P. (2006). Rapid specific detection and quantification of bacteria and archaea involved in mineral sulfide bioleaching using real-time PCR. *Biotechnol. Bioeng.* 94, 330–336. doi: 10.1002/bit.20845

Lovley, D. R., and Phillips, E. J. P. (1987). Rapid assay for microbially reduced ferric iron in aquatic sediments. *Appl. Environ. Microbiol.* 53, 1536–1540.

Lunau, M., Lemke, A., Walther, K., Martens-Habbena, W., and Simon, M. (2005). An improved method for counting bacteria from sediments and turbid environments by epifluorescence microscopy. *Environ. Microbiol.* 7, 961–968. doi: 10.1111/j.1462-2920.2005.00767.x

Muyzer, G., Teske, A., Wirsen, C. O., and Jannasch, H. W. (1995). Phylogenetic relationships of *Thiomicrospira* species and their identification in deep-sea hydrothermal vent samples by denaturing gradient gel electrophoresis of 16S rDNA fragments. *Arch. Microbiol.* 164, 165–172. doi: 10.1007/BF025 29967

Nadkarni, M., Martin, F. E., Jacques, N. A., and Hunter, N. (2000). Determination of bacterial load by real-time PCR using a broad range (universal) probe and primer set. *Microbiology* 148, 257–266. doi: 10.1099/00221287-148-1-257

Okibe, N., Gericke, M., Hallberg, K. B., and Johnson, D. B. (2003). Enumeration and characterization of acidophilic microorganisms isolated from a pilot plant stirred tank bioleaching operation. *Appl. Environ. Microbiol.* 69, 1936–1943. doi: 10.1128/AEM.69.4.1936-1943.2003

Olson, G. J., Brierley, J. A., and Brierley, C. L. (2003). Bioleaching review part B: progress in bioleaching: applications of microbial processes by the minerals industries. *Appl. Microbiol. Biotechnol.* 63, 249–257. doi: 10.1007/s00253-003-1404-6

Remonsellez, F., Galleguillos, F., Moreno-Paz, M., Parro, V., Acosta, M., and Demergasso, C. (2009). Dynamic of active microorganisms inhabiting a bioleaching industrial heap of low-grade copper sulfide ore monitored by real-time PCR and oligonucleotide prokaryotic acidophile microarray. *Microbiol. Biotechnol.* 2, 613–624. doi: 10.1111/j.1751-7915.2009.00112.x

Rohwerder, T., Schippers, A., and Sand, W. (1998). Determination of reaction energy values for biological pyrite oxidation by calorimetry. *Thermochim. Acta* 309, 79–85. doi: 10.1016/S0040-6031(97)00352-3

Sand, W., Hallmann, R., Rohde, K., Sobotke, B., and Wentzien, S. (1993). Controlled microbiological in-situ stope leaching of a sulphidic ore. *Appl. Microbiol. Biotechnol.* 40, 421–426. doi: 10.1007/BF00170404

Sand, W., Jozsa, P.-G., Kovacs, Z.-M., Såsåran, N., and Schippers, A. (2007). Long-term evaluation of acid rock drainage mitigation measures in large lysimeters. *J. Geochem. Explor.* 92, 205–211. doi: 10.1016/j.gexplo.2006.08.006

Schippers, A. (2007). "Microorganisms involved in bioleaching and nucleic acid-based molecular methods for their identification and quantification," in *Microbial Processing of Metal Sulfides*, eds E. R. Donati and W. Sand (Dordrecht: Springer), 3–34.

Schippers, A., and Bosecker, K. (2005). "Bioleaching: analysis of microbial communities dissolving metal sulfides," in *Methods in Biotechnology: Microbial Processes and Products*, Vol. 18, ed. J.-L. Barredo (Totowa, NJ: Humana Press Inc).

Schippers, A., Hallmann, R., Wentzien, S., and Sand, W. (1995). Microbial diversity in uranium mine waste heaps. *Appl. Environ. Microbiol.* 61, 2930–2935.

Schippers, A., Nagy, A. A., Kock, D., Melcher, F., and Gock, E. D. (2008). The use of FISH and real-time PCR to monitor the biooxidation and cyanidation for gold and silver recovery from a mine tailings concentrate (Ticapampa, Peru). *Hydrometallurgy.* 94, 77–81. doi: 10.1016/j.hydromet.2008.05.022

Spolaore, P., Joulian, C., Gouin, J., Morin, D., and d'Hugues, P. (2011). Relationship between bioleaching performance, bacterial community structure and mineralogy in the bioleaching of a copper concentrate in stirred-tank reactors. *Appl. Microbiol. Biotechnol.* 89, 441–448. doi: 10.1007/s00253-010-2888-5

Tamura, K., Stecher, G., Peterson, D., Filipski, A., and Kumar, S. (2013). MEGA6: molecular evolutionary genetics analysis version 6.0. *Mol. Biol. Evol.* 30, 2725–2729. doi: 10.1093/molbev/mst197

Wakeman, K., Auvinen, H., and Johnson, D. B. (2008). Microbiological and geochemical dynamics in simulated-heap leaching of a polymetallic sulfide ore. *Biotechnol. Bioeng.* 101, 739–750. doi: 10.1002/bit.21951

Webster, G., Newberry, C. J., Fry, J., and Weightman, A. J. (2003). Assessment of bacterial community structure in the deep sub-seafloor biosphere by 16S rDNA-based techniques: a cautionary tale. *J. Microbiol. Methods* 55, 155–164. doi: 10.1016/S0167-7012(03)00140-4

Wittwer, C. T., Herrmann, M. G., Moss, A. A., and Rasmussen, R. P. (1997). Continuous fluorescence monitoring of rapid cycle DNA amplification. *BioTechniques* 22, 130–138.

Zammit, C. M., Mutch, L. A., Watling, H. R., and Watkin, E. L. J. (2011). The recovery of nucleic acid from biomining and acid mine drainage microorganisms. *Hydrometallurgy* 108, 87–92. doi: 10.1016/j.hydromet.2011.03.002

Zhang, R., Wei, M., Ji, H., Chen, X., Qiu, G., and Zhou, H. (2009). Application of real-time PCR to monitor population dynamics of defined mixed cultures of moderate thermophiles involved in bioleaching of chalcopyrite. *Appl. Microbiol. Biotechnol.* 81, 1161–1168. doi: 10.1007/s00253-008-1792-8

Conflict of Interest Statement: The authors declare that the research was conducted in the absence of any commercial or financial relationships that could be construed as a potential conflict of interest.

frontiers in Microbiology

ORIGINAL RESEARCH
published: 05 January 2017
doi: 10.3389/fmicb.2016.02132

Multiple Osmotic Stress Responses in *Acidihalobacter prosperus* Result in Tolerance to Chloride Ions

*Mark Dopson[1], David S. Holmes[2,3], Marcelo Lazcano[2,3], Timothy J. McCredden[4], Christopher G. Bryan[4], Kieran T. Mulroney[4], Robert Steuart[4], Connie Jackaman[4] and Elizabeth L. J. Watkin[4]**

[1] Centre for Ecology and Evolution in Microbial Model Systems, Linnaeus University, Kalmar, Sweden, [2] Facultad de Ciencias Biologicas, Universidad Andres Bello, Santiago, Chile, [3] Center for Bioinformatics and Genome Biology, Fundacion Ciencia y Vida, Santiago, Chile, [4] School of Biomedical Sciences, Curtin Health Innovation Research Institute, Curtin University, Perth, WA, Australia

OPEN ACCESS

Edited by:
Axel Schippers, Federal Institute for Geosciences and Natural Resources, Germany

Reviewed by:
Sabrina Hedrich, Federal Institute for Geosciences and Natural Resources, Germany
Cecilia Susana Demergasso, Catholic University of the North, Chile

***Correspondence:**
Elizabeth L. J. Watkin
e.watkin@curtin.edu.au

Specialty section:
This article was submitted to Extreme Microbiology, a section of the journal Frontiers in Microbiology

Received: *29 September 2016*
Accepted: *19 December 2016*
Published: *05 January 2017*

Citation:
Dopson M, Holmes DS, Lazcano M, McCredden TJ, Bryan CG, Mulroney KT, Steuart R, Jackaman C and Watkin ELJ (2017) Multiple Osmotic Stress Responses in Acidihalobacter prosperus Result in Tolerance to Chloride Ions. Front. Microbiol. 7:2132. doi: 10.3389/fmicb.2016.02132

Extremely acidophilic microorganisms (pH optima for growth of ≤3) are utilized for the extraction of metals from sulfide minerals in the industrial biotechnology of "biomining." A long term goal for biomining has been development of microbial consortia able to withstand increased chloride concentrations for use in regions where freshwater is scarce. However, when challenged by elevated salt, acidophiles experience both osmotic stress and an acidification of the cytoplasm due to a collapse of the inside positive membrane potential, leading to an influx of protons. In this study, we tested the ability of the halotolerant acidophile *Acidihalobacter prosperus* to grow and catalyze sulfide mineral dissolution in elevated concentrations of salt and identified chloride tolerance mechanisms in *Ac. prosperus* as well as the chloride susceptible species, *Acidithiobacillus ferrooxidans*. *Ac. prosperus* had optimum iron oxidation at 20 g L^{-1} NaCl while *At. ferrooxidans* iron oxidation was inhibited in the presence of 6 g L^{-1} NaCl. The tolerance to chloride in *Ac. prosperus* was consistent with electron microscopy, determination of cell viability, and bioleaching capability. The *Ac. prosperus* proteomic response to elevated chloride concentrations included the production of osmotic stress regulators that potentially induced production of the compatible solute, ectoine uptake protein, and increased iron oxidation resulting in heightened electron flow to drive proton export by the F_0F_1 ATPase. In contrast, *At. ferrooxidans* responded to low levels of Cl^- with a generalized stress response, decreased iron oxidation, and an increase in central carbon metabolism. One potential adaptation to high chloride in the *Ac. prosperus* Rus protein involved in ferrous iron oxidation was an increase in the negativity of the surface potential of Rus Form I (and Form II) that could help explain how it can be active under elevated chloride concentrations. These data have been used to create a model of chloride tolerance in the salt tolerant and susceptible species *Ac. prosperus* and *At. ferrooxidans*, respectively.

Keywords: salt, acidophile, biomining, bioleaching, proteomics, pyrite, chalcopyrite, environmental stress

INTRODUCTION

Acidophilic and extremely acidophilic microorganisms have pH optima for growth of ≤5 and ≤3, respectively, and comprise a phylogenetically and phenotypically diverse group of microorganisms from all three domains of life (reviewed in Aguilera et al., 2016; Dopson, 2016; Golyshina et al., 2016). As a group, they comprise species across wide temperature ranges for growth (from eurypsychrophilic to thermophiles), with the ability to exploit organic and/or inorganic electron donors and carbon sources, and can utilize molecular oxygen, ferric iron, and sulfate as electron acceptors. Acidophilic microorganisms have generated considerable interest as: (i) they catalyze the dissolution of sulfide minerals for recovery of valuable metals, termed "biomining" or "bioleaching" (Vera et al., 2013); (ii) they can cause uncontrolled sulfide mineral oxidation leading to the release of toxic, acidic and metal containing waters, called "acid mine drainage" (Mendez-Garcia et al., 2015); (iii) they are a source of extremozymes for use in biotechnologies (Elleuche et al., 2014); (iv) liposomes from these species have been investigated as a method for drug delivery (Jensen et al., 2015); and (v) these microorganisms may be analogs for early life on earth and potential life on other planets (Bauermeister et al., 2014).

Acidithiobacillus ferrooxidans was the first microorganism recognized to generate acid mine drainage (Colmer and Hinkle, 1947) and has since been identified in many acidic environments playing an important role during heap bioleaching of sulfide minerals. *At. ferrooxidans* fixes carbon dioxide for cellular carbon and couples ferrous iron, inorganic sulfur compound, and hydrogen oxidation to the reduction of either molecular oxygen or ferric iron. The type strain genome sequence is available (Valdes et al., 2008) and the genetic basis of many aspects of its metabolism has been elucidated (Osorio et al., 2008, 2013; Quatrini et al., 2009; Esparza et al., 2010; Ponce et al., 2012). *Acidihalobacter prosperus* (originally described as "*Thiobacillus prosperus*") is another autotrophic and acidophilic species capable of growth via oxidation of ferrous iron and inorganic sulfur compounds (Huber and Stetter, 1989; Cardenas et al., 2015). The *Ac. prosperus* type strain was isolated from a volcanic marine environment and is halotolerant, being able to grow in chloride concentrations from 0.04 to 0.6 M (2.3–35 g L^{-1}; Nicolle et al., 2009). The underlying mechanisms for *Ac. prosperus* growth are far less well-understood than for *At. ferrooxidans*, although the recent publication of its genome sequence (Ossandon et al., 2014) now aids investigation of this species.

Acidophiles employ a number of methods to maintain their intracellular pH near to neutral despite a proton ion gradient of up to 10,000 fold across the cytoplasmic membrane (reviewed in Slonczewski et al., 2009; Zammit and Watkin, 2016). These mechanisms include: (i) primary proton pumps that export protons during electron transport; (ii) cytoplasmic membranes that are highly resistant to the influx of protons; (iii) an inside positive membrane potential that creates a chemiosmotic gradient that reduces proton influx by electrostatic repulsion; (iv) alterations in cytoplasmic membrane structure; (v) proton-consuming reactions such as carboxylases; and (vi) cytoplasmic buffering. Osmotic stress occurs when the soluble extracellular salts differ from the concentration within the cell that either leads to cellular dehydration or lysis (Zammit and Watkin, 2016). Typical acidophile biomining strains are highly sensitive to anions and in particular chloride that have been demonstrated to inhibit ferrous iron oxidation by a *Leptospirillum ferriphilum*-dominated culture (Gahan et al., 2010) and the bioleaching ability of an undefined mixed acidophile consortium (Shiers et al., 2005). One exception is the salt tolerant industrial isolate, *L. ferriphilum* Sp-Cl and its genome sequence will aid in discovering adaptations to high salt concentrations in acidophiles (Issotta et al., 2016). The greater sensitivity to the membrane permeable anion chloride is due to its ability to cross the cell membrane. This reduces the transmembrane potential resulting in an influx of protons and acidification of the cytoplasm (Suzuki et al., 1999). Other anions such as SO_4^{2-}, and cations such as Na^+, have little effect beyond their impact on osmotic potential (Blight and Ralph, 2004; Shiers et al., 2005; Davis-Belmar et al., 2008; Rea et al., 2015; Boxall et al., 2016).

The isolation and investigation of halotolerant/halophilic acidophiles has long been a goal due to their potential use for biomining in countries where freshwater is limited and the use of seawater would be beneficial (Zammit et al., 2012; Rea et al., 2015). The major constituents of standard seawater are; Cl^- (0.56M) and Na^+ (0.48M) with SO_4^{2-} at much lower concentrations (0.03M; Millero et al., 2008). Given the sensitivity of acidophiles to Cl^-, those to be utilized in biomining with seawater must be able to tolerate the dual stresses of low pH and high Cl^- concentrations. Adaptations to high salt concentrations exhibited by halophilic/halotolerant microorganisms include: (i) accumulation of cytoplasmic potassium; production of osmoprotectants in the cytoplasm to maintain an even turgor pressure inside and outside of the cell; (ii) alterations in the cell membrane, and (iii) an increase in acidic amino acids on the surface of proteins resulting in an elevated negative potential that aids in keeping the protein in solution (Shivanand and Mugeraya, 2011; Oren, 2013; Graziano and Merlino, 2014). In addition, changes in the surface electrostatic potential of a halophilic/halotolerant electron transport proteins is likely to affect their interactions with redox partners as has been shown for the interaction of the blue copper protein amicyanin with methylamine dehydrogenase (Ma et al., 2007; Choi et al., 2011). The combined effect of low pH and an anion such as chloride is to collapse the inside positive membrane potential involved in pH homeostasis (Alexander et al., 1987; Suzuki et al., 1999). However, the mechanisms halo-acidophiles utilize to combat these combined stresses are poorly understood and the majority of the studies to date have focused on species susceptible to increased salt while halotolerant acidophiles have been neglected.

Acidophilic bacteria have proven to be recalcitrant to the development of genetic methods, such as the creation of knockout mutants, and such techniques are only recently becoming more common (Wen et al., 2014; Yu et al., 2014). As a result, many acidophile studies have utilized "omics" techniques, including proteomics to investigate not only whole communities

(Belnap et al., 2011; Mueller et al., 2011; Goltsman et al., 2013) but also specific responses in a single species (Baker-Austin et al., 2010; Mykytczuk et al., 2011; Potrykus et al., 2011; Mangold et al., 2013). In this study, iron oxidation and biomining studies along with a proteomic strategy are used to investigate the differing responses to chloride by the salt susceptible and tolerant acidophiles *At. ferrooxidans* and *Ac. prosperus*, respectively.

MATERIALS AND METHODS

Strains and Growth Conditions

At. ferrooxidans ATCC 23270^T and *Ac. prosperus* DSM 5130^T were obtained from Deutsche Sammlung von Mikroorganismen und Zellkulturen GmbH (DSMZ) and grown under the following conditions. *At. ferrooxidans*^{T} was cultured in pH 1.8 basal salts medium (BSM) (Plumb et al., 2002) and *Ac. prosperus*^{T} in DSMZ media 477 with 12.5 g/L NaCl (pH 2.5). Filter sterilized (0.2 μm Minisart, Sartorius Stedim) substrates (50 mM $FeSO_4 \cdot 7 H_2O$ and 5 mM $K_2S_4O_6$) were added to both media. Cultures were incubated on a rotary shaker at 120 rpm at 30°C. The effect of NaCl on the iron oxidizing activity of *At. ferrooxidans*^{T} and *Ac. prosperus*^{T} was investigated by addition of NaCl to the media to achieve the required Cl^- concentrations. Cells were counted using a Helber bacteria counting chamber (Hawksley) at 400-fold magnification. Iron(II) oxidation was determined in *At. ferrooxidans*^{T} using spectrophotometry (Govender et al., 2012) and in *Ac. prosperus*^{T} experiments by titration against $CeSO_4$ (Dopson and Lindström, 1999).

Electron Microscopy

At. ferrooxidans^T and *Ac. prosperus*^{T} cells (80 mL) were removed from log phase planktonic grown cultures, filtered (8.0 μm pore size nitrocellulose filters; Miltex™) to remove iron hydroxysulfate precipitate, and concentrated by centrifugation for 20 min at 48,000 × g at 4°C. Cell pellets were washed and resuspended with growth media and then 5.0×10^6 cells were collected by centrifugation for 20 min at 48,000 × g at 4°C and resuspended in 100 μL of the appropriate growth media. Of this concentrated culture, 30 μL was pipetted onto an A1 SEM aluminum stub and incubated at 37°C for 10–40 min (until the surface appeared barely dry). Twenty Five microliters of 2.5% gluteraldehyde in BSM pH 2.5 was pipetted onto the surface of the stubs and then incubated at 4°C for 3 h. The sample stub was then washed by gently pipetting Invitrogen Gibco Ultrapure Distilled Water over the surface. Samples were dehydrated by sequential 30 min incubations with 70, 90, and 100% ethanol at 37°C before being transferred to a desiccator for 24 h. Stubs were coated with a 5 nm layer of platinum and imaged using a Zeiss Neon 40ESB Crossbeam Electron Microscope. Cell debris was differentiated from inorganic precipitates using SEM-EDX Spectra.

Determination of Cell Viability by Flow Cytometry

A single dye viability assay was developed for cells with an internal positive membrane potential. SYTO 9 is natively fluorescent although the fluorescence increases by a factor of ten when bound to DNA (Ankarcrona et al., 1995; Knowles et al., 1996). SYTO9 will cross the membrane of cells with an inside negative membrane potential via passive diffusion. However, the inside positive membrane potential of live acidophiles will exclude SYTO9. Cells of non-viable acidophiles will lose their membrane potential and SYTO 9 will be able to cross the membrane by passive diffusion, binding to the DNA, and fluorescing brighter. The difference in fluorescence intensity between live and dead cells is 10-fold (Supplemental File 1). The cell viability assay was carried out by first removing ferric iron precipitates from cultures by filtration using 8.0 μm Miltex™ nitrocellulose filters followed by centrifugation at 700 × g for 1 min at 4°C. Cells were harvested from the supernatant by centrifugation at 48,000 × g for 20 min at 4°C and re-suspended in either BSM, pH 1.8 (*At. ferrooxidans*^{T}) or DSMZ 477 media, pH 2.5 (*Ac. prosperus*^{T}). Cell suspensions were adjusted to a density of 5.0×10^5 cells/mL. SYTO 9 (ThermoFisher, Eugene, OR) was added to a concentration of 5 μM and the samples were incubated, protected from light, for 15 min. Three controls were prepared: (i) "no stain," a 1 mL aliquot of cells was incubated at 4°C until time of acquisition with no further handling; (ii) "untreated," a 1 mL aliquot of cells was incubated at 4°C for 15 min prior to acquisition, at which time it was stained with 5 μM SYTO 9, and (iii) "heat treated," a 1 mL aliquot was heated to 60°C for 120 min and then incubated in 80% vol/vol molecular biology grade ethanol at room temperature for 60 min and then stained with 5 μM SYTO 9. To confirm the non-viability of this sample, a 200 μL aliquot was inoculated into 800 μL of appropriate growth media with 50 mM $FeSO_4.7 H_2O$ and 5 mM $K_2S_4O_6$ and incubated for 48 h at 30°C.

Samples were acquired in technical triplicates on an Attune Acoustic Flow Cytometer (ThermoFisher) using Attune Cytometric software version 1.2.5. on high sensitivity mode at a flow rate of 25 μL/min. Acquisition was terminated once 10,000 events on all gates were collected or 3 min had elapsed. Photomultiplier tube (PMT) voltages for forward scatter and side scatter were adjusted such that the bacterial population was clearly visible, with no truncation of relevant populations. PMT voltages were set on an unstained aliquot of cells with mean fluorescence intensity (MFI) of $\sim 10^2$ arbitrary fluorescence units excited at 488 nm with a 515–545 nm filter. Gating strategies and the determination of the fluorescence properties of populations of interest were established using FlowJo v10.0 (FlowJo LLC) and an unpaired *t*-test between conditions was performed using the GraphPad Prism v6 Software Suite (Graphpad Software, Inc.).

Bioleaching of Sulfide Minerals

Milled concentrates (<0.75 μm) of pyrite (FeS_2), chalcopyrite ($CuFeS_2$), and pentlandite [$(Ni,Fe)_9S_8$] were sterilized by gamma irradiation (50 kGray). The elemental compositions of the concentrates were determined using inductively coupled plasma—atom emission spectroscopy (ICP-AES) after borax flux and re-dissolution in 5% (vol/vol) HNO_3. The pyrite concentrate contained (wt/wt) 36.6% Fe, 0.24% Cu, 0.04% Ni, and 39.8% S; the chalcopyrite contained 26.6% Fe, 26.8% Cu, and 29.8% S; and the pentlandite contained 40.7% Fe, 0.73% Cu, 7.01% Ni, and 35.4% S. *Ac. prosperus*^{T} was incubated in 100 mL of DSM

144 media containing increasing concentrations of NaCl and 0.5% (wt/vol) of the respective sulfide mineral concentrates. The cultures were incubated at 30°C with shaking at 130 rpm and evaporation was compensated for by the addition of sterile deionized water acidified to pH 2.5 with sulfuric acid. Leachates were assayed for pH and ORP (vs. Ag/AgCl) using Ionode pH (IJ44A) and ORP (IJ64) electrodes connected to a TPS SmartCHEM pH reader; Fe(III) concentration using the method of Govender et al. (2012); and Cu and Ni concentrations using flame atomic absorption spectrophotometry (Avanta Σ) with standards supplied by FLUKA chemicals.

Proteomic Analysis of Growth at High or Low Chloride Concentrations

Two liter cultures of the isolates were grown as described above with low and high concentrations of NaCl (0 and 8 g/L for *At. ferrooxidans*^{T} and 3.5 and 30 g/L for *Ac. prosperus*^{T}). To avoid alterations within the proteome as a result of differences in the growth phase, cultures were harvested by centrifugation for 20 min at 48,000 × g and 4°C during mid-exponential phase as determined by Fe^{3+} concentrations. Cell pellets were washed in acidified ultrapure water (HpH_2O, pH 1.8 or 2.5), re-pelleted by centrifugation for 20 min at 48,000 × g and 4°C, and stored at −80°C.

The *At. ferrooxidans*^{T} total soluble proteome was analyzed by 2D-PAGE as described by Mangold et al. (2011) except the initially extracted proteins were concentrated through methanol precipitation and 400 μg of protein was added to each IPG strip. Two dimensional gels were run in duplicate for cells grown in high salt and four gels were run for cells grown at low salt. Images of gels were taken on a PerkinElmer ProXPRESS and analyzed using Progenesis Same Spots program (Non-Linear Dynamics, USA). The two stained gels, of proteins isolated from cells grown in high NaCl concentrations, were aligned to the four stained gels, of proteins isolated from cells grown in low NaCl concentrations. Protein spots that showed change in abundance >1.8-fold and $p < 0.05$ were included in the identification process. Protein spots were analyzed at the Proteomics Node of the Lotterywest State Biomedical Facility within the Western Australian Institute for Medical Research. Protein samples were trypsin digested and analyzed by tandem mass spectrometry using a 5800 Proteomics Analyser (AB Sciex, USA) and peptides identified using Mascot sequence matching software with Ludwig NR Database and taxonomy set to bacteria.

Differential expression of the *Ac. prosperus*^{T} proteome was analyzed by isobaric tags for relative and absolute quantification (iTRAQ). The cell pellet was suspended in lysis buffer [0.2% vol/vol IGEPAL, 0.2% vol/vol Triton X, 0.2% wt/vol CHAPS, 75 mM NaCl, 1 mM EDTA, protease inhibitors; in phosphate buffered saline (PBS)] and sonicated using Misonix Ultrasonic Liquid Processor S-4000 (Sonica LLC) with the following parameters; Amplitude 30% and 5 s cycles (pulse on and off) for a total of 2 min. Cellular debris was removed by centrifugation at 13,000 ×g for 10 min at 4°C and the supernatant stored at −80°C. iTraq analysis was performed by Proteomics International as follows: protein samples were acetone diafiltrated, reduced, alkylated, and trypsin digested according to the iTRAQ protocol (Applied Biosystems) and labeled using the iTRAQ reagents. Peptides were desalted on a Strata-X 33 μm polymeric reversed phase column (Phenomenex) and dissolved in a buffer containing 10 mM KH_2PO_4 pH 3 in 10% vol/vol acetonitrile before separation by strong cation exchange liquid chromatography (SCX) on an Agilent 1100 High Performance Liquid Chromatography system using a PolySulfoethyl column (4.6 × 100 mm; 5 μm; 300 A). Peptides were eluted with a linear gradient of 0 to 400 mM KCl. Eight fractions containing the peptides were collected and after desalting on Strata-X columns were loaded onto a Agilent Zorbax 300SB-C18, 3.5 μm column (Agilent Technologies) running on an Shimadzu Prominence nano HPLC system (Shimadzu). Peptides were resolved with a gradient of 10–40% vol/vol acetonitrile (0.1% vol/vol trifluoroacetic acid) over 160 min. The resultant spots were analyzed on a 5600 Triple Time of Flight mass spectrometer (AB Sciex). Spectral data were analyzed against a protein sequence database for the whole genome (Ossandon et al., 2014) using ProteinPilot™ 4.5 Software (AB Sciex).

Rusticyanin Discovery, Multiple Alignments, and Model Building

The amino acid sequence of the rusticyanin protein of *At. ferrooxidans*^{T} (locus tag: AFE_3146) was used as a query in a BlastP search (Altschul et al., 1997) to predict similar proteins (genes) in the genome of *Ac. prosperus*^{T} (Ossandon et al., 2014). Predicted protein sequences were aligned with Clustal Omega (Sievers et al., 2011) using the server at http://www.ebi.ac.uk/Tools/msa/clustalo/. Predictions of peptide signal and subcellular location were carried out using SignalP 4.1 (Petersen et al., 2011) and Cello (Yu et al., 2006) using the servers at http://www.cbs.dtu.dk/services/SignalP/ and http://cello.life.nctu.edu.tw/, respectively.

Three dimensional models of the structures of Rus Forms I and II from *Ac. prosperus*^{T} were constructed using the experimentally determined structure of rusticyanin from *At. ferrooxidans*^{T} (PDB "1RCY") as a template (Walter et al., 1996). Electrostatic potentials of all three rusticyanins were determined using SWISS MODEL and visualized in Swiss-PDBViewer using the Swiss Model server at https://swissmodel.expasy.org/ (Bordoli et al., 2008). Default parameters were used [dielectric constant (solvent) 80.000, using only charged residues] using the Coulomb computational method with a dielectric constant (protein) 1.000 and solvent ionic strength (mol/L) 0.0.

RESULTS AND DISCUSSION

Iron Oxidation by *At. ferrooxidans* and *Ac. prosperus* in the Presence of Chloride

Ac. prosperus^T maintained activity (as defined by iron oxidation) at a higher concentration of NaCl compared to *At. ferrooxidans*^{T} (**Figure 1**). *At. ferrooxidans*^{T} ferrous iron oxidation was ∼25% inhibited in the presence of 8 g L^{-1} NaCl and ∼65% inhibited

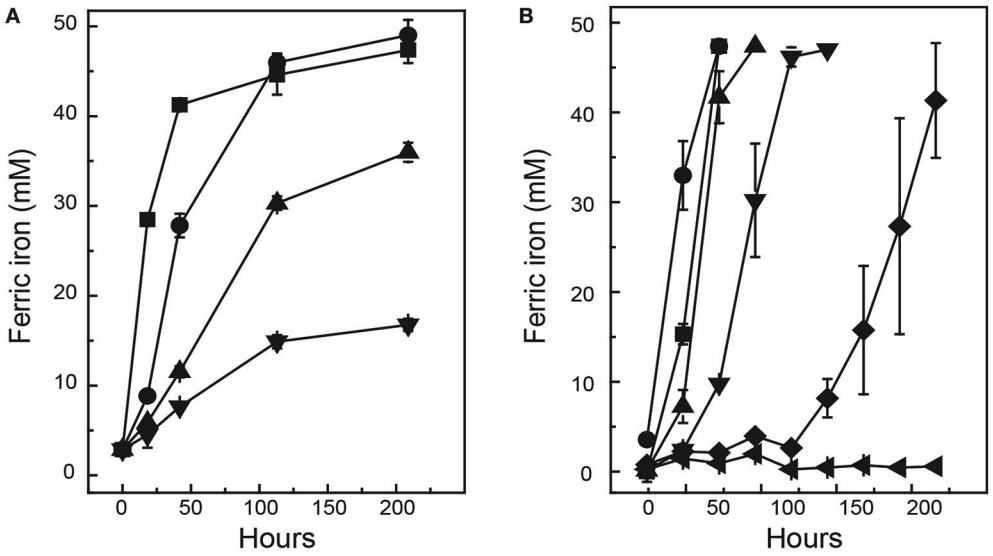

FIGURE 1 | Effect of NaCl upon of ferric iron generation during growth of *At. ferrooxidans*^{T} (A) and *Ac. prosperus*^{T} **(B)**. Symbols for *At. ferrooxidans*^{T}: ■, 0 g L^{-1}; ●, 6 g L^{-1}; ▲, 8 g L^{-1}; and ▼, 10 g L^{-1} while the symbols for *Ac. prosperus*^{T} are: ■, 3.8 g L^{-1}; ●, 20 g L^{-1}; ▲, 35 g L^{-1}; ▼, 50 g L^{-1}; ♦, 60 g L^{-1}; and ◄, 75 g L^{-1}. Data are averages ± *SD* of duplicate biological replicates and one to three technical replicates.

with the addition of 10 g L^{-1} NaCl (**Figure 1A**). In contrast, *Ac. prosperus*^{T} had the highest rate of ferric iron generation in the presence of 20 g L^{-1} NaCl. In addition, while *Ac. prosperus*^{T} ferrous iron oxidation in the presence of 50 g L^{-1} NaCl was less rapid, the ferrous iron was completely oxidized within 96 h (**Figure 1B**). Scanning electron micrographs indicate that *At. ferrooxidans*^{T} was healthier at 0 g L^{-1} NaCl compared to 3.5 g L^{-1} NaCl with many of the *At. ferrooxidans*^{T} cells lysed at the higher concentration. The lysed cells were confirmed as organic in nature by SEM-EDX Spectra (data not shown). In comparison *Ac. prosperus*^{T} cells appeared more healthy in the presence of 30 g L^{-1} NaCl compared with 12.5 g L^{-1} NaCl (**Figure 2**). An optimum NaCl concentration of 20 g L^{-1} (342 mM) suggests *Ac. prosperus*^{T} is a "slight halophile" (Ollivier et al., 1994).

A single dye viability assay using SYTO9 was developed based on positively charged SYTO 9 being excluded by live cells with an inside positive membrane potential. The cell viability of *At. ferrooxidans*^{T} grown at 3.5 g L^{-1} NaCl decreased by 50% ($P < 0.01$) compared to 0 g L^{-1} NaCl whereas *Ac. prosperus*^{T} had a 30% increase ($P < 0.001$) in viable cells when grown at 30 g L^{-1} NaCl compared to 12.5 g L^{-1} NaCl (Supplemental File 1).

Ac. prosperus Catalyzed Sulfide Mineral Bioleaching in the Presence of Chloride

Previous studies have indicated that the ability of *At. ferrooxidans*^{T} to leach metal sulfides in the presence of chloride is completely inhibited in the presence of ∼3.5 g/L NaCl (Deveci, 2002; Deveci et al., 2008; Zammit et al., 2012; Bevilaqua et al., 2013). Due to the potential use of halo-acidophiles to carry out biomining in arid environments where saline groundwater is used (Zammit et al., 2012; Rea et al., 2015), the ability of *Ac. prosperus*^{T} to catalyze metal release from sulfide mineral concentrates was evaluated (**Figure 3**). The generation of ferric iron during *Ac. prosperus*^{T} catalyzed pyrite bioleaching was more rapid in the presence of 15 and 30 g L^{-1} NaCl compared to either 3.8 or 50 g L^{-1} NaCl. The pyrite bioleaching in the presence of NaCl confirmed that *Ac. prosperus*^{T} is a slight halophile. Ferric iron generation from pentlandite was similar in the presence of 15, 30, and 50 g L^{-1} NaCl and more rapid than observed at 3.5 and 75 g L^{-1} NaCl. Nickel release was greatest at 30 g L^{-1} NaCl (**Figure 3**). However, this trend was not supported for ferric iron generation and copper release from chalcopyrite where the leaching rates were very low and there was no statistically significant difference between 3.5 and 75 g L^{-1} NaCl. This lack of difference in leaching rates was potentially due to the advantages of chalcopyrite bioleaching in chloride systems as opposed to sulfate systems (reviewed in Watling, 2014). However, not all studies find an advantage with higher chloride ions at temperatures below 50°C (Dutrizac and Macdonald, 1971).

Ac. prosperus Proteomic Response to the Presence of Chloride

Differential expression of the total soluble proteome from *Ac. prosperus*^{T} cultures grown in the presence of 3.5 and 30 g L^{-1} NaCl identified 617 proteins in each of the proteomes of which 125 were differentially expressed ($P < 0.05$; **Table 1** plus the complete data set in Supplemental File 2). The COG classifications with the highest number of differentially expressed proteins were cell envelope integrity, protein synthesis, energy acquisition, central carbon metabolism, and protein fate (Supplemental File 3). This likely reflected the need to adjust the cell envelope to maintain cellular integrity and the increased

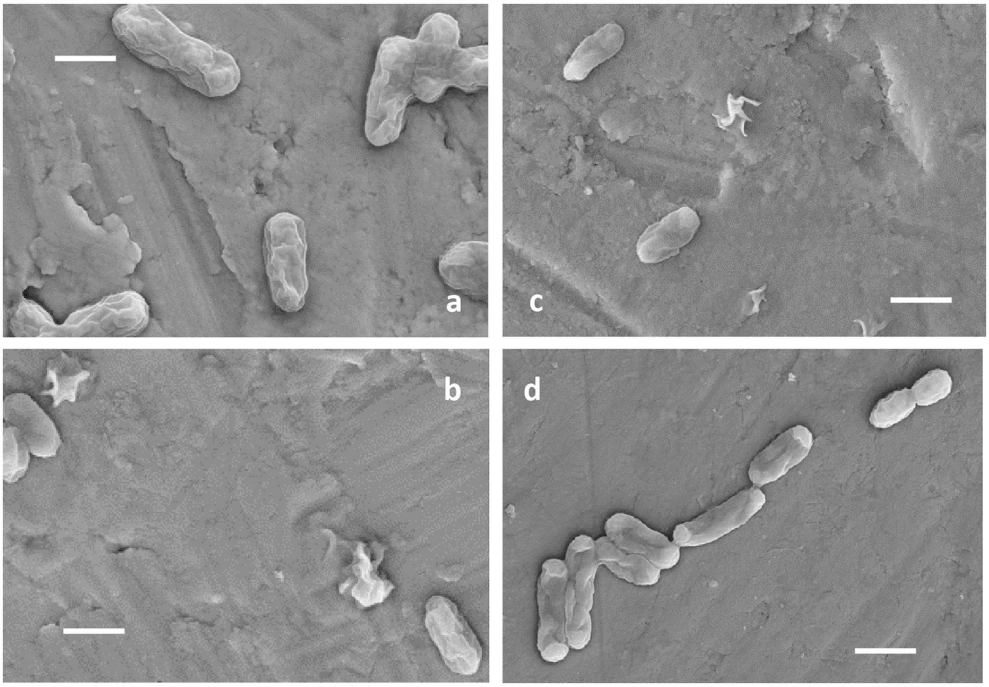

FIGURE 2 | Electron micrographs of *At. ferrooxidans*^{T} grown in the presence of 0 g L^{-1} (A) and 3.5 g L^{-1} NaCl **(B)** and *Ac. prosperus*^{T} in the presence of 12.5 g L^{-1} **(C)**, and 30 g L^{-1} NaCl **(D)**. All scale bars are 1 μm.

energy required to maintain pH and osmotic balance (reviewed in Slonczewski et al., 2009; Zammit and Watkin, 2016).

Growth in high salt compared to low salt resulted in the unique identification of the osmolarity response regulator, OmpR. This regulator senses alterations in the membrane surface tension as a result of changes in the medium osmolarity (Cai and Inouye, 2002). A further regulatory protein, PilG which acts to control the transcription of many genes including osmotically inducible (Bouvier et al., 1998) and osmotic control (Lucht et al., 1994) genes, was 5.7 ± 1.2 fold up-regulated. On exposure to osmotic stress microorganisms will accumulate compatible solutes of which the most common is ectoine (Empadinhas and da Costa, 2008) and its ABC transporter was 55.3 ± 1.6 fold up-regulated in high salt conditions.

Another known response to osmotic stress is the production of proteins involved in the maintenance of the cell membrane integrity (reviewed: Zammit and Watkin, 2016). Growth in high salt conditions resulted in up-regulation of many *Ac. prosperus*^{T} membrane integrity proteins. These included cytoskeleton protein RodZ (7.6 ± 1.1 fold) that is linked to maintaining cell shape (Bendezu et al., 2009); the cell membrane integrity Tol-Pal system (Lloubes et al., 2001; Zakharov et al., 2004) proteins BtuB (5.6 ± 0.8 fold), SecB (4.6 ± 0.8 fold), YbgF (3.7 ± 0.3 fold), and TolB (2.2 ± 0.3 fold); the MlaD outer membrane lipid asymmetry maintenance protein (5.8 ± 2.6 fold) and MlaC phospholipid ABC transporter (10.5 ± 1.8 fold) that maintain outer membrane integrity (Malinverni and Silhavy, 2009); a Gram-negative porin (5.6 ± 0.2 fold) and SurA (4.8 ± 1.0 and 4.5 ± 0.7 fold) involved in outer membrane protein folding (Vertommen et al., 2009). Additionally, several proteins that form the cell membrane had higher levels of abundance including MurA (unique in high salt conditions); RfaD and DdL (both unique) involved in lipopolysaccharide and peptidoglycan biosynthesis, respectively; and a peptidoglycan-associated lipoprotein (8.4 ± 3.3 fold). An increase in membrane biosynthesis proteins in the presence of chloride has also been observed in *Acidithiobacillus caldus* (Guo et al., 2014).

A second group of *Ac. prosperus*^{T} proteins with increased concentrations in response to high salt conditions were related to the stress response. These proteins included protein folding chaperones such as DnaK (7.0 ± 1.1 fold) and GrpE (4.3 ± 0.8 fold) that form a homolog of the eukaryotic Hsp70 chaperone (Mayer and Bukau, 2005); HscA (unique) that forms part of a chaperone similar to DnaK (Silberg et al., 1998); and GroL (9.2 ± 3.7 fold) that acts under stress conditions (Chuang and Blattner, 1993). A further group of up-regulated proteins were involved in oxidative stress and included a AhpC/TSA family protein (7.9 ± 1.4 fold), ruberythrin (3.3 ± 1.5 fold), and a Dyp-type peroxidase family protein (1.1 ± 0.2 fold). These proteins may have been produced due to the increased metabolic and electron transport rate (see below) necessary to remove protons from the cytoplasm. This response has previously been observed in the acidophiles *At. caldus* (Zammit et al., 2012; Guo et al., 2014), *Acidimicrobium ferrooxidans* (Zammit et al., 2012), and *Leptospirillum ferrooxidans* (Parro et al., 2007). The final up-regulated proteins involved in the stress response to chloride were an ATP-dependent Clp protease (4.3 ± 0.9 fold) that degrades proteins (Katayama et al., 1988); GroS (15.7 ± 3.7 fold) that

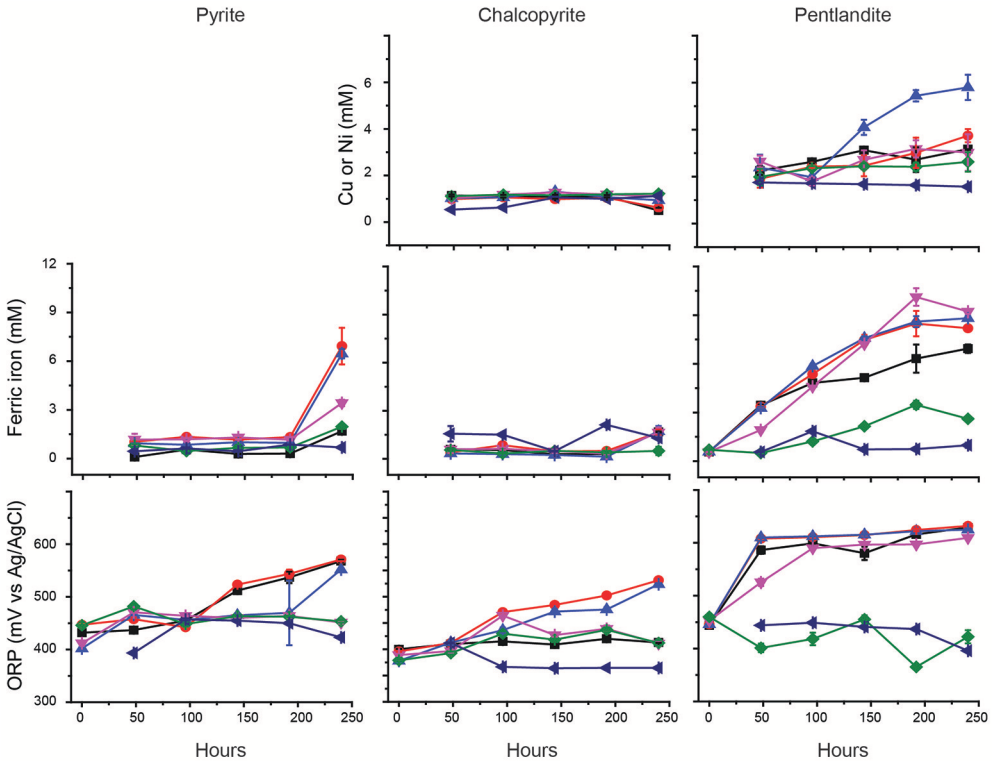

FIGURE 3 | Effect of NaCl on the bioleaching of pyrite, chalcopyrite, and pentlandite by *Ac. prosperus*^{T}: ■, 3.8 g L^{-1}; ●, 15 g L^{-1}; ▲, 30 g L^{-1}; ▼, 50 g L^{-1}; ♦, 75 g L^{-1}; and ◄ abiotic control in the presence of 15 g L^{-1} NaCl (chosen as closest to the optimal NaCl concentration for *Ac. prosperus*^{T} growth). The figure shows the copper and nickel concentrations during chalcopyrite and pentlandite leaching, respectively. Data are averages ± *SD* of triplicate biological replicates and three technical replicates.

acts in concert with GroE in the response to DNA mutation (Al Mamun et al., 2012); ADP-ribose pyrophosphatase, NudF (7.4 ± 2.5 fold) that if deleted increases sensitivity to heat stress (Krisko et al., 2014); and RNA polymerase-binding transcription factor, DksA (7.0 ± 2.0 fold) that is induced at low pH (Stancik et al., 2002).

Metabolic and electron transport proteins with a higher concentration in high salt conditions included rusticyanin (9.7 ± 2.3 fold) and cytochrome c_1 (unique) involved in ferrous iron oxidation (Quatrini et al., 2009). As mentioned above, these proteins were likely used during proton exclusion from the cytoplasm. In addition, ATP synthase subunit b had an 8.2 ± 3.5 fold higher concentration in high salt conditions. In addition to synthesizing ATP, the *Enterococcus hirae* ATPase extrudes protons from the cytoplasm to regulate pH (Shibata et al., 1992) and increasing the concentration of subunit b may result in the same function.

Proteins with a statistically higher concentration in low salt conditions generally had much lower fold differences (**Table 1**). These proteins included OmpA (0.5 ± 0.3 fold) and AsmA (0.3 ± 0.1 fold) involved in OMP assembly that were likely decreased in high salt conditions to reduce pores in the outer membrane that allow influx of chloride, as has been reported for OmpC and OmpF in *E. coli* (Csonka and Hanson, 1991). In addition, the ATPase α-subunit (0.7 ± 0.2 fold) had a higher concentration in low salt conditions, potentially as the complex was being used to produce ATP rather than extrude protons (Shibata et al., 1992). In a similar vein, several central carbon metabolism (e.g., enolase; 0.4 ± 0.1 fold), Calvin-Benson-Bassham cycle (e.g., ribulose bisphosphate carboxylase large chain; 0.7 ± 0.3 fold), and ribosomal (e.g., 50S ribosomal protein L23, RplW; 0.5 ± 0.3 fold) proteins had higher concentrations as energy production via ferrous iron oxidation was likely utilized for cellular growth rather than as a response to osmotic and pH stress.

At. ferrooxidans Proteomic Response to the Presence of Chloride

At. ferrooxidans^T response to growth in high (8 g/L) and low (0 g/L) salt conditions was investigated by two-dimensional polyacrylamide gel based proteomics (Supplemental File 4) that identified a total of 24 statistically valid up-regulated proteins during growth in high salt conditions (Supplemental File 5 with proteins discussed in the text in **Table 2**). *At. ferrooxidans*^{T} growth in high salt exhibited several similar strategies as employed by *Ac. prosperus*^{T} such as the increased abundance of peptidyl-prolyl *cis-trans* isomerase (two protein spots that

TABLE 1 | Up- and down-regulated *Ac. prosperus*^{T} proteins in the presence of high (30 g L^{-1}) and low (3.5 g L^{-1}) concentrations of sodium chloride.

Accession[a]		Fold[b]	*SE*[c]
UP-REGULATED IN HIGH SALT CONDITIONS			
Osmoregulation, Cell Envelope, and Its Integrity			
WP_038086993	Osmolarity response regulator, OmpR	Unique[d]	NA[e]
WP_038089003	UDP-N-acetylglucosamine 1-carboxyvinyltransferase, murA	Unique	NA
WP_038093711	ADP-L-glycero-D-mannoheptose-6-epimerase, RfaD	Unique	NA
WP_038088939	D-alanine–D-alanine ligase, DdL	Unique	NA
WP_038089461	Ectoine ABC transporter solute-binding protein	55.3	1.6
WP_052064239	MlaC, ABC transporter	10.5	1.8
WP_052064215	Peptidoglycan-associated lipoprotein OmpA	8.4	3.3
WP_038091948	Cytoskeleton protein RodZ	7.6	1.1
WP_038087491	ATP-dependent zinc metalloprotease, FtsH	6.3	2.3
WP_038089009	Outer membrane lipid asymmetry maintenance protein MlaD	5.8	2.6
WP_070079811	Pilus Assembly Protein PilG	5.7	1.2
WP_038093779	BtuB, Outer membrane cobalamin receptor protein	5.6	0.8
WP_065089743	Gram-negative porin	5.6	0.2
WP_052064070	Probable peptidyl-prolyl cis-trans isomerase, SurA	4.8	1.0
WP_038088090	Preprotein translocase subunit SecB	4.6	0.8
WP_065089354	Chaperone SurA	4.5	0.7
WP_038086391	3-ketoacyl-(Acyl-carrier-protein) reductase	3.9	0.4
WP_065089408	Tol-pal system protein YbgF	3.7	0.3
WP_065089387	Translocation protein TolB	2.2	0.3
Stress Response			
WP_065089122	Chaperone protein HscA	Unique	NA
WP_038091761	50S ribosomal protein L25/general stress protein Ctc	21.0	11.1
WP_038092421	10 kDa chaperonin, GroES	15.7	3.7
WP_038092418	60 kDa chaperonin, GroEL	9.2	3.7
WP_038092694	AhpC/TSA family	7.9	1.4
WP_038086510	ADP-ribose pyrophosphatase, NudF	7.4	2.5
WP_038086634	RNA polymerase-binding transcription factor, DksA	7.0	2.0
WP_065089055	Molecular chaperone, DnaK	7.0	1.1
WP_065089054	Heat shock protein, GrpE	4.3	0.8
OBS10750	ATP-dependent Clp protease	4.3	0.9
WP_038086793	Ribosome recycling factor	3.9	0.5
WP_038089562	Rubrerythrin protein	3.3	1.5
WP_065089340	Dyp-type peroxidase family	1.1	0.2
Metabolism and Energy Conservation			
OBS09221	Cytochrome c_1 family	Unique	NA
WP_065089467	Rusticyanin protein	9.7	2.3
WP_038087805	ATP synthase subunit b	8.2	3.5
WP_038092630	SirA-like protein	6.6	3.3
WP_038089319	50S ribosomal protein L29	3.8	0.4
WP_038088471	Sulfur oxidation protein, SoxZ	2.9	0.3
UP-REGULATED IN LOW SALT CONDITIONS			
Osmoregulation			
WP_052064171	OmpA	0.5	0.3
WP_038092666	Protein AsmA	0.3	0.1
Cell Envelope and Its Integrity			
OBS10484	UDP-glucose pyrophosphorylase, GalU	0.1	0.0

(Continued)

TABLE 1 | Continued

Accession[a]		Fold[b]	*SE*[c]
Metabolism and Energy Conservation			
WP_038093510	Ribulose bisphosphate carboxylase large chain	0.7	0.3
WP_065089545	ATP synthase subunit alpha	0.7	0.2
WP_038089302	50S ribosomal protein L23, RplW	0.5	0.3
WP_038093481	Glyceraldehyde-3-phosphate dehydrogenase	0.4	0.0
WP_038091971	Enolase	0.4	0.1
WP_065089725	SoxAX cytochrome complex subunit A	0.4	0.2
WP_038089305	50S ribosomal protein L2, RplB	0.2	0.0
WP_038094109	50S ribosomal protein L10	0.2	0.0
OBS10998	Translation initiation factor IF-3	0.2	0.1
WP_038089313	30S ribosomal protein S3, RpsC	0.1	0.0
WP_038093513	Ribulose bisphosphate carboxylase small chain	0.1	0.0
WP_038089345	30S ribosomal protein S13, RpsM	0.1	0.0
WP_070077256	Major carboxysome shell protein 1A	0.1	0.0
WP_038093488	Fructose-1,6-bisphosphate aldolase	0.1	0.0

[a] *Accession numbers refers to the identified protein within the non-redundant protein sequence database for Acidihalobacter prosperus.*
[b] *Average fold up-regulation of the four independent pairwise comparisons between the duplicate high and low salt proteomes.*
[c] *Standard error of the mean of the average fold up-regulation for the four independent comparisons between treatments.*
[d] *Unique protein not expressed in low salt conditions.*
[e] *NA, not available as the protein was unique.*

TABLE 2 | *At. ferrooxidans*^{T} proteins with statistically supported altered abundance when grown in high or low NaCl concentration.

UniProt[a]	Protein	*P*-value[b]	Fold[c]
UP-REGULATED IN HIGH SALT CONDITIONS			
Cell Envelope and Its Integrity			
B7JA08	Survival protein SurA	0.049	3.4
B7J3E4	Periplasmic solute binding protein	0.038	2.8
B7J3E4	Periplasmic solute binding protein	0.04	2.6
B7J541	PpiC-type peptidyl-prolyl *cis-trans* isomerase	0.026	2.8
B7J541	PpiC-type peptidyl-prolyl *cis-trans* isomerase	3.9 E-04	2.5
B7J3E4	Periplasmic solute binding protein	0.007	2.3
Stress			
B7J9P4	Ribosome recycling factor	0.009	4.0
B7J4U6	Heat shock protein Hsp20	0.026	2.5
B7J942	Serine protease, DO/DeqQ family	0.123	2.0
Metabolism and Energy Conservation			
B7JBC9	Glyceraldehyde-3-phosphate dehydrogenase, type I	0.004	4.0
B7J3E6	Sulfur/pyrite/thiosulfate/sulfide-induced protein	0.001	2.9
B7J6R4	Enolase	0.026	2.2
B7JBC9	Glyceraldehyde-3-phosphate dehydrogenase, type I	0.050	2.0
UP-REGULATED IN LOW SALT CONDITIONS			
Cell Envelope and Its Integrity			
B7J3E4	Periplasmic solute binding protein	3.71 E-04	3.1
B7J8H1	Major outer membrane protein 40	0.005	1.8
Stress			
B7J7L4	Glycine cleavage system H protein	0.007	1.9
Metabolism and Energy Conservation			
P0C918	Rusticyanin (Form I)	0.006	2.5
B7J913	50S ribosomal protein L9	0.022	1.8

[a] *Uniprot accession number, refers to the identified protein within this database.*
[b] *Significance as calculated by ANOVA.*
[c] *Average fold up-regulation between the high and low salt proteomes.*

were 2.8 and 2.5 fold up-regulated in 8 vs. 0 g/L salt) which is involved in outer membrane protein folding (Vertommen et al., 2009). Another three protein spots with increased abundance were identified as periplasmic solute binding proteins that are involved in the maintenance of the cell envelope integrity (2.8, 2.6, and 2.3 fold). However, the periplasmic solute binding protein also had a 3.1 higher concentration in low salt conditions suggesting that it had undergone regulation via post-translational modification. Several *At. ferrooxidans*^{T} stress proteins with higher concentrations in 8 g/L NaCl included heat shock protein Hsp20 (2.5 fold) that aids in reducing protein denaturation (Lindquist and Craig, 1988); ribosome recycling factor (4.0 fold) also observed when *Ac. prosperus*^{T} was cultured in high salt conditions; and a serine protease, DO/DeqQ family protein (2.0 fold) that has a chaperone function and also has a higher concentration in the *At. ferrooxidans* response to heat stress (Ribeiro et al., 2011). Finally, the major outer membrane protein 40 had 1.8 fold lower concentration in high salt conditions, potentially to reduce the influx of chloride (Csonka and Hanson, 1991).

In contrast to the increase in rusticyanin seen in *Ac. prosperus*^{T} when cultured in high salt conditions, *At. ferrooxidans*^{T} had a 2.5 fold decrease implying a reduction in iron oxidation (Quatrini et al., 2009) as was demonstrated in the growth experiments, where a reduction of iron oxidation by 25% was observed.

Rusticyanin Tolerance to Increased Salt Concentration

Iron oxidation in the well-studied acidophile *At. ferrooxidans*^{T} involves a protein complex that transfers electrons from iron to oxygen (Castelle et al., 2008; Li et al., 2015) and includes the copper protein rusticyanin encoded in the *rus* operon (Levicán et al., 2002). Rusticyanin is located in the periplasmic space where the pH is low. A cluster of genes has been detected in *Ac. prosperus* V6 (DSM 14174) that has similarity to the *rus* operon of *At. ferrooxidans*^{T} (Nicolle et al., 2009) and it is hypothesized that expression of the rusticyanin gene is actively involved in Fe oxidation, presumably in a similar way to that described for *At. ferrooxidans*^{T}. However, a major difference in the two systems is that iron oxidation in *At. ferrooxidans*^{T} is inhibited by low concentrations of chloride (Blake et al., 1991; Harahuc et al., 2000), whereas chloride is required for expression of rusticyanin in *Ac. prosperus* V6 (Nicolle et al., 2009) and maximum iron oxidation in *Ac. prosperus*^{T} was seen at 20 g/L NaCl.

Using the rusticyanin gene of *At. ferrooxidans*^{T} (locus tag: AFE_3146) as a query, two rusticyanin genes, termed Form I and Form II (locus tags: Thpro_021557 and Thpro_020703, respectively) were predicted in the genome of *Ac. prosperus*^{T} (Ossandon et al., 2014). Relative to the rusticyanin of *At. ferrooxidans*^{T}, Form I was detected with a score of 142, a query coverage of 100%, an *E*-value of 2e-48, and an identity of 46%. The same parameters for Form II were 116, 89%, 2e-38, and 43%. The extent of sequence similarity and coverage suggest that the two forms of Rus in *Ac. prosperus*^{T} are encoded by genes that are orthologs of *rus* from *At. ferrooxidans*^{T}. Both Rus Forms I and II are predicted to contain signal peptides and to reside in the periplasm. If this is true, then they are most likely to be subjected to the low pH and high salt conditions typical for *Ac. prosperus*. However, the genetic contexts of the two Forms differ (Supplemental File 6). Form I is embedded in a gene cluster very similar to the classical *rus* operon of *At. ferrooxidans*^{T} (Valdes et al., 2008). This supports the hypothesis that Form I Rus is involved in iron oxidation in a manner similar to that described for *At. ferrooxidans*^{T}. In contrast, the gene encoding Form II Rus is found as a singleton gene with no other known genes involved in iron oxidation in the gene neighborhood (Supplemental File 6). The function of this Rus remains unknown. However, because of its sequence similarity to Rus from *At. ferrooxidans*^{T}, it can be speculated that it is also involved in iron oxidation, perhaps under different growth conditions from Form I Rus.

As Form I Rus increases in abundance (9.7 ± 2.3 fold) when *Ac. prosperus*^{T} is subjected to high salt conditions, both its primary amino acid sequence and its predicted tertiary structure were interrogated for clues that might suggest how it maintains activity in high salt conditions. Form II Rus (no change in abundance with increasing salt concentration) and Rus from *At. ferrooxidans*^{T} (2.5 fold decrease) were included for comparison (**Figure 4**). Four critical amino acids (two histidines, one cysteine, and one methionine) have been shown to be ligands in the inner sphere coordinating the copper ion in Rus in *At. ferrooxidans*^{T} and many other members of the family of small blue copper proteins (Gray et al., 2000). The ligands Cys, Met, and one of the histidines are close to each other at the C terminal end in the primary sequence whereas the other histidine is far away from them in the amino acid chain. The loop length that connects these ligands has been shown to be important for coordination of the copper in related blue copper proteins (Gough and Chothia, 2004). Also, as observed in other small blue copper proteins including Rus from *At. ferrooxidans*^{T}, both Form I and Form II Rus from *Ac. prosperus*^{T} are predicted to contain the so-called Greek key β-barrel (data not shown). This is a rigid structure formed by an extended network of hydrogen bonds and tertiary interactions between amino acid side chains (Gray et al., 2000). This rigidity is transmitted to the metal ion and is essential for electron transfer. As shown in **Figure 4**, these ligands, their relative positions in the primary amino acid sequence, and the length of the connecting loop are conserved in Forms I and II Rus from *Ac. prosperus* and in Rus from *At. ferrooxidans*^{T}. Due to the conservation of these properties between the acidophilic *At. ferrooxidans*^{T} and the haloacidophilic *Ac. prosperus*^{T}, it is unlikely that they contribute to salt tolerance in Rus Form I (and perhaps Form II).

The number and distribution of positively (His, Lys, and Arg) and negatively charged (Asp and Glu) amino acids in Rus Forms I and II differ from that observed for Rus of *At. ferrooxidans*^{T} (**Figure 4**). This is in agreement with an observation made earlier for Rus from *Ac. prosperus* V6 (Nicolle et al., 2009). In order to examine whether these differences in charged amino acids could affect the surface electrostatic potential of the different Rus, three dimensional models of the structures of Rus Forms I and II were constructed using the experimentally determined structure of rusticyanin from *At. ferrooxidans*^{T} (PDB "1RCY")

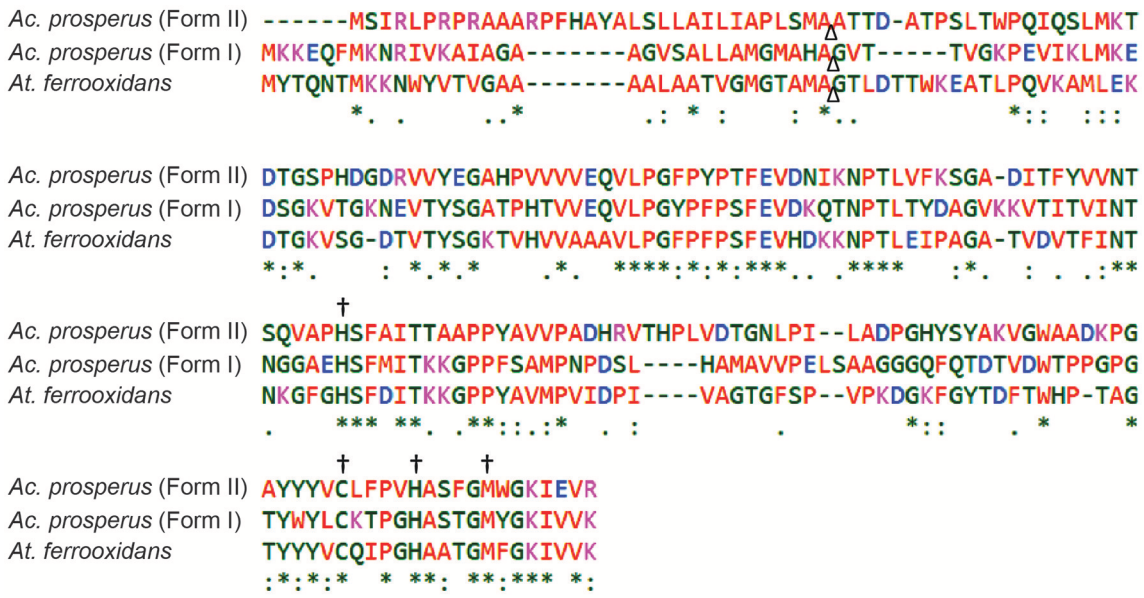

FIGURE 4 | Clustal Omega multiple alignment of rusticyanins from *At. ferrooxidans*^{T} (locus tag: AFE_3146), *Ac. prosperus*^{T} Form I (locus tag: Thpro_021557) and *Ac. prosperus*^{T} Form II (locus tag: Thpro_020703). An * (asterisk) indicates positions which have a single, fully conserved residue. (A), (colon) indicates conservation between groups of strongly similar properties, a. (period) indicates conservation between groups of weakly similar properties. A Δ (triangle) indicates the position of cutting of the peptide signal using *At. ferrooxidans*^{T} as reference. The meaning of the colors is described in (Sievers et al. (2011), Mol Sys Bio 7:539). A † (dagger) indicates the four conserved amino acids that bind the copper ion.

as a template (Walter et al., 1996). The predicted surface electrostatic potentials of Rus Forms I and II of *Ac. prosperus*^{T} (**Figures 5B,C**) are significantly more negative compared to that of Rus from *At. ferrooxidans*^{T} (**Figure 5A**). In the case of Form I Rus, this negative electrostatic potential is widely distributed over the surface of the entire molecule, including around the copper ion. In contrast, in Form II, it is principally distributed around the copper ion. It has been well-established that the electrostatic field directly influences the electrostatic properties of the metal-binding site of blue copper proteins, being a major determinant of the redox potential of the copper ion (Olsson et al., 2003). It is possible that the noticeable negative shift in surface electrostatic potential of Rus Forms I and II could help stabilize them in high salt conditions and assist in the maintenance of an appropriate redox potential of the copper ion. It could also help to repel negatively charged chloride ions in the immediate environment of the proteins.

The increased negative surface electrostatic potential of Form I rusticyanin of *Ac. prosperus*^{T} likely affects its interactions with its redox partners that, based upon amino acid sequence similarities and gene neighborhood conservation, are predicted to be the same as in *At. ferrooxidans*^{T} [i.e., a high molecular weight *c*-type cytochrome Cyc2 located in the external membrane, a periplasmic diheme cytochrome *c* Cyc1, and a periplasmic diheme cytochrome Cyc_{42} (Cyc1A; Bruscella et al., 2007; Castelle et al., 2008)]. Although the potential changes evidently still permit electron transfer, their nature requires experimental verification. The redox partners of Rus Form II are not known.

Other changes in amino acid sequence between Rus of *At. ferrooxidans*^{T} and *Ac. prosperus*^{T} might reveal clues regarding stabilization and activity of Rus at high salt concentrations such as changes in the outer coordination sphere (Cascella et al., 2006; Warren et al., 2012), but these await discovery and investigation. Although a reasonable argument can be made that an increase in the negativity of the surface potential of Rus Form I (and Form II) could help explain salt tolerance perhaps by modulating the environment of copper ion and very likely by affecting its interaction with redox partners, significant effort is still required to understand and experimentally validate these ideas. However, the current suggestions do lead to testable hypotheses and can be used a basis for guiding future research.

Model of *Ac. prosperus* Responses to Chloride

When challenged by elevated salt concentration, acidophiles experience both osmotic stress and an acidification of the intracellular pH (reviewed in Zammit and Watkin, 2016). This is due to a collapse of the inside positive membrane potential as a result of Cl^- crossing the cell membrane, leading to an influx of protons. Notwithstanding the caveat that the iTRAQ analysis of *Ac. prosperus*^{T} in high salt will identify many more proteins than the 2D-PAGE analysis of *At. ferrooxidans*^{T}, the response of the two species were distinct (**Figure 6**). *At. ferrooxidans*^{T} responded to even low levels of Cl^- with a generalized stress response and decreased iron oxidation which was confirmed by a reduced abundance of the protein rusticyanin. However,

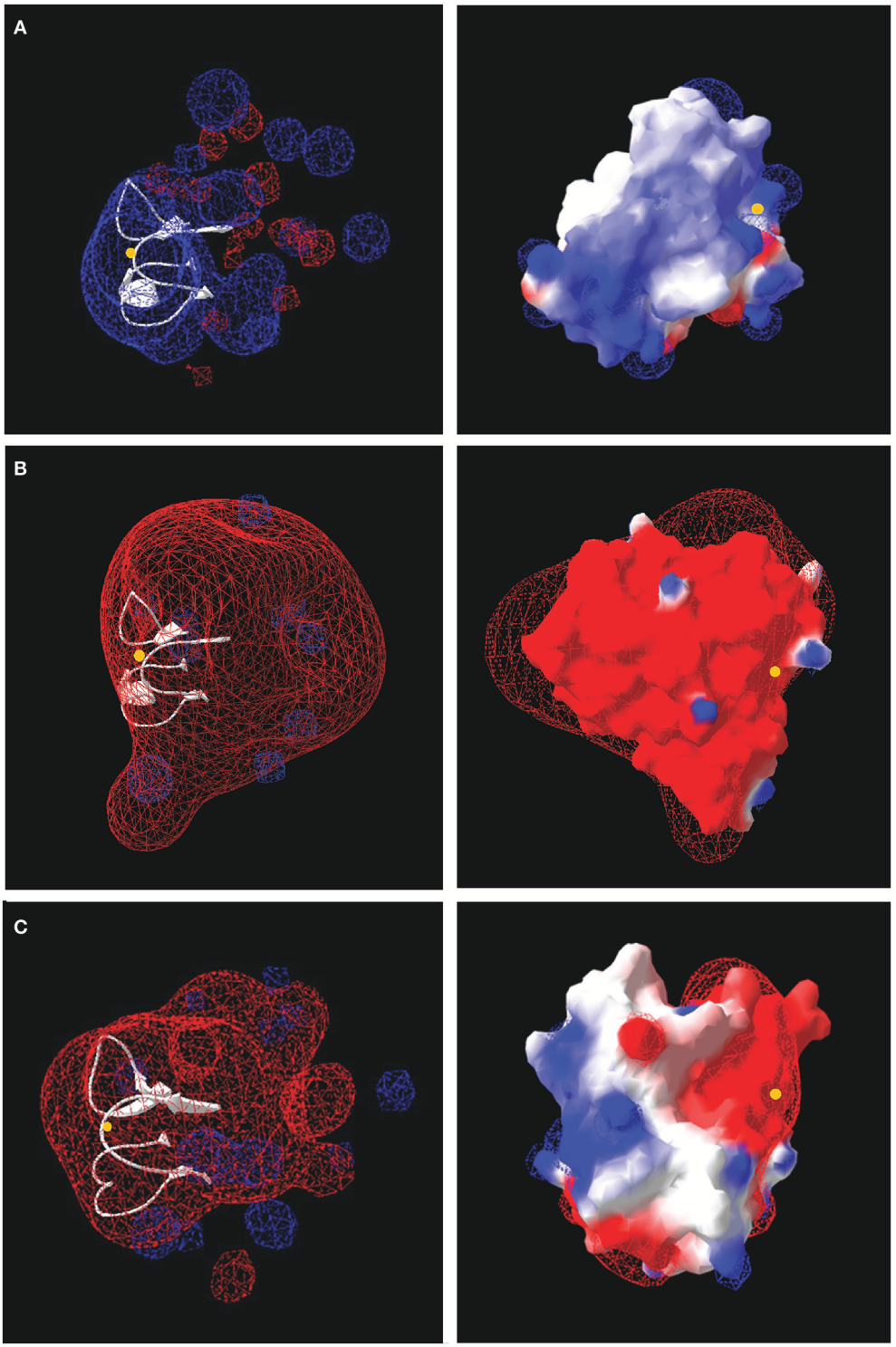

FIGURE 5 | Models of the electrostatic surface potential of rusticyanin of: (A) *At. ferrooxidans*^{T}; **(B)** *Ac. prosperus*^{T} Form I, and **(C)** *Ac. prosperus*^{T} Form II. The surface is colored according to the protein electrostatic potential from red (negative) to blue (positive); the copper ion is shown as a yellow dot. The models on the left hand side are rendered transparent to show (in white) the critical protein folds that binds the copper ion. The models on the right have been rotated 180° (*y*-axis) compared with the models on the left to provide a different perspective.

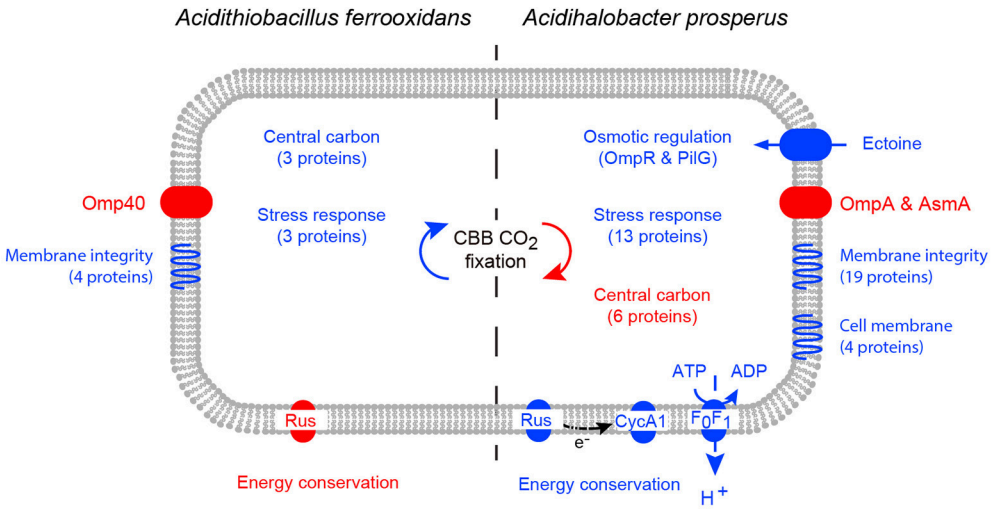

FIGURE 6 | A model of the cellular response of *At. ferrooxidans*^{T} (left) and *Ac. prosperus*^{T} (right) to increased NaCl levels. Increases in protein abundance in high NaCl conditions are represented by blue and decreases in protein abundance in high NaCl conditions are represented by red. Differential protein expression was determined by 2D-PAGE for *At. ferrooxidans*^{T} and iTraq for *Ac. prosperus*^{T}.

despite the reduced ability to generate energy there was an increase in central carbon metabolism and carbon fixation. The most significant responses to increased salt concentration by *Ac. prosperus*^{T} were an increase in abundances of osmotic stress regulators; uptake of the compatible solute ectoine protein and increased iron oxidation as confirmed by the raised abundance of the proteins rusticyanin and cytochrome c_1 that consumes cytoplasmic protons and/or provides reducing power for the stress response. Both central carbon metabolism and carbon fixation decreased suggesting the increased ability to generate energy is utilized for the potential efflux of protons via the F_0F_1 ATPase at the expense of ATP suggested by the greater abundance of the ATP synthase subunit b.

AUTHOR CONTRIBUTIONS

EW, MD, CB, and DH conceived and designed the experiments. EW, TM, KM, and ML performed the experiments. MD, EW, DH analyzed the data. EW, MD, DH, RS, and CJ contributed to the reagents/materials/analysis tools. MD, EW, and DH wrote the paper. All authors read and approved the final manuscript.

ACKNOWLEDGMENTS

EW was funded by an Ian Potter Foundation Travel Grant. This project was partially funded by a Bioplatforms Australia Omics grant. DH and ML were funded by Conicyt Basal CCTE PFB16 and Fondecyt 1130683.

SUPPLEMENTARY MATERIAL

The Supplementary Material for this article can be found online at: http://journal.frontiersin.org/article/10.3389/fmicb.2016.02132/full#supplementary-material

REFERENCES

Aguilera, A., Olsson, S., and Puente-Sánchez, F. (2016). "Physiological and phylogenetic diversity of acidophilic eukaryotes," in *Acidophiles: Life in Extremely Acidic Environments*, eds R. Quatrini and D. B. Johnson (Poole, UK: Caister Academic Press), 107–118.

Alexander, B., Leach, S., and Ingledew, W. J. (1987). The relationship between chemiosmotic parameters and sensitivity to anions and organic acids in the acidophile *Thiobacillus ferrooxidans*. *J. Gen. Microbiol.* 133, 1171–1179. doi: 10.1099/00221287-133-5-1171

Al Mamun, A. A., Lombardo, M. J., Shee, C., Lisewski, A. M., Gonzalez, C., Lin, D., et al. (2012). Identity and function of a large gene network underlying mutagenic repair of DNA breaks. *Science* 338, 1344–1348. doi: 10.1126/science.1226683

Altschul, S. F., Madden, T. L., Schaffer, A. A., Zhang, J., Zhang, Z., Miller, W., et al. (1997). Gapped BLAST and PSI-BLAST: a new generation of protein database search programs. *Nucleic Acids Res.* 25, 3389–3402. doi: 10.1093/nar/25.17.3389

Ankarcrona, M., Dypbukt, J. M., Bonfoco, E., Zhivotovsky, B., Orrenius, S., Lipton, S. A., et al. (1995). Glutamate-induced neuronal death:a succession of necrosis or apoptosis depending on mitochondrial function. *Neuron* 15, 961–973. doi: 10.1016/0896-6273(95)90186-8

Baker-Austin, C., Potrykus, J., Wexler, M., Bond, P. L., and Dopson, M. (2010). Biofilm development in the extremely acidophilic archaeon '*Ferroplasma acidarmanus*' Fer1. *Extremophiles* 14, 485–491. doi: 10.1007/s00792-010-0328-1

Bauermeister, A., Rettberg, P., and Flemming, H. C. (2014). Growth of the acidophilic iron-sulfur bacterium *Acidithiobacillus ferrooxidans* under Mars-like geochemical conditions. *Planet. Space Sci.* 98, 205–215. doi: 10.1016/j.pss.2013.09.009

Belnap, C. P., Pan, C., Denef, V. J., Samatova, N. F., Hettich, R. L., and Banfield, J. F. (2011). Quantitative proteomic analyses of the response of acidophilic

microbial communities to different pH conditions. *ISME J.* 5, 1152–1161. doi: 10.1038/ismej.2010.200

Bendezu, F. O., Hale, C. A., Bernhardt, T. G., and De Boer, P. A. (2009). RodZ (YfgA) is required for proper assembly of the MreB actin cytoskeleton and cell shape in *E. coli*. *EMBO J.* 28, 193–204. doi: 10.1038/emboj.2008.264

Bevilaqua, D., Lahti, H., Suegama, P. H., Garcia, O. Jr., Benedetti, A. V., Puhakka, J. A., et al. (2013). Effect of Na-chloride on the bioleaching of a chalcopyrite concentrate in shake flasks and stirred tank bioreactors. *Hydrometallurgy* 138, 1–13. doi: 10.1016/j.hydromet.2013.06.008

Blake, R. C. II, White, K. J., and Shute, E. A. (1991). Effect of divers anions on the electron-transfer reaction between iron and rusticyanin from *Thiobacillus ferrooxidans*. *Biochemistry* 30, 9443–9449. doi: 10.1021/bi00103a008

Blight, K. R., and Ralph, D. E. (2004). Effect of ionic strength on iron oxidation with batch cultures of chemolithotrophic bacteria. *Hydrometallurgy* 73, 325–334. doi: 10.1016/j.hydromet.2003.12.006

Bordoli, L., Kiefer, F., Arnold, K., Benkert, P., Battey, J., and Schwede, T. (2008). Protein structure homology modeling using SWISS-MODEL workspace. *Nat. Protoc.* 4, 1–13. doi: 10.1038/nprot.2008.197

Bouvier, J., Gordia, S., Kampmann, G., Lange, R., Hengge-Aronis, R., and Gutierrez, C. (1998). Interplay between global regulators of *Escherichia coli*: effect of RpoS, Lrp and H-NS on transcription of the gene osmC. *Mol. Microbiol.* 28, 971–980. doi: 10.1046/j.1365-2958.1998.00855.x

Boxall, N. J., Rea, S. M., Li, J., Morris, C., and Kaksonen, A. H. (2016). Effect of high sulfate concentrations on chalcopyrite bioleaching and molecular characterisation of the bioleaching microbial community. *Hydrometallurgy*. doi: 10.1016/j.hydromet.2016.07.006. [Epub ahead of print].

Bruscella, P., Appia-Ayme, C., Levicán, G., Ratouchniak, J., Jedlicki, E., Holmes, D. S., et al. (2007). Differential expression of two bc1 complexes in the strict acidophilic chemolithoautotrophic bacterium *Acidithiobacillus ferrooxidans* suggests a model for their respective roles in iron or sulfur oxidation. *Microbiology* 153, 102–110. doi: 10.1099/mic.0.2006/000067-0

Cai, S. J., and Inouye, M. (2002). EnvZ-OmpR interaction and osmoregulation in *Escherichia coli*. *J. Biol. Chem.* 277, 24155–24161. doi: 10.1074/jbc.M110715200

Cardenas, J.-P., Ortiz, R., Norris, P. R., Watkin, E., and Holmes, D. S. (2015). Reclassification of '*Thiobacillus prosperus*' (Huber and Stetter 1989) as *Acidihalobacter prosperus* gen. nov., sp. nov., a member of the family *Ectothiorhodospiraceae*. *Int. J. Syst. Evol. Microbiol.* 65, 3641–3644. doi: 10.1099/ijsem.0.000468

Cascella, M., Magistrato, A., Tavernelli, I., Carloni, P., and Rothlisberger, U. (2006). Role of protein frame and solvent for the redox properties of azurin from *Pseudomonas aeruginosa*. *Proc. Natl. Acad. Sci. U.S.A.* 103, 19641–19646. doi: 10.1073/pnas.0607890103

Castelle, C., Guiral, M., Malarte, G., Ledgham, F., Leroy, G., Brugna, M., et al. (2008). A new iron-oxidizing/O_2-reducing supercomplex spanning both inner and outer membranes, isolated from the extreme acidophile *Acidithiobacillus ferrooxidans*. *J. Biol. Chem.* 283, 25803–25811. doi: 10.1074/jbc.M802496200

Choi, M., Sukumar, N., Mathews, F. S., Liu, A., and Davidson, V. L. (2011). Proline 96 of the copper ligand loop of amicyanin regulates electron transfer from methylamine dehydrogenase by positioning other residues at the protein-protein interface. *Biochemistry* 50, 1265–1273. doi: 10.1021/bi101794y

Chuang, S. E., and Blattner, F. R. (1993). Characterization of twenty-six new heat shock genes of *Escherichia coli*. *J. Bacteriol.* 175, 5242–5452. doi: 10.1128/jb.175.16.5242-5252.1993

Colmer, A. R., and Hinkle, M. E. (1947). The action of certain microorganisms in acid mine drainage: a preliminary report. *Science* 106, 253–256. doi: 10.1126/science.106.2751.253

Csonka, L. N., and Hanson, A. D. (1991). Prokaryotic osmoregulation: genetics and physiology. *Annu. Rev. Microbiol.* 45, 569–606. doi: 10.1146/annurev.mi.45.100191.003033

Davis-Belmar, C. S., Nicolle, J. L. C., and Norris, P. R. (2008). Ferrous iron oxidation and leaching of copper ore with halotolerant bacteria in ore columns. *Hydrometallurgy* 94, 144–147. doi: 10.1016/j.hydromet.2008.05.030

Deveci, H. (2002). Effect of salinity on the oxidative activity of acidophilic bacteria during bioleaching of a complex Zn/Pb sulphide ore. *Eur. J. Miner. Proc. Environ. Prot.* 2, 141–150.

Deveci, H., Jordan, M. A., Powell, N., and Alp, I. (2008). Effect of salinity and acidity on bioleaching activity of mesophilic and extremely thermophilic bacteria. *Trans. Nonferr. Met. Soc. China* 18, 714–721. doi: 10.1016/S1003-6326(08)60123-5

Dopson, M. (2016). "Physiological and phylogenetic diversity of acidophilic bacteria," in *Acidophiles: Life in Extremely Acidic Environments*, eds R. Quatrini and D. B. Johnson (Poole, UK: Caister Academic Press), 79–92.

Dopson, M., and Lindström, E. B. (1999). Potential role of *Thiobacillus caldus* in arsenopyrite bioleaching. *Appl. Environ. Microbiol.* 65, 36–40.

Dutrizac, J. E., and Macdonald, R. J. C. (1971). The effect of sodium chloride on the dissolution of chalcopyrite under simulated dump leaching conditions. *Metallurgical Mater. Trans. B* 2, 2310–2312. doi: 10.1007/BF02917578

Elleuche, S., Schroder, C., Sahm, K., and Antranikian, G. (2014). Extremozymes - biocatalysts with unique properties from extremophilic microorganisms. *Curr. Opin. Biotechnol.* 29, 116–123. doi: 10.1016/j.copbio.2014.04.003

Empadinhas, N., and da Costa, M. S. (2008). Osmoadaptation mechanisms in prokaryotes: distribution of compatible solutes. *Int. Microbiol.* 11, 151–161. doi: 10.2436/20.1501.01.55

Esparza, M., Cardenas, J. P., Bowien, B., Jedlicki, E., and Holmes, D. S. (2010). Genes and pathways for CO2 fixation in the obligate, chemolithoautotrophic acidophile, *Acidithiobacillus ferrooxidans*. *BMC Microbiol.* 10:229. doi: 10.1186/1471-2180-10-229

Gahan, C. S., Sundkvist, J.-E., Dopson, M., and Sandström, Å. (2010). Effect of chloride on ferrous iron oxidation by a *Leptospirillum ferriphilum*-dominated chemostat culture. *Biotechnol. Bioeng.* 106, 422–431. doi: 10.1002/bit.22709

Goltsman, D. S., Dasari, M., Thomas, B. C., Shah, M. B., Verberkmoes, N. C., Hettich, R. L., et al. (2013). New group in the *Leptospirillum clade*: cultivation-independent community genomics, proteomics, and transcriptomics of the new species "*Leptospirillum* group IV UBA BS." *Appl. Environ. Microbiol.* 79, 5384–5393. doi: 10.1128/AEM.00202-13

Golyshina, O., Ferrer, M., and Golyshin, P. N. (2016). "Diversity and physiologies of acidophilic archaea," in *Acidophiles: Life in Extremely Acidic Environments*, eds R. Quatrini and D. B. Johnson (Poole, UK: Caister Academic Press), 93–106.

Gough, J., and Chothia, C. (2004). The linked conservation of structure and function in a family of high diversity: the monomeric cupredoxins. *Structure* 12, 917–925. doi: 10.1016/j.str.2004.03.029

Govender, E., Harrison, S. T. L., and Bryan, C. G. (2012). Modification of the ferric chloride assay for the spectrophotometric determination of ferric and total iron in acidic solutions containing high concentrations of copper. *Miner. Eng.* 35, 46–48. doi: 10.1016/j.mineng.2012.05.006

Gray, H. B., Malmstrom, B. G., and Williams, R. J. (2000). Copper coordination in blue proteins. *J. Biol. Inorg. Chem.* 5, 551–559. doi: 10.1007/s007750000146

Graziano, G., and Merlino, A. (2014). Molecular bases of protein halotolerance. *Biochim. Biophys. Acta* 1844, 850–858. doi: 10.1016/j.bbapap.2014.02.018

Guo, X., Jiang, C., Luo, Y., Zhang, M., Poetsch, A., and Liu, S. (2014). Proteomic and molecular investigations revealed that Acidithiobacillus caldus adopts multiple strategies for adaptation to NaCl stress. *Chin. Sci. Bull.* 59, 301–309. doi: 10.1007/s11434-013-0039-y

Harahuc, L., Lizama, H. M., and Suzuki, I. (2000). Selective inhibition of the oxidation of ferrous iron or sulfur in *Thiobacillus ferrooxidans*. *Appl. Environ. Microbiol.* 66, 1031–1037. doi: 10.1128/AEM.66.3.1031-1037.2000

Huber, H., and Stetter, K. O. (1989). *Thiobacillus prosperus* sp. nov., represents a new group of halotolerant metal-mobilizing bacteria isolated from a marine geothermal field. *Arch. Microbiol.* 151, 479–485. doi: 10.1007/BF00454862

Issotta, F., Galleguillos, P. A., Moya-Beltrán, A., Davis-Belmar, C. S., Rautenbach, G., Covarrubias, P. C., et al. (2016). Draft genome sequence of chloride-tolerant *Leptospirillum ferriphilum* Sp-Cl from industrial bioleaching operations in northern Chile. *Stand. Genomic Sci.* 11, 1–7. doi: 10.1186/s40793-016-0142-1

Jensen, S. M., Christensen, C. J., Petersen, J. M., Treusch, A. H., and Brandl, M. (2015). Liposomes containing lipids from *Sulfolobus islandicus* withstand intestinal bile salts: an approach for oral drug delivery? *Int. J. Pharmaceut.* 493, 63–69. doi: 10.1016/j.ijpharm.2015.07.026

Katayama, Y., Gottesman, S., Pumphrey, J., Rudikoff, S., Clark, W. P., and Maurizi, M. R. (1988). The two-component, ATP-dependent Clp protease of *Escherichia coli*. Purification, cloning, and mutational analysis of the ATP-binding component. *J. Biol. Chem.* 263, 15226–15236.

Knowles, R. B., Sabry, J. H., Martone, M. E., Deerinck, T. J., Ellisman, M. H., Bassell, G. J., et al. (1996). Translocation of RNA granules in living neurons. *J. Neurosci.* 16, 7812–7820.

Krisko, A., Copic, T., Gabaldon, T., Lehner, B., and Supek, F. (2014). Inferring gene function from evolutionary change in signatures of translation efficiency. *Genome Biol.* 15:R44. doi: 10.1186/gb-2014-15-3-r44

Levicán, G., Bruscella, P., Guacunano, M., Inostroza, C., Bonnefoy, V., Holmes, D. S., et al. (2002). Characterization of the petI and res operons of *Acidithiobacillus ferrooxidans*. *J. Bacteriol.* 184, 1498–1501. doi: 10.1128/JB.184.5.1498-1501.2002

Li, T. F., Painter, R. G., Ban, B., and Blake, R. C. II. (2015). The multicenter aerobic iron respiratory chain of *Acidithiobacillus ferrooxidans* functions as an ensemble with a single macroscopic rate constant. *J. Biol. Chem.* 290, 18293–18303. doi: 10.1074/jbc.M115.657551

Lindquist, S., and Craig, E. A. (1988). The heat-shock proteins. *Annu. Rev. Genet.* 22, 631–677. doi: 10.1146/annurev.ge.22.120188.003215

Lloubes, R., Cascales, E., Walburger, A., Bouveret, E., Lazdunski, C., Bernadac, A., et al. (2001). The Tol-Pal proteins of the *Escherichia coli* cell envelope: an energized system required for outer membrane integrity? *Res. Microbiol.* 152, 523–529. doi: 10.1016/S0923-2508(01)01226-8

Lucht, J. M., Dersch, P., Kempf, B., and Bremer, E. (1994). Interactions of the nucleoid-associated DNA-binding protein H-NS with the regulatory region of the osmotically controlled proU operon of *Escherichia coli*. *J. Biol. Chem.* 269, 6578–6586.

Ma, J. K., Wang, Y., Carrell, C. J., Mathews, F. S., and Davidson, V. L. (2007). A single methionine residue dictates the kinetic mechanism of interprotein electron transfer from methylamine dehydrogenase to amicyanin. *Biochemistry* 46, 11137–11146. doi: 10.1021/bi7012307

Malinverni, J. C., and Silhavy, T. J. (2009). An ABC transport system that maintains lipid asymmetry in the gram-negative outer membrane. *Proc. Natl. Acad. Sci. U.S.A.* 106, 8009–8014. doi: 10.1073/pnas.0903229106

Mangold, S., Potrykus, J., Björn, E., Lövgren, L., and Dopson, M. (2013). Extreme zinc tolerance in acidophilic microorganisms from the bacterial and archaeal domains. *Extremophiles* 17, 75–85. doi: 10.1007/s00792-012-0495-3

Mangold, S., Valdes, J., Holmes, D. S., and Dopson, M. (2011). Sulfur metabolism in the extreme acidophile *Acidithiobacillus caldus*. *Front. Microbiol.* 2:17. doi: 10.3389/fmicb.2011.00017

Millero, F. J., Feistel, R., Wright, D. G., and McDougall, T. J. (2008). The composition of standard seawater and the definition of the reference-composition salinity scale. *Deep Sea Res. I* 55, 50–72 doi: 10.1016/j.dsr.2007.10.001

Mayer, M. P., and Bukau, B. (2005). Hsp70 chaperones: cellular functions and molecular mechanism. *Cell. Mol. Life Sci.* 62, 670–684. doi: 10.1007/s00018-004-4464-6

Méndez-García, C., Peláez, A. I., Mesa, V., Sánchez, J., Golyshina, O. V., and Ferrer, M. (2015). Microbial diversity and metabolic networks in acid mine drainage habitats. *Front. Microbiol.* 6:475. doi: 10.3389/fmicb.2015.00475

Mueller, R. S., Dill, B. D., Pan, C., Belnap, C. P., Thomas, B. C., Verberkmoes, N. C., et al. (2011). Proteome changes in the initial bacterial colonist during ecological succession in an acid mine drainage biofilm community. *Environ. Microbiol.* 13, 2279–2292. doi: 10.1111/j.1462-2920.2011.02486.x

Mykytczuk, N. C., Trevors, J. T., Foote, S. J., Leduc, L. G., Ferroni, G. D., and Twine, S. M. (2011). Proteomic insights into cold adaptation of psychrotrophic and mesophilic *Acidithiobacillus ferrooxidans* strains. *Antonie van Leeuwen* 100, 259–277. doi: 10.1007/s10482-011-9584-z

Nicolle, J. L. C., Simmons, S., Bathe, S., and Norris, P. R. (2009). Ferrous iron oxidation and rusticyanin in halotolerant, acidophilic '*Thiobacillus prosperus*'. *Microbiology* 155, 1302–1309. doi: 10.1099/mic.0.023192-0

Ollivier, B., Caumette, P., Garcia, J. L., and Mah, R. A. (1994). Anaerobic bacteria from hypersaline environments. *Microbiol. Rev.* 58, 27–38.

Olsson, M. H., Hong, G., and Warshel, A. (2003). Frozen density functional free energy simulations of redox proteins: computational studies of the reduction potential of plastocyanin and rusticyanin. *J. Am. Chem. Soc.* 125, 5025–5039. doi: 10.1021/ja0212157

Oren, A. (2013). Life at high salt concentrations, intracellular KCl concentrations, and acidic proteomes. *Front. Microbiol.* 4:315. doi: 10.3389/fmicb.2013.00315

Osorio, H., Mangold, S., Denis, Y., Nancucheo, I., Johnson, D. B., Bonnefoy, V., et al. (2013). Anaerobic sulfur metabolism coupled to dissimilatory iron reduction in the extremophile *Acidithiobacillus ferrooxidans*. *Appl. Environ. Microbiol.* 79, 2172–2181. doi: 10.1128/AEM.03057-12

Osorio, H., Martinez, V., Nieto, P. A., Holmes, D. S., and Quatrini, R. (2008). Microbial iron management mechanisms in extremely acidic environments: comparative genomics evidence for diversity and versatility. *BMC Microbiol.* 8:203. doi: 10.1186/1471-2180-8-203

Ossandon, F. J., Cardenas, J. P., Corbett, M., Quatrini, R., Holmes, D. S., and Watkin, E. (2014). Draft genome sequence of the iron-oxidizing, acidophilic, and halotolerant "*Thiobacillus prosperus*" type strain DSM 5130. *Genome Announce.* 2:e01042-14. doi: 10.1128/genomeA.01042-01014

Parro, V., Moreno-Paz, M., and González-Toril, E. (2007). Analysis of environmental transcriptomes by DNA microarrays. *Environ. Microbiol.* 9, 453–464. doi: 10.1111/j.1462-2920.2006.01162.x

Petersen, T. N., Brunak, S., Von Heijne, G., and Nielsen, H. (2011). SignalP 4.0: discriminating signal peptides from transmembrane regions. *Nat. Methods* 8, 785–786. doi: 10.1038/nmeth.1701

Plumb, J. J., Gibbs, B., Stott, M. B., Robertson, W. J., Gibson, J. A. E., Nichols, P. D., et al. (2002). Enrichment and characterisation of thermophilic acidophiles for the bioleaching of mineral sulphides. *Miner. Eng.* 15, 787–794. doi: 10.1016/S0892-6875(02)00117-6

Ponce, J. S., Moinier, D., Byrne, D., Amouric, A., and Bonnefoy, V. (2012). *Acidithiobacillus ferrooxidans* oxidizes ferrous iron before sulfur likely through transcriptional regulation by the global redox responding RegBA signal transducing system. *Hydrometallurgy* 127–128, 187–194. doi: 10.1016/j.hydromet.2012.07.016

Potrykus, J., Rao Jonna, V., and Dopson, M. (2011). Iron homeostasis and responses to iron limitation in extreme acidophiles from the *Ferroplasma* genus. *Proteomics* 11, 52–63. doi: 10.1002/pmic.201000193

Quatrini, R., Appia-Ayme, C., Denis, Y., Jedlicki, E., Holmes, D., and Bonnefoy, V. (2009). Extending the models for iron and sulfur oxidation in the extreme acidophile *Acidithiobacillus ferrooxidans*. *BMC Genomics* 10:394. doi: 10.1186/1471-2164-10-394

Rea, S. M., Mcsweeney, N. J., Degens, B. P., Morris, C., Siebert, H. M., and Kaksonen, A. H. (2015). Salt-tolerant microorganisms potentially useful for bioleaching operations where fresh water is scarce. *Miner. Eng.* 75, 126–132. doi: 10.1016/j.mineng.2014.09.011

Ribeiro, D. A., Maretto, D. A., Nogueira, F. C., Silva, M. J., Campos, F. A., Domont, G. B., et al. (2011). Heat and phosphate starvation effects on the proteome, morphology and chemical composition of the biomining bacteria *Acidithiobacillus ferrooxidans*. *World J. Microbiol. Biotechnol.* 27, 1469–1479. doi: 10.1007/s11274-010-0599-9

Shibata, C., Ehara, T., Tomura, K., Igarashi, K., and Kobayashi, H. (1992). Gene structure of *Enterococcus hirae (Streptococcus faecalis)* F1F0-ATPase, which functions as a regulator of cytoplasmic pH. *J. Bacteriol.* 174, 6117–6124. doi: 10.1128/jb.174.19.6117-6124.1992

Shiers, D. W., Blight, K. R., and Ralph, D. E. (2005). Sodium sulphate and sodium chloride effects on batch culture of iron oxidising bacteria. *Hydrometallurgy* 80, 75–82. doi: 10.1016/j.hydromet.2005.07.001

Shivanand, P., and Mugeraya, G. (2011). Halophilic bacteria and their compatible solutes - osmoregulation and potential applications. *Curr. Sci.* 100, 1516–1521.

Sievers, F., Wilm, A., Dineen, D., Gibson, T. J., Karplus, K., Li, W., et al. (2011). Fast, scalable generation of high-quality protein multiple sequence alignments using Clustal Omega. *Mol. Syst. Biol.* 7:539. doi: 10.1038/msb.2011.75

Silberg, J. J., Hoff, K. G., and Vickery, L. E. (1998). The Hsc66-Hsc20 chaperone system in *Escherichia coli*: chaperone activity and interactions with the DnaK-DnaJ-grpE system. *J. Bacteriol.* 180, 6617–6624.

Slonczewski, J. L., Fujisawa, M., Dopson, M., and Krulwich, T. A. (2009). Cytoplasmic pH measurement and homeostasis in bacteria and archaea. *Adv. Microb. Physiol.* 55, 1–79. doi: 10.1016/S0065-2911(09)05501-5

Stancik, L. M., Stancik, D. M., Schmidt, B., Barnhart, D. M., Yoncheva, Y. N., and Slonczewski, J. L. (2002). pH-dependent expression of periplasmic proteins and amino acid catabolism in *Escherichia coli*. *J. Bacteriol.* 184, 4246–4258. doi: 10.1128/JB.184.15.4246-4258.2002

Suzuki, I., Lee, D., Mackay, B., Harahuc, L., and Oh, J. K. (1999). Effect of various ions, pH, and osmotic pressure on oxidation of elemental sulfur by *Thiobacillus thiooxidans*. *Appl. Environ. Microbiol.* 65, 5163–5168.

Valdes, J., Pedroso, I., Quatrini, R., Dodson, R. J., Tettelin, H., Blake, R., et al. (2008). *Acidithiobacillus ferrooxidans* metabolism: from genome sequence to industrial applications. *BMC Genomics* 9:597. doi: 10.1186/1471-2164-9-597

Vera, M., Schippers, A., and Sand, W. (2013). Progress in bioleaching: fundamentals and mechanisms of bacterial metal sulfide oxidation–part A. *Appl. Microbiol. Biotechnol.* 97, 7529–7541. doi: 10.1007/s00253-013-4954-2

Vertommen, D., Ruiz, N., Leverrier, P., Silhavy, T. J., and Collet, J. F. (2009). Characterization of the role of the *Escherichia coli* periplasmic chaperone SurA using differential proteomics. *Proteomics* 9, 2432–2443. doi: 10.1002/pmic.200800794

Walter, R. L., Ealick, S. E., Friedman, A. M., Blake, R. C. II, Proctor, P., and Shoham, M. (1996). Multiple wavelength anomalous diffraction (MAD) crystal structure of rusticyanin: a highly oxidizing cupredoxin with extreme acid stability. *J. Mol. Biol.* 263, 730–751. doi: 10.1006/jmbi.1996.0612

Warren, J. J., Lancaster, K. M., Richards, J. H., and Gray, H. B. (2012). Inner- and outer-sphere metal coordination in blue copper proteins. *J. Inorg. Biochem.* 115, 119–126. doi: 10.1016/j.jinorgbio.2012.05.002

Watling, H. R. (2014). Chalcopyrite hydrometallurgy at atmospheric pressure: 2. Review of acidic chloride process options. *Hydrometallurgy* 146, 96–110. doi: 10.1016/j.hydromet.2014.03.013

Wen, Q., Liu, X. M., Wang, H. Y., and Lin, J. Q. (2014). A versatile and efficient markerless gene disruption system for *Acidithiobacillus thiooxidans*: application for characterizing a copper tolerance related multicopper oxidase gene. *Environ. Microbiol.* 16, 3499–3514. doi: 10.1111/1462-2920.12494

Yu, C. S., Chen, Y. C., Lu, C. H., and Hwang, J. K. (2006). Prediction of protein subcellular localization. *Proteins* 64, 643–651. doi: 10.1002/prot.21018

Yu, Y. Y., Liu, X. M., Wang, H. Y., Li, X. T., and Lin, J. Q. (2014). Construction and characterization of tetH overexpression and knockout strains of *Acidithiobacillus ferrooxidans*. *J. Bacteriol.* 196, 2255–2264. doi: 10.1128/JB.01472-13

Zakharov, S. D., Eroukova, V. Y., Rokitskaya, T. I., Zhalnina, M. V., Sharma, O., Loll, P. J., et al. (2004). Colicin occlusion of OmpF and TolC channels: outer membrane translocons for colicin import. *Biophys. J.* 87, 3901–3911. doi: 10.1529/biophysj.104.046151

Zammit, C. M., Mangold, S., Jonna, V. R., Mutch, L. A., Watling, H. R., Dopson, M., et al. (2012). Bioleaching in brackish waters - effect of chloride ions on the acidophile population and proteomes of model species. *Appl. Microbiol. Biotechnol.* 93, 319–329. doi: 10.1007/s00253-011-3731-3

Zammit, C. M., and Watkin, E. L. J. (2016). "Adaptation to extreme acidity and osmotic stress," in *Acidophiles: Life in Extremely Acidic Environments*, eds R. Quatrini and D. B. Johnson (Poole, UK: Caister Academic Press), 49–62.

Conflict of Interest Statement: The authors declare that the research was conducted in the absence of any commercial or financial relationships that could be construed as a potential conflict of interest.

The reviewer CSD declared a past co-authorship with one of the authors DH to the handling Editor, who ensured that the process met the standards of a fair and objective review. The reviewer SH and the handling Editor declared their shared affiliation, and the handling Editor states that the process nevertheless met the standards of a fair and objective review.

Advantages of publishing in Frontiers

OPEN ACCESS
Articles are free to read, for greatest visibility

COLLABORATIVE PEER-REVIEW
Designed to be rigorous – yet also collaborative, fair and constructive

FAST PUBLICATION
Average 85 days from submission to publication (across all journals)

COPYRIGHT TO AUTHORS
No limit to article distribution and re-use

TRANSPARENT
Editors and reviewers acknowledged by name on published articles

SUPPORT
By our Swiss-based editorial team

IMPACT METRICS
Advanced metrics track your article's impact

GLOBAL SPREAD
5'100'000+ monthly article views and downloads

LOOP RESEARCH NETWORK
Our network increases readership for your article

Frontiers
EPFL Innovation Park, Building I • 1015 Lausanne • Switzerland
Tel +41 21 510 17 00 • Fax +41 21 510 17 01 • info@frontiersin.org
www.frontiersin.org

Find us on